BNL-NCS-51694
UC-34c
(Physics-Nuclear — TIC-4500)

IAEA ADVISORY GROUP MEETING ON BASIC AND APPLIED PROBLEMS OF NUCLEAR LEVEL DENSITIES

Held at
BROOKHAVEN NATIONAL LABORATORY
Upton, Long Island, New York 11973
April 11-15, 1983

BNL-NCS--51694
DE84 004474

Edited by
M.R. Bhat

June 1983

Jointly Sponsored by the
IAEA and the DIVISION OF HIGH ENERGY AND NUCLEAR PHYSICS
OF THE UNITED STATES DEPARTMENT OF ENERGY

NATIONAL NUCLEAR DATA CENTER
BROOKHAVEN NATIONAL LABORATORY
ASSOCIATED UNIVERSITIES, INC.
UNDER CONTRACT NO. DE-AC02-76CH00016 WITH THE
UNITED STATES DEPARTMENT OF ENERGY

Printed in the United States of America
Available from
National Technical Information Service
U.S. Department of Commerce
5285 Port Royal Road
Springfield, VA 22161

NTIS price codes:
Printed Copy: A19; Microfiche Copy: A01

TABLE OF CONTENTS

TABLE OF CONTENTS (cont'd)

TABLE OF CONTENTS (cont'd)

PREFACE

This meeting was organized under the auspices of the International Atomic Energy Agency (IAEA) and the Division of High Energy and Nuclear Physics of the U.S. Department of Energy to consider in detail the present state of knowledge of nuclear level densities. This would include both the results of basic research on nuclear level densities and their application for practical problems. The basic research on nuclear level densities has been concerned with various phenomenological and microscopic models, their validation by comparison with measurements, and the extraction of level density parameters from experimental data. Neutron cross-sections are needed for a number of applications for fission and fusion reactors, intense high energy neutron sources, and related problems of neutron shielding and gamma-ray production. The many measurements of these cross-sections are supplemented by nuclear model calculations in which the nuclear level density is an important parameter.

The Meeting was divided into a number of sessions to consider these topics in review or contributed papers. At the end of these sessions, the attendees formed two workshop groups: the first on nuclear level density theories and nuclear model reaction cross-section calculations and the second on the extraction of nuclear level density information from experimental data. The reports of these workshop groups discussing the present status of these subjects and providing specific recommendations for future work were

approved in a plenary session on the last day of the Meeting and are included in this volume.

I would like to thank J.J. Schmidt and V.G. Pronyaev of the Nuclear Data Section, IAEA for their help in the organization of this Meeting. Grateful thanks are also due to my associates on the Local Organization Committee, April Donegain, Judy Badal, and Arleen Lancsarics for taking care of the many details that went into the successful functioning of the Meeting.

June 15, 1983 M. R. Bhat

ORGANIZATION OF THE IAEA ADVISORY GROUP MEETING ON BASIC AND APPLIED PROBLEMS OF NUCLEAR LEVEL DENSITIES

ORGANIZING COMMITTEE

V. G. Pronyaev, Chairman
E. D. Arthur
M. R. Bhat
F. H. Fröhner
S. M. Grimes
R. C. Haight
K. Harada
A. V. Ignatyuk
S. S. Kapoor
J. E. Lynn
E. Menapace
P. Ribon
G. Rohr
V. G. Soloviev

CONFERENCE CHAIRMAN: J. E. Lynn

SCIENTIFIC SECRETARY V. G. Pronyaev

WORKSHOP CHAIRMEN: S. M. Grimes
F. H. Fröhner
H. Vonach

LOCAL ORGANIZING COMMITTEE

M. R. Bhat
B. A. Magurno
S. F. Mughabghab
S. Pearlstein
F. M. Scheffel

ADMINISTRATIVE SECRETARY

April Donegain

Opening Remarks from the IAEA

V.G. Pronyaev

On behalf of the Director General of the International Atomic Energy Agency I would like to welcome all of you to this IAEA Advisory Group Meeting on Basic and Applied Problems of Nuclear Level Densities. We meet together to discuss on the one hand such classical and fundamental questions of the description of many-body systems as the Level Density of Atomic Nuclei. On the other hand it is well known that chiefly through the statistical model of nuclear eactions this fundamental quantity has a strong impact on the results of calculations and evaluations particularly of neutron reaction cross-sections needed for many practical applications. The level density formulae needed for such calculations have to be simple enough for use in the rather lengthy model calculations of the cross sections, but at the same time they have to reflect all the basic features of the level density behaviour. Past developments have shown that it is very difficult to satisfy both these conditions simultaneously. To discuss ways of solution of this problem will be one of the main tasks of our meeting from my point of view.

As you know the preparations of this meeting were carried out under rather difficult circumstances. Mainly due to this fact there occurred some delay in various stages of preparation of the meeting. Finally problems were resolved and I would like to thank all of you who contributed to this for your

understanding and assistance. On behalf of the IAEA I would like to express particular gratitude to the Brookhaven National Laboratory as host laboratory and to the National Nuclear Data Centre and personally to Mulki Bhat and Sol Pearlstein for their help in organizing this meeting and to the U.S. Department of Energy for the generous financial contribution to our meeting. I am also very grateful to the Members of the Organizing Committee of this meeting for their help and fruitful suggestions on the elaboration of the Meeting Programme.

Thank you for your attention. I wish you all a pleasant and scientifically interesting and successful meeting.

WORKSHOP REPORTS

Workshop I

NUCLEAR LEVEL DENSITY THEORIES AND NUCLEAR MODEL REACTION CROSS-SECTION CALCULATIONS

S.M. Grimes - Chairman
A.M. Anzaldo Meneses
M. Divadeenam
C.Y. Fu
D.G. Gardner
M.A. Gardner
H. Gruppelaar
M. Hillman
C. Jacquemin
H. Jahn
A.S. Jensen
C. Kalbach
D.G. Madland
E. Menapace
V.G. Pronyaev
V.S. Ramamurthy
G. Reffo
G. Rohr
K-H. Schmidt
B. Strohmaier
J. Treiner

1. Introduction

The earliest theoretical work in the field of nuclear level densities dates back to the 1930's. In spite of nearly fifty years of increasingly sophisticated models, many unanswered questions remain. This committee assessed the current status of level density models in use today and compiled some recommendations for future work. Recent work in this area has resulted in some promising new approaches to level density calculations; these should be utilized and the results compared with data to evaluate the need for more refinements.

2. Phenomenological Models

The work of Bethe led to the development of the Fermi gas model for level densities. An analytic form for the level density resulted from this work and it is this form which is normally fit to experimental data today. Current work on phenomenological representations of nuclear level densities attempts to build on this framework by finding simple functional relations which give the level density parameters for various nuclei. These forms must include the important physical features if they are to give the proper values to be used for extrapolation into new regions. The most important such effects are a) shell effects, b) odd-even effects, c) collective enhancements and d) microscopic effects (isospin dependence, finite size corrections).

Several alternate forms have been proposed to take shell effects into account. It appears that various approaches, which incorporate these effects into an energy dependence of the level density parameter, an energy shift or a combination of both, agree on the fact that shell effects anneal out rapidly

with energy. The different techniques agree reasonably well on the rate at which this occurs. An important input parameter for these calculations is the ground state shell correction. At present there is no complete agreement on the definition of these quantities because of uncertainties in the form of the energy expression of the liquid drop model. Theoretical estimates of this parameter from microscopic models are known to contain some unresolved uncertainties.

Pairing effects can be included in the framework of the superconducting model (BCS). Most BCS treatments do not include the expected J-dependence and exciton number dependence of the pairing gap; all levels at a given excitation are assumed to have the same gap energy. There are indications that the simplest correction for odd-even or even-even mass differences is not always adequate. This problem is possibly coupled to problems with ground state shell corrections discussed above. Pairing correlations tend to wash out subshell effects and to reduce but not eliminate major shell effects.

Collective enhancements to level densities at low energies are well established. Agreement has not yet been reached on the detailed energy dependence of such enhancements. Simple prescriptions based on the adiabatic approximation are probably valid at low energies. Extrapolations to higher energies are risky because of the possible change of parameters with energy and the violation of unitarity caused by adding in levels at low energy even though they are already present (at an unknown higher energy) in the spectrum.

Microscopic systematics have been investigated recently. Two new features which have emerged from these studies are the observation of finite size and isospin dependence effects on the level density parameter "a".

Studies of these effects should improve our ability to extrapolate the parameter away from the lines of stability.

Papers in this volume by Arthur, Jensen, Menapace, Ramamurthy, Reffo, Rohr and Treiner deal with current applications of phenomenological level density models.

3. Microscopic Fermi-gas Model

Microscopic Fermi gas models utilize shell model single-particle schemes and the BCS quasiparticle approach to calculate level densities with the inclusion of shell and pairing effects. The numerical values of the level density resulting from this type of calculation can often be fit with a conventional Fermi gas form. Use of such a model therefore allows a test of the assumed energy dependence of the level density as well as providing a means of calculating the level density parameter. Unlike phenomenological models the microscopic model also predicts the parity ratio and spin cutoff parameter as functions of energy.

Our insufficient knowledge of input parameters as well as complications of collective states cause difficulty with this approach; extrapolation of these calculations to nuclei off the stability line is somewhat risky because of these problems. These calculations are fast and easy to perform however, and will be valuable both for the direct use of the level densities themselves as well as the guidance they can provide on the systematics to be expected in phenomenological level density parameter expressions. Presentations by Arthur and Menapace at this conference discuss calculations of this type.

4. Non-Fermi-gas Methods

Alternative methods to the traditional Fermi-gas are also available for calculating nuclear level densities. These include direct iterative techniques, number theoretical methods and Hamiltonian moment expansions. These are much less widely used than Fermi gas procedures but can be useful in evaluating level densities.

Direct iterative techniques are those which involve direct tabulation of the level energies, spins and parities. They are therefore valuable in checking the mathematical approximations (principally the saddle point approximation) made in applying the Fermi gas formalism. They are rather demanding in terms of computer time, since to calculate the parameters of N levels, for example, more than $N^{1/2}$ arithmetic manipulations must be performed. It is clear that such techniques are not at present sufficiently fast that they can routinely be used for level density calculations. They do have two special virtues: levels can easily be classified as to exciton number and the pairing energy can be calculated separately for each state. An additional advantage is that the J-distribution is obtained exactly. A disadvantage is that the two-body force (beyond pairing) cannot easily be incorporated in such a procedure. Further improvements in computer performance may make the computer limitations less significant. These calculations can continue to serve as benchmarks for checking approximations in various other methods; it remains to be seen whether future theoretical developments will allow a more general two-body force to be included, such as perhaps a spreading width as a function of energy. A code LEVBCS6 (See

Appendix) which makes such calculations is available from M. Hillman of Brookhaven.

Number theoretical approaches have been used at Karlsruhe to calculate nuclear level densities. They have been used to yield not only total level densities but also level densities as a function of exciton number. As yet they have not been used with a two-body interaction. They therefore do not predict collective states and need the enhancement factors required for Fermi gas calculations. Those using these techniques believe that future work will allow inclusion of collective states. Work at present is focussed on obtaining analytical forms for the level density; no computer code is available at present for general distribution. The talk by Anzaldo Meneses at this conference discusses this technique.

Both number theoretical and microscopic Fermi gas methods can calculate the level density for arbitrary single particle spectra. Thus, neither is tied to the Bethe level density formula and shell effects can be included with either approach. Also, by appropriate choice of single particle energies, the average effect of two-body forces (in the Hartree-Fock sense) can be included in the calculation. More subtle consequences of the two-body force, such as shifts in the average single particle energy with temperature, cannot be incorporated in these "one-body" approaches. It is therefore important to make detailed comparisons of such calculations with data and with the results of calculations including the full two-body force to improve our understanding of the relative importance of the various effects of the two-body force. Such comparisons should include spin cutoff parameters and parity ratios as well as level densities.

Moment methods are being investigated by groups in Europe, Canada and in the United States. These calculations have the important advantage that a complete two-body force can be included in the calculations. This allows, in principle, the nucleus to assume the appropriate deformation and puts the collective states in the appropriate energy regions. Obviously, this can occur only if we include a large enough number of active nucleons (a small enough core) and a two-body interaction and single particle spectrum which are correct. To some extent we may be guided by shell-model results, but because we normally use a much larger basis in level density calculations there are indications that the two-body force strength may have to be modified. This makes a priori calculations difficult at present, but as we gain experience with such large bases a better understanding of renormalization effects may emerge, allowing systematic rules to be formulated.

A severe problem at present is that these calculations take approximately two hours on modern computers. This effectively prohibits parameter searches and makes it impossible to use for problems which require level density information for numerous nuclei. The calculations are much faster if only a one-body Hamiltonian is used; in some cases, this could be used to check the results from other approaches. It is very important to continue efforts to speed up these calculations, because we must explore the effects of varying various parameters. Until better information on input parameters is available, this method will not be used widely. It is clear that an improvement in computer performance would greatly facilitate use of moment techniques. Efforts should continue to find better theoretical techniques for evaluating moments. Since nearly all of the time is used to calculate the

highest moments, development of approximation techniques for these would save considerable time.

There is increasing demand for level densities for nuclei off the stability line or for nuclei which are highly deformed (as are of interest in studies of fission or heavy-ion reactions). Both of these situations can be difficult to deal with Fermi gas models. A correct treatment of the two-body force is particularly important in calculating level densities in these situations. Moment methods are able to deal with these nuclei without fundamental difficulty, if we have the appropriate input parameters Contributions to these proceedings by Grimes, Halemane and Jacquemin discuss the use of such techniques.

5 Exciton Level Densities

Calculations of cross sections for pre-equilibrium reactions require level or state densities as a function of exciton number. Unified models, which treat the pre-equilibrium and equilibrium reactions consistently, require not only exciton level densities but also a consistent total level density.

The Williams formula (Nucl. Phys. A166, 231 (1971)) is frequently used in pre-equilibrium model calculations. There are, however, small differences in the way the Pauli corrections are evaluated, as indicated in the contributions of Anzaldo Meneses and Kalbach to this conference. Normally, pairing and shell corrections have been neglected.

At this conference, progress was reported in the inclusion of these corrections in microscopic exciton calculations as reported by Fu and Reffo.

To include these effects in the Williams formula, a simple parameterization is needed for these shifts. Examples of such attempts are the work of Grimes (Phys. Rev. C13, 2224(1976)) and Fu (this conference), for pairing corrections and Kalbach (this conference), for shell effects.

For reasons of consistency the sum over all possible particle-hole components should be equal to the total level density, which can be deduced from measurements. This is a necessary constraint for unified model calculations, that leads to constraints on the adopted expressions for the particle-hole level densities and their spin distributions. The easiest way to do this is by renormalizing the Williams formula to a phenomenological expression for the level density as discussed by Gruppelaar at this conference.

In these unified models a simple expression for the spin distribution of the particle-hole level density is required. It has been found from combinatorial calculations that the square of the spin cut-off parameter is proportional to the exciton number for small exciton numbers (Reffo, this conference). At high exciton numbers it is expected that the spin cut-off parameter is less dependent and perhaps even independent of the number of excitons.

In some precompound models protons and neutrons are explicitly considered. This requires use of an appropriate particle-hole level density formula, e.g. the one proposed by Ericson (Advan. Phys. 9, 425 (1960)), with additional corrections for Pauli blocking etc. This also leads to modified expressions of the internal transition rates, as discussed by Kalbach (this conference).

In other calculations where the multi-step-direct cross section is to be differentiated from the multi-step-compound cross-section, separate particle-hole state densities for bound and unbound states in the continuum are needed. Progress in this area has also been reported (Kalbach this conference).

6. Recommendations

As this summary indicates many areas of research in nuclear level density theory are active. There remain numerous problems, however, and we make the following recommendations:

(i) Work should continue on phenomenological models. Particular emphasis should be placed on comparisons with as wide a range of data as possible, including not only isolated resonance counts but also evaporation spectra. Detailed examination of the recently discovered size and isospin effects should be continued. Studies of the systematics of level density parameters should incorporate as much as possible the trends and parameter dependence suggested by microscopic models. The phenomenological models will continue to be widely used, because of the difficulty of most other approaches.

(ii) Studies of microscopic Fermi gas calculations should be carried out systematically in given mass regions to determine appropriate single particle sets. Equivalently, number theoretical methods could be used. The purpose of these studies is twofold: to better understand the relative importance of various two-body

force effects and to obtain information on the systematics of the variation of single particle energies with neutron and proton numbers. Again, the comparisons should be with as broad a range of data as possible, including parity ratios and spin cutoff parameters.

(iii) Calculations including the full two-body force exactly as well as in approximate forms should be continued. Proposals to include random phase approximation correlations in one-body calculations are worth investigating. Parameter studies for moment method calculations are quite difficult, given the present length of the calculations, but are needed in order to make these calculations more useful. A high priority should be given to efforts to speed up these calculations. Comparisons with data over as wide a range as possible should be made.

(iv) More work on parameterizing pairing and shell corrections to exciton level densities in the Williams formula is needed. Nearly all calculations of reactions utilize this closed form for the exciton level densities.

(v) Additional examination of the consequences of requirements of self consistency for exciton and total level densities on the spin and parity distributions is needed. Methods such as the combinatorial or number theoretical approach could be used for these studies. One stringent requirement on the particle-hole spin distribution functions is that they lead to simultaneous consistency between

exciton and total formula for both the state and level densities. The spin dependence of the transition state densities which appear on the internal transition rates also needs to be studied. Care also needs to be exercised in summing particle hole state densities for comparison with total state densities. Most pre-equilibrium model calculations treat only configurations with a fixed value of the difference between p and h while total state densities correspond to sum over all values of p and h independently. It would also be useful to look at two-body and collective effects on exciton level densities; this may be possible with moment methods.

(vi) Some further effort is required to study the dependence of the spin cut-off parameter on exciton number and energy; similarly the exciton number dependence of the yrast line needs to be established.

(vii) In summary, the field of nuclear level densities remains an active one, with many new developments and some continuing problems. We note that mean square deviations of the order of a factor of two between calculated and experimental neutron resonance spacings persist even after all the recent refinements in the calculations have been included. This can arise either from an inherent scatter of this order in the experimental values or a physical feature missing in the calculations. This aspect consequently deserves further consideration. Level density calculations are not only of applied interest but involve many questions of basic nuclear physics.

APPENDIX

Microscopic Level Density Codes

CODE/COMPUTER	AUTHOR	PHYSICS INCORPORATED - INPUT/OUTPUT	COMMENTS
NILS IBM 370 CDC-7600	Grimes Physics Dept. Ohio Univ.	Partition and Saddle Point approximations. Pairing included via BCS Formalism. Input: Neutron, Proton Pairing Energies. Single-Particle Energies: Nilsson/Seeger + Perish/Seeger + Howard. Output: Numerical value of level density as a function of E, spin-cutoff parameter, parity ratio. Best fit value of "a" and δ by fitting to the data.	The code is fast. Parameter search possible. Single-Particle Energies for deformed well possible by inputting deformation parameter. Collective bands are not included. Available for distribution.
LEVBCS6 CDC IBM 60 UNIVAX 1110	Hillman BNL	Combinatorial calculation of level densities with BCS pairing and spin distribution. Input: Z,N,E_{max}, G. Single-Particle data in code. These can be changed. Output: Level densities in energy bins vs. spin J.	The code has been used in conjunction with Hauser-Feshbach program. G is the only parameter. G's are available based on neutron capture resonances. Available for distribution.

Microscopic Level Density Codes (continued)

CODE/COMPUTER	AUTHOR	PHYSICS INCORPORATED - INPUT/OUTPUT	COMMENTS
SYDMNP CDC IBM	Hillman BNL	Saddle-point approximation method, direct iterative solution of Non-linear equations. Input: Z,N, E_{max} Output: Level density one MeV apart.	Not tested. Inclusion of Pairing planned. Available for distribution.
SCALJ UNIVAC	Jacquemin Univ. of Paris	Fixed J level densities approximated by Gaussian. Exactly calculated centroids and widths. Input: One-Fermion Energies, Two-body matrix elements in reduced form. Output: Centroids E(n,J) and variances $\Lambda^2(n,J)$ for each particle number and J value.	Higher order moments impractical. Quasi-particle code exists, which is quite similar. The code is very fast. Available for distribution.
CONFJ UNIVAC	Jacquemin Univ. of Paris	Fixed J level densities approximated by sum over configurations. Exactly calculated centroids and widths.	Careful selection of configurations of interest required.

Microscopic Level Density Codes (continued)

CODE/COMPUTER	AUTHOR	PHYSICS INCORPORATED - INPUT/OUTPUT	COMMENTS
		Input: One-Fermion Energies, Two-body matrix elements. Output: Fixed J configuration centroids and widths.	Large memory (200,000 words) needed. Available for distribution.
PREMZP UNIVAC	Jacquemin Univ. of Paris	Exact level densities. Non-interacting Fermions. Fixed J, Parity and isospin etc. Input: Single-Particle Energies (Spherical or Rotational). Output: Level densities as a function of A,J,Π,T etc.	Inclusion of residual interaction, pairing etc. are planned. Available for distribution.
NUDENS IBM 370/168	Maino, et al. ENEA, Bologna	Nilsson-BCS with Blocking effect at finite temperatures. Input: $N, Z, E_2, E_4, B, \Delta_n, \Delta_z(T=0)$ $\hbar\omega_{vib}$, N_0. E_{x_i}.	Applicable in the energy range of 4 MeV <Ex<20 MeV. Zero temperature blocking effect to be considered.

Microscopic Level Density Codes (continued)

CODE/COMPUTER	AUTHOR	PHYSICS INCORPORATED - INPUT/OUTPUT	COMMENTS
		Output: $E_F(N), E_F(Z), T, \Delta_n(T), \Delta_z(T)$, $S(T)$, Ω, the intrinsic state density and "a", the phenomenological level density parameter.	Will be available after cleaning and testing.

Workshop II

EXTRACTION OF NUCLEAR LEVEL DENSITY INFORMATION FROM EXPERIMENTAL DATA

F.H. Fröhner/H. Vonach -- Chairmen

M.R. Bhat

R.C. Haight

J.E. Lynn

E. Menapace

S.F. Mughabghab

S. Pearlstein

V.G. Pronyaev

P. Ribon

G. Rohr

Conclusions and Recommendations

A. Resolved Resonance Parameters (Chairman: F.H. Fröhner)

1. The most direct method of level density determination is resonance counting in the resolved resonance region, but

   - the count must always be corrected for levels missing because of counting statistics and resolution effects (unresolved multiplets). Corrections range from 15% (^{238}U) to 30-40% or more for less will studied nuclei. Uncorrected level densities are worthless for most purposes.
   - one obtains only 1 point of the ρ vs. E curve, and that for only 1 or 2 spins.

2. Required accuracies of ρ for applications-oriented cross-sections calculations are of the order of 10% for wide energy ranges (e.g. 0.1 to 15 or 20 MeV), a few percent for the unresolved resonance region (up to 200 or 300 keV). These accuracies are not reached yet; existing results differ often by factors of 1.3 to 2. The main cause is inadequate methods of statistical analysis of resonance parameters.

3. Missing-level estimators not based on the Porter-Thomas distribution are now recognized as unreliable. This is true not only for simple ladder statistics but also for sophisticated variants such as Dyson's Δ_3 statistic (see papers in this volume by Fröhner, Ribon). Evaluators and compilers of level densities are

urged to use methods based on the Porter-Thomas distribution as done for example in the recent evaluations of V. Benzi, G. Maino and E. Menapace, Nuovo Cimento, A66, 1, (1981) and Rohr (this volume).

4. Some recent shell-model calculations seemed to indicate an enhancement over the simple Porter-Thomas distribution for very weak levels but according to others this discrepancy vanishes if due account is taken of the slow energy variation of the mean width (see e.g. T.A. Brody et al. Rev. Mod. Phys. 53, 385 (1981) Fig. 10 or J.J.M. Verbaarschot and P.J. Brussaard, Phys. Lett. 87B, 155 (1979)). All experimental data support the Porter-Thomas hypothesis so far.

5. Missing-level estimation codes should be checked against the test material (E_0, $2g\Gamma_n$ values) of the NEADB benchmark exercise initiated by P. Ribon. This test material, available from the 4 Nuclear Data Centers, includes the effects of finite resolution and counting statistics. Results could also be compared to those of the estimators already checked and available from the 4 Centers, viz. BAYESZ (M. Moore), ESTIMA (E. Fort et al.) and MISDO (G. Rohr). (See Appendix).

6. The essential input for level density estimation consists of evaluated sets of resonance parameters, notably those in Neutron

Cross-Sections Vol. I, 4th ed. (formerly BNL-325). It is strongly recommended that periodic publication of this useful document continue. Concern was expressed about the drawn-out publication cycle, and the National Nuclear Data Center (BNL) is urged to explore whether supplements could be issued between subsequent publications (or at least the updated file of evaluated resonance parameters be made available to requesters). The compilation of experimental resonance parameters in the EXFOR files of the 4 Data Centers in conjunction with improved retrieval techniques and formats is of additional value. These activities should under no circumstances be weakened because of new tasks.

7. Much information on level densities is contained in high-resolution proton resonance data. The 4 Centers are urged to compile these resonance parameters so that they become accessible with similar ease and completeness as has been achieved for neutron resonance parameters in recent years.

8. It is strongly recommended that estimates of level densities should not be published or compiled without specification of the energy range and the method utilized in the estimation process.

9. Compilation and publication of level spacing results should primarily take the form of tables of level spacings, not of "a" values.

10. The experimental data base for neutron resonance parameters is quite extensive. Gaps exist, however, in particular for higher actinides (^{242m}Am,...) and fission products, where only very few or no resonances are known. These gaps should be filled by linac and similar other measurements. Among the important fissile nuclides ^{239}Pu is an example where the level density uncertainty could be reduced drastically with polarization data similar to those obtained at LANL for ^{235}U. In spite of the difficulties to polarize radioactive samples, this avenue should be seriously studied by experimenters.

11. Although virtually no reliable information on p-wave level densities has so far been extracted from neutron resonance data, the methods (high-resolution differential elastic scattering measurements) used at ORNL e.g. for ^{56}Fe appear to have the potential for further development. Experimenters are urged to study the possibility to make sufficiently complete partial-wave assignments in favorable cases, e.g. in the Fe region, so that p-wave level densities can be established.

B. Non-Resonant Reactions (Chairman: H. Vonach)

1. Important level density information can be derived from high resolution nuclear research studies identifying individual nuclear levels, from the study of the energy differential particle emission cross-sections in compound nucleus reactions, and from cross-

section fluctuations in the excitation functions of compound nucleus reactions to isolated final states. By combination of these methods it is possible to derive the total level density as a function of excitation energy over an extended energy range and to get additional information on the spin dependence of the level density. This allows a much more detailed testing of the phenomenological and theoretical level density model than the comparison with the neutron resonance data alone which provide the level density for just one energy and one or two spin values.

2. Study Of Resolved Levels In High Resolution Nuclear Reactions.

2.1 The energy range, where nuclear level schemes are approximately complete is still rather small covering the first 15-50 levels and extending to 1-5 MeV depending on A and the type of nucleus.

2.2 Reliable correction procedures for missing levels could considerably extend the energy accessible to the level counting method. Such procedures however are only available for the extraction of level densities from high-resolution particle spectra obtained from compound nucleus reactions, whereas as yet no methods have been developed for correcting either particle spectra from direct reactions or the level schemes derived from high resolution γ-spectroscopy for such missing levels. As a consequence, the completeness of nuclear level schemes above ~ A-70 has to be judged very cautiously.

2.3 Most existing high-resolution measurements of particle spectra have been performed with an energy resolution ~ 10 keV which is about a factor of 3 worse than the presently achievable values. Thus improved knowledge of the level densities could be obtained by further experiments with these techniques.

2.4 New high-resolution measurements of particle spectra in the A=40-60 region where reliable corrections for missing levels are possible, can probably extend the range accessible to level counting to a point where reliable extrapolation to the neutron binding energy is possible.

2.5 Discrete states are often identified by the gamma rays from (n,γ) reactions. The technique of average resonances guarantees that all states in a limited range of spin and parity will be observed up to several MeV.

3. Determination of Level Densities From Energy-Differential Particle Emission Cross-Sections

3.1 Level densities with an accuracy comparable to the resonance data can be derived in the energy range between the region of resolved levels and the neutron binding energy from such particle spectra over the whole mass-range. For actinides the presence of fission neutrons is an additional complication, which however, can be largely overcome by careful difference measurements.

3.2 These measurements of particle spectra can be performed using conventional experimental techniques and require only accuracies (~10%) which can be obtained routinely.

3.3 It is however most important to choose both the type of reaction and the bombarding energy in a way that minimizes the contribution of non-compound processes. For heavy nuclei (A>70) this means that (α,n) and (p,n) reactions should be used, for lighter nuclei (p,α), (α,p), (n,α) and (n,p) reactions will also provide good level density information.

3.4 In order to obtain the full information contained in the measured spectra the results should be analyzed by means of the statistical model with rigorous treatment of angular momemtum effects and both cross sections for populating resolved levels and those for populating the unresolved region used in the analysis as described in one of the contributions to this meeting. (Vonach).

3.5 Results should be reported both in terms of the directly measured particle emission cross-sections and as level density values versus excitation energy with realistic uncertainty estimates taking into account the errors in the statistical model analysis due to uncertainties of various needed input quantities.

3.6 Up to now very few of the results reported in the literature meet these requirements; probably this is the case for the Livermore and recent USSR (p,n) measurements.

3.7 Most other measurements of particle spectra have either not been analyzed specifically for the purpose of deriving level densities or have been analyzed in a way which does not correspond to the present state of the art.

3.8 Thus reanalysis of a number of such measurements can provide important information on the level density of a considerable number of nuclei.

3.9 In addition to this reanalysis, many new measurements of particle spectra are needed if we want to get a body of data comparable in scope to the neutron resonance data. The most efficient way to do this seems to be further measurements of (p,n) and (α,n) reactions and analysis of the data by means of the procedures mentioned before.

3.10 The proposed measurements will not only provide total level densities up to the neutron binding energy, but in addition, information on the spin-cutoff factor can be obtained both by comparison with the resonance data and from measurements of angular distributions in (α,n) reactions.

3.11 Absolute values of nuclear level densities up to about two times the neutron binding energy can be derived from neutron emission spectra in (p,n) and (α,n) by means of the Grimes method (see contribution of H. Vonach to this meeting).

3.12 Extraction of level densities from composite particle spectra suffers still from the lack of adequate procedures for this purpose. For the simplest case of neutron emission from compound nuclei with excitation energies below the 3n threshold it should be possible to develop such procedures.

3.13 Thus also for the excitation energy range up to twice the neutron binding energy new measurements of (p,n) and (α,n) reactions seem to be the most promising way to improve our knowledge on level densities.

3.14 For very high excitation energies (up to 100 MeV) measurements of α particle emission spectra have proved to be a very valuable method especially for heavy nuclei.

4. Extraction Of Level Density Information From Cross-Section Fluctuations

4.1 Absolute level densities of a number of nuclei in the mass-range A=20-60 have been derived from cross-section fluctuations at excitation energies around 20 MeV.

4.2 Most of these measurements have been performed more than 10 years ago. Because of the considerable improvements in energy resolution of Tandem accelerators since that time, measurements should now be possible both to lower excitation energies and to somewhat heavier nuclei.

4.3 It would be especially desirable to have new fluctuation measurements in the energy region of ~ 15-20 MeV and compare these results with measurements by means of the Grimes method on the same nuclei to get a better idea of the systematic errors of both these methods.

5. Determination Of Level Densities of Fissionable Nuclei At High Deformations

For calculations of the cross-section behavior of fissionable nuclides, it is necessary to have information on the density of intrinsic levels at the nuclear deformations corresponding to the peaks in the fission barrier. In the first place it is necessary to obtain this information experimentally from the analysis of cross sections, where the fission reaction is induced either by neutrons or by charged-particle transfer reactions. There is still room for much improvement in the experimental accuracy of our knowledge of these cross sections. From the characteristic energy dependence of these fission cross sections, barrier heights can be deduced quite accurately; these form the reference point for the

dependence of barrier level density on excitation energy. From the cross-sections at higher energy the barrier level density, or rather its effective ratio to the normal level density of the residual nucleus following neutron emission, can be determined. The broad outlines of this program have been carried out, but there is still a need for more careful analysis, particularly to check the fairly detailed model spectra of the barrier states at low excitation and to determine the energy dependence of the associated spin cut-off factor. For this last purpose careful analysis of the angular distribution of fission products is required.

APPENDIX

Codes for extracting level density information from experimental data.

Table A - Computer programs for extraction of level densities and strength functions from resolved resonance parameters by techniques based on the reduced-width distribution.

Code	Author	Estimation method*	p-level admixture	Unresolved multiplets	Available from
BAYESZ CRAY-1	M. Moore (LANL)	moment methods, eq. (23) highly automatic	treated eqs. (49)	treated approximately	NEADB
ESTIMA IBM 3033-11	E. Fort (Cadarache)	maximum likelihood, eq. (20)	excluded by threshold	neglected	NEADB
MISDO	G. Rohr (Geel)	maximum likelihood, eq. (20)	excluded by threshold	neglected	NEADB
CAVE	M. Stefanon (Bologna)	maximum likelihood, grid search	yes	neglected	Author
STARA-83 IBM 3033-11	F. Fröhner (KFK)	maximum likelihood, eq. (50)	yes	treated see eq. (24)	Author

* Equation numbers given are those of F. H. Fröhner's paper in this volume, where additional information can be found.

Table B - Codes for extracting level density information from energy differential particle emission spectra in compound nucleus reactions.

Code	Author	Models/References
CERBERO FORTRAN IV, 240 K bytes	F. Fabbri et al. CNEN, Bologna, Italy	Spherical OP + HF (single-step) RT IFI (74) 36 (74) and RT/RI (77) 6 (1977)
ERINNI FORTRAN IV, 240 K bytes	F. Fabbri et al. CNEN, Bologna, Italy	Spherical OP + HF (two-step) RT/FI (77) 4 (1977)
GNASH FORTRAN IV, CDC-7600 49 K words, SCM + 260 K words LCM	P.G. Young et al. Los Alamos, USA	EM(1st step) + HF (multi-step) LA-6947 (1977)
HAUSER - 5 FORTRAN IV 336 k Bytes	F.M. Mann HEDL, Hanford, USA	EM (1st step) + HF (two-step) HEDL-TME 78-83 (1978)
STAPRE FORTRAN IV 45 K words	M. Uhl et al. Inst. f. Radiumf. Vienna, Austria	EM (1st step) + HF (multi-step) IRK-76/01 and Addenda
TNG FORTRAN 300 K bytes	C. Y. Fu Oak Ridge, USA	EM (1st step) + HF (multi-step) ORNL/TM-7042

Abbreviations: OP ... optical model EM ... exciton model (for preequilibrium emission)
HF ... Hauser-Feshbach model

All codes are available from the NEA DATA BANK, F-91191 Gif-Sur-Yvette, Cedex, France.

INVITED AND CONTRIBUTED PAPERS

APPLIED USES OF NUCLEAR LEVEL DENSITIES

Robert C. Haight

University of California
Lawrence Livermore National Laboratory
Livermore, CA 94550

ABSTRACT

General and specific applications of nuclear level densities are described. Areas of particular applied interest are fission reactors, fusion reactors, and astrophysics.

I. INTRODUCTION

Nuclear level densities are a crucial ingredient in nuclear reaction models and in neutron transport calculations. Fermi's Golden Rule expresses the general importance of the density of final states, ρ, which includes the nuclear level density, in relating the transition rate w between initial and final states to the matrix element H_{if}:

$$w = \frac{2\pi}{\hbar} |H_{if}|^2 \rho$$

For applications in nuclear science the approach of Hauser and Feshbach [1] restates this rule in a form that describes cross sections:

$$\sigma_{cc'}^{J^\pi} = \sigma_{c,CN}^{J^\pi}(E) \cdot \frac{T_{c'}^{J^\pi}}{\sum_{c''} T_{c''}^{J^\pi}} \quad \text{where}$$

$\sigma_{cc'}^{J^\pi}$ = the cross section for the reaction c→c' with total angular momentum J and parity π,

$\sigma_{c,CN}^{J^\pi}(E)$ = the compound nucleus formation cross section through the reaction channel c,

$T_{c'}^{J^\pi}$ = the transmission function for decay of the compound nucleus through the exit channel c',

$\sum_{c''} T_{c''}^{J^\pi}$ = the sum of transmission functions through all possible channels, namely the channel of interest plus all competing channels.

As an example of the transmission function, consider the neutron (inelastic scattering) channel which may be written:

$$T_{n'}^{J^\pi}(E^*) = \sum_{\nu} T_{n'}^{J^\pi}(E_\nu^*) + \int_{\varepsilon_{min}}^{\varepsilon_{max}} T_{n'}^{J^\pi}(E^*)\cdot\rho(\varepsilon,J^\pi)d\varepsilon$$

where the transmission functions are summed over discrete levels ν, of the residual nucleus, and integrated over unresolved levels. The density of unresolved levels of particular J^π and excitation energy ε is represented by $\rho(\varepsilon,J^\pi)$.

The representation of nuclear level densities is only one ingredient out of many required to generate nuclear data for applications. Optical model parameters for calculating the particle transmission functions as well as strength functions for gamma and beta emission, coefficients of fractional parentage, and specification of the reaction mechanism itself are also necessary. In analogy to the study of a great cathedral, the nuclear level density is like the north transept: it is crucial to the spiritual, historical, and aesthetic unity of the building but it is not the whole cathedral. And at times other parts of the building may be more important for "applications" to religion, to architectural progress, and to the human condition.

In other parts of the nuclear reaction "cathedral," significant advances are taking place and these will influence the developments in the area of nuclear level densities. One need point only to the calculation of optical model parameters from the fundamental nucleon-nucleon interaction as pioneered by Brieva and Rook [2] and by Jeukenne, Lejeune, and Mahaux [3]. Work at many laboratories is now extending and refining this approach so that in a few years one can expect a firm basis for and a few changes in the phenomenological approach that we have followed for decades. Similarly new approaches to strength functions as guided by studies of giant resonances and by moment-method calculations (e.g. ref. 4) are providing a much improved understanding of the continuum.

Unlike the analogy of the cathedral, where one area complements and may give new dimension to the others, these developments restrict the range of physically reasonable parameters used in conjunction with representations of the level density. The shape, for example, of the optical model potential is no longer a free parameter but rather is constrained from other data (mainly electron scattering) through a model that folds the nuclear mass distribution with a nucleon-nucleon interaction which itself is constrained by data and meson-exchange models. The possibilities of "fixing-up" a nuclear reaction calculation so that it agrees with data are therefore more limited. Consequently we may in the near future be able to define more precisely the level densities obtained from experiment.

With the prospect of better experimental determinations of level densities, one can pose more strongly the question of whether a given representation is physically reasonable. At the applied level, this question is whether the representation agrees with experimental data. We should also ask how the representation corresponds with our understanding of a quantum-mechanical system of interacting fermions: Is the representation physically reasonable at this level? New approaches from microscopic calculations (e.g. ref. 5) are beginning to shed light on this latter question.

In this paper, I focus on some applications of nuclear level densities for applications. Certain applications are so general as to be treated together and they are collected in section II. Other applications are more application-specific, such as those to fission reactors, fusion reactor development, and astrophysics. Section III gives some of these specific applications. The representations of level densities and their interpretation from a basic physics perspective are discussed by others at this meeting.

II. GENERIC APPLICATIONS

This section treats broad-ranging applications of nuclear level densities.

A. Neutron Transport Applications

Nuclear level densities can be used to describe cross sections in the resonance region. [In the ENDF/B system of evaluated nuclear data, nuclear level densities (or average spacings) are employed explicitly to specify cross sections in the unresolved resonance region. Interestingly enough, ENDF/B does not explicitly use level densities anywhere else.] This specification also requires average competitive widths, reduced neutron widths, radiation widths, and fission widths. For example the fission cross section is given by the following expression: [6]

$$\sigma_{n,f}(E) = \sum_{\ell=0}^{NLS} \sigma_{n,f}^{\ell}(E)$$

with

$$\sigma_{n,f}^{\ell}(E) = \frac{2\pi^2}{k^2} \sum_{J}^{NLS_\ell} \frac{g_J}{\overline{D}_{\ell,J}} \left\langle \frac{\Gamma_n \Gamma_f}{\Gamma} \right\rangle_{\ell,J}$$

where $\overline{D}_{\ell,J}$ is the mean level spacing (inverse of the level density) for a given ℓ and J, and

$$\left\langle \frac{\Gamma_n \Gamma_f}{\Gamma} \right\rangle_{\ell,J} = \left(\frac{\overline{\Gamma}_{n_{\ell,J}} \overline{\Gamma}_{f_{\ell,J}}}{\overline{\Gamma}_{\ell,J}} \right) R_{f\ell,J}$$

where the $R_{f\ell,J}$ is the fission fluctuation integral and the $\overline{\Gamma}$'s are average widths.

From these expressions, cross sections can be calculated by processing codes. The result is processed data that should account for the fluctuations in the cross section, self-shielding effects, and so forth. To this end, the values used for the parameters including the level density could be taken as parameters and adjusted to fit the microscopic data as well as integral experiments. A more satisfying approach and the one usually followed is to fix those parameters (such as the level density) that can be obtained from resolved resonances for s- and p-wave neutrons and then letting the less well known parameters vary until good agreement with the integral experiments is found. Because this region is just above the resolved resonance region, the extrapolation of known quantities such as the s-wave strength function is usually reliable.

B. Nuclear Reactions Calculations

The compound nuclear reaction mechanism is able to account for a wealth of nuclear cross section data, especially neutron data, if the energy of the compound nucleus is not too high, say less than 20 MeV or so. Other reaction mechanisms, such as direct or pre-compound mechanisms, account for only a small fraction of the total reaction cross section at these energies.

There are many motivations for wanting to calculate reaction cross sections. One is simply to make sense out of experimental data. To understand the effects of thresholds and competing reactions, to deduce information on spins and parities from angular distributions, and to deduce information about the level density itself--all require detailed calculations. A second motivation is to understand the contribution of a particular reaction mechanism so that the effects of a different mechanism can be isolated. For example one often wants to subtract the compound nuclear reaction contribution to investigate direct or pre-compound mechanisms.

The major motivation for many calculations, however, is to provide nuclear data for applications. Because experimental data often do not exist for a particular reaction on a target isotope at a given energy, the cross sections must be calculated. The result is an interpolation or extrapolation from existing data or a true ab initio calculation. Extensions of existing data can thereby by made to unmeasured or unmeasurable regions in energy, isotope, excitation energy, or other nuclear property such as deformation. In the cases where experimental data exist and are discrepant, a reaction model calculation may help to decide which data are physically reasonable and which are clearly erroneous.

Hauser-Feshbach calculations have been performed in many cases to provide evaluated nuclear data for applications. The two examples given here illustrate the importance of level densities in those calculations.

The cross section for the $^{51}V(n,p)^{51}Cr$ reaction has been measured several times by activation techniques. The experimental results are discrepant, and they extend only from 13 to 18 MeV, while the threshold for the reaction is 1.7 MeV. An evaluated data file for this and other reactions on vanadium was achieved [7] using Hauser-Feshbach calculations. The results are reproduced in Fig. 1.

This calculation first of all showed that the shape of the excitation function measured from 13 to 18 MeV is reasonable. A less smooth excitation function that might have been conjectured from the single-energy measurements was ruled out. The calculation also demonstrated that the magnitude of the experimental values could be reproduced with a compound nuclear reaction model. To within the uncertainties of the parameters, including the level densities, the cross sections are again reasonable. Finally the calculation was able to extend the (n,p) cross section over the energy range from threshold to 13 MeV where there are no measured data. The calculational results show that the preceeding version of ENDF did not correctly take into account the threshold effects and thereby gave unreasonable values for the cross section from 5 to 13 MeV. This example shows how level densities are able to extend cross section data to unmeasured energies.

A second example is from the analysis of proton emission spectra from neutron-induced reactions. The pre-compound part of the spectrum is of interest, and, to isolate it, one must calculate the expected compound nuclear component. The results from one such analysis are shown in Fig. 2 for 15-MeV neutrons incident on isotopes of Cr, Fe, Ni, and Cu [8]. The difference between the compound nuclear (Hauser-Feshbach) calculation and the experimental spectra, especially above 8 MeV proton energy, are interpreted in terms of a pre-compound reaction mechanism (Fig. 3). It is important to know how the nuclear level density varies with energy in this application: one could describe the measured spectra as compound nuclear evaporation if a very unusual form were chosen for the level density of the residual nuclei. Measurements of the spectra at lower incident neutron energy together with results of charged-particle experiments rule out such an unusual form, however. This is an example of how the nuclear level densities are used to extend our knowledge of reaction mechanisms.

III. SPECIFIC EXAMPLES

A. Fission Reactors

The cross section for fission induced by fast neutrons is basic to all fission reactors, even those with a small fraction of fast neutrons. For ^{235}U, the fission cross section from 100 keV to 6 MeV has structure which is not fully understood even now. And if that cross section, which has been studied so often, cannot be calculated reliably from a basic model,

how then can the fission cross section for unmeasured isotopes be calculated with confidence?

A recent attempt [9] to understand the structure in the ^{235}U fission cross section was based on a Hauser-Feshbach calculation of the competition between fission and inelastic scattering. In this work the densities of levels at the fission barriers in the compound nucleus ^{236}U were varied until good agreement was obtained with the experimental fission cross section. The resulting level densities and the calculated cross section are shown in Figs. 4 and 5.

The remarkable features of the deduced level densities at the fission barriers are their shapes which were used to explain the structure in the fission cross section between 1 and 2 MeV. An alternative analysis could have attributed this structure to the shape of the level density in ^{235}U reached by inelastic scattering. In either case there is an indication of an anomaly at low excitation where collective levels and single-particle excitations compete. It is possible that structure in the level density is a characteristic of nuclei at very high deformations such as at the fission barrier; however, information there on nuclear structure properties including the level density is almost non-existent.

A second area of application of level densities in fission reactors is the calculation of cross sections for the fission products. These data are needed for predicting the neutronic performance of a reactor after the buildup of fission products and they are also used in analyzing the consequences of accidents.

Fission products can affect criticality parameters, sodium void and Doppler coefficients, the required enrichment for the fuel loading, and the breeding ratio. The importance of fission products on these quantities depends of course on the concentration of these products and therefore is greatest after long burn-ups. Short-lived products do not have a great effect. In fact, most of the important products have undergone beta-decay so that they are stable and measurements can be made on them. Compound nuclear reaction calculations are used in these cases to fill in the unmeasured regions and to decide between discrepant data sets [10].

For accident analysis, the inventory of radioisotopes is required. Many of these isotopes are fission (and subsequent beta-decay) products. Others result from neutron-induced reactions on those products. The nuclear data required to predict the abundance of the latter generally must be calculated. Great accuracy is usually not required in these calculations because other uncertainties in the accident analysis (in the models of dispersal of the isotope, its chemical form, and how it enters biological systems) are large.

A third area of potential importance to fission reactors is the calculation of the fission neutron spectrum. In principle the spectrum could be obtained from statistical emission of neutrons from the excited fission fragments after averaging over the fragment charge and mass distribution. A kinematic transformation from the fragment rest frame to the laboratory frame then would yield the observed neutron spectrum. In practice a representative spectrum is calculated, to avoid the complexity of the many possible combinations of fragments, and then the kinematic transformations are made [11]. The more ambitious approach of treating

each fragment separately would put additional demands on the representation of level densities because most of the fragments are far from the valley of stability. Extrapolations from stable nuclei are therefore less reliable. In addition the excitation energies of interest are lower because of the lower neutron separation energies. Similar problems are encountered in astrophysical applications as discussed below.

Finally, many other evaluations for fission reactor applications depend on Hauser-Feshbach calculations and therefore on level densities. Cross sections for neutron transport, especially inelastic scattering and radiative capture, are coordinated through this reaction mechanism and calculation. Evaluations of dosimetric reaction cross sections also rely heavily on this approach. While these applications depend on level density information in "well-known" regions, they are the most demanding in terms of the accuracy required. For this reason, the level density is often normalized at a few points so that the Hauser-Feshbach calculation agrees with the experimental data. It would indeed be a triumph of nuclear science if ab initio or even independent, empirical approaches to the level density gave results that required no further normalization.

B. Fusion Reactor Applications

Fusion reactors with deuterium or deuterium-tritium fuel will produce copious quantities of 14-MeV neutrons. For many reasons one can expect the effects of these neutrons to be much different than those in a fission reactor: The average number is higher, which is important in the context of threshold reactions; the energy of the neutrons for a given reactor power is higher than that of a fission reactor by a factor of 7 or so; and, for magnetic confinement schemes, the neutrons interact practically not at all with the low-density fuel but rather impinge uncollided with structural and blanket components. Nuclear data needs for fusion have been summarized by many authors previously (see e.g. refs. 12 and 13).

Much of the nuclear data for fusion reactor applications will of necessity be provided by calculations employing level density representations. The reasons are technical as well as economic. One area where calculations will provide most of the data is for neutron energies between about 10 and 14 MeV. In this energy region most experimental neutron sources are not monoenergetic but contain low-energy neutrons from breakup of the projectile or the target in the neutron source. It is thus very difficult to measure, for example, the neutron emission spectrum for incident neutron energies in this range.

Another area of technical necessity is cross section data for broad-spectrum neutron sources for radiation damage studies. A source using a reaction such as d+Li can produce a very large and useful flux of neutrons with a broad peak centered at 14 MeV. The range of the neutron energies is large, however, and neutrons at higher energies (to 35 MeV or beyond) are also produced. Data in this higher energy range are very scarce [14], yet they are needed to analyze the radiation damage effects.

The economic incentive for calculating the required data is large since the nuclear data needs for fusion are so extensive [11]. To have confidence in the calculational results, one must have an accurate

representation of the reaction and therefore accurate nuclear level densities. Because these applications extend the current models beyond the experimental data, some further experiments will be necessary to confirm the calculational results.

One area of recent progress is the production of hydrogen and helium by neutron reactions with candidate materials for fusion reactors. These reactions generally have an effective threshold of several MeV and are less important in fission reactors. Recent measurements with a variety of new techniques have provided not only the integrated gas-production cross sections but also the spectra of charged particles from the (n,p), (n,d), and (n,alpha) reactions. Examples of these data are shown in Figs. 2 and 3. It is a remarkable success of Hauser-Feshbach calculations that they can describe the major part of the charged-particle emission spectra quite well (see for example the calculations in Fig. 2). The remaining part of the emission spectra at the high energy end are attributed to precompound particle emission. The success of these calculations is especially important to give confidence in predicting cross sections at lower incident neutron energies which will be important in fusion reactors but where experimental measurements are difficult because of present-day source intensities.

Cross sections at higher energies for d+Li neutron sources present a different type of challenge in that level densities at much higher excitations are required. For example, one of the materials considered as a dosimeter is cobalt. Cross sections as a function of incident energy are required to unfold the neutron flux spectrum from the observed activities. These cross sections have been calculated [15], and the results are given in Fig. 6. The excitation energies of the residual nuclei are well above those encountered with 14-MeV neutrons incident: For an incident energy of 40 MeV, level densities are required up to 40 MeV in ^{59}Co, 29 MeV in ^{58}Co, about 36 MeV in ^{59}Fe and so forth. Because of level densities increase very rapidly with increasing excitation energy, a small inaccuracy in the values at lower energies can become a very significant error after this extrapolation. Unfortunately there are few neutron data to confirm the calculational results at these higher energies. One must instead rely on charged-particle-induced reaction data.

To round out the perspective of the importance of level densities, some note must be made of reactions which are not described well by Hauser-Feshbach calculations. The pre-compound component of particle emission already mentioned is one such process that is beyond the compound nuclear reaction picture. Another is tri-nucleon emission where other mechanisms, perhaps direct reactions, are significant [16]. Finally the reaction mechanisms in light nuclei are influenced by resonances and final state interactions, that is by non-statistical effects. Another way of stating this problem is that the level density can be so low as to be an inappropriate concept from the beginning.

C. Astrophysical Nuclear Reaction Applications

Nuclear reactions in astrophysical systems take place over a wide range in time scales, densities, temperatures, and elemental compositions.

Thus it is not surprising that reactions of importance occur with nuclides in the valley of stability (s-process, helium burning, etc.), very neutron-rich nuclides (r-process, fission), and neutron-deficient species (rp and p-processes). The energies at which the reactions take place (usually tens of keV or more) and the spread in this energy from the Maxwellian distribution usually imply that the compound-nuclear reaction mechanism is predominant.

Neutron-induced reactions on nuclides near the valley of stability are important in s-process nucleosynthesis, which is where the neutron-induced reaction rates are slow compared to beta-decay half lives. To parameterize the data near the valley of stability, nuclear level densities are used with Hauser-Feshbach calculations [17]. This approach yields a consistent description of the measured neutron capture cross sections to within a factor of 2 or so. It also serves as a calculational tool for predicting unmeasured capture cross sections as well as those for (n,p) and (n,alpha) reactions, very few of which have been measured at the low energies of interest in astrophysics.

Calculations of proton capture in the rp and p-process are carried out in a similar manner [18]. Here the data on the proton capture cross sections are usually at higher energies than of astrophysical interest. The calculations then are used to extend the data to those low energies.

Understanding the r-process, that is rapid neutron capture on time scales short compared with beta-decay half-lives, requires the calculation of reactions on neutron-rich nuclides far from the valley of beta-stability. Here there are no experimental data to guide the calculations. Neutron capture is the most important process and inelastic scattering and (n,2n) reactions should be considered. To carry out such calculations one needs nuclear level densities that are extrapolated from stable or nearly stable nuclides. Since this extrapolation is large, significant uncertainties can be introduced. An additional challenge is that the excitation energies of interest are in general lower than those in stable nuclei where the nuclear level density can be obtained from resolved resonances. This is because the neutron separation energy is less and in fact becomes zero at large neutron excesses where the nuclides become unstable to neutron emission (the so-called "neutron-drip line"). The nuclear level density at the neutron separation energy therefore decreases as the neutron excess increases and eventually becomes an inappropriate concept.

An example of Hauser-Feshbach calculations to predict neutron-capture cross sections in cadmium isotopes for the r-process is given in Fig. 7 [19]. The isotope $^{130}Cd(Z=48, N=82)$ is of particular importance since it is a "resting point" in r-process nucleosynthesis: it must beta decay before elements of higher atomic number can be formed. It is therefore partly responsible for the abundance peak at A = 128 to 130. For this nucleus, the level density at the neutron separation energy is so low that there may be no compound nuclear resonance available for resonance neutron capture. An alternative mechanism, direct neutron capture, may in fact be dominant (see Fig. 7). For more neutron-rich isotopes, the level densities are even lower. This example then points out some of the challenges and the difficulties in using nuclear level densities for astrophysical processes far from the valley of beta-stability.

IV. CONCLUSION

This brief report of some of the uses of nuclear level densities illustrates their broad use in a wide variety of applied fields. In future applications, their use will require more accurate representations and extensions to nuclear regimes beyond the frontiers of our present experience: to nuclides far from the valley of beta-stability, to higher excitations, and to large deformations.

ACKNOWLEDGMENTS

The author wishes to thank R. M. White, G. J. Mathews, R. J. Howerton, R. W. Bauer, R. Schenter, E. Arthur, D. Finch, B. Magurno, and O. Ozer for helpful comments. The work was performed under the auspices of the U.S. Department of Energy by the Lawrence Livermore National Laboratory under contract number W-7405-ENG-48.

REFERENCES

1. W. Hauser and H. Feshbach, Phys. Rev. 87, 366 (1952).

2. F. A. Brieva and J. R. Rook, Nucl. Phys. A291, 299, 317 (1977).

3. J. P. Jeukenne, A. Lejeune, and C. Mahaux, Phys. Rev. C 16, 80 (1977).

4. B. J. Dalton, S. M. Grimes, J. P. Vary, and S. A. Williams (eds.), Theory and Applications of Moment Methods in Many-Fermion Systems, Plenum, New York (1979).

5. S. D. Bloom, C. D. Goodman, S. M. Grimes, and R. F. Hausman, Jr., Phys. Lett. 107B, 336 (1981).

6. M. K. Drake (ed), Data Formats and Procedures for the ENDF Neutron Cross Section Library, Brookhaven National Laboratory Report BNL-50274 (1970).

7. P. Guenther, D. Havel, R. Howerton, F. Mann, D. Smith, A. Smith, and J. Whalen, "Fast Neutron Cross Sections of Vanadium and an Evaluated Neutronic File," Argonne National Laboratory Report ANL/NDM-24 (1977).

8. S. M. Grimes, R. C. Haight, K. R. Alvar, H. H. Barschall, and R. R. Borchers, Phys. Rev. C 19, 2127 (1979).

9. R. M. White and J. C. Browne, Proc. Int. Conf. on Nuclear Data for Science and Technology, Antwerp, Belgium, (1982) (to be published).

10. R. Schenter and F. Mann, Private Communication.

11. D. G. Madland and J. R. Nix, Nucl. Sci. and Eng. 81, 213 (1982).

12. E. T. Cheng, D. R. Mathews, and K. R. Schultz, "Magnetic Fusion Energy Program Nuclear Data Needs," General Atomic Co. Report GA-16886 (1982).

13. R. C. Haight, Proc. Int. Conf. on Nuclear Cross Sections for Technology, ed. J. L. Fowler, C. H. Johnson, and C. D. Bowman, NBS special publication 594, Knoxville, TN (1980) pp. 228-238.

14. R. C. Haight, Proc. Symp. on Neutron Cross Sections from 10 to 40 MeV, Brookhaven National Laboratory Report BNL-NCS-50681 (1977) 201.

15. E. Arthur, P. G. Young, and W. K. Matthes, Proc. Symp. on Neutron Cross Sections from 10 to 50 MeV, Brookhaven National Laboratory Report BNL-NCS-51245 (1980) 751.

16. S. M. Qaim, R. Wölfe, and H. Liskien, Phys. Rev. C 25, 203 (1982).

17. J. A. Holmes, S. E. Woosley, W. A. Fowler, and B. A. Zimmerman, Atomic Data and Nuclear Data Tables 18, 306 (1976).

18. S. E. Woosley, W. A. Fowler, J. A. Holmes, and B. A. Zimmerman, Atomic and Nuclear Data Tables 22, 371 (1978).

19. G. J. Mathews, A. Mengoni, F.-K. Thielemann, and W. A. Fowler, Astrophysical Journal (to be published).

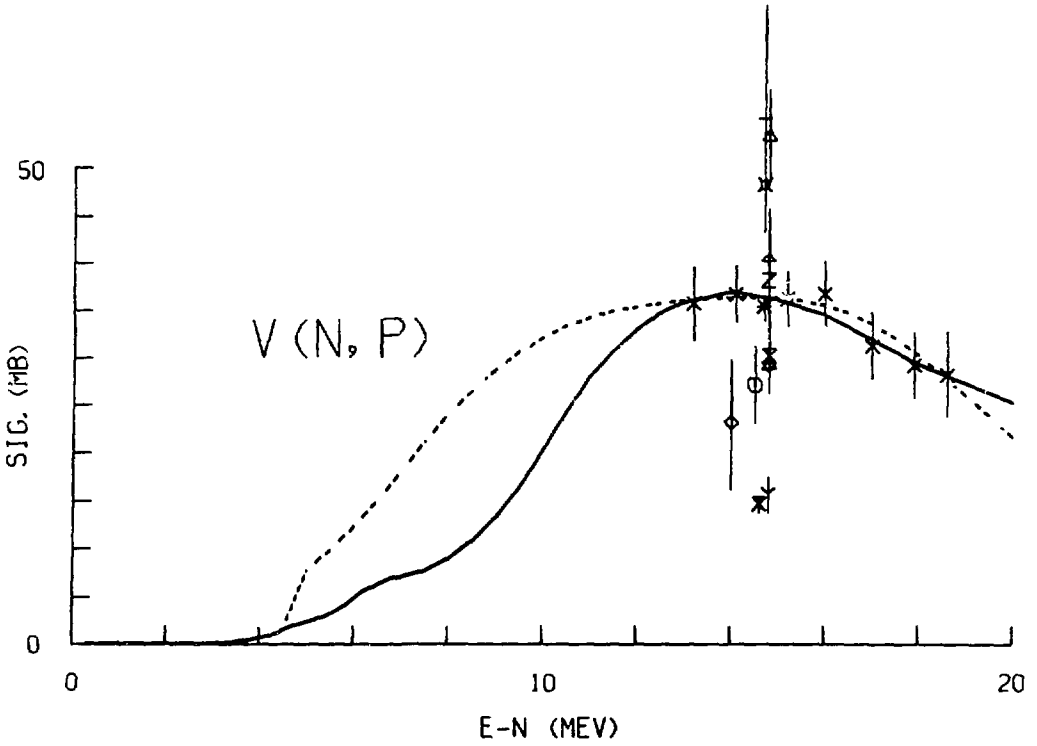

Fig. 1. Measurements and evaluations of the $^{51}V(n,p)$ cross section [7]. The solid curve is the result of Hauser-Feshbach calculations. The dashed curve is the ENDF/B-IV evaluation.

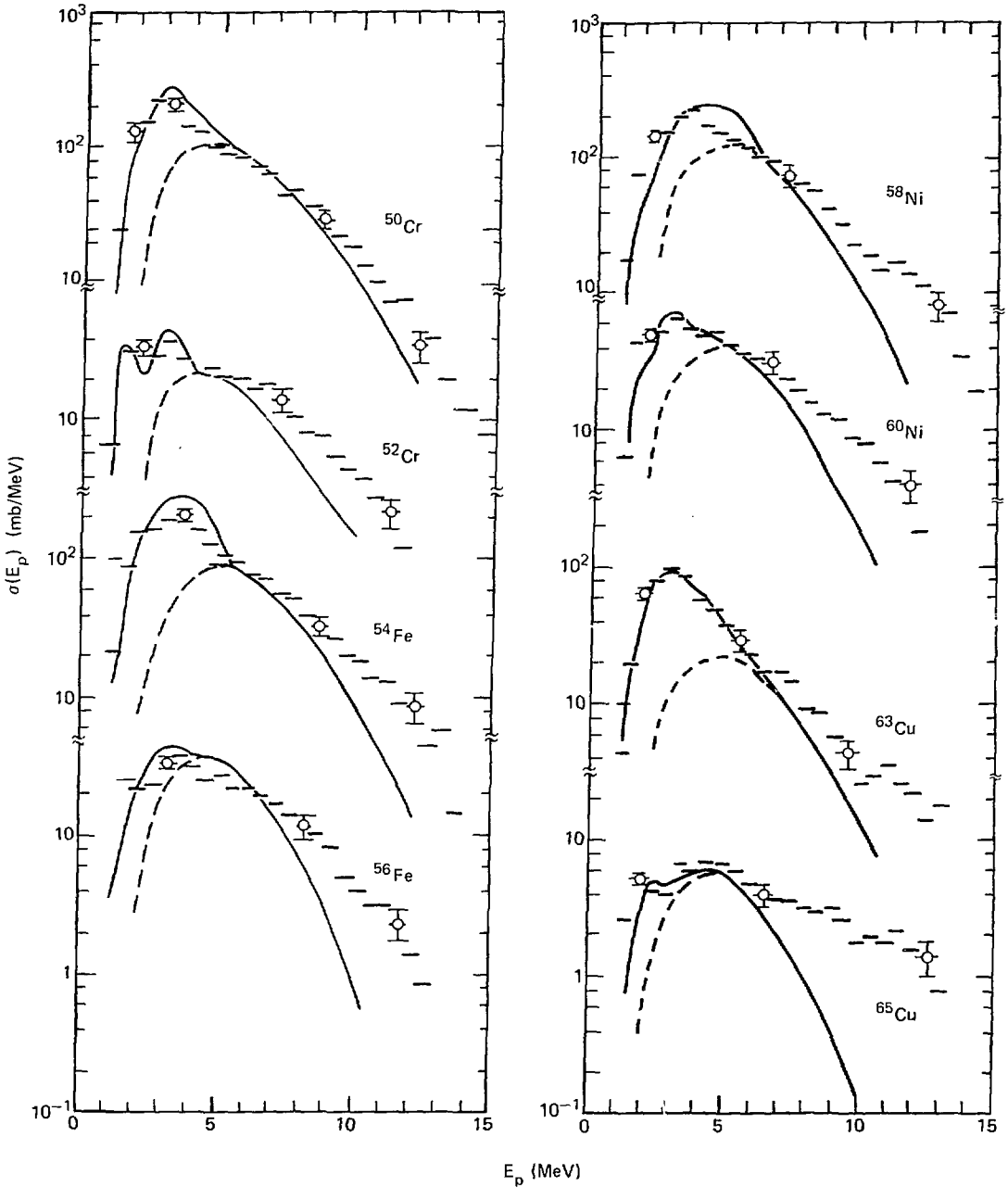

Fig. 2. Proton emission spectra from isotopes bombarded with 15-MeV neutrons [8]. The solid curves are Hauser-Feshbach calculations. The dashed curves are the calculational results for emission from the initial compound nucleus.

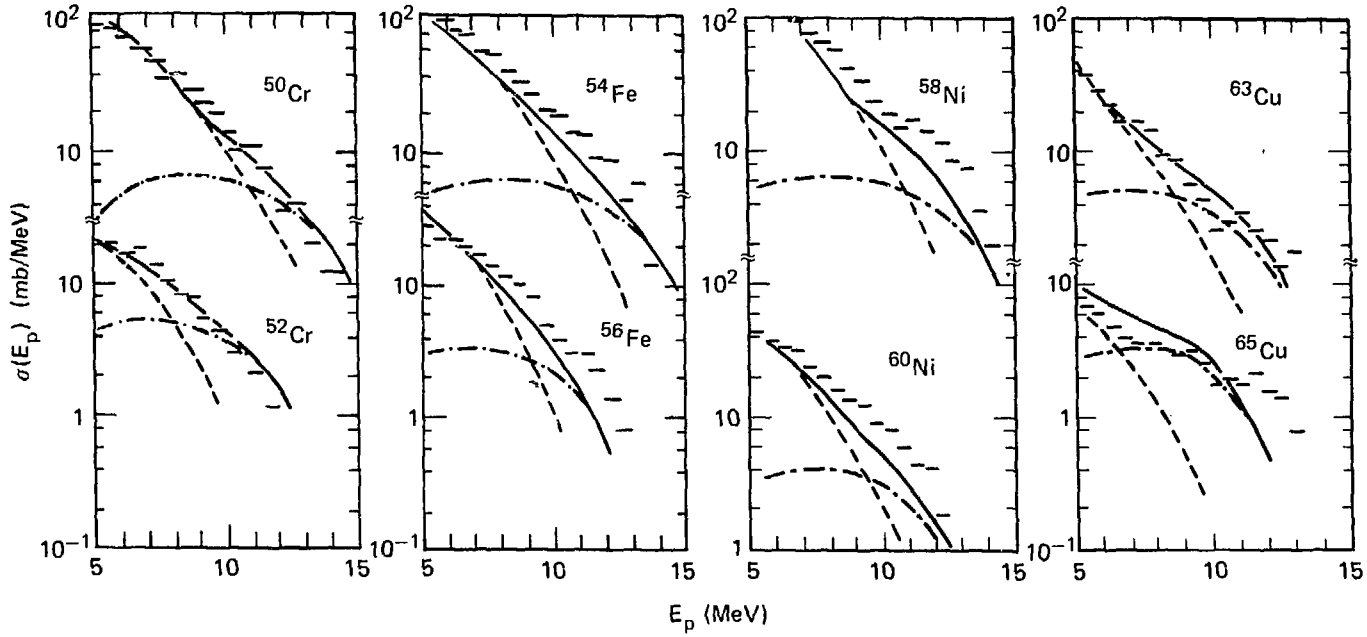

Fig. 3. The high-energy part of the proton emission spectrum in Fig. 2. The dashed curves are Hauser-Feshbach calculations; the dot-dashed curves are pre-equilibrium calculations; and the solid curves are the sum of compound plus pre-compound calculations.

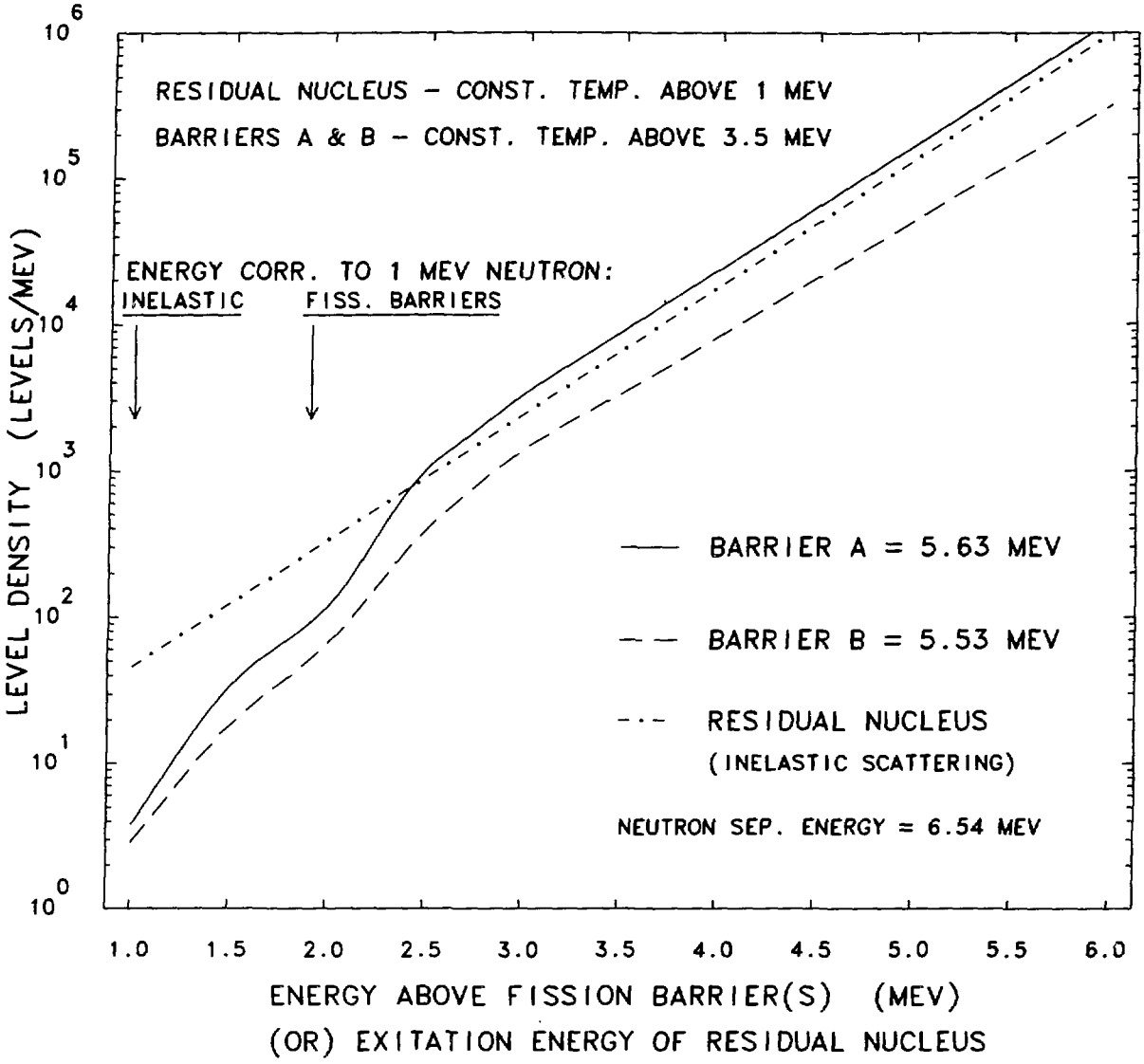

Fig. 4. Level densities used to calculate the $^{235}U(n,f)$ cross section [9].

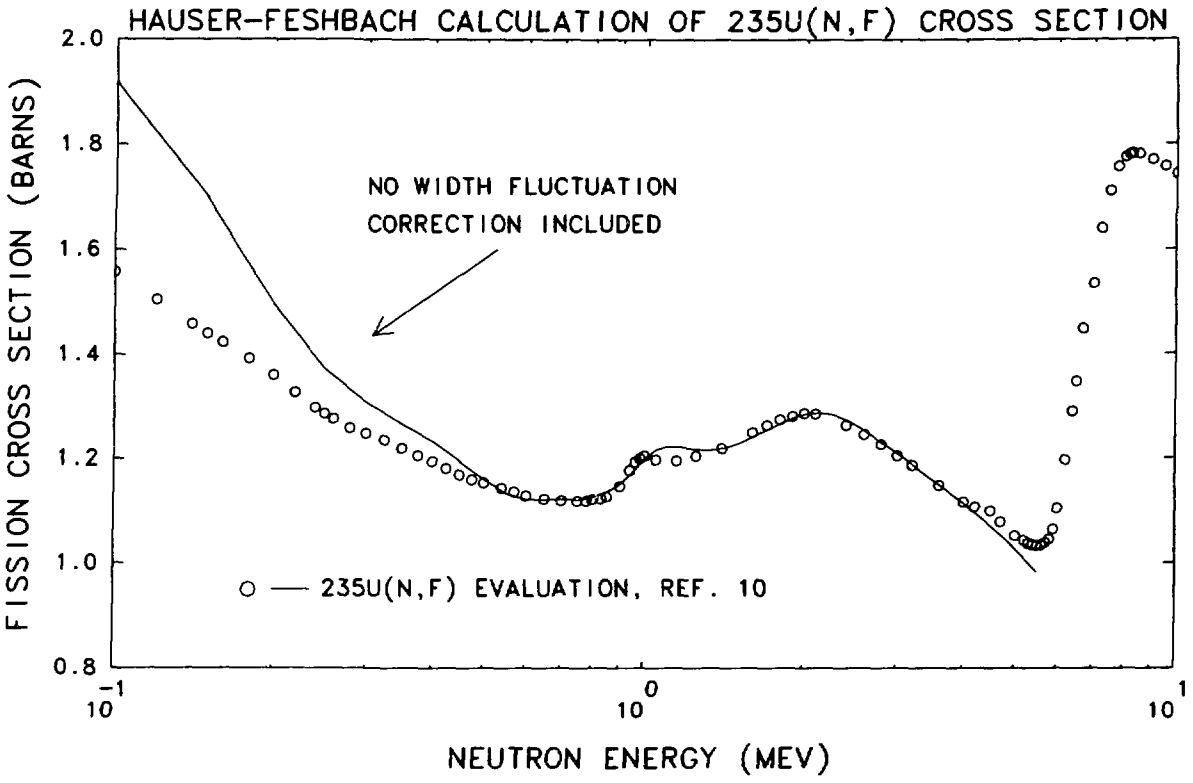

Fig. 5. Calculated cross section for $^{235}U(n,f)$ using the level densities of Fig. 4. The structure in the range 1-2 MeV requires structure in the level densities.

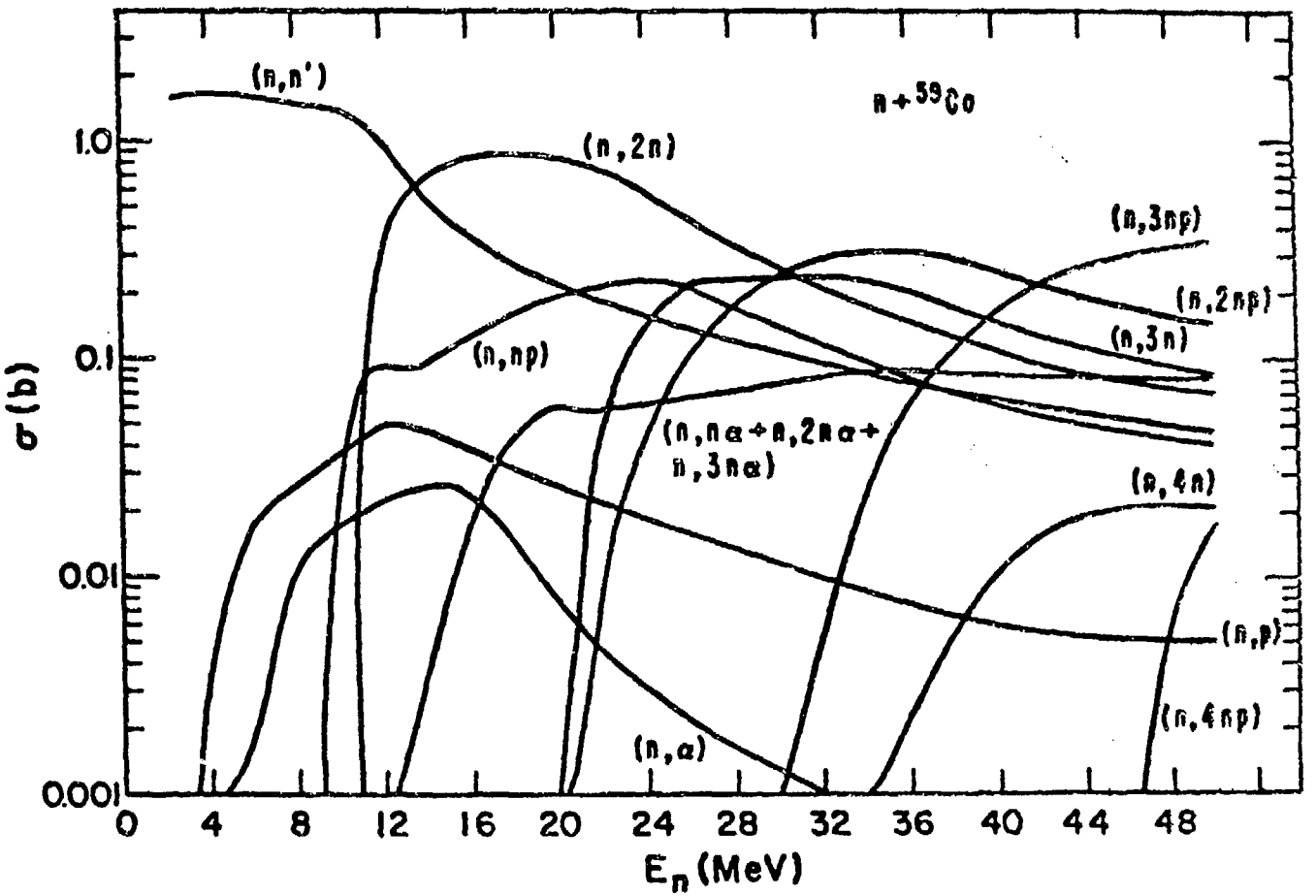

Fig. 6. Activation cross sections for neutron reactions with ^{59}Co [15]. The curves result from Hauser-Feshbach calculations.

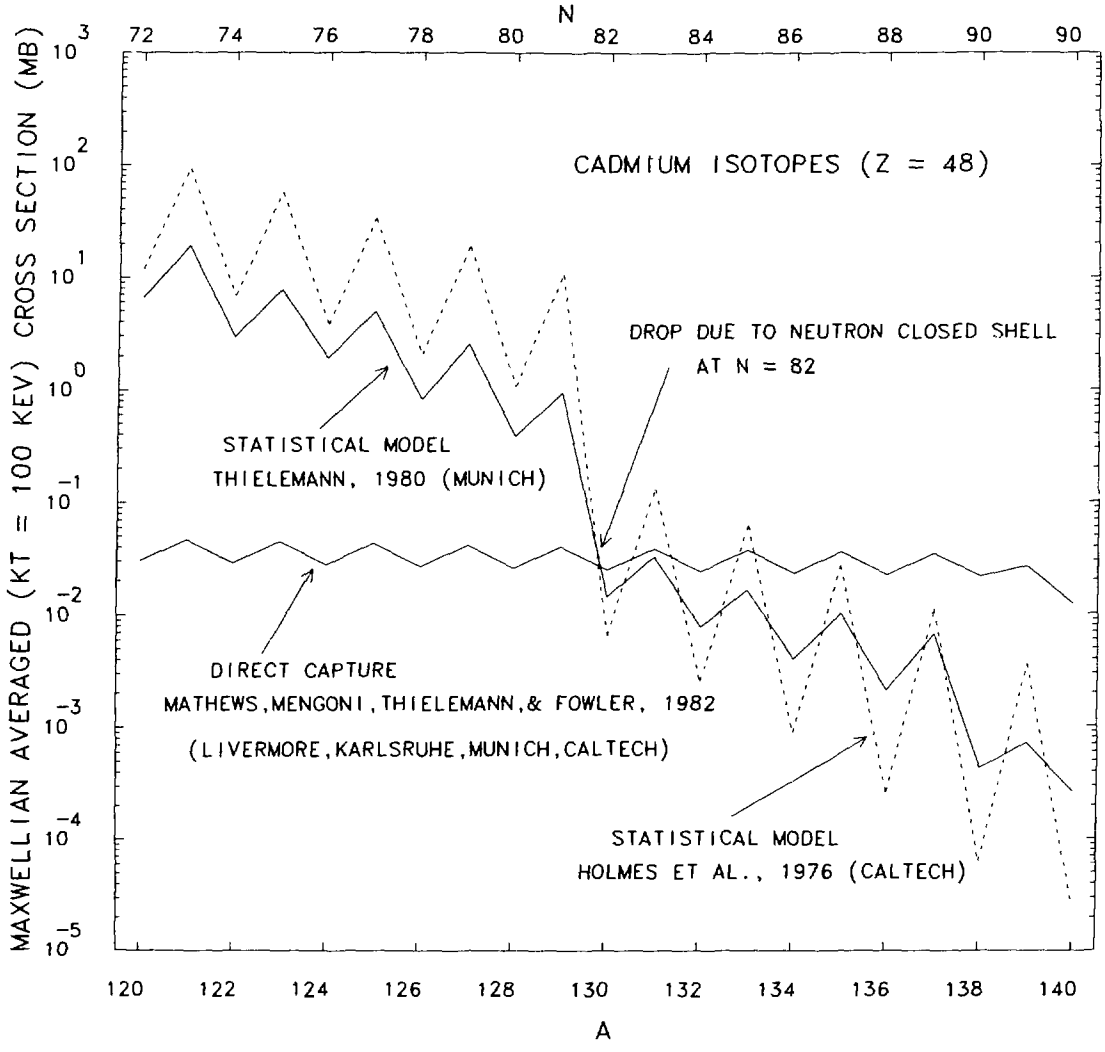

Fig. 7. Maxwellian-average cross sections for neutron capture by neutron-rich isotopes of cadmium [19]. The direct capture mechanism becomes larger than the statistical mechanism for the heavy isotopes where the level density at the neutron separation energy becomes small.

MOMENT METHOD CALCULATIONS OF NUCLEAR LEVEL DENSITIES

S.M. Grimes

Physics Department, Ohio University
Athens, Ohio 45701, U.S.A.

ABSTRACT

A summary of the limitations of level density calculations which omit the two-body force is presented. An alternative procedure which allows inclusion of such forces is now available. Some early results with these moment methods suggest that they will be very useful in level density calculations. Significant remaining problems include the uncertainty in some of the input parameters and the computer time demands of these calculations.

INTRODUCTION

Most calculations of nuclear level densities utilize the Fermi gas model [1]. This formalism is based on the assumptions that the nucleons are non-interacting Fermions bound in a well. Obvious virtues of such a picture include the fact that the methods of statistical mechanics can be used to calculate the level density and the limited number of parameters needed by the model. In the original formulation, only one parameter, a, denoting the average single particle state density multiplied by $\pi^2/6$, is needed in the model.

More recent refinements have allowed pairing and shell effects to be incorporated into the model [2]. The non-interacting Fermions may be replaced by the quasi-particles of superconductivity theory. This allows inclusion of pairing effects in a one-body approach. Another recent modification is to relax the assumption that the single particle states are equidistant and put in single particle states with shell gaps where appropriate. In principle this forces us to give up an analytic expression for the level density. We can carry out the calculation numerically on a modern computer and the results can often be fit with the original form, where we use a (the level density parameter) and δ (the energy shift) as fitting parameters. Deviations from this form normally occur only for low energies, where pairing and shell effects are most important. At these energies a constant temperature form (exponential) is often used to represent the level density and is matched in height and slope to the Fermi gas form at an energy of a few MeV.

Some problems with the Fermi gas model remain, however, even after we incorporate pairing and shell effects. Many low-lying levels of the nucleus are collective states and these will not be located properly in a calculation which ignores the two-body force. It has been suggested [3] that this deficiency could be remedied by adding rotational or vibrational levels to the low-lying spectrum. Two difficulties are associated with this solution to the problem. The fundamental problem is that this represents "double-counting" in that our original calculation had the correct total number of levels in the basis. Omission of two-body forces resulted in levels not being brought down to low excitation, but the levels are present in the spectrum at higher energies. If we add in levels, we should subtract them from the level density at higher energies. This, of course, cannot be done since we do not know precisely from which energy region they should be removed.

An additional difficulty is that such levels can be added only if we know the collective parameters (separation between levels in a band) for the nucleus in question and their energy dependence. We often know the information required at low energy, but are not in as good a position at higher energies. Calculations by Moretto [4] indicate that at high energies both deformed and spherical nuclei have levels with a range of deformations with the most likely shape being spherical. This result is plausible, since at high energies one would expect deformed and spherical nuclei to become similar in their nuclear properties. The rate at which this limit is approached is not well known, however, making use of a model with ad hoc deformation parameters difficult.

A closely related problem occurs when one uses Fermi gas parameters found for nuclei on the stability line to extrapolate to nearby nuclei off the stability line. Since the deformation parameter can change very rapidly as a function of N and Z, this extrapolation procedure could lead to serious errors in level density calculations.

Some indication of additional problems comes from studies of the spin cutoff parameter and the positive-parity negative-parity ratio of nuclear levels [5]. Both of these parameters are necessary to define the level density distribution as a function of spin and parity. It appears that the Fermi gas model does not always predict these parameters correctly even when the total number of levels is correctly given. Our information is not sufficiently complete to let us determine how extensive these discrepancies are, but it appears as though the spin cutoff parameter and parity ratio may be more sensitive to two body forces than is the total level density.

SPECTRAL DISTRIBUTION THEORY

The theory of spectral distributions allows the inclusion of two-body forces in level density calculations in an enormous basis. It is routine to include two-body forces in shell model calculations, but these involve diagonalization of a large matrix and are therefore limited to a basis of 10^4 or less. Level densities are often needed in bases which have as many as 10^{10} levels or more. Even if we could diagonalize a very large matrix, this would not be an efficient way to proceed. We actually do not

want all 10^{10} eigenvalues or eigenfunctions but only the distribution of levels with energy. French and collaborators [6] have developed a method which yields the level density (and spin cutoff and parity ratio) directly, without requiring a diagonalization. This formalism utilizes the assumptions that the Hamiltonian is two-body (actually a combination of one- and two-body parts) and that the distribution of levels with energy for such a Hamiltonian is nearly Gaussian. If we can calculate the total number of levels in our basis and also the average energy ($\langle H \rangle$) and dispersion ($[\langle H^2 \rangle - \langle H \rangle^2]^{1/2}$), we can make a Gaussian expansion of the level density.

We clearly depart from the typical Fermi gas approach in two ways: two-body forces are included and we deal with a finite (though large) basis. This latter difference may appear troublesome, since a finite basis obviously has no levels beyond a particular energy (that of the highest level). The Fermi gas form yields a level density which increases indefinitely with energy.

Actually, the limited basis assumption is physically more realistic [7]. For a nucleus such as ^{56}Fe with 56 nucleons and a binding energy of 8 MeV/nucleon, the nucleus will be totally dissociated into constituent nucleons at 8 x 56 = 448 MeV. For energies lower than this, many levels will have more than one nucleon in an unbound state and will have an extremely short lifetime. These are arrangements of 26 protons and 30 neutrons but probably do not live long enough to be considered excited states of ^{56}Fe. Thus, a level density which reaches a peak and then declines to 0 with increasing energy is actually more realistic physically than the traditional Fermi gas level density. The peak and region of negative slope, of course, will be at very high energies ($E \gtrsim 4A$ MeV).

Because these Gaussians span an enormous energy range, the shape of the predicted level density for moderate energies ($E \lesssim 30$ MeV) does not show dramatic effects of this cutoff. Indeed, it has been shown [5] that a Fermi gas form and a Gaussian are nearly indistinguishable over a wide energy range for proper choice of parameters. Fig. 1 illustrates this similarity. The Fermi gas form for $a = 4$ and $\delta = 0$ is fitted with Gaussians corresponding to two different dimensionalities with appropriate values for the average energy and width. Discrepancies between the two forms are extremely small over a 10-15 MeV range of energy. This similarity indicates that the general agreement of level density data with the Fermi gas form does not provide an argument against the spectral distribution approach.

Calculation of the parameters which enter the spectral distribution expansion is not difficult. The number of states in the basis will be the binomial coefficient

$$\binom{N_0}{m} = \frac{N_0!}{m!\,(N_0 - m)!}$$

where m is the number of particles and N_0 the total number of particle states available. We may obtain $\langle H \rangle$ and $\langle H^2 \rangle$ through use of a relation called the propagator theorem:

The expectation value of an n-body operator will be an n+1 order polynomial in the particle number.

As an example, consider the application of a one-body Hamiltonian to a system of 20 single particle states. By putting 10 particles in these states, we generate $\binom{20}{10} = 184756$ states, and evaluating the average energy would seem to be difficult. According to the propagator theorem, the average energy will be a two-term polynomial in the particle number. Thus,

$$\langle H \rangle = C_0 + C_1 m$$

If we define $\langle H \rangle$ to be 0 for 0 particles, then $C_0 = 0$. To evaluate $\langle H \rangle$ for a one particle system ($= \langle H \rangle_1$), we need a twenty term sum

$$\langle H \rangle_1 = \Sigma \varepsilon_i / 20$$

From the above form it is obvious that $C_1 = \langle H \rangle_1$. Thus,

$$\langle H \rangle = \left\{ \frac{\Sigma \varepsilon_i}{20} \right\} m$$

and we can evaluate the average energy for a system of 184756 states by multiplying two numbers together. For a one-body operator, the validity of the theorem can be appreciated immediately: we have the average energy of the system being given by the product of the average energy per particle times the number of particles.

For a realistic nuclear Hamiltonian, the situation is somewhat more complicated. The Hamiltonian is a two-body operator and $\langle H^2 \rangle$ is a four-body operator. Thus, for a latter operator, a five term polynomial will be required. In addition, we want information about the energy dependence of the spin cutoff parameter, $\langle J_z{}^2 \rangle$, the average of the square of the z projection of the angular momentum. This requires, in addition to $\langle J_z{}^2 \rangle$, the expectation values of $\langle HJ_z{}^2 \rangle$ and $\langle H^2 J_z{}^2 \rangle$. These are two-body, four-body, and six-body operators, respectively.

The binomial coefficients $\binom{N_0}{m}$ are symmetric about a reflection through $m = N_0/2$, i.e. $\binom{N_0}{m} = \binom{N_0}{N_0 - m}$. Dimensionalities are therefore smallest for particle numbers which are small or near N_0. For example, the dimensionality for no particles or for $m = N_0$ will be one, for one particle or $N_0 - 1$ will be N_0, and for two or $N_0 - 2$ will be $\frac{N_0(N_0 - 1)}{2}$. It is therefore easiest to evaluate the moments for systems which are either nearly full or nearly empty. Evaluation of the moments of operators of higher rank is complicated not only by the complexity of the operator itself but also the fact that we need to evaluate it for systems with larger dimensionalities. It might appear that we face an additional problem in that H is not a diagonal operator in the shell model basis. Unitarity implies that the trace of an operator is the same in any representation, diagonal or

not, so we are free to calculate the moments (normalized traces) in our non-diagonal basis.

Obviously, the utility of a Gaussian expansion for a level density depends on how nearly Gaussian the level density is. It is fairly easy to check the Gaussian assumption for one-body Hamiltonians. As an example, consider the system consisting of 20 single particle states, all spaced at equal intervals. For one particle, the level density is constant with energy, but for two particles, the distribution already is close to Gaussian, as can be seen from Fig. 2. The addition of more particles to the system causes the distribution to become even more Gaussian (Fig. 3) until we reach 10 particles. As the number is further increased, we find that $\rho(E)$ for m particles is the reflection in energy of $\rho(E)$ for 20 - m particles. Thus, as long as m is more than 2 and less than 18 in this example, the level density is nearly Gaussian. Since we have assumed non-interacting particles and have used an equidistant level spacing, we have essentially the same situation as a Fermi gas, with the one difference being the truncated basis. The contribution from higher energy single particle states will not be important at low energies, so our level density should agree with the classic Fermi gas in the low energy region. This is an alternative way of demonstrating the result presented in Fig. 1; the Fermi gas and Gaussian forms are very similar over a range of 10 MeV or more.

This comparison does not, of course, show that the level density has a Gaussian distribution with energy for an arbitrary two-body Hamiltonian. Specific Hamiltonians, for example a pairing Hamiltonian in a basis of originally degenerate states, do give non-Gaussian distributions. It has been shown that most two-body interactions yield a distribution of levels with energy which is essentially Gaussian [8]. An example of a shell model calculation for which all eigenvalues have been obtained and compared with a Gaussian distribution is shown in Fig. 4. Note the very nearly Gaussian behavior of this level distribution.

In a larger system the diagonalization cannot be carried out. In such a case the deviations from Gaussian form may still be investigated. Calculated values for $\langle H^3 \rangle$ and $\langle H^4 \rangle$ may be compared with those predicted by a Gaussian distribution based on the calculated $\langle H \rangle$ and $\langle H^2 \rangle$ values. Corrections to the Gaussian distribution could be calculated by incorporating the known $\langle H^3 \rangle$ and $\langle H^4 \rangle$ values into a Hermite polynomial expansion.

An alternative procedure for investigating these possible discrepancies is to partition the space into configurations. If we consider an sd shell nucleus and do a calculation involving the $d_{5/2}$, $s_{1/2}$, $d_{3/2}$ and $f_{7/2}$ orbitals, the moments could be calculated for the entire distribution, resulting in a single expansion. Another possibility is to group states into configurations and calculate the moments for each of these separately. In the above example, one configuration could be all states with particles only in the sd shell, a second would include all states with one particle in the $f_{7/2}$ orbital and a third would encompass those states with two particles in the $f_{7/2}$ shell. This division results in configurations identified by the number of particles in each of two groups of orbitals. One could also divide the space into three (or more) groups of orbitals,

making the total level density the sum of an even larger number of component distributions. Any such decomposition results in the expansion of the level density as the sum of a number of configuration distributions, each centered on a separate centroid. If each of these is carried out to order $\langle H^n \rangle$, the resultant summed distribution will have the correct moments to that order of the total distribution. In addition, it carries some information about higher moments of the distribution. For example, if each configuration is expressed as a Gaussian, the summed distribution will deviate in general from a Gaussian form, although the deviations will be small in most cases. Similarly, a configuration expansion to order $\langle H^4 \rangle$ will give a combined distribution which has correct moments through $\langle H^4 \rangle$ but also incorporates some information about higher moments.

Calculation of moments beyond $\langle H^2 \rangle$ becomes increasingly difficult with the propagator theorem. The higher order operators require more sums, some of which have many more terms than the corresponding sums for lower rank operators. An alternative approach, called the random vector method, has recently been developed [9,10]. This procedure utilizes a Monte Carlo approach to calculate higher moments of the Hamiltonian. Slater determinants are selected at random from either the entire basis or a particular configuration as desired. Amplitudes are chosen at random and the vector $|r\rangle$ is normalized. The expectation value $\langle r|H|r\rangle$ is then calculated and a new vector $|r'\rangle$ constructed:

$$|r'\rangle = H|r\rangle - \langle r|H|r\rangle \; |r\rangle$$

It can be seen that this vector is orthogonal to $|r\rangle$ by construction. We normalize this vector and then construct a third vector $|r''\rangle$

$$|r''\rangle = \cos\theta \; |r\rangle + \sin\theta \; |r'\rangle ,$$

where θ is determined so that $\langle r''|H|r''\rangle$ has the correct value of $\langle H \rangle$ as calculated with the propagator theorem. It can be shown that a θ can be found which meets this condition unless $|r\rangle$ is an eigenvector of H or unless all components of $|r\rangle$ have values of $\langle H \rangle$ which are on the same side of the correct value of $\langle H \rangle$. By choosing our vectors to have 15 components we make the second situation extremely unlikely and the first condition is never fulfilled in a shell model basis (the real eigenvectors have many more than 15 components). By forcing the vector to have the correct value of $\langle H \rangle$, we drastically reduce the dispersion in $\langle H^2 \rangle$, $\langle H^3 \rangle$, and $\langle H^4 \rangle$. We normally require approximately fifty such random vectors in order to obtain statistical convergence on the higher moments of the Hamiltonian.

The use of this correction algorithm is absolutely vital to making calculations with the random vector technique. Total calculation time for the level density parameters of one nucleus is about 1.5 hours with the correct technique; without it, convergence of the higher moments would be sufficiently poor that more than 100 times as many random vectors would be required for convergence.

A calculation of the level density parameters of ^{28}Si has recently been completed using the random vector technique [11]. The basis included

the $d_{5/2}$, $s_{1/2}$, $d_{3/2}$ and $f_{7/2}$ states with the single particle energies based on energies of the appropriate spin and parity in ^{17}O. Thus, ^{28}Si was treated as twelve active nucleons outside a ^{16}O core. The two-body matrix elements were based on the interaction of Petrovich et al. [12]. Initial calculations with this potential showed that inclusion of the $f_{7/2}$ state caused considerable broadening of the distribution. Although the slope of the level density function was approximately correct for the sd calculation, the $sdf_{7/2}$ calculation, notwithstanding the larger number of states in the basis, had too slow a rise for small values of the energy. By trial and error, it was found that a reduction of 35% in the strength of the two-body interaction gave an appropriate slope for the level density.

This renormalization is not unexpected. As the basis is enlarged, more couplings become possible and each shell model state is spread over a wider energy range. Most interactions used in shell model calculations have an implicit or explicit renormalization to make the force larger to compensate for basis truncation effects. As we enlarge the basis beyond that used in conventional shell model calculations, we expect that the force strength should be reduced. A similar finding in a spectral distribution calculation has recently been reported by Verbaarschot et al. [13].

Calculations were performed with two different partition of the space. The first (two partition) expansion corresponded to specifying the number of particles in the sd orbitals and the number in the $f_{7/2}$ orbitals. A second expansion (three partition) was carried out with the number of particles specified in (a) the $d_{5/2}$ and $s_{1/2}$, (b) the $d_{3/2}$, and (c) the $f_{7/2}$ orbital separately. The value of making the calculation with different partitions is that the results can be compared to check for convergence.

Fig. 5 presents a comparison of the calculated level density for ^{28}Si for these two partitions with measured values. The open circles at low energy represent points determined by counting the levels tabulated in Endt and van der Leun [14] while the open square is calculated from the levels in Ref. 14 by Beckermann [15] by estimating how many levels at this energy had spins and parties such that they probably would have been missed. The points at energies about 20 MeV were deduced from Ericson fluctuation measurements and are due to Singh et al. [16], Shaw, Katsanos, and Vandenbosch [17], and Eberhard and Mayer-Böricke [18]. Table I presents a comparison of level density parameters from ^{28}Si inferred from the present data with parameters obtained by Beckerman [15] and Roeders et al. [19].

The present calculations would give a poor fit to the data if we chose the energy zero based on the first predicted level in the calculation. Thus, we shift the scale so as to normalize the integral of the calculation to the experimental integral over the the first eight MeV of excitation. This produced about a 3 MeV shift in the energy scale. One possible explanation for the need for such a shift is the fact that ^{28}Si has only two energy levels below 4.5 MeV, making a continuous approximation difficult to apply. This normalization procedure accounts for the difference of about 20% in the two- and three-component distributions at 20 MeV. In fact, these distributions were virtually identical at this point and differed by 20% at

low energy. Our normalization procedure transfers this discrepancy to higher energy. This difference is an estimate of the numerical convergence uncertainty produced by our configuration decomposition. This discrepancy is smaller than the estimated error in the experimental points ($\sim$ 50%) and is also smaller than the uncertainty produced by the uncertainty in theoretical input parameters.

We find generally good agreement between calculation and experiment for the level density. Some refinement of parameters could result from an effort to match theory and experiment more exactly, but given the uncertainty in the experimental values, such a procedure would be premature at this time.

The parity ratio and spin cutoff parameter were also calculated and are presented in Figs. 6 and 7, respectively. The crosses are calculated from the levels listed in Endt and van der Leun [14]. The various lines show the results for the two partitions with four moments of the Hamiltonian and for one partition with two moments. The agreement is good for the parity ratio but it appears the calculation approaches the asymptotic value too slowly with energy. For the spin cutoff parameter, the Δ points are from Ref. 20. A slight tendency to overestimate the spin cutoff parameter is seen, but the agreement is generally good.

SUMMARY

Spectral distribution methods allow a calculation of the level density and related parameters for a nucleus with inclusion of the two-body force. This allows collective levels to be placed in their proper position (if our input parameters are correct) and makes extrapolations to nuclei off the stability line more reliable, since the two-body force incorporates the differences between n-n, n-p and p-p interactions. We therefore require two-body force parameters in addition to the single particle energies needed for a Fermi gas calculation. The need for extra input is a disadvantage, but it is the price we must pay for a more detailed description of the nucleus. It also affords us an opportunity, in that it allows comparison with shell model calculations and thereby makes possible a study of basis truncation effects. A significant remaining problem is the need to speed up the calculations. The slowness of the present calculations makes parameter searches extremely difficult. Undoubtedly, some improvement will come as faster computers are developed. More efficient calculational procedures are also needed, however. We are presently investigating the effects of correcting random vectors for both $\langle H \rangle$ and $\langle H^2 \rangle$. This may lead to more rapid convergence of $\langle H^3 \rangle$ and $\langle H^4 \rangle$ and cut down the computer time requirement significantly.

Although much additional work is needed, spectral distribution methods show promise as a technique for improving our ability to calculate nuclear level densities. Other benefits, including a better understanding of basis truncation effects and the physics of the two body interaction itself, may also result from these investigations.

REFERENCES

1. H.A. BETHE, Phys. Rev. 50, 332 (1936).

2. J.R. HUIZENGA and L.G. MORETTO, Ann. Rev. Nucl. Sci. 22, 427 (1972).

3. J.R. HUIZENGA, A.M. BEHKAMI, R.W. ATCHER, J.S. SVENTEK, H.C. BRITT and H. FREIESLEBEN, Nucl. Phys. A223, 589 (1974).

4. L.G. MORETTO, Nucl. Phys. A182, 641 (1972).

5. S.M. GRIMES, Proceedings of the International Conference on Theory and Application of Moment Methods in Many-Fermion Systems, edited by B.J. Dalton, S.M. Grimes, J.P. Vary and S.A. Williams, Plenum Press (1980), p. 17.

6. J.B. FRENCH and K.F. RATCLIFF, Phys. Rev. C3, 94 (1971).
J.B. FRENCH, "Nuclear Structure", A. Hassain, Harun-al-Raschid and M. Islam, eds. (North Holland, Amsterdam, 1967).
F.S. CHANG, J.B. FRANCE and T.H. THIO, Ann. Phys. (N.Y.) 66, 137 (1966).

7. S.M. GRIMES, Proceedings of the Europhysics Conference on Neutron-Induced Reactions, Slovak Academy of Sciences (1982), p. 79.

8. J.B. FRENCH, Proceedings of the International Conference on the Theory and Application of Moment Methods in Many-Fermion Systems, edited by B.J. Dalton, S.M. Grimes, J.P. Vary and S.A. Williams, Plenum Press (1980), p. 1;
J.N. GINOCCHIO, ibid, p. 109.

9. S.M. GRIMES, S.D. BLOOM, R.F. HAUSMAN, JR. and B.J. DALTON, Phys. Rev. C19, 2378 (1979).

10. S.D. BLOOM and R.F. HAUSMAN, JR., Proceedings of the International Conference on the Theory and Application of Moment Methods in Many-Fermion Systems, edited by B.J. Dalton, S.M. Grimes, J.P. Vary, and S.A. Williams, Plenum Press (1980), p. 151.

11. S.M. GRIMES, S.D. BLOOM, H.K. VONACH and R.F. HAUSMAN, JR., Physical Review C (in press) (1983).

12. F. PETROVICH, H. McMANUS, V.A. MADSEN and J. ATKINSON, Phys. Rev. Lett. 22, 895 (1969).

13. J.J.M. VERBAARSCHOT, G.S. TIMMER and P.J. BRUSSARD, Nucl. Phys. A378, 205 (1982).

14. P.M. ENDT and C. VAN DER LEUN, Nucl. Phys. A310, 1 (1978).

15. M. BECKERMAN, Nucl. Phys. A278, 333 (1977).

16. P.P. SINGH, R.E. SEGEL, L. MEYER-SCHUTZMEISTER, S.S. HANNA and R.G. ALLAS, Nucl. Phys. 65, 577 (1965).

17. R.W. SHAW, JR., A.A. KATSANOS and R. VANDENBOSCH, Phys. Rev. 184, 1089 (1969).

18. K.A. EBERHARD and C. MAYER-BÖRICKE, Nucl. Phys. A142, 113 (1970).

19. J.D.A. ROEDERS, L.W. PUT, A.G. DRENTJE and A. VAN DER WOUDE, Nucl. Phys. A112, 561 (1968).

20. S.M. GRIMES, C.H. POPPE, C. WONG and B.J. DALTON, Phys. Rev. C18, 1100 (1978).

TABLE I

LEVEL DENSITY PARAMETERS FOR ^{28}Si

Previous Values (fitted to data)		
Beckerman *	$a = 2.168$	$c = .00187$
Roeders et al. **	$a = 3.11$	$\delta = 3.5$
Present Result **	$a = 2.87$	$\delta = 2.57$

* Based on the form $ce^{2\sqrt{au}}$

** Based on the form $\dfrac{e^{2\sqrt{a(u-\delta)}}}{24\sqrt{2}\,\sigma\, a^{1/4}(u-\delta)^{5/4}}$

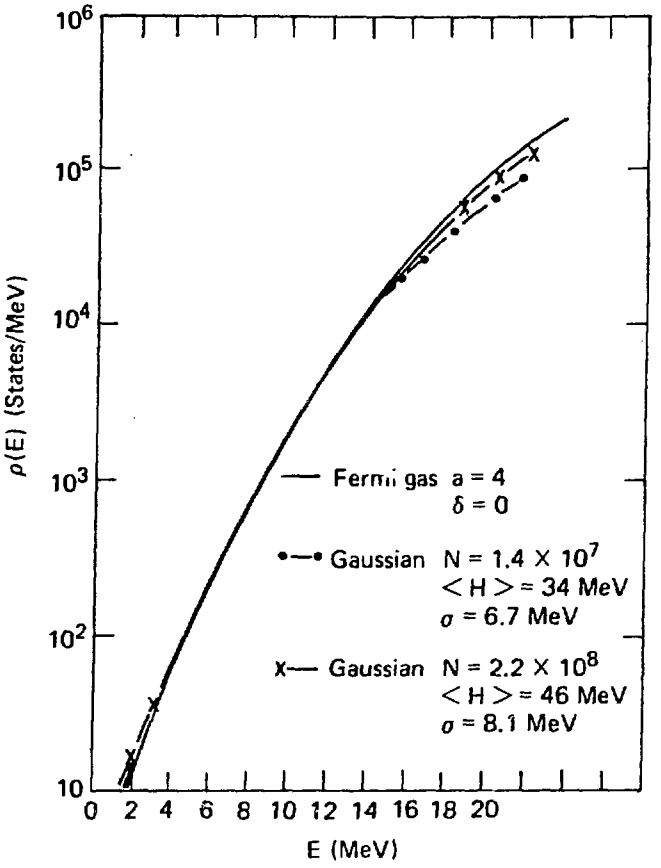

Figure 1: Illustration of the similarity between the Gaussian and Fermi gas level density forms. The solid line represents the energy dependence of the Fermi gas form for a = 4 and δ = 0; the x-dashed and dot-dashed lines indicate fits to this form for Gaussians with two different dimensionalities. Note the close agreement over a wide energy range.

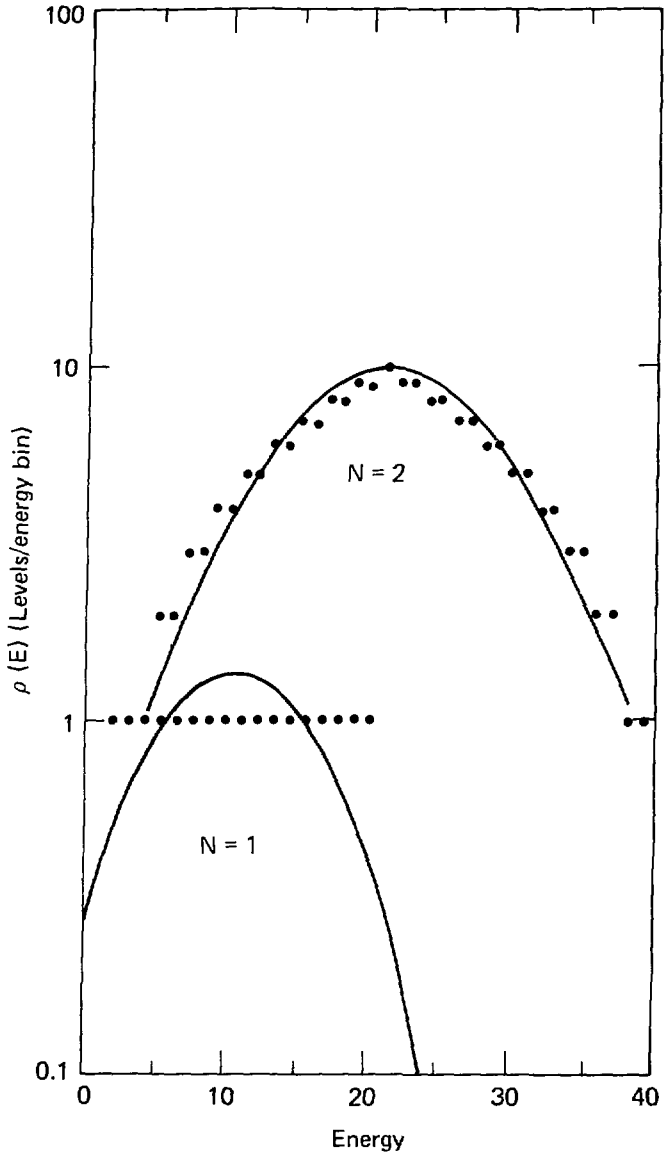

Figure 2: Level density for systems of one or two particles in a set of equidistant single particle levels. The lower curve is the Gaussian fit to the exact level density (dots) of a one particle system in a basis of twenty levels with energies of 1, 2, . . ., 20 energy units. The curve on top is the corresponding fit to the level density of the two-particle system.

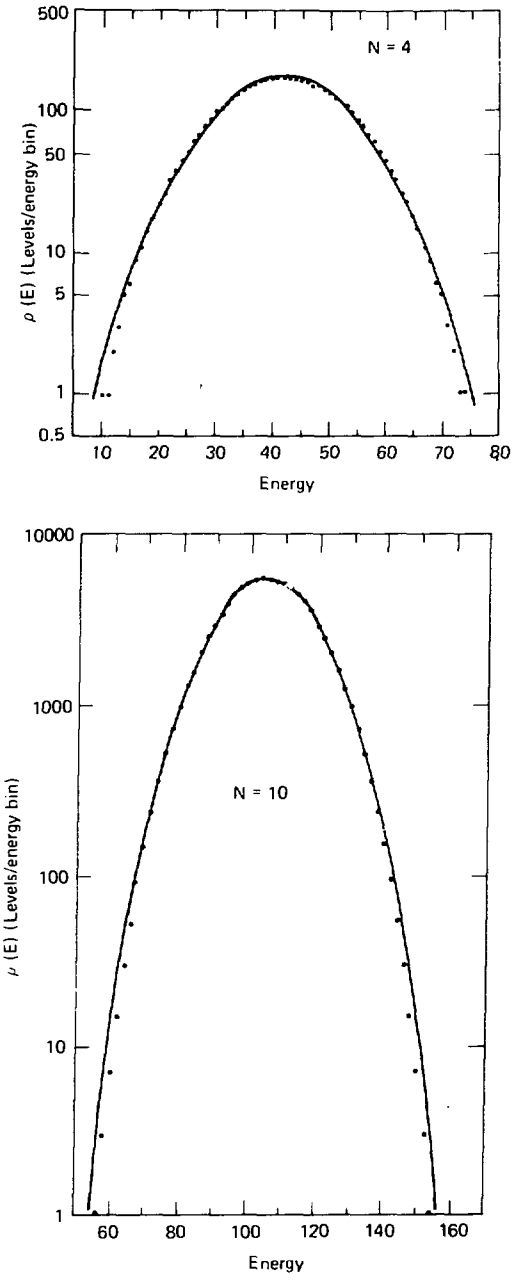

Figure 3: Same as Fig. 2 for systems with 4 or 10 particles in the same single particle basis.

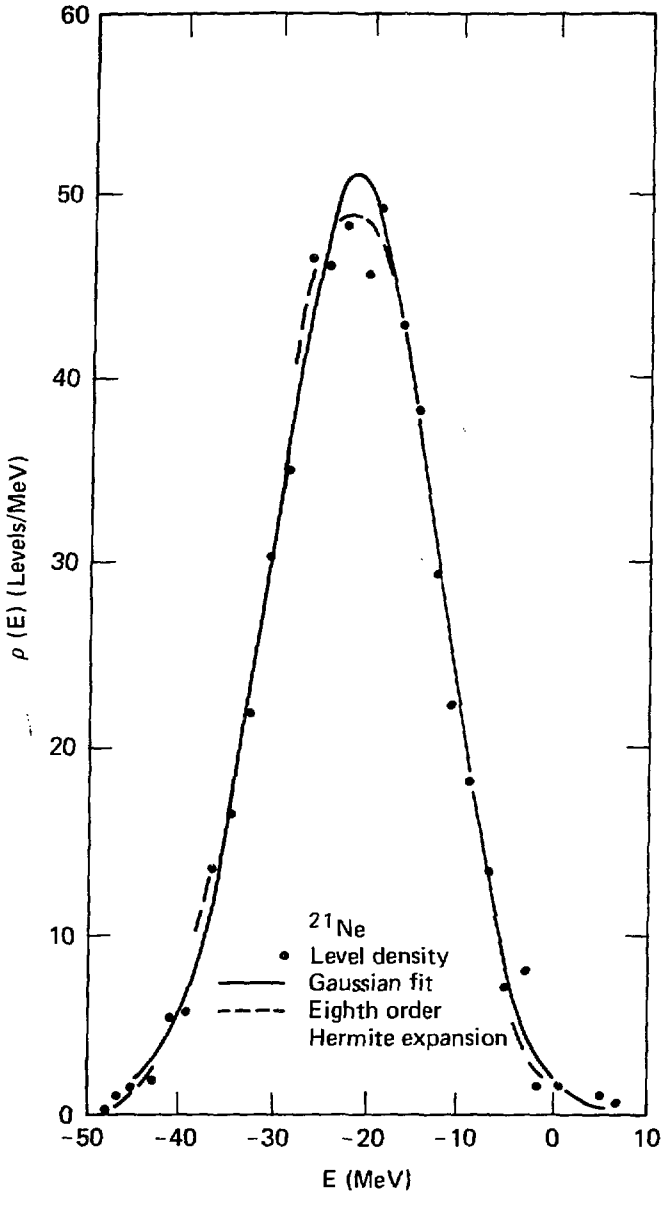

Figure 4: Fit of a Gaussian function to the level density of ^{21}Ne. Eigenvalues for ^{21}Ne calculated with an ^{16}O core are grouped in bins and plotted with a dot; the solid line is the corresponding Gaussian fit, while the dashed line shows the modest changes produced by including Hermite polynomials through eighth order in the expansion.

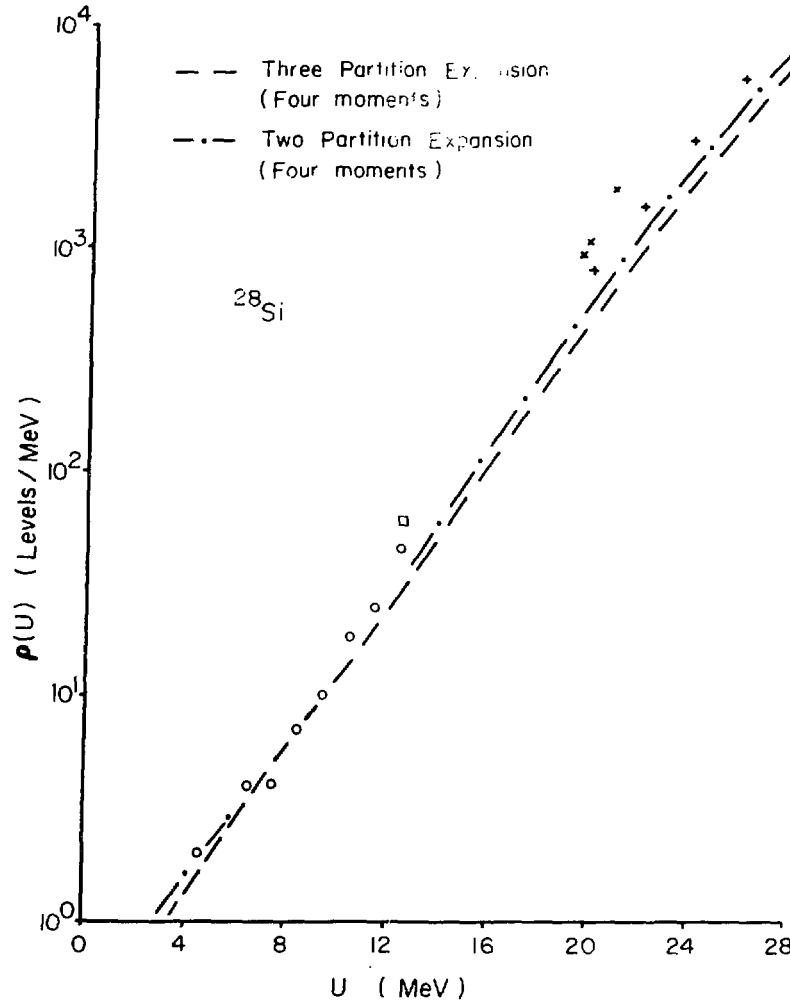

Figure 5: Comparison of the calculated level density of ^{28}Si with measured values. The dashed and dot-dash lines represent spectral distribution calculations as explained in the text; the points represent values from level counting (0,□) or Ericson fluctuation measurements (x,+).

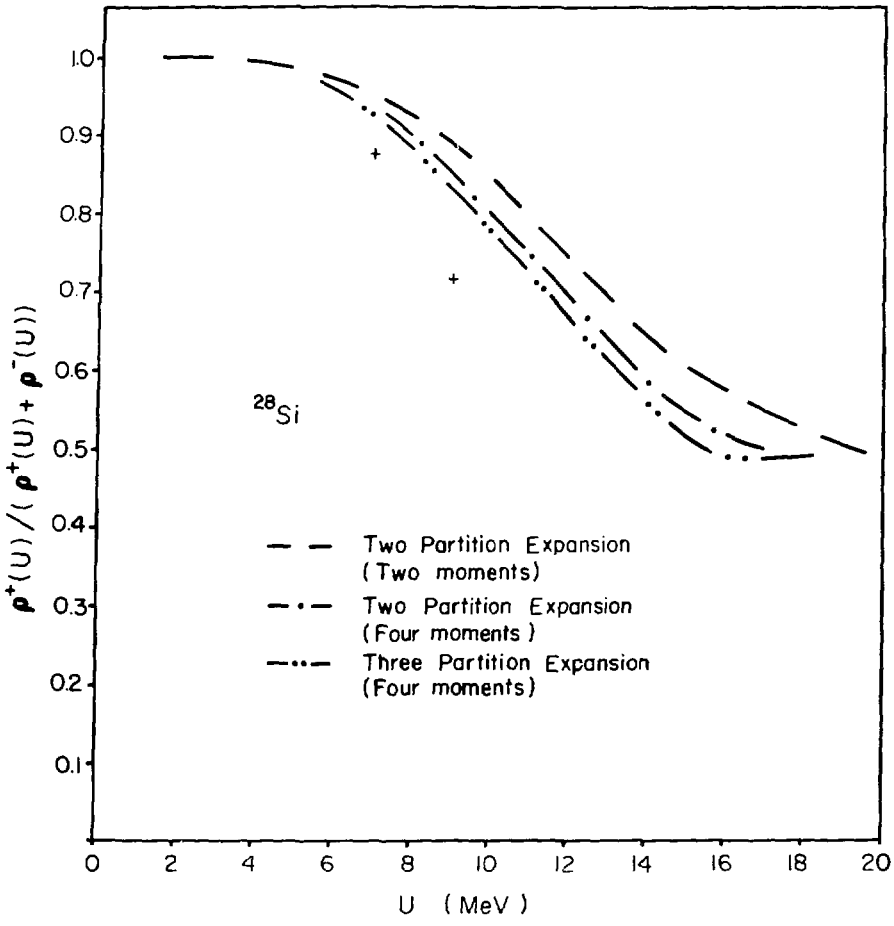

Figure 6: Comparison of calculated and measured values of the parity ratio. The crosses are values deduced from level counting; the lines are spectral distribution calculations explained in the text.

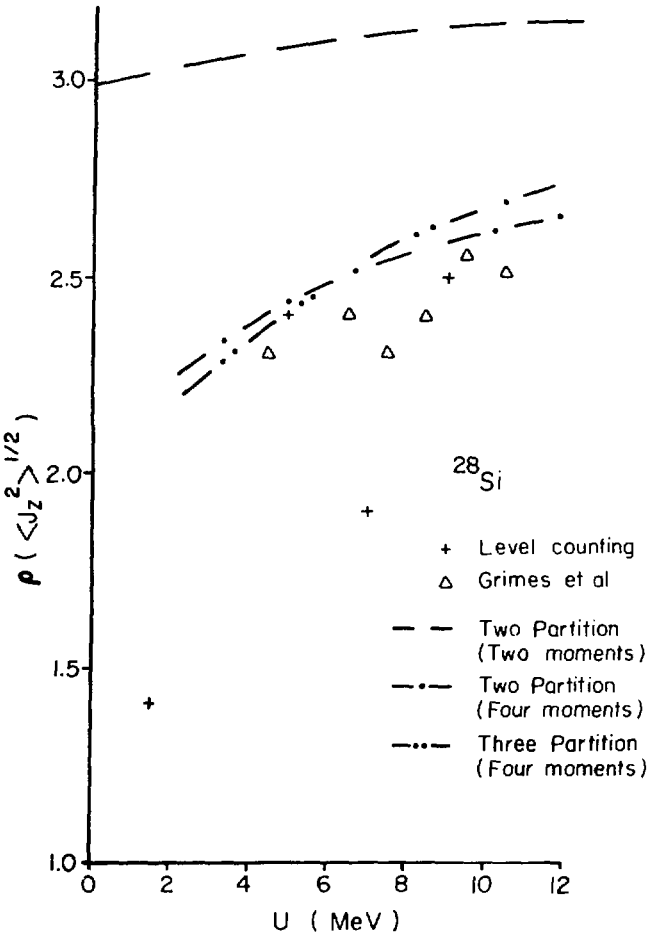

Figure 7: Comparison of calculated and measured values for the spin cutoff parameter. Crosses represent values obtained from level counting and triangles values deduced from angular distributions of (α,n) reactions. The lines represent spectral distribution calculations as explained in the text.

A NILSSON-BCS MICROSCOPIC APPROACH FOR LEVEL DENSITIES, EXTENDED TO ODD NUCLEI, AND RELATED PHENOMENOLOGICAL PARAMETERS

G. Maino and E. Menapace

E.N.E.A., Via Mazzini 2, 40138 Bologna (ITALY)

ABSTRACT

A phenomenological and analytical formula for nuclear level densities is proposed, that reproduces microscopic Nilsson-BCS calculations, with inclusion of the blocking effect for odd N and/or Z nuclei. A simple energy dependence of the level density parameter "a" is obtained in the interval ranging from 4 to 20 MeV for a number of nuclei in the mass region $124 \leq A \leq 160$.

INTRODUCTION

A reliable knowledge of nuclear level densities over a wide range of excitation energies and in a broad mass region, is required by cross-section and emission spectrum calculations. The experimental information - mainly from the analyses of s-wave neutron resonances and from the cumulative number of discrete levels - is rather poor in many cases to permit an accurate determination of the adjustable parameters in the usual level density formulae based on the Fermi gas model |1| . Microscopic approaches to nuclear level densities, starting from realistic single-particle states and including residual interactions as the pairing correlation in the BCS approximation |2| , are based on more realistic assumptions, but require a lot of computing time. As a compromise, in the last few years many efforts were accomplished to obtain reliable but still closed-form expressions for the level densities, that would take into account shell and pairing effects |3,4,5,6| .

In ref. |7| a mixed theoretical-phenomenological method is proposed and an analytical formula is given able to reproduce both the experimental data at the neutron binding energies and the theoretical calculations, based on a Nilsson or Woods-Saxon level spectrum and the BCS treatment of the pairing in-

teraction. In particular, the level density parameter "a" was found to depend on the excitation energy. Subsequent works |8,9| essentially confirmed the simple exponential dependence of the "a" parameter, proposed in |7|.

In the present paper, a very simple expression for the level density is suggested, similar to that of ref.|7|, starting from NBCS microscopic calculations that take into account the blocking effect of single-particle levels due to unpaired nucleon(s) in odd-A and odd-odd nuclei |10| , as the main difference with respect to the previously quoted papers.

THEORY

In the frame of NBCS microscopic calculations of the grand partition function and of the saddle-point approximation to the Laplace inverse transform, the level density is given by |11|:

$$\rho_{NBCS}(U,J) = \frac{e^{S}}{(2\pi)^{3/2}|D|^{1/2}} \cdot \frac{e^{-J(J+1)/2\sigma^2}}{\sigma^3} \cdot F_{coll}(U,J) \qquad (1)$$

where U is the excitation energy in MeV, J the angular momentum in $\hbar$ units, S the nuclear entropy related to the intrinsic degrees of freedom, D a 3x3 determinant, σ the spin cut-off factor. Expressions for S,D and σ ,with blocking effects, are reported in ref.|10|.

The collective enhancement factors are (see ref.|12| where the symbols are explained):

$$F_{coll}(U,J) = \begin{cases} \dfrac{1}{(2\pi)^{3/2}} \cdot \dfrac{(2J+1)}{\left[1-\exp(-\hbar\omega/T)\right]^{g}} & \text{for vibrational contr.} \quad (2a) \\[2ex] \dfrac{1}{(2\pi)^{3/2}} \cdot \sigma_{/\!/}^2 \cdot \displaystyle\sum_{K=-J}^{J} \exp\left[-K^2\left(\frac{1}{2\sigma_{/\!/}^2} - \frac{1}{2\sigma_{\perp}^2}\right)\right] & \text{for rotational contr.} \quad (2b) \end{cases}$$

The form.(1), taking into account the blocking effect for odd N and/or Z nuclei, was checked by calculations of level densities at the neutron binding energies for 148 nuclei in the mass region $90 \leq A \leq 250$ |11| and comparisons with the empirical s-wave neutron resonance spacings. The theoretical results agree within a 30% with the experimental data and represent a considerable improvement with respect to the usual "unblocked" treatment of odd nuclei.

This microscopic method can be applied with confidence in the excitation energy range 4-20 MeV, where the involved approximations are still valid. At lower energies, any statistical approach fails and would have to be replaced, e.g., by combinatorial techniques; above 20 MeV the present rough treatment of the collective degrees of freedom could be inadequate. Moreover, a constant nuclear deformation, corresponding to the ground-state shape, is assumed over the whole energy range. This assumption is justified only for nuclear tempera

tures below 1-1.5 MeV |13|, (for the nuclei in Table I, the excitation energy of 20 MeV corresponds to about 1 MeV of temperature).

A very simple expression is adopted to reproduce these NBCS calculations, in the energy range 4-20 MeV:

$$\rho(U,J) = \frac{e^{2\sqrt{aU}}}{2\sqrt{2}\, a^{1/4}\, U^{5/4}} \cdot \frac{e^{-J(J+1)/2\sigma^2}}{\sigma^3} \cdot F_{coll}(U,J) \qquad (3)$$

The following energy dependence

$$a = \tilde{a}\,(1 - e^{-\gamma U}) \qquad (4)$$

is derived from the microscopic entropy of form.(1), by means of the relation $a=S^2/4U$, with a proper choice of the adjustable parameters $\tilde{a}$ and γ .

The collective enhancement factors are the same of form.(2a,2b). The spin cut-off factor σ is approximated by the rigid body value:

$$\sigma^2 = K\, A^{5/3} \sqrt{U/a} \qquad (5)$$

with A mass number and K a constant.

Note that in form.(3), we do not introduce the odd-even mass difference parameter δ , which usually appears in Fermi gas-like formulae. This is why the difference between the treatments of even and odd nuclei is introduced "ab initio" in our microscopic blocked formalism, whose results are phenomenologically reproduced by form.(3,4). An advantage of the present approach, with respect to the Gilbert-Cameron expression, is that form.(3,4) can be extended to low energies, possibly with a suitable change of the adjustable parameters $\tilde{a}$ and γ .

RESULTS

The formalism of the previous section has been applied to the analysis of nuclei with mass number $124 \leq A \leq 160$, corresponding to the second peak in the yield of fission product nuclei. In Table I the phenomenological parameters, obtained from a fit of the experimental information and of the microscopic calculations, are listed. At the excitation energies here considered, shell effects are expected to be not negligible |14| ; since form.(3,4) are very simple, the possible shell effects are loaded on the mass dependence of the $\tilde{a}$ and γ parameters. Figs. 1 and 2 show, respectively, $\tilde{a}$ versus the neutron number N and γ versus the mass number A. The level density parameter $\tilde{a}$ changes strongly around the shell closure N=82, while the γ parameter is smooth over the whole mass region. An higher mean value $\langle\gamma\rangle$ for odd than for even nuclei is found as expected on the basis of a faster increase of the level density with the

excitation energy for the odd nuclei. All the data of fig. 2 are approximated to some extent, within the statistical errors, to an overall mean value $\langle\gamma\rangle = (0.21\pm0.06)\ \mathrm{MeV}^{-1}$. The microscopic spin cut-off factor is reproduced at energies higher than the neutron binding energy by form.(5) with K = 0.018. At lower energies, the discrepancies may be considerable, as shown in fig. 3. However, the introduction of the blocking effect, that reduces the pairing correlations in the odd nuclei, involves a microscopic calculated spin cut-off factor closer to the rigid body value (see fig. 3, ^{154}Eu in comparison with ^{155}Eu).

Finally, in fig. 4 the theoretical NBCS and the phenomenological level densities $\rho(U,J=1/2)$ for ^{151}Sm are drawn and compared with the relation of ref.|7|.

REFERENCES

1. A. Gilbert and A.G.W. Cameron, Can.J.Phys.43,1446 (1965).
2. J.R. Huizenga and L.G. Moretto, Annu. Rev. Nucl. Sci. 22, 427 (1972).
3. A.S. Jensen and J. Sandberg, Phys. Scripta 17, 107 (1978).
4. S.K. Kataria, V.S. Ramamurthy and S.S. Kapoor, Phys. Rev. C18, 549 (1978).
5. Yu.N. Shubin, Sov.J.Nucl.Phys.30, 643 (1979).
6. K. Junker, J. Hadermann and N.C. Mukhopadhyay, in Proc.Intern. Symp. on Physics and Chemistry of Fission, Jülich (1979), International Atomic Energy Agency, Vienna (1980), vol. I, p. 445.
7. A.V. Ignatyuk, G.N. Smirenkin and A.S. Tishin, Sov. J. Nucl. Phys. 21, 255 (1975).
8. N. Cârjan, H. Delagrange and A. Fleury, Phys. Rev. C19, 2267 (1979).
9. K.H. Schmidt, H. Delagrange, J.P. Dufour, N. Cârjan and A. Fleury, Zeit. Phys. A308, 215 (1982).
10. G. Maino, E. Menapace and A. Ventura, Nuovo Cim. A57, 427 (1980).
11. V. Benzi, G. Maino and E. Menapace, Nuovo Cim. A66, 1 (1981).
12. S. Bjørnholm, A. Bohr and B.R. Mottelson, in Proc. Intern. Symp. on Physics and Chemistry of Fission, Rochester, N.Y. (1973), International Atomic Energy Agency, Vienna (1974), vol. I, p. 367.
13. P. Quentin and H. Flocard, Annu. Rev. Nucl. Part. Sci. 28, 523 (1978).
14. L.G. Moretto, Nucl. Phys. A182, 641 (1972).

TABLE I

Phenomenological level density parameters, deduced from microscopic NBCS calculations.

Nucleus	N	Z	$\tilde{a}$ (Mev^{-1})	γ (MeV^{-1})	$\Delta\gamma$ (MeV^{-1})
^{124}Te	72	52	14.4	0.21	0.04
^{126}Te	74	52	14.1	0.21	0.05
^{127}Te	75	52	16.4	0.31	0.11
^{130}I	77	53	15.3	0.45	0.19
^{132}Xe	78	54	14.8	0.20	0.02
^{131}Ba	75	56	16.4	0.26	0.04
^{136}Ba	80	56	14.3	0.19	0.01
^{137}Ba	81	56	16.3	0.29	0.06
^{138}Ba	82	56	13.7	0.19	0.02
^{139}Ba	83	56	14.1	0.23	0.03
^{139}La	82	57	15.5	0.33	0.10
^{141}Ce	83	58	15.8	0.22	0.02
^{142}Pr	83	59	17.4	0.29	0.07
^{143}Nd	83	60	16.2	0.21	0.03
^{144}Nd	84	60	16.1	0.21	0.02
^{145}Nd	85	60	18.2	0.30	0.05
^{146}Nd	86	60	17.3	0.21	0.02
^{147}Nd	87	60	18.4	0.23	0.01
^{151}Nd	91	60	18.8	0.24	0.03
^{148}Pm	87	61	20.1	0.34	0.10
^{150}Sm	88	62	17.8	0.19	0.02
^{151}Sm	89	62	19.2	0.23	0.02

Nucleus	N	Z	$\tilde{a}$ (MeV^{-1})	γ (MeV^{-1})	$\Delta\gamma$ (MeV^{-1})
^{152}Sm	90	62	17.8	0.19	0.02
^{153}Sm	91	62	19.0	0.24	0.03
^{155}Sm	93	62	18.6	0.23	0.03
^{152}Eu	89	63	19.7	0.29	0.06
^{153}Eu	90	63	17.9	0.22	0.03
^{154}Eu	91	63	19.8	0.25	0.10
^{155}Eu	92	63	17.8	0.21	0.03
^{156}Eu	93	63	18.8	0.26	0.07
^{153}Gd	89	64	19.4	0.23	0.02
^{155}Gd	91	64	19.2	0.24	0.03
^{156}Gd	92	64	17.9	0.19	0.02
^{157}Gd	93	64	18.9	0.23	0.03
^{158}Gd	94	64	17.6	0.19	0.02
^{159}Gd	95	64	18.0	0.24	0.04
^{161}Gd	97	64	18.6	0.26	0.06
^{160}Tb	95	65	17.9	0.30	0.08

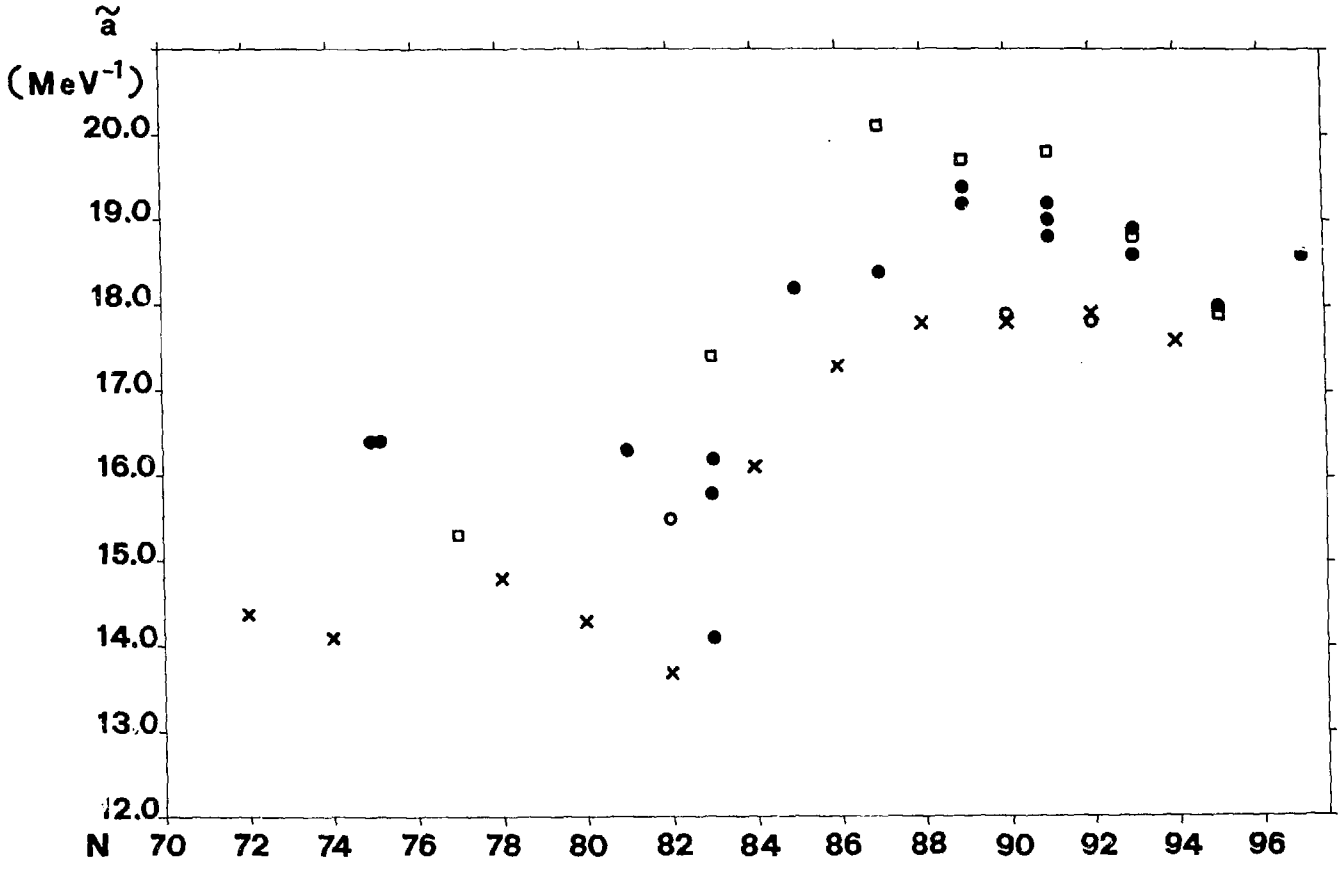

Fig. 1 - The level density parameter $\tilde{a}$ as a function of the neutron number N, for: x even-even nuclei; ● odd N-even Z nuclei; O even N-odd Z nuclei; □ odd-odd nuclei.

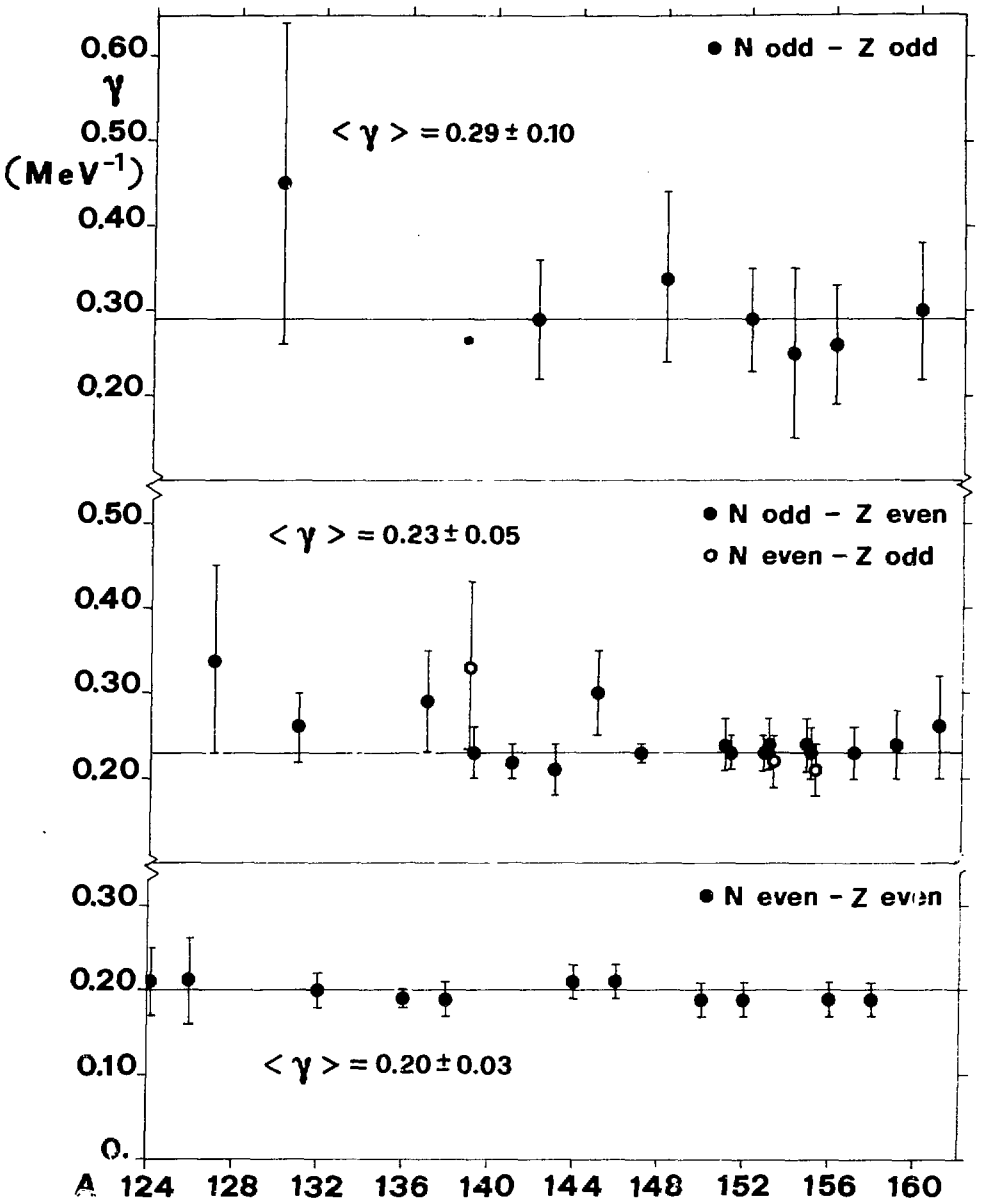

Fig. 2 - The parameter γ versus the mass number A.

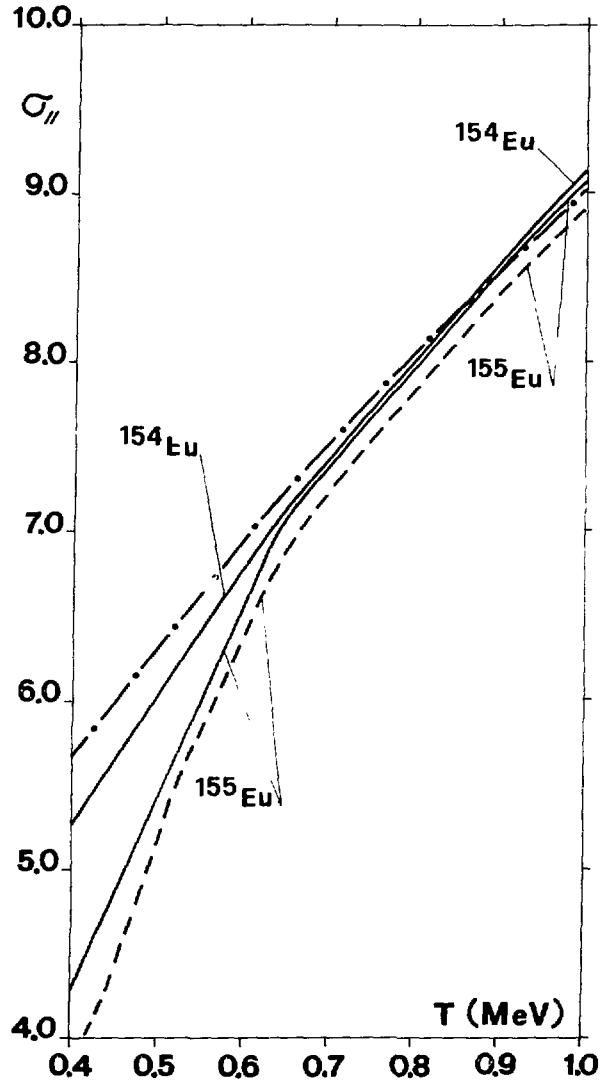

Fig. 3 - The spin cut-off factor $\sigma_{//}$ versus the temperature T for ^{154}Eu and ^{155}Eu. Solid lines: NBCS calculations with blocking effect; dashed line: NBCS calculations without blocking effect; dot-dashed line; rigid body value $\sigma = | 0.018\ A^{5/3} T |^{1/2}$.

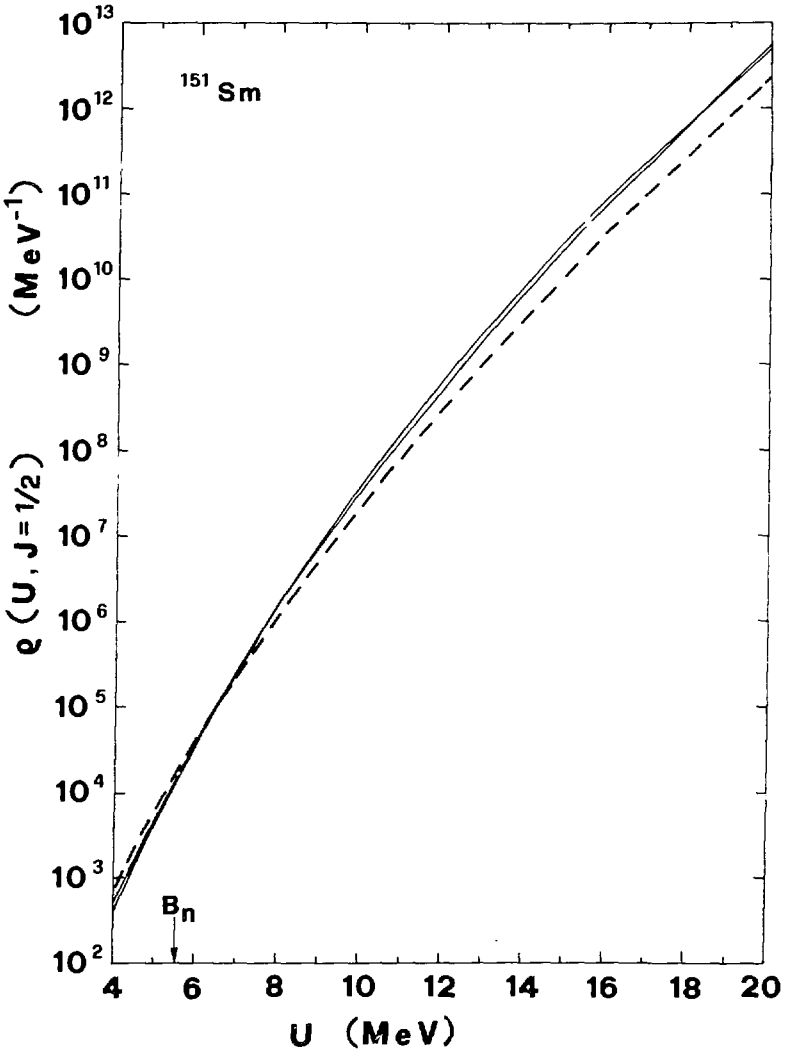

Fig. 4 - The level density $\rho(U,J=1/2)$ for ^{151}Sm as a function of the excitation energy. Solid lines: NBCS calculations with blocking effect and related phenomenological expression (form.3,4) with the parameters as in Table I. Dashed line: calculations as in ref.|7|.

LEVEL DENSITY APPROACH TO PERTURBATION THEORY AND INVERSE-ENERGY-WEIGHTED SUM-RULES

T. Raya Halemane

Physics Department
State University College
Fredonia, New York 14063, U.S.A.

ABSTRACT

The terms in the familiar Rayleigh-Schrodinger perturbation series involve eigenvalues and eigenfunctions of the unperturbed operator. A level density formalism, that does not involve computation of eigenvalues and eigenfunctions, is given here for the perturbation series. In the CLT (central limit theorem) limit the expressions take very simple linear forms. The evaluation is in terms of moments and traces of operators and operator products.

INTRODUCTION

In a conventional shell-model calculation, the dimensionalities of the matrices to be constructed and diagonalized become too large to handle too quickly as the number of nucleons is increased and the model space is extended to allow more excitations. It is desirable to approach the problem from a different angle focusing on the simplicities available in a many-particle system. A level density approach can make good use of the central limit theorem operating in such spaces [1,2]. We give here such a procedure [3] for perturbation theory.

THEORY

Let the Hamiltonian H of a nucleus be perturbed by αK where α is a small parameter and K is the perturbing operator. Let E and E_α denote the corresponding eigenvalues of H and $H_\alpha \equiv H + \alpha K$ respectively. Let E_α be expressed as a power series in α by

$$E_\alpha = \sum_{n=0}^{\infty} \alpha^n S_n(E) = E + \alpha S_1(E) + \alpha^2 S_2(E) + \cdots \tag{1}$$

(where $S_o(E) \equiv E$). This implies that the $S_n(E)$ are the same as the terms in the Rayleigh-Schrodinger perturbation series. That is,

$$S_1(E) = \langle E | K | E \rangle \tag{2}$$

$$S_2(E) = -\sum_{E' \neq E} \frac{|\langle E' | K | E \rangle|^2}{E' - E} \tag{3}$$

We shall now obtain [3] expressions for $S_n(E)$ in terms of the level density $\rho(W)$ of the Hamiltonian H. This, along with the moment calculating techniques [1] of the spectral distribution methods [2] will make it possible to calculate $S_n(E)$ without having to diagonalize the Hamiltonian matrix. Let ρ and ρ_α denote the density (normalized to unity) of eigenvalues of H and H_α by ρ and ρ_α respectively and the corresponding p^{th} moments by M_p and $M_p(\alpha)$. Now $M_p(\alpha)$ can be written in two different ways. By the standard definition of moment,

$$M_p(\alpha) = \int_{-\infty}^{\infty} x^p \rho_\alpha(x)\, dx \tag{4}$$

However, the perturbation $H \to H_\alpha$ takes the eigenvalue E to E_α. The number of eigenvalues E which thus go to E_α is $\rho(E)dE$. Then the pth moment goes to

$$M_p(\alpha) = \int_{-\infty}^{\infty} (E_\alpha)^p \rho(E)\, dE \tag{5}$$

Using Leibnitz theorem in differential calculus and combinatorial arguments it can be shown from (4) and (5) that for all integers n > o

$$\int_{-\infty}^{\infty} E^p \frac{\partial^n \rho_\alpha}{\partial \alpha^n}\Big|_{\alpha=0} dE = \frac{\partial^n M_p(\alpha)}{\partial \alpha^n}\Big|_{\alpha=0} = \sum_{t=1}^{n} \int_{-\infty}^{\infty} E^p \frac{\partial^t}{\partial E^t}\left[\rho(E)\, c_t^n(E)\right] dE \tag{6}$$

where

$$c_t^n(E) = (-1)^t \frac{n!}{t!} \sum_P S_{i_1}(E) S_{i_2}(E) \cdots\cdots S_{i_t}(E) \tag{7}$$

where the partitions P are such that

$$\sum_{k=1}^{t} i_k = n \quad , \quad i_k \geq 1 \tag{8}$$

It then follows that

$$S_n(E) = -\frac{1}{n!}\frac{1}{\rho(E)}\left[\frac{\partial^n F_\alpha(E)}{\partial\alpha^n}\bigg|_{\alpha=0} - \sum_{t=1}^{n-1}\frac{\partial^t}{\partial E^t}\left\{\rho(E)\, e^n_{t+1}(E)\right\}\right] \tag{9}$$

Here $F_\alpha(E)$ is the distribution function $\int_{-\infty}^{E}\rho_\alpha(x)dx$.

For n = 1 and n = 2 equ. (9) gives

$$S_1(E) = -\frac{1}{\rho(E)}\frac{\partial F_\alpha(E)}{\partial\alpha}\bigg|_{\alpha=0} \tag{10}$$

$$S_2(E) = -\frac{1}{2\rho(E)}\left[\frac{\partial^2 F_\alpha}{\partial\alpha^2}\bigg|_{\alpha=0} - \frac{\partial}{\partial E}\left\{\frac{1}{\rho(E)}\left(\frac{\partial F_\alpha}{\partial\alpha}\bigg|_{\alpha=0}\right)^2\right\}\right] \tag{11}$$

By looking at their Rayleigh-Schrodinger forms it is clear that $S_1(E)$ is the expectation value K(E) of operator K at energy E and $S_2(E)$ is the inverse-energy-weighted sum.

In a many-particle model space consisting of m particles distributed over N single-particle states, the central limit theorem (CLT) dictates that in the limit of large particle number, the smoothed eigenvalue distributions for most Hamiltonian operators in the model space become close to Gaussian [1]. In this limit it can be shown that

$$S_1(E) \equiv K(E) \xrightarrow{CLT} \langle K\rangle + \frac{\langle\langle K(H-\langle H\rangle)\rangle\rangle}{\sigma^2}(E-\xi) \tag{12}$$

$$S_2(E) \xrightarrow{CLT} (1-\xi^2)\frac{\sigma_K^2}{2\sigma^2}(E-\xi) \tag{13}$$

Where we use the notation that for any operator G, << G >> denotes the trace over the model space and < G > denotes the average expectation value. ξ is the centroid and σ^2 is the variance of the distribution $\rho(W)$. Thus

$$\xi \equiv M_1 \equiv \langle H\rangle\,, \quad \text{and} \quad \sigma^2 \equiv M_2 - M_1^2 \equiv \langle H^2\rangle - \langle H\rangle^2$$

Also, $\xi \equiv \langle (H - \langle H \rangle)(K - \langle K \rangle) \rangle / \sigma_K \sigma$ is the correlation coefficient between H and K with σ_K^2 representing the variance of K.

The CLT results can be extended [3] to incorporate corrections due to deviations of $\rho(x)$ from Gaussian. These involve higher order moments and correlations of H and K.

Applications of this theory to perturbations of model interaction Hamiltonians and to moment of inertia in nuclei has been made [3] with encouraging results.

REFERENCES

1 J. B. FRENCH, "Nuclear Symmetries and Distributions" in Dynamic Structure of Nuclear States edited by D. J. Rowe, L. E. H. Trainor, S. S. M. Wong and T. W. Donnelly (University of Toronto, Toronto, Ontario, Canada, 1972).

2 J. B. FRENCH, "Statistical Nuclear Spectroscopy" in Nuclear Spectroscopy edited by G. F. Bertsch and D. Kurath, Lecture Notes in Physics Vol. 119 (Springer, Berlin, 1980) and references therein.

3 T. R. HALEMANE, "A statistical approach to perturbation theory and inverse-energy-weighted sum rules", J. Math. Phys., 22, 2961 (1981).

BRUTE FORCE LEVEL DENSITY

S. Raman

Physics Division

Oak Ridge National Laboratory

P.O. Box X, Oak Ridge, Tennessee 37830 USA

Since the text of this paper was not available by the deadline of May 31, 1983, the Editor regrets having to omit it from the Proceedings of the Meeting.

APPLICATION OF NUMBER THEORETICAL METHODS FOR THE CALCULATION OF NUCLEAR LEVEL DENSITIES

A.M. Anzaldo Meneses*

Kernforschungszentrum Karlsruhe GmbH
Institut für Neutronenphysik und Reaktortechnik
P.O.Box 3640 D-7500 Karlsruhe
Federal Republic of Germany
*DAAD-Stipendiat.On leave from the UNAM
(Universidad Nacional Autónoma de México)

ABSTRACT

The application of certain mathematical methods of number theory to compute the nuclear level density is a well established procedure since many years.

The analytical calculations provide closed formulas which have the advantage , on one side, to show the physical meaning of the appearing parameters and, on the other side, to provide simple analytic relations useful for applications. In this work, the most relevant contributions related to number theory are briefly reviewed. The asymptotic calculation of the partition function (needed to estimate the entropy at the saddle point) is an example of the usefulness of the standard methods of number theory for level density studies. The application of such methods led recently to more general results than the usual Bethe-formula or similar relations.

INTRODUCTION

It was clear very early [1],[2],[3],[4] that for large excitation energy there is a strong relation between the computation of the so-called "partitions of integer numbers" in number theory [5] and the calculation of the nuclear level density. For example, for the simple case of a system of N independent fermi particles on equidistant energy levels $\varepsilon_k = k$ for $k=1,2,3,\ldots$, the number

$p(N,E)$ of partitions of an integer number E in parts not exceeding N is related to the number $\rho(N,\mathcal{E})$ of partitions of an integer number $\mathcal{E}$ in N different parts by the relation:

$$p(N,E) = \rho(N,\mathcal{E}) \tag{1}$$

where E is the excitation energy and $\mathcal{E} = N(N+1)/2 + E$ is the total energy . This relation can be easily proved using the relations :

$$\sum_{E,N} p(N,E)\, e^{\mu N - \beta E} = \prod_{k=0}^{\infty} \frac{1}{1 - xy^k} \tag{2a}$$

and

$$\sum_{\mathcal{E},N} \rho(N,\mathcal{E})\, e^{\mu N - \beta \mathcal{E}} = \prod_{k=1}^{\infty} (1 + xy^k) \tag{2b}$$

And using the following representations of Euler [6] :

$$1 + \sum_{N=1}^{\infty} \frac{x^N y^N}{(1-y)\cdot\ldots(1-y^N)} = \prod_{k=1}^{\infty} \frac{1}{1 - xy^k} \tag{3a}$$

and

$$1 + \sum_{N=1}^{\infty} \frac{x^N y^{N(N+1)/2}}{(1-y)\ \ldots\ (1-y^N)} = \prod_{k=1}^{\infty} (1 + xy^k) \tag{3b}$$

Moreover, for unrestricted partitions we have the celebrated asymptotic representation of Hardy and Ramanujan and Rademacher [5] :

$$p(E) = \frac{1}{\pi\sqrt{2}} \sum_{k=1}^{\infty} A_k(E) k^{1/2} \left[\frac{d}{dx} \frac{\sinh\left\{\pi/k\left(\frac{2}{3}(x-1/24)\right)^{1/2}\right\}}{(x-1/24)^{1/2}}\right] \tag{4}$$

which gives practically the exact value for $p(E)$ after the consideration of the first terms. The leading term in eq.(4) $(A_1(E)=1)$ gives :

$$p(E) \approx \frac{1}{\sqrt{48}\,(E-1/24)} \exp\left\{\pi\sqrt{2(E-1/24)/3}\right\} \tag{5}$$

essentially the well known result [1], [3] . The number 1/24 is also included in some computations of the nuclear level density for this simple problem [7] .

After these first studies to deduce simple analytical representations for the nuclear level density, like relation (5), there has been little progress in this sense, although the mathematical methods of analytic number theory have experienced several important advances. In the next sections recent results for the level densities will be described. These results have been deduced using methods of the modern number theory.

THE PARTICLE-HOLE STATE DENSITY

The computation of the particle-hole state density $\mathcal{W}_{ph}(E)$ for a Fermi system with p particles and h holes for the equidistant spacing model is possible through the application of techniques used for the calculation of restricted partitions of integer numbers (the so-called "Ferrar graphs", see ref. [5]). One finds :

$$\frac{q^{ph}}{(q)_p\,(q)_h} = \sum_E \mathcal{W}_{ph}(E)\, q^E \qquad (6)$$

where $(q)_p = (1-q)(1-q^2)\ \ldots\ (1-q^p)$, which is symmetric on p and h .

From eq.(6) follows the exact recurrence relation :

$$\mathcal{W}_{ph}(m+p+h-1) - \mathcal{W}_{ph}(m+h-1) - \mathcal{W}_{ph}(m+p-1) + \mathcal{W}_{ph}(m-1) =$$

$$= \mathcal{W}_{p-1,h-1}(m)\ , \qquad m = 1,2,\ldots\ , \qquad (7)$$

And after the application of the saddle-point method to eq.(6), follows the relation :

$$\mathcal{W}_{ph}(E) \approx \frac{(E - A(p,h))^{p+h-1}}{p!\ h!\ \ (p+h-1)!} \qquad (8)$$

where

$$A(p,h) = ph - p(p+1)/4 - h(h+1)/4 \qquad (9)$$

which is symmetric also in p and h like the exact $\mathcal{W}_{ph}(E)$. Relation (9) differs from the result of Williams [8] :

$$A(p,h) = (p^2+h^2)/4 + (p-h)/2 - h/2 \qquad (10)$$

which is only valid for p = h .

The result given by eqs.(8) and (9) agrees also with the first term of the exact analytic expressions given in [9] for low p and h .

It can be proved also that :

$$\sum_p \frac{q^{ph}}{(q)_p\,(q)_h} = \sum_{n=0}^{\infty} p(n)\, q^n \qquad (11)$$

for p(n) equal to the number of unrestricted partitions of n .

The calculations using the recurrence relation (7) are also in agreement with the combinatorial computations of Böhning [10] using :

$$\mathcal{W}_{ph}(E) = \sum_{m=0}^{E-ph} p(p,m)\; p(h,E-ph-m) \qquad (12)$$

The application of similar techniques to compute $\mathcal{W}_{ph}(E)$ for arbitrary energy spectra is under study.

NUCLEAR LEVEL DENSITY FORMULAE

The use of the methods of analytic number theory can be applied to obtain an asymptotic expression for the partition function which leads to a more rigorous and more general result for the nuclear level density. The partition function is expressed with the help of a Dirichlet series and the parameters given by the analytical properties of the series determine the asymptotic representation of the level density .

The starting point is the usual relation for the nuclear level density inclu ding pairing effects and obtained with help of the saddle point method [11] . The nuclear level density reads :

$$\rho(N_n,N_p,\mathcal{E}) = \frac{\exp(S)}{(2\pi)^{3/2}\,(\det|\partial^2\mu_i\mu_j S|)^{1/2}} \qquad (13)$$

where $\mathcal{E}$ is the total energy, $N_{n,p}$ is the number of neutrons (protons), $\mu_{n,p}$ are the Lagrange parameters for neutrons (protons), to be determined, S is the entropy and $\det|\partial^2 \mu_i \mu_j S|$ is a certain determinant.

The entropy is given by :

$$S = \ln Z(\mu_n, \mu_p, \beta) + \beta\mathcal{E} - \mu_n N_n - \mu_p N_p \qquad (14)$$

where $Z(\mu_n, \mu_p, \beta)$ is the partition function given by :

$$\ln Z = -\beta \sum_k (\varepsilon_k - \lambda - E_k) - \beta \frac{\Delta^2}{G} + 2 \sum_k \ln(1 + \exp(-\beta E_k)) \qquad (15)$$

The quasiparticle energies E_k are given in terms of the single-particle energies ε_k, the chemical potential λ and the energy gap Δ by :

$$E_k = \sqrt{(\varepsilon_k - \lambda)^2 + \Delta^2} \qquad (16)$$

G is related to Δ by the equation :

$$\frac{2}{G} = \sum_k \frac{1}{E_k} \operatorname{tgh}(\beta E_k/2) \qquad (17)$$

The saddle point equations are :

$$\partial_{\mu_n} \ln Z_n = N_n \ , \quad \partial_{\mu_p} \ln Z_p = N_p \ , \ - \partial_\beta \ln Z = \mathcal{E} \ , \qquad (18)$$

if $\ln Z = \ln Z_n + \ln Z_p$, from which it is possible to obtain :

$$S_{n,p} = 2 \left(1 - \beta \partial_\beta \sum_k \ln(1 + \exp(-\beta E_k)) \right)_{n,p} \qquad (19a)$$

$$\mathcal{E}_{n,p} = \sum_k \varepsilon_k \left(1 - \frac{\varepsilon_k - \lambda}{E_k} \operatorname{tgh}(\beta E_k/2)\right)_{n,p} - \frac{\Delta^2_{n,p}}{G} \ , \qquad (19b)$$

$$N_{n,p} = \sum_k \left(1 - \frac{\varepsilon_k - \lambda}{E_k} \operatorname{tgh}(\beta E_k/2)\right)_{n,p} \qquad (19c)$$

where the subscripts n,p denotes neutrons and protons respectively and $S = S_n + S_p$, $\mathcal{E} = \mathcal{E}_n + \mathcal{E}_p$.

To compute these expressions asymptotically it is useful to define the "quasiparticle partition function" :

$$\hat{Z}(\beta) = \prod_k (1 + \exp(-\beta E_k)) \qquad (20)$$

and rewrite :

$$S = 2\,(1 - \beta\partial_\beta)\,\ln \hat{Z}\,(\beta) \qquad (21)$$

The estimation of $\hat{Z}(\beta)$ goes as follows :
First $|\varepsilon_k - \lambda| = \hat{\varepsilon}_k$ are substituted by integral multiples of some energy unit $1/g$:

$$\hat{\varepsilon}_k = e_k/g \ , \quad \text{for } e_k \text{ positive integers} \qquad (22)$$

thus :

$$\ln \hat{Z} = \sum_n a_n \ln\left(1 + \exp\left(-\beta\sqrt{(n/g)^2 + \Delta^2}\right)\right) \qquad (23)$$

where :

a_n = degeneracy of $\hat{\varepsilon}_k$, if $n = e_k$ for some e_k

and

$a_n = 0$ otherwise

We apply the Mellin transformation [12] :

$$\exp\left(-\beta m\sqrt{((n/g)^2 + \Delta^2)}\right) = \frac{1}{2\pi i}\int_{c-i\infty}^{c+i\infty} dz\,\left(\frac{n}{g}\right)^{-z}\frac{\Delta}{\sqrt{\pi}}\left(\frac{2\Delta}{\beta m}\right)^{(z-1)/2} \qquad (24)$$

$$\cdot\ \left(\frac{z}{2}\right) K_{(z+1)/2}\,(\Delta\beta m)$$

where $K_\nu(t)$ is a modified Bessel function of the second kind.
We define the Dirichlet series :

$$D(t) = \sum_n \frac{a_n}{n^t} \qquad (25)$$

Which will be assumed to be analytic except for simple real poles at the points $\alpha_0 > \alpha_1 > \ldots > \alpha_N > 0$ with residues A_0, A_1, etc. . And after some contour integrations it is possible to find [13]:

$$\ln Z = \sum_i A_i (1-2^{-\alpha_i}) \zeta(\alpha_i+1) \Gamma(\alpha_i) (\beta/g)^{-\alpha_i} + D(0) \ln Z + O(\beta^{-\alpha_{N+1}}) \tag{26}$$

where $\zeta(x)$ denotes the Riemann ζ-function .
And for the entropy at the saddle-point :

$$S = 2D(0)\ln 2 + \sum_i (1-2^{-\alpha_i}) \Gamma(\alpha_i+1) \zeta(1+\alpha_i) 2A_i (\beta/g)^{-\alpha_i} (1+\frac{1}{\alpha_i}) + O(\beta^{-\alpha_{N+1}}) \tag{27}$$

which leads after some algebra to :

$$S = \sum_j M_j(\alpha_i, A_i)\, E^{m_j(\alpha_i)} \quad , \quad m_j > m_{j+1} \tag{28}$$

This is a descending series of the excitation energy $E = \mathcal{E} - \mathcal{E}_0 - \delta P$ ($\mathcal{E}_0$ is the ground state energy and δP is a correction for pairing and shell effects). The coefficients $M_j(\alpha_i, A_i)$ and the exponents $m_j(\alpha_i)$ are given by the Lagrange equations for $\mathcal{E}$ and for N. The leading term is of the form :

$$2^{\frac{1}{1+\alpha_0}} (1+\frac{1}{\alpha_0}) \left((1-2^{-\alpha_0}) \zeta(1+\alpha_0) \Gamma(1+\alpha_0) A_0 \right)^{\frac{1}{1+\alpha_0}} E^{\frac{\alpha_0}{1+\alpha_0}} \tag{29}$$

With equation (28) we have thus an explicit analytic expression for the entropy which shows how the relevant characteristics of the discrete single particle spectrum determines the nuclear level density for large excitation energies.
This formalism can be directly applied if the single particle energies have an explicit analytical expression . We show below several examples without the inclusion of pairing effects .

Constant single-particle level density.

In this case the Dirichlet series reads :

$$D(s) = \frac{1}{2}\left(\zeta(s,x) + \zeta(s,1-x)\right), \text{for } 0<x\leq 1/2 \qquad (30)$$

where $\zeta(s,x)$ is the generalized Riemann ζ-function. This series leads to :

$$\rho(E) = g\left(\frac{g^2}{g_n\, g_p}\right)^{1/2} \frac{6^{1/4}}{12} \frac{\exp(\pi\sqrt{2gE/3})}{(gE)^{5/4}} \qquad (31)$$

which is the well known [1] Bethe-formula for the nuclear level density with $g = g_n + g_p$. In this case $M(\alpha,A)$ is $\pi\sqrt{2g/3}$ and $m(\alpha)$ is 1/2 .

Constant single particle level density with constant degeneracy e .

For this example :

$$D(s) = \frac{1}{2}\, e\left(\zeta(s,x) + \zeta(s,1-x)\right), \text{for } 0<x\leq 1/2 \qquad (32)$$

This series leads to the entropy :

$$S = \pi\sqrt{\frac{2e}{3}\left(E - \frac{1}{24}e + \frac{1}{2}\, ex(1-x)\right)} \qquad (33)$$

which is in complete agreement with the result of Rosenzweig [14] . In Fig.1. one can see the effect of the filling of the last energy level on the entropy.

Periodic single-particle spectra.

The Dirichlet series is given now by :

$$D(s) = \sum_{l=1}^{e} \left(\zeta(s,x_o+m(l)) + \zeta(s,1-x_o+m(l))\right) \qquad (34)$$

The single-particle energies are given by (see ref. [15]):

$$\varepsilon_k = k + m(l), \quad \sum_{l=1}^{e} m(l) = 0 \quad , \; k=0,1,\ldots, \; l=1,2,\ldots,e \qquad (35)$$

And the entropy is :

$$S = \pi\left\{\frac{2e}{3}\left(E - \frac{1}{24}e + \frac{1}{2}\, xe(1-x) + \sum_{l=1}^{n} m(l) + \frac{1}{2}\sum_{l=1}^{e} m^2(l)\right)\right\}^{1/2}, \qquad (36)$$

which is in agreement with ref. [15] .

Harmonic Oscillator.

The Dirichlet series depend now also on the chemical potential μ :

$$D(s) = \frac{2}{(\hbar\omega)^s} \left(\zeta(s-2,1/2) + \left(\frac{\mu^2}{(\hbar\omega)^2} - \frac{1}{4}\right)\zeta(s,1/2)\right), \quad (37)$$

for the single particle energies $\varepsilon_k = (k + 3/2)\hbar$, $k=0,1,\ldots$

For the entropy we have :

$$S = \left[\frac{\pi^2}{6}\left((3N)^{2/3}+\frac{1}{4}\right)\right)\left(E+\varepsilon_{shell}-\frac{13}{960}\right)\right]^{1/2}\left(1+\frac{7}{5}\left((3N)^{2/3}+\frac{1}{4}\right)^{-1}\cdot\right.$$

$$\left.\cdot\left(E + \varepsilon_{shell}-\frac{13}{960}\right)\right) \quad (38)$$

where

$$\varepsilon_{shell}=\frac{1}{24}(3N)^{2/3}(-1 + 12x(1-x)) \quad (39)$$

and

$$\varepsilon = E + \tilde{\varepsilon}_0 + \varepsilon_{shell} \quad (40)$$

with:

$$\tilde{\varepsilon}_0 = \frac{1}{4}(3N)^{4/3} + \frac{1}{8}(3N)^{2/3} \quad (41)$$

These last two equations are in agreement with the results of [16] .

The consideration of a harmonic oscillator potential with the inclusion of deformation is also possible. In general , it is possible to deduce explicit analytic expressions for every algebraic representation of the single-particle energy levels.

THE SHELL CORRECTION METHOD

The mathematical treatment applied in the preceding section provides also a method to study the closely related Strutinsky calculations for ground state shell corrections [17] .

The effect of the shell structure on the potential energy surface is expressed usually in the form :

$$\delta U = U - \tilde{U} \quad (42)$$

where U is the total single particle energy sum given by :

$$U = \int_{-\infty}^{\lambda} dy\ y g(y) \quad , \quad N = \int_{-\infty}^{\lambda} dy\ g(y) \tag{43}$$

with

$$g(y) = \frac{1}{2\pi i} \int_{-i}^{i} d\beta\ e^{\beta y}\ Z_o(\beta) \tag{44}$$

using the partition function:

$$Z_o(\beta) = \sum_k e^{-\beta \varepsilon_k} \tag{45}$$

The smoothed energy $\tilde{U}$ is determined by the system :

$$\tilde{U} = \int_{-\infty}^{\tilde{\lambda}} d\varepsilon\ \varepsilon\ \tilde{g}(\varepsilon) \quad , \quad N = \int_{-\infty}^{\tilde{\lambda}} d\varepsilon\ \tilde{g}(\varepsilon) \tag{46}$$

where $\tilde{g}(\varepsilon)$ is the smoothed level density function :

$$\tilde{g}(\varepsilon) = \frac{1}{\gamma} \sum_k \mathcal{C}_M\left(\frac{1}{\gamma}(\varepsilon - \varepsilon_k) \right) \tag{47}$$

defined by the energy-smoothing parameter γ and by the smearing functions :

$$\mathcal{C}_M(x) = P_M(x) W(x) \tag{48}$$

where $P_M(x)$ is a so-called curvature polynomial of M-th degree and $W(x)$ is a weight function .

To compute $\tilde{g}(\varepsilon)$ the partition function $Z_o(\beta)$ is estimated using the Mellin transformation :

$$e^{-\beta\varepsilon} = \frac{1}{2\pi i} \int_{c-i}^{c+i} ds (\beta\varepsilon)^{-s} \Gamma(s) \ , \ \mathrm{Re}\ \beta\varepsilon > 0 \ , \ c > 0$$

to find :

$$Z_o(\beta) = \sum_{j=1}^{n} B_j \Gamma(\lambda_j) \beta^{-\lambda_j} + D_o(0) + O(\beta^{-\lambda_n + 1}) \tag{49}$$

where :

$$D_o(s) = \sum_k \frac{b_k}{\varepsilon_k^s} \quad , \quad \varepsilon_k \neq \varepsilon_m \text{ for } k \neq m \tag{50}$$

b_k is the degeneracy of the level ε_k and we assume that $D_o(s)$ has only simple poles at $s = \lambda_j > \lambda_{j+1} > 0$ with residues B_j. We obtain in this way :

$$\tilde{g}(\varepsilon) = \sum_j B_j \varepsilon^{\lambda_j - 1} + D_o(0)\,\delta(\varepsilon) \qquad (51)$$

without the introduction of any parameters in addition to those defining the single-particle spectrum.
Thus, for the smoothed single-particle level density of a cubic box potential of side L, one finds :

$$\tilde{g}(\varepsilon) = \frac{\sqrt{\varepsilon}}{4\pi^2}\left(\frac{2mL^2}{\hbar^2}\right)^{3/2} - \frac{3}{8}\left(\frac{2mL^2}{\hbar^2}\right) + \frac{3}{8}\left(\frac{2mL^2}{\hbar^2}\right)^{1/2}\frac{1}{\sqrt{\varepsilon}} - \frac{1}{8}\delta(\varepsilon) \qquad (52)$$

which agrees with the result of reference [18] obtained using a semiclassical procedure.

Another example very easy to compute is the isotropic harmonic oscillator with a constant spin-orbit interaction with hamiltonian :

$$H = -\frac{\hbar^2}{2M}\nabla^2 + \frac{1}{2}M\omega^2 r^2 - k\hbar\omega\vec{l}\cdot\vec{\sigma} \qquad (53)$$

leading to:

$$\tilde{g}(\varepsilon) = \frac{(1-k^2)\,\varepsilon^2}{3(\hbar\omega)^3(1-k^2)^2} - \frac{k^3\varepsilon}{(\hbar\omega)^2(1-k^2)^2} + \frac{10k^4-9k^2-3}{12\hbar\omega(1-k^2)^2} + \frac{5k^3-2k^5}{12(1-k^2)^2}\,\delta(\varepsilon) \qquad (54)$$

which is also in agreement with the semiclassical calculation of the same quantity [19] .

CONCLUSIONS

From this paper it is possible to see that the methods of

the modern analytical number theory represent a very useful tool to study the nuclear level density and the possibility to represent it through simple analytical formulas. These formulas are of a more general nature than those normally used in the present literature.

Particularly, it is easy to see that the obtained asymptotic expression for the entropy (eq.(28)) will lead to more general relations than for the case of only one pole . But even for only one pole we obtain a more general expression than the usual Bethe formula. It must be stressed that the analytic properties of the Dirichlet series D(t) depend only on the structure of the quasiparticle spectra and that the knowledge of this would determine entirely the nuclear level density through the parameters appearing in eq.(28).

The usual assumptions of a continuous single particle level density were not required, representing thus another advantage of this method. Of special interest is the possibility to study through the analytic behaviour of D(t) very important contributions as those arising from the shell structure of the spectra and their expected disappearance for very high excitation energies.

The so-called a-parameter defined by:

$$a = S^2/4E \qquad (55)$$

can also be calculated in terms of the general characteristics of the single particle spectrum. Preliminary calculations using deformed single-particle potentials of the Nilsson type reproduce qualitatively the energy dependence of the a-parameter reported in references [20] , [21] and [22]. Figure 1 shows the results of reference [20] computed numerically for a single-component system having particle numbers 40 and 50 with a Nilsson spectrum. Figure 2 shows the parametrized energy dependence of the a-parameter of reference 21 for ^{210}Po and ^{232}U . Figure 3 shows the energy dependence of the a-parameter of the neutron channel (a_n) derived from an analysis of cross-sections for the reaction ^{206}Pb(α,f) from ref.[22] . It is clear that the observed energy dependence can be well reproduced by the expansion given by equation (28).

REFERENCES

1. H.A. Bethe, Phys.Rev. 50(1936) 332.
2. N. Bohr, Natur 137(1936) 1 .
3. C. van Lier, G.E. Uhlenbeck, Physica 4(1937) 531.
4. S. Goudsmit, Phys.Rev. 51(1937) 64.
5. C.E. Andrews, "The Theory of Partitions", Addison Wesley Publishing Co., Reading, Massachussetts (1976).
6. L. Euler, "De Partitione Numerorum", Novi Commentarii academiae scientiarum Petropolitanae, 3(1750) 125 .
7. K. Husimi, Proc.Phys.Math.Soc.Japan, 20(1938) 912.
8. F. Williams, Nucl.Phys. A166(1971) 231.
9. H. Gupta, A.E. Gwyther, J. Miller,"Tables of Partitions", University Press Cambridge(1962) .
10. M. Böhning, Nucl.Phys. A152(1970) 529.
11. M. Sano, S. Yamasaki, Progr. Theor. Phys. 29(1963) 397.
12. F. Oberhettinger,"Tables of Mellin Transforms", Springer Verlag, Berlin (1974).
13. A.M. Anzaldo Meneses, in Proceedings of the Conference on "Nuclear Data for Science and Technology"Antwerp(1982).
14. N. Rosenzweig, Phys.Rev. 108(1957) 817.
15. P.B. Kahn, N. Rosenzweig, Phys.Rev. 187(1969) 1193.
16. A. Bohr, B.R.Mottelson,"Nuclear Structure",vol.II. W.A. Benjamin, Inc.,Reading, Massachusetts (1975).
17. V.M. Strutinsky, F.A. Ivantjuk, Nucl.Phys. A255(1975) 405.
18. R.K. Bhaduri, C.K. Ross, Phys.Rev.Lett. 27(1971) 606.
19. B.K. Jennings, R.K. Bhaduri, M. Brack, Nucl.Phys. A253 (1975) 29.
20. A.V. Ignatyuk, Y.N. Shubin, Sov.Jour.Phys. 8(1969) 660.
21. M. Ploszajczak, M.E. Faber, Phys.Rev.C25(1982) 1538.
22. M.G. Itkis et al., Yad. Fiz. 16(1972) 1150.

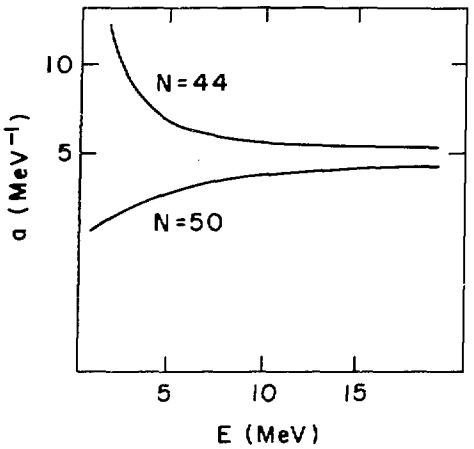

Fig. 1. This figure shows the energy dependence of the a-parameter for a single component system. From reference [20].

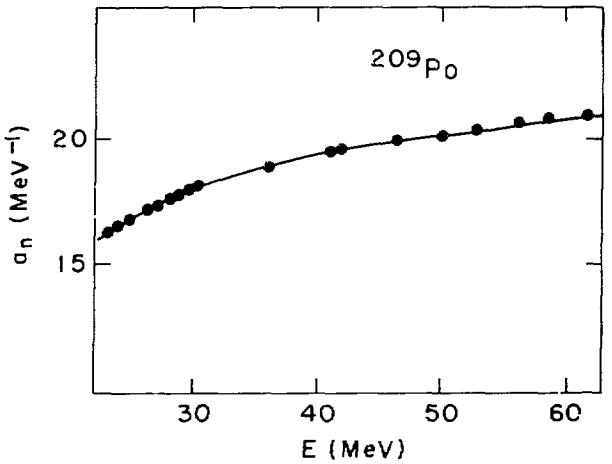

Fig. 3. Energy dependence of the a-parameter of the neutron channel (a_n) derived from an analysis of cross-sections for the reaction $^{206}Pb(\alpha,f)$. From reference [22].

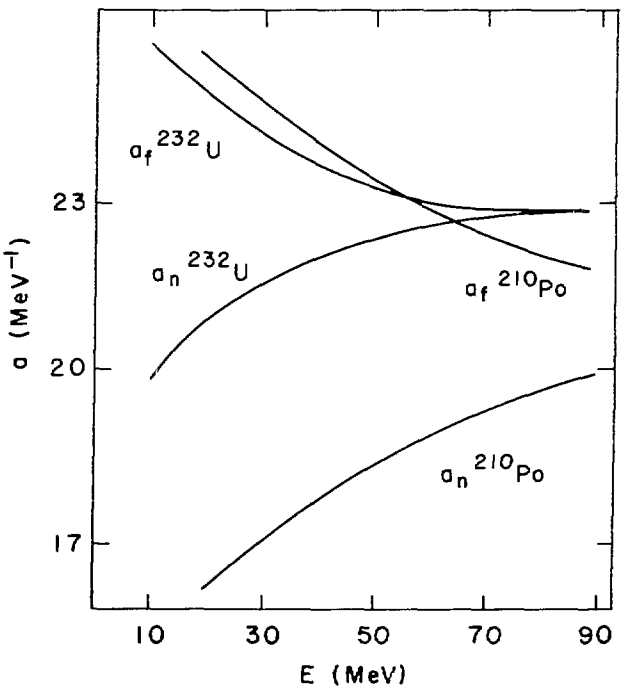

Fig. 2. In this figure a_f is the a-parameter at the fission saddle point deformation and a_n is the a-parameter at equilibrium. From reference [21].

EXACT CALCULATION OF LEVEL DENSITIES FOR NON INTERACTING MANY-FERMION SYSTEMS

C. JACQUEMIN

Division de Physique Théorique[+], Institut de Physique Nucléaire, F-91406 ORSAY

ABSTRACT

We have developed a recursive method to exactly calculate level densities of many fermion systems in large model spaces. A short review of the method is given.Some illustrative calculations are made for Calcium isotopes and lead 208. Results of saddle points approximation are compared to exact ones for Calcium isotopes.

The spectral distribution method which has been extensively studied for many years has proved to be very usefull for describing the statistical properties of many fermions systems [1] . However, in any application of the method it would be very usefull to distinguish between the physical approximations made through the choice of the model hamiltonian and the numerical ones made in the derivation of the state densities [2] . For non interacting fermions systems exact calculations have already been made [3] which involve a tedious one by one counting of configurations and are therefore strongly limited to small models spaces.

In this work we introduce a recursive method to exactly calculate states densities of non-interacting fermions. As it avoid any detailed counting it apply to large model space. Furthermore, in addition to the energy dependance of state densities with respect to excitation energy, its dependance with respect to total angular momentum, isospin, parity, number of particle-hole can be exactly calculated.

The one fermion space, denoted by $S(1)$, is made of ℓ subshells, and may contain particle and hole protons and neutrons states. The subshells are specified by their energies $\{(\varepsilon\nu)\nu = 1,\ldots, \ell\}$, angular momenta $\{(j\nu)\nu = 1,\ldots, \ell\}$, parities $\{(\pi\nu)\nu = 1,\ldots,\ell\}$, and isospins $\{(\tau\nu)\nu = 1,\ldots, \ell\}$. One also considers a complementary quantum number $\{(b\nu)\nu = 1,-,\ell\}$ to distinguish between hole subshells ($b\nu = -1$) and particle ones ($b\nu = +1$). A one-fermion state of $S(1)$ is completly specified by its angular momentum projection m and the subshell ν to which it belongs. Such a one fermion state is denoted by α and its various quantum numbers by $m(\alpha) = m$, $\varepsilon(\alpha) = \varepsilon\nu$, $J(\alpha) = J\nu$, ... and so on.

IPNO/TH 83-17

[+]Laboratoire associé au C.N.R.S

For scalar state densities the basic recursion relations write [4] :

$$\rho^{\alpha}(n,E) = \rho(n-1,E-\varepsilon(\alpha)) - \rho^{\alpha}(n-1,E-\varepsilon(\alpha))$$
$$n\rho(n,E) = \sum_{\alpha}\rho^{\alpha}(n,E) \qquad (1)$$

Here the scalar state density $\rho(n,E)$ is the number of n-fermions Slater determinant whose energy is E, $\rho^{\alpha}(n,E)$ is the number of those Slater determinants in which the one-fermion state α is occupied. The recursion relations (1) start with $\rho(1,E)$ which is known once $S(1)$ is specified and $\rho^{\alpha}(1,E) = \delta(E-\varepsilon(\alpha))$. These recursion relations are easily generalized to a set of one-body operators commuting two by two. For the operators H_0 and J_z for instance they write :

$$\rho^{\alpha}(n,E,M) = \rho(n-1,E-\varepsilon(\alpha),M-m(\alpha)) - \rho^{\alpha}(n-1,E-\varepsilon(\alpha),M-m(\alpha))$$
$$n\rho(n,E,M) = \sum_{\alpha}\rho^{\alpha}(n,E,M) \qquad (2)$$

From which the level density $\Omega(n,E,J)$ is then obtained by :

$$\rho^{\alpha}(n,E,J) = \rho(n,E,M=J) - \rho(n,E,M'=J+1) \qquad (3)$$

To calculate a fixed parity state density one writes it as a two dimensional vector whose upper component is the positive parity state density and lower component the negative parity one. The set of equations (1) then writes :

$$\vec{\rho}^{\alpha}(n,E) = P_{\alpha}\{\vec{\rho}(n-1,E-\varepsilon(\alpha)) - \vec{\rho}^{\alpha}(n-1,E-\varepsilon(\alpha))\}$$
$$\vec{\rho}(n,E) = n^{-1}\sum_{\alpha}\vec{\rho}^{\alpha}(n,E) \qquad (4)$$

Here P_{α} is a two by two matrixes which is equal to the unity matrix if $\pi(\alpha) = +1$ and to :

$$\begin{vmatrix} 0 & 1 \\ 1 & 0 \end{vmatrix} \qquad \text{if } \pi(\alpha) = -1.$$

The method shortly reviewed above has been applied to some calcium isotopes and to lead 208. The phenomenological one-fermion spaces which have been taken from Bohr-Mottelson [5], are displayed in Table 1.

For calcium isotopes one has calculated fixed J and parity level densities (Fig.1). One notice that the level density is alternatively dominated by its positive parity component and its negative one. This occurs for all J values and all Ca isotopes ($39 \leqslant A \leqslant 45$) and is due to the structure of the one fermion model space. Indeed the hole states (s,d shell) have a positive parity while the particle states (f,p shell) a negative one. As a result the 1p-1h, 2p-2h, 3p-3h, state which appears successively with excitation energy have negative parity, positive parity and so on.

Approximate scalar state densities $\tilde{\rho}(n,E)$ can be obtained by use of the saddle point approximation from which fixed J level densities $\tilde{\Omega}(n,E,J)$ are deduced by the spin cut-off formula :

$$\tilde{\Omega}(n,E,J) = \frac{\tilde{\rho}(n,E)}{\sigma(E)\sqrt{2\pi}} \left[e^{-\frac{J^2}{2\sigma^2(E)}} - e^{-\frac{(J+1)^2}{2\sigma^2(E)}} \right]$$

where the spin cut-off factor $\sigma(E)$ is the square root of the the fixed energy mean value of J_z^2. Comparison has been made (Fig.2) of these approximate densities [6] with the exactly calculated ones for calcium isotopes. The saddle point approximation systematically overevaluate scalar densities ; relative error which is more than 40% at 10 MeV decreases to less than 15% at 50 MeV. In addition to that the spin cut-off factor approximation overevaluate ($\approx$ 20%) the relative intensities of low J values and underevaluate (-10%) those of large J values (i.e. $J \geqslant 2\sigma(E)$).

For lead 208, one has carried out calculation of state densities with fixed parity and fixed number of neutron (protons) hole and particle (Fig.3). Comparing these results to those of Calcium isotopes one notice that (one particle- one hole states excepted) positive and negative parity densities have almost equal values. As for the calcium case this is due to the one fermion space structure but here, hole states and particle states have not a definite parity.

To conclude this short review of the proposed method let us say that the residual interaction may be approximately taken into account. The set of recursive equations 1 can be completed by similar equations relating k-body propagation functions $\rho^{\alpha_1,\ldots,\alpha_k}(n,E)$. These functions are used to calculate the moments of the residual interaction V over eigenstates of H_0 with eigen-energy E_0. Approximate level densities are then obtained as sums over E_0 of gaussian partial ones. Numerical calculations of such densities are one progress.

REFERENCES

1. J.B. FRENCH, Theory and Applications of Moments Methods in Many Fermions Systems, B.J DALTON, S.M. GRIMES, J.P. VARY, S.A. WILLIAMS, Plenum Press, N.Y..

2. H.A. BETHE, Phys. Rev. 50, 332 (1936).

3. M. WILLIAM and J.C. GROVER, Phys. Rev. 185, 4 (1969) 1303.

4. C. JACQUEMIN, Zeit. Phys. A290, 251 (1979).

5. A. BOHR and B.R. MOTTELSON, Nuclear Structure, Vol. 1 325, 328.

6. S.K. KATARIA, V.S. RAMAMURTHY and S.S. KAPOOR, Phys. Rev. C18, 549 (1978).
Private communication.

TABLE 1

One body model space and hamiltonian. For calcium 40 (col.1) neutron and proton spaces and hamiltonian are identical. The first three subshells (s, d shell) are hole ones the four last (f,p shell) are particle ones. For lead 208 neutron space (col.2) and proton space (col.3) are very differents. These model spaces deduced from experiment have been taken from ref.[5].

CALCIUM											
LEAD											
proton neutron			neutron holes			neutron particles			proton holes			proton particles		
d	$5/2^+$	0.0	p	$1/2^-$	1.7	g	$9/2^+$	1.6	s	$1/2^+$	2.4	h	$9/2^-$	1.7
s	$1/2^+$	3.0	f	$5/2^-$	2.3	i	$11/2^+$	2.5	d	$3/2^+$	2.8	f	$7/2^-$	2.7
d	$3/2^+$	5.6	p	$3/2^-$	2.6	d	$5/2^+$	3.2	h	$11/2^-$	3.8	i	$13/2^+$	3.5
f	$7/2^-$	13.0	i	$13/2^+$	3.3	j	$15/2^-$	3.3	d	$5/2^+$	4.1			
p	$3/2^-$	15.0	f	$7/2^-$	4.0	s	$1/2^+$	3.5	g	$7/2^+$	5.9			
p	$1/2^-$	17.2	h	$9/2^-$	5.1	g	$7/2^+$	4.0						
f	$5/2^-$	18.4				d	3/2	4.1						

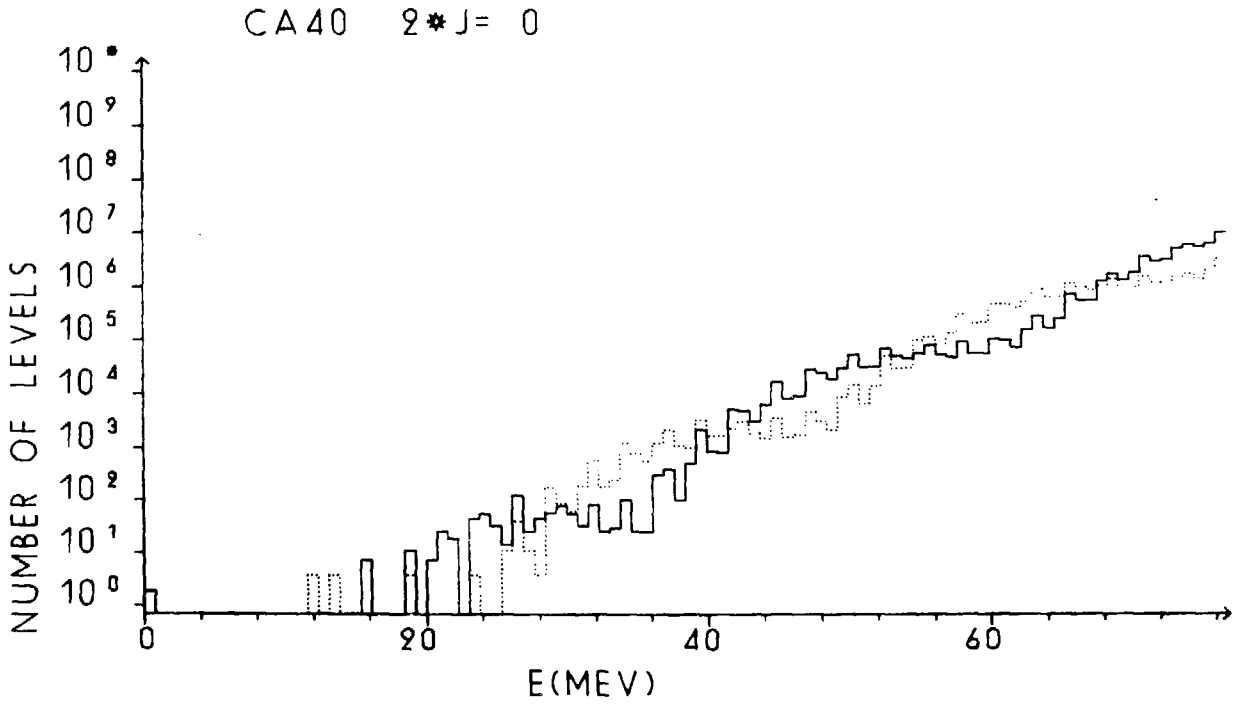

Figure 1 : Exactly calculated level density of Calcium 40 for J = 0. The continuous line is for positive parity states, dotted line for negative ones. The model one particle space and one-body hamiltonian are specified in Table 1 column 1. They have been taken identical for neutrons and protons.

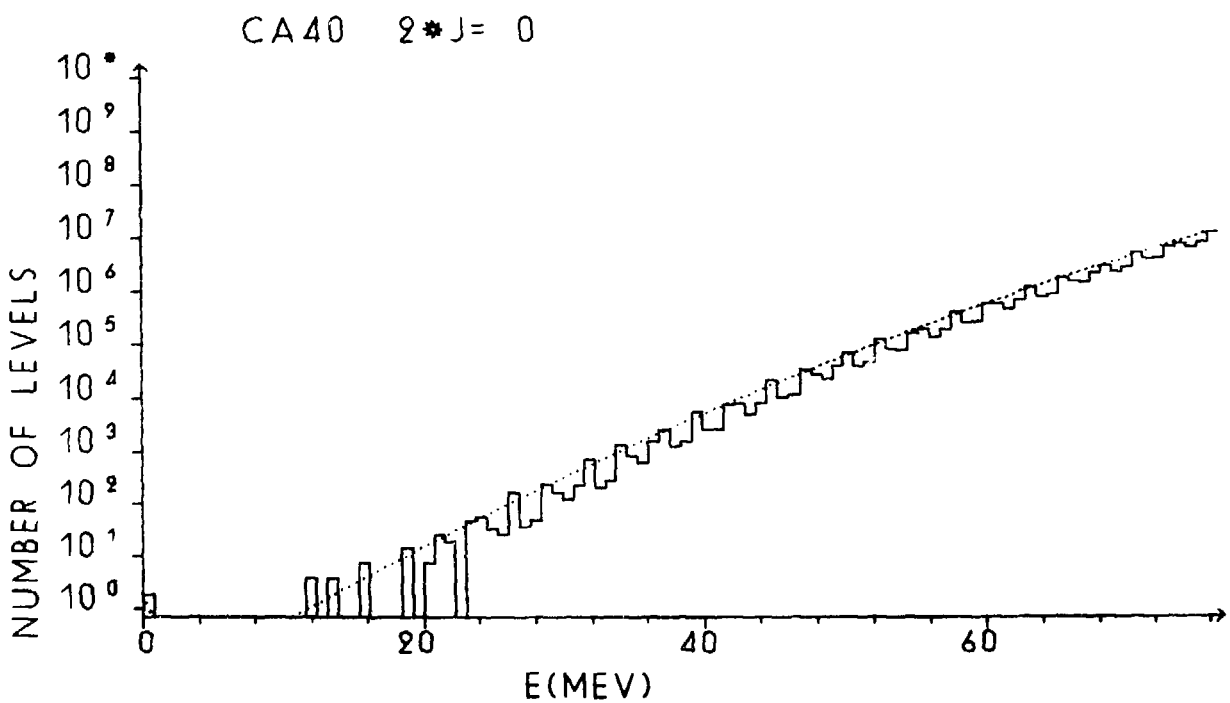

Figure 2 : Comparison of exactly and approximatly calculated level densities for Calcium 40 and J = 0. The continuous line is for exact calculation and the dotted line for approximated one. Approximate results are obtained by the use of the saddle point approximation to calculate the inverse Laplace transform of the grand-partition function, together with the use of spin cut-off factor approximation.

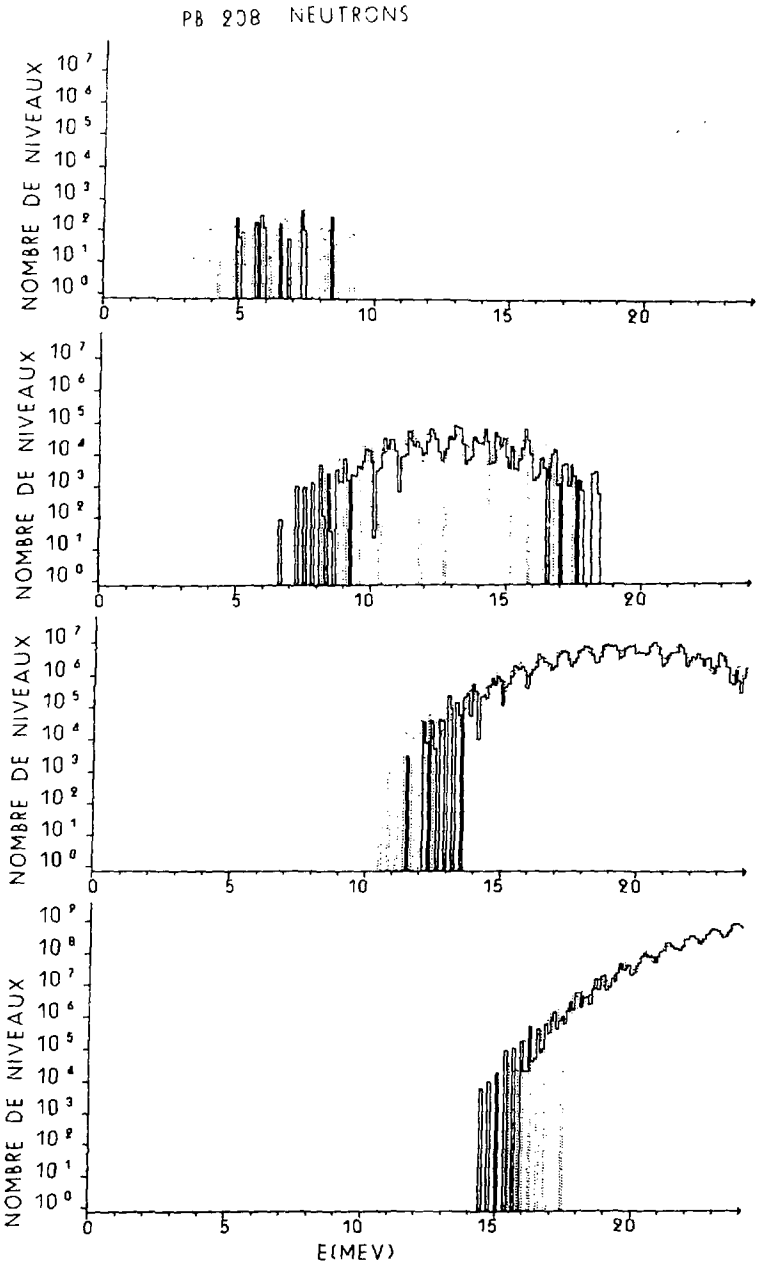

Figure 3 : Fixed parity, fixed number of particle-hole state densities for lead 208. From top to bottom are 1p-1h, 2p-2h, 3p-3h and 4p-4h. Exactly calculated partial state densities. The model one particle spaces an one-body hamiltonian are specified in Table 1 column 2 (neutrons) and column 3 (protons).

PARTICLE-HOLE STATE DENSITIES FOR PREEQUILIBRIUM REACTION CALCULATIONS AND FOR CLOSED AND OPEN CONFIGURATIONS

C. Kalbach

Triangle Universities Nuclear Laboratory
Physics Department
Duke University
Durham, North Carolina 27706, U.S.A.

ABSTRACT

The current status of simple state densities for fixed numbers of quasiparticle degrees of freedom is discussed. The state densities are derived for the case of equally spaced single particle states. Special emphasis is given to the case in which states with unbound particle degrees of freedom are differentiated from the remaining configurations. Some important details are discussed and open problems, particularly relating to deviations from the simple equi-spacing model, are considered.

I. INTRODUCTION

State densities for systems with fixed numbers of quasiparticle degrees of freedom play the same role in preequilibrium reaction calculations that total state densities play in compound nucleus (or equilibrium) reactions. They determine the relative phase space for emission into different exit channels and thus the relative yields of different types of particles and the energy distributions of the emitted particles.

But quasiparticle state densities do more. They also are used to describe the redistribution of the projectile's energy within the composite nucleus and the competition between particle emission and the residual interactions which accomplish the redistribution.

While quasiparticle (or particle-hole) state densities play a role similar to total state densities, so too they are beset with some of the same problems. For the sake of simplicity

in reaction calculations, the state density formulae are usually derived in a very simple model with a simple set of single particle states assuming particles (fermions) which are non-interacting. Then, almost as an afterthought, phenomena such as pairing interactions and shell structure must be introduced in some approximate way. In addition, there are other problems, such as taking the finite depth of the nuclear potential into account, which are peculiar to preequilibrium studies using particle-hole state densities.

The purpose of this talk is to review the state of quasiparticle state densities in their most commonly used form for preequilibrium reaction calculations and then to go on to discuss how these results are extended when it is necessary to differentiate between states which do and do not have unbound particle degrees of freedom or, to put it differently, between closed and open configurations. This differentiation is useful in certain calculations of angular distributions for particles emitted in the preequilibrium phase of a reaction. [1-3]

There are more realistic microscopic approaches to particle-hole state densities which can serve as guides for the simpler, more phenomenological models. They will, however, not be discussed in this paper which is restricted to state density formulae suitable for routine use in phenomenological preequilibrium reaction models.

II. QUASIPARTICLE STATE DENSITIES IN THE EQUI-SPACING MODEL

While a few calculations of particle-hole state densities have been done using a realistic set of single particle states (see e.g. [4-7]), by far the majority of calculations for use in preequilibrium reaction models are done using a set of equally spaced single particle states. This set, at least initially, is assumed to be infinitely deep. The rationale for using the equi-spacing model (or ESM) is that it is simple. For the most part the degrees of freedom in a real nucleus sample the single particle states in the neighborhood of the Fermi level, and the density of the single particle states in the equi-spacing model is supposed to represent an average of the density for realistic levels taken in the neighborhood of the Fermi level. Corrections to the state densities to account for both long and short range deviations from the ESM can be included later.

General Results

What we seek to calculate in quasiparticle state densities is the density of distinguishable configurations available to a particular nucleus at a fixed excitation energy and with fixed numbers of particle and hole degrees of freedom.

When the Pauli exclusion principle is neglected, the result can be arrived at using simple combinatorial techniques starting from the single particle state density by folding in additional degrees of freedom. The result is given by Ericson [8]. To include the Pauli principle requires much more sophistication. Williams [9] works from partition functions and uses the Cauchy residue theorem (rather than the saddle point method of integration). His result has the same basic form as Ericson's but contains the added correction function A(p,h) which includes the Pauli blocking effect. Williams' result for a single type of fermion is

$$\omega(p,h,E) = \frac{g^n \left(E-A(p,h)\right)^{n-1}}{p!\ h!\ (n-1)!}\ , \tag{1}$$

where n=p+h is the total number of degrees of freedom consisting of p particles and h holes. The quantity g is the single particle state density, and E is the excitation energy of the system. The exact form of A(p,h) used in calculations varies somewhat from group to group and is discussed below.

Williams also generalized his result to the case of two distinguishable types of fermions. Letting the subscripts π and ν denote protons and neutrons respectively, the result becomes

$$\omega(p_\pi,h_\pi,p_\nu,h_\nu,E) = \frac{g_\pi^{n_\pi}\ g_\nu^{n_\nu}\ \left(E-A(p_\pi,h_\pi,p_\nu,h_\nu)\right)^{n-1}}{p_\pi!\ h_\pi!\ p_\nu!\ h_\nu!\ (n-1)!} \tag{2}$$

Williams' work was extended by Běták and Dobeš [10] to include the limitations imposed by the finite depth of the nuclear potential. Equations (1) and (2) allow hole degrees of freedom to be arbitrarily deep. Eliminating those states which have holes deeper than the assumed well depth, V, produces the state density

$$\omega(p,h,E) = \frac{g^n}{p!\ h!\ (n-1)!} \sum_{j=0}^{h} (-1)^j \binom{h}{j}$$

$$\left(E-A_{0,j}(p,h)-jV\right)^{n-1}\ \Theta\left(E-A_{0,j}(p,h)-jV\right) \tag{3}$$

where $\Theta(E)$ is the Heaviside function which is zero for a negative argument and unity otherwise. The subscripts on the A function indicate the number of particle and hole degrees of freedom whose minimum energy is specified by some condition other than the exclusion principle. The form of Eq. (3) can be seen more clearly if it is expanded and the zeroth order term factored out. This gives

$$\omega(p,h,E) = \frac{g^n \left(E-A(p,h)\right)^{n-1}}{p!\ h!\ (n-1)!} \left[1 - h \left(\frac{E-V}{E}\right)^{n-1} \Theta(E-V) + \frac{h\ (h-1)}{2} \left(\frac{E-2V}{E}\right)^{n-1} \Theta(E-2V) \ \ldots \right] \tag{4}$$

Here the A's have been neglected in all but the leading term. The first term is the infinite well result, the second term subtracts those states which have a hole with excitation energy (measured relative to the Fermi surface) greater than V. But any states which have two such holes have been counted twice; those with three have been counted three times, and so on. This requires the extra terms. For convenience in further calculations Eq. (4) is rewritten as

$$\omega(p,h,E) = \frac{g^n \left(E-A(p,h)\right)^{n-1}}{p!\ h!\ (n-1)!} f(p) \ , \tag{5}$$

$$f(p) = \sum_{j=0}^{h} (-1)^j \binom{h}{j} \left(\frac{E-jV}{E}\right)^{n-1} \Theta(E-jV) \ . \tag{6}$$

Exactly the same correction function can be applied to Eq. (2) for the case of two types of fermions.

Densities of States Accessible in Residual Interactions

In preequilibrium models such as the exciton model it is generally recognized that the particle-hole states are not eigenstates of the system. While the main part of the nucleon-nucleon interaction is assumed to have gone into the potential well in which the single particle states exist, residual interactions will cause transitions from one particle-hole state to another. For energy conserving, two-body interactions the transitions which can occur involve either the creation or annihilation of a particle-hole pair (a third degree of freedom must be involved to conserve energy) or the exchange of energy between degrees of freedom leaving n unchanged. These types of interactions are denoted by the subscripts +, - and 0, respectively. Their rates are given by time-dependent perturbation theory and have the form

$$\lambda_+(p,h,E) = \frac{2\pi}{\hbar} M^2 \ \omega_+(p,h,E) \ , \tag{7}$$

where M is some appropriate average effective matrix element and ω_+ is the average number of final states accessible to an initial state specified by p, h and E in a pair creation interaction. Thus for many reaction calculations it is crucial to have the densities of accessible final states ω_+ and ω_-.

The scattering interactions in the one fermion model are not important because they leave the system in the same class of states, but in the model with two types of fermions they can lead to the transformation of a proton particle-hole pair into a neutron pair.

These densities of accessible final states (or transition state densities, as they are also called) have evolved in the same way as the full particle-hole state densities. The first results [11] were for an infinite well and did not include the effects of Pauli blocking. Later Dobeš and Běták [12] derived both exact (relatively intractible) results and approximate results which include Pauli blocking. They used the Darwin-Fowler method of statistical mechanics. Similar results can be obtained by combinatorial methods starting from the full state densities. The results vary in detail but have the same basic form. The results corresponding to the results for closed and open configurations to be considered later are

$$\omega_+(p,h,E) = \frac{g^3}{2(n+1)} \frac{\left(E-A(p+1,h+1)\right)^{n+1}}{\left(E-A(p,h)\right)^{n-1}} \tag{8}$$

$$\omega_0(p,h,E) = \frac{g^2 \left(E-A(p,h)\right)}{2n} \left\{p(p-1)+4ph+h(h-1)\right\} \tag{9}$$

$$\omega_-(p,h,E) = \frac{g\ ph(n-2)}{2} \tag{10}$$

The results of Dobeš and Běták [12] and of Obložinský *et al* [13] differ in that they replace $A(p+1,h+1)$ in ω_+ with $A(p,h)$ and add extra Pauli blocking corrections to each of the three equations For ω_0 each of the three terms in the sum has a slightly different correction function.

The results of Eqs. (8)-(10) can be easily generalized to the case of two types of fermions. The main difference is that there are separate rates for creation of proton and neutron particle-hole pairs and for annihilation of proton and neutron pairs. Further there is the possibility of converting a proton pair to a neutron pair or vice versa while leaving the exciton number n unchanged. The appropriate transition state densities are

$$\omega_{\pi+}(p_\pi,h_\pi,p_\nu,h_\nu,E) = \frac{g_\pi^2}{2(n+1)} \left(\frac{n_\pi\ g_\pi + 2n_\nu\ g_\nu}{n}\right) \frac{\left(E-A(p_\pi+1,h_\pi+1,p_\nu,h_\nu)\right)^{n+1}}{\left(E-A(p_\pi,h_\pi,p_\nu,h_\nu)\right)^{n-1}} \tag{11}$$

$$\omega_{\pi\nu}(p_\pi,h_\pi,p_\nu,h_\nu,E) = \frac{p_\pi\ h_\pi\ g_\nu^2}{n}\left(\frac{E-B(p_\pi,h_\pi,p_\nu,h_\nu)}{E-A(p_\pi,h_\pi,p_\nu,h_\nu)}\right)^{n-1}$$

$$\{2\left(E-B(p_\pi,h_\pi,p_\nu,h_\nu)\right)$$

$$+\ n\ \left|A(p_\pi,h_\pi,p_\nu,h_\nu)-A(p_\pi-1,h_\pi-1,p_\nu+1,h_\nu+1)\right|\} \qquad (12a)$$

$$B(p_\pi,h_\pi,p_\nu,h_\nu) =$$

$$\max\left(A(p_\pi,h_\pi,p_\nu,h_\nu),A(p_\pi-1,h_\pi-1,p_\nu+1,h_\nu+1)\right) \qquad (12b)$$

$$\omega_{\pi-}(p_\pi,h_\pi,p_\nu,h_\nu,E) = \frac{p_\pi\ h_\pi}{2}\left((n_\pi-2)g_\pi + 2n_\nu\ g_\nu\right) \qquad (13)$$

where the subscripts $\pi+$, $\pi\nu$ and $\pi-$ denote creation of a proton pair, transformation of a proton pair into a neutron pair and destruction of a proton pair.

Finite well depth corrections can be introduced into the transition state densities as well. This is commonly done by multiplying Eqs. (8)-(13) by the correction function, f, appropriate to the final class of states.

The Pauli Correction Function

The previous subsections have indicated the general form of the quasiparticle or particle-hole state densities. But, as has already been mentioned, there is some difference in the way in which the correction function A(p,h) is evaluated by different groups.

The first question is the location of the Fermi level. Williams [9] has taken the Fermi level to coincide with the last occupied single particle state in the ground state of the nucleus in question. This is illustrated in Fig. 1. The excitation energies (in units of 1/g) of the single particle states accessible by the particle degrees of freedom are then 1,2,3,4... while the energies for the hole degrees of freedom are 0,1,2,3... Williams' result for A(p,h) is then

$$A(p,h) = (p^2+h^2+p-3h)/4g \qquad (14)$$

This has the obvious disadvantage that it is not symmetric in particles and holes. On the other hand, Eq. (14) can be rewritten in terms of $E_{Pauli}(p,h)$, the minimum energy that the configuration must have in order to satisfy the requirements of the exclusion principle given by the sum of the excitation energies of the first p excited particle states and the first h excited hole states. This gives

$$A(p,h) = E_{Pauli}(p,h) - \{p(p+1)+h(h+1)\}/4g \ . \tag{15}$$

Thus the lack of symmetry between particles and holes in A(p,h) was in the Pauli energy. It is thus possible to move the Fermi level to its correct position half way between the last filled and first vacant single particle states in the ground state of the nucleus (see Fig. 1) and reevaluate the Pauli energy. This gives

$$A(p,h) = \frac{p^2+h^2}{2g} - \frac{p(p+1)+h(h+1)}{4g} \tag{16}$$

Each time a particle is emitted or absorbed by the system, the Fermi level must be moved accordingly.

The second question was discussed in [14]. Equation (16), and indeed all of the energy correction functions discussed so far have assumed that the number of particle degrees of freedom may be different from the number of hole degrees of freedom. Thus, typically, for a nucleon induced reaction the first states of the composite nucleus are p,h=2,1 states. These are loosely referred to as 2-particle, 1-hole states, yet it is clear that each time a particle is excited above the Fermi level a hole must be created below it. Thus, strictly speaking, the number of particles must be equal to the number of holes. The apparent discrepancy disappears when the need to differentiate between particles and particle degrees of freedom on the one hand and between holes and hole degrees of freedom on the other is recognized. When a nucleon projectile enters a nucleus, the Fermi level moves up. This leaves a hole just below it (see Fig. 2). The projectile indeed is a degree of freedom. It can give up excitation energy in a two-body interaction and still remain a particle. The hole cannot. It is fixed at the Fermi surface and is not a degree of freedom. It is, so to speak, passive. Yet it has an effect on the energy required for the configuration by the Pauli principle. Thus to properly calculate the Pauli energy for Eq. (15) it is necessary to define

$$p_m = \text{maximum}(p,h) \tag{17}$$

$$E_{Pauli} = p_m^2/g \tag{18}$$

with equal contributions to the Pauli energy coming from particles and holes. Thus the function A(p,h) becomes

$$A(p,h) = \frac{p_m^2}{g} - \frac{p(p+1)+h(h+1)}{4g} \tag{19}$$

with an analogous expression for systems with two types of

fermions [14].

The form of $A_{i,j}(p,h)$ is discussed in Section III.

While the effects considered here are not large, it is useful to think carefully about such details, particularly when attempting to derive quantities such as state densities for open and closed configurations from the full particle-hole state densities.

Numerical Results

In actually calculating particle-hole state densities in the equi-spacing model with an infinite well depth, the only adjustable parameter is the density of single particle states, g. When protons and neutrons are treated as indistinguishable, g is usually taken from the level density parameter $a=\pi^2 g/6$. Thus quite commonly the single particle state density used is

$$g = A/(13\ \text{MeV}) \tag{20}$$

which corresponds roughly to $a=A/(8\ \text{MeV})$. Sometimes g is taken from the Gilbert and Cameron [15] values for a. Similarly, for the distinguishable case Eq. (20) becomes

$$g_\pi = Z/(13\ \text{MeV}) \tag{21a}$$

$$g_\nu = N/(13\ \text{MeV}) \tag{21b}$$

When finite well depth corrections are included, the depth of the potential well is also needed. It is usually taken to be of the order of 38 to 40 MeV.

Figure 3 shows the dependence of the particle-hole state density on the number of particle and hole degrees of freedom. Calculations are shown using Eq. (1) both with $A(p,h)=0$ and with $A(p,h)$ given by Eq. (19). At low particle numbers the state density increases rapidly with the number of particle degrees of freedom due to the E^{n-1} dependence. Eventually, however, the factorials in the denominator cause the curve to turn over. Including the effects of the exclusion principle has little effect on the very simple states where there should be little blocking, but it drastically reduces the state densities for more complex states and causes a shift downward in the peak particle number. The peak in the curves in Fig. 3 represents the most probable configuration at equilibrium since all states should be populated with equal likelihood. It is designated by $p,h=\bar{p},\bar{h}$.

The corresponding transition state densities are shown in Fig. 4. The most important thing to notice is that they are such that they will tend to push the system toward the most probable equilibrium states. Pair creation is dominant for the simple states while pair destruction dominates for the most

complex states.

A test for the consistency of the full state density with the transition state densities is that they satisfy the steady state equilibrium condition

$$\omega(p,h,E)\ \omega_{+}(p,h,E) = \omega(p+1,h+1,E)\ \omega_{-}(p+1,h+1,E) \qquad (22)$$

This guarantees that if the system is at statistical equilibrium the residual interactions will not disturb that equilibrium. Equation (22) is satisfied by the state density expressions from Eqs. (1), (8) and (10). The same is true if the finite well depth corrections are included by replacing Eq. (1) with Eq. (5), multiplying Eq. (8) by $f(p+1,h+1)$ and Eq. (10) by $f(p-1,h-1)$.

Deviations from the Equi-Spacing Model

For particle-hole state densities, just as for total state densities, it is sometimes necessary to include such physical effects as pairing and shell structure in order to obtain suitable accuracy in reaction calculations.

With regard to the pairing interaction, the convention here as in evaporation calculations has been to subtract a pairing energy from the excitation energy. In the equilibrium case this is supposed to correct for the effect of the pairing interaction on the ground state of the nucleus, since the pairing effects are presumed to have washed out at the relatively high excitation energies typically encountered. This seems to be appropriate for the moderately complex states in the particle-hole scheme, but not for the very simple states populated in the early stages of a reaction. For the simple states Grimes [16,17] has proposed using a pairing correction determined from the number of unpaired nucleons in the state in question relative to the ground state of the nucleus. The difficulty is that most calculations are still done using state densities for one type of fermion whereas the preequilibrium pairing corrections should depend on how the excitons, or degrees of freedom, are distributed among protons and neutrons.

Extending Grimes' suggestion, the proton pairing energy may be found by taking the minimum number of unpaired protons in the particle-hole configuration (0, 1 or 2) and subtracting the number (0 or 1) in the ground state of the same nucleus. This number of extra unpaired nucleons is then multiplied by δ_{π}, the usual pairing shift appearing in, for instance, the Gilbert and Cameron [15] or Nemirovsky and Adumchuk [18] prescriptions. The preequilibrium proton pairing correction appropriate to the very simple, few-exciton states becomes

$$\Delta_\pi(p_\pi, h_\pi) = 0 \quad \text{for odd } Z$$
$$= 2\delta_\pi \quad \text{for even } Z \text{ and odd } p_{\pi m}$$
$$= 0 \quad \text{for even } Z \text{ and even } p_{\pi m} \tag{23}$$

and similarly for the neutron pairing correction. The utility of this prescription coupled with the usual equilibrium-type corrections for the more complex states is currently being tested in reaction model calculations. It is interesting to note, however, that the average of Eq. (23) over all possible p values gives the usual equilibrium pairing correction.

Inclusion of shell structure effects also requires the use of state densities for two types of fermions. A simple approach which has been checked against numerical calculations based on realistic sets of single particle states but is only now being compared with data in reaction calculations is the so-called shell-shifted equi-spacing model or S^2-ESM [14]. It is illustrated in Fig. 5. In this model the usual ESM state density expressions are employed, but the Pauli energy in the two-fermion-type counterpart of Eq. (15) is evaluated from the states in the S^2-ESM. The Fermi level is, of course, given its physical location relative to the shell gap. Additional shell corrections may be applied by using different g-values for proton particles, proton holes, neutron particles and neutron holes. These are obtained by averaging in the S^2-ESM scheme over a suitable energy interval.

Finally corrections to the single particle state density g for long range deviations from the ESM have occasionally been employed. Most frequently this involves using different g-values for particles and holes. These can be chosen assuming that the density of single particle states varies as the square root of their energy measured from the bottom of the well and using the average energies for particle and hole degrees of freedom as in Ref. [2]. Alternatively the effective single hole state density can be chosen so that there are A states between the bottom of the well and the Fermi level [10]. This gives $g_{hole}=A/V$. In this scheme the particle value is A/(14 MeV).

III. CLOSED AND OPEN CONFIGURATIONS

In calculating angular distributions for particles emitted in preequilibrium reactions it is often convenient to know how often the system passes through a series of particle-hole states all of which contain an unbound particle degree of freedom since under these conditions the angular distribution is expected to be forward peaked rather than symmetric about 90°. To do that calculation it is necessary to distinguish between those quasiparticle configurations which contain an unbound particle degree of freedom and those which do not.

Derivation of the Density of Unbound Particle-Hole States

The density of states containing an unbound particle (what will be loosely termed the density of unbound states) is most easily derived in the infinite well depth limit assuming that there can be no more than one unbound particle. It is then given by

$$\omega^{(u)}(p,h,E) = \int_{S+A(1,0)}^{E-A(p-1,h)} \omega(1,0,e)\ \omega(p-1,h,E-e)\ \Theta\{E-A(p-1,h)-e\}\ de \qquad (24)$$

where S is the energy mid-way between the last bound and first unbound single particle states, and S+A(1,0) is the minimum energy required for the state density $\omega(1,0,e)$.

In Eq. (24) the integrand is the density of states specified by p and h which has one particle degree of freedom at energy e. By integrating this from what is essentially S up to the maximum allowed energy, all unbound particles in this class of states are counted. If there are no states with two or more unbound particles, then the result is the density of unbound or open configurations. It has the form

$$\omega^{(u)}(p,h,E) = \frac{g^n\ \left(E-A_{1,0}(p,h)-S\right)^{n-1}}{(p-1)!\ h!\ (n-1)!}\ \Theta\left(E-A_{1,0}(p,h)-S\right) \qquad (25)$$

where it has been assumed that $A(1,0)+A(p-1,h)=A_{1,0}(p,h)$. Equation (25) looks like Eq. (1) for the full quasiparticle state density. There is a slight change in the Pauli blocking term, the excitation energy is reduced by the amount S, and p! has become (p-1)! because the unbound particle is now assumed to be distinguishable from the others.

When there can be more than one unbound particle (roughly speaking if E>2S) then the integral in Eq. (24) counts doubly unbound states twice and triply unbound states three times. The problem is almost identical with the correction for the finite potential well depth where states with holes below a certain depth were to be eliminated. Here states with particles above a certain height are to be counted. Mathematically the solutions have the same form so that the density of particle unbound states is no longer given by Eq. (25) but becomes

$$\omega^{(u)}(p,h,E) = \frac{g^n}{p!\ h!\ (n-1)!} \sum_{i=1}^{p} \sum_{j=0}^{h} (-1)^{i+j+1} \binom{p}{i} \binom{h}{j}$$

$$\left(E-A_{i,j}(p,h)-iS-jV\right)^{n-1}\ \Theta\left(E-A_{i,j}(p,h)-iS-jV\right) \qquad (26)$$

or, neglecting the A's in all but the leading term [19]

$$\omega^{(u)}(p,h,E) = \frac{g^n \left(E-A_{1,0}(p-1,h)-S\right)^{n-1}}{(p-1)!\ h!\ (n-1)!} f_1(p) \tag{27}$$

$$f_1(p) = \frac{1}{p} \sum_{i=1}^{p} \sum_{j=0}^{h} (-1)^{i+j+1} \binom{p}{i} \binom{h}{j} \left(\frac{E-iS-jV}{E-S}\right)^{n-1} \theta(E-iS-jV). \tag{28}$$

The quantity $\omega^{(u)}(p,h,E)$ contains all states specified by p and h that have at least one unbound particle degree of freedom.

The density of bound states (those that do not have an unbound particle degree of freedom even though E may be greater than S) are denoted $\omega^{(b)}(p,h,E)$ and are found by simple difference:

$$\omega^{(b)}(p,h,E) = \omega(p,h,E) - \omega^{(u)}(p,h,E). \tag{29}$$

Densities of States Accessible in Residual Interactions

As before, in order to do reaction calculations it is often necessary to have the transition state densities; the densities of states accessible in the residual two-body interactions. Now, however, instead of one hierarchy of states there are two, one for bound states and the other for unbound states. This is illustrated in Fig. 6. Thus instead of one transition state density for pair creation, there are four: $\omega_+^{(uu)}$, $\omega_+^{(ub)}$, $\omega_+^{(bu)}$, and $\omega_+^{(bb)}$. Here the first superscript denotes the bound or unbound character of the initial state and the second the character of the final state in the interaction. Similar considerations exist for exciton scattering and pair annihilation.

The procedure which has been used is to derive these transition state densities from the state densities for open and closed configurations ignoring the finite well depth corrections and corrections for multiple counting of multiply unbound states. The necessary state densities are given by Eqs. (1), (25), (29) and the analog of Eq. (25) for states with two or more unbound particles. This procedure, described in Ref. [2], yields the simplest results, to which correction functions can be applied.

The state density $\omega_+^{(uu)}(p,h,E)$ contains three distinct contributions: one from excitation by the unbound particle, one from excitation by one of the bound particles and one from excitation by a hole,

$$\omega^{(u)}(1,0,e)\ \omega(p-1,h,E-e) \rightarrow \omega^{(u)}(2,1,e)\ \omega(p-1,h,E-e)$$

$$\omega(1,0,e)\ \omega^{(u)}(p-1,h,E-e) \rightarrow \omega(2,1,e)\ \omega^{(u)}(p-1,h,E-e)$$

$$\omega(0,1,e)\ \omega^{(u)}(p,h-1,E-e) \rightarrow \omega(1,2,e)\ \omega^{(u)}(p,h-1,E-e)$$

If, however, $E>2S$ so that there can be multiply unbound states, then transitions of the type

$$\omega^{(u)}(1,0,e)\ \omega^{(u)}(p-1,h,E-e) \rightarrow \omega^{(u)}(2,1,e)\ \omega^{(u)}(p-1,h,E-e)$$

have been counted twice, once in each of the first two cases considered above. To remove this double counting of transitions, contributions from this fourth category need to be subtracted. The resulting transition state density then becomes

$$\omega_{+}^{(uu)}(p,h,E) = \frac{g^3}{2n(n+1)} \frac{1}{\left(E-A_{1,0}(p,h)-S\right)^{n-1}}$$

$$\left\{(n+1)\left(E-A_{1,0}(p+1,h+1)-S\right)^{n+1} - 2(p-1)\left(E-A_{2,0}(p+1,h+1)-2S\right)^{n+1}\right\}$$

$$= \frac{g^3}{2n(n+1)} \frac{(n+1)X_1^{n+1}(p+1) - 2(p-1)X_2^{n+1}(p+1)}{X_1^{n-1}(p)} \tag{30}$$

Here and in subsequent equations the notation

$$X_i(p) = \left(E - A_{i,0}(p,h) - iS\right)\ \Theta\left(E-A_{i,0}(p,h)-iS\right) \tag{31}$$

is employed. The subscript i denotes the number of unbound particles required in each energy term. The functions x_i used in Refs. [2] and [19] are related to the present functions by the relation $X_i(p) = x_{i+1}(p)$. In a similar way, the other transition state densities needed in preequilibrium calculations can be derived.

The results of Eq. (30) and the other necessary transition state densities do not yet contain corrections for the multiple counting of multiply unbound states in $\omega^{(u)}(p,h,E)$ and the similar corrections to $\omega^{(2u)}(p,h,E)$, the density of states with two or more unbound particles. Neither do they contain the finite well depth corrections.

Clearly it would be preferable from a theoretical viewpoint to derive all of the transition state densities using the more exact quasiparticle state densities of Eqs. (3), (26) and the analogous expression for states with two or more unbound particles (rather than Eqs. (1), (25) and their analog). This, however, has not yet been done. Instead, a procedure involving use of the correction functions f, f_1 and f_2 (the analog of f_1 for doubly unbound states) has been employed.

The method used in Ref. [2] was to correct the particle-

hole state densities for the initial states which appear in the denominators using the appropriate f functions. In the numerator the f function for the initial state was also applied as was a special correction function for the final state of the degrees of freedom involved in the interaction. In [19] a somewhat similar procedure was adopted, although for bound initial states populating unbound final states only the correction functions for the initial states were applied and for $\omega_+(bu)$ the finite well depth corrections were included in the limits of integration.

In the present report a different method is employed. As before the initial state densities appearing in the denominator are corrected with their appropriate f functions. The numerator of each integral contributing to a transition state density is, however, corrected by two f functions, one each for the initial and final states considered in that integral. Thus, for instance, the first three contributions to $\omega_+^{(uu)}$ are all corrected by the product $f_1(p)\cdot f_1(p+1)$ while the term which corrects for double counting of transitions is corrected by $f_2(p)\cdot f_2(p+1)$. This has the advantage that the resulting transition state densities satisfy a number of consistency conditions which were not met by the earlier results. This is discussed in more detail below.

The resulting corrected transition state densities for the transitions indicated by arrows in Fig. 6 are

$$\omega_+^{(uu)}(p,h,E) = \frac{g^3}{2n(n+1)} \frac{1}{X_1^{n-1}(p)\cdot f_1(p)} \Big[(n+1)X_1^{n+1}(p+1)\cdot f_1(p)\cdot f_1(p+1) - 2(p-1)X_2^{n+1}(p+1)\cdot f_2(p)\cdot f_2(p+1)\Big] \tag{32}$$

$$\begin{aligned}\omega_+^{(ub)}(p,h,E) = {} & \frac{g^3}{2n(n+1)} \frac{1}{X_1^{n-1}(p)\cdot f_1(p)} \Big[X_1^{n-1}(p)\cdot f_1(p)\cdot f(p+1)\cdot \\ & \{\tfrac{n^2}{2}[X_0(p+1)-X_1(p)]^2+\tfrac{n}{2}[X_0^2(p+1)-X_1^2(p)]+X_0(p+1)\cdot X_1(p)\} \\ & - 2X_1^{n+1}(p+1)\cdot f_1(p)\cdot f_1(p+1) \\ & - (p-1)X_2^{n-1}(p)\cdot f_2(p)\cdot f_1(p+1)\cdot \\ & \{\tfrac{n^2}{2}[X_1(p+1)-X_2(p)]^2+\tfrac{n}{2}[X_1^2(p+1)-X_2^2(p)]+X_1(p+1)\cdot X_2(p)\} \\ & + 2(p-1)X_2^{n+1}(p+1)\cdot f_2(p)\cdot f_2(p+1)\Big]\end{aligned} \tag{33}$$

$$\omega_+^{(bu)}(p,h,E) = \frac{g^3\ h}{2n(n+1)} \frac{1}{X_0^{n-1}(p)\cdot f(p) - pX_1^{n-1}(p)\cdot f_1(p)}$$

$$\left[X_1^{n+1}(p+1)\cdot f(p)\cdot f_1(p+1) - pX_2^{n+1}(p+1)\cdot f_1(p)\cdot f_2(p+1)\right] \tag{34}$$

$$\omega_+^{(bb)}(p,h,E) = \frac{g^3}{2n(n+1)} \frac{1}{X_0^{n-1}(p)\cdot f(p) - pX_1^{n-1}(p)\cdot f_1(p)}$$

$$\left[nX_0^{n+1}(p+1)\cdot f(p)\cdot f(p+1) - pX_1^{n-1}(p)\cdot f_1(p)\cdot f(p+1)\cdot \left\{\frac{n}{2}^2\left[X_0(p+1)-X_1(p)\right]^2+\frac{n}{2}\left[X_0^2(p+1)-X_1^2(p)\right]+X_0(p+1)\cdot X_1(p)\right\} - p(n-1)X_1^{n+1}(p+1)\cdot f_1(p)\cdot f_1(p+1) + p(p-1)X_2^{n-1}(p)\cdot f_2(p)\cdot f_1(p+1) \left\{\frac{n}{2}^2\left[X_1(p+1)-X_2(p)\right]^2+\frac{n}{2}\left[X_1^2(p+1)-X_2^2(p)\right]+X_1(p+1)\cdot X_2(p)\right\}\right] - \omega_+^{(bu)}(p,h,E) \tag{35}$$

$$\omega_0^{(ub)}(p,h,E) = \frac{g^2}{2n} \frac{1}{X_1^{n-1}(p)\cdot f_1(p)}$$

$$\left[(p+2h-1)X_1^{n-1}(p)\cdot f_1(p)\cdot f(p)\left\{nX_0(p)-(n-2)X_1(p)\right\} - 4(n-1)X_1^n(p)\cdot f_1^2(p) + 4(p-1)(n-2)X_2^n(p)\cdot f_2^2(p) - (p-1)(p+2h-2)X_2^{n-1}(p)\cdot f_2(p)\cdot f_1(p)\cdot \left\{nX_1(p)-(n-2)X_2(p)\right\}\right] \tag{36}$$

$$\omega_0^{(bu)}(p,h,E) = \frac{g^2}{2n} \frac{1}{X_0^{n-1}(p)\cdot f(p) - pX_1^{n-1}(p)\cdot f_1(p)}$$

$$\left[(p+2h-1)X_1^{n-1}(p)\cdot f_1(p)\cdot f(p)\left\{nX_0(p)-(n-2)X_1(p)\right\} - 4(n-1)X_1^n(p)\cdot f_1^2(p) + 4(p-1)(n-2)X_2^n(p)\cdot f_2^2(p) - (p-1)(p+2h-2)X_2^{n-1}(p)\cdot f_2(p)\cdot f_1(p) \left\{nX_1(p)-(n-2)X_2(p)\right\}\right] \tag{37}$$

$$\omega_-^{(uu)}(p,h,E) = \frac{g\ (p-1)h}{2} \frac{1}{X_1^{n-1}(p)\cdot f_1(p)}$$
$$\Big[(n-1)X_1^{n-1}(p)\cdot f_1(p)\cdot f_1(p-1)$$
$$- 2(p-2)X_2^{n-1}(p)\cdot f_2(p)\cdot f_2(p-1)\Big] \tag{38}$$

$$\omega_-^{(ub)}(p,h,E) = \frac{g\ h(h-1)}{2} \frac{1}{X_1^{n-1}(p)\cdot f_1(p)}$$
$$\Big[X_1^{n-1}(p)\cdot f_1(p)\cdot f(p-1)$$
$$- (p-1)X_2^{n-1}(p)\cdot f_2(p)\cdot f_1(p-1)\Big] \tag{39}$$

$$\omega_-^{(bu)}(p,h,E) = \frac{g\ p(p-1)h}{4} \frac{1}{X_0^{n-1}(p)\ f(p) - pX_1^{n-1}(p)\cdot f_1(p)}$$
$$\Big[X_1^{n-3}(p-1)\cdot f(p)\cdot f_1(p-1)\{(n-2)(n-3)X_1^2(p-1)$$
$$-2(n-1)(n-3)X_1(p-1)\cdot X_0(p)+(n-1)(n-2)X_0^2(p)\}$$
$$- 4X_1^{n-1}(p)\cdot f_1(p)\cdot f_1(p-1)$$
$$- (p-2)X_2^{n-3}(p-1)\cdot f_1(p)\cdot f_2(p-1)\{(n-2)(n-3)X_2^2(p-1)$$
$$-2(n-1)(n-3)X_2(p-1)\cdot X_1(p)+(n-1)(n-2)X_1^2(p)\}$$
$$+ 4(p-2)X_2^{n-1}(p)\cdot f_2(p)\cdot f_2(p-1)\Big] \tag{40}$$

$$\omega_-^{(bb)}(p,h,E) = \frac{g\ ph}{2} \frac{1}{X_0^{n-1}(p)\cdot f(p) - pX_1^{n-1}(p)\cdot f_1(p)}$$
$$\Big[(n-2)X_0^{n-1}(p)\cdot f(p)\cdot f(p-1)$$
$$- \{2(p-1)+(h-1)+(p-1)(n-3)\}X_1^{n-1}(p)\cdot f_1(p)\cdot f_1(p-1)$$
$$+ \{2(p-1)(p-2)+(p-1)(h-1)\}X_2^{n-1}(p)\cdot f_2(p)\cdot f_2(p-1)\Big]$$
$$- \omega_-^{(bu)}(p,h,E) \tag{41}$$

These results differ from those of Refs. [2] and [19] not only in the way that finite well depth corrections and corrections for multiple counting of multiply unbound states are made. They differ also in the way that the effects of multiply unbound states on the transitions are accounted for. Transitions to bound states are not possible in a single two-body interaction if the initial state has more than one unbound

particle. In the earlier papers this was accounted for by multiplying $\omega_+^{(ub)}$, $\omega_0^{(ub)}$ and $\omega_-^{(ub)}$ by the factor $1-m(p)$ where $m(p)$ is the fraction of the unbound initial states that have two or more unbound particles. The strength thus removed from these transitions was added back into the corresponding unbound-to-unbound transition state densities. In this work the correction is considered directly by requiring the initial state to have only one unbound particle. In addition, corrections for double counting of transitions were generally not included in the earlier papers. It is important to note, however, that in the limiting case of $E<V$ and $E<2S$ the present results do agree with the results of Ref. [19]. (In Ref. [2] the distinguishability of bound from unbound particle degrees of freedom was generally not recognized.

Consistency Checks

The present total and transition state densities for closed and open configurations, either with or without the f functions, satisfy a number of consistency criteria.

With respect to the steady state equilibrium condition there are now five relations which are satisfied. They are

$$\omega^{(u)}(p,h,E)\ \omega_+^{(uu)}(p,h,E) = \omega^{(u)}(p+1,h+1,E)\ \omega_-^{(uu)}(p+1,h+1,E) \tag{42}$$

$$\omega^{(u)}(p,h,E)\ \omega_+^{(ub)}(p,h,E) = \omega^{(b)}(p+1,h+1,E)\ \omega_-^{(bu)}(p+1,h+1,E) \tag{43}$$

$$\omega^{(b)}(p,h,E)\ \omega_+^{(bu)}(p,h,E) = \omega^{(u)}(p+1,h+1,E)\ \omega_-^{(ub)}(p+1,h+1,E) \tag{44}$$

$$\omega^{(b)}(p,h,E)\ \omega_+^{(bb)}(p,h,E) = \omega^{(b)}(p+1,h+1,E)\ \omega_-^{(bb)}(p+1,h+1,E) \tag{45}$$

$$\omega^{(u)}(p,h,E)\ \omega_0^{(ub)}(p,h,E) = \omega^{(b)}(p,h,E)\ \omega_0^{(bu)}(p+1,h+1) \tag{46}$$

In addition, if the original expressions for ω_+ and ω_- given in Section II indeed represent averages over bound and unbound states alike, then the following two conditions should be (and are) satisfied by the present results:

$$\omega(p,h,E)\ \omega_+(p,h,E) = \omega^{(u)}(p,h,E)\left[\omega_+^{(uu)}(p,h,E) + \omega_+^{(ub)}(p,h,E)\right] + \omega^{(b)}(p,h,E)\left[\omega_+^{(bu)}(p,h,E) + \omega_+^{(bb)}(p,h,E)\right] \tag{47}$$

and the analogous expression for pair destruction.

The Pauli Correction Function

In addition to the functions $A(p,h)$ discussed in Section II, it is also necessary to define the quantities $A_{i,j}(p,h)$ where i particles and j holes are considered to have their minimum energy requirements specified by some other criterion in addition to the Pauli exclusion principle and to therefore, in some sense, be distinguishable from the remaining particles and holes.

The work of Williams implies that the energy correction used in quasiparticle state densities can be divided into two parts. The first part (which is subtracted from the excitation energy) is the minimum energy required for the configuration. The second part includes a term of the type $p(p+1)/4g$ for each distinguishable type of degree of freedom. This second part is added back to the excitation energy.

The minimum energy required for a configuration with i unbound particles and j holes below the bottom of the potential well is

$$\frac{(p_m-i)^2 + i^2 + (p_m-j)^2 + j^2}{2g} + iS + jV$$

Here it is assumed that S is the excitation energy midway between the last bound and first unbound single particle states and that V is defined similarly. The i particles must occupy single particle states with energies $S+1/2g$, $S+3/2g$ $S+5/2g$ ... Taking the sum of the lowest i single particle states gives the minimum energy requirement for having i unbound particles. Similar considerations apply for the j holes below the bottom of the potential well. Recalling that the terms iS and jV are subtracted from the excitation energy directly, they should not be included in $A_{i,j}(p,h)$ which thus takes on the form

$$A_{i,j}(p,h) = \frac{(p_m-i)^2+i^2+(p_m-j)^2+j^2}{2g} - \frac{(p-i)(p-i+1)+i(i+1)+(h-j)(h-j+1)+j(j+1)}{4g}. \tag{48}$$

Numerical Results

Before performing calculations for systems in which unbound particle degrees of freedom are to be distinguished, a value of S must be chosen. For neutrons S should clearly be the separation or binding energy. For charged particles there is the ambiguity of whether or not to include the Coulomb barrier. If the equations of this section, derived for one distinguishable type of fermion, are used to describe a physical system with both protons and neutrons, then there is the question of whether to use the lowest of the neutron and proton values or, perhaps, an average. Fortunately all of these physically reasonable choices give very similar results for preequilibrium reaction energy spectra [2]. The value adopted in Ref. [2] is

$$S = \text{minimum}(B_n, B_p+C_p, B_\alpha+C_\alpha) \tag{49}$$

where the B's are binding energies and the C's are Coulomb barriers.

Figure 7 shows results for the density of states with at least one unbound particle compared with the full particle-hole state density. It can be seen that the proportion of the states which are unbound falls off dramatically as the number of degrees of freedom increases.

Figure 8 is taken from Ref. [19] and shows the rates for transitions between bound and unbound configurations. These are proportional to the corresponding transition state densities. While these latter are evaluated from expressions somewhat different from the ones given here, the qualitative trends are expected to be the same. As in Sect. II it is seen that pair creation dominates over pair destruction in the early stages of the reaction. In addition, a preference for unbound states to populate other unbound states in pair creation is also noticed.

As a further check on the validity of the present equations, results of calculations performed for a system with $gE=21.0$ and $gS=5.0$ have been compared with the results obtained by direct counting. Equations (5), (27), (32)-(41) and the analog of (27) for states with two or more unbound particles were used both with the approximate correction functions of Eqs. (6) and (28) (and the corresponding result for f_2) and with "exact" correction functions in which the appropriate $A_{i,j}$'s have been included in each energy term. A value of $gV>21.0$ was assumed. The results of this comparison are given in Table I.

It is interesting to note that while $\omega(2,1,21)$ and $\omega^{(2u)}(2,1,21)$ are essentially exactly reproduced, $\omega^{(u)}(2,1,21)$ is overestimated by 4 or 5%. This, in turn, causes a 30 to 35% underestimate in $\omega^{(b)}(2,1,21)$. A possible explanation is that the general state density formulae are most accurate when either none or all of the particle degrees of freedom are required to

be unbound. This is related to the fact that unbound particle degrees of freedom are not truly distinguishable from the other particle degrees of freedom in the same sense that particles and holes or proton and neutron degrees of freedom are distinguishable. In particular, in addition to counting doubly unbound states twice, Eq. (25) for $\omega^{(u)}(p,h,E)$ also counts states with two different unbound particles occupying the same single particle state (simply because of the way in which the Pauli blocking correction is made). Perhaps a better way to correct for double counting is to subtract all contributions to Eq. (25) which have a second particle with energy greater than S but where that second unbound particle is treated as indistinguishable from the other p-2 particles. This gives the density of states with one and only one unbound particle. To get the desired density of states with one *or more* unbound particles, the density of states with two or more must be added back in. This latter state density will have the same sort of correction as the density of unbound states itself whenever p>2. Thus the density of states with at least one unbound particle is

$$\omega^{(u)}(p,h,E) = \frac{g^n\left(E-A_{1,0}(p,h)-S\right)^{n-1}}{(p-1)!\ h!\ (n-1)!}\,\Theta\left(E-A_{1,0}(p,h)-S\right)$$

$$- \frac{g^n\left(E-A_{1,0}(p,h)-2S\right)^{n-1}}{(p-1)!\ h!\ (n-1)!}\,\Theta(\ldots) + \omega^{(2u)}(p,h,E) \qquad (50)$$

$$\omega^{(u)}(p,h,E) = \frac{g^n}{h!\ (n-1)!}\left[\sum_{i=1}^{p} \frac{\left(E-A_{i,0}(p,h)-iS\right)^{n-1}}{i!\ (p-i)!}\,\Theta(\ldots)\right.$$

$$\left. - \sum_{i=1}^{p-1} \frac{\left(E-A_{i,0}(p,h)-(i+1)S\right)^{n-1}}{i!\ (p-i)!}\,\Theta(\ldots)\right] \qquad (51)$$

which corresponds to Eq. (27) but with

$$f_1(p) = \frac{1}{p}\left[\sum_{i=1}^{p} \binom{p}{i}\left(\frac{E-A_{i,0}(p,h)-iS}{E-A_{1,0}(p,h)-S}\right)^{n-1}\Theta\left(E-A_{i,0}(p,h)-iS\right)\right.$$

$$\left. - \sum_{i=1}^{p-1} \binom{p}{i}\left(\frac{E-A_{i,0}(p,h)-(i+1)S}{E-A_{1,0}(p,h)-S}\right)^{n-1}\Theta(\ldots)\right] \qquad (52)$$

where the finite well depth corrections have been neglected and the Heaviside functions abbreviated. The f_2's are similar.

Using these new correction functions to recalculate the full quasiparticle state densities and the corresponding transition state densities produces the results shown in the last column of Table I. Now all of the quasiparticle state

densities for the p,h=2,1 states are essentially exactly reproduced.

In spite of the improvement in $\omega^{(u)}(p,h,E)$ resulting from using the improved correction for double counting of doubly unbound states, the corresponding transition state densities still show serious discrepancies with the direct counting results. The most obvious remaining difficulty is that the multiple counting corrections are applied only in an approximate way while the transition state densities frequently involve taking relatively small differences between large numbers so that any errors in making the corrections are greatly magnified. Clearly it would be advantageous to rederive the transition state densities using Eq. (51) for $\omega^{(u)}(p,h,E)$ as a starting point.

Deviations from the Equi-Spacing Model

Both the long and short range deviations from the equi-spacing model which were considered in Sect. II can also, at least in principle, be included here. The only one which has seriously been considered, however, is the use of different effective single particle state densities for different kinds of degrees of freedom. In Refs. [2] and [19] separate effective single particle state densities are defined for unbound particles, for other particle degrees of freedom and for hole degrees of freedom.

Pairing effects can presumably be handled as was suggested in Sect. II, except that the extra requirement of having an unbound particle may increase the minimum number of unpaired particles an unbound configuration may have (compared to the corresponding number for the full quasiparticle state density). This has not yet been investigated.

Inclusion of shell structure effects through the shell-shifted equi-spacing model as well as any reasonable inclusion of pairing corrections would require derivation of state densities analogous to those considered in this section but for two types of fermions. This has not yet been done.

IV. SUMMARY AND CONCLUSIONS

Simple expressions for the densities of states with fixed numbers of particle and hole degrees of freedom appropriate for use in preequilibrium reaction calculations have been reviewed. Full state densities as well as transition state densities have been considered, as have state densities for open and closed systems.

Derivations have all been based on the simple equi-spacing model for the single particle states. Within the context of this model the basic mathematical form for the state densities

considered are well understood, but many details need further study. In particular, transition state densities for bound and unbound configurations with more accurate corrections for multiple counting of multiply unbound states should be studied.

In terms of deviations from the simple ESM, work remains to be done to confirm and perhaps improve on the prescription for handling preequilibrium pairing corrections proposed by Grimes [16,17]. (In this connection please see also the contribution of C. Y. Fu to this conference.) Work to study the utility of making shell corrections in the context of the shell-shifted equi-spacing model is still in a relatively early stage and needs to be completed. The advisability of using different effective single particle state densities for particles and holes and perhaps, also, for bound and unbound particle degrees of freedom likewise needs investigation.

The question of angular momentum in particle-hole state densities for preequilibrium reaction calculations has not been addressed here but is considered, for example, in the contribution of H. Gruppelaar to this conference.

ACKNOWLEDGEMENTS

This work was supported under the auspices of the U. S. Department of Energy for Los Alamos National Laboratory. The author would like to acknowledge the hospitality of the Triangle Universities Nuclear Laboratory and the Duke University Physics Department. Without strength from the Lord Jesus Christ at a time of physical weakness, the author would have been unable to give this talk or to prepare this paper.

REFERENCES

1. C. KALBACH and F. M. MANN, "Phenomenology of Continuum Angular Distributions. I. Systematics and Parameterization," Phys. Rev. C, 23 112 (1981).

2. C. KALBACH, "Phenomenology of Continuum Angular Distributions. II. Griffin Preequilibrium Model," Phys. Rev. C, 23, 124 (1981).

3. H. FESHBACH, A. KERMAN and S. KOONIN, "The Statistical Theory of Multi-Step Compound and Direct Reactions," Ann. Phys. (N.Y.), 125, 429 (1980).

4. F. C. WILLIAMS, JR., A. MIGNEREY and M. BLANN, "Partial State Densities from Realistic Single-Particle States," Nucl. Phys., A207, 619 (1973).

5. K. ALBRECHT and M. BLANN, "Realistic Partial State Densities for Proton-Neutron Configurations in Nuclei Near Closed Shells," Phys. Rev. C, 8, 1481 (1973).

6. J. F. BERGER and M. MARTINOT, "Shell Effects on State Densities with Given Numbers of Excited Protons and Neutrons," Nucl. Phys., A226, 391 (1974).

7. S. M. GRIMES, J. D. ANDERSON, J. W. McCLURE, B. A. POHL and C. WONG, "(^{3}He,n) Reaction to the Continuum Near A=50," Phys. Rev. C, 5, 830 (1972), and "Odd-Even Effects in Pre-Equilibrium Processes," Phys. Rev. C, 7, 343 (1973).

8. T. ERICSON, "The Statistical Model and Nuclear Level Densities," Adv. Phys., 9, 425 (1960).

9. F. C. WILLIAMS, JR., "Particle-Hole State Density in the Uniform Spacing Model," Nucl. Phys., A166, 231 (1971).

10. E. BĚTÁK and J. DOBEŠ, "The Finite Depth of the Nuclear Potential Well in the Exciton Model of Preequilibrium Decay," Z. Phys. A, 279, 319 (1976).

11. F. C. WILLIAMS, JR., "Intermediate State Transition Rates in the Griffin Model," Phys. Lett., 31B, 184 (1970).

12. J. DOBEŠ and E. BĚTÁK, "A Statistical Derivation of the Density of Final States for the Exciton Model," Nucl. Phys., A272, 353 (1976).

13. P. OBLOŽINSKÝ, I. RIBANSKÝ and E. BĚTÁK, "Intermediate-State Transition Rates in the Exciton Model," Nucl. Phys., A226, 347 (1974).

14. C. KALBACH, "The Shell-Shifted Equi-Spacing Model for Particle-Hole State Densities," Nuov. Cim., 29A, 283 (1975).

15. A. GILBERT and A. G. W. CAMERON, "A Composite Nuclear-Level Density Formula with Shell Corrections," Can. J. Phys., 43, 1446 (1965).

16. S. M. GRIMES, J. D. ANDERSON, J. C. DAVIS and C. WONG, "Nonequilibrium Contributions to the ^{51}V(p,n)^{51}Cr Reaction for $18 \leq E_p \leq 26$ MeV," Phys. Rev. C, 8, 1770 (1973).

17. S. M. GRIMES, J. D. ANDERSON and C. WONG, "Odd-Even Effects in Pre-Equilibrium (p,n) Reactions," Phys. Rev. C, 13, 2224 (1976).

18. P. C. NEMIROVSKY and Y. V. ADUMCHUK, "Neutron and Proton Pair Interaction Energy," Nucl. Phys., 39, 551 (1962).

19. C. KALBACH, "Bound and Unbound Particles in Griffin Model State Densities," Phys. Rev. C, 24, 819 (1981).

TABLE I

Calculated Numbers of States
Compared with the Results of Direct Counting

Quantity	Direct Counting	Calculations		
		Approx. f's [a]	f's with A's	Revised f's with A's
$(1/g)\omega(2,1)$	90.	90.25	90.25	90.25
$(1/g)\omega^{(u)}(2,1)$	80.	83.3	84.8	80.25
$(1/g)\omega^{(b)}(2,1)$	10.	7.0	5.4	10.00
$(1/g)\omega^{(2u)}(2,1)$	20.	20.25	20.25	20.25
$(1/g)\omega_{+}^{(uu)}(1,0)$	80.	83.3	84.8	80.25
$(1/g)\omega_{+}^{(ub)}(1,0)$	10.	7.0	5.4	10.00
$(1/g)\omega_{+}^{(uu)}(2,1)$		14.5	15.3	17.7
$(1/g)\omega_{+}^{(ub)}(2,1)$	4.35	3.4	2.9	0.7
$(1/g)\omega_{+}^{(bu)}(2,1)$	16.6	22.8	31.0	20.4
$(1/g)\omega_{+}^{(bb)}(2,1)$	16.5	95.	112.	64.
$(1/g)\omega_{0}^{(ub)}(2,1)$	3.08	6.6	6.1	7.6
$(1/g)\omega_{o}^{(bu)}(2,1)$	24.7	52.	64.	41.
$(1/g)\omega_{-}^{(uu)}(2,1)$	1.	1.00	1.00	1.00
$(1/g)\omega_{-}^{(ub)}(2,1)$	0.	0.00	0.00	0.00
$(1/g)\omega_{-}^{(bu)}(2,1)$	1.	1.00	1.00	1.00
$(1/g)\omega_{-}^{(bb)}(2,1)$	0.	0.00	0.00	0.00

[a] A value of $gS'=5.5$ (the value corresponding to the first unbound single particle state) was used in evaluating f_1 and f_2 rather than the value of 5.0 which was used elsewhere in the calculations.

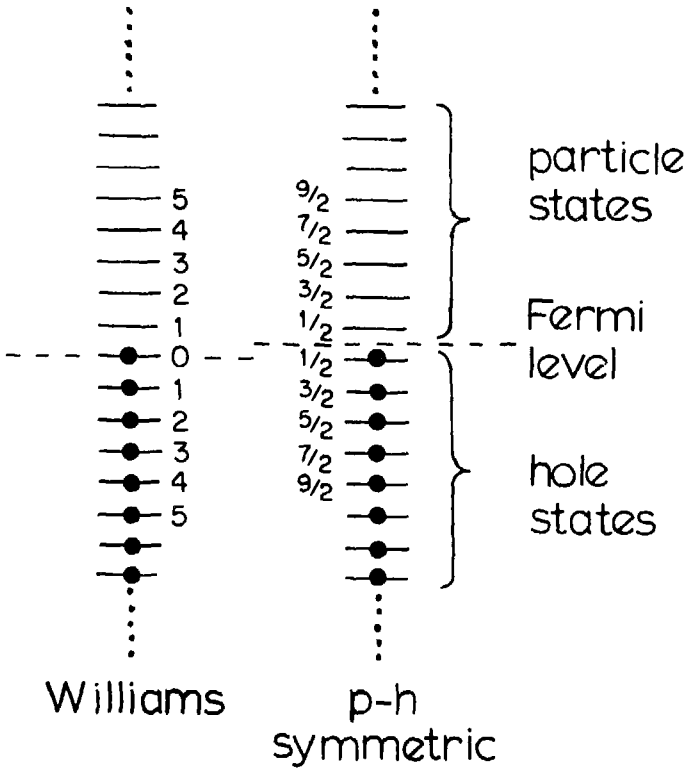

Fig. 1. Schematic diagram showing the placement of the Fermi level for calculations of particle-hole state densi-ties. The excitation energies of the single particle states available to the particle and hole degrees of freedom are also indicated.

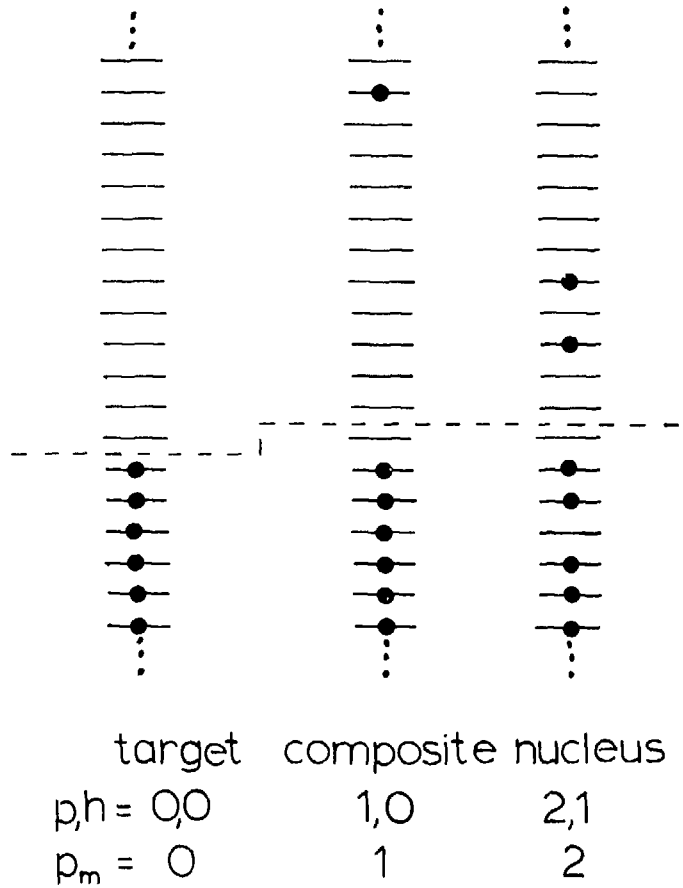

Fig. 2 Schematic diagram of the first stage of a nucleon induced reaction. The quantities p and h denote the numbers of particle and hole degrees of freedom while p_m is the number of particle-hole pairs relative to the ground state of the nucleus. The target nucleus is shown in its ground state, and the composite nucleus is shown both before and after the initial pair creation interaction.

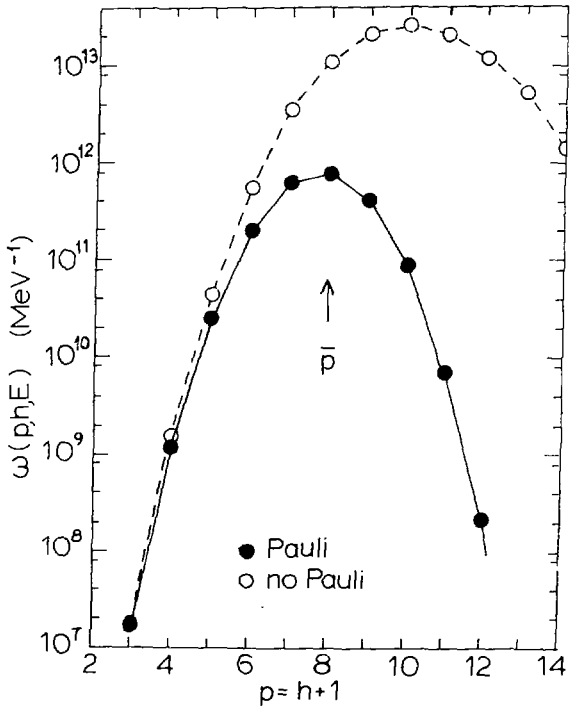

Fig. 3. Particle-hole state densities as a function of the number of particle (and hole) degrees of freedom for a ^{55}Co nucleus at an excitation energy of 43.3 MeV. At this energy finite well depth corrections are insignificant. A single particle state density of g=4.23/MeV was used.

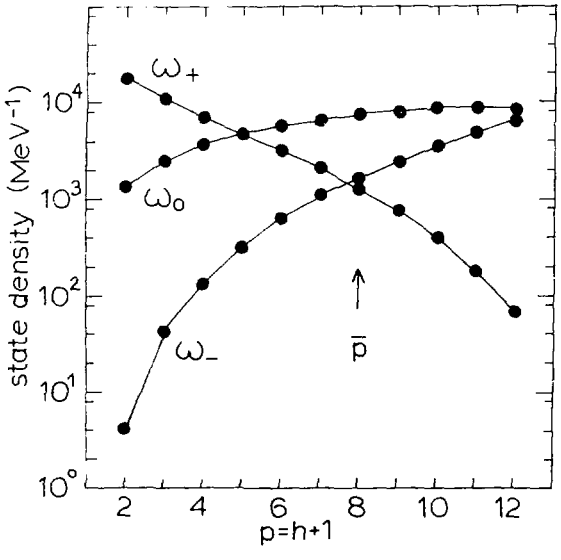

Fig. 4. Transition state densities as a function of the number of particle (and hole) degrees of freedom for a ^{55}Co nucleus at 43.3 MeV of excitation and g=4.23/MeV.

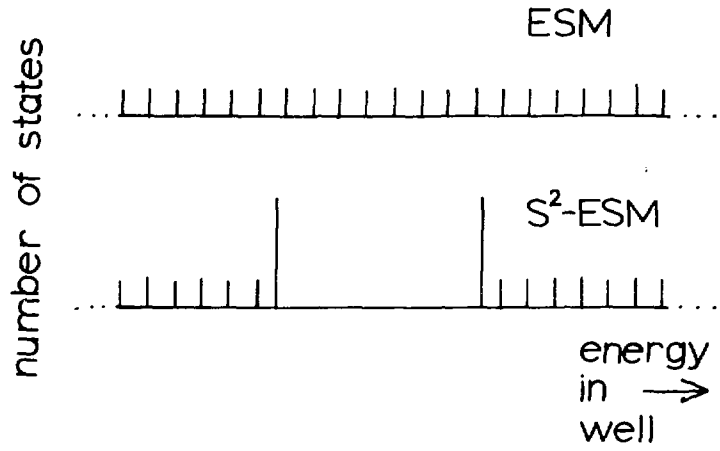

Figure 5. Single particle states for one type of fermion as a function of energy in the potential well for the equi-spacing and shell-shifted equi-spacing models.

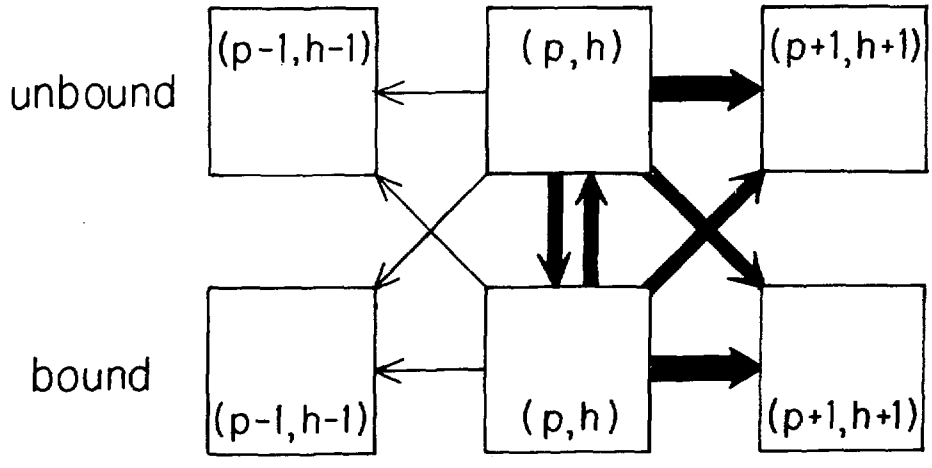

Figure 6. Schematic drawing of the two hierarchies of states one with and one without unbound particle degrees of freedom The arrows indicate the types of transitions which must be considered in preequilibrium reaction calculations.

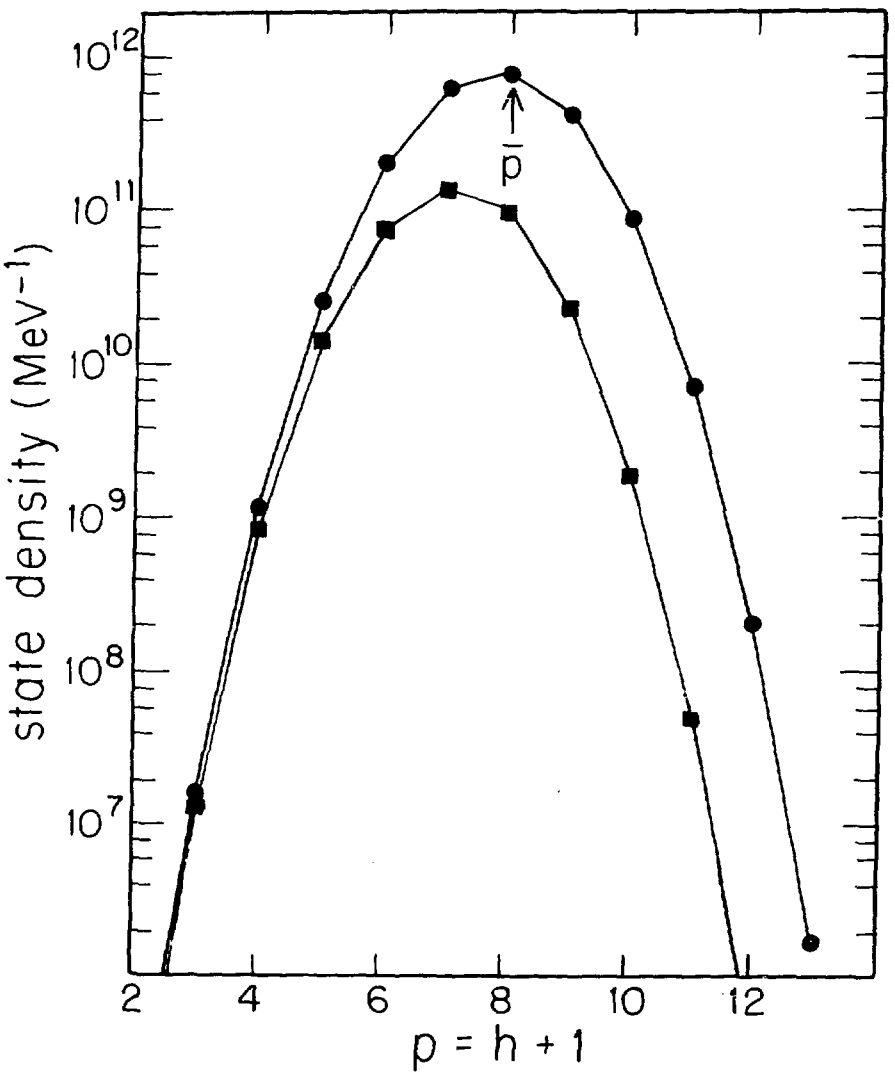

Figure 7. Particle-hole state densities for particle-unbound configurations compared to the full particle-hole state densities as a function of the number of particle (and hole) degrees of freedom. The calculations are for the system considered in Figure 3. The squares are for the unbound states.

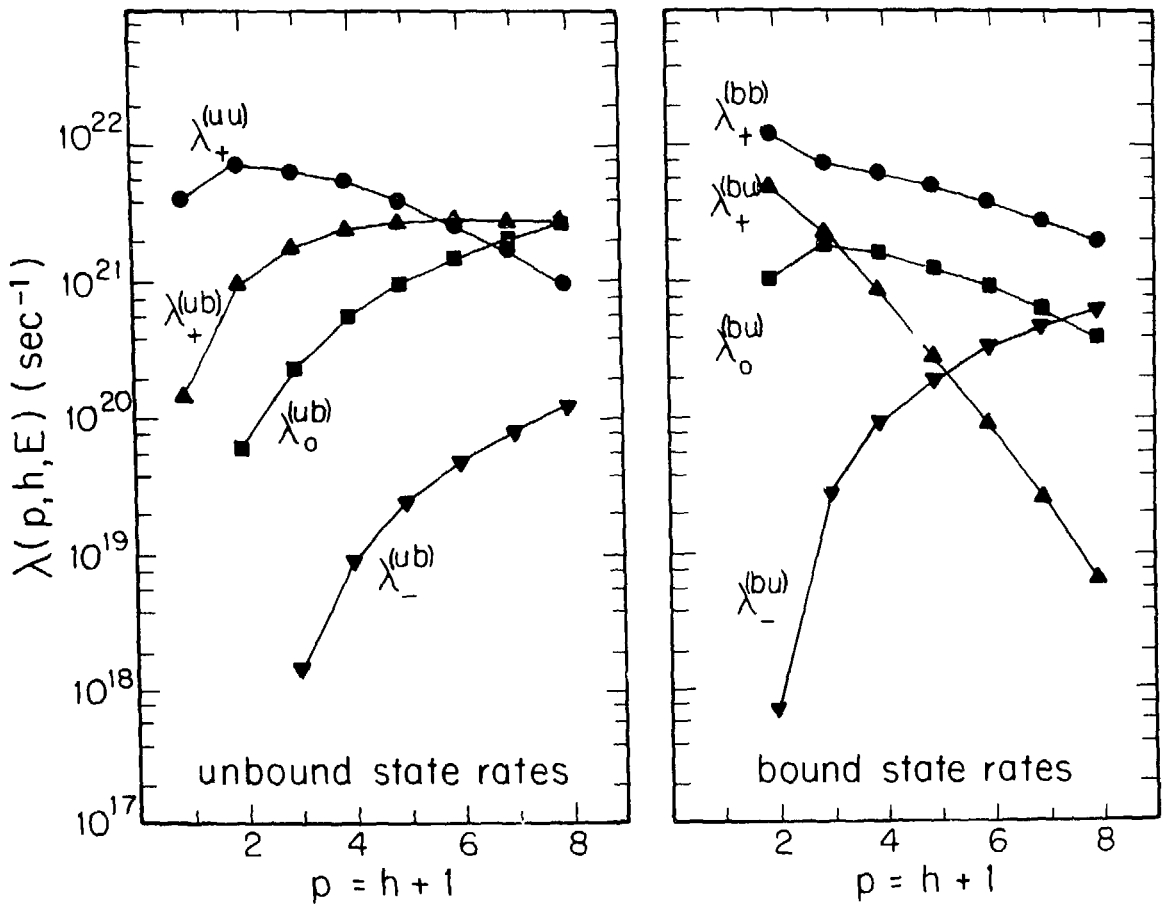

Figure 8. Residual two-body interaction rates as a function of the number of particle (and hole) degrees of freedom in the initial configuration. These rates are proportional to the corresponding average density of accessible final states. Calculations are for the system considered in Figures 3 and 4.

LEVEL DENSITY IN UNIFIED PREEQUILIBRIUM AND EQUILIBRIUM MODELS

H. Gruppelaar

Netherlands Energy Research Foundation ECN, P.O.Box 1,
1755 ZG Petten, The Netherlands

ABSTRACT

In this paper the use of phenomenological level-density formulas in statistical pre-equilibrium and equilibrium models is discussed with the aim to obtain a simple expression for insertion in a proposed "unified" model. A renormalized particle-hole level-density formula that is asymptotically equal to the backshifted Fermi-gas expression of Dilg et al. is suggested. Furthermore, the relations between various statistical models are discussed. It is shown that the Hauser-Feshbach, Weisskopf-Ewing and (pre-)equilibrium exciton models can be derived from the unified model mentioned before. However, some factors containing spin cut-off parameters remain. These problems are due to assumptions with regard to the spin distribution of the level density and the spin population during equilibration of the composite state.

INTRODUCTION

In statistical models for predicting nuclear cross sections phenomenological formulas are adopted for the description of the level density in the energy range where "discrete" level scheme information is not available or incomplete. The most commonly used level-density formulas in statistical Hauser-Feshbach (HF) model codes are based on those of Gilbert and Cameron [1] or Dilg et al. [2]. These formulas describe the *level density* as a function of excitation energy, spin and parity by means of a factorized expression:

$$\rho(E,J,\pi) = R(J)P(\pi)\rho_0(E) \tag{1}$$

with

$$R(J) = \frac{(2J+1)}{2\sigma^2} \exp\left[-\frac{(J+\frac{1}{2})^2}{2\sigma^2}\right], \tag{2}$$

where σ is the spin cut-off parameter; $P(\pi)$ is the parity distribution that is assumed to be 0.5 in this paper. The *state density* is given by

$$\omega(E) = \sum_{J,\pi} (2J+1)\rho(E,J,\pi) \approx \sqrt{2\pi}\ \sigma\ \rho_o(E). \tag{3}$$

In this paper we will frequently use the notation

$$\rho(E,J,\pi) = f(J,E)\omega(E), \tag{4}$$

where

$$f(J,E) = \frac{1}{\sigma\sqrt{2\pi}} R(J)P(\pi). \tag{5}$$

The energy dependence of f is due to the spin cut-off parameter σ.

At high energies the HF-model approaches the more simple Weisskopf-Ewing (WE) expression in which the state density† $\omega(E)$ occurs. In pre-equilibrium models the state density $\omega(n,E)$ is assumed to be a function of the exciton number n. In these models the formula of Williams [3] is usually adopted. When the exciton model is used to calculate the equilibrium part of the cross sections as well (PE model) it is required that

$$\sum_n \omega(n,E) = \omega(E). \tag{6}$$

Assuming that the system is in equilibrium before emission is possible it follows that the exciton model is equivalent to the WE model (provided that the spin cut-off factor is independent of energy).

Recently, there are some attempts (e.g.[4]) to include spin and parity conservation into the exciton model to obtain a "unified" model (UM). For these series of models it is required that the *level density of n excitons* satisfies the condition

$$\sum_n \rho(n,J,\pi,E) = \rho(J,\pi,E). \tag{7}$$

With these definitions the HF-, PE- and WE-models should follow as limiting cases of the unified model.

In this paper we first discuss some problems with regard to a satisfactory phenomenological expression for the n-dependent level density $\rho(n,J,\pi,E)$, for use in unified statistical-model codes. Next, we discuss the relation between the various models, mentioned before. This shows some difficulties, originating from the spin distribution of the level density. A summary of the discrepancies is given in the last section.

† In this paper we assume that the state density ω is used in the WE model, rather than the total level density ρ_o. The difference is irrelevant when the spin cut-off parameter is independent of energy.

LEVEL DENSITY IN HF MODELS

In the two most frequently used expressions [1,2] the level density is described by a Fermi-gas type of formula (at least at high energies), with an energy shift

$$U = E-\Delta \tag{8}$$

to account for odd-even effects. The expressions of Gilbert-Cameron (GC) and Dilg et al. (D) are denoted as

$$\omega_{GC}(U) = \frac{\sqrt{\pi}}{12} \frac{\exp 2\sqrt{aU}}{a^{1/4} U^{5/4}} \quad (U \geq U_x), \tag{9}$$

$$\omega_D(U) = \frac{\sqrt{\pi}}{12} \frac{\exp 2\sqrt{aU}}{a^{1/4} (U+t)^{5/4}}, \tag{10}$$

respectively. Eq.(9) is accompanied by a low-energy part that smoothly joins it at the dividing energy U_x. The nuclear temperature t in Eq.(10) satisfies the relation

$$U = at^2-t. \tag{11}$$

The main difference between GC and D arises from different expressions for the energy shift: in Eq.(9) Δ=P is taken as a tabulated pairing energy [1], in Eq.(10) Δ is assumed to be a fit parameter. In the two formulas there are additional fit parameters (only a in case of Eq.(10)) that are used to obtain agreement with the low-energy "discrete" level scheme and the level spacing of resolved (neutron) resonances. Therefore, there are at least two energies, e.g. $E = E_c$ (cut-off energy of discrete level scheme) and $E \approx B$ (neutron binding energy), where the two equations give almost the same level density.

We note that the expressions for the spin cut-off factor are also different in Refs.[1,2]:

$$\sigma^2_{GC}(E) = c\, a\, t\, A^{2/3} \quad (U \geq U_x), \tag{12}$$

where c = 0.0888 [1] or c = 0.146 [5], and

$$\sigma^2_D(E) = 0.01495\, t A^{5/3} \tag{13}$$

(assuming $I_{eff} = I_{rigid}$, r_o = 1.25 fm, see [2]).

At high energies these expressions converge to

$$\sigma^2_{GC}(E) \simeq c\sqrt{aU}\, A^{2/3}, \tag{14}$$

$$\sigma^2_D(E) \simeq 0.118\sqrt{aU}\, A^{2/3}, \tag{15}$$

where it has been assumed that a=0.1265 A MeV^{-1} (corresponding to g=A/13 MeV^{-1}, see Eqs.19,20). We conclude that Eqs.(14) and (15) are almost the same, apart from the uncertain numerical constants. At low energies ($U << U_x$) the value of GC for σ^2 is not well-defined. It has been proposed [6] to follow a linear function of energy to match the experimental spin distribution at low energies (near E_c) and the theoretical value at U_x-P.

The differences between the GC and D formulas may become quite large at high energies (E >> B) or in between E_c and B. This is illustrated in Table I. This might affect the computed cross sections significantly, see Table II.

STATE DENSITY IN EXCITON MODELS

The particle-hole state density of Williams [3] is given as

$$\omega(n,E) = g \frac{\{gU-A(p,h)\}^{p+h-1}}{p!h!(p+h-1)!} , \tag{16}$$

where n=p+h and A is a Pauli correction factor:

$$A(p,h) = (p^2+h^2+p-3h)/4. \tag{17}$$

Williams has shown [3] that the sum over all excitons is asymptotically equal to (cf. Table I)

$$\omega(E) = \sum_n \omega(n,E) \simeq \frac{1}{\sqrt{48}} \frac{\exp 2\sqrt{aU}}{U} , \tag{18}$$

where the relation between a and g is given by

$$a = \frac{\pi^2}{6} g. \tag{19}$$

As the numerical factors in front of Eqs.(9,10,18) are almost the same, the main differences occur in the denominators: $a^{1/4}U^{5/4}$, $a^{1/4}(U+t)^{5/4}$ and U, respectively.

In the application of Eq.(16) it is often assumed that

$$g = A/13 \ MeV^{-1}, \tag{20}$$

neglecting shell effects. However, this seems to be too rough at low excitation energies. Furthermore, a pairing energy correction (U=E-P) is frequently assumed, where P is taken from Ref.[1]. This leads to problems, in particular at low excitation energies, where Eq.(16) vanishes.

For these and other reasons we have suggested in Ref.[7] to require that the summed particle-hole level density agrees with the experimental level density. This is most easily accomplished by means of a renormalization of the Williams formula:

$$\omega_R(n,E) = \sqrt{\frac{\pi}{3}} \frac{U}{a^{1/4}(U+t)^{5/4}} \omega(n,E), \tag{21}$$

with the property that at high energies its sum over all n approaches the backshifted Fermi-gas formula, Eq.(10). The introduction of Eq.(21) into the exciton model hardly complicates the calculations [7]. It appeared (see Table I) that the parameters a and Δ of Dilg et al. are almost the same as those for this "renormalized Williams formula". We note that a renormalization to the Gilbert-Cameron formula is much more involved, at least at low energies.

LEVEL DENSITY IN UNIFIED MODELS

Introduction of the renormalized Williams' formula Eqs.(16,21) into a "unified" model satisfies condition (7). However, the spin distribution is also a function of n with the requirement

$$\rho(E,J,\pi) = \sum_n R(n,J)P(\pi)\rho_o(n,E)$$

$$\approx \sum_n f(n,J)\omega(n,E). \tag{22}$$

For the n-dependent spin cut-off factor it is assumed that (cf. [1])

$$\sigma^2(n) = n\langle m^2\rangle \simeq 0.24\ n\,A^{2/3}. \tag{23}$$

This is consistent with Eq.(12) when c=0.146. Recently, it has been found [8] that $\sigma^2(n) \approx 0.28\ nA^{2/3}$, based upon combinatorial calculations. We note that $\sigma^2(n)$ is independent of energy, in contrast with Eqs.(12-15). This is consistent with the definition of the equilibrium exciton number

$$\bar{n} = 1.09\ \sqrt{gE}. \tag{24}$$

However, the value of $\sigma^2(\bar{n})$ exceeds the value of $\sigma^2_{GC}(E)$. In order to account for pairing effects it seems better to *limit* the value of $\sigma^2(n)$ to the equilibrium value Eqs. (12-15). For instance, Eq. (12) should be used when n exceeds

$$\tilde{n} = 0.780\ \sqrt{gE}\ . \tag{25}$$

With this restriction and assuming that terms with $n \ll \tilde{n}$ give a negligible contribution, condition (22) is satisfied.

Also the pairing-energy correction is n-dependent. Again this could be a linear function of n at low values of n |4| with a saturation near equilibrium. When the renormalised Williams' formula Eq. (21) is used the energy shift Δ is a fit parameter. There seems no need to make this parameter n-dependent.

We summarize that the use of Eq. (21) combined with Eqs. (22,23) and a limitation on $\sigma^2(n)$ provides a useful formula for insertion into a unified model. A similar approach could be made based upon the Gilbert-Cameron formula, cf. Ref. |4|.

RELATION BETWEEN HF AND WE MODELS

The HF formula for continuum emission can be written as:

$$\sigma_{ab}(E,\varepsilon)d\varepsilon = \pi\lambda\!\!\!^{-2} \sum_{J\Pi} \frac{2J+1}{(2s+1)(2I+1)}$$

$$\frac{\sum_{\ell j} T^{a}_{\ell j}(E) \sum_{I'\ell'j'\pi'} T^{b}_{\ell' j'}(\varepsilon)\rho_b(I',\pi',E')d\varepsilon}{\sum_{I'b'\ell'j'\pi'} \int T^{b'}_{\ell' j'}(\varepsilon')\rho_{b'}(I',\pi',E')d\varepsilon'}, \qquad (26)$$

where:

a	= index of incoming particle with c.o.m. energy E,
b	= index of outgoing particle with c.o.m. energy ε,
J,Π	= spin and parity of compound state,
I	= spin of the target,
ℓ,j,s	= orbital angular momentum, channel spin and intrinsic spin of incident particle,
ℓ',j',s'	= same quantities for emitted particle(s),
E'	= residual energy of excited state after emission of particle b,
$T^{a}_{\ell j}(\varepsilon)$	= transmission coefficient of particle a with quantum numbers ℓ and j,
ρ_b	= level density in final nucleus reached by particle b.

The summation in Eq. (26) is restricted by spin- and parity conservation laws. In the denominator a summation is made over all outgoing particles b'. Eq.(26) can be reduced to the more simple WE-expression by ignoring the j-dependence of T_ℓ and assuming that the spin-parity dependence of $\rho(I,\pi,E)$ can be factorized as $\rho(I,\pi,E) \propto (2I+1)\omega(E)$, where ω is the state density.† It then follows that (see, e.g. [9]):

$$\sigma_{ab}(E,\varepsilon)d\varepsilon = \sigma_a(E) \frac{(2s_b+1)\,\mu_b\,\varepsilon\,\sigma_b(\varepsilon)\,\omega_b(E')d\varepsilon}{\sum_{b'} (2s_{b'}+1)\,\mu_{b'} \int \varepsilon'\sigma_{b'}(\varepsilon')\,\omega_{b'}(E')d\varepsilon'}, \qquad (27)$$

where σ_a is the compound-formation cross section and μ_b is the reduced mass of the outgoing particle.

In the derivation of the WE-formula from the HF-formula the spin cut-off of the level density has been neglected. Inserting Eq. (4) into Eq. (26) and using the approximation

$$\sum_{I'j'} f(I',E) \approx (2s'+1)(2J+1)(2\ell+1)\, f(J,E) \qquad (28)$$

we may obtain a somewhat more accurate expression.

---

†See footnote in INTRODUCTION.

First we note that from Eq. (27) it follows that:

$$\sum_{I'\ell'j'\pi'} T^{b}_{\ell'j'}(\varepsilon)\rho_b(I',\pi'E') \approx \frac{2\mu_b}{\pi\hbar^2}(2s_b+1)f(J,E_b')\varepsilon\,\sigma_b(\varepsilon)\,\omega_b(E'_b) \qquad (29)$$

In the denominator usually the neutron emission dominates. This gives a similar factor $f_n(J,\langle E'\rangle_n)$ at an "average" excitation energy $\langle E'\rangle_n$ of the target. The remaining J-dependence in Eq. (26) is $(2J+1)f_b(J,E_b')/f_n(J,\langle E'\rangle_n)$. Once more Eq. (28) is applied, leading to:

$$\sigma_{ab}(E,\varepsilon)d\varepsilon = \frac{f_b(I,E_b')}{f_n(I,\langle E'\rangle_n)}\,\sigma_{ab}^{WE}(E,\varepsilon)d\varepsilon. \qquad (30)$$

The factor f_b/f_n is a weak function of the target spin I with a significant energy dependence (see Table III). Since most of the spectrum is emitted in a narrow evaporation peak we may further approximate Eq. (30) by replacing $f_b(I,E_b')$ by $f_b(I,\langle E'\rangle_b)$. This is denoted by

$$\sigma_{ab}(E,\varepsilon)d\varepsilon = \frac{f_b(I,\langle E'\rangle_b)}{f_n(I,\langle E'\rangle_n)}\sigma_{ab}^{WE}(E,\varepsilon)d\varepsilon. \qquad (31)$$

Eq. (30) has been derived previously by Schmittroth [10] for the (n,γ) reaction. When $\sigma^2(E)$ is independent of energy the exact WE formula is obtained. From Eq. (31) it follows that for neutron scattering the WE formula is retained as well. This is indeed its most important application. However, for charged-particle reaction cross sections Eq. (30) is an *improved* version of the WE formula. Similar factors are needed in the exciton model; see below.

RELATION BETWEEN WE AND PE MODELS

The Weisskopf-Ewing formula can be written as:

$$\sigma_{ab}(E)d\varepsilon = \sigma_a\,\frac{W_b(\varepsilon)d\varepsilon}{W_t}, \qquad (32)$$

where the emission rate is given by:

$$W_b(\varepsilon) = \frac{\mu_b}{\pi^2\hbar^3}(2s_b+1)\,\varepsilon\,\sigma_b(\varepsilon)\,\frac{\omega_b(E')}{\omega_c(E)} \qquad (33)$$

with ω_c the state density of the compound nucleus at the incident energy. The total emission rate is given by

$$W_t = \sum_{b'}\int W_{b'}(\varepsilon')d\varepsilon'. \qquad (34)$$

In this notation Eq. (2) is quite close to the formulation of the (pre-)

equilibrium exciton model, where:

$$\sigma_{ab}(E) = \sigma_a \frac{\sum_n W_b(n,\varepsilon)\tau(n)}{\sum_n W_t(n)\tau(n)} \tag{35}$$

with

$$W_b(n,\varepsilon) = \frac{\mu_b}{\pi^2\hbar^3}(2s_b+1)\ Q_b(n)\ \varepsilon\,\sigma_b(\varepsilon)\ \frac{\omega_b(n-b,E')}{\omega_c(n,E)} \tag{36}$$

and

$$W_t(n) = \sum_{b'} \int W_b(n,\varepsilon')d\varepsilon'. \tag{37}$$

The factor $Q_b(n)$ accounts for the fact that for low values of n there is enhanced emission of particle a; at equilibrium $Q_b(n)$ approaches unity [11].

The mean life $\tau(n)$ is the time-integrated occupation probability:

$$\tau(n) = \int_0^\infty q(n,t)dt. \tag{38}$$

The occupation probability follows from a master equation:

$$\frac{dq(n,t)}{dt} = q(n-2,t)\lambda_+(n-2)+q(n+2,t)\lambda_-(n+2) + \\ -q(n,t)\ [W_t(n) + \lambda_+(n) + \lambda_-(n)], \tag{39}$$

where $\lambda_\pm(n)$ are internal transition rates. The mean life times $\tau(n)$ satisfy the equation

$$-q(n,t=0) = \tau(n-2)\lambda_+(n-2) + \tau(n+2)\lambda_-(n+2) \\ -\tau(n)\ [W_t(n) + \lambda_+(n) + \lambda_-(n)], \tag{40}$$

with initial condition

$$q(n,t=0) = \delta_{nn_o}, \tag{41}$$

where n_o is the initial exciton number. From Eqs. (40,41) it follows that the denominator of Eq. (35) equals unity (conservation of probability); thus:

$$\sigma_{ab}(E) = \sigma_a \sum_n W_b(n,\varepsilon)\tau(n). \tag{42}$$

This equation approaches to the WE formula when

$$\tau_{eq}(n) = \frac{\omega_c(n,E)}{\omega_c(E)\ W_t}, \tag{43}$$

assuming that Eq. (6) holds and $Q_b(n)=1$. This result is obtained by looking

for the stationary solution of the master equation (39), i.e. $\frac{dq(n,t)}{dt} = 0$ and $W_t(n) = 0$. Assuming detailed balance and $\lambda_{\pm}(n)$ proportional to $\omega_c(n\pm 2)$, it is found that

$$q(n,eq) = \omega_c(n,E)/\omega_c(E). \tag{44}$$

Substituting this into Eq. (40) as the "initial" condition we find that Eq. (43) is the approximate solution of Eq. (40).

We note that in order to obtain Eq. (30) rather than Eq. (32), the emission rates need to be multiplied by a factor proportional to $f_b(I,E')$. This will be studied in more detail in the next section.

UNIFIED MODEL

In the usual exciton model the formation of a "composite" state is described by the compound-formation cross section summed over all possible states:

$$\sigma_c = \sum_{J\Pi} \sigma_c^{J\Pi} \tag{45}$$

It is imagined that this process takes place immediately and that the decay starts at t=0 from the composite state with $n = n_o$, i.e. $q(n,t=0)=\delta_{nn_o}$. If we extend this picture to include angular-momentum conservation, it is clear that the occupation probability at t=0 should be:

$$q(n,J,\Pi,t=0) = \frac{\sigma_c^{J\Pi}}{\sigma_c} \delta_{nn_o}, \tag{46}$$

i.e. the spin-parity population is completely determined by the compound-formation process.

Analogous to the usual exciton model (cf. Eq. 35) we assume in the "unified" model (cf. [4]):

$$\sigma_{ab}\, d\varepsilon = \sigma_a \sum_{J\Pi} q(n_o,J,\Pi,t=0) \frac{\sum_n W_b^{J\Pi}(n,\varepsilon)\tau^{J\Pi}(n)d\varepsilon}{\sum_n W_t^{J\Pi}(n)\, \tau^{J\Pi}(n)}, \tag{47}$$

where $\tau^{J\Pi}$ follows from a time-integrated master equation like Eq. (39), subjoined with J,Π-indices. This simple extension holds, since the internal transitions should not change the total angular momentum and parity of the system. The denominator of Eq. (47) equals $q(n,J,\Pi,t=0)$; therefore we have:

$$\sigma_{ab} d\varepsilon = \sigma_a \sum_{J\Pi} \sum_n W_b^{J\Pi}(n,\varepsilon)\tau^{J\Pi}(n)d\varepsilon . \tag{48}$$

The expression for the emission rate is straightforward:

$$W_b^{J\Pi}(n,\varepsilon) = \frac{1}{2\pi\hbar} \sum_{I'\ell'j'\pi'} T^b_{\ell'j'}(\varepsilon)\, Q_b(n)\, \frac{\rho_b(n-b,I',\pi',E')}{\rho_c(n,J,\Pi,E)} \,. \tag{49}$$

We note that the J-dependence of this quantity is rather weak, since after summation over I' the numerator becomes approximately equal to f(n-b,J), partly compensating the factor f(n,J) in the denominator:

$$W_b^{J\Pi}(n,\varepsilon) \approx \frac{f(n-b,J)}{f(n,J)}\, W_b(n,\varepsilon). \tag{50a}$$

Since $\sigma^2(n)$ is proportional to n at low values of n, the ratio of f-factors is proportional to $[n/(n-b)]^{3/2}$. At values of $n > \tilde{n}$ Eq. (50a) needs to be replaced by (cf. Eq. 29):

$$W_b^{J\Pi}(n,\varepsilon) \approx \frac{f_b(J,E')}{f_c(J,E)}\, W_b(n,\varepsilon), \tag{50b}$$

where the ratio of f-factors is proportional to $(E/E')^{3/4}$.

For the solution of the J-dependent master equation we also need to know the internal transition rates. As a first estimate we may follow the "golden rule":

$$\lambda_\pm^{J\Pi}(n) = \frac{2\pi}{\hbar} \left|\overline{M^{J\Pi}}\right|^2 \rho_c(n\pm 2,J,\Pi). \tag{51}$$

Lack of knowledge about the average matrix element prevents the solution of the spin- and parity-dependent master equation. However, in two limiting cases, at t=0 and at equilibrium we may draw some conclusions without a detailed knowledge of $\lambda_\pm^{J\Pi}(n)$.

At t=0 we know the initial occupation probability from Eq. (46). Following the same arguments as given for the justification of Eq. (44) it follows that after a long lapse of time (t_{eq}) the occupation probability becomes:

$$q(n,J,\Pi,t_{eq}) = \frac{\rho_c(n,J,\Pi,E)}{\rho_c(J,\Pi,E)}\, q(n_o,J,\Pi,t=0), \tag{52}$$

approaching $q(n_o,J,\Pi,t=0)$ for values of n close to $\bar{n}$. This indicates that (when the preequilibrium emission is small) the spin-parity population "equilibrates" from $q(n_o,J,\Pi,t=0)\delta_{nn_o}$ at t=0 to Eq. (52) at $t = t_{eq}$.

The mean lifetime can be written as $\tau^{J\Pi}(n) = s(n,J,\Pi)\tau(n)$. Neglecting the (weak) spin-parity dependence of W_t we find from conservation of probability:

$$\sum_n s(n,J,\Pi) W_t(n)\tau(n) = q(n_o,J,\Pi,t=0). \tag{53}$$

The simplest possibility is

$$\tau^{J\Pi}(n) = q(n_o,J,\Pi,t=0)\ \tau(n), \tag{54}$$

corresponding to the solution of the master equation with $W^{J\Pi}$ and $\lambda_{\pm}^{J\Pi}$ independent of J and Π [i.e. constant spin-parity population $q(n_o,J,\Pi,t=0)$ at all values of n]. Assuming that the system is in equilibrium before emission is possible (and $W^{J\Pi}$ independent of J and Π) we find:

$$\tau^{J\Pi}(n) = \frac{f_c(n,J)}{f_c(J,E)}\, q(n_o,J,\Pi,t=0)\, \tau(n)\,, \tag{55}$$

together with Eq. (43).

Constant spin-parity population

Substitution of Eq. (54) into Eq. (48) leads to the following replacement in the HF formula (Eq. 26):

$$\rho(I',\pi',E') \rightarrow \sum_n \frac{\rho_b(n-b,I',\pi',E')}{f(n,J)} \frac{\tau(n)}{\omega_c(n,E)}\, Q_b(n)\,, \tag{56}$$

to obtain the unified model* with "constant spin-parity population". This model is considered in the limits of the exciton model (summation over spins and parities) and of the HF-model (Eq. 43), first by assuming that $\sigma^2(n)$ is proportional to n, valid at $n < \tilde{n}$. This leads to an additional factor in the exciton-model emission rates given by Eq. (50a) and to the following replacement in the HF model:

$$\rho(I,\pi',E') \rightarrow \sum_n \frac{\rho_b(n-b,I',\pi',E')}{f(n,J)}\, Q_b(n)\,, \tag{57a}$$

However, for values of n near $\bar{n}$ the approximation (50b) should be used in the exciton model, consistent with the improved WE relation, Eq. (30). Furthermore, the terms in Eq. (57a) with $n < \tilde{n}$ are very small with respect to the terms near equilibrium; therefore (57a) should be replaced by:

$$\rho(I',\pi',E') \rightarrow \frac{\rho_b(I',\pi',E')}{f_c(J,E)}\,. \tag{57b}$$

This shows that assuming a constant spin-parity population agrees with the HF model. The relations between the various models are illustrated in Fig. 1.

Other approximations

Assuming that Eq. (55) holds also for the non-equilibrium case one has

---

* A further simplication is possible by replacing J by I in Eq. (56).

to make the following replacement in the HF formula (Eq. 26):

$$\rho(I',\pi',E') \rightarrow \sum_n \rho_b(n-b,I',\pi',E')\ Q_b(n)\ \tau(n)/\omega_c(n,E) \tag{58}$$

to obtain a unified model with "equilibrium spin population". This prescription was followed by Fu [4]. It leads to consistent equilibrium models, see Fig. 2. However, the model does not correspond to the preequilibrium exciton model, unless Eq. (36) is multiplied with a factor proportional to $f_b(n-b,I)$. This leads to large discrepancies at low values of n. Application of Eq. (58) overestimates the precompound part and enhances α-emission (b=4).

In most statistical-model codes a preequilibrium option is introduced without subdividing the spin distribution of the level density into n-dependent distributions. The exciton model is then used to obtain the precompound parts of the cross sections. However, there is an inconsistency, since in these "extended" HF codes each exciton component is multiplied with a spin factor $f_b(I,E')$; to obtain consistency these factors also need to be introduced in the exciton model (see Fig. 3). However, that seems to be incorrect at low values of n (cf. Fig. 1).

CONCLUSION

We have considered the phenomenological formulas of Gilbert and Cameron [1], Dilg et al. [2] and Williams [3] for the level density in statistical equilibrium and pre-equilibrium models. In spite of the significant differences (see Table I) between the first two formulas, both are frequently used in Hauser-Feshbach calculations. Summation over all excitons in Williams' formula gives the total state density that is easily renormalised to the formula of Dilg et al. We propose to use this "renormalised Williams" formula Eq. (21) in unified-model calculations. The recommended spin cut-off parameter is given in Eq. (23) with a limitation to the equilibrium value of Dilg et al. [2].

The various statistical models: Hauser-Feshbach, Weisskopf-Ewing and the exciton model are limiting cases of a proposed unified model. This is easily demonstrated when it is assumed that the spin cut-off parameter is independent of n and E. Otherwise, additional spin factors occur in the various models, depending upon the assumptions with regard to the "equilibration" of the spin population. We have studied these assumptions, summarized in Figs. 1 to 3. In all cases the right equilibrium models are obtained, with an improvement of the WE model as given in Eq. (30). However, different spin factors occur in the preequilibrium emission rates of the exciton model. Since the assumption of a constant spin-parity population seems to be correct at the lowest values of n, we prefer this description (Fig. 1), leading to factors $[(n/n-b)]^{3/2}$ in the emission rates.

Further study with regard to the spin population during equilibration might be needed to establish the present views.

The author would like to thank Dr. J.M. Akkermans, Drs. H.A.J. van der Kamp and Mr. D. Nierop for some useful contributions to this paper.

REFERENCES

1. A. Gilbert and A.G.W. Cameron, "A composite nuclear level density formula with shell corrections", Can. J. Phys. 43, 1446 (1965).

2. W. Dilg, W. Schantl, H. Vonach and M. Uhl, "Level density parameters for the back-shifted Fermi-gas model in the mass range $40 < A < 250$", Nucl. Phys. A217, 269 (1973).

3. F.C. Williams, "Particle-hole state density in the uniform spacing model", Nucl. Phys. A166, 231 (1971).

4. C.Y. Fu, "A consistent nuclear model for compound and precompound reactions with conservation of angular momentum", Proc. Int. Conf. Nuclear Cross Sections for Technology, Knoxville (1979), NBS-Sp-594, p. 757 (1980) and ORNL/TM-7042.

5. U.E. Facchini and E. Saetta-Menichella, "Level density parameter values from neutron and proton resonances", Energ. Nucl. 15, 54 (1968).

6. H. Gruppelaar, A.J. Janssen and J.W.M. Dekker, "Intercomparison of recent evaluations for the capture cross sections of some fission-product nuclides, ECN-12, App. 2 (1976).

7. H. Gruppelaar, C. Costa, D. Nierop and J.M. Akkermans, "Calculation and processing of continuum particle-emission spectra and angular distributions", Proc. Int. Conf. Nuclear Data for Science and Technology, Antwerp (1982), D. Reidel Publ. Co., Dordrecht, Holland, p. 537 (1983).

8. G. Reffo and M. Herman, "Spin distribution of exciton levels for spherical nuclei", Lett. al Nuovo Cim. 34, 261 (1982).

9. H. Goldstein, "Statistical-model theory of neutron reactions and scattering", in: J.B. Marion and J.L. Fowler, Fast Neutron Physics, Vol. II, p. 1525 (1963) Interscience Publishers, New York.

10. F. Schmittroth, "Neutron capture calculations for $E_n = 100$ keV to 4 MeV", HEDL-TME-73-79, 1973, Hanford Engineering Development Laboratory.

11. C. Kalbach, "The Griffin model, complex particles and direct nuclear reactions", Z. für Physik A283, 401 (1977).

TABLE I

Comparison of various level-density formulas for ^{93}Nb (MeV^{-1})

E (MeV)	Williams g = 6.10 Δ = -0.299	Asymt. formula g = 6.10 Δ = -0.299	Dilg et al. g = 6.79 Δ = -0.521	Williams × f(E) g = 6.72 Δ = -0.591	Gilbert-Cameron g = 7.66 P = 0.72
0.2	2.93	3.59	3.10	2.94	4.58
0.4	4.61	5.45	4.78	4.62	5.96
0.6	7.09	8.18	7.20	7.10	7.77
0.8	10.7	12.1	10.7	10.7	10.1
1.0	15.9 *	17.6	15.5 *	15.8 *	13.2 *
2.0	90.2	95.4	84.2	89.6	49.5
3.0	398	400	367	394	185
4.0	1 490	1 510	1 380	1 480	696
5.0	4 960	4 960	4 630	4 920	2 610
6.0	15 100	15 000	14 300	15 000	9 610
7.0	42 800	42 100	41 300	42 600	32 500
8.0	114 000	112 000	113 000	114 000	102 000
9.0	291 000 *	282 000	292 000 *	291 000 *	300 000 *
10.0	710 000	684 000	728 000	726 000	837 000
12.0	3.81×10^6	3.62×10^6	$4\ 07\times10^6$	4.07×10^6	5.74×10^6
14.0	18.1×10^6	17.1×10^6	20.3×10^6	20.0×10^6	34.1×10^6
16.0	78.3×10^6	73.5×10^6	91.8×10^6	90.4×10^6	181×10^6
18.0	313×10^6	292×10^6	384×10^6	377×10^6	875×10^6
20.0	$1\ 170\times10^6$	$1\ 090\times10^6$	$1\ 500\times10^6$	$1\ 470\times10^6$	$3\ 910\times10^6$

* Fitting points at $E_c = 1.15$ MeV ($N_c = 9.5$) and $B = 8.83$ MeV ($D_{obs} = 41.17$ eV).

TABLE II

Effect of using GC and D formulas on ^{93}Nb+n cross sections (mb) calculated with the HF model

Cross section (only first emission)	E = 10 MeV		E = 20 MeV	
	GC	D	GC	D
$\sigma(n,n')$	1814	1814	1648	1653
$\sigma(n,p)$	4.6	5.6	25.8	18.0
$\sigma(n,\alpha)$	2.7	2.9	3.7	6.5
$\sigma(n,\gamma)$	1.6	0.9	0.7	0.5

TABLE III

Ratio of spin cut-off factors f(I,E')/f(I,E) at E=15 MeV

E' (MeV)	I=0	I=1	I=2	I=3
1	7.56	7.05	6.13	4.97
3	3.33	3.23	3.04	2.78
6	1.99	1.96	1.90	1.82
9	1.46	1.46	1.43	1.40
12	1.18	1.18	1.17	1.16
15	1.00	1.00	1.00	1.00

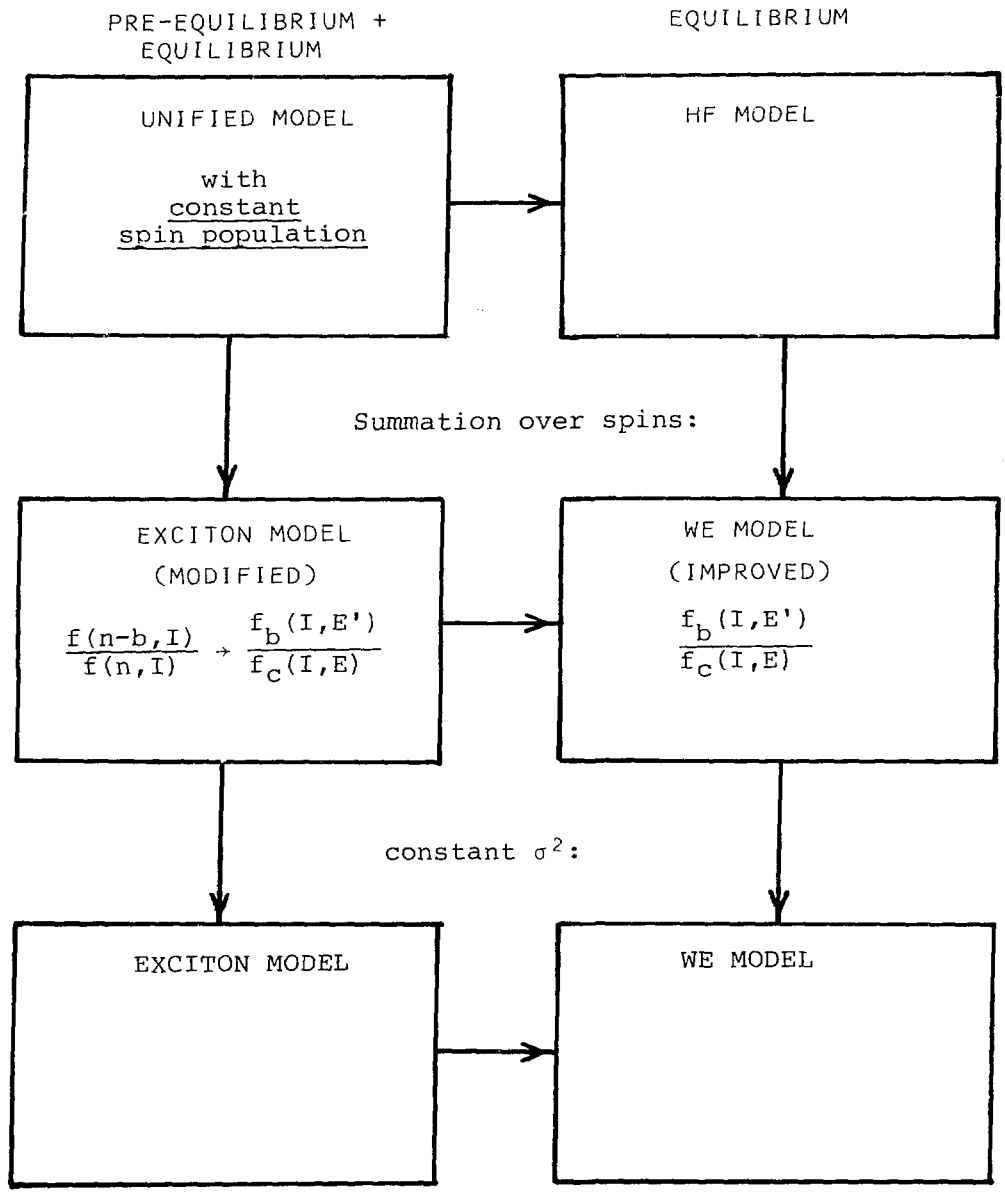

Fig. 1. Relation between various models, assuming a *constant spin-parity population*. At low values of n the emission rates in the exciton model are multiplied with a factor $f(n-b,I)/f(n,I)$; at n close to $\bar{n}$ this factor becomes $f_b(I,E')/f_c(I,E)$.

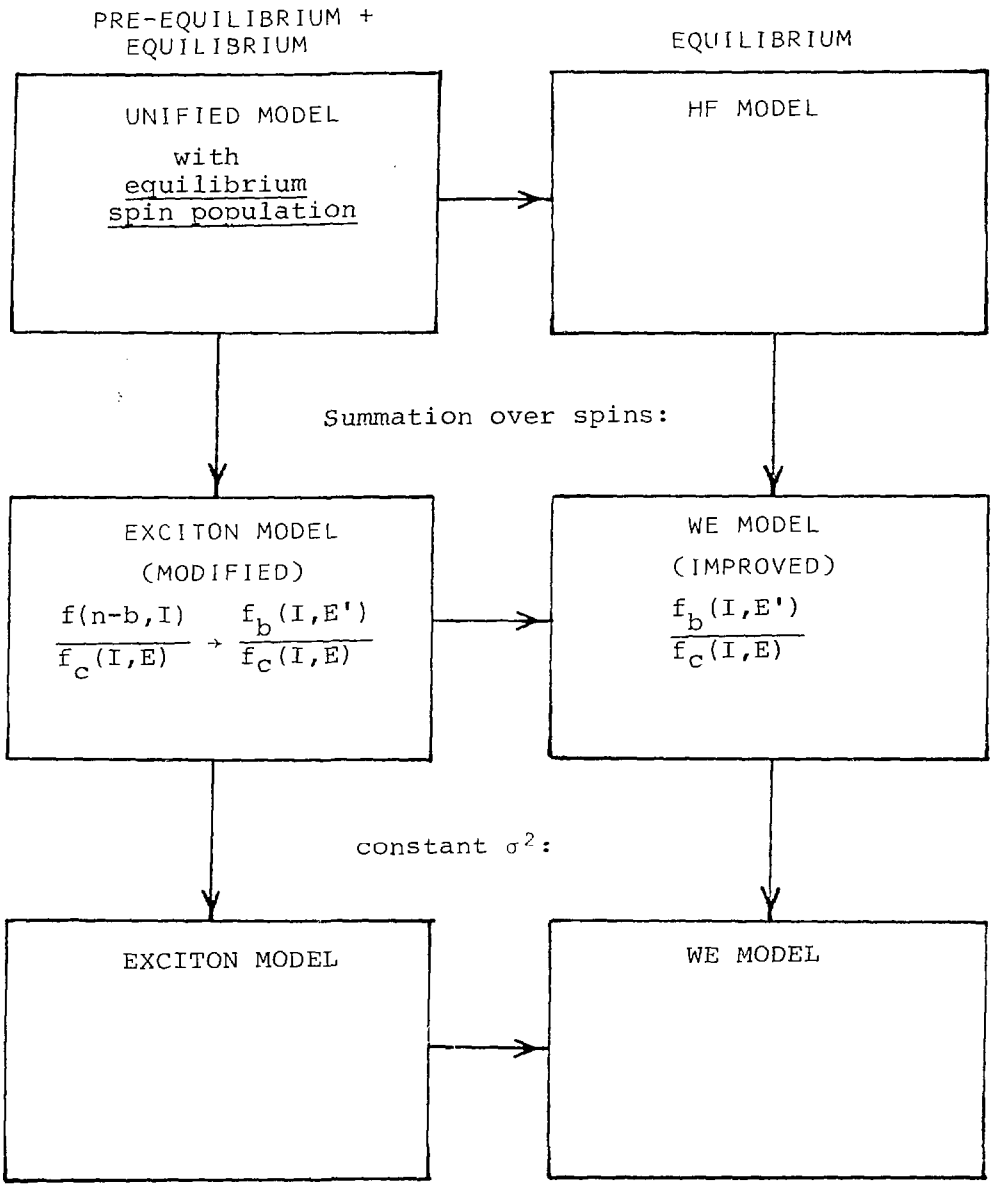

Fig. 2. Relation between various models, assuming the *equilibrium spin population*. At low values of n the emission rates in the exciton model are multiplied with a factor proportional to $f_b(n-b,I)$; at n close to $\bar{n}$ this factor becomes $f_b(I,E')$, independently of n.

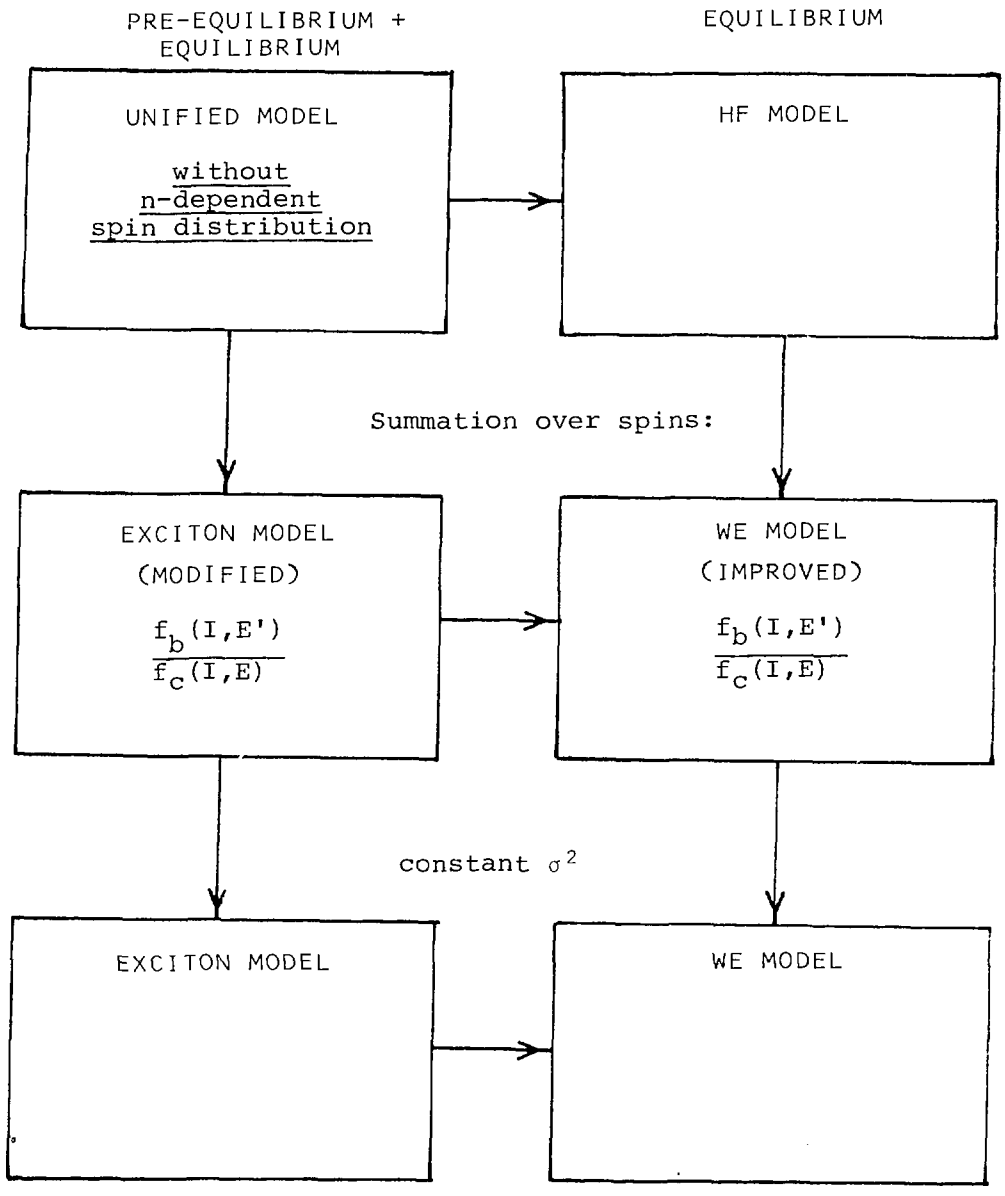

Fig. 3. Relation between various models, assuming that the *spin distribution is independent of n*. The emission rates in the exciton and WE models are multiplied with a factor proportional to $f_b(I,E')$.

ENERGY DEPENDENCE OF THE ROTATIONAL ENHANCEMENT FACTOR IN THE LEVEL DENSITY

G. Hansen and A. S. Jensen

Institute of Physics, University of Aarhus, DK-8000 Aarhus C, Denmark

ABSTRACT

The one-shell SU3-energies are given and the corresponding level density is calculated approximately by use of a distribution function for the SU3-quantum numbers. The calculation is extended to include many shells by a renormalization procedure and an effective one-shell interaction. The traditional level density is then obtained from the related mean-field Hamiltonian which corresponds to a deformed harmonic oscillator potential. Various rotational enhancement factors are considered. Numerical results are obtained and comparison between SU3- and traditional level density allow the first computation of the energy dependence of the rotational enhancement factor. A transition from axial to spherical level density is found. A simple parametrization is suggested in terms of a deformation dependent half value energy and a transition width.

INTRODUCTION

The nuclear level density often crucially enters both in analyses of experimental results and in theoretical calculations. It is therefore a much studied quantity [1-4]. One particularly interesting and not yet understood problem is how much the collective degrees of freedom contribute.

The collective states of even-even nuclei dominate the spectrum at the very low excitation energies where the nature of the individual states are known. If this situation extends to higher energies, the rotational bands build on top of each deformed intrinsic state should be counted in addition to the intrinsic excitations. The resulting level density expression [6] retain its structure for small spin values. It contains at least one constant, i.e. the single particle level density

at the Fermi energy. Therefore, if this constant is unknown, it does not matter from a practical point of view whether the rotations are counted or not. The problem was not solved, but its solution apparently would not have any practical implication.

The advent of the computer soon made it possible to calculate the level density directly from the microscopic single particle spectrum. This was done by counting only intrinsic excitations [7-10] as if ref.6 had been forgotten. Also the microscopic formulation [11] of the spin dependence was done without any consideration of the collective states.

Actual numerical calculations [12] based on a realistic single particle potential and the collective rotations included for deformed nuclei demonstrated the importance of the rotational contribution of the level density. Together with the lack of qualitative understanding of a series of fission cross sections [13] this called for a general theoretical framework [14] describing the role of collective degrees of freedom in the nuclear level density.

Afterwards the inclusion of the collective states have become practically mandatory in calculations [15] and analyses [16]. However, the problem is still unsolved, since ref.14 only describes how to completely omit or fully include the collective contributions, argues that these are the correct limits for very low and very high excitations and estimates a characteristic energy in the transition region in the case of collective rotations.

Then a quantitative investigation appeared [17,18] of the full energy dependence of the vibrational enhancement factor, i.e. the ratio of the correct level density to that where the vibration is completely neglected. A similar investigation for collective rotations is very desirable, since the rotational enhancement factor amounts to one to two orders of magnitude and the transition occurs within the physically interesting excitation energy region [14]. To our knowledge the only existing attempt is the phenomenologically extracted information [19] from measured fission cross sections. Since the result is independent of deformation it contradicts the simple estimate of ref.14.

In this paper we present the first calculation of the energy dependence of the rotational enhancement factor. We use the Elliott SU3-model [20], which can be analytically solved for one oscillator shell. We then include many shells and calculate the corresponding level density containing all states without reference to their collectivity. Then the mean field is calculated and the ordinarily derived microscopic level density obtained both when collective rotations are included and completely discarded. Comparison of the "exact" and usual level density as function of energy then gives the desired information about the rotational enhancement factor.

The paper is organized in the following way. In section 2 is described the details of the necessary theory. Section 3 contains the nu-

merical results, a discussion of the accuracy of the applied approximations and methods and extracts the rotational enhancement factor as function of deformation and excitation energy. Section 4 gives a brief summary of the results together with the conclusions and a few of the implications.

THEORY

The behaviour of the rotational enhancement factor can be investigated quantitatively in model calculations. The model requirements are then that it is possible and preferably easy to find (i) the total level density, including all states, as function of excitation energy and (ii) the corresponding traditional level density both with and without rotational contribution. This means that the model Hamiltonian must be soluble and the corresponding mean field obtainable. The calculations should be as simple as possible to allow maximum or at least a certain amount of flexibility. These reasonable conditions lead almost uniquely to the SU3-model and the related deformed harmonic oscillator mean field.

One Shell SU3-Model

The SU3-Hamiltonian is given by [20,21]

$$H=H_o-\tfrac{1}{2}\kappa\tilde{Q}\cdot\tilde{Q} \tag{1}$$

$$\tilde{Q}\cdot\tilde{Q}\equiv\sum_{i,k,\mu}(-1)^{\mu}\tilde{Q}_{\mu}(i)\tilde{Q}_{-\mu}(k) \tag{2}$$

$$\tilde{Q}_{\mu}\equiv\sqrt{\frac{4\pi}{5}}\left[\left(\frac{r}{b}\right)^2 Y_{2\mu}(\theta_r,\phi_r)+\left(\frac{b}{\hbar}\right)^2 p^2 Y_{2\mu}(\theta_p,\phi_p)\right] \tag{3}$$

where H_o is the one-body spherical harmonic oscillator Hamiltonian and κ is the strength of the two-body quadrupole-quadrupole interaction. The particle positions and momenta are given in spherical coordinates (r,θ_r,ϕ_r) and (p,θ_p,ϕ_p). The length b is given in terms of the nucleon mass m and the frequency ω_o of H_o as $b^2=\frac{\hbar}{m\omega_o}$. The matrix elements of $\tilde{Q}_{\mu}$ within one shell are identical to those of the ordinary quadrupole operator, i.e. the first term in eq.(3).

If we have k particles in the oscillator shell of principal quantum number N, the eigenvalues of H are given by

$$E^N_{\lambda\mu L}=\hbar\cdot\omega_o(N+\tfrac{3}{2})k+\tfrac{3}{2}\kappa(L(L+1)-2C_{\lambda\mu}) \tag{4}$$

$$C_{\lambda\mu}=\frac{2}{3}(\lambda^2+\lambda\mu+\mu^2+3(\lambda+\mu)) \tag{5}$$

where $(\lambda\mu)$ is the SU3-quantum numbers and the angular momentum L assumes the values

$$L=K,K+1,\cdots\cdots,K+\max\{\lambda,\mu\},\ K\neq 0$$

$$K=\min\{\lambda,\mu\},\ \min\{\lambda,\mu\}-2\cdots\cdots\cdots,\begin{cases}1\\0\end{cases}$$

$$L=\max\{\lambda,\mu\},\max\{\lambda,\mu\}-2,\cdots\cdots\cdots,\begin{cases}1\\0\end{cases}\ K=0 \tag{6}$$

The number of L-values $n_{\lambda\mu}(L)$ for a given (λ,μ) can be written [22]

$$n_{\lambda\mu}(L)=\left[\frac{\lambda+\mu-L}{2}\right]-\left[\frac{\lambda+1-L}{2}\right]-\left[\frac{\mu+1-L}{2}\right]+1 \tag{7}$$

where [x] is the integer part of x for x _ 0 and zero otherwise.

When the values and degeneracies of $(\lambda\mu)$ are known, we have the full energy spectrum and therefore the level density. This information can be obtained in two ways, either from tables which in general would limit applications to fairly light systems, or from a computer program. The latter possibility is clearly the most flexible, but it represents simultaneously a substantial amount of numerical and mathematical difficulties. Instead of choosing one of these options we shall push the analytical derivation a little further at the expense of several approximations.

Level Density in the One-Shell SU3-Model

The level density ρ as function of energy E and angular momentum L is given by

$$\rho(E,L)=\sum_i \delta(E-E_i)\cdot\delta(L-L_i) \tag{8}$$

where the summation index i runs over all SU3-states, except the trivial degeneracy (2L+1) due to the projection of angular momentum on an external axis. The degeneracy g(N) of the harmonic oscillator shell N is

$$g(N)=2(N+1)(N+2) \tag{9}$$

Where spin up and down of both neutrons and protons is included. The total number of levels is therefore

$$\iint\rho(E,L)(2L+1)dEdL=\frac{g(N)!}{k!(g(N)-k)!}\equiv\binom{g(N)}{k} \tag{10}$$

When all SU3-states are known, eq.(8) can in principle be used directly to calculate the level density. This is possible in special cases used as test examples. In general we use instead the distribution func-

tion [23] $P_{\lambda\mu}$ which approximately describes the number of times (the degeneracy) the SU3-quantum numbers (λ,μ) occur in the spectrum for each set of the remaining quantum numbers (angular momentum and its projections). The number $D_{\lambda\mu}$ of these sets, the dimension of (λ,μ), enters by an interesting coincidence in the definition of the distribution function

$$P_{\lambda\mu}=fD_{\lambda\mu}\exp(-\frac{C_{\lambda\mu}}{\sigma^2}) \tag{11}$$

$$D_{\lambda\mu}=\tfrac{1}{2}(\lambda+1)(\mu+1)(\lambda+\mu+2) \tag{12}$$

$$\sigma^2 = \frac{k(g(N)-k)}{g(N)-1}\langle d^2\rangle_N \tag{13}$$

$$\langle d^2\rangle_N=\langle(n_x-n_y)^2\rangle_N=\frac{1}{6}N(N+3) \tag{14}$$

where d is the difference between the number of oscillator quanta for one particle in two different directions and f is a normalization constant found by the requirement

$$\binom{g(N)}{k}=\sum_{\lambda\mu}D_{\lambda\mu}\cdot P_{\lambda\mu} \tag{15}$$

The factor $D_{\lambda\mu}$ is from the angular momentum summation and λ and μ run over the possible values [20,21] consistent with k particles in the shell N, i.e.

$$2\mu+\lambda+3m_1=kN$$

$$2\lambda+\mu\leq 2\lambda_o+\mu_o \tag{16a}$$

$$2\lambda+\mu+3m_2=(g(N)-k)N$$

$$2\mu+\lambda\leq 2\mu_o+\lambda_o \tag{16b}$$

where m_1 and m_2 are non-negative integers and (λ_o,μ_o) are the (λ,μ)-values of the ground state.

The right hand side of eq.(15) is now estimated by replacing the summation by an integration

$$\binom{g(N)}{k}=f\iint_{\Omega}d\lambda d\mu g(\lambda,\mu)D^2_{\lambda\mu}\exp(-C_{\lambda\mu}/\sigma^2) \tag{17}$$

where the density of points in the (λ,μ)-plane is found from eq.(16) to be $g(\lambda,\mu)=\frac{1}{3}$. The integrand has maximum exponent in the point $\lambda=\mu=-1+\sigma\sqrt{\frac{3}{2}}$ which in the case of interest is in the interior of Ω. Expansion to second order of the exponent around this point then leads to

$$f=\frac{8\sqrt{2}}{9\pi\sigma^8}\binom{g(N)}{k}\exp(3-\frac{2}{\sigma^2}) \tag{18}$$

The level density eq.(8) is then approximated by

$$\rho(E,L)=\sum_{\lambda\mu} P_{\lambda\mu} \sum_{L'} n_{\lambda\mu}(L')\delta(E-E^N_{\lambda\mu L'})\cdot\delta(L-L') \tag{19}$$

which, in case we don't need the spin distribution, can be integrated to give

$$\rho(E)\equiv\int\rho(E,L)dL=\sum_{\lambda\mu} P_{\lambda\mu} \sum_{L} n_{\lambda\mu}(L)\cdot\delta(E-E^N_{\lambda\mu L}) \tag{20}$$

SU3-Model, Many Shells

The Hamiltonian in eq.(1) has non-vanishing matrix elements between oscillator shells of principal quantum number differing by an even number. An exact analytic solution can therefore not be obtained.

It is convenient to work with the spherical one-shell solutions and fortunately this can be justified at least for small deformations. The corresponding effective interaction is namely approximately given by [24]

$$H=H_o-\tfrac{1}{2}(1+2\eta)\kappa\tilde{Q}\cdot\tilde{Q} \tag{21}$$

where $\tilde{Q}$ only acts within shells and η, a number to be determined later, may depend on particle number and shell. Thus the energy spectrum is simply that of eq.(4) where κ is renormalized to $(1+2\eta)\kappa\equiv\kappa_R$ and N and k assume appropriate values.

Level Density in the Many-Shell SU3-Model

The partition function $Z(\beta)$ for A particles can now be calculated for the Hamiltonian in eq.(21). It is conveniently expressed in terms of the partition functions Z_k for given distributions $\{k\}$ of the A particles in the oscillator shells

$$Z(\beta)=\sum_{\{k\}} Z_k(\beta) \tag{22}$$

Then Z_k is in turn a product of one-shell partition functions $Z_{N_k}(\beta)$ over the shells containing particles

$$Z_k(\beta)=\prod_{N_k} Z_{N_k}(\beta) \tag{23}$$

where N_k means the shell N with the number of particles given from the distribution $\{k\}$.

The level density $\rho_{SU3}(E)$ as function of excitation energy for given A is then the inverse Laplace transform of Z

$$\rho_{SU3}(E)=\frac{1}{2\pi i}\int_{-i\infty}^{i\infty} Z(\beta)e^{\beta E}d\beta=\sum_{\{k\}}\frac{1}{2\pi i}\prod_{N_k} Z_{N_k}(\beta)e^{\beta E}d\beta \tag{24}$$

The integral is evaluated in the saddle point approximation as

$$\rho_{SU3}(E)=\sum_{\{k\}}\rho_k(E) \tag{25}$$

$$\rho_k(E)=\left[2\pi\sum_{N_k}\frac{\partial^2 \ln Z_{N_k}(\beta_{N_k})}{\partial\beta^2_{N_k}}\right]^{-\frac{1}{2}}\prod_{N_k} Z_{N_k}(\beta_{N_k})e^{\beta E} \tag{26}$$

where the saddle point β_{N_k} is a solution of the equation

$$\sum_{N_k}\frac{\partial \ln Z_{N_k}(\beta_{N_k})}{\partial\beta_{N_k}}+E=0 \tag{27}$$

Let us therefore first calculate the one-shell partition function of k particles in the shell N

$$Z_{N_k}(\beta)=e^{-\beta\hbar\omega_o(N+3/2)k}\sum_{\{\lambda\mu\}}e^{\beta 3\kappa_R C_{\lambda\mu}}\cdot\sum_L n_{\lambda\mu}(L)e^{-\frac{3}{2}\beta\kappa_R L(L+1)} \tag{28}$$

When the number of active particles, min{k,g(N)-k}, is less than or equal to three, we calculated Z_{N_k} exactly. Otherwise the distribution function $P_{\lambda\mu}$ is used, $n_{\lambda\mu}$ is approximated by a continuous function and the summations over $(\lambda\mu)$ and L are replaced by integrals. This leads to

$$Z_{N_k}(\beta)\simeq e^{-\beta\hbar\omega_o(N+3/2)k}\int_\Omega\frac{1}{3}d\lambda d\mu P_{\lambda\mu}e^{\beta 3\kappa_R C_{\lambda\mu}}\cdot G(\lambda,\mu,\kappa_R,\beta) \tag{29}$$

where the density of points account for the factor $\frac{1}{3}$ (see eqs.(16) and (17)), the angular momentum integration results in G, calculated in appendix A and the integration area Ω is confined by the lines

$$\begin{aligned}&\lambda=-\tfrac{1}{2}\\&\mu=-\tfrac{1}{2}\\&\lambda+2\mu=\lambda_o+2\mu_o+\tfrac{1}{2}\sqrt{3}\\&2\lambda+\mu=2\lambda_o+\mu_o+\tfrac{1}{2}\sqrt{3}\end{aligned} \tag{30}$$

Compared to eq.(16) Ω is enlarged in order to treat the boundary contribution in a better approximation.

The first and second derivatives of Z_{N_k} needed in eq.(26) can then be written as

$$\frac{\partial \ln Z_{N_k}}{\partial\beta}=-\hbar\omega_o(N+\tfrac{3}{2})k+\frac{e^{-\beta\hbar\omega_o(N+\frac{3}{2})k}}{Z_{N_k}}\int_\Omega\frac{1}{3}d\lambda d\mu P_{\lambda\mu}e^{3\beta\kappa_R C_{\lambda\mu}}(3\kappa_R G C_{\lambda\mu}+\frac{\partial G}{\partial\beta}) \tag{31}$$

$$\frac{\partial^2 \ln Z_{N_k}}{\partial\beta^2} = -(\hbar\omega_o(N+\frac{3}{2})k+\frac{\partial \ln Z_{N_k}}{\partial\beta})^2 + \frac{e^{-\beta\hbar\omega_o(N+\frac{3}{2})k}}{Z_{N_k}}$$

$$\cdot\int_\Omega \frac{1}{3} d\lambda d\mu P_{\lambda\mu} e^{3\beta\kappa_R C_{\lambda\mu}}((3\kappa_R C_{\lambda\mu}\cdot G+2\frac{\partial G}{\partial\beta})3\kappa_R C_{\lambda\mu}+\frac{\partial^2 G}{\partial\beta^2}) \tag{32}$$

In the actual calculations are the integrals eqs.(29) and (31) evaluated by numerical integration whereas the second derivative of $\ln Z_{N_k}$ is found by numerical differentiation of the first derivative.

The SU3-level density is now given by eqs.(25)-(32). It is expressed as function of excitation energy for a given number of nucleons. We have been working with the micro-canonical ensemble of exact nucleon number and not the traditional grand-canonical ensemble.

Traditional Level Density

The Hamiltonian corresponding to the ordinary quadrupole-quadrupole interaction is given by

$$H = H_o - \tfrac{1}{2}\kappa Q\cdot Q \tag{33}$$

$$Q_\mu = \sqrt{\frac{16\pi}{5}}\left(\frac{r}{b}\right)^2 Y_{2\mu}(\theta_r,\phi_r) \tag{34}$$

In one-shell calculations is it equivalent to that of eq.(1). The related Hartree mean-field is the deformed harmonic oscillator

$$H_H = \frac{p^2}{2m} + \tfrac{1}{2}m(\omega_x^2 x^2+\omega_y^2 y^2+\omega_z^2 z^2) \tag{35}$$

where the frequencies are expressed in terms of the deformation parameters, ε_o and ε_2

$$\omega_x^2=\omega_o^2(1+\frac{2}{3}(\varepsilon_o-\varepsilon_2)) \tag{36a}$$

$$\omega_y^2=\omega_o^2(1+\frac{2}{3}(\varepsilon_o+\varepsilon_2)) \tag{36b}$$

$$\omega_z^2=\omega_o^2(1-\frac{4}{3}\varepsilon_o) \tag{36c}$$

$$\varepsilon_o=3\frac{\kappa}{\hbar\omega_o}\langle Q_o\rangle$$

$$\varepsilon_2=3\sqrt{6}\frac{\kappa}{\hbar\omega_o}\langle Q_2+Q_{-2}\rangle \tag{37b}$$

Here $\langle\,\rangle$ denote expectation value with respect to the eigenfunction of H_H and

$$\langle Q_o\rangle=2S_z\frac{\omega_o}{\omega_z}-S_x\frac{\omega_o}{\omega_x}-S_y\frac{\omega_o}{\omega_y} \tag{38a}$$

$$<Q_2 + Q_{-2}> = \frac{1}{2}\sqrt{6}\left[S_x \frac{\omega_o}{\omega_x} - S_y \frac{\omega_o}{\omega_y}\right] \tag{38b}$$

where all information about the occupied single particle states is contained in the quantities S_K

$$S_x = \sum_{i\ occ} (n_x(i)+\tfrac{1}{2}), \text{ etc.} \tag{39}$$

For given values of S_K, the lowest lying states are occupied, are the selfconsistent set of equations (36)-(38) solved to give ε_o and ε_2. The single particle energy spectrum of H_H is then given by

$$\varepsilon_{n_x n_y n_z} = \hbar\omega_x(n_x+\tfrac{1}{2})+\hbar\omega_y(n_y+\tfrac{1}{2})+\hbar\omega_z(n_z+\tfrac{1}{2}) \tag{40}$$

where n_K are non-negative integers. Each of these levels is fourfold degenerate, neutrons and protons of spin up and down.

The intrinsic level density $\rho_i(E,A)$, corresponding to the spectrum in eq.(40), is expressed as usual [4,5] in the saddle point approximation. From this intrinsic level density we can calculate the level density for an assumed given rotational symmetry [14]. After integration over spin we can express the resulting level density in terms of ρ_i and the spin cut-off factors σ_x, σ_y and σ_z. In case of axial symmetry we name them $\sigma_{||} \equiv \sigma_z$ and $\sigma_\perp = \sigma_x = \sigma_y$. The following possibilities will be considered:

(i) spherical symmetry
(ii) axial and R-symmetry
(iii) axial symmetry without R symmetry
(iv) no rotational symmetry
(v) only time reversal symmetry
(vi) only time reversal symmetry and parity invariance

The corresponding level densities are given as function of excitation energy and nucleon number by [14]

$$\rho_1 \equiv (2\pi)^{-\frac{1}{2}}\sigma_{||}\rho_i$$
$$\rho_2 \equiv \sigma_\perp^2 \rho_1$$
$$\rho_3 \equiv 2\sigma_\perp^2 \rho_1$$
$$\rho_4 \equiv \sqrt{8\pi}\ \sigma_x\sigma_y\sigma_z\rho_1$$
$$\rho_5 \equiv \frac{1}{2}\rho_4$$
$$\rho_6 \equiv \frac{1}{4}\rho_4 \tag{41}$$

The spin cut-off factor $\sigma_{||}$ is obtained microscopically simultaneously with ρ_i whereas $\sigma_\perp$ is approximated by the rigid body expression for the given deformation.

The Values of κ and η

The selfconsistency conditions eqs.(36)-(38) can explicitely be solved to first order in the deformation parameters to give

$$\langle Q_o \rangle = \frac{2S_z - S_x - S_y}{1 - 6\frac{\kappa S_o}{\hbar\omega_o}} \tag{42}$$

$$\langle Q_2 + Q_{-2} \rangle = \frac{\sqrt{6}}{2} \frac{(S_x - S_y)}{1 - 6\frac{\kappa S_o}{\hbar\omega_o}} \tag{43}$$

where we consistently have neglected terms of second order in the difference between two of the quantities S_κ and introduced S_o by

$$S_o = \frac{1}{3}(S_x + S_y + S_z) \tag{44}$$

When the expectation values in eqs.(42) and (43) are calculated by using a spherical oscillator potential we obtain results where the denominator is changed to unity. The same is true when only the moments of the last (partially) filled shell is used in the evaluation. Thus an effective one-shell interaction of the same form as in eq.(33) can be found [24] by the requirement of identical Hartree mean-field solutions of eq.(33) and eq.(21). Then the deformation parameters $\kappa\langle Q_o \rangle$ and $\langle Q_2 + Q_{-2} \rangle$ of the deformed harmonic oscillator must remain unchanged for the effective interaction (eq.(21)) for all shells and particle configurations. These two conditions are identical and therefore the operators Q only should act within the shell while the strength is renormalized to κ_R

$$\kappa_R = \kappa(1+2\eta) \equiv \frac{\kappa}{1 - 6\frac{\kappa S_o}{\hbar\omega_o}} \tag{45a}$$

For the one-shell calculations in question it is equivalent to change Q (eq.(33)) into $\tilde{Q}$ (eq.(3))

This first order calculation [24] can easily be improved by exact evaluation of $\langle \tilde{Q} \rangle$ and $\langle Q \rangle$. Then eq.(45a) is generalized to

$$(1+2\eta)\langle \tilde{Q}_o \rangle \equiv \langle Q_o \rangle \tag{45b}$$

$$(1+2\eta)\langle Q_2 + Q_{-2} \rangle = \langle Q_2 + Q_2 \rangle \tag{45c}$$

where the expectation values $\langle Q \rangle$ depend on κ and the total number of particles, and the expectation values $\langle \tilde{Q} \rangle$ of the one-shell operators $\tilde{Q}$ depend on both shell quantum number and particle configuration. For an axially symmtric case is eq.(45c) the identity zero equals zero and eq.(45b) is used to determined η as function of N and k. For triaxial configurations is it

not possible to fulfill both eq.(45b) and 45c). As an approximation we then use eq.(45b) and ignore the hopefully less important eq.(45c).

A particular value of η results for the partially filled shell in the ground state configuration. Using this value throughout for all N and k is probably a reasonable approximation, because a contribution from a larger η-value always has a corresponding contribution from a smaller η-value.

The procedure is now to calculate the traditional level density from the Q•Q-interaction with a given κ. Then perform the many-shell SU3-calculation with an effective one-shell interaction of strength determined from eq.(45b). The desired information about rotational enhancement factors can then be extracted by comparison.

An especially interesting value for the strength κ is the so-called selfconsistent value $\kappa_{s.c.}$ (see ref. 24):

$$\kappa_{s.c.} = \frac{\hbar\omega_o}{12} \frac{\left(\frac{2}{S_z^2} - \frac{1}{S_x^2} - \frac{1}{S_y^2}\right)}{S_x^2 - S_y^2 - 2S_z^2} S_x S_y S_z \tag{46a}$$

which for small deformations (first order in $S_\kappa - S_o$) reduces to

$$\kappa_{s.c.} \approx \frac{\hbar\omega_o}{12S_o} = \frac{1}{4mA} \frac{\hbar^2}{\langle r^2 \rangle} \approx \frac{12\,\mathrm{MeV}}{A^{5/3}} \tag{46b}$$

where $\langle r^2 \rangle = \frac{3}{5}(1.2\ \mathrm{fm})^2 A^{2/3}$ is used. This value where the solutions to the Hartree mean-field Hamiltonian are reasonable approximations to those of the original two-body Hamiltonian, can be obtained in many ways [25,26, 3]. It arises most simply from the quadrupole-quadrupole interaction (not the SU3-operator) by assuming equal ratios of half axes of Hartree potential and density distributions. The quadrupole moment of the last partially filled shell is then to first order equal to that of the remaining fully occupied lower lying shells. In other words $\kappa_R = 2\kappa$ or $\eta = 1/2$ for $\kappa = \kappa_{s.c.}$. In the actual calculations we used this first order strength $\kappa_R = 2\kappa_{s.c.}$ and the resulting value of κ from eq.(45b).

NUMERICAL RESULTS

Various approximations and numerical methods are used in these model calculations. It is for our purpose extremely important to have estimates of the resulting inaccuracies, because we want to study differences between the SU3- and the ordinary level density. Thus first we investigate the reliability of our procedure and then we continue to study the level densities themselves.

Inaccuracies of the Approximations

The most important simplifications was achieved by introduction of the distribution function $P_{\lambda\mu}$ (eq.(11)). It is calculated for 8 particles in the N=4 shell and compared to the exact distribution of the SU3-quantum numbers in fig. 1. The overall agreement is satisfactory. The scattering around the approximation is about 30% (in $P_{\lambda\mu}$) when $C_{\lambda\mu}$ is less than 100. It increases to a factor of about 10 at $C_{\lambda\mu}\approx 500$ where the number of representations is insignificantly small for our purpose. Because small $C_{\lambda\mu}$ corresponds to large energies (see eq.(4)), the accuracy of the approximation using the distribution function improves with increasing excitation energy. On the other hand, this approximation breaks down at low excitation energy. The example in fig.1 is typical.

The normalization constant f, determined by eq.(18), is slightly underestimated by not more than 10%. Thus the line on fig. 1 should be moved a little bit upwards in order to represent the correct total number of levels. Still the accuracy of $P_{\lambda\mu}$ quoted above holds.

The angular momentum summation is replaced by an integral (see app. A) for shells containing more than three active particles. The resulting function G is shown in fig. 2 for two cases and compared with exact calculations. For small β (large temperature) is the approximation very accurate over a large region of λ-values whereas a systematic underestimate up to 20% occurs for large β and large λ/μ.

The accuracy of the calculated level density is now investigated in one-shell calculations. Fig. 3 compare an exact result with those where all described approximations are used and where only the $P_{\lambda\mu}$-distribution is used instead of the exact values. Most of the inaccuracy arises from the distribution function. The remaining uncertainty is less than about 10%. At very low excitation energy is the level density underestimated by a factor of 4 but in the important (for our purpose) energy region above 20 MeV we have obtained a relative approximation of better than 25%.

In the many-shell calculations are particle excitations restricted to less than 10 $\hbar\omega_0$. This implies that the level density is underestimated for excitation energies larger than about 11 $\hbar\omega_0$=11·41 MeV/$A^{1/3}$.

Level Density Results

As we treat shells with up to three active particles exactly the accuracy of the SU3-level density is a one-shell problem up to around 4 $\hbar\omega_0$. For energies between 4 $\hbar\omega_0$ and 8 $\hbar\omega_0$ uncertainties from two shells will appear and uncertainties from three shells will show up in the region above 8 $\hbar\omega_0$.

The calculated SU3-level density is for energies below 4 $\hbar\omega_0$ at the most underestimated by a factor 4 and at the most overestimated by a factor 1.2. The corresponding factors for the two higher energy regions are (6, 1.5) and (8, 1.7), respectively. These numbers are the really extreme

limits and most of the contributing configurations are very accurately determined. Under normal circumstances are ρ_{SU3} determined in the respective energy regions to within factors of 1.2, 1.5 and 2.0.

The largest part of these uncertainties arises from the distribution function $P_{\lambda\mu}$. However, the accuracy may be better than these uncertainty estimates as indicated by a comparison with calculations where the distribution is used for three active particles. The level density changed by less than 10%.

We concentrated on the N=5 oscillator shell and supplemented with a few cases for N=4. In fig. 4 is shown typical examples with the strength of the interaction $\kappa_R=2\kappa_{s.c}$. The low energy ($E\leq 15$ MeV) behaviour is in general not reliable due to the inaccuracy of the distribution function. In the high energy region above 80 MeV is ρ_{SU3} smaller than the level density corresponding to a spherical shape. This is due to the restriction of particle excitations to less than 10 $\hbar\omega_0$ and the general decrease of accuracy at high excitation energy.

In spite of these unreliable limits we clearly observe the general trend that ρ_{SU3} increases slower than the other level densities in the intermediate energy region.

For all four nuclei, ρ_{SU3} furthermore follows the axial and R-symmetric level density ρ_2 in a certain energy range above the very uncertain low energies. By increasing the energy, ρ_{SU3} turn away from ρ_2, and after a while approaches the spherical level density ρ_1. This behaviour is exactly as anticipated for axially symmetric nuclei and for those easily understood in terms of an energy dependent rotational enhancement factor. The triaxial nuclei seems to make the transition to the spherical level density in two steps. The first transition to the intermediate axial level density occurs at low energy where our calculations are inaccurate due to the distribution function and from then on they behave like axially symmetric nuclei.

The Rotational Enhancement Factor

The rotational enhancement factor R is defined as the ratio between the "correct" level density (ρ_{SU3}) where all degrees of freedom are properly included and the level density of a spherical nucleus (ρ_1 in eq. (41)) where collective rotations do not exist. This function of energy is in principle easily extracted from our calculations. The inaccuracies of the level densities are, however, inherited in the process and thereby complicating the determination of R.

Let us first consider axially symmetric nuclei and extract R_a. Its fundamental behaviour is a decrease from a certain value at low energy towards unity at large energy. One characteristic parameter of such a function is the half-value energy $E_{\frac{1}{2}}^a$ where R_a is reduced to half the value at low energy. The numerical computations support the expression

$$E^a_{\frac{1}{2}} = \frac{A \cdot \hbar^2}{\gamma_a} \left(\frac{\omega_x + \omega_y}{2} - \omega_z\right)^2 \tag{47}$$

where $\gamma_a = (14 \pm 3)$ MeV. Provided the excitation energy is equal A/γ_a times the temperature squared, eq.(47) is of the same form and numerically in good agreement with the simple estimate of ref.14. The uncertainty in γ_a contains both the computational inaccuracies and the fluctuations in nucleon number.

The calculations furthermore show that the width of the transition region roughly is proportional to $\left(\frac{\omega_x+\omega_y}{2} - \omega_z\right)^2$. The inaccuracy in the width determination is larger than that of $E^a_{\frac{1}{2}}$ due to the larger uncertainty at high excitation energy. It nevertheless suggests the parametrization

$$R_a = (1-f_a) + f_a \cdot \frac{\rho_2}{\rho_1} \tag{48}$$

$$f_a = \frac{1}{1+\exp((E-E^a_{\frac{1}{2}})/d_a)} \tag{49}$$

$$d_a = \frac{\hbar^2}{\nu_a}\left(\frac{\omega_x+\omega_y}{2} - \omega_z\right)^2 \tag{50}$$

where $\nu_a = (1.2 \pm 0.5)$ MeV. The uncertainty in ν_a reflects again both numerical inaccuracy and (of special importance here) variation with nucleon number. Thus a better parametrization of d_a may exist.

The above parametrization of the rotational enhancement factor can be expressed in terms of the axis ratio $q \equiv (\omega_x+\omega_y)/2\omega_z$. Using the volume conservation condition and the value $\hbar\omega_0 = 41$ MeV$/A^{1/3}$ we find

$$E^a_{\frac{1}{2}} \approx 120 \text{ MeV} \cdot A^{1/3} \; (q-1)^2 \cdot q^{-4/3} \tag{51a}$$

$$d_a \approx 1400 \text{ MeV } A^{-2/3} (q-1)^2 \cdot q^{-4/3} \tag{51b}$$

It is then tempting to use eq.(51) as a crude generalization to arbitrary axially symmetric quadrupole shapes. It is, however, also very dangerous due to the absolute lack of results for deformations of $q \geq 1.25$ and the possible model dependence of the obtained results for the smaller deformations.

In the SU3-model is only rather few nuclei axially symmetric. We have therefore also investigated triaxial nuclei and chosen to concentrate on the same mass region. As indicated by the results in fig. 4 is the rotational enhancement factor defined in eqs.(47)-(50) apparently also applicable to triaxial nuclei in the transition region around $E^a_{\frac{1}{2}}$.

In fig. 5 is it compared to the "exact" enhancement for a few nuclei. The average parameter set is fairly good except perhaps at the end of the transition region. An improvement is of course obtained by individual parameter adjustment but the agreement is only marginally better.

There is apparently no difference at these energies (above 20 MeV) between the axial and triaxial nuclei. The low-energy transition from triaxial to axial level density must of course be present. although at the moment it is outside our reach. The total enhancement factor R can then be imagined parametized as a product of R_a and R_t where

$$R_t(E \to 0) \approx \frac{\rho_6}{\rho_2} = \sqrt{\frac{\pi}{2}}\sigma_z$$

$$R_t(E^a_{\frac{1}{2}} - 2d_a \ln 3) \approx 1$$

$$R_t(\omega_x = \omega_y) = 1 \tag{52}$$

This can be achieved analogously to eqs.(48)-(50) by the definitions

$$R_t \equiv 1 - f_t + f_t \frac{\rho_6}{\rho_2} \tag{53}$$

$$f_t = \frac{1}{1+\exp\left(\frac{E-E^t_{\frac{1}{2}}}{d_t}\right)} \tag{54}$$

$$E^t_{\frac{1}{2}} = \frac{A \cdot \hbar^2}{\gamma_t}(\omega_x - \omega_y)^2 \tag{55}$$

$$d_t = \frac{\hbar^2}{\nu_t}(\omega_x - \omega_y)^2 \tag{56}$$

where $\gamma_t > 1$ MeV and $\nu_t > 0.01$ MeV are the limits from the numerical results. Thus it is possible that $(\gamma_t, \nu_t) = (\gamma_a, \nu_a)$.

Clearly both forms and actual values in eqs.(55) and (56) are suggestions from symmetry and plausibility arguments without any support (except the limits) in numerical computations. However, it is important to stress, that a functional form of R similat to that of R_a (or R_t) for triaxial nuclei is inconsistent with the numerical results, but consistent with $R = R_a \cdot R_t$.

SUMMARY AND CONCLUSIONS

The energy dependence of the rotational enhancement factor is investigated in a model calculation. It consists of a two-body quadrupole--quadrupole interaction. The total level density is calculated as function of energy for several nuclei. From the Hartree mean-field of the Hamiltonian is the traditional level density evaluated both with and without collective rotational contributions. By comparison is the rotational enhancement factor then extracted.

To make the computations possible in practice a number of approximations had to be done. The two most essential of these are use of an effective one-shell quadrupole-quadrupole interaction and a continous distribution function for the quantum numbers of the eigensolutions. Only the average over different angular momenta is considered and degeneracy with respect to the nucleon spin and isospin is assumed. Thus the excitation energy, the total nucleon number and to a certain extent the deformation are the independent variables.

A number of other approximations are also applied, i.e. substitution of integrals for discrete summations, saddle point approximation to calculate the inverse Laplace transform, rigid body values of the x and y spin cut-off parameters and the full rotational enhancements in terms of simple factors σ_κ.

The price paid to obtain the numerical results is rather high in terms of inaccuracies. They are consequently carefully estimated and concluded to be small enough to allow important deductions. First of all a transition from axial- to spherical level density does apparently occur for all axially symmetric nuclei. The transition region extends over an energy interval consistent with the estimate of ref. 14. Triaxial nuclei seems to make two transitions, i.e. one at low excitation energy to the axial level density and then another similar to that of axially symmetric nuclei.

The transitions are then attempted parametrized in terms of simple analytical, energy dependent rotational enhancement factors. The introduced parameters are estimated together with the related uncertainties arizing from both numerical inaccuracies and fluctuations in nucleon number. The resulting level density is given in an easily applicable form in terms of the axes ratio of ellipsoidally deformed shapes. However, only ground state deformations (resulting from the self-consistency requirement for κ) of N=5 and a few N=4 nuclei are investigated. Extrapolations to very different nuclei and deformations (in particular much more deformed) may therefore, although not expected, turn out to be erroneous.

The quoted parameter uncertainties do not include a possible model dependence. It is conceivable that the transitions discussed here depend on the two-body interaction for example through the resulting softness of appropriate deformation degrees of freedom.

The qualitative main conclusion of this investigation is that the nuclear level density increases significantly slower with excitation energy in a transition region than the traditional mean-field based microscopic or macroscopic level densities with or without rotational enhancements. Thus the nuclear temperature ($\frac{1}{T}=\partial \ln\rho/\partial E$) should consequently be significantly larger in the region. Including this effect in the various analyses, where the level density enters, is almost inevitably leading to different numerical results for the deduced parameters. It may even lead to qualitatively different interpretations of the physics involved in the process considered.

ACKNOWLEDGEMENT

We want to thank B. Mottelson for suggesting this type of investigation and A. Miranda for an independent similar suggestion and subsequent discussions.

APPENDIX A

The Contibution of the Partition Function from the Orbital Angular Momentum.

According to eq.(28) the following factor Z_L, is the contribution to the one shell partition function from the orbital angular momentum for a given SU3-representation

$$Z_L(\beta)=\sum_{L=o}^{\lambda+\mu} n_{\lambda\mu}(L)e^{-\frac{3}{2}\beta L(L+1)\cdot\kappa_R} \tag{A.1}$$

where the function $n_{\lambda\mu}$ is given in eq.(7).

To give a simple analytical expression, G, for $Z_L(\beta)$ we substituted the summation by an integral

$$\sum_{L=o}^{\lambda+\mu} \sim \int_{-\frac{1}{2}}^{\lambda+\mu+\frac{1}{2}} dL \tag{A.2}$$

and approximated $n_{\lambda\mu}$ by the following continous function $\tilde{n}_{\lambda\mu}$

$$\tilde{n}_{\lambda\mu}(L) = \begin{cases} \dfrac{|L|+\frac{1}{2}}{2} & , -\frac{1}{2} \le L \le \min\{\lambda,\mu\}=M1 \\ \dfrac{1+\min\{\lambda,\mu\}}{2} & , M1 < L \le \min\{\max\{\lambda,\mu\}+1,\lambda+\mu\}=M2 \\ \dfrac{\lambda+\mu+\frac{3}{2}-L}{2} & , M2 < L \le \lambda+\mu+\frac{1}{2} \end{cases} \tag{A.3}$$

The integration can now be done analytically and with $\alpha = 3\beta\kappa_R$ we get for $\kappa_R > 0$.

$$\begin{aligned} G(\lambda,\mu,\alpha)= & \frac{1}{4}\sqrt{\frac{\pi}{\alpha}}\, e^{\alpha/4}\, \mathrm{erf}(\tfrac{1}{2}\sqrt{\alpha})+\frac{1}{4\alpha}(2-e^{-\alpha(\frac{1}{2}+M1)(\frac{3}{2}+M1)}-e^{\alpha/4}) \\ & +\sqrt{\frac{\pi}{\alpha}}\, e^{\alpha/4}\,\frac{1+M1}{4}(\mathrm{erf}((1+M2)\sqrt{\alpha})-\mathrm{erf}((1+M1)\sqrt{\alpha})\} \\ & +\frac{1}{4\alpha}\{e^{-\alpha(\frac{1}{2}+\lambda+\mu)(3/2+\lambda+\mu)}-e^{-\alpha(\frac{1}{2}+M2)(3/2+M2)}\} \\ & +\frac{\lambda+\mu+2}{4}\sqrt{\frac{\pi}{\alpha}}\, e^{\alpha/4}\{\mathrm{erf}((1+\lambda+\mu)\sqrt{\alpha})-\mathrm{erf}((1+M2)\sqrt{\alpha})\} \end{aligned} \tag{A.4}$$

REFERENCES

1. H.A.Bethe, Rev.Mod.Phys. 9 (1937) 69

2. T.Ericson, Adv.of Physics 9 (1960) 425

3. A.Bohr and B.Mottelson, Nuclear Structure, Vol.I and II (Benjamin, New York, 1969 , 1975)

4. V.S.Stavinsky, Sov.J.Part.Nucl. 3 (1972) 417

5. J.R.Huizenga and L.G.Moretto, Ann.Rev.Nucl.Sci. 22 (1973) 378

6. T.Ericson, Nucl.Phys. 6 (1958) 62

7. P.Decowski, W.Grochulski, A.Marcinkovksi, K.Siwek and Z.Wilhelmi, Nucl.Phys. A110 (1968) 129

8. A.V.Ignatyuk and Y.N.Shubin, Sov.J.Nucl.Phys. 8 (1969) 660

9. L.G.Moretto, Nucl.Phys. A182 (1972) 641

10. A.S.Jensen and Jens Damgaard, Nucl.Phys. A203 (1973) 378

11. L.G.Moretto, Nucl.Phys. A185 (1972) 145

12. T.Dössing and A.S.Jensen, Nucl.Phys. A222 (1974) 493

13. B.B. Back, Ole Hansen, H.C.Britt, J.D.Garrett and B.Leroux, Proc. Third IAEA Symp.on Physics and Chemistry of Fission, Rochester 1973, p.3

14. S.Bjørnholm, A.Bohr and B.Mottelson, Proc.Third IAEA Symp on Physics and Chemistry of Fission, Rochester 1973, p.367

15. J.R.Huizenga, A.N.Behkami, R.W.Atcher, J.S.Sventek, H.C.Britt and H.Freiesleben, Nucl.Phys. A223 (1974) 589

16. A.Gavron, H.C.Britt, E.Konecny, J.Weber and J.B.Wilhelmy, Phys.Rev. C13 (1976) 2374

17. A.V.Ignatyuk, IAEA-190, Proc.Consultant Meeting on Nuclear Theory in Neutron Nuclear Data Evaluation, Trieste, 1975, p.211

18. A.V.Ignatyuk, K.K.Istekov, and G.N.Smirekin, Sov.J.Nucl.Phys.30, 1979) 626

20. J.P.Elliott, Proc.Roy.Soc. A245 (1958) 128

21. M.Harvey, Adv.Nucl.Phys.1 (1968)

22. J.P.Draayer, D.L.Pursey and S.A.Williams, Nucl.Phys. A119 (1968) 577

23. I.Kanestrøm, Nucl.Phys.83 (1966) 380, A91 (1967) 199

24. M.Harvey, Phys.Lett. 40B (1972) 77

25. M.Baranger and K.Kumar, Nucl.Phys. A110 (1968) 490

26. D.R.Bes and R.A.Sorensen, Adv. in Nucl.Phys. 2 (1969)

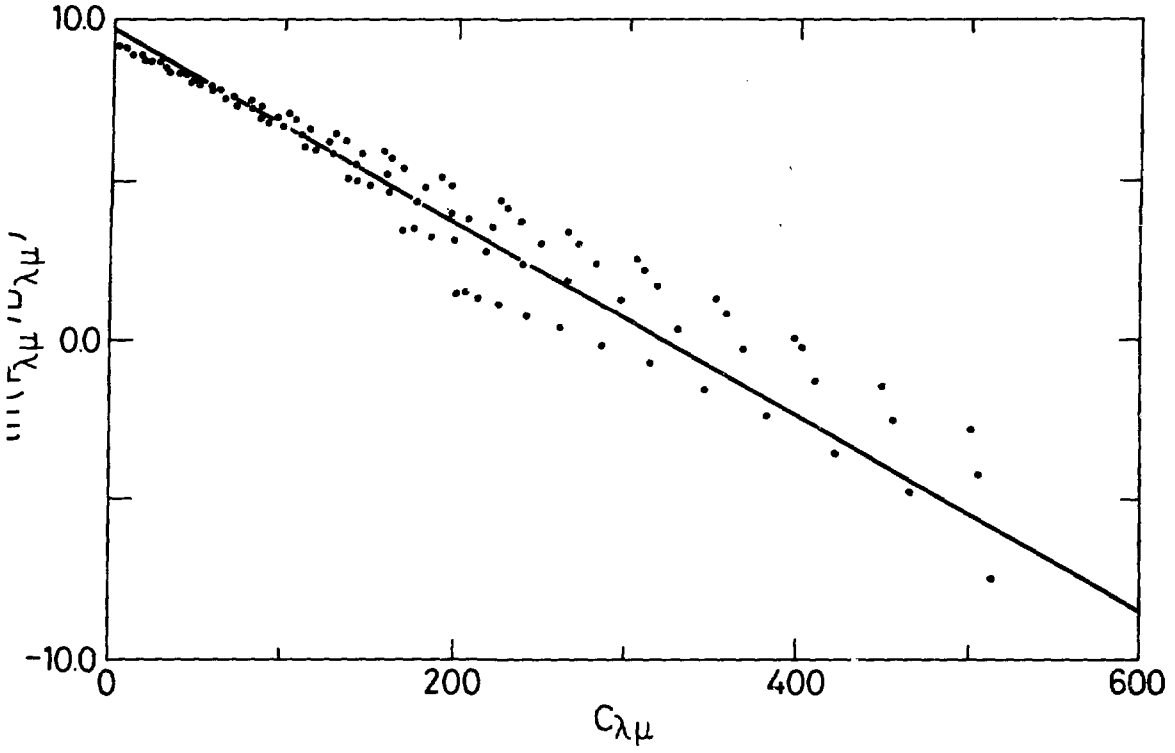

Fig. 1 The degeneracy of the occuring SU3-quantum numbers (λ,μ) divided by the dimension of the set as function of the expectation value $C_{\lambda\mu}$ of the Casimir operator. The line is the approximation described by the distribution function $P_{\lambda\mu}$ from eq.(11).

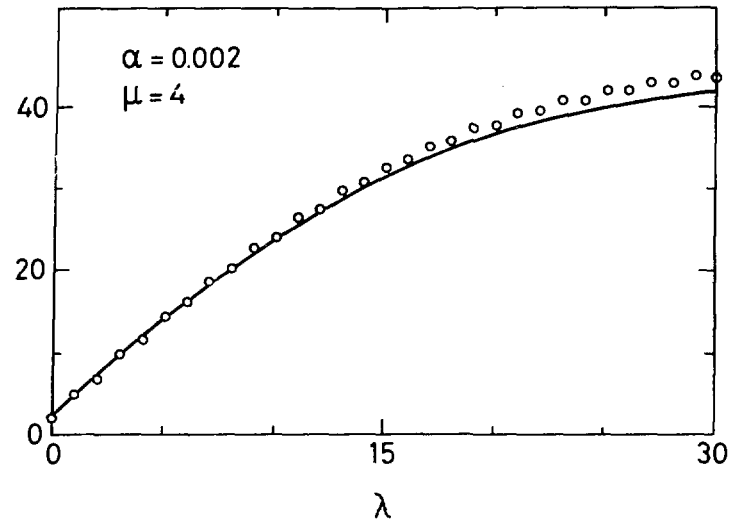

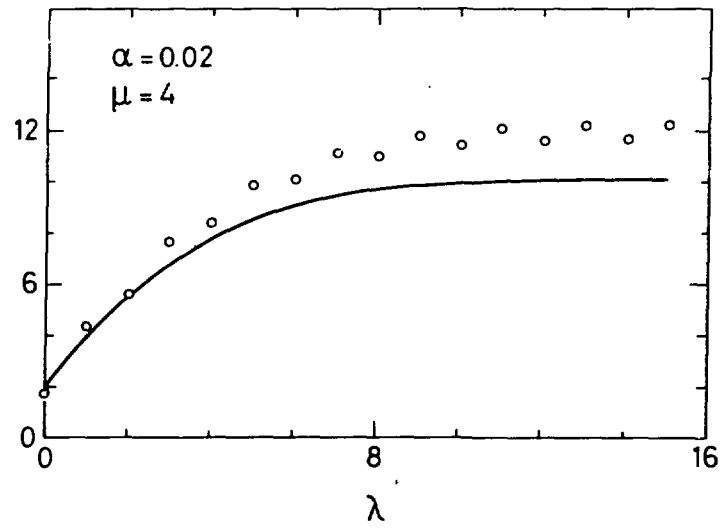

Fig. 2 The angular momentum partition function as function of λ for fixed μ and $\alpha=3\beta\kappa_R$. The circles are the exact values (see eq.(A.1)) and the line is the approximation G of eq.(A.4).

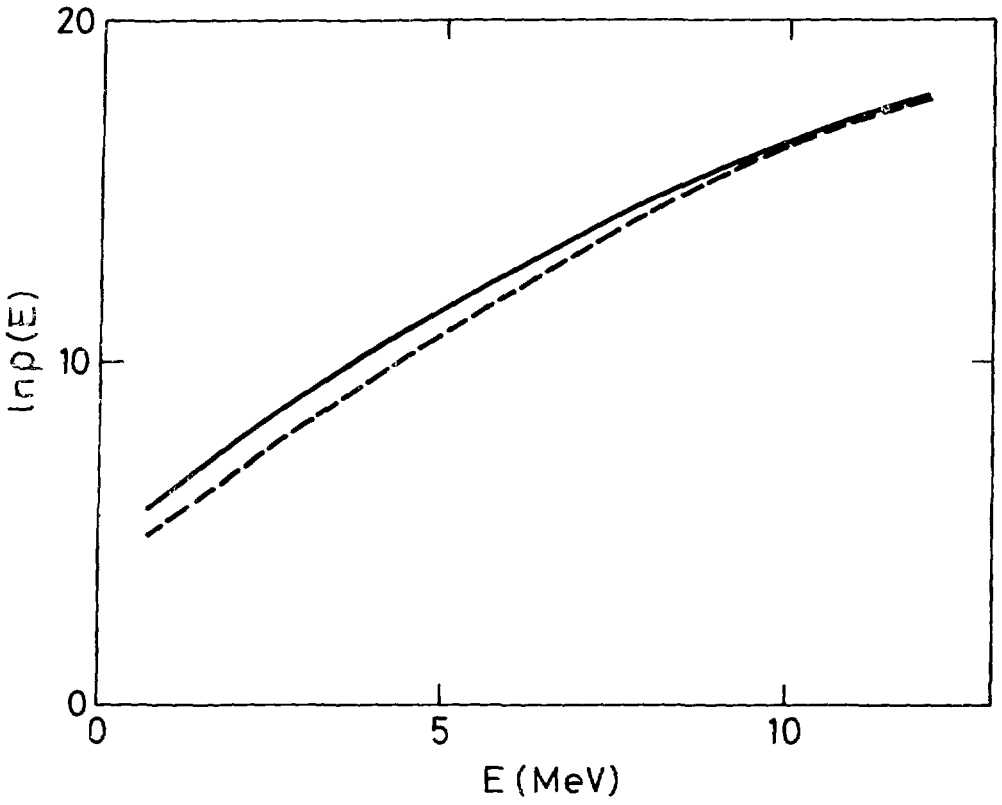

Fig. 3 The SU3-level density as function of mean excitation energy for mass number A=88, 8 particles in the N=4 oscillator shell with κ=0.004645 MeV. The full line is the exact calculation, and the dashed line is obtained with the distribution function $P_{\lambda\mu}$ as the only approximation. Applying all the approximations described and used in the text leads to a curve which on this figure can not be distinguished from the dashed line.

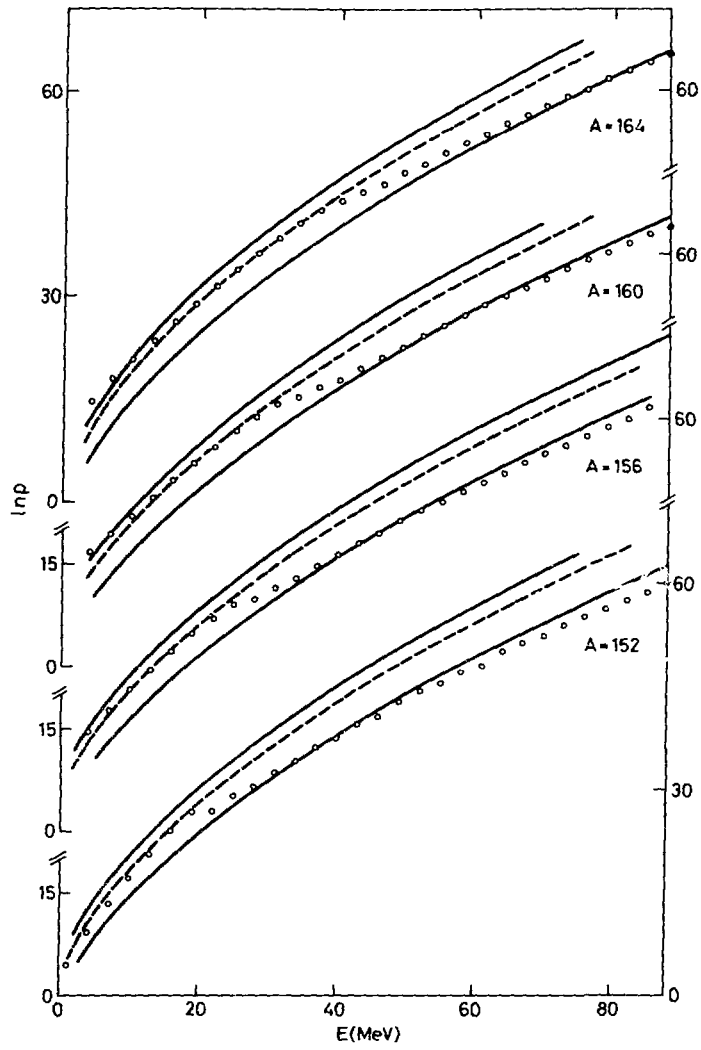

Fig. 4 The SU3-level density (circles) as function of energy for four nucleon numbers A. The three lines for each nucleus are ρ_1 (spherical), ρ_2 (axial- and R-symmetry) and ρ_6 (triaxial for quadrupole degrees of freedom). The strenght $\frac{1}{2}\kappa_R$ is equal to the selfconsistent value from eq.(46a). The SU3 ground states of A=152 and 164 are axially symmetric and those of A=156 and 160 are triaxial.

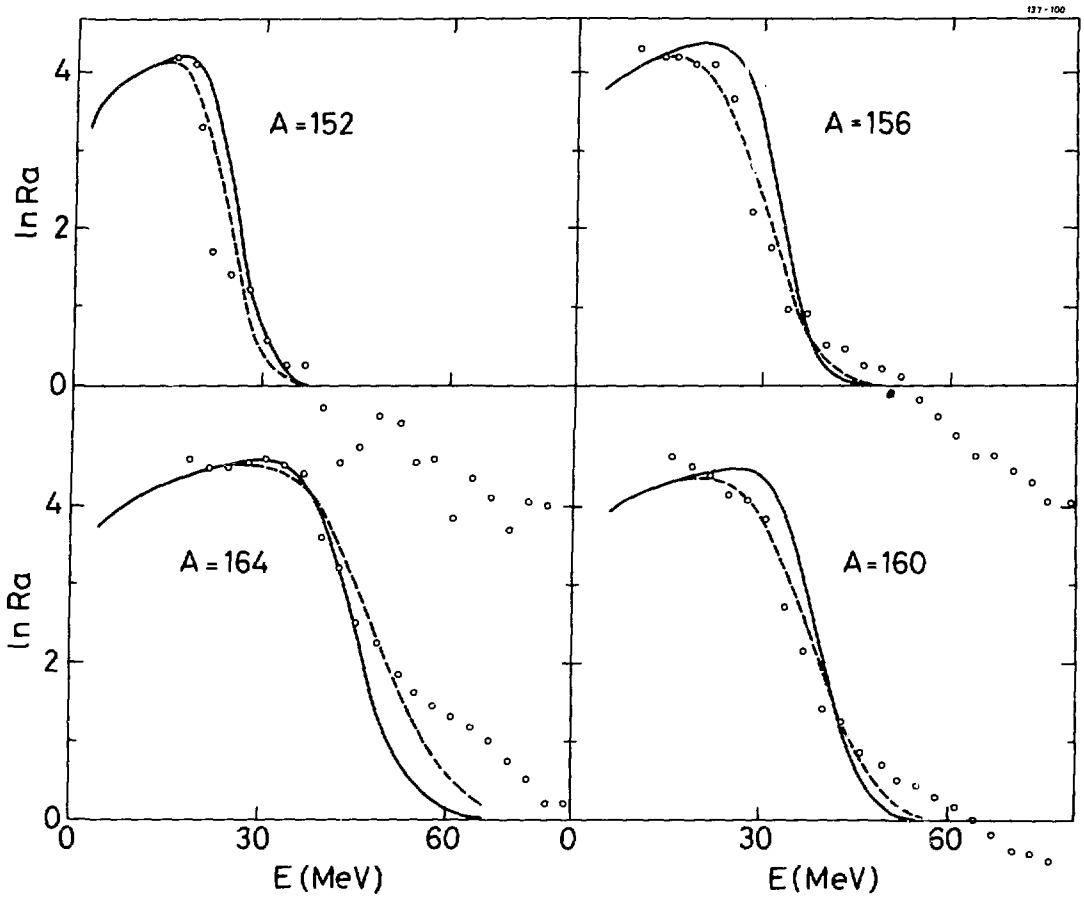

Fig. 5 Energy dependence of the axial rotational enhancement factor (circles) for the four nuclei in fig. 4. The full line is the parametrization from eqs.(47)-(50) with the average parameters. The dashed line is the same parametrization with the following individual parameters in MeV from A=152-164: (γ_a, ν_a)=(15.5, 0.8), (16.9, 0.8), (15.9, 0.8), (14.0, 0.8).

REVIEW OF RECENT PHENOMENOLOGICAL APPROACHES TO THE DESCRIPTION OF NUCLEAR LEVEL DENSITIES

V.S. Ramamurthy, S.K. Kataria and S.S. Kapoor

Nuclear Physics Division
Bhabha Atomic Research Centre
Trombay, Bombay 400085, India

ABSTRACT

The phenomenological approaches to the nuclear level density problem are discussed in the light of recent numerical calculations based on sophisticated microscopic models of nuclei. Recent semiempirical prescriptions to take into account shell and pairing corrections, collective effects and finite size and shape corrections to nuclear level densities are reviewed. Uncertainties and possible improvements are also discussed.

1. INTRODUCTION

In the last few years, a number of semi-empirical formulae [1-8] have been proposed for the calculation of the nuclear level densities, which take into account the nuclear shell, pairing and collective effects. While the different formulae idffer in detail, all of these exploit the possible separation of the nuclear thermodynamic properties into a smooth macroscopic part and a shell and pairing contribution in analogy with a similar separation [9] in the calculations of nuclear masses and deformation potential energies. Analyses of available experimental data have shown that the proposed formulae can explain most of the systematics in the available neutron resonance spacing data and excitation functions. These formulae contain an important feature [10,11], that the shell and pairing effects on the nuclear level densities disappear at moderate excitation energies, and in a hot nucleus the thermodynamic properties are determined by a smooth macroscopic part alone. Another feature brought out by these formulae is that the shell independent part of the level densities also exhibits

significant deviations from the conventional linear dependence of the level density parameter on the mass number of the nuclei, arising from the finite size of the nuclei, finite binding of the nucleons in nuclei and the diffuseness of the nuclear surface. We present here a comparative review of the different semi-empirical level density formulae proposed in the recent years incorporating both the local nuclear structure effects, namely shell and pairing corrections and the global mass, charge and deformation dependences.

2. WHY PHENOMENOLOGY?

In the past, there has been considerable success in accounting for the thermodynamic properties of excited nuclei on the basis of numerical calculations starting from the single-particle spectrum given by a shell model calculation [12-17]. This approach takes into account in a natural way the influence of both shell and pairing effects and also their dependence on the excitation energy. However, for practical applications there exist a few inherent drawbacks in this approach. First ofcourse, is the requirement of detailed shell model calculations for all nuclei, resulting in a considerable computational effort. While this in itself is not a big constraint, because of a number of single particle level schemes currently available in literature and easy accessibility of fast computers, this is a step which one will like to gladly dispense with for routine calculations. A more intrinsic drawback of microscopic calculations is as follows: In all these calculations, the quantity on which the calculated level density crucially depends is the density of single particle states near the Fermi level. This is not a quantity which is crucially adjusted in any calculation of shell model energy level schemes. In fact, differences to the extent of 10-20% are known to exist between the calculated average single particle state density near the Fermi level for the various level schemes currently being used in literature for the calculation of nuclear shell correction energies and level densities. Even the ground state shell correction energies evaluated from different single particle level schemes are found to be appreciably different. A similar dependence of the calculated level density parameters on the nucleon-nucleon effective interaction used in a self-consistent modified Thomas-Fermi calculation has been demonstrated by Barranco and Treiner [18]. It is therefore necessary to adopt a normalization procedure which ensures that the structure independent part of the calculated level densities are consistent with a macroscopic model estimate and the structure dependent part is consistent with the experimental ground state shell and pairing corrections. Another objection which can be raised against these microscopic calculations of level densities is that they are carried out in the independent particle model approximation and therefore do not

include effects arising from coherent motion of nucleons of a collective nature. At present, therefore, one cannot fully rely on these microscopic calculations of level densities but allow for some parametric adjustments to fit the experimental level densities. Alternately, one can look for simpler phenomenological descriptions which take into account, to the necessary extent, the main features of the above microscopic calculations while remaining sufficiently simple and convenient for practical applications. Some of the well known experimental features of nuclear level densities are their extremely rapid increase with excitation energy, dependence on nuclear shell effects and odd-even effects. New features which have been brought out by the microscopic theories are the excitation energy dependence of shell and pairing effects and an enhancement of the level densities due to collective rotations and vibrations of nuclei, so well known in the structure of low lying nuclear levels.

3. THE MODEL

The statistical properties of excited nuclei are to a large extent similar to those of a degenerate ideal Fermi gas as has been demonstrated by the success of the model in describing excitation functions, evaporation spectra etc. [12-17]. Simple analytical relations for the density of states $\omega(E_x)$ and for the density of levels $\rho(E_x, I)$ of a nucleus with a given excitation energy E_x and angular momentum I, have been obtained in the framework of the above model [11,12]. On the assumption that the single particle states are equispaced with a density g, one has

$$\omega(E_x) = \frac{\sqrt{\pi}}{12} \frac{1}{\underline{a}^{1/4} E_x^{5/4}} \exp\left(2\sqrt{\underline{a} E_x}\right) \tag{1}$$

$$\rho(E_x, I) = \frac{(2I+1)}{2\sqrt{2\pi}\,\sigma^3} \omega(E_x) \exp\left[-\frac{I(I+1)}{2\sigma^2}\right] \tag{2}$$

where $\underline{a} = (\pi^2/6) g$ and σ^2 is known as the spin cut off parameter. One also has for the other thermodynamic functions of hthe nucleus,

$$E_x = \underline{a} T^2$$

$$S = 2\underline{a} T$$

$$\sigma^2 = m_f^2 g T \tag{3}$$

where T is the thermodynamic temperature, S is the entropy, and

m_f^2 is the average value of the square of the projection of the angular momentum of the single particle states lying close to the Fermi energy, which can also be associated with the moment of inertia of the nucleus $\mathcal{J}_0$ by the relation $\mathcal{J}_0 = g m_f^2$. In the framework of the Fermi gas model, based on the semi-classical approximation, the parameter a is related to the mass number A of the nucleus by

$$\underline{a} = 2\left(\frac{\pi}{3}\right)^{4/3} \frac{m r_0^2}{\hbar^2} A$$
$$\text{and} \quad \mathcal{J}_0 = \frac{2}{5} m r_0^2 A^{5/3} \tag{4}$$

where m is the nucleon mass and r_0 is the radius parameter. Nuclear shell and pairing effects and collective effects result in deviation of the level densities from those calculated as above. These are the deviations which are of current interest and form the focal point of all recent phenomenological formulae.

For the general case of many Fermion system whose partition function is known, the state density can be expressed by the relation [12,17]

$$\omega = \frac{\exp(S)}{(2\pi)^{3/2} D^{1/2}} \tag{5}$$

where S is the thermodynamic entropy and D is a determinant of second derivatives of the logarithm of the grand partition function. Both S and D are dependent on the thermodynamic temperature of the nucleus and the density of single particle states near the Fermi energy. Inclusion of shell and pairing corrections and finite size corrections usually involve a redetermination of the entropy S and the coefficient D. On the otherhand, collective effects are expected to manifest themselves as enhancement factors of the calculated level densities. One can therefore write in general,

$$\rho_{obs}(E_x, I) = \rho_{shell+pairing}(E_x, I)\, K_{coll} \tag{6}$$

Additional enhancement factors can be introduced with each additional loss of symmetry of the nuclear shape [19,20,21]. We discuss below phenomenological prescriptions proposed for the calculation of the different terms in the above formula.

4. NUCLEAR SHELL EFFECTS ON LEVEL DENSITIES

One of the well known deviations of experimental level densities from the predictions of the Fermi gas model is that

arising from nuclear shell effects. Early in 1956, Newton [22] analysed available neutron resonance spacing data and showed that not only the fitted level density parameters show appreciable deviations from the expected linear dependence on the mass number but also the deviations could be correlated to the density of single particle states near the Fermi level. A subsequent analysis by Cameron and coworkers [23,24] further demonstrated that the deviations from the Fermi gas model are correlated to the ground state shell correction energies. Based on this observation they proposed a semi-empirical formula of nuclear level densities which has been commonly used in the past for reaction rate calculations. In retrospect, however, this formula missed an important physical feature, namely, the excitation energy dependence of nuclear shell effect on the thermodynamic properties of nuclei [10,11]. The recently developed semi-empirical formulae essentially incorporate this feature by treating the level density parameter $\underline{a}$ as dependent on both the ground state shell correction energy and the excitation energy of the nucleus. We discuss below two prescriptions, one by Ignatyuk et al [1] and the other by the present authors [3,4], the other investigations in this area being essentially minor modifications of either one of these. Both of these start from the now well established feature of microscopic shell model calculations of the thermodynamic properties of excited nuclei that a plot of the square of the calculated entropy versus excitation energy shows an asymptotic behaviour such that at high enough excitation energies, it exhibits the linear relationship of the Fermi gas model provided the excitation energy is measured from an effective Liquid drop model ground state [10,11,25]. Defining an effective level density parameter $\underline{a}^{eff} = S^2/(4E_x)$ to describe the energy dependence of the parameter, Ignatyuk et al [1] use the formula

$$\underline{a}^{eff}(E_x) = \underline{a}^{LDM}\left[1 - f(E_x)\,\delta W/E_x\right] \qquad (7)$$

where $\underline{a}^{LDM}$ is the asymptotic value of $\underline{a}$ at high excitation energies and δW is the ground state shell correction energy. The dimensionless function $f(E_x)$ determines the trend of the excitation energy dependence of $\underline{a}^{eff}$ at lower excitation energies.

$$f(E_x) \rightarrow 1 \quad \text{as} \quad E_x \rightarrow \infty$$
$$f(E_x)/E_x \rightarrow \text{Constant} \quad \text{as} \quad E_x \rightarrow 0 \qquad (8)$$

From calculations of $f(E_x)$ carried out for a number of nuclei, an approximate relation of the form

$$f(E_x) = 1 - \exp(-\gamma E_x) \tag{9}$$

was deduced as a universal behaviour. A value of $\gamma = 0.054$ was deduced by fitting the formula to available experimental neutron resonance spacing data. Thus the main improvement of Ignatyuk et al [1] is the introduction of an excitation energy dependence of the level density parameter, a feature which was missing in earlier formulae. It should be pointed out here that the proper asymptotic excitation energy dependence of the square of the thermodynamic entropy of a nucleus is

$$S^2 = 4\,\underline{a}^{LDM}(E_x - \delta W) \tag{10}$$

and not

$$S^2 = 4a^{eff}E_x \qquad \text{where} \quad \underline{a}^{eff} = \underline{a}^{LDM}\left(1 - \frac{\delta W}{E_x}\right) \tag{11}$$

as can be seen from microscopic calculations for model single particle level schemes and shell model level schemes [10,11,25]. However, this different is perhaps of little consequence in level density calculations for practical applications. An alternate form which exhibits a better asymptotic behaviour is the back shift Fermi-gas model proposed by Hurwitz and Bethe [26]. A global fit to the neutron resonance data has also been attempted by Dilg et al [27] incorporating an energy shift. However, an excitation energy independent shift is valid only asymptotically and it is necessary to have an excitation energy dependent shift to extend the validity in the low excitation energy region also. One can write in such a case

$$S^2 = 4a^{LDM}\left[E_x - \delta W\, h(E_x)\right] \tag{12}$$

with $h(E_x) \rightarrow 1$ as $E_x \rightarrow \infty$

As can be seen later, the function $h(E_x)$ can be identified with the function $f(E_x)$ introduced by Ignatyuk et al. In an alternate approach, the present authors [3,4] start from a Fourier expansion of the shell fluctuations in the single particle level density

$$\begin{aligned} G(\epsilon) &= g(\epsilon) + \delta g(\epsilon) \\ &= g(\epsilon) + \sum_m g_m \cos(m\omega\epsilon - \phi_m) \end{aligned} \tag{13}$$

where ω is a parameter characteristic of the wavelength of shell oscillations and therefore of the major shell spacing.

For the range of temperatures of interest in nuclear reaction analysis, it was shown that g(E) can be well approximated by a constant value g_o and one can neglect all terms with $m > 1$. The following approximate expressions were obtained for the entropy and excitation energy as a function of the thermodynamic temperature of the nucleus.

$$S = \frac{1}{3}\pi^2 g_o T + \frac{\Delta_{gs}}{T}\left[\frac{\pi^2\omega^2T^2 \cosh \pi\omega T}{\sinh^2 \pi\omega T} - \frac{\pi\omega T}{\sinh \pi\omega T}\right]$$

$$= 2\underline{a}^{LDM} T + \frac{\Delta_{gs}}{T} F \qquad (14)$$

$$E_x = \frac{1}{6}\pi^2 g_o T + \Delta_{gs}\left[\frac{\pi^2\omega^2T^2 \cosh \pi\omega T}{\sinh^2 \pi\omega T} - 1\right] \qquad (15)$$

$$= \underline{a}^{LDM} T^2 + \Delta_{gs} G$$

where

$$\underline{a}^{LDM} = \frac{\pi^2}{6} g_o$$

From the known mass dependence of the major shell spacing in nuclei proportional to $A^{-1/3}$ a mass dependence of the parameter ω of the form $\omega = \omega_o A^{1/3}$ was also introduced. Least square fit to experimental neutron resonance spacing data results in a value of $\omega_o = 0.185$ MeV^{-1} and $\underline{a}^{LDM} = 0.14A$ MeV^{-1}. This value of ω_o corresponds to a major shell spacing of about $34.5A^{-1/3}$ MeV in good agreement with the values used in literature [28,29]. The value of $\underline{a}^{LDM} \simeq A/7$ is also close to the values generally used in literature. Typical mean square deviations of the calculated level spacings from the experimental neutron resonance spacing values defined as

$$\chi^2 = \sum (\ln D_{th}/D_{exp})^2/N$$

for about 100 spherical nuclei is of the order of 0.4, indicating an average discrepancy of a factor 2 between experiment and calculation. The prescriptions of both Ignatyuk et al [1] and the present authors incorporate similar features namely, the excitation energy dependence of the thermodynamic properties of nuclei, in particular, the washing out of shell effects at high excitation energies, but in different ways. It is therefore of interest to relate the two parameters introduced by Ignatyuk et al and by the present authors respectively. For this, we write the $\underline{a}^{eff}$ values as defined by Ignatyuk et al in terms of the $S - \bar{E}_x$ relationship given by us.

$$\underline{a}^{eff} = S^2/(4E_x)$$

$$= \left[2\underline{a}^{LDM} T + \frac{\Delta_{gs}}{T} F\right]^2 / \left[4(\underline{a}^{LDM} T^2 + \Delta_{gs} G)\right] \qquad (16)$$

$$\simeq \underline{a}^{LDM}\left[1+\frac{\Delta_{gs}}{E_x}(F-G)\right]$$

Thus

$$f(E_x)=F-G=1-\frac{\pi\omega T}{\sinh \pi\omega T}\simeq\frac{\pi^2\omega^2T^2}{6}+\cdots \qquad (17)$$

Comparing with eq.(9)

$$\gamma E_x=\frac{\pi^2\omega^2T^2}{6}\simeq\frac{\pi^2\omega^2}{6}\frac{E_x}{\underline{a}^{LDM}}$$

$$\gamma=\frac{\pi^2\omega^2}{6}\frac{1}{\underline{a}^{LDM}}\simeq 0.4\,A^{-1/3} \qquad (18)$$

The value of γ thus obtained for nuclei in the actinide region are indeed close to the value obtained by Ignatyuk et al [1]. But the above relation in addition brings out a weak mass dependence of the parameter γ. A similar mass dependence of the parameter γ has also been obtained by Schmidt et al [8]. On the assumption that the influence of major shell effects is determined by the ratio of the average single particle energy difference between shell closures at the Fermi level and the nuclear temperature, they obtain

$$\frac{1}{\gamma}\simeq\frac{0.4}{\underline{a}^{LDM}}A^{4/3}$$

$$\gamma\simeq 0.35\,A^{-1/3} \qquad (19)$$

One can therefore conclude that in the Ignatyuk's formalism, it is perhaps necessary to include a weak mass dependence of the form $\gamma=\gamma_0 A^{-1/3}$ in a least square determination of the parameters, and then the two formalisms of Ignatyuk et al and of the present authors would have similar physical features. By a similar consideration, it is also possible to relate the function $h(E_x)$ of eqn.12, to the parameters of Ignatyuk et al and Kataria et al. By definition,

$$h(E_x)=\frac{1}{\delta W}\left[E_x-\frac{S^2}{4\,\underline{a}^{LDM}}\right]$$

$$=\frac{1}{\delta W}\left[\underline{a}^{LDM}T^2+\Delta_{gs}G-\frac{2\underline{a}^{LDM}T+\frac{\Delta_{gs}}{T}F}{4\,\underline{a}^{LDM}}\right]$$

$$= F - G \equiv f(E_x)$$

Thus the energy dependent function $h(E_x)$ can be identified as the function $f(E_x)$ introduced by Ignatyuk et al on (F-G) introduced by Kataria et al. This simple modification of the back shifted Fermi-gas model will extend the range of validity of the model to low excitation energy region also.

5. EVEN-ODD EFFECTS

Apart from nuclear shell effects, another well known feature of nuclear level densities is the odd-even effect. The experimental level densities of even nuclei are systematically lower than those of their odd neighbours. A very early prescription to incorporate this feature in level density calculations is to use an effective excitation energy defined as

$$E_x^* = E_x - \begin{cases} \delta_Z + \delta_N & \text{for even-even nuclei.} \\ \delta_Z \text{ , } \delta_N & \text{for nuclei with even Z or N.} \\ 0 & \text{for odd-odd nuclei.} \end{cases}$$

in the relations of the Fermi gas model. δ_Z and δ_N are the even-odd differences in the nuclear masses [23]. It is well known that residual interactions of the correlation type, in much the same way as the correlation interactions of electrons in a superconductor, are responsible for the observed even-odd mass differences. The same mathematical apparatus has also been employed in studying the statistical properties of excited nuclei [12-14,30]. The most characteristic feature of the superfluid model is the existence of a critical temperature at which the nucleus undergoes a phase transition from the superconducting to the normal state. Above the critical temperature, the thermodynamical properties are identical to those of a non-interacting system with an effective excitation energy $E_x^* = E_x - E_c$ where E_c is the ground state condensation energy which must be expended in order to destroy the pair correlations in a cold system. Though microscopic calculations of condensation energies yield results strongly dependent on the number of nucleons and on the single particle level scheme used, the energy difference between adjacent odd and even systems is about 1 MeV, in reasonable agreement with the phenomenological shifts δ_Z and δ_N. There however remains some ambiguity in defining the reference system as the odd-odd or even-even system and may influence the determination of the parameters of the model.

Below the critical temperature, the behaviour of the thermodynamic functions differs considerably from the above simplified picture. Some experimental evidence for the presence of two regions with different excitation energy dependence of the thermodynamic functions has been obtained by Ignatyuk et al in the fission channel level densities [31]. While, even from the theoretical point of view the exact nature of the phase transition from the superconducting to the normal phase is not known, simple analytical prescription have been proposed to mock the energy dependence of the thermodynamic functions in the superconducting phase also [30]. One can therefore say on the whole, that even-odd effects in level densities can be reasonably incorporated in phenomenological level density expressions, though the microscopic basis for this is only at present qualitative.

6. MACROSCOPIC SYSTEMATICS OF LEVEL DENSITY PARAMETERS

An important feature brought out by the recent phenomenological formulae is that in addition to excitation energy dependent shell and pairing corrections, even the macroscopic part of the level density parameters exhibits deviations from the conventional linear dependence on the mass number of the nuclei. In particular, an $A^{2/3}$ dependence, arising from the finite size of the nuclei, is often looked for. However, there is some ambiguity in literature in the determination of the coefficient of the $A^{2/3}$ term from least square fits to the experimental data. While the present authors [3] extract a negative coefficient for the $A^{2/3}$ term, Ignatyuk et al [21] conclude that the statistical significance of the data is not sufficient to uniquely determine the coefficient, while not being inconsistent with a positive $A^{2/3}$ term, indicated by simple models of the distribution of single particle levels in potential wells. Kataria and Ramamurthy [32] have studied the distribution of energy eigenvalues in realistic Woods-Saxon potential wells and showed that there is a complicated interplay of various effects arising from the finite size of the nucleus, binding of the nucleons in nuclei and the diffuseness of the nuclear surface leading to the observed dependence of the level density parameter $\underline{a}^{LDM}$ on the mass number of the nucleus. A general leptodermous expansion for the density of single particle levels in thin-skinned potential wells has also been investigated by Ramamurthy et al [33] and used to study the various corrections to the macroscopic level density parameters. It was shown that for a determination of the $A^{2/3}$ term, it is necessary to make explicit assumptions regarding the mass and charge dependence of the parameters of the potential wells such as the depth, the radius and the surface diffuseness. With droplet model potential

parameters [32,33], the calculated level density parameter values were found to be still lower than the experimental values. Recently Toke and Swiatecki [34] have obtained finite size corrections to the macroscopic part of the level density parameters making use of the Thomas-Fermi model of the nucleus. However, it has been showed by Ramamurthy et al [33] that not only it is necessary to add semi classical corrections to these calculations, but one should also incorporate in these calculations the mass and charge dependence of the parameters of the matter distributions such as the central density and the surface diffuseness parameter. A simple dependence on powers of $A^{1/3}$ is perhaps an over simplification. The results of Kataria and Ramamurthy [32] obtained from a study of levels in realistic Woods-Saxon potentials clearly demonstrate this point and have even lead to the postulation of a separation energy dependence of a^{LDM} [5,32]. Such a dependence also leads to interesting isospin dependence of the level density parameters [32,35]. Further investigations along these lines are required to clearly bring out the mass and charge dependence of the macroscopic part of the level density parameter.

7. COLLECTIVE CONTRIBUTIONS TO NUCLEAR LEVEL DENSITIES

It is well known that nuclei exhibit near their ground state many low energy collective levels, rotational and vibrational. In general, each intrinsic level may therefore be expected to give rise to a band of collective levels and the total level spectrum for a given angular momentum is to be obtained as a sum over a set of intrinsic states. Such an analysis has been performed by Ericson [19] and Bjornholm et al [20] and shown that in nuclei having static deformations in their ground state, the level densities are enhanced over those for spherical nuclei because of the contributions from the available rotational degrees of freedom. For the spherical nuclei themselves, the availability of the vibrational degree of freedom enhances the level densities over those calculated on the basis a static shell model. Phenomenological determination of the coefficients of the level density increase K_{rot} and K_{vib} due to the collective modes in excited nuclei is usually based on the adiabatic assumption [20].

$$K_{rot} = \mathcal{J}_{\perp} T \qquad \text{for deformed nuclei}$$

$$= 1 \qquad \text{for spherical nuclei}$$

$$K_{vib} = \exp\left[1.7\left(\frac{3 m_0 A\, C_{drop}}{4\pi\, \sigma_{drop}\, C}\right)^{2/3} T^{4/3}\right]$$

where $\mathcal{J}_\perp$ is the perpendicular moment of inertia, T is the temperature of the excited nucleus, σ_{drop} is the coefficient of the surface tension in the liquid drop model, and the ratio c/c_{drop} characterizes the difference between the restoring force coefficients of the excited nucleus and the corresponding coefficients of the liquid drop model [21]. K_{rot} ranges from 45 to 65 for nuclei with A values ranging from 150 to 250, rigid body moment of inertia and excitation energies equal to the neutron binding energy. While there have been some indications from microscopic shell model calculations of level densities [36-38] for such collective enhancements, the inherent uncertainties of such calculations mentioned earlier, and the results of phenomenological analysis [1,3] do not substantiate collective enhancements of a magnitude indicated by the above equations. The problem is further complicated by the expected but as yet unknown excitation energy dependence of the effect. This aspect of the problem requires further investigation both from the theoretical point of view and experimental analysis.

8. SUMMARY

The semi-empirical nuclear level density formulae proposed in the last few years incorporate several new features not contained in earlier formulae, the most important ones of these being the excitation energy dependent shell and pairing corrections, enhancement of level densities due to the collective degrees of freedom, and corrections arising from the finite size of nuclei. The need for these new features have come partly from the available experimental data and partly from theoretical models. In spite of their simplicity, these formulae contain all the essential features of the detailed microscopic calculations. The formulae, however, do involve a few free parameters, whose values can not, at present, be obtained from theoretical models alone, without recourse to a comparison to the experimental data. Since the experimental data are so incomplete, confined to a narrow range of nuclei around the beta stability line and a narrow range of excitation energies, there is a need for reliable theoretical estimates of the parameters of the formulae. Several investigations are currently in progress along these lines.

REFERENCES

1. A.V. Ignatyuk, G.N. Smirenkin and A.S. Tishin, "Phenomenological description of the energy dependence of the level density parameter", Yad. Fiz. 21, 485 (1975) [Sov. J. Nucl. Phys. 21, 255 (1975)].

2. A.V. Ignatyuk, "Statistical characteristics of excited nuclei", in Proc. IAEA Consultants meeting on the use of Nuclear Theory in Neutron Nuclear Data Evaluation, International Centre for Theoretical Physics, Trieste, Italy, Dec. 8-11, 1975 IAEA-190. Vol.1, 211 (1976).

3. V.S. Ramamurthy, S.K. Kataria and S.S. Kapoor, "On a new semiempirical nuclear level density formula with shell effects", in Proc. IAEA Consultants meeting on the use of Nuclear Theory in Neutron Nuclear Data Evaluation, International Centre for Theoretical Physics, Trieste, Italy, Dec.8-11, 1975, IAEA-190, Vol.2, 117 (1976).

4. S.K. Kataria, V.S. Ramamurthy and S.S. Kapoor, "Semi-empirical nuclear level density formula with shell effects", Phys. Rev. C18, 549 (1978).

5. S.K. Kataria and V.S. Ramamurthy, "Macroscopic level density parameters of nuclei", Phys. Rev. C22, 2263 (1980).

6. A.S. Jensen and J. Sandberg, "Analytic nuclear level density formula with shell and pairing effects", Phys. Scripta. 17, 107 (1978).

7. W. Reisdorf, "Analysis of fissionability data at high excitation energies. I. The level density problem", Z. Phys. A300, 227 (1981).

8. K.H. Schmidt, H. Delagrange, J.P. Dufour, N. Carjan and A. Fleury, "Influence of shell structure and pairing correlations on the nuclear state density" Z. Phys. A308, 215 (1982).

9. V.M. Strutinski, "Shell effects in nuclear masses and deformation energies", Nucl. Phys. A95, 420 (1967).

10. V.S. Ramamurthy, S.S. Kapoor and S.K. Kataria, "Excitation energy dependence of shell effects on nuclear level densities and fission fragment anisotropies", Phys. Rev. Letters 25, 386 (1970).

11. V.S. Ramamurthy, S.S. Kapoor and S.K. Kataria, "Shell effects on nuclear level densities", Phys. Rev. C5, 1124 (1972).

12. T. Ericson, "The statistical model and nuclear level densities", Adv. Phys. 9, 425 (1960).

13. H. Bethe, "Nuclear Physics B: Nuclear Dynamics, Theoretical", Rev. Mod. Phys. 9, 69 (1937).

14. J.R. Huizenga and L.G. Moretto, "Nuclear level densities", Ann. Rev. Nucl. Sci. 22, 427 (1972).

15. V.S. Ramamurthy, "Theories and approximations of nuclear level densities", Nuclear Theory for Applications, International Centre for Theoretical Physics, Trieste, (1980) 186,

16. A. Bohr and B.R. Mottelson, Nuclear Structure, Vol.II, New York, Benjamin, 1975.

17. J.W. Lynn, The Theory of Nuetron Resonance Reactions, Clarendon Press, Oxford, 1975.

18. M. Barranco and J. Treiner, "Self-consistent description of nuclear level densities", Nucl. Phys. A351, 269 (1981).

19. T. Ericson, "On the level density of deformed nuclei", Nucl. Phys. 6, 62 (1958).

20. S. Bjornholm, A. Bohr and B.R. Mottelson, "Role of Symmetry of the nuclear shape in rotational contributions to nuclear level densities", Physics and Chemistry of fission, Rochester, IAEA (1973) Vol. I, 367.

21. A.V. Ignatyuk, K.K. Istekov and G.N. Smirenkin, "The role of collective effects in the systematics of nuclear level densities", Yad. Fiz. 29, 875 (1979) /Sov. J. Nucl. Phys. 29, 450 (1979)/.

22. T.D. Newton, "Shell effects on the spacing of nuclear levels", Can. J. Phys. 34, 804 (1956).

23. A. Gilbert and A.G.W. Cameron, "A composite nuclear level density formula with shell corrections", Can. J. Phys. 43, 1446 (1965).

24. P.J. Brancazio and A.G.W. Cameron, "Relation between nuclear level density parameters and mass shell corrections", Can. J. Phys. 47, 1029 (1969).

25. P.B. Kahn and N. Rosenzweig, "Theory of nuclear level density for periodic independent-particle energy level schemes", Phys. Rev. 187, 1193 (1969).

26. H. Hurwitz and H.A. Bethe, "Neutron Capture Cross sections and level density", Phys. Rev. 81 898 (1951).

27. W. Dilg, W. Schantle, H. Vonach and M. Uhl, "Level density parameters for the backshifted Fermi gas model in the mass range $40 < A < 250$", Nucl. Phys. A217, 269 (1973).

28. P.A. Seeger and R.C. Perisho, Los Alamos Scientific Laboratory Repprt No. LA-3751 (unpublished).

29. P.A. Seeger and W.M. Howard, "Semiempirical atomic mass formula", Nucl. Phys. A238, 491 (1975).

30. A.V. Ignatyuk and Yu. N. Shubin, Izv. Akad. Nauk USSR, Ser. Fiz. 37, 1947 (1975) [Bull. USSR Acad. Sci. Ser. Phys. 37, 127 (1975)].

31. A.V. Ignatyuk, M.G. Itkis, V.N. Okolovich, G.N. Smirenkin and A.S. Tishin, "Fission of pre-actinide nuclei-Excitation functions for the (α,f) reaction", Yad. Fiz. 21, 1185 (1975) [Sov. J. Nucl. Phys. 21, 612 (1975)].

32. S.K. Kataria and V.S. Ramamurthy, "Macroscopic Systematics of nuclear level densities", Nucl. Phys. A349, 10 (1980).

33. V.S. Ramamurthy, M. Asghar and S.K. Kataria, "Mean distribution of single particle levels in thin-skinned potential wells and the macroscopic level density parameters of nuclei", Nucl. Phys. A398, 544 (1983).

34. J. Toke and W.J. Swiatecki, "Surface layer corrections to the level density formula for a diffuse Fermi gas", Nucl. Phys. A372 141 (1982).

35. J. Treiner, "Macroscopic nuclear level densities from Thermal Thomas-Fermi method", Workshop on semi classical methods in Nuclear Physics, Grenoble, March 18-20, 1981.

36. J.R. Huizenga, A.N. Behkami, J.S. Sventek and R.W. Atcher, "Comparison of neutron resonance spacings with microscopic theory for spherical nuclei", Nucl. Phys. A223, 577 (1973).

37. J.R. Huizenga, A.N. Bekhami, R.W. Atcher, J.S. Sventek, H.C. Britt and H. Freiesleben, "Comparison of neutron resonance spacings with microscopic theory for nuclei with static deformation", Nucl. Phys. A223, 589 (1973).

38. T. Dossing, A.S. Jensen, "Nuclear level densities with collective rotations included", Nucl. Phys. A222, 493 (1974).

LIMITS AND VALIDITY OF THE PHENOMENOLOGICAL GILBERT-CAMERON LEVEL DENSITY APPROACH

G. Reffo

E.N.E.A., Via Mazzini 2, 40138 Bologna (ITALY)

ABSTRACT

The level density models studied and the methods adopted for practical purposes are briefly reviewed, with special emphasis on the problem of pairing correction and spin distribution of p-h level density.

INTRODUCTION

The interest in high energy cross sections for medical and technological purposes has stimulated a renewed interest in level density studies.

Recently, a large amount of works have been carried out on this subject, that it is now particularly useful to start a critical comparison of results. To this end I will briefly review and comment the work done recently, which is specifically aimed at cross section calculation need.

We follow simultaneously several paths and use different approaches depending on the purpose.

For our applicative purposes, namely cross section calculations, the Gilbert-Cameron /1/ approach is used, supplied by the local systematics we have determined for all involved parameters /2/.

Nilsson model is also used to supply information on deformation dependence of the spin cut off /2/ and on the local systematics for the level density parameter, lacking experimental information.

Interacting Boson Approximation by Arima-Iachello /3/ can be used to fill gaps or to clarify doubtful situations in the discrete level region, when evaluation of very important cross sections is requested.

At the same time research efforts /4/, /5/ are carried on in the framework of the superconductivity model and by means of combinatorial calculations. We have investigated the important properties of the density of nuclear levels

and quasi-particle states as well as the possibility to fit by means of the usual simple formulae, very sophysticated theoretical calculations, which, hopefully, should not be involved in very complicated cross section codes.

THEORETICAL BACKGROUND AND RESULTS

Nilsson-BCS-Combinatorial Approach to Particle-Hole State Density

The recent developments in the understanding and formulation of preequilibrium reaction mechanisms should be coupled with reliable particle-hole (p-h) spin dependent level density $\rho_{ph}(E,J)$ in order to draw more meaningful conclusions.

As an example, angular distributions of emitted particles are very sensitive not only to exciton number, but also to spin distribution of exciton levels, see fig. 1.

Usual theoretical expressions for exciton level density are expected to work better for higher exciton numbers and at higher excitations where the underlying statistical assumptions are better satisfied. On the contrary, at lower incident energies (which are of technological interest as well) preequilibrium contributions are mostly dominated by the early steps of the intranuclear cascade, characterized by lower exciton numbers.

In any case one expects that, for consistency reasons, whatever the excitation energy, the sum over all p-h states of $\rho_{ph}(E)$ be equal to the total level density $\rho(E)$.

As an example, in ^{93}Nb the ratio between Gilbert-Cameron /1/ and the usual Williams formula /6/ tends to one only above 10 MeV excitation, whereas it raises up to $\sim$ 10 below 1 MeV excitation.

This example raises the doubt that, unless appropriate actions are taken, many preequilibrium investigations might be biased. This also indicates that more precise $\rho_{ph}(E)$ estimates should be adopted, expecially at lower excitations and in the region of discrete levels.

We have investigated this subject by means of combinatorial calculations in the framework of the superconductivity model. Details of the model are given in ref. /4/.

The work is not completed. At the moment only spherical nuclei have been considered; however some useful conclusions /7/ may be anticipated here.

- $\sum_{ph}\rho_{ph}(E)$ of our theoretical approach reproduced satisfactorily the density of discrete levels of all investigated isotopes like in fig. 2.

- The spin distribution of exciton levels was proved /4/ to be consistent with the law

$$f(E,J) = \frac{(2J+1)\exp\left[-J(J+1)/2\sigma_n^2(E)\right]}{2\sigma_n^2(E)} \qquad (1)$$

(see figs. 3, 4), where neglecting a weak energy dependence, the spin cut off was found to be $\sigma_n^2 = .28A^{2/3}n$ (n being the exciton number p+h) in excellent agreement with our preceding Nilsson model calculations /4/ which gave $\langle m^2 \rangle = .24A^{2/3}$.

- Yrast lines were deduced for each exciton configuration, see fig. 4 and were found /4/ to have approximately a parabolic trend in J . The Yrast line for total level density (as obtained by summation over all exciton numbers and as used in compound nucleus calculations) was found to be in perfect agreement with the predictions of Augustiniak and Marcinkowski /8/, see fig. 5.

Recently this author observed that:

- the theoretical level densities calculated /7/ for different exciton configurations start above certain energy thresholds, exciton dependent, see fig. 6. The energy gap G for the lowest configuration possible was found to be the sum of the shell gap S and pairing correction Δ . In particular, the difference G-S was found in excellent agreement with the pairing correction of Gilbert- and Cameron.

For higher exciton configurations, the pairing correction was found to be exciton and, thereby, energy dependent. Analysis of the data obtained is still in progress and we are confident it is possible to provide with a closed expression for $\Delta = \Delta(n,E)$.

Glibert-Cameron Phenomenological Approach

For applicative purposes we have been using since many years the phenomenological approach by Gilbert and Cameron /1/. This choice is justified by the flexibility and simplicity of the formulae involved, which are particularly suited to big cross section computer codes.

In particular this approach allows for a pretty reliable fit of all available experimental information in the excitation energy range up to a few MeV above neutron resonances. Only two free parameters are sufficient to completely characterize total level density, while all involved parameters a, U_x, T (level density parameter, matching energy and nuclear temperature respectively) obey to well known global, as well as local, systematic trend which are predictable in terms of nuclear models /2/. Our local systematics allow for a precision $\leq$30% in D_{OBS} (observed neutron resonance spacing) predictions.

Microscopic calculations of a and spin cutoff σ^2 performed by means of the single particle levels from the Nilsson model /2/, allowed for precise model guided local systematics of a and for the dependence of σ^2 on neutron, and proton numbers, as well as on the deformation parameter.

In addition, by way of definition, the parameter a turns out to be nuclear temperature and, thereby, excitation energy dependent, in particular its behaviour fluctuates rapidly and encreases with energy,at low temperatures, becoming asymptotic at high temperatures. These results well agree with those of ref. /9/.

A few drawbacks, however, affect this approach. Its parameter systematics, even if model guided, should be cautiously extrapolated, away from the stability valley. All this cannot be neglected in cross section calculations at high incident energies.

In addition, the whole approach is expected to gradually lose its prediction power at increasing excitation energies, far from the normalization interval, if the energy dependence of the parameter a , and the residual interactions are not properly accounted for.

As an example to illustrate the latter statement, one recalls the well known residual e-o effect which this author finds it affects the parameter, a over the whole periodic table, see fig. 7 .

This evidence can be explained as one usually corrects total excitation energy only for the pairing energy of the last pair, whereas our combinatorial calculations showed that more than one pair can be broken at the neutron resonance energy where a values are deduced. In particular, the number of broken pairs depends on the isotope considered and particularly on the resonance energy and on the shell gap. As a possible way to account for the pairing correction to total excitation, when dealing with total level density, this author suggests one should introduce the concept of an 'effective" energy dependent pairing, which is defined as the weighted average over all exciton configurations possible at that energy.

$$\Delta_{eff}(E) = \frac{\sum_{ph} \Delta_{ph} \rho_{ph}(E)}{\sum_{ph} \rho_{ph}(E)} \qquad (2)$$

Nilsson-BCS Microscopic Approach for Level Densities

The difficulty of taking into proper account the pairing interaction is overcome by Maino et al. /5/, /9/ using the Nilsson-BCS approach with inclusion of blocking effect even at finite temperatures. This lead to two important results.

- A microscopic level density approach was found able to predict D_{OBS} with a precision comparable to that obtained with a local systematics of ref. /2/. This having the advantage of more reliable extrapolations away from the stability valley.
- A fit could be found to the theoretical BCS calculations by means of the

Gilbert-Cameron high energy formula, provided an energy dependence of a is allowed for, of the type

$$a = a_o(1-e^{-\gamma E}) \qquad (3)$$

a_o and γ being fit parameters.

Maino and Menapace /9/ show that a_o vs. neutron number has the usual trend with the characteristic deeps at magic numbers, and depression in the region of rare earths.

The usual e-o effect however, is still evident in fig. 1, ref. /9/, while γ values are found constant with mass number A , but depending on the various e-e, o-o or e-o, o-e combination possibilities, see fig. 2 of ref./9/.

This result is not surprising because even if the pairing interaction is appropriately accounted for in the hamiltonian system of the BCS approach of ref./9/, this was not included in the Gilbert-Cameron formula adopted by ref. /9/, where it was assumed $\Delta=0$ in all cases. This way, formula 3 is inclusive of the energy dependence of $a=a(E)$ as well as of the energy dependence of the effective pairing correction $\Delta=\Delta(E)$ (which are not easily separable) and therefore the fit parameters a and γ are consequently affected. Consistency with BCS treatment of the pairing interaction would not be obtained anyhow, even including usual pairing corrections. In fact, at the moment, lacking a close form for (2) one cannot easily reach the aim this way, unless resorting to detailed combinatorial calculations.

In principle, the sign of the pairing correction could be checked fitting to BCS calculations a Gilbert-Cameron type formula with different assumptions about the appropriate pairing and verifying which one is in better agreement over the whole excitation energy range.

The trend of the energy dependence found for a(E), which exhibits a characteristic "knee" at some critical energy, confirms and explains the necessity for a composite formula approach like Gilbert-Cameron's in order to reproduce the change in slope of level density.

Effective Excitation Energy

The problem of the effective excitation energy is characteristic of Fermi gas models and it may greatly affect parameter systematics, and their validity over the whole energy and mass range.

In fact our parameter systematics /2/, are valid only locally, in energy, because uncertainties from model approximations are moved to the fit parameters involved.

The most important parameter involved in macroscopic approaches, based on the Fermi gas assumption, is the level density parameter a . It is derived mostly from the mean neutron resonance spacing D_{OBS}.

Values of a derived from particle spectra analysis are very useful to test the overall validity of level density approaches and inherent parametrization. One has to be cautious however, because in this case, large uncertainties may come from the assumptions underlying the reaction model adopted.

The total amount of potential energy to be introduced in order to determine the effective excitation energy becomes crucial when it is comparable with the total excitation energy available and causes a breakdawn of the statistical models approaching it.

Both the energy dependence of a vs. E and the corrections for the residual and the long range interactions affect not only the absolute value of a , but also the energy trend of $\rho(E)$. As an example, in the case of e-o or o-e nuclei, the ratio of the entropies S , according to the two usual assumptions on the sign for the pairing correction, is $S(B-\Delta)/S(B+\Delta) = 1$ at the resonance energies B , but by no means this ratio is conserved over the whole excitation energy range.

Another question mark may be arised whether the pairing interaction may be introduced "a posteriori", as a correction to total excitation energy or it must be introduced "a priori" in the total Hamiltonian of the system as it is done in the framework of the superconductivity approaches.

Some useful indications may be found in Weiszäcker mass formulae /10/ for the total energy of the ground states.

As it is known introduction of the corrections for the Coulomb energies and the energies due to neutron-proton mass differences into the total energy of ground states of an isobar family, move ground state energies according to characteristic parabolas in the plane (E,T_z) , see Fig. 8.

In particular, the vertex of the parabolas are shifted from each other by an amount Δ equal to the binding energy of the last nucleon pair. In fact, the ground states of e-e isobars having all nucleons bound into pairs are the lightest of all isobars and therefore are distributed on the lowest parabola, whereas the ground states of o-o isobars having the last nucleons unpaired are the heaviest and therefore accupy the highest parabola.

In addition the energetically lowest states with a given isobaric spin T (isobaric analogue states) are all placed at the same excitation energy if counted from an appropriate origin in the energy axis.

The particular regularities and simmetries of these parabolas indicate that equal level densities are expected for all isobars of a family at excitation energies differing from each other by the amount of pairing + Coulomb + simmetry + n-p mass difference energy. In particular, this means that the same level density parameter a characterizes the whole family, in agreement with Fermi gas prediction that $a \propto A$.

From all the above observations one deduces that the concept of effective energy which implies "a posteriori" corrections to total excitation energy, applies to ground as well as to isobaric analogue states.

Excitation energies may be referred to a whatever origin in the energy axis, provided all simmetry properties and energy gaps between isobar ground states are respected.

CONCLUDING REMARKS

From our efforts on combinatorial calculations in the framework of the superconductivity model, we cannot yet be sure whether or not a parametrization exists (with parameters obeying to model systematics) which allow for a safe and reliable use of Williams or any other similar expression in the whole excitation energy range. However the results of our studies cast light on the spin distribution of p-h levels and on the way to treat pairing corrections $\Delta(p,h,E)$ exciton and energy dependent.

From the studies on superconductivity models it has been proven that Gilbert-Cameron composite formula for total level density is valid over the whole energy range provided a suitable energy dependence of $\underline{a}$ is adopted. The form of energy dependence of the level density parameter $\underline{a}$ was determined and it was also proven that both parameters involved a_o and γ obey to systematic trends, but these must be reconsidered.

An idea how to treat in a comprehensive way the level density parameter systematics and the problem of effective excitation energies (to be used in connection with a Gilbert-Cameron type formulae) comes from considerations on the masses of the ground and isobaric analogue states.

Like the Fermi gas model this approach predicts that $\underline{a}$ only depends on mass number A.

Being rather high the global energy correction for residual and long range interactions, the range of validity of the Fermi gas statistical assumptions is shifted to higher excitations, which makes the formalism more useful for the determination of asymptotic values a_o and for emitted particle spectra analysis.

The more comprenhensive concept of effective energy, above indicated, becomes necessary for introducing into the level density, rotations in the isospin space. These play a rôle in weighting reaction channels which involve competitions of particle with different charge quantum numbers.

On the whole one may say that exception made for exiton level density, in all other cases with introduction of proper improvements, a Gilbert-Cameron type formula can be found reliable in the whole energy range and for all cross section computational needs in reactor technology.

REFERENCES

1. A. Gilbert, A.G.W. Cameron, Can. J. Phys. 43, 1446 (1965)
2. G. Reffo, "Parameter Systematics for Statistical Theory Calculations of Neutron Reaction Cross Sections", CNEN Report RT/FI(78)11, 1978 and IAEA Report SMR-43 (1980) and also Proc. of the Int. Conf. on Theory and Applications of Moment Methods in Many Fermion Systems, ed. by B.J. Dalton, S.M. Grimes, J.P. Vary, S.A. Williams, Plenum Press N.Y. 1980.
3. A. Arima, F. Iachello, Ann. Rev. of Nucl. and Part. Sci., 31, 75(1981).
4. G. Reffo, M. Hermann, Lettere al Nuovo Cimento, 34, 261 (1982).
5. V. Benzi, G. Maino and E. Menapace, Nuovo Cimento A57, 427 (1980).
6. F.C. Williams jr., Nucl. Phys. A166, 231 (1971).
7. G. Reffo, M. Herman, to be published.
8. W. Augustiniak, A. Marcinkowski, Acta Phys. Pol. B, 10, 357 (1969).
9. G. Maino, E. Menapace, contributed paper to this meeting.
10. J. Jänecke, Nucl. Phys. 73, 97 (1965).
11. Y.L. Kammerdienen, report UCRL-51232, 1972.
12. D. Hermsdorf et al., INDL (GDR-2/L), 1974.
13. C.M. Lederer, V.S. Shirley, table of isotopes Wiley Interscience Publications (1978).

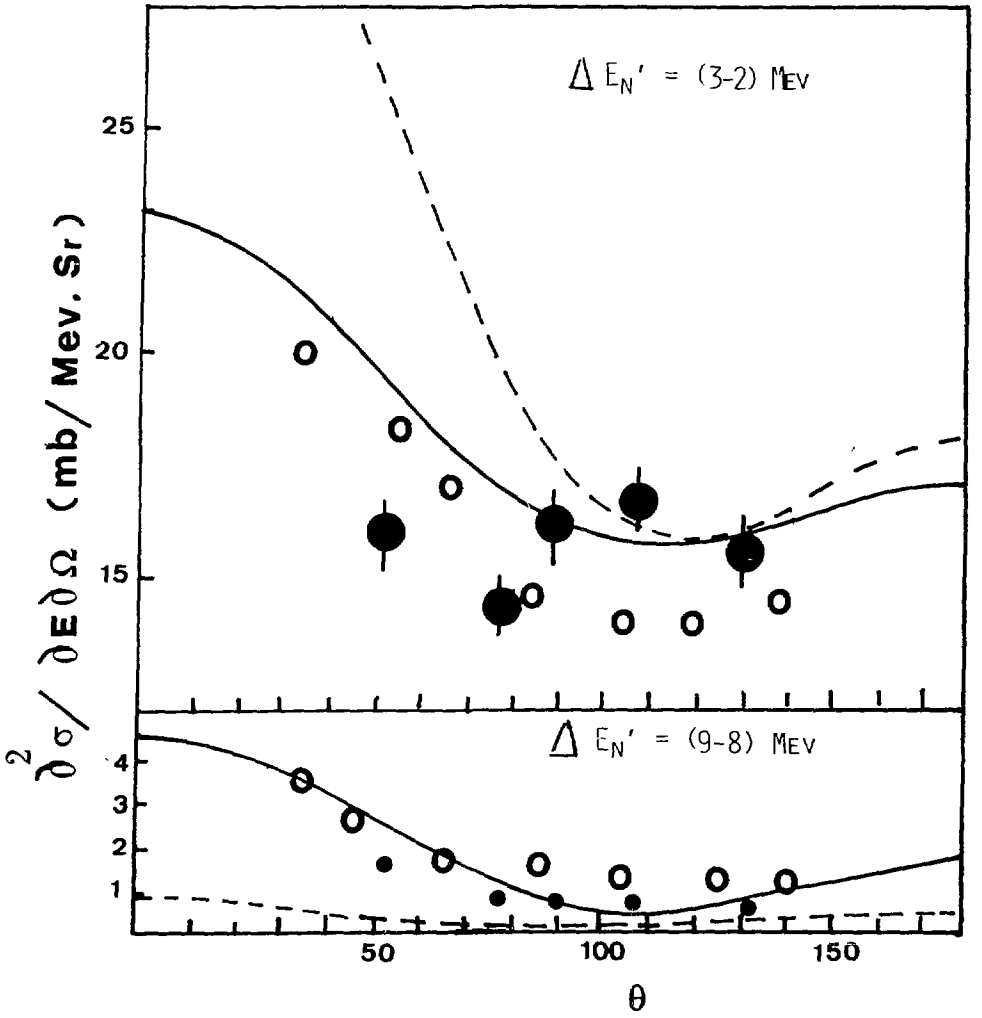

Fig. 1 - Neutron angular distribution in the reaction n + ^{56}Fe at 14.5 MeV. Full line is obtained with inclusion of spin conservation, dashed line without. ● experimental data from ref.11. ○ Experimental data from ref. 12.

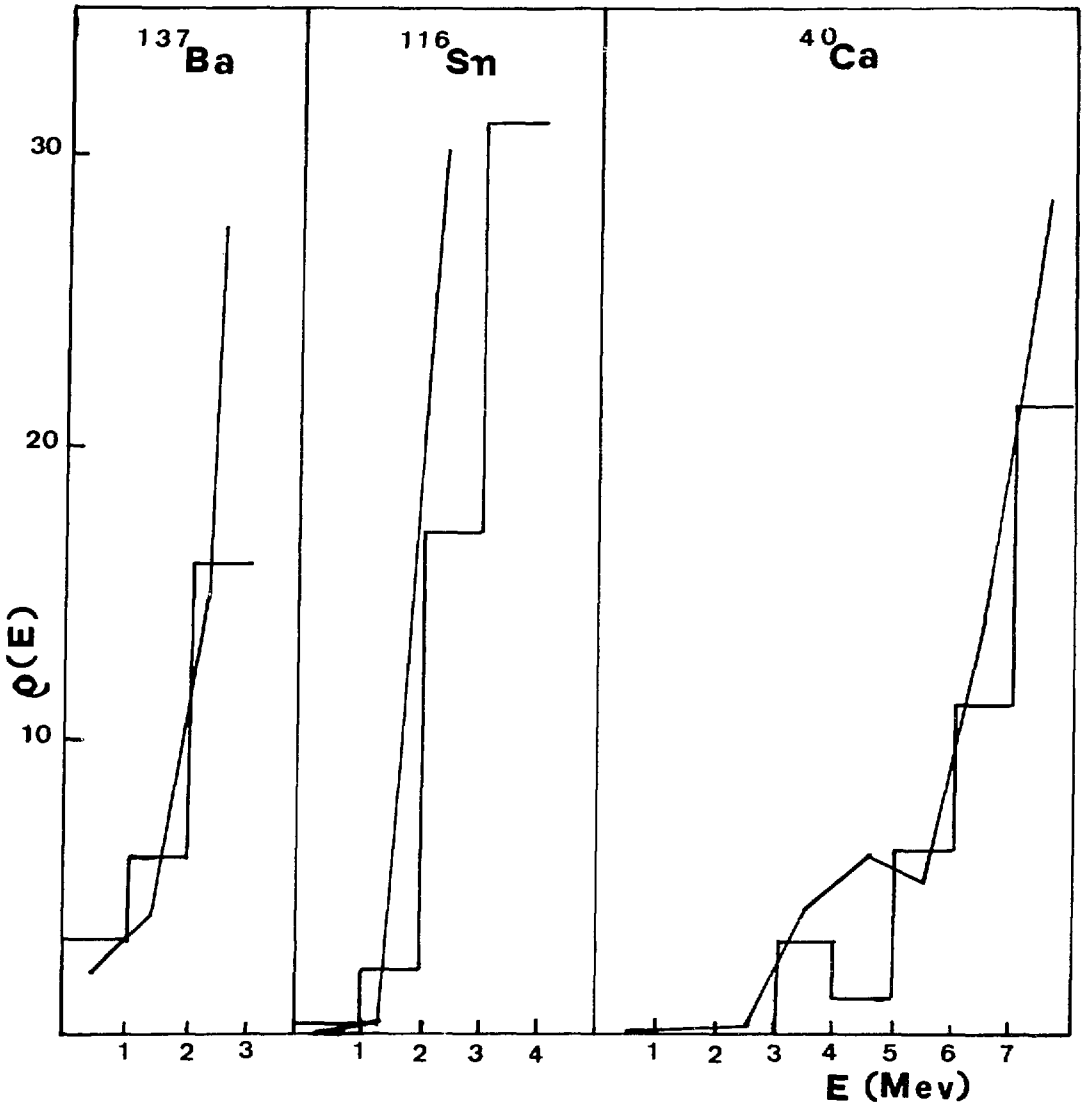

Fig. 2 - Total level density from combinatorial calculations and density of discrete levels from ref. 13. ⌐ represents data from ref. 13.

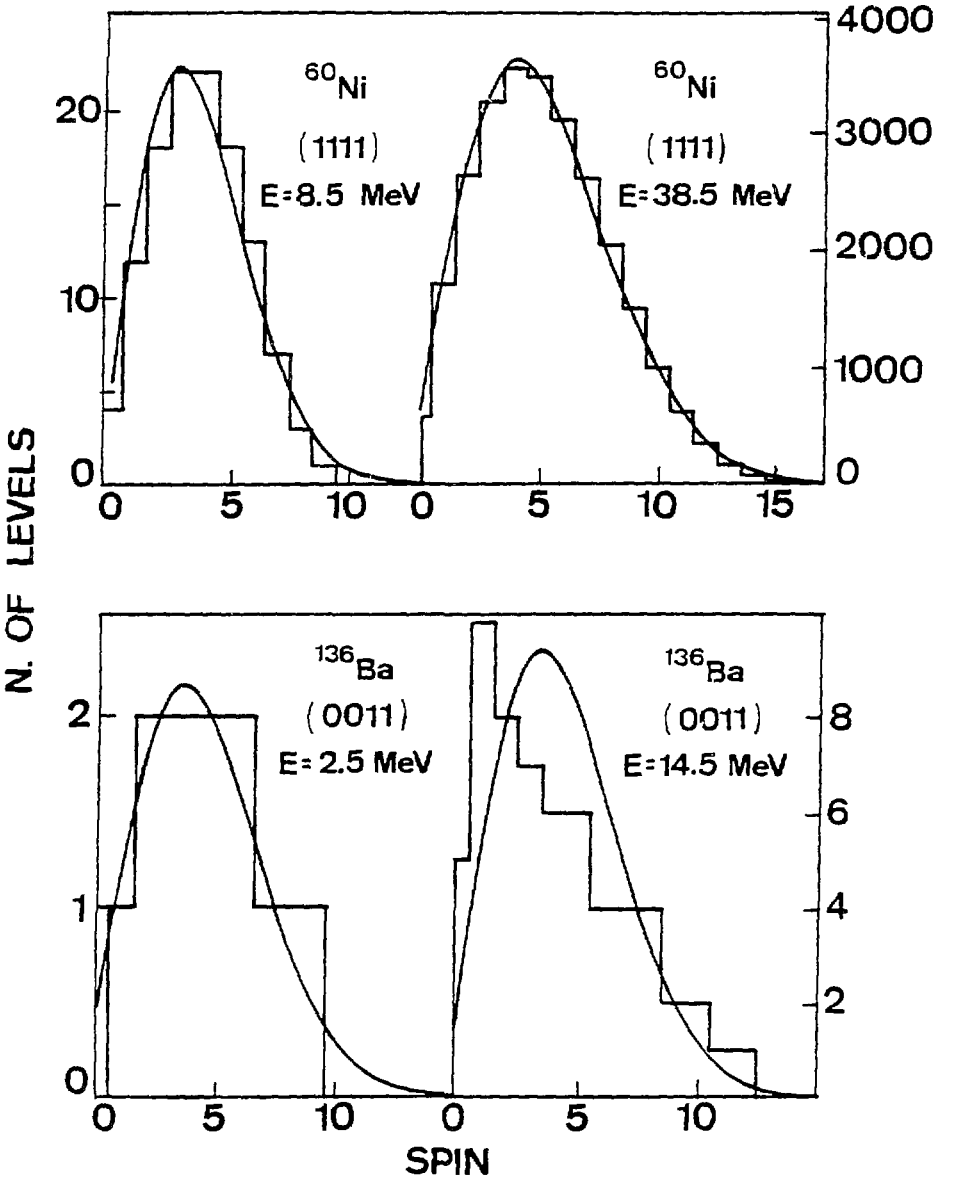

Fig. 3 - Comparison of spin distribution of the exciton levels (confined to energy interval of 1 MeV) obtained from present combinatorial calculations (histograms) with prediction of law 1 .

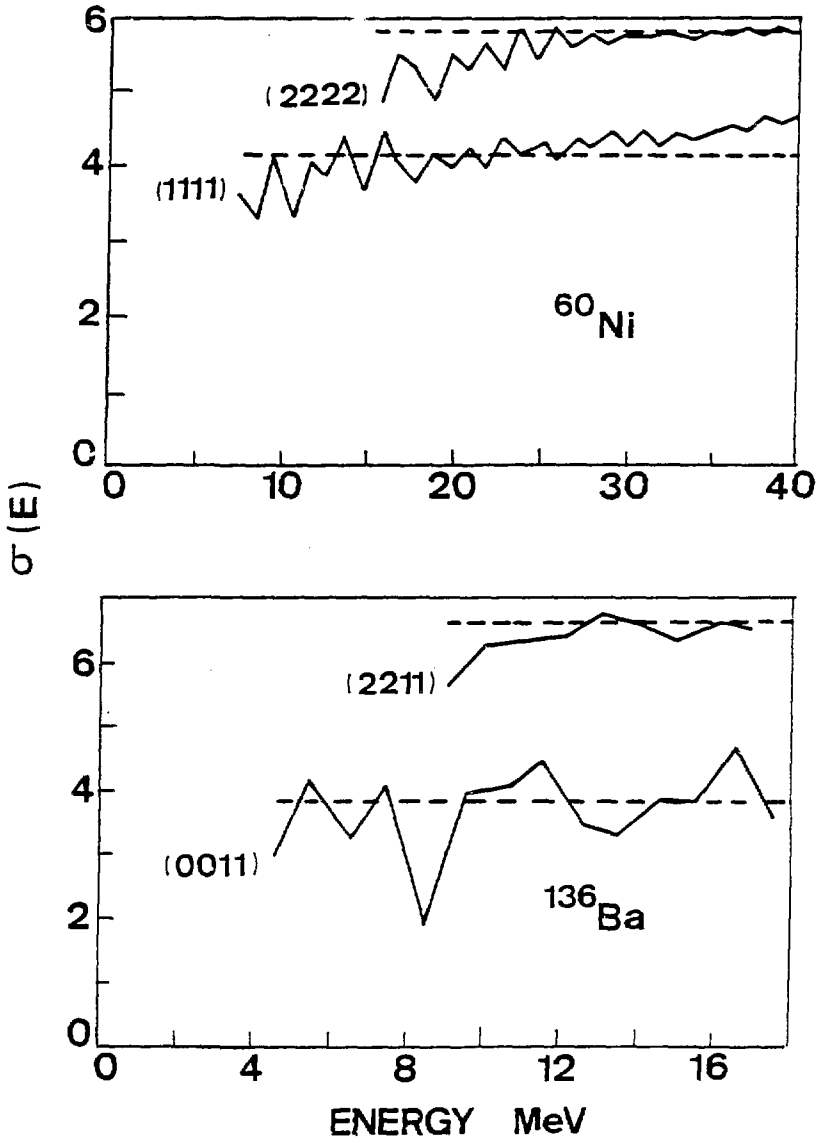

Fig. 4 - Energy dependence of spin cut off parameter according to present calculations. Dashed lines correspond to $\sigma^2 = .28n\ A^{2/3}$.

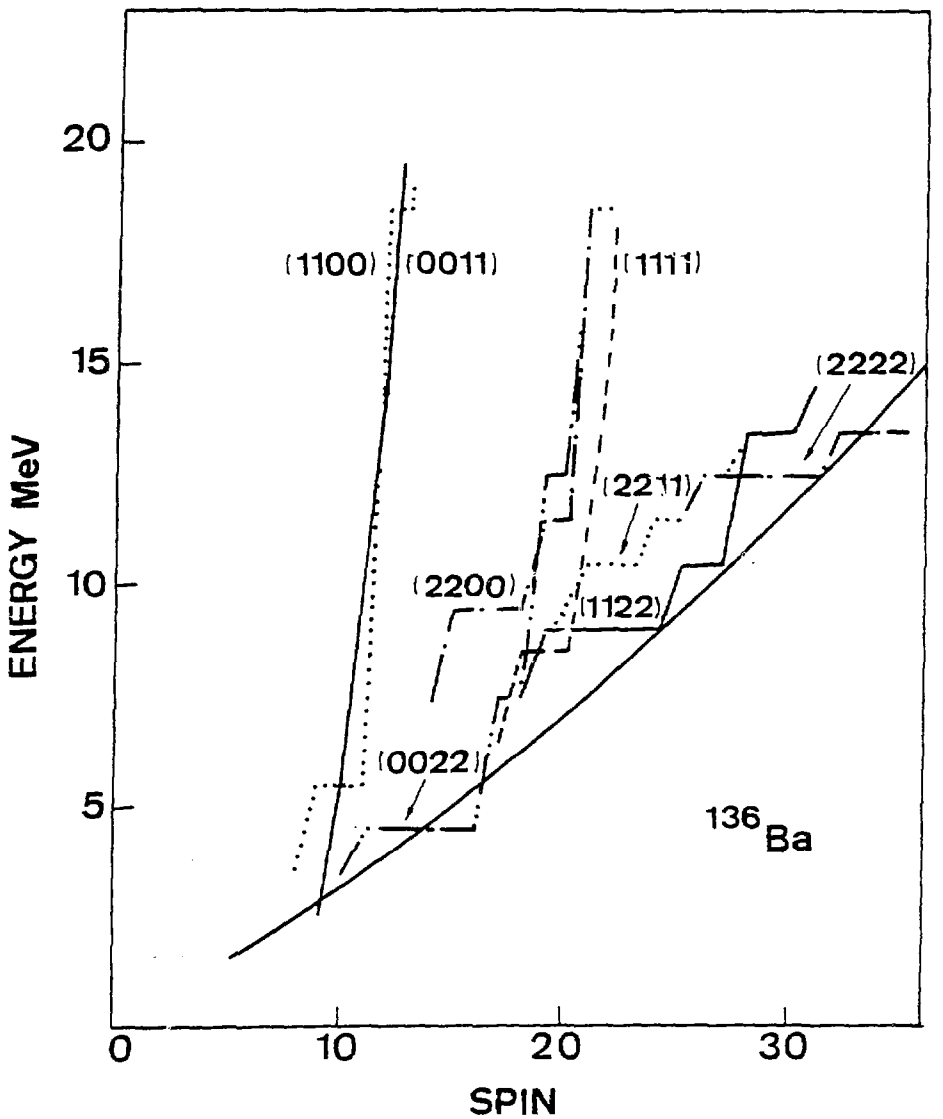

Fig. 5 - Yrast lines for certain exciton numbers in ^{130}Ba.

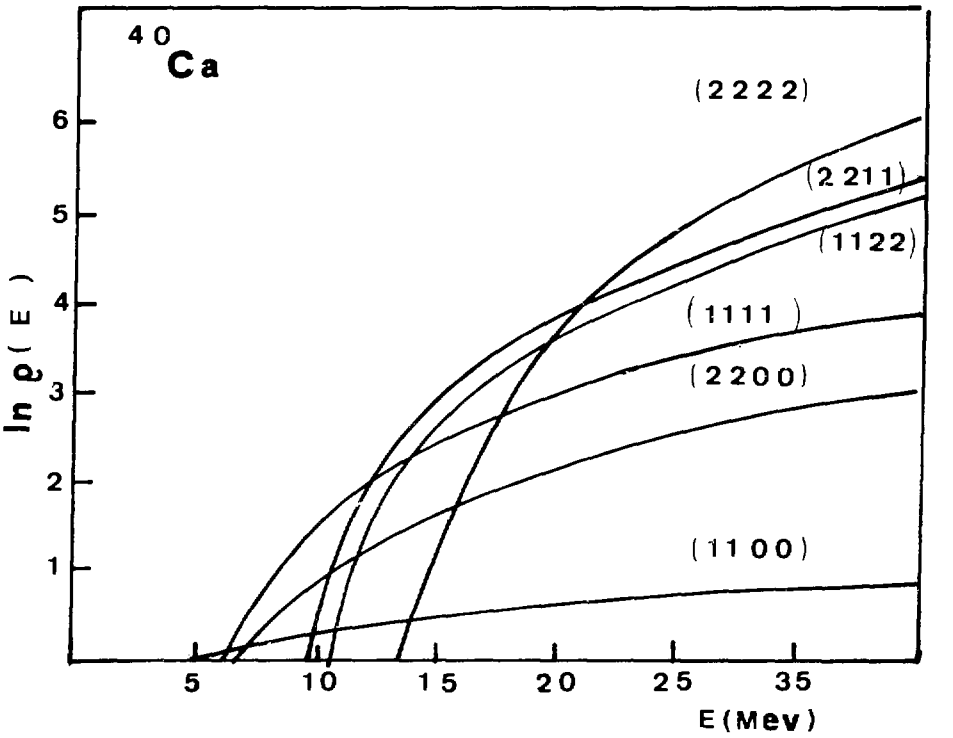

Fig. 6 - Level density from Nilsson-BCS and combinatorial calculations for a few p-h configurations. The sequence of 4 digits indicates neutron and proton p-h configurations respectively.

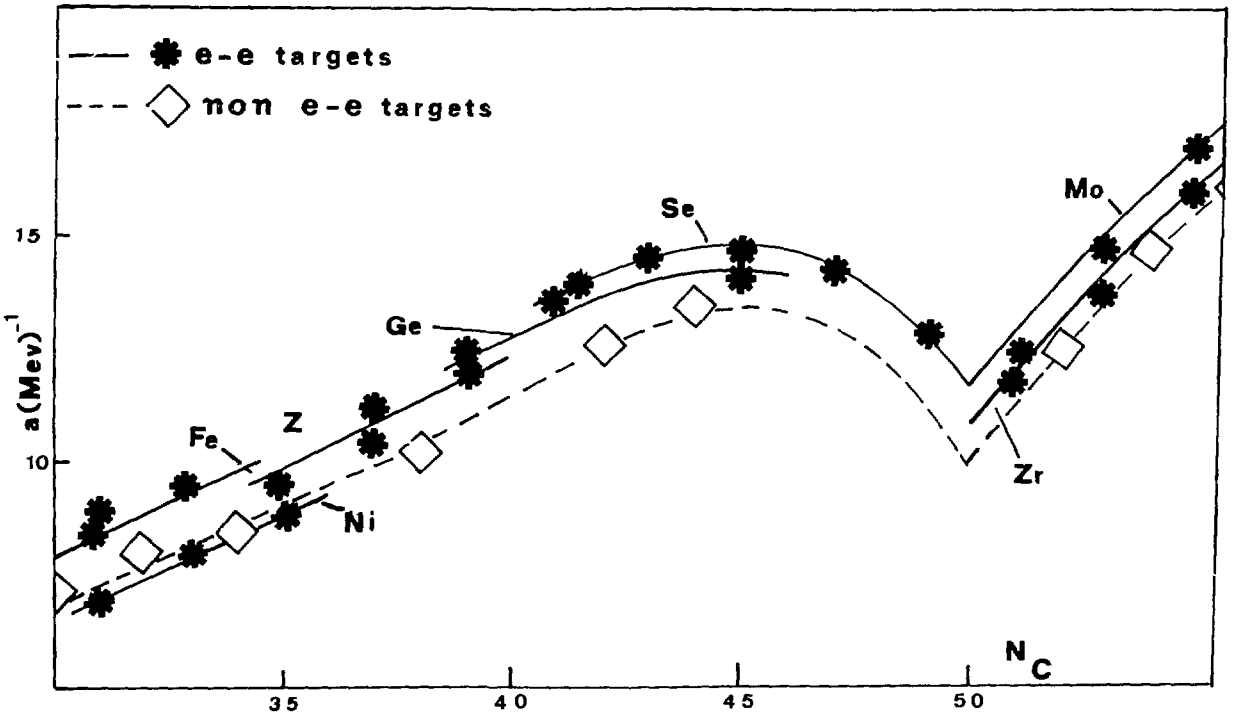

Fig. 7 - Typical e-o effects on local systematics for the level density parameter a according to ref./2/.

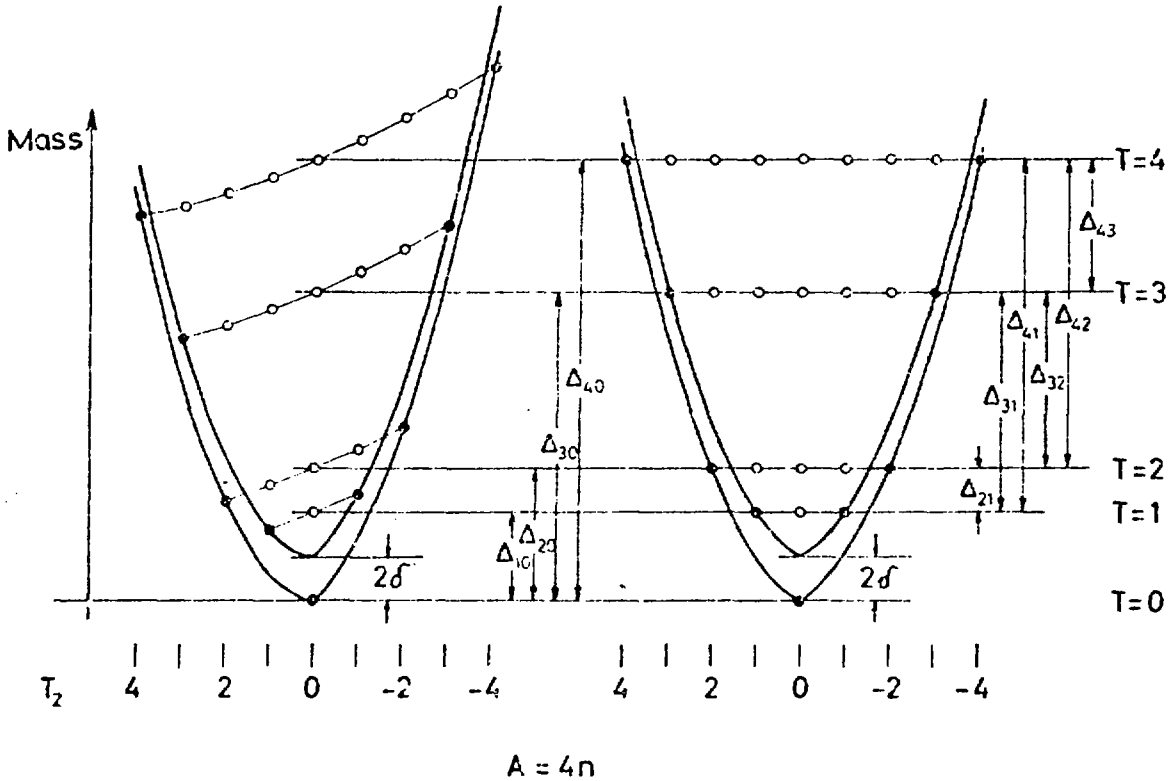

Fig. 8 - Typical distribution of ground and isobaric analogue states for e-e and o-o isobars. The left hand side is without any corrections, the right-hand side is corrected with regard to n-p mass difference and the different Conlomb energies. Δ is the pairing energy. $\Delta_{TT'}$ are the energy differences between isobaric analogue states.

STATISTICAL INFERENCE OF LEVEL DENSITIES FROM RESOLVED RESONANCE PARAMETERS

F.H. Fröhner

Kernforschungszentrum Karlsruhe
Institut für Neutronenphysik und Reaktortechnik
Postfach 3640, D-7500 Karlsruhe
West Germany

ABSTRACT

Level densities are most directly obtained by counting the resonances observed in the resolved resonance range. Even in the best measurements, however, weak levels are invariably missed so that one has to estimate their number and add it to the raw count. The main categories of missing-level estimators are discussed in the present review, viz. (i) ladder methods including those based on the theory of Hamiltonian matrix ensembles (Dyson-Mehta statistics), (ii) methods based on comparison with artificial cross section curves (Monte Carlo simulation, Garrison's autocorrelation method), (iii) methods exploiting the observed neutron width distribution by means of Bayesian or more approximate procedures such as maximum-likelihood, least-squares or moment methods, with various recipes for the treatment of detection thresholds and resolution effects. The language of mathematical statistics is employed to clarify the basis of, and the relationship between, the various techniques. Recent progress in the treatment of resolution effects, detection thresholds and p-wave admixture is described.

1. INTRODUCTION

Accurate information on level densities, apart from providing test material for level density theories [1-4], is indispensable for level-statistical calculations of average partial cross sections. These are roughly proportional to the level density if the relevant mean partial widths are known for instance from analysis of high-resolution neutron (or proton) resonance data. The level densities themselves are also most directly obtained in the resolved resonance region just above the neutron (or proton) separation energy, where it seems simple enough to count the resonances observed in a given energy interval.

Weak levels are always missing, however, because of limited counting statistics and finite instrumental resolution. The preponderance of small values in the Porter-Thomas distribution of entrance-channel widths [5] and hence of weak levels aggravates the problem. As a consequence even the best contemporary high-resolution resonance data, for instance the ^{238}U transmission data shown in Fig. 1, are affected by about 20 % missing s-wave levels, and 30 or 40 % are quite common for less well studied nuclei. Level densities uncorrected for missing levels are therefore useless for most purposes. Nor does it help to take only the low-energy portion of the cumulative level count N(E) with its typical nicely linear behaviour. This linearity is frequently mistaken as an indication that no levels are missed. Of course it indicates merely that the missing fraction does not depend on energy.

The whole problem of level density estimation is truly an evaluator's item - replete with missing data, shaky statistical models suggested by rather abstract spectral theories, rigorous equations which are so intractable that approximations must be invoked, logical and numerical traps etc. Even benchmark calculations have recently made their appearance in this field [7], showing that (and why [8]) impeccably conceived and carefully tested programs can produce less than satisfactory results. Liou [9] has reviewed a number of level density estimation techniques, giving a short functional description of each one. In the present paper (which updates and expands a recent similar review [10]) the emphasis will be on the probability-theoretical aspects. Since the very concept of level density is statistical it seems appropriate to use the tools of mathematical statistics to develop and to compare methods for the estimation of level densities and missing levels. It will then be seen that many of the seemingly quite different techniques which exist are mere variants of the same basic approach.

2. THEORY OF LEVEL STATISTICS

Strictly speaking there is nothing random or statistical about resonance energies or widths. They are determined as eigenvalues and by the eigenfunctions of a Schrödinger equation with suitable boundary conditions. A statistical description is justified only by the complexity of the spectra which reflects the complicated interaction between the many nucleons in the nuclear systems we consider here. The square roots of the reduced neutron (proton, photon,...) widths, for instance, are essentially surface integrals over rapidly oscillating eigenfunctions in the 3A-dimensional configuration space associated with the A nucleons of a given nucleus. Without any further information one can therefore expect them to be normally distributed around zero. This hypothesis leads immediately to the Porter-Thomas distribution [5] for the reduced widths Γ,

$$p(\Gamma|\langle\Gamma\rangle)d\Gamma = \frac{e^{-x}}{\sqrt{\pi x}}\,dx\ , \qquad 0 < x \equiv \frac{\Gamma}{2\langle\Gamma\rangle} < \infty \quad . \tag{1}$$

where $\langle\Gamma\rangle$ is the ensemble average (for clarity we omit the usual sub- and superscripts for reduced widths). Recently there were reports that in

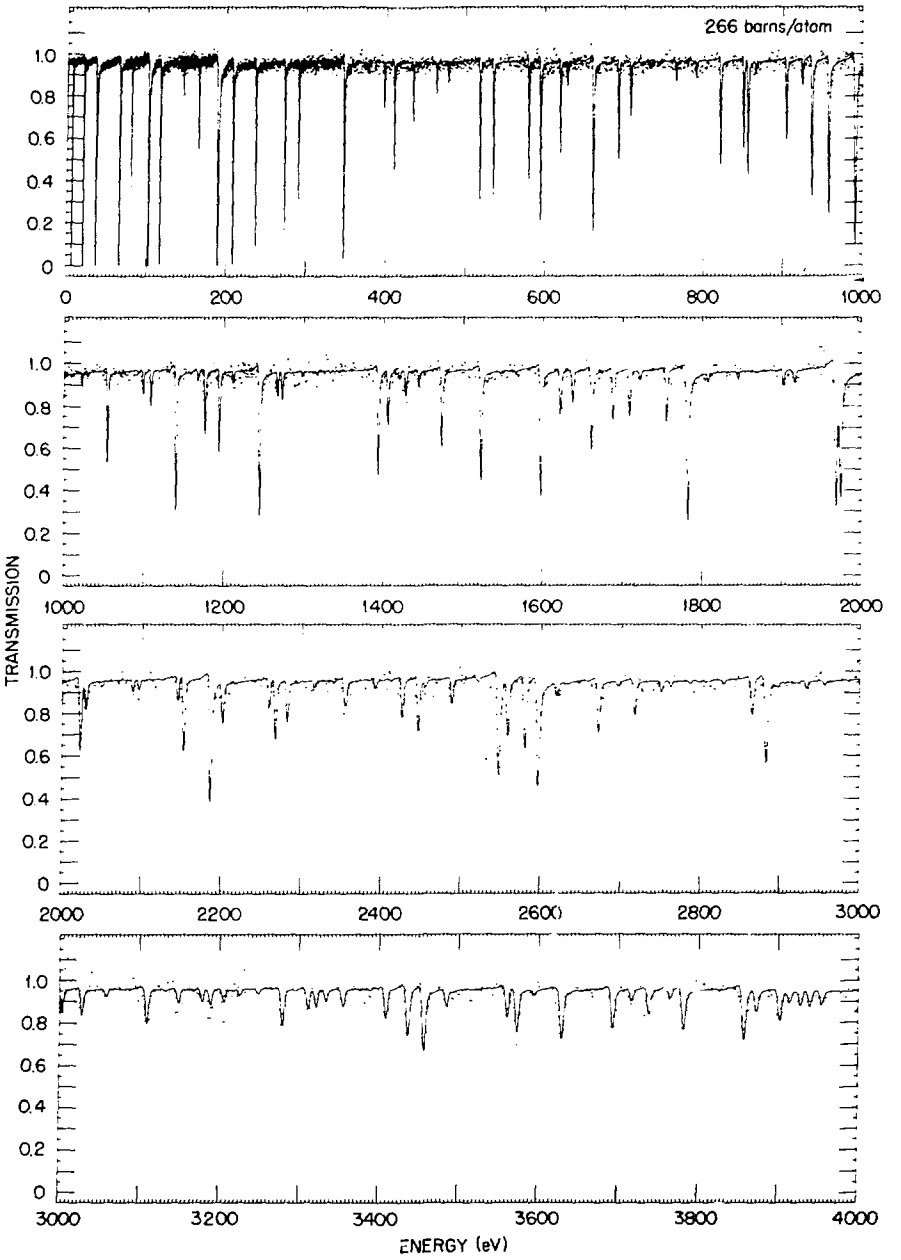

Fig. 1 - Points: high-resolution resonance data (transmission of neutrons through 0.76 mm of ^{238}U measured by time-of-flight), Curve: calculated from ENDF/B-IV total cross sections, Doppler broadened to 300 K (from Olsen et al. 1976, Ref. 8)

large-scale shell model calculations including two-body residual interactions the width distributions deviated from (1) [11, 12]. According to other studies [13, 14] the deviations vanished, however, if the secular variation of the average reduced width was properly taken into account (or if the sampling was restricted to reasonably narrow energy bins). So far all experimental neutron, proton and photon resonance data support local validity of the Porter-Thomas hypothesis.

The level spacing distribution is much more difficult to find. The level energies are the eigenvalues of a Hamiltonian matrix H which can be taken as real and symmetric since the nuclear interaction is invariant under time reversal. Furthermore, the probability density function p(H) must be invariant under rotations in Hilbert space because all representations of H, including the diagonal form, are equally valid. The additional requirement that the matrix elements be independent of each other yields the Gaussian orthogonal ensemble (see [15]). This independence is, however, unfounded physically and leads to an unrealistic semi-circular dependence of level density on energy. Dyson (see [15]) introduced the circular orthogonal ensemble by assuming that some unitary (otherwise unspecified) matrix function S of H has its eigenvalues distributed uniformly around the unit circle. He showed that with this very general assumption one can reproduce any reasonable energy dependence of the level density. Mello et al. [16] studied the more physical statistical shell model where not the elements of H but only those of the residual (two-body) interaction are considered as random variables. Both the orthogonal ensembles and the statistical shell model (or two-body random ensemble) yield a level spacing distribution that is very close to Wigner's famous surmise (see [14, 15])

$$p(D|\langle D\rangle)dD = 2xe^{-x^2}dx, \qquad 0 < x \equiv \frac{\sqrt{\pi}}{2}\frac{D}{\langle D\rangle} < \infty , \tag{2}$$

where $\langle D\rangle$ is the ensemble average. In addition to the level repulsion (improbability of small spacings) implied by (2) all random-matrix models predict that nuclear level sequences possess "nearly crystalline" regularity or stiffness in the sense that the cumulative level count N(E) follows closely a straight line with slope $\rho = 1/\langle D\rangle$, excursions by more than one unit being extremely unlikely. This implies that spacings are correlated in such a way that a large spacing is followed by a short one more often than not and vice versa. The mean-square deviation from a best-fit straight line in an interval containing N levels, called the Δ_3 statistic by Dyson and Mehta [17], has the expectation value

$$\langle\Delta_3\rangle = \frac{1}{\pi^2}\ \{\ln(2\pi N) + \gamma - \frac{\pi^2}{8} - \frac{5}{4}\} \tag{3}$$

(γ = 0.5772... is Euler's constant) and the variance

$$\mathrm{var}\ \Delta_3 = \frac{1}{\pi^4}\ \left(\frac{4\pi^2}{45} + \frac{7}{24}\right) \simeq 0.012\ . \tag{4}$$

Absence of levels or presence of spurious levels from other sequences obviously increases Δ_3. One has therefore tried to use it as a test statistic for the purity of level sequences. According to Dyson the best test statistic for the presence of spurious or missing levels in an almost

pure and complete level sequence is (see [18])

$$F_\lambda = \sum_{\mu \neq \lambda} \text{ar cosh} \frac{I/2}{|E_\mu - E_\lambda|} , \tag{5}$$

where μ runs through all levels between $E_\lambda - I/2$ and $E_\lambda + I/2$ and I is an arbitrary test interval (for instance 20 times $\langle D \rangle$). Expectation value and variance are, with $m \equiv \pi I/(2\langle D \rangle)$,

$$\langle F_\lambda \rangle = m - \ln m - \gamma + 2 , \tag{6}$$

$$\text{var } F_\lambda = \ln m , \tag{7}$$

if E_λ is a true member of the sequence. If it is the energy of a spurious level in an otherwise pure sequence one gets

$$\langle F_\lambda \rangle = m , \tag{8}$$

so that a spurious or missing level should produce, on average, a peak or a dip of magnitude ln m in an almost constant trend. The catch, however, lies in the words "on average" (see [19]). In practice one finds that the Δ_3 and F_λ test criteria for purity and completeness are often satisfied for samples that are known to be neither pure nor complete.

3. ESTIMATION BASED ON LEVEL POSITIONS ALONE

It was already stated that simple ladder estimators such as a straight line fitted to the linear portion of the level number staircase curve N(E) are usually rather worthless, and this is true also if they appear under the more pretentious name of Δ_3 statistic.

The seemingly straightforward approach of fitting the Wigner distribution (2) to the observed distribution of level spacings is ruled out by the bad distortion of the latter if 20 % or more of all levels are missing. Unfortunately none of the tests described so far permits unambiguous identification of spurious or missed levels. Nevertheless, as the Columbia group demonstrated, one can purify almost pure level sequences further by a combination of all available tests [19]. Such an ambitious program involves much judgement and is therefore not easily cast into the form of a computer code. Moreover, as already mentioned the tests based on orthogonal-ensemble theory are not as sensitive as one might expect [20-22]. For instance evaluated ^{238}U resonance parameters, after application of the Δ_3 test, yielded a seemingly pure and complete sequence of s-wave levels [23]. The mean spacing corresponding to the slope of the fitted straight line,

$$\langle D \rangle = 24.78 \pm 0.14 \text{ eV},$$

(see Fig. 2) was obtained from the W statistic recommended by Dyson and Mehta [17] as the optimal estimator for nearly pure level sequences,

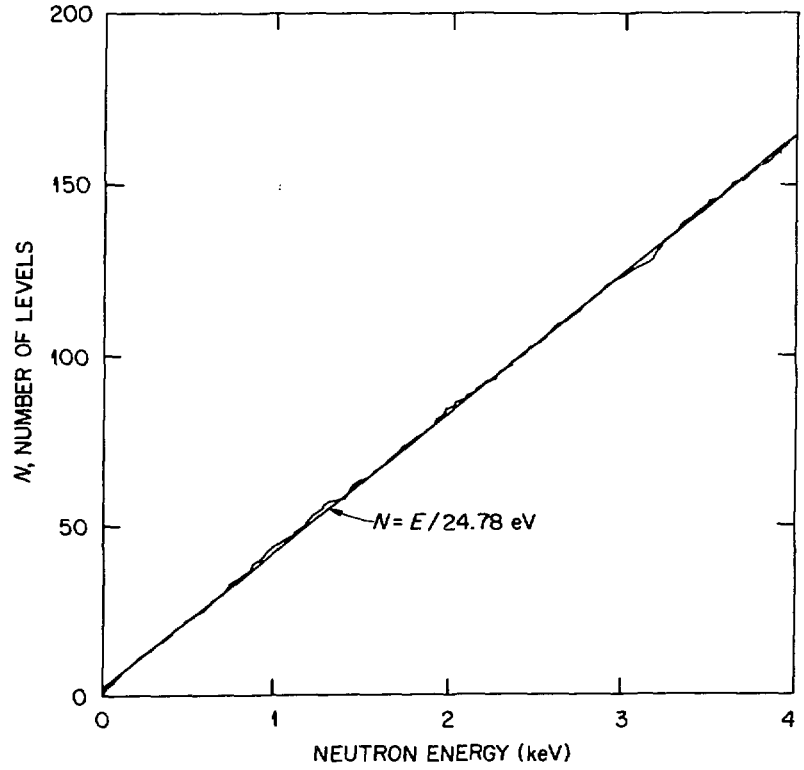

Fig. 2 - Cumulative number of s-wave levels versus neutron energy according th the evaluation of de Saussure et al., Ref. 23. There is no indication from the Δ_3 test that many weak levels are missing as shown clearly by the reduced-width distribution.

$$W = \sum_{\lambda=1}^{N} \sqrt{1 - \left(\frac{E_\lambda - \overline{E}}{I/2}\right)^2} \quad , \quad \langle D \rangle = \frac{\pi I}{4 \langle W \rangle} \quad , \tag{9}$$

where I and $\overline{E}$ are length and midpoint of the energy interval considered. As will be seen below, however, the width distribution shows quite clearly that about 20 % of the levels are missing. Similar discrepancies for the stable iron isotopes [24] can be traced back to the same weakness of the Δ_3 and other related statistics. Now if the ladder tests suggested by orthogonal-ensemble theory are of such doubtful value already in these favorable cases, where levels are well separated and only one spin is possible for s-wave resonances (so that level repulsion is fully effective) they are quite useless for resonance data afflicted by severe level overlap and unknown level spins such as those for ^{233}U, ^{239}Pu and other fissile target nuclei with two superimposed s-wave sequences.

4. ESTIMATION BASED ON LEVEL POSITIONS AND WITHS

For the last-mentioned nuclei Monte Carlo techniques have proven useful. One generates artificial cross sections from resonance parameters sampled from the relevant distributions. By varying the mean widths and spacings one tries to make the artificial, Doppler and resolution broadened cross section curves statistically as similar as possible to the measured data. The number of unrecognisable and unresolved levels in the artificial cross section can then be taken as estimate for the number missed in the real data (see e. g. [25, 26]).

The difficult judgement of the statistical similarity between experimental and artificial cross sections was put on a quantitative basis by Garrison [27]. He uses the same energy grid and also the same cross section bin structure for both cross section curves and then generates a bivariate distribution in matrix form by considering all pairs of data points that are separated by the same energy difference ΔE (which is to be chosen as comparable to the mean level spacing). If the two cross sections of such a pair fall into the i-th and the k-th cross section bin the value one is added to the (i,k) matrix element. The two matrices thus created from the experimental and the artificial cross section are then compared by means of either a maximum-likelihood or a chi-square criterion to determine the degree of statistical similarity between both. Varying the level density and the mean widths one can maximise the statistical similarity. This method can cope with data that are quite badly affected by missing levels and unresolved doublets. Garrison's estimate for ^{235}U,

$$\langle D \rangle = 0.38 \pm 0.04 \text{ eV}$$

[27], deduced from spin-merged data, is consistent with the value

$$\langle D \rangle = 0.44 \pm 0.04 \text{ eV}$$

found later by Moore et al. from spin-separated data measured with polar-

ised beam and sample [20], whereas previous, less quantitative comparisons with Monte Carlo generated cross sections had given much higher values [25]. It is obvious, however, that simpler techniques are required for routine extraction of level densities from the vast body of modern resonance parameter data.

5. ESTIMATION BASED ON WIDTHS

In contrast to the spacing distribution the neutron width distribution is only slightly affected by missing levels. The upper part of the Porter-Thomas distribution, corresponding to the strong levels, can usually be regarded as unperturbed. It is then possible to estimate the mean width from this part, for instance by a straightforward least-squares fit [28]. The expected number of missing levels and the level density can be calculated once the mean width is known. This, in essence, is the basis of the best level density estimation techniques available at present, even if they employ more refined methods. In order to introduce the relevant principles of probability theory we begin with a discussion of the simplest parameter estimation problem involving the Porter-Thomas distribution.

5.1 Unperturbed Porter-Thomas Distribution

Suppose we have a sample of reduced neutron widths $\Gamma_1, \Gamma_2, \ldots \Gamma_N$ from a pure Porter-Thomas distribution. The joint probability that in a random sample of size N, drawn from the distribution (3) with given $\langle\Gamma\rangle$, the sample values lie in the infinitesimal intervals $d\Gamma_1$ at Γ_1, $d\Gamma_2$ at $\Gamma_2, \ldots$ $d\Gamma_N$ at Γ_N is

$$L(\Gamma_1,\ldots\Gamma_N|\langle\Gamma\rangle)d\Gamma_1\ldots d\Gamma_N = \prod_{i=1}^{N} p(\Gamma_i|\langle\Gamma\rangle)d\Gamma_i \ . \tag{10}$$

The joint probability density function L is called the likelihood function. It specifies the relative probabilities for different samples if the parent distribution and its parameter(s) are given. Our problem, however, is just the reverse. We want the probability density function not for the sample (that is given) but for the parameter $\langle\Gamma\rangle$ of the parent distribution. The recipe for the necessary inversion of conditional probabilities is provided by Bayes' theorem (see e. g. [29]) which thus constitutes the very basis for all scientific inference from experimental (uncertainty-affected) data. It states that the required (a-posteriori) probability is the product of the likelihood function and the a-priori probability for the estimated parameter(s). Writing $p_0(\langle\Gamma\rangle)d\langle\Gamma\rangle$ for our a-priori probability we get

$$p(\langle\Gamma\rangle|\Gamma_1,\ldots\Gamma_N)d\langle\Gamma\rangle \propto L(\Gamma_1,\ldots\Gamma_N|\langle\Gamma\rangle)p_0(\langle\Gamma\rangle)d\langle\Gamma\rangle \ . \tag{11}$$

This distribution, the Bayesian solution to the estimation problem, is the optimal solution: it contains the complete information about $\langle\Gamma\rangle$ which can

be extracted from the sample, including all error information. Its usefulness depends, however, on knowledge of the prior probability, and this is often unknown in the case of continuous parameters. In our case $\langle\Gamma\rangle$ is a scale factor. Jaynes [30], arguing that the prior probability cannot depend on the scale chosen, showed that for scale parameters the appropriate prior probability is $d\langle\Gamma\rangle/\langle\Gamma\rangle = d \ln \langle\Gamma\rangle$, thus giving a rigorous group-theoretical proof for a conjecture due to Jeffreys [29]. Next the question arises which value of $\langle\Gamma\rangle$ should be quoted as the best estimate, the maximum (mode) of p or the expectation value or something else? The recommended Porter-Thomas distribution should of course be the same whether we estimate $\langle\Gamma\rangle$ or $1/\langle\Gamma\rangle$ (both must be equally possible for a scale parameter). The Jeffreys-Jaynes prior probability suggests that we consider $\ln\langle\Gamma\rangle$ as the basic parameter, hence L as its probability density function. The maximum of L with respect to $\ln\langle\Gamma\rangle$ is then determined by

$$\frac{d\,L}{d\,\ln\langle\Gamma\rangle} = \langle\Gamma\rangle \frac{d\,L}{d\langle\Gamma\rangle} = \frac{1}{\langle\Gamma\rangle}\frac{d\,L}{d(1/\langle\Gamma\rangle)} = 0 , \tag{12}$$

which shows that in each case we have to maximise the likelihood function, and that the recommended value is in fact the same in all three cases.

We could have avoided Bayes' theorem and the Jeffreys-Jaynes prior probability by use of the more familiar maximum-likelihood technique (see e. g. [29]). Writing down L explicitly for the Porter-Thomas distribution one sees that L is a product of one factor containing the sample values and a second factor which depends only on the true mean $\langle\Gamma\rangle$ and the sample average

$$\overline{\Gamma} \equiv \frac{1}{N}\sum_{i=1} \Gamma_i . \tag{13}$$

The factorisation shows that $\overline{\Gamma}$ is a minimal sufficient statistic, i. e. it is a number that can be calulated from the sample, contains all information about $\langle\Gamma\rangle$ that the sample contains and has the smallest scatter around its expectation value among all possible sufficient statistics. Small scatter is one property which a useful estimator must have. The second property is that it should be unbiased which means that its expectation value should be equal to the estimated true value. The sample average $\overline{\Gamma}$ has both properties. Furthermore it maximises the likelihood function, i. e. the value to be recommended is, as might have been expected,

$$\langle\Gamma\rangle = \overline{\Gamma} . \tag{14}$$

The statistic $\overline{\Gamma}$ has a χ^2-distribution with N degrees of freedom [31],

$$p(\overline{\Gamma}|\langle\Gamma\rangle)d\overline{\Gamma} = \Gamma(N/2)^{-1}e^{-y}y^{N/2-1}dy ,$$
$$0 < y \equiv \frac{N\,\overline{\Gamma}}{2\langle\Gamma\rangle} < \infty \tag{15}$$

(where $\Gamma(N/2)$ is a gamma function, not a width), as follows upon substitution of $\xi_i = \sqrt{\Gamma_i/(2\langle\Gamma\rangle)}$ and integration in the space of the ξ_i over all angles, for fixed radius. Now (15) is seen to be basically the distribution

of the ratio $\overline{\Gamma}/\langle\Gamma\rangle$. It can be interpreted either as the distribution of $\overline{\Gamma}$ for given $\langle\Gamma\rangle$ or, equally well, as that of $\langle\Gamma\rangle$ for given $\overline{\Gamma}$,

$$p(\overline{\Gamma}|\langle\Gamma\rangle)d\overline{\Gamma} = p(\langle\Gamma\rangle|\overline{\Gamma})d\langle\Gamma\rangle \quad . \tag{16}$$

The importance of this distribution lies in the fact that it contains the uncertainty information about the $\langle\Gamma\rangle$ estimate. One can establish confidence limits for any confidence level P by demanding that y-integration over (15) yield the value P between, and equal values (1-P)/2 below and above the limits, and then converting y-limits to $\langle\Gamma\rangle$-limits. ($P \approx 0.68$ corresponds to the error bars of $\pm$ 1 standard deviation usually quoted for Gaussian distributions.)

Exactly the same estimate and the same associated probability distribution would have been obtained immediately with the Bayesian approach, i. e. by insertion of the Porter-Thomas distribution (1) and of the Jeffreys-Jaynes prior in Bayes' theorem, Eq. (11), and determination of the most probable value of $\ln\langle\Gamma\rangle$. In fact, the Bayesian and the maximum-likelihood solution coincide whenever a scale parameter (or a position parameter, with constant prior probability density [30]) is estimated. It should be understood, however, that in more general cases the maximum-likelihood solution only approximates the rigorous Bayesian solution (which is the price one has to pay for not working with the correct prior probability).

5.2. Porter-Thomas Distribution with Given Threshold

Let us now consider a less academic case. We assume that the sample contains only reduced widths that exceed a given detection threshold Γ_c. If the threshold depends on energy we must start from the bivariate distribution (properly normalised to unity)

$$p(\Gamma_i,E_i|\langle\Gamma\rangle,\Gamma_c)d\Gamma_i dE_i = \frac{1}{\overline{\mathrm{erfc}\sqrt{x_c}}}\frac{e^{-x_i}}{\sqrt{\pi x_i}}dx_i\frac{dE_i}{E_b-E_a} \quad ,$$

$$x_c \equiv \frac{\Gamma_c(E)}{2\langle\Gamma\rangle} < x_i \equiv \frac{\Gamma_i}{2\langle\Gamma\rangle} < \infty \ , \quad E_a < E_i < E_b \quad , \tag{17}$$

where the bar over the complementary error function denotes the energy average in the interval $(E_a \ldots E_b)$. The joint probability to obtain the given sample of level energies and entrance-channel widths is

$$L\ d\Gamma_1\ldots d\Gamma_N dE_1\ldots dE_N = \left(\frac{2}{\sqrt{\pi}\ \overline{\mathrm{erfc}\sqrt{x_c}}}\right)^N e^{-\xi^2} d^N\xi\ \frac{dE_1\ldots dE_2}{(E_b-E_a)^N} \tag{18}$$

where $\xi^2 = (N/2)(\overline{\Gamma}/\langle\Gamma\rangle)$ is the sqared radius and $d^N\xi$ is the volume element in the space of the ξ_i defined before. Factorising L one sees again that the sample average $\overline{\Gamma}$ is a minimal sufficient statistic. As before its distribution can be obtained by integration over all angles in the space of

the ξ_i for fixed level energies E_i. The resulting solid angle factor must then be averaged over level energies. The final distribution can again be interpreted either as that for $\overline{\Gamma}$ or as that for $\langle\Gamma\rangle$. Since the energy-averaged solid-angle factor does not depend on $\langle\Gamma\rangle$ one finds in the latter case

$$p(\langle\Gamma\rangle|\overline{\Gamma},\Gamma_c)d\langle\Gamma\rangle \propto \left(\overline{\mathrm{erfc}\sqrt{yz}}\right)^{-N} e^{-y} y^{N/2-1} dy ,$$

$$0 < y \equiv \frac{N\,\overline{\Gamma}}{2\langle\Gamma\rangle} < \infty, \qquad z \equiv \frac{\Gamma_c(E)}{\overline{\Gamma}} . \tag{19}$$

Since we estimate a scale factor again, the maximum-likelihood solution coincides with the rigorous Bayesian solution. Maximising L with respect to $\langle\Gamma\rangle$ one obtains

$$\overline{\Gamma} = \langle\Gamma\rangle\left(1 + \frac{2}{\sqrt{\pi}} \frac{\overline{e^{-x_c} x_c}}{\overline{\mathrm{erfc}\sqrt{x_c}}}\right) . \tag{20}$$

The factor in parantheses corrects for threshold effects. Since it depends on $\langle\Gamma\rangle$ one must solve iteratively, for instance with the Newton-Raphson method. Once $\langle\Gamma\rangle$ is known one knows also $\mathrm{erfc}\sqrt{x_c}$ and thus the estimated true number of levels, $N/\mathrm{erfc}\sqrt{x_c}$.

Although this may not be readily apparent from the available documentation (20) is the basis of the algorithms developped by

- Fuketa and Harvey [32] (with $\Gamma_c/\Gamma = c \cdot E^b$, c and b being given constants characterising experimental conditions),
- Fort et al. [33] (ESTIMA code, Γ_c = const, chosen so as to exclude practically all p-wave levels),
- Rohr et al. [34] (MISDO, modified Fuketa-Harvey code with threshold chosen so as to restrict p-wave admixture to a given small fraction).

In none of these algorithms, however, is the $\langle\Gamma\rangle$-uncertainty calculated from the exact distribution (19).

Another approximate estimation procedure is the moment method. One equates the sample moments with the true (ensemble) moments of the probability distribution whose parameters one tries to estimate. Moore [20] derived a missing-level estimator by equating the first two moments of the distribution of $\sqrt{\Gamma}$ (essentially the width amplitude) with their expectation values, for a sharp width threshold Γ_c,

$$\overline{\sqrt{\Gamma}} \equiv \frac{1}{N}\sum_{i=1}^{N}\sqrt{\Gamma_i} = \int_{\Gamma_c}^{\infty}\sqrt{\Gamma}\,p(\Gamma)d\Gamma \Big/ \int_{\Gamma_c}^{\infty}p(\Gamma)d\Gamma\ , \tag{21}$$

$$\overline{\Gamma} \equiv \frac{1}{N}\sum_{i=1}^{N}\Gamma_i = \int_{\Gamma_c}^{\infty}\Gamma\,p(\Gamma)d\Gamma \Big/ \int_{\Gamma_c}^{\infty}p(\Gamma)d\Gamma\ . \tag{22}$$

Inserting (1) explicitly one gets

$$\frac{\overline{\Gamma}}{(\overline{\sqrt{\Gamma}})^2} = \sqrt{\frac{\pi}{2}}\,e^{x_c}\mathrm{erfc}\sqrt{x_c}\left(\sqrt{\frac{\pi}{2}}\,e^{x_c}\mathrm{erfc}\sqrt{x_c} + \sqrt{2x_c}\right)\ . \tag{23}$$

For given sample averages this is an equation for x_c which can be solved by iteration. If, in addition, the threshold Γ_c is known one obtains $\langle\Gamma\rangle = \Gamma_c/(2x_c)$. Moore, on the other hand, prescribes a value for x_c (e. g. 1/8 for the ^{238}U sample considered in [36]) which determines the right-hand side of (23). He then varies the threshold and thus the number N of levels included, beginning with a high threshold. Lowering the threshold he includes weaker and weaker levels in the sample averages until the left-hand side of (23) equals the fixed number on the right-hand side. The true number of levels is then estimated as $N/\mathrm{erfc}\sqrt{x_c}$. The mean level spacing found with this estimator for ^{238}U was

$$\langle D\rangle = 20.9 \pm 1.5 \text{ eV}.$$

This is to be compared with the 24.78 ± 0.14 eV obtained from essentially the same data base by means of the ortogonal-ensemble statistics Δ_3 and W (see Sect. 3.). The 19% discrepancy corresponds to weak levels that are clearly missing from the width distribution but did not show up in the Δ_3 test because they were fairly uniformly distributed over the energy range covered (0 to 4 keV). This illustrates the insensitivity of the orthogonal-ensemble test statistics mentioned before and the general superiority of estimation procedures based on the width distribution.

An estimator similar to the one devised by Moore could be based on (20). Assuming with Moore that the threshold does not depend on energy one can rewrite (20) as

$$\frac{\overline{\Gamma}}{2\Gamma_c} = \frac{1}{x_c}\left(1 + \frac{2}{\sqrt{\pi}}\,\frac{e^{-x_c}\,x_c}{\mathrm{erfc}\sqrt{x_c}}\right)\ . \tag{24}$$

For given right-hand side one can again vary the threshold Γ_c and thereby also the number N of widths included in the statistic Γ until both sides of (24) are equal. With the final value of N the estimated true number of levels is $N/\mathrm{erfc}\sqrt{x_c}$ as before. For given threshold, however, it is not more difficult to find $\langle\Gamma\rangle$ and thus $\mathrm{erfc}\sqrt{x_c}$ from (19). This rigorous (Bayesian) approach has the additional advantage that confidence limits can easily be calculated from the correct distribution (19) whereas for Moore's missing-level estimator and the simpler one based on (24) the correct error estimation recipe is not so obvious.

5.3. Porter-Thomas Distribution with Unknown Threshold

The missing-level estimators discussed in the preceding section require thresholds to be set on the basis of experimental characteristics [32] or of prior knowledge about strength functions [33, 34] or by judging how far the unperturbed part of the width distribution extends [20, 28]. It will be shown now that for a pure Porter-Thomas distribution the threshold can be automatically estimated from the resonance parameters themselves without any other prior knowledge. We adopt the notation

$$u_i \equiv \operatorname{erfc} \sqrt{x_i} \quad , \qquad u_c(E) \equiv \operatorname{erfc} \sqrt{x_c(E)} \quad , \tag{25}$$

so that $u_c(E)$ is the fraction of observed levels in the interval dE at E. In this representation the bivariate distribution of level energies and reduced neutron widths (normalised to unity) assumes the simple form

$$p(\Gamma_i, E_i \,|\, \langle\Gamma\rangle, \Gamma_c) d\Gamma_i dE_i = \frac{du_i}{\overline{u_c}} \frac{dE_i}{E_b - E_a} \quad ,$$

$$0 < u_i < u_c(E_i) \quad , \qquad E_a < E_i < E_b \quad . \tag{26}$$

This means that in an (E,u)-diagram the sample points (E_i, u_i) are uniformly distributed below the threshold $u = u_c(E)$ as shown schematically in Fig. 3.

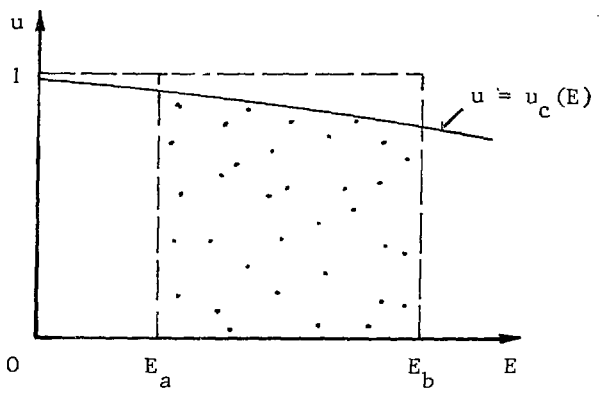

Fig. 3 - Threshold and distribution of sample points in (E,u) representation

Next we factorise , pulling out the energy average denoted by the overbar,

$$u_c(E) \equiv \overline{u_c}\, f(E) \quad , \tag{27}$$

and assume the energy dependence f(E) to be known. This function can easily be obtained from the resonance data with adequate precision by least-squares fitting of a suitable test function to the cumulative level numbers

N(E). Choosing a polynomial we can write for the fitted function and its derivative

$$\overline{N}(E) - \overline{N}(E_a) = \rho\overline{u_c} \int_{E_a}^{E} f(E)dE = c_1(E-E_a) + c_2(E-E_a)^2 + \ldots \quad (28)$$

$$\frac{d\overline{N}}{dE} = \rho\overline{u_c}\, f(E) = c_1 + 2c_2(E-E_a) + \ldots \quad (29)$$

where the coefficients c_n are known from the fit. The apparent level density $u_c\rho$ is easily expressed by known quantities if we put $E = E_b$ in (28) and utilise $f(E) = 1$. One finds

$$f(E) = \frac{c_1 + 2c_2(E-E_a) + \ldots}{c_1 + c_2(E_b-E_a) + \ldots} \quad (30)$$

A parabolic fit ($c_3 = c_4 = \ldots = 0$), corresponding to a linear energy dependence of u_c, is usually quite adequate. Fig. 4 shows examples for parabolic fits.

Clearly $\langle\Gamma\rangle$ is a scale parameter again but the role of $\overline{u_c}$ is less clear. Not knowing the prior probability we cannot invoke Bayes' theorem. Instead we try to find sufficient statistics by factorisation of L, and then their probability distribution by integration over as many widths and energies as possible. We start with a constant threshold, $f(E) = 1$. The joint probability for the whole sample is

$$L(\Gamma_1,\ldots\Gamma_N|\langle\Gamma\rangle,\Gamma_c)d\Gamma_1\ldots d\Gamma_N = \frac{1}{u_c^N}\frac{e^{-N\overline{\Gamma}/(2\langle\Gamma\rangle)}}{\langle\Gamma\rangle^{N/2}}\prod_{i=1}^{N}\frac{d\Gamma_i}{\sqrt{2\pi\Gamma_i}}H(\Gamma_1-\Gamma_c) \quad (31)$$

where H is the Heaviside function and Γ_1 the smallest width. This shows that $\overline{\Gamma}$ and Γ_1 are jointly sufficient statistics. Integration over all angles in the (N-1)- dimensional space spanned by $\xi_2,\ldots\xi_N$ results in the distribution

$$p(\overline{\Gamma},\Gamma_1|\langle\Gamma\rangle,\Gamma_c)d\overline{\Gamma}d\Gamma_1 \propto \frac{du_1}{u_c^N}e^{-y}y^{(N-1)/2-1}dy \quad , \qquad y \equiv \frac{N\overline{\Gamma}-\Gamma_1}{2\langle\Gamma\rangle} \quad . \quad (32)$$

This is the product of the joint probability that Γ_1 lies in $d\Gamma_1$ and all other widths are larger, viz.

$$p(u_1 > u_2 > \ldots u_N|u_c)du_1 = N\left(\frac{u_1}{u_c}\right)^{N-1}\frac{du_1}{u_c} \quad , \quad (33)$$

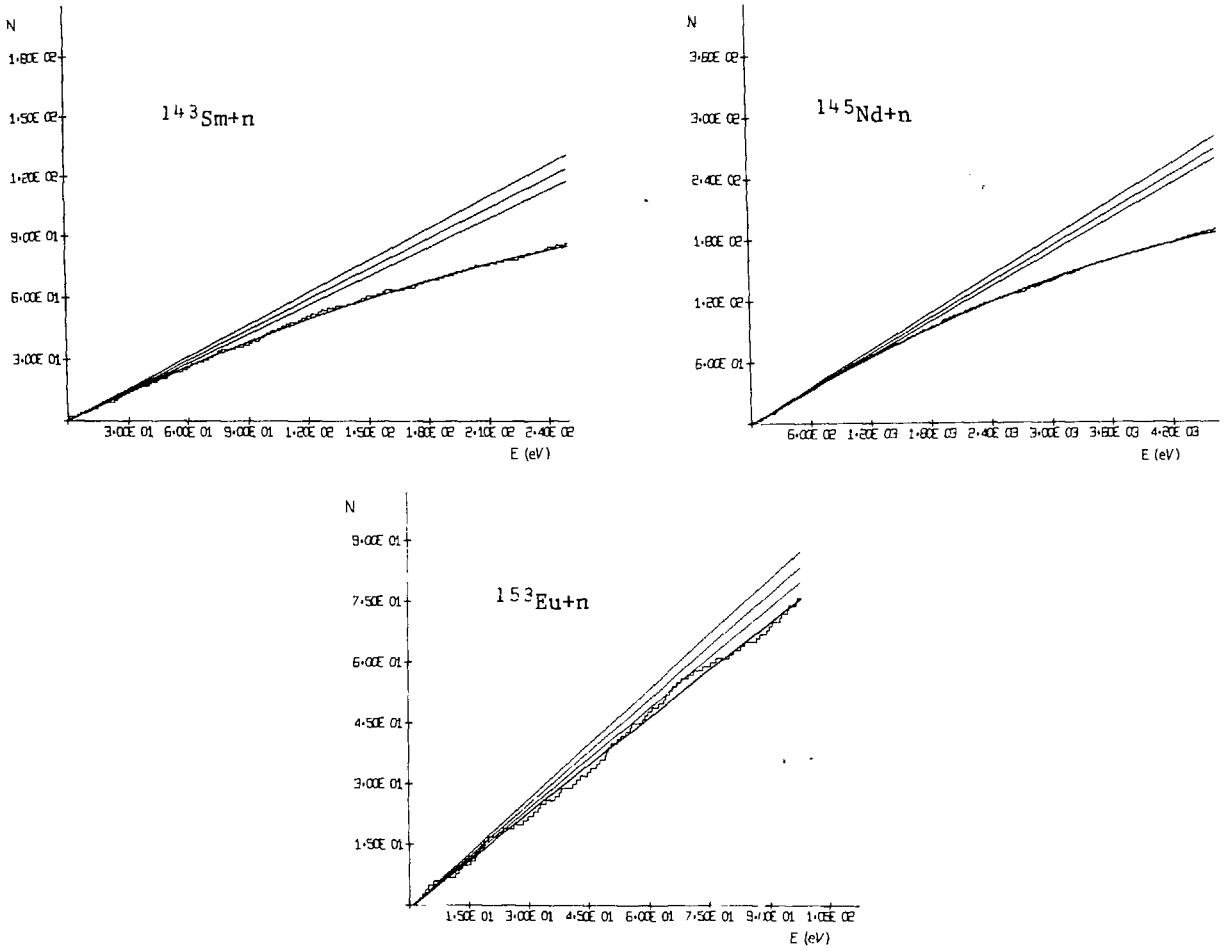

Fig. 4 - Examples for parabolic fits to level number staircase curves N(E). Straight lines: STARA estimates and confidence limits for the level density corrected for missing levels (from Ref. 35), maximum-likelihood approach.

and the probability that the sum of these other widths is $N\overline{\Gamma}-\Gamma_1$ given that Γ_1 is the lower threshold, viz.

$$p(\overline{\Gamma}|\langle\Gamma\rangle,\Gamma_1)d\overline{\Gamma} \propto \frac{1}{u_1^{N-1}} e^{-y} y^{(N-1)/2-1} dy \quad . \tag{34}$$

Going to $\langle\Gamma\rangle$ and u_c as variables one finds from (32) the joint distribution of the estimated parameters,

$$p(\langle\Gamma\rangle,u_c|\overline{\Gamma},\Gamma_1)d\langle\Gamma\rangle du_c \propto \frac{u_1}{u_c^N} e^{-y} y^{(N-1)/2-1} dy \frac{du_c}{u_c} ,$$

$$0 < y \equiv \frac{N\overline{\Gamma}-\Gamma_1}{2\langle\overline{\Gamma}\rangle} < \infty \quad , \quad 0 < u_c < 1 \quad . \tag{35}$$

For given Γ_1 the probability becomes maximal if u_c is minimal, i. e. $u_c = u_1$. This estimate is biased, however, being always low. Calculating the expectation value of u_1/u_c from (33) one finds that

$$u_c = \frac{N+1}{N} u_1 = \frac{N+1}{N} \operatorname{erfc}\sqrt{x_1} \tag{36}$$

is an unbiased estimator of the observable fraction of levels. Differentiation of L with respect to $\langle\Gamma\rangle$ yields

$$\frac{1}{N-1} \sum_{i=1}^{N} \Gamma_i = \langle\Gamma\rangle \left(1 + \frac{2}{\sqrt{\pi}} \frac{e^{-x_1}\sqrt{x_1}}{\operatorname{erfc}\sqrt{x_1}}\right) . \tag{37}$$

Thus $\langle\Gamma\rangle$ can be found from (37) whereupon u_c and the estimated true number of levels N/u_c follow from (36). If the threshold depends on energy (37) remains valid but instead of (36) one finds

$$\overline{u_c} = \frac{N+1}{N} \frac{\operatorname{erfc}\sqrt{x_1}}{f(E_1)} \quad . \tag{38}$$

In both (37) and (38) the subscript 1 refers now to the sample point which relatively speaking is closest to the threshold, i. e. which has the highest ratio $u_i/f(E_i)$ (but not necessarily the smallest Γ_i).

So far we assumed thresholds to be sharp. In reality, however, thresholds are diffuse. It is then better to base the estimation not on all members of the sample, but to discard the points in the region of the diffuse threshold. It is not difficult to derive the corresponding equations. If the sample members are enumerated in descending order of $u_i/f(E_i)$ and the estimation is based on the members k to N only one finds as generalisation of Eqs. (37) and (38)

$$\frac{1}{N-k} \sum_{i=k+1}^{N} \Gamma_i = \langle\Gamma\rangle\left(1 + \frac{2}{\sqrt{\pi}} \frac{e^{-x_k}\sqrt{x_k}}{\mathrm{erfc}\sqrt{x_k}}\right) , \tag{39}$$

$$\overline{u_c} = \frac{N+1}{N+1-k} \frac{\mathrm{erfc}\sqrt{x_k}}{f(E_k)} . \tag{40}$$

One can begin the estimation with the outermost point (k=1) and then move inward point by point to check the stability of the results against threshold variations. It should be pointed out that the rigorous result presented here differs from the maximum-likelihood result given in [8], especially for small samples.

Another way to deal with diffuse thresholds is to replace the Heaviside function in (31) by a function with smooth edges. This precludes a rigorous solution and one has to use the maximum-likelihood approximation, as is done in the STARA code [35]. Fig. 5 shows results for ^{238}U, obtained from the same data base as the mean level spacings quoted before (24.78 ± 0.14 eV [23], 20.9 ± 1.5 eV [36]). The average s-wave level spacing estimated with STARA was [35]

$$\langle D\rangle = 20.4 \pm 0.3 \text{ eV} ,$$

in good agreement with the value from Moore's missing-level estimator.

5.4 Porter-Thomas Distribution Distorted by Unresolved Multiplets

The level density estimators based on the observed width distribution which we discussed so far gave satisfactory results when tried on Monte Carlo generated resonance parameter sets, with reduced widths sampled from the Porter-Thomas distribution, resonance energies from the Wigner distribution or orthogonal-ensemble theory, and levels with a reduced width below some critical value rejected as missing. It came, therefore, as an unpleasant surprise when in the recent NEADB benchmark exercise [5] all of them systematically underestimated the level density by 4-8 % in cases which must be considered as quite favorable, viz. large, almost pure s-wave samples resembling those observed for actinides.

The NEADB test material was prepared as follows. Level widths and energies were produced by Monte Carlo sampling as usual, but not distributed. Instead, they were utilised by P. Ribon to generate Doppler- and resolution-broadened cross sections which were in addition subjected to simulated counting statistics. These "experimental" data (but not the original parameters) were handed over to H. Derrien who tried to recover the resonance parameters by multi-level shape analysis. His extracted resonance energies, neutron widths, spins and parities were then distributed to the participants. They contained thus not only threshold effects due to counting statistics in a very realistic way but also resolution effects in the form of resonance parameters that had been extracted from peaks mistaken for singlets while actually they were doublets and triplets. This latter effect is totally absent in resonance parameters directly obtained by Monte Carlo

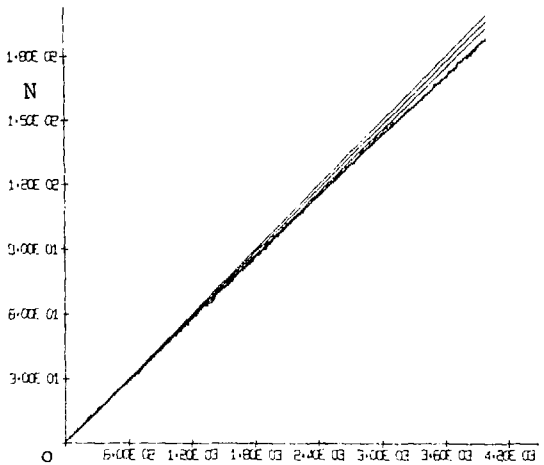

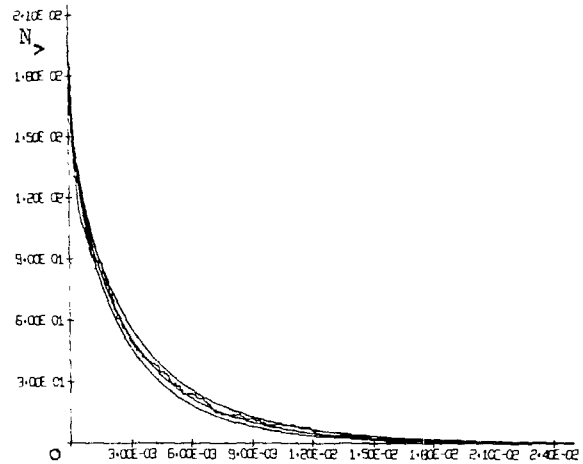

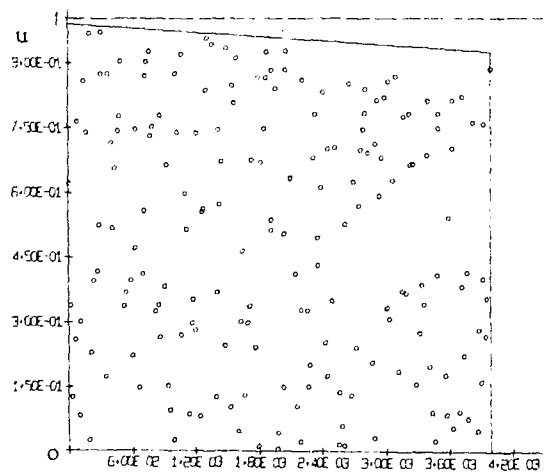

Fig. 5 - STARA results for $^{238}U+n$.

Top left: Level number staircase curve with parabolic fit and straight lines giving estimated level density and confidence limits (see text).

Top right: Integral Porter -Thomas distribution with confidence limits and data staircase curve showing scarcity of small levels.

Bottom: Uniformly distributed sample points in (E,u) diagram below automatically estimated detection threshold.

(from Ref. 35)

sampling. That it was significant can be seen in Table I which shows characteristics of benchmark test material representing almost pure s-wave samples together with STARA results. Strength functions were estimated correctly but level densities were underestimated. One recognises that adding the true numbers of levels lost in unresolved multiplets (disclosed after the benchmark exercise) to the estimated missing-level numbers one gets almost exactly the correct numbers in all three cases. The conclusion is that most of the bias in the STARA results was due to unrecognised multiplets that had been analysed as singlets.

Table I - Characteristics of NEADB benchmark data and STARA results. Numbers in parantheses give STARA results modified by addition of the true number of levels lost in multiplets to the original STARA estimates of missing levels.

Benchmark Case	S_0 (10^{-4})	$\langle D \rangle$ (eV)	all levels	missing levels	lost in multiplets	origin
5A	2.22 2.23±.30	1.85 2.02±.08 (1.84)	173 158±2 (174)	33 26±2 (42)	16 0 (16)	true STARA (")
5B	2.47 2.52±.25	1.43 1.56±.05 (1.42)	224 204±1 (226)	50 30±1 (52)	22 0 (22)	true STARA (")
5C	1.79 1.81±.25	1.82 1.90±.09 (1.77)	170 162±3 (175)	40 32±3 (45)	13 0 (13)	true STARA (")

Let us now consider the problem that levels are missed not because of a detection threshold but because limited instrumental resolution causes pairs, triples etc. of closely spaced levels to be mistaken for single peaks. We assume that this happens whenever spacings are smaller than some critical separation D_c which of course must be of the order of the instrumental resolution. The fraction of levels lost in unresolved multiplets is then

$$q = \int_0^{D_c} p(D)dD \ , \tag{41}$$

where $p(D)dD$ is the level spacing distribution. If one assumes that the apparent neutron width extracted from an unresolved multiplet peak is equal to the sum of the true component widths one can show that the observed width distribution is given by [8]

$$p(\Gamma|\langle\Gamma\rangle,q)d\Gamma = (1-q)(1+v)\frac{e^{-x}}{\sqrt{\pi x}}dx\ , \quad 0 < x \equiv \frac{\Gamma}{2\langle\Gamma\rangle} < \infty \tag{42}$$

with

$$v = \sqrt{\pi}z\ e^{z}\ (1 + \mathrm{erf}\ z), \quad z = q\sqrt{x} \tag{43}$$

in the case of a single Porter-Thomas distribution. The distortion factor $(1-q)(1+v)$ multiplying the undistorted width distribution reduces the relative frequency of small widths and increases that of large ones as was to be expected (Fig. 6).

It is quite easy to modify the estimators described so far (and the corresponding codes) by replacing the unperturbed Porter-Thomas distribution everywhere by the distorted distribution (42), (43). This analytic treatment of resolution effects is much more convenient than Monte Carlo cross section simulations. It is used in a new version of the STARA code for statistical resonance analysis which gave the improved benchmark results [8] shown in Table II.

Table II - Comparison between NEADB benchmark values and STARA-81 results obtained with analytical estimation of levels lost in unrecognised multiplets.

Benchmark Case	S_0 (10^{-4})	$\langle D\rangle$ (eV)	origin
5A	2.22	1.849	true
	2.20±.30	1.81±.19	STARA-81
5B	2.47	1.428	true
	2.49±.30	1.44±.05	STARA-81
5C	1.79	1.824	true
	1.78±.22	1.86±.09	STARA-81

5.5. Mixtures of Level Sequences

So far we treated only a single s-wave level sequence as occurs for target nuclei with spin 0. For target nuclei with nonzero spin one has two s-wave level sequences. It is well known that the quantities $g\Gamma$ of the mixed sample (g being the spin factor) are again members of a Porter-Thomas distribution provided that the strength function is the same for both sequences and their level densities can be taken as proportional to 2J+1, J being the resonance spin quantum number. This means that the methods discussed so far are applicable to all isotopically pure s-wave samples, from both even and odd nuclei.

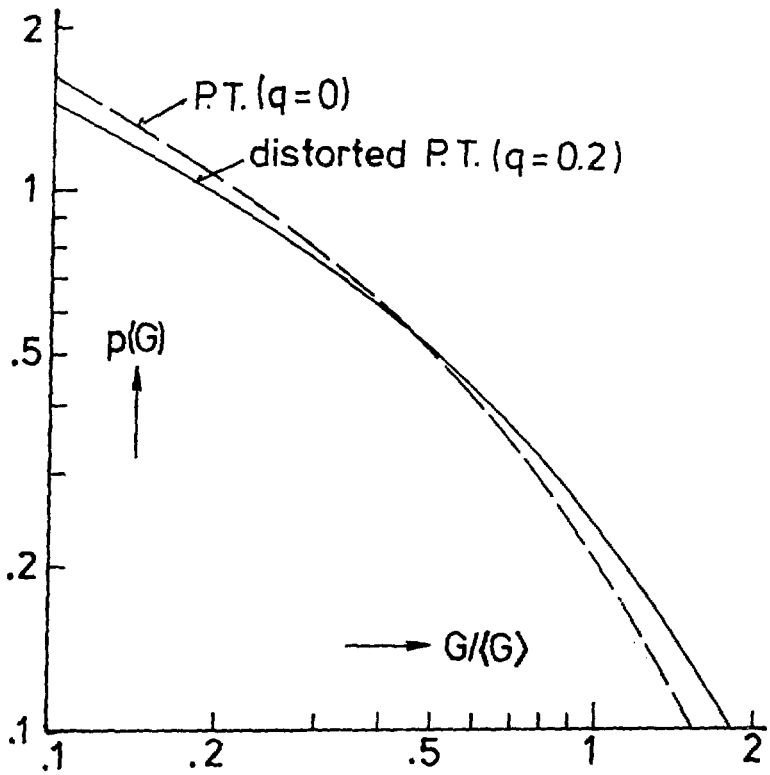

Fig. 6 - Undistorted Porter-Thomas distribution (perfect resolution, q = 0) and Porter-Thomas distribution distorted by 20 % missing levels lost in unrecognised multiplets (q = 0.2), according to the analytic approximation Eqs. (42), (43).

The problem of p-wave admixture with unidentified level parities is more difficult. One can use artificial thresholds to reject practically all p-wave levels (which usually have very small widths) as is done in ESTIMA [33], MISDO [345] and in the original version of STARA [35], or one can estimate the p-wave strength function together with the s-wave strength function and the level density, as is done in Stefanon's CAVE code [37] where the maximum of the likelihood function is determined by a simple grid search procedure. We shall look first at the simplest possible estimation problem involving an s-wave distribution $p_0(G|G^0)$ and a p-wave distribution $p_1(G|G^1)$ of neutron widths, where we use the notation

$$G \equiv g\Gamma_n\sqrt{1\ eV/E}\ (= g\Gamma_n^{\ell}v_{\ell}(E))\ , \qquad G^{\ell} \equiv \langle g\Gamma_n^{\ell}\rangle\ , \qquad (44),(45)$$

g is the statistical spin factor, Γ_n the neutron width and v_ℓ the centrifugal-barrier penetrability (equal to 1 for the s-wave). As we assume that spins and parities are not or not always known we cannot calculate reduced widths from the $g\Gamma_n$-values which resonance analysis yields (because this would require division by v_ℓ which depends on parity). For s-wave levels G is, however, just the reduced neutron width times the spin factor. For zero target spin both p_0 and p_1 are Porter-Thomas distributions (p_1 at least in good approximation) and we can write

$$p(G_i,E_i|G^0,G^1)dG_i dE_i = \left(w_0\frac{e^{-G/(2G^0)}}{\sqrt{2\pi GG^0}} + w_1\frac{e^{-G/(2G\ v_1(E_i))}}{\sqrt{2\pi\ GG^1v_1(E_i)}}\right)\frac{dG_i dE_i}{E_b-E_a} \qquad (46)$$

where w_0, w_1 are the a-priori probabilities that a given resonance is excited by the s- or the p-wave, viz.

$$w_0 = \begin{cases}\frac{\rho_0}{\rho_0+\rho_1}\\ 1\\ 0\end{cases}, \quad w_1 = \begin{cases}\frac{\rho_1}{\rho_0+\rho_1}\\ 0\\ 1\end{cases} \quad \text{for} \begin{cases}\text{unknown parity}\\ \text{s-wave level}\\ \text{p-wave level}\end{cases} \qquad (47)$$

where ρ_0, ρ_1 are the densities of s- and p-wave levels ($\rho_1 = 3\ \rho_0$ for target spin zero and approximate (2J+1)-dependence of the level densities). The likelihood function becomes maximal for

$$G^0 = \langle g\Gamma_n^0\rangle = \frac{\sum_i \tilde{w}_{0i}G_i}{\sum_i \tilde{w}_{0i}}\ , \qquad G^1 = \langle g\Gamma_n^1\rangle = \frac{\sum_i \tilde{w}_{1i}G_i/v_\ell(E_i)}{\sum_i \tilde{w}_{1i}} \qquad (48)$$

where $\tilde{w}_0$, $\tilde{w}_1$ are the a-posteriori probabilities that a level with given E_i and G_i belongs to the s- or the p-wave part,

$$\tilde{w}_0 = \frac{w_0p_0}{w_0p_0+w_1p_1}\ , \qquad \tilde{w}_1 = \frac{w_1p_1}{w_0p_0+w_1p_1}\ . \qquad (49)$$

Both estimated parameters occur in the a-posteriori weights so that the eqs. (48) are coupled and must be solved iteratively. For a pure s-wave

sample ($\rho_l = 0$) the weighted average for $l = 0$ reduces to the unweighted sample average (14). Since we estimate scale parameters, the maximum-likelihood solution is rigorous and the probability distribution for them is just the likelihood function, from which confidence limits (and the covariance) can be calculated.

Eqs. (48) suggest a general approach for samples of mixed parity: Start with guess values for the parameters, calculate the a-posteriori probabilities for each member of the sample and go through the estimation procedure for pure s- and pure p-wave samples separately, with weighted G-values weighted by w_0 and w_1, respectively. This yields improved estimates for $\langle g\Gamma_n^0\rangle$ and $\langle g\Gamma_n^1\rangle$ with which improved posterior probabilities can be calculated. Repeat the process until convergence is achieved. Moore adopted this prescription to generalise his missing-level estimator to mixed parities. The generalised estimator is implemented in the code BAYESZ, available from the neutron data centres. BAYESZ handles also resolution effects in a simple approximation.

It should be clear by now how the formulae derived for single Porter-Thomas distributions can be generalised. We shall only state the result for given, energy-dependent threshold: The maximum-likelihood equations to be solved for the two parameters $\langle g\Gamma_n^0\rangle$ and $\langle g\Gamma_n^1\rangle$ are (ℓ=0, 1)

$$G^\ell = \langle g\Gamma_n^\ell\rangle = \frac{\sum_i \tilde{w}_{\ell i} G_i / v_\ell(E_i)}{\sum_i \tilde{w}_{\ell i}} \left(1 + \frac{1}{\sum_i \tilde{w}_{\ell i}} \frac{2}{\sqrt{\pi}} \sum_i \frac{w_{\ell i} \exp(-x_{c\ell})\sqrt{x_{c\ell}}}{w_{0i}\,\mathrm{erfc}\sqrt{x_{c0}} + w_{1i}\,\mathrm{erfc}\sqrt{x_{c1}}}\right)^{-1} \tag{50}$$

where

$$x_{c\ell} = \frac{G_c(E)}{2\langle g\Gamma_n^\ell\rangle v_\ell(E)} \tag{51}$$

It is not clear at present how much better the more rigorous Bayesian and maximum-likelihood methods are compared to ad hoc techniques such as Moore's missing-level estimator or the simple approach of finding $\langle g\Gamma_n^0\rangle$ and the s-wave level density from a least-squares fit to the upper, unperturbed part of the width distribution, then subtracting the extrapolated s-wave distribution from the lower part and fitting the remainder with an average p-wave width. For small samples differences may become noticeable. In any case the more rigorous methods give clearer recipes for error estimation.

6. SUMMARY

Level density estimation methods have been reviewed with emphasis on the mathematical and statistical aspects. A new rigorous solution is given for the problem of simultaneous estimation of mean width and level density (or true number of levels) for a Porter-Thomas distribution affected by a detection threshold with known energy dependence but unknown height.

The generalisation to mixed (s- and p-wave) resonance samples is also indicated briefly.

A number of conclusions can be drawn from experience with experimental data and benchmark test material:

- Estimators based on level energies (ladder statistics) are not useful except with extremely pure single sequences.

- Estimators based on the reduced-width (Porter-Thomas) distribution work well. Rigorous solutions for the parameter estimation problem can be given for simple models (known sharp detection threshold, sharp threshold with known energy dependence but unknown height), maximum-likelihood solutions are possible also for more complex models (diffuse threshold, p-level admixture).

- Resolution effects (levels missed in unresolved multiplets) can be treated analytically at least for pure (or almost pure) s-wave samples.

- Estimators should be tested with the NEADB benchmark test material (available from the neutron data centres). Simple tests with Monte Carlo generated resonance parameters are not sufficiently sensitive to resolution effects.

- New estimators could also be compared with well tested and documented codes such as BAYESZ, ESTIMA and MISDO (all available from the neutron data centres).

ACKNOWLEDGEMENT

It is a pleasure to acknowledge valuable discussions with F. Perey on the group-theoretical approach to prior probabilities.

REFERENCES

1. A.M. Anzaldo Meneses, Proc. Conf. on Nucl. Data for Sci. and Technol., Antwerp (1982), p. 534

2. O. Bohigas, R.U. Haq and A. Pandey, Proc. Conf. on Nucl. Data for Sci. and Technol., Antwerp (1982), p. 809

3. V.S. Ramamurthy, this meeting

4. G. Rohr, this meeting

5. C.F. Porter and R.G. Thomas, Phys. Rev. 104(1959)483

6. D.K. Olsen, G. de Saussure, R.B. Perez, E.G. Silver, R.W. Ingle and H. Weaver, Report ORNL/TM-5256. Oak Ridge (1976); D.K. Olsen, G. de Saussure, R.B. Perez, E.G. Silver, F.C. Difilippo, R.W. Ingle and H. Weaver, Nucl. Sci. Eng. 62(1977)479;

7. P. Ribon and A. Thompson, Proc. Conf. on Nucl. Data for Sci. and Technol., Antwerp (1982), p. 628

8. F.H. Fröhner, IAEA Meeting on Uranium and Plutonium Isotope Resonance Parameters, INDC(NDS)-129/GJ, Vienna (1981), p. 103

9. H.I. Liou, Conf. on Nucl. Data Eval. Meth. and Proced., Brookhaven 1980, BNL-NCS-51363 (1981), p. 463

10. F.H. Fröhner, Proc. Conf. on Nucl. Data for Sci. and Technol., Antwerp (1982), p. 623

11. R.R. Whitehead, A. Watt, D. Kelvin and A. Conkie, Phys. Lett. 76B(1978)149

12. S.M. Grimes and S.D. Bloom, Phys. Rev. C23(1981)1259

13. J.J.M. Verbaarschot and P.J. Brussaard, Phys. Lett. 86B(1979)155

14. T.A. Brody, J. Flores, J.B. French, P.A. Mello, A. Pandey and S.S.M. Wong, Rev. Mod. Phys. 53(1981)385, in particular Fig. 10

15. C.E. Porter (ed.), Statistical Theories of Spectra, New York - London (1965)

16. P.A. Mello, J. Flores, T.A. Brody, J.B. French, S.S.M. Wong, Proc. Conf.on Interact. of Neutrons with Nuclei, Lowell (1976), vol. I, p. 496

17. F.J. Dyson and M.L. Mehta, J. Math. Phys. 4(1963)701

18. M.L. Mehta, Statistical Properties of Nuclei (ed. J.B. Garg), New York - London (1972), p. 179

19. H.I. Liou, H.S. Camarda and F. Rahn, Phys. Rev. C5(1972)450

20. M.S. Moore, J.D. Moses, G.A. Keyworth, J.W.T. Dabbs and N.W. Hill, Phys. Rev. C18(1978)1328

21. E.Fort, H. Derrien and D. Lafond, Meeting on Neutron Cross Sections of Fission Product Nuclei, Bologna 1979, RIT/FIS-LDN(80)1, p. 121

22. P. Ribon, this meeting

23. G. de Saussure, D.K. Olsen, R.G. Perez and F.C. Difilippo, Report ORNL/TM-6152 (1978)

24. J.S. Story and R.W. Smith, Trieste Winter Courses 1982, ITCP Trieste, to be published,
J.L. Rowlands, R.W. Smith, J.M. Stevenson and W.H. Taylor, Proc. Conf. on Nucl. Data for Sci. and Technol., Antwerp (1982), p. 85

25. A. Michaudon, H. Derrien, P. Ribon, M. Sanché, Nucl. Phys. 69(1965)545

26. H. Derrien and B. Lucas, Nucl. Cross Sections and Technol., NBS Spec. Publ. 425, Washington D.C. (1975) vol. II, p. 637

27. J.D. Garrison, Phys. Rev. Letters 29(1972)1189

28. H. Weigmann, Proc. Conf. on Nuetron Physics and Nuclear Data, Harwell (1978), p. 969

29. H. Jeffreys, Theory of Probability, Oxford (1939)

30. E.T. Jaynes, Trans. Systems Sci. and Cybern. 4(1968)227

31. D.D. Slavinskas and Kennett, Nucl. Phys. 85(1966)641

32. T. Fuketa and J.A. Harvey, Nucl. Inst. Meth. 33(1965)107

33. P. Ribon, E. Fort, J. Krebs, Tran Quoc Thuong, CEA-N-1832 167L (1975)

34. G. Rohr, L. Maisano and R. Shelley, Meeting on Neutron Cross Sections of Fission Product Nuclei, Bologna 1979, RIT/FIS-LDN(80)1, p. 197;
G. Rohr, this meeting

35. F.H. Fröhner, Meeting on Neutron Cross Sections of Fission Product Nuclei, Bologna 1979, RIT/FIS-LDN(80)1, p. 145

36. G.A. Keyworth and M.S. Moore, Neutron Physics and Nuclear Data, (Conf. Proc.), Harwell (1978), p. 241

37. C. Coceva and M. Stefanon, Nucl. Phys. A315(1979)

EXTRACTION OF INFORMATION ON NUCLEAR LEVEL DENSITIES FROM THE RESONANCE REGION

P. Ribon

CEN - SACLAY

B.P. No. 2

F-91190 Gif-Sur-Yvette, France

Since the text of this paper was not available by the deadline of May 31, 1983, the Editor regrets having to omit it from the Proceedings of the Meeting.

EXTRACTION OF LEVEL DENSITY INFORMATION FROM NON-RESONANT REACTIONS

H. Vonach

Institut für Radiumforschung und Kernphysik
Vienna, Austria

ABSTRACT

The currently used methods to derive nuclear level density from study of non-resonant nuclear reactions are critically reviewed. The problem of extracting level densities from the particle spectra observed in compound nucleus reactions are addressed in some detail. Problems discussed include optimum choice of experimental conditions to minimize non-compound contributions, procedures to invert the equations of the statistical model with angular momentum conservation in order to derive specific level density information from comparison of model calculations with measured particle emission cross-sections, choice of optical model parameters for such calculations and uncertainty estimates for level densities derived in this way including the uncertainties in the input parameters for the model calculations. Other methods for deriving level densities like level counting in the region of resolved levels or the analysis of nuclear level widths derived from Ericson fluctuations, blocking experiments or other methods are discussed only briefly with respect to their most important methodological problems. Finally, after a short summary of the level density results achieved from the study of nuclear reactions, suggestions are made how our knowledge of nuclear level densities could be improved in the most efficient way by further use of the discussed methods.

1. INTRODUCTION

In this talk I want to give a survey on the various methods which can be used to determine nuclear level densities

from the study of nuclear reactions except for the area of resonance reactions which are delt with in other lectures.
The main topic of this lecture will thus be the discussion of the procedures which have to be used to derive absolute values of the level density of nuclei as function of their excitation energy from the directly observed quantities and the problem how to get reliable uncertainty estimates for the deduced level densities taking into account both the experimental errors and the theoretical uncertainties inherent to the various procedures for deducing the level density values. Lack of time will not permit me to do this in full detail for all methods which have to be addressed. Therefore I will cover just one problem, the determination of level densities from energy-differential particle emission cross-sections in compound nucleus reactions in some detail, because it appears to me that this area is the most promising one to improve our knowledge on level densities. For the other methods I will to a large extent have to refer to the relevant literature. Also because of the limited time I will restrict myself to the determination of the total level density $\rho(U)$ and cannot address the interesting question of the spin and parity dependence of level densities. In addition to the mentioned problem of how to deduce level densities in the best possible way from the various experiments I will, however, try to give a summary on the results which have so far been accumulated by their use and discuss the question what seems to be the most efficient way to improve our present still very incomplete knowledge of nuclear level densities.

2. DETERMINATION OF LEVEL DENSITIES FROM COUNTING OF RESOLVED LEVELS IDENTIFIED BY THEIR POPULATION IN NUCLEAR REACTIONS

At low excitation energy the level density can be determined by direct counting of the number of levels per unit energy. The individual levels of nuclei may be identified either from high-resolution measurements of charged particle spectra emitted in nuclear reactions like (p,α) or (d,p) or from high-resolution measurements of the γ-radiation emitted in reactions like thermal neutron capture, $(n,n'\gamma)$ or $(n,p\gamma)$. In the first case (s. fig. 1) each level populated in the reaction manifests itself in a particle group of the corresponding energy, in the second case the gamma-energy corresponds to the energy differences between all pairs of levels and the level scheme has to be established by means of Rytz' combination principle and/or additional coincidence measurements. (Fig. 2) Quantitatively there are two problems inherent to this method. First of all there is certainly a loss of levels when the average level spacing approaches the experimental energy resolution. Secondly and this is the more difficult pro-

blem there is the possibility that levels may escape detection because they are too weakly populated. These problems have up to now only been solved for one group of such experiments: for high resolution measurements of the particles emitted in compound nucleus reactions. Thus high-resolution magnetic spectrograph measurements of charged particles from compound nucleus reactions e.g. nuclear reactions like (p,α) or (p,p') in medium mass nuclei offer the best possibilities to derive rather complete nuclear level schemes up to relatively high excitation energies. In such reactions most levels are populated with comparable cross sections [1] and the possible loss of levels because of too low cross-section can either be neglected or estimated reliably from the known spin distribution of the levels [2]. Likewise procedures for correcting the loss of levels due to unresolved levels and estimating the uncertainty of this correction have been given [3]. Accordingly these reactions have allowed to use the level counting method up to densities of ∿ 50/MeV [1,4] (s. fig. 3). With the presently achievable resolution of ∿ 3 keV in such measurements this can certainly be extended to densities of 100/MeV. Unfortunately they are restricted to nuclei below ∿ A = 70 as for heavier nuclei almost all compound nuclei decay by neutron emission and charged particle emission proceeds predominantly by direct processes.

For heavier nuclei the situation becomes somewhat more difficult. Up to now no method has been developed to estimate the number of levels escaping detection in direct reactions. This number is certainly also very sensitive to the experimental conditions especially background and counting statistics. Thus in heavy nuclei we cannot hope to get reliable level density information from study of just one charged particle reaction. We can, however, hope to get better information by investigating the same nucleus by different reactions which populate different classes of levels (e.g. (d,p), (d,t) and (d,d') for populating particle, hole and collective states.

Likewise no procedure has been developed so far to estimate the number of missed levels if level schemes are derived from high resolution measurements of γ-spectra from either slow neutron capture or (p,nγ) and (n,n'γ) reactions. The latter reactions proceed mainly by means of compound nucleus formation and are therefore non-selective as discussed before. Accordingly it has been found that such reactions may successfully be used to identify reliably about the 20 lowest levels of many nuclei. At higher excitation energies the increasing complexity of the gamma spectra results in a loss of levels, the amount of which is hard to estimate.

Thus in most medium and heavy nuclei levels have been investigated by a number of methods, each of which is rather incomplete (s. fig. 4) and one has to make a somewhat qualitative judgement on the excitation energy up to which most (e.g. more than 90%) of the levels have been identified.

The results obtained so far by this method are summarized

in fig. 5, which shows my certainly somewhat subjective estimate on the present status of the level counting method for those nuclei for which also neutron resonance data exist. This figure shows two important points:

1) The energy range accessible to direct counting is still rather small, especially for the heavier nuclei. For most nuclei the level counting data give us just one significant piece of data, an average value of the level density in the low energy range or more precisely the integral over the level density between U = 0 and $U_{max} \sim$ 1-5 MeV

2) This integral information is available, however, for the whole mass range with reasonable statistical accuracy.

Actually there are of course many more levels known than indicated in fig. 5, but excitation energy regions where only a part of the levels has been identified cannot be used for deriving the level densities because no reliable procedures for estimating the fraction of missed levels are available, except for the discussed case of charged particles emitted in compound reactions in light and medium weight nuclei A < 70. For these cases (s. fig. 3) reasonable corrections for missing level can be applied which increases the usable excitation energy range by 1-2 MeV compared to figure 2.

After this description of the present situation I want to add a few words on the future possibilities. Unlike the resonance method the level counting method has by far not been pushed to its limits. Up to now most measurements of charged particle spectra have been performed with resolutions around 10 keV, whereas 2-3 keV have been achieved with magnetic spectrographs of the Q3D type and high-quality Tandem-van de Graaff beams [5]. With this resolution it should be possible to determine level densities up to ∿ 100 - 200 levels/MeV which correspond to excitation energies of 7 MeV in ^{56}Fe or 5 MeV in ^{55}Mn. Unfortunately no experiments of this kind seem to be planned at present.

3. DETERMINATION OF LEVEL DENSITIES FROM ENERGY DIFFERENTIAL PARTICLE EMISSION CROSS-SECTIONS IN COMPOUND NUCLEUS REACTIONS

3.1 BASIC CONCEPTS FOR DEDUCING LEVEL DENSITIES FROM PARTICLE SPECTRA FROM COMPOUND NUCLEUS REACTIONS

Now I will proceed to the main topic of this talk, the extraction of level density information from the study of compound nucleus reactions. This is the oldest method for obtaining nuclear level densities. Nevertheless the results obtained so far are somewhat disappointing compared to the enormous amount of work that has gone into the development and use of the method and I will try to explain why this has been so.

In order to better see the essential points we will first start with a very simplified picture of a compound nucleus reac-

tion neglecting all angular momentum effects by assuming the spin of all levels involved to be zero. The result of such a reaction is shown schematically in figure 6. The compound nucleus will decay to all accessible levels of the residual nuclei which can be reached by particle emission and the decay probability to any specific energy level is determined only by a barrier transmission factor and a phase space factor for the emitted particle.

Thus we get:

$\sigma_{Lev}(\varepsilon_a, \varepsilon_b)$ = cross-section for population of a certain level of the residual nucleus by emission of particle b with energy ε_b

$$\sigma_{Lev}(\varepsilon_a, \varepsilon_b) = \sigma_c(\varepsilon_a) \frac{p_b^2 \cdot \sigma_{inv_b}(\varepsilon_b)}{G} \qquad (1)$$

with $$G = \sum_{b'} \sum_{\varepsilon_{b'n}} p_{b'n}^2 \cdot \sigma_{inv_{b'}}(\varepsilon_{b'n}) \qquad (2)$$

$\varepsilon_a, \varepsilon_b$ channel energies for bombarding and emitted particle

σ_c = cross-section for compound nucleus formation

p_b^2 = square of particle momentum

$\sigma_{inv_b}(\varepsilon_b)$ = cross-section for the inverse reaction to the considered decay channel that is absorption of particle b by the residual nucleus in the considered excited level and formation of compound nucleus

If the excitation energy of the compound nucleus is sufficiently high we may replace the sums over levels in G by integrals over a level density $\rho_{b'}(U)$ of the residual nuclei reached by the emission of the different particles (n,p and α)

$$G = \sum_{b'} \int_0^{U_{max}} p_{b'}^2 \quad \sigma_{inv_{b'}}(\varepsilon_{b'}) \cdot \rho_{b'}(U_{b'}) \cdot dU_{b'} \qquad (3)$$

$$U_{max} = U_c - B_{b'} \text{ (Separation energy of particle b')} \qquad (4)$$

and $$\varepsilon_{b'} = U_{max} - U_{b'} \text{(Channel energy of emitted particle)} \qquad (5)$$

If we consider particle emission into an energy bin $d\varepsilon_b$ we have to sum equation (1) over all levels in the corresponding excitation energy bin $dU = d\varepsilon_b$ and we get for the energy differential particle emission cross-section

$$\frac{d\sigma}{d\varepsilon_b}(\varepsilon_a, \varepsilon_b) = \sigma_c(\varepsilon_a) \cdot \frac{p_b^2 \cdot \sigma_{inv_b}(\varepsilon_b) \; \rho_b(U_{max} - \varepsilon_b)}{G} \qquad (6)$$

If we measure the spectra of emitted particles for such reactions e.g. the α-spectra we will in general get both information of type (1) and (6) that is cross-sections for population of resolved levels or groups of such levels and particle emission cross-sections leading into the excitation regions where the levels are no longer known.

From such data we can get the following level density informations:

1) From the cross-sections σ_{Lev} we can determine the quantity G, which is dominated by the neutron emission term

$$\int_0^{U_{max}} p_n^2 \, \sigma_{inv_n}(\varepsilon_n) \, \rho_n(U) dU$$

$\rho_n(U)$ being the level density reached by neutron decay of the compound nucleus. As fig. 6 shows, the main part of the integral comes from a relatively small energy region just below U_{max} and it is qualitatively obvious that from our knowledge of G we can extract a value of ρ_n at an excitation energy corresponding to about the centroid of the neutron spectrum.

Quantitatively it can be shown that the integral can be used to derive a value of ρ_n at the excitation U_{max}-2T, which is to first order independent of the assumed energy dependence of the level density (T being the inverse logarithmic derivative of the level density in the region of neutron emission).

2) Knowing the so-called Hauser-Feshbach denominator G we can simply invert eq. (6) in order to calculate the level density of the compound nucleus reached by the emission of the measured particle

$$\rho_b(U_b) = \frac{\frac{d\sigma}{d\varepsilon_b}(U_{max}-U_b) \cdot G}{p_b^2 \cdot \sigma_{inv_b}(U_{max} - U_b)} \qquad (7)$$

Actually the situation is somewhat more complicated because of angular momentum effects. Absorption of the bombarding particle leads to formation of compound nuclei with different spins and parities. Thus we have different kinds of compound nuclei, each of which decays in different ways to the accessible levels of the residual nuclei determined in addition to the factors mentioned before by the centrifugal barrier depending on the angular momentum difference between the compound nucleus and the respective level of the residual nucleus. The observed cross-sections are of course those due to the decay of all kinds of compound levels. Thus equ. (1) and (6) have to be replaced by a sum of terms corresponding to the different kinds of compound nuclei whereby each of those terms has basically the same structure as equ. (1) and (6).

The well-known formulas, again for angle-integrated cross-sections are [6].

$$\sigma_{Lev}(\varepsilon_a, U_b, I_b, \pi_b) = \sum_{J\pi} \sigma_{cJ\pi}(\varepsilon_a) \frac{F_b(J,\pi, \varepsilon_b, I_b, \pi_b)}{G(J,\pi)} \tag{8}$$

$$\text{and} \quad \frac{d\sigma}{d\varepsilon_b}(\varepsilon_a, \varepsilon_b) = \sum_{J\pi} \sigma_{cJ\pi}(\varepsilon_a) \frac{\sum_{I_b,\pi_b}^{\pi_b} F_b(J,\pi, \varepsilon_b, I_b, \pi_b) \cdot \rho_b(U_b, I_b, \pi_b)}{G(J,\pi)} \tag{9}$$

with $\sigma_{cJ\pi}$ = cross section for formation of compound nuclei with angular momentum J and parity π by absorption of particle a with energy ε_a. In terms of transmission coefficients it is given by

$$\sigma_{cJ\pi}(\varepsilon_a) = \frac{\pi}{k_a^2} \cdot \sum_{S_a = |I_a - i_a|}^{I_a + i_a} \sum_{I_a = |J - S_a|}^{J+S_a} \frac{(2J+1) T_a^{l_a}(\varepsilon_a) \cdot \delta_{\pi_a \pi}^{(-1)^{l_a}}}{(2i_a+1)(2I_a+1)}$$

and $F_b(J,\pi,\varepsilon_b,I_b, \pi_b)$ = decay probability of compound nucleus with quantum numbers J,π by emission of particle b to the selected residual level with excitation energy U_b and quantum numbers I_b, π_b. It is the sum over the contributions of particles of all angular momenta allowed by the conservation laws of J and π. Thus in term of transmission coefficients it can be written as

$$F_b(J,\pi,\varepsilon_b,I_b, \pi_b) = \sum_{S_b = |I_b - i_b|}^{I_b + i_b} \sum_{l_b = |J - S_b|}^{J+S_b} T_b^{l_b}(\varepsilon_b) \cdot \delta_{\pi \cdot \pi_b}^{(-1)^{l_b}} \tag{10}$$

and $G(J,\pi)$ is again the sum over all decay probabilities which can be expressed in terms of sums respectively integrals over the level densities of the residual nuclei ρ_b (U,I,π) which now in principle depends also on J and π

$$G(J,\pi) = \sum_b \int_0^{U_{b\,max}} \sum_{I_b,\pi_b} F_b(J,\pi, \varepsilon_b, I_b, \pi_b) \cdot \rho_b(U_b, I_b, \pi_b) dU_b \tag{11}$$

$\rho_b(U_b,I_b,\pi_b)$ = spin and parity dependent level density for residual nucleus reached by emission of particle b. We will assume it to be independent of parity and parametrize in the usual way as a product of a total level density ρ_{tot} (U) and a conventional normalized spin distribution function $f(I_b,\pi_b)$. This results in

$$\rho_b(U_b,I_b,\pi_b) = \rho_{tot}(U_b) \cdot f(I_b,\pi_b) \tag{12}$$

$$\text{with} \quad f(I_b,\pi_b) = \frac{1}{4\sigma^2(U)} (2I_b+1) \exp\left[-I_b(I_b+1)/2\sigma^2(U_b)\right] \tag{13}$$

σ being the so-called spin cutoff-factor.
The quantities I_a, i_a, I_b and i_b are the spins of the target, projectile, residual nucleus and emitted particle respectively, S_a and S_b are the channel spins in the entrance and exit channels, l_a and l_b are the orbital angular momenta and π_a, π_b the parities in the entrance and exit channels. The quantities

$\delta^{(-1)^{l_b}}_{\pi,\pi_b}$ and $\delta^{(-1)^{l_a}}_{\pi_a,\pi}$ are 1 ore zero depending whether its two arguments are equal or not and serve to insure parity conservation. Though eq. (8) and (9) are considerably more complicated than equ. (1) and (6) they are very similar in structure. Each term of the sum in equ. (8) and (9) has exactly the same structure as equ. (1) and (6). Therefore we can use the described procedure for extraction of level densities from particle emission spectra also in the frame-work of the rigorous angular-momentum conserving theory.

We proceed again in two steps

1) We use equ. (8) to calculate the total level density $\rho_{n_{tot}}(U_{max}-2T)$ of the compound nucleus reached by neutron emission at an excitation energy corresponding to the centroid of the neutron spectra. This is done by assuming a suitable functional form for the energy dependence of $\rho_{ntot}(U)$ and adjusting the absolute normalization until the cross-section calculated by means of equ. (8) matches the measured value. To first order the level density ρ_n at the excitation energy $U_{max}-2T$ is still independent of the choice of the functional form for $\rho_n(U)$ (s. fig. 7), it does, however, depend to some extent on our choice of the spin-cutoff factor and this has to be taken into account in the uncertainty analysis.

2) Using the $\rho_{ntot}(U)$ derived from (1) and a guess for the wanted level density $\rho_{btot}(U_b)$ we calculate $\frac{d\sigma}{d\varepsilon_b}(\varepsilon_b)$. Comparison of these calculated values with the measured ones allows us to derive the level density $\rho_{btot}(U_b)$ as

$$\rho_{b_{tot}}(U) = (\rho_{btot}(U))_{assumed} \left(\frac{(\frac{d\sigma}{d\varepsilon_b})_{meas}}{(\frac{d\sigma}{d\varepsilon_b})_{calc}} \right)_{\varepsilon = U_{b\,Max} - U} \tag{14}$$

Finally it has to be mentioned that equ. (8) and (9) do not take into account the partial isospin conservation which has been observed in compound nucleus reactions [7,8]. Extensions of the Hauser-Feshbach formalism to include complete or partial isospin conservation have been given [9,10], which, however, are only of restricted practical value because of the large uncertainty in the actual amount of isospin mixing. Fortunately the deviations from equ. (8) and (9) due to isospin conservation are rather small (< 10%) except for (p,p') reactions which have also large contamination from non-compound particles and thus should not be used for extraction of level densities. Thus use of equ. (8) and (9) is completely adequate in most cases; possible deviations due to isospin conservation should, however, be considered in the uncertainty analysis (s. 3.2.5).

3.2 PRACTICAL IMPLEMENTATION OF THE METHODS DERIVED IN 3.1

Before we can actually use equ. (8) and (9) for the determination of level densities we have to solve 3 problems:

1) Check the measured cross-sections for contamination by non-compound reactions and if necessary apply corrections,

2) choose appropriate optical potentials for the calculation of the trans-

mission coefficients for the incident and all emitted particles,
3) choose appropriate level densities as starting point for the calculation.
In the following I will make some general remarks to these questions and also as a practical example show the analysis of a recent measurement of $\frac{d\sigma}{d\varepsilon_\alpha}$ for the $^{56}Fe(n,\alpha)^{53}Cr$ reaction at E_n = 14.1 MeV. Finally I will address the problem how to estimate the uncertainty of the level density values derived by the described procedure.

3.2.1 CONTAMINATION OF EVAPORATION SPECTRA BY NON-COMPOUND PARTICLES

All measured particle spectra are to some extent "contaminated" by contributions of both direct and preequilibrium reaction. Quantitatively, however, this contamination depends strongly on the type of reaction and the incident and outgoing particle energy showing the following general trend:
1) Inelastic scattering reactions like (n,n'), (p,p') or (α,α') always contain relatively large non-compound contributions, reactions of the type (n,p) or (p,n) are considerably better and reactions of the type (α,nucleon) or (nucleon,α) have the smallest non-compound cross-sections. In addition we have to keep in mind that above about A = 70 emission of charged particles from compound nuclei becomes so much inhibited by the coulomb barrier, that non-compound contributions dominate for all types of reactions.

Thus for up to about A = 70 the reactions (α,n), (α,p), (n,α) and (p,α) are about equally well suited for level density determinations whereas above A = 70 preferably the (α,n) and (p,n) reactions should be used.
2) For all reactions precompound emission strongly increases with incident particle energy.
3) Non-compound emission is always most important for the high-energy ends of the emitted particle spectra. Thus it is advisable always to use the lowest bombarding energy compatible with the excitation energy-range which is to be studied and to use the highest energy levels from the region of resolved levels for the level density calculations according to equ. (9).

Non-compound contributions to the spectra manifest themselves in the angular distribution. Whereas compound nucleus theory predicts exact symmetry of $\frac{d^2\sigma}{d\varepsilon\, d\Omega}$ around θ = 90°, both direct and preequilibrium reactions are forward peaked. As an example fig. 7 shows the angular distribution for the $^{56}Fe(n,\alpha)$ reaction, which clearly shows the gradual increase of non-compound reactions with increasing α-energy. Because of this difference in angular distributions only cross-section measurements from the backward hemisphere should be used for calculations of $\frac{d\sigma}{d\varepsilon}$.

3.2.2 CHOICE OF OPTICAL POTENTIALS

The transmission coefficients needed both for the entrance channel (for calc of $\sigma_{cJ\pi}$) and for the exit channels have to be calculated from appropriate optical potentials. There exists a large variety of such potentials derived from differential elastic and total reaction cross-sections. In choosing among these potentials we should avoid to use potentials outside the mass and energy range of the data which were used to derive them and always check that the potentials predict the correct total reaction

(non-elastic) cross-sections for all energies relevant for the analysis.

For the emitted particle this means that, if possible, we should use potentials derived from low energy data like the neutron potentials derived by A. Smith's group for many elements from 0.5-5 MeV elastic and inelastic scattering [11]. For cases where no such potentials are available one has to use one of the common global potentials [12-14]. For protons the global potentials of [15] and [16] have been found satisfactory down to the lowest energies of interest at least for medium mass nuclei (A = 40-70). For α-particles this is true for the Satchler-McFadden potential [17], however, it has recently been found [18], that the widely used Huizenga-Igo potential [19] seriously overestimates the total reaction cross-sections at low energies and should no longer be used for the analysis of evaporation spectra.

For the incident particles with their higher energies the choice of the potential is not critical as most of the common global potentials predict very similar reaction cross-sections above 10 MeV and we may use the mentioned global neutron [12-14], proton [15,16] and α-particle [17] potentials also for the calculation of the compound nucleus formation cross-sections, $\sigma_{cJ\pi}$. We have to keep in mind, however, that these cross-sections only describe the formation of a composite system of total angular momentum J, which may decay partly by direct or precompound particle emission. Thus in the presence of such reactions the $\sigma_{cJ\pi}$ value calculated from the optical potentials have to be reduced by an appropriate factor. As no detailed knowledge exists how these non-compound processes effect the different J states one can only reduce all $\sigma_{cJ\pi}$ values by a common factor $1 - f_D - f_{PE}$, f_D and f_{PE} being the fractions of direct and preequilibrium processes in the total reaction cross-section. The preequilibrium fraction f_{PE} can be estimated from either the exciton [20] or hybrid model [21], the direct fraction f_D is only important for inelastic scattering to collective states where it may be estimated from DWBA calculations except for deformed nuclei where coupled channel calculations may be necessary.

3.2.3 CHOICE OF LEVEL DENSITIES

In order to use equ. (8) and (9) for deriving level densities we have to start with initial values for the level densities that is both for the total level densities $\rho_{tot}(U)$ and the spin distribution functions $f(J,\pi)$ of all residual nuclei populated in the reaction.

The starting values for the total level densities $\rho_{tot}(U)$ do not strongly influence the final result and are thus uncritical, the backshifted Fermi-Gas [22], the Gilbert-Cameron model [23] or just the constant temperature part of the Gilbert-Cameron model can be used. If the corresponding information is available, these parameters should be adjusted to reproduce the total proton to neutron emission ratio of the compound nuclei.

For the spin distribution - lacking more detailed knowledge - it seems best to use the standard form of equ. (13) and choose values of the spin cut-off-factor σ which correspond to an effective moment of inertia equal to the full rigid body moment as calculated with a nuclear radius constant of $r_o = 1.25$ fm. For medium mass nuclei (A ∿ 40 - 70) there is considerable evidence that these moments of inertia are correct to better 30 %; for heavier nuclei the evidence is much weaker and there are indications that moments of

inertia may be smaller than the rigid body values by up to 50%. It has to be pointed out that the choice of the spin dependence of the level density does effect the values of σ_{Lev} and $\frac{d\sigma}{d\varepsilon}$ calculated from equ. (8) and (9) to some extent and (see section 3.2.5) our uncertainty in the distribution function $f(J,\pi)$ will produce a corresponding error in the $\rho_{tot}(U)$ values calculated from equ. (8) and (9).

3.2.4 ACTUAL PROCEDURE FOR DERIVING LEVEL DENSITIES

In this section I will demonstrate the procedures described in the preceding sections for a definite example, the analysis of our recent measurement of the double differential α-emission cross-sections in the reaction $^{56}Fe(n,\alpha)$ for E_n = 14.1 MeV.

Fig. 8 shows the angular distribution for different energies of the emitted α-particles and fig. 9a gives the angle-integrated cross-section $\frac{d\sigma}{d\varepsilon\alpha}$ derived from the data in the backward hemisphere assuming symmetry around 90°. The figure also shows the position of the resolved levels in the residual nucleus ^{53}Cr. From fig. 8 we conclude that for the highest α-energies non-compound reactions are already dominating. We thus decide to restrict our analysis to the α-energy range 6-12 MeV corresponding to excitation energies of 2-8 MeV in ^{53}Cr. The upper limit is given by the neutron binding energy of ^{53}Cr (7.9 MeV).

Starting with a parameter set (transmission coefficients, level densities) which has succesfully been used to describe neutron cross-sections for many nuclei in the ^{56}Fe region [24] we calculate first the cross-section $\sum_{U=2.1}^{3.1} \sigma_{Lev}$ contributing to the α-emission cross-section in the 11-12 MeV bin. According to the deviation of this first guess from the measured value (~25%) we slightly adjust the level density ρ_n and ρ_p of the residual nuclei ^{56}Fe and ^{56}Mn reached by neutron and proton emission until we get agreement with the measured value while simultaneously preserving the right neutron to proton emission ratio. This agreement is reached with the level density parameters as listed in table 1. While this parameter set is by no means unique we may use it to derive the one uniquely determined quantity $\rho_n(U-2T)$ (s. fig. 7) and get for the nucleus ^{56}Fe, which is reached by neutron emission

$$\rho_{^{56}Fe}(11\ \text{MeV}) = 2.65 \cdot 10^3\ \text{levels/MeV}$$

which is in good agreement with an extrapolation of the level counting results shown in fig. 10.

In the second step of the analysis we calculate the α-emission cross-section $\frac{d\sigma}{d\varepsilon\alpha}(\varepsilon_\alpha)$ using the level density parameters of table 1 by means of equ. (9) and determine the level density of ^{53}Cr, the residual nucleus reached by α-emission from equ. (14) as indicated in fig. 9a and 9b.

3.2.5 DETERMINATION OF UNCERTAINTIES FOR THE LEVEL DENSITY VALUES

Realistic uncertainties for the level densities derived by use of equ. (8) and (9) must take into account the experimental errors of the measured particle emission cross-section, the uncertainties in our estimate of the

contribution of non-compound reactions and the uncertainties in the calculated cross-sections due to the parameter uncertainties (s. sect. 3.2.2 and 3.2.3). Detailed consideration of the various sources of errors gives the following result

1) For the method of determining $\rho_n(U-2T)$ from the cross-sections σ_{Lev} to resolved levels I have summarized the error contributions in table 2. The error contributions due to our incomplete knowledge of the optical model parameters and the spin distribution function $f(J,\pi)$ of the nuclear levels can be estimated from calculations of σ_{Lev} using different optical potentials and varying the nuclear moments of inertia within the limits of our present knowledge (s. sect. 3.2.2 and 3.3.2); the uncertainty due to contribution of non-compound reactions to the measured particle spectra has already been discussed in section 3.2.1, uncertainties due to neglect of isospin effects can be estimated by calculations assuming complete isospin conservation . This will, however, only be necessary for reactions involving protons in the entrance or exit channel and target nuclei of small neutron excess. The uncertainty in the compound formation cross-sections due to prior direct and preequilibrium particle emission (s. sect. 3.2.3) will in general be dominated by the uncertainty of the preequilibrium fraction f_{PE} which can in most cases not be estimated to better than 30% of its value.

2) In order to discuss the relevant uncertainties for the level densities derived for the nucleus populated by the measured particles we rewrite equ. (14) in a somewhat different form

$$\rho(U) = \frac{[\frac{d\sigma}{d\varepsilon} / \sigma_{Lev}]_{meas}}{[\frac{d\sigma}{d\varepsilon} / \sigma_{Lev}]_{calc}} \cdot \rho_{assumed}(U) \qquad (15)$$

This equ. is obtained from equ. (14) by multiplication with the ratio $\sigma_{Lev_{meas}} / \sigma_{Lev_{calc}}$ which is unity as the parameters of the calculation are adjusted to reproduce σ_{Lev}. This form of the equ. shows clearly that the level density at excitation energy U is essentially obtained as quotient of 2 ratios each of which is more accurate than its constituents due to the cancellation of uncertainties e.g. absolute cross-section normalization factor in the experimental values and a number of theoretical uncertainties common to the calculation of σ_{Lev} and $\frac{d\sigma}{d\varepsilon}$. The remaining uncertainties are summarized in table 3, they can be estimated as discussed before.

The error estimates obtained in this way for our example, the reaction $^{56}Fe(n,\alpha)$, are also shown in fig. 9b and fig. 10. These uncertainties are about typical for what can be obtained with presently available techniques of measurements and analysis and we may summarize the situation as follows.

1) Level desities accurate to 15-25% can be derived from equ. (9) for a residual nucleus in a compound nucleus reaction from the emission cross-sections of the particles populating it.

2) Level densities for the residual nucleus formed by neutron emission can be derived from the cross-section for formation of resolved levels of any of the residual nuclei with somewhat larger uncertainties.

3) These uncertainties are, however, only achievable if the contribution of non-compound reactions can be kept sufficiently small (< 20-30% for the worst parts of the spectra used for the analysis).

4) Only a relatively small fraction of the total uncertainties of $\rho(U)$ is due to the experimental errors of the measured particle emission cross-sections. This means that the presently achievable accuracy of $\sim 10\%$ for energy-differential particle emission cross-sections is sufficient in most cases.

The discussed error estimates can and should be checked experimentally by the use of different reactions and bombarding energies in the study of one nucleus (s. fig. 12).

3.3 ACCESSIBLE EXCITATION ENERGY RANGE

The accessible range for extraction of level densities from $\frac{d\sigma}{d\varepsilon}$ measurement (equ. (9)) is limited to energies below the neutron binding energy, as for higher excitation and correspondingly lower particle energies the experimental spectra are "contaminated" by particles from cascade reactions (e.g. our $^{56}Fe(n,\alpha)$ spectrum will contain contributions from the $^{56}Fe(n,n'\alpha)$ reaction).

The alternative procedure to determine $\rho_n(U)$ from σ_{Lev} according to equ. (8) is in principle applicable to arbitrarily high excitation energy. In practice unfortunately two effects limit the maximum obtainable excitation energy also to about the neutron binding energy.

1) Due to the exponential dependence of the nuclear level density on excitation energy the cross-section for any selected level or group of levels decreases exponentially with excitation energy and measurements become difficult if cross-sections decrease below about 1μb/Sr which corresponds to about 10^5 competing levels. This number is reached at about 15 MeV around mass 50 and it decreases strongly with A.

2) As already discussed, "contamination" by non-compound reactions increases strongly with increasing bombarding energy and eventually such contributions will become important for all resolved levels of any residual nucleus and this imposes another limit on the maximum excitation energy accessible to this method of level density measurement. This limit is mostly even lower than the limit due to restriction 1 even for the reactions which have the lowest non-compound contributions like (α,n) or (n,α). This may also be seen from our example. As fig. 8 shows we are just at the limit where non-compound reactions start to become important for the population of all resolved levels at the chosen bombarding energy of 14 MeV which permits study of the level density $\rho_n(U)$ of ^{56}Fe up to 11 MeV which is about the neutron binding energy of that nucleus. Thus also the method of extracting level densities from resolved levels is in practice restricted to excitation energies not much larger than the neutron binding energy.

3.4 DERIVATION OF LEVEL DENSITY INFORMATION FOR EXCITATION ENERGIES ABOVE THE NEUTRON BINDING ENERGY

3.4.1 GRIMES' METHOD

The excitation energy range accessible to the application of equ. (8) (cross-sections to resolved levels) can be increased considerably by a modification proposed by S. Grimes [25-27].

Instead of measuring excitation functions to a few isolated levels he

measures in (p,n) and (α,n) reactions the total cross-section for population of all levels below the neutron binding energy that is sum of all excitation functions for all levels with excitation energies below the neutron binding energy.

This has two advantages:

1) The count-rate is increased by factors of 10^4 to 10^6 compared to measurement of excitation functions for individual levels. This increases the excitation energy range by about 5 MeV for heavy nuclei and allows to study level density up to about two times the neutron binding energy for most nuclei.

2) The influence of direct reactions is also reduced, as most of the levels included in the summation have rather high excitation energies and their direct cross-sections are thus much smaller than for the low lying levels used in the study of isolated level excitation functions. Moreover corrections even for these small direct contributions can be derived from the measured neutron spectra.

The price one has to pay for these advantages is a more difficult way of analysis and the introduction of additional uncertainties in the determination of the absolute values of the level densities. Instead of using equ. (8) directly one has to sum it over all levels below the neutron binding energy. The measured quantity (neutrons populating all levels below the neutron binding energy) is thus given by

$$\sigma_n(\text{neutrons with energies above } \varepsilon_a + B_a - B_n) = \Sigma\, \sigma_{Lev}(\varepsilon_a, U, I, \pi) \qquad (16)$$

where the summation extends over all levels from the groundstate to the neutron binding energy and

$\sigma_{Lev}(\varepsilon_a, U, I, \pi)$ is given by equ. (8).

The summation can of course only be performed as an integral over the level density.

This results in

$$\sigma_n = \int_{U=0}^{B_n} \sum_{J=0}^{\infty} \sum_{\pi} \rho_n(U, I, \pi)\, \sigma_{Lev}(\varepsilon_a, U, I, \pi) \qquad (17)$$

Thus in order to calculate the level density of some nucleus for excitation energies above the neutron binding energy one has already to know the level density below the neutron binding energy B_n. As a consequence the limited accuracy of the level density data for energies below B_n causes corresponding errors in the results obtained for the level densities at higher excitation energies.

3.4.2 ANALYSIS OF COMPOSITE EVAPORATION SPECTRA

At high bombarding energies compound nuclei will decay by successive emission of several particles and the observed particle emission spectra will be the superposition of the particle spectrum emitted by the first compound nucleus and the spectra emitted in all later stages of the reaction. In principle such composite evaporation spectra can also be calculated in terms of the statistical model of nuclear reactions. The necessary generalizations of equ. (8) and (9) are rather straight-forward and have been given in the lite-

rature [28-30]. However, obviously such spectra do depend on the level densities of all residual nuclei populated in successive stages of the reaction. Furthermore the fraction of the total reaction cross-sections leading to pre-equilibrium particle emission increases strongly with bombarding energy and this creates additional difficulties for the interpretation of the spectra from multistage compound reactions. Thus in many cases it is not possible to extract useful information on the level densities of the individual nuclei from such measurements.

Thus it appears that at present extraction of level density information from composite spectra with reasonable accuracy is possible only in 2 special situations

a) If the composite spectrum contains only two components that is if the excitation energy of the compound nucleus is kept below the 3n threshold. In this case the particle spectra depend only on two level densities, the level density of the first c.n. in the region between the binding energies for one and two neutrons and the level density of the second compound nucleus in the energy region below the neutron binding energy, which can be determined by the methods described before.

The best way to do such measurements (s. sect. 3.2.1) is the observation of the neutron spectra from compound nuclei formed by either α-particle or proton bombardment. It can be expected that such measurements,which can be combined with absolute level density measurements according to Grimes' method (s. sect. 3.4.1), can supply reasonably accurate level densities up to about two times the neutron binding energy for the whole mass range. However, the necessary procedures for quantitative extraction of level density values and deriving reliable error estimates have still to be worked out.

Existing data on such two component evaporation spectra are mostly measurements of secondary neutron spectra from nuclei irradiated with 14 MeV neutrons [31-34] which have large precompound contributions (∿ 30%). In addition these measurements have mostly been analyzed either by means of the approximate Lang-LeCouteur relation [35] or by visual comparison with model calculations and the result obtained in this way must be considered somewhat uncertain.

b) A second favourable region for level density studies from composite evaporation spectra is the investigation of α-particle spectra from (α,α') and (p,α) reactions at very high bombarding energies and thus compound nucleus excitation energies (50-100 MeV) [36-38]. It has been shown in the pioneering work of Halpern and coworkers [36] that such reactions are especially useful for determining nuclear level densities at high excitation energies because of two features:

1) At excitation energies above ∿ 40 MeV the α-particle spectra emitted at backward angles do contain well defined evaporation parts, which can be separated from the precompound background reasonably well also for the heaviest nuclei (s. fig. 11).

2) The α-emission probability decreases strongly with decreasing excitation energy as expected from the energy dependence of the nuclear temperature according to the Fermi-Gas model. Thus one can approximately neglect the α-emission in the later stages of the evaporation process and analyze the evaporation spectra with equ. (9). Measurements of this kind have so far concentrated on the region around the A = 208 shell where they have produced inter-

esting results on the energy dependence of the shell effects in the level density, but the method should be applicable for the whole range of medium and heavy nuclei.

3.5 PRESENT STATUS OF LEVEL DENSITY INFORMATION FROM PARTICLE EMISSION SPECTRA

A huge amount of work has been devoted to the determination of nuclear level densities from evaporation spectra in compound nucleus reactions. However, many of the experiments used reactions which have a large contamination by non-compound reactions like (n,n') or (p,p') and much of the early work on neutron spectra seems to suffer from large unidentified systematic errors. Most measurements of α-spectra from (p,α), (n,α) or (α,α') reactions have used in their analysis the Huizenga-Igo potential [19] which does not adequately describe the α-absorption cross-section at low energy [18].

In addition most experiments have not been analyzed in the optimum way. Most authors have analyzed their results by the use of the so-called Weisskopf approximation (equ. (6)) and completely neglected angular momentum effects. Those authors which did compare their results with correct treatment of spin and parity conservation have mostly restricted themselves to finding sets of level density parameters for which they get reasonable agreement between measured and calculated particle spectra and have not quantitatively extracted level density information in the way described in section 3.2.

Thus it appears that at present only (p,n) experiments have reached sufficient quality both in the experimental data and the procedure used in the extraction of level densities as to produce level density information comparable in accuracy with the neutron resonance work. There has been some discrepancy between the early (p,n) work of the Wisconsin group [39-41] and the later Livermore work of Grimes [25-27] . Careful (p,n) experiments in Russia and lately also in East Germany [42-47] - which may be considered as the most important experimental contribution in the field of level density in the last decade - have, however, clearly confirmed the Livermore work both with respect to measured primary data and procedures used to correct for the "contamination" of non-compound particles. Extraction of level densities was done mostly by use of the Weisskopf approximation which in this special case, however, seems justified because of the small orbital angular momenta involved in this type of reaction, although it still has the disadvantage that it does not provide an absolute normalization for the level density. Thus these experiments [25-27, 42-47] have provided a consistent set of level density measurements between the region of resolved levels and the neutron binding energy for about 10 nuclei in the mass range A = 50-209.

The results indicate that the energy dependence of the nuclear level density at low energy seems to be closer to a constant temperature than to the Fermi-Gas predictions (fig. 12-14) for all nuclei investigated. Comparison with neutron resonance data for the nucleus ^{181}W seems to confirm the assumption of an effective moment of inertia equal to the full rigid body moment also for heavy nuclei; this, however, should be checked by experiments on other nuclei.

In addition to the discussed (p,n) data there exists a considerable amount of data which - if reanalyzed with the procedures described before -

will probably make a significant contribution to our knowledge of level densities. In this connection I would like to mention especially the (α,n) measurement of the Livermore group [25-27], the (p,α) and (α,p) results of the Huizenga [48-50] and Porile [51-54] groups, the (n,α) and (n,p) results of the Livermore group [55-58] and the Hamburg (n,α) results [59-60].

No relevant information can probably be extracted from the very discrepant rather old inelastic neutron data nor from the (p,p') data which mostly suffer from serious non-compound "contamination".

Thus we may summarize the situation as follows. Only for relatively few nuclei we have level density data of an accuracy comparable to that obtainable from average neutron resonance spacings. For a somewhat larger number of nuclei such information is probably obtainable by reanalysis of existing experimental results. This refers to the situation below the neutron binding energy.

Above the neutron binding energy we have at present only the discussed results of the "Grimes method" on a few nuclei and the somewhat uncertain results derived from the neutron emission spectra from the interaction of 14 MeV neutrons with nuclei [31-34]. The latter data can probably be improved considerably by a consistent evaluation combined with a reanalysis in terms of the exact statistical model formalism.

4. DETERMINATION OF LEVEL DENSITIES FROM MEASUREMENTS OF LEVEL WIDTHS IN THE REGION OF OVERLAPPING LEVELS

4.1 PRINCIPLE OF THE METHOD

The average width $\Gamma_{J\pi}(U_c)$ of a compound nucleus of spin J and exitation energy U_c (in the region of overlapping levels) and its level density $\rho(U_c,J,\pi)$ are connected by the relation [49, 61].

$$\Gamma_{J\pi}(U_c) = \frac{1}{2\pi\,\rho(U_c,J,\pi)} \cdot G(J,\pi) \qquad (18)$$

with $G(J,\pi)$ defined by equ. (11).

This relation can be used to derive absolute level densities at high excitation energies. In this method the compound nucleus level width (from fluctuation studies) is measured as a function of the compound nucleus excitation energy U_c and the level density of the compound nucleus at that excitation energy is calculated from equ. (18). This method of course requires that the level densities of the residual nuclei in the low excitation energy region are already known (from measurements of particle emission spectra) and $G(J,\pi)$ can be calculated.

In the following we will first discuss the problem of deriving level widths $\Gamma_{J\pi}(U_c)$ from various experimental methods and then discuss the procedures for calculating the level density from the level width by use of equ. (18).

4.2 MEASUREMENT OF LEVEL WIDTHS OF HIGHLY EXCITED NUCLEI

4.2.1 DETERMINATION OF LEVEL WIDTHS FROM FLUCTUATION MEASUREMENTS

Level widths of highly excited compound nuclei (in the region of overlapping levels $\Gamma_J/D_J \gg 1$ for all relevant J values) can be determined as follows in the framework of the fluctuation theory of Ericson [61,62,63].
1) An excitation function for some isolated residual level e.g. the (p, α_0) or (p,p_1) excitation function is measured with high energy resolution in small energy increments (s. fig. 16).
2) Fluctuation theory predicts that the "average period" of such fluctuating excitation functions is equal to the average level width. This average period can be determined in a number of ways [63], the most reliable of which seems to be the determination of the half-width of the auto-correlation function. The auto-correlation function defined as [63]

$$C(\varepsilon) = \langle\sigma(E + \varepsilon)\, \sigma(E)\rangle - \langle\sigma\rangle^2 \qquad (19)$$

(< > means average over the energy interval ΔE covered by the measurement of all excitation function)
is calculated and its half-width determined (fig. 16). For such measurements it is of course necessary that the energy resolution in the excitation function measurements is at least somewhat better than the width to be measured [63]. This condition can be relaxed to a certain extent, however, if the so-called fluctuation attentuation method is used [64].
3) The half width determined in this way gives the average width of the compound levels contributing to the special reaction channel selected by the choice of the excitation function used for the analysis. It is in general an average over several J values and both parities. The J values contributing to the average and their relative weight depend on the type of reaction chosen and on spin and parity of the selected residual level. The weighting factors have been calculated from the statistical theory of nuclear reactions by Gadioli et al. [65]. They obtained

$$1/\Gamma^2_{meas} = \sum_J P_J/\Gamma_J^2 \;/\; \sum_J P_J \qquad (20)$$

with $$P_J = \sum_{S_1 l_2 S_2 l_2} \exp[J(J+1)/2\sigma_c^2]\; T_{a l_1}^2(\varepsilon_a) T_{b l_2}^2(\varepsilon_b) \qquad (21)$$

where σ_c is the spin-cutoff factor of the compound nucleus at its excitation energy U_c and the summation extends over all combinations $S_1 l_1$ and $S_2 l_2$ connecting the entrance and exit channel respectively with the compound spin J.

4.2.2 OTHER METHODS FOR DETERMINING LEVEL WIDTHS

In special cases the so-called blocking effect can be used to measure directly average life-times of compound nuclei [66-69] if these times are in the range of 10^{-16}–10^{-17} sec and single crystal targets are available. Due to these limitations such life-time measurements have so far only been performed for Germanium and Uranium; not much more can be expected in future.

Recently it has been pointed out [10] that the width Γ of the compound states manifests itself also in the spectra of atomic electrons ejected coherently prior to and after nuclear scattering. The authors show that in principle Γ can be derived from coincidence measurements between nuclear reaction products and atomic electrons. The necessary measurements of energy spectra of very slow electrons (.1-10 keV), however, will also be quite difficult. This method would make it possible to measure much smaller Γ values than accessible to the fluctuation method.

4.3 DETERMINATION OF LEVEL DENSITIES FROM LEVEL WIDTHS

The total level densities $\rho_{tot}(U_c)$ of the compound nuclei at their excitation energies U_c can be calculated from the measured level width $\Gamma_{meas}(U_c)$ using equ. (18) as follows:
We assume the compound level density $\rho_c(U_c,J_c,\pi_c)$ to be given by

$$\rho_c(U_c,J_c,\pi_c) = \rho_{tot}(U_c)\,\frac{1}{4\sigma_c^2}\,(2J_c+1)\exp[-J_c(J_c+1)/2\sigma_c^2] \qquad (22)$$

is independent of parity.
Then equ. (18) can be rewritten as

$$\Gamma_{J\pi}(U_c) = \frac{1}{\sigma_{tot}(U_c)}\,\frac{2\sigma_c^2\exp[J_c(J_c+1)/2\sigma_c^2]}{\pi(2J_c+1)}\,G(J,\pi) \qquad (23)$$

which can be combined with equ. (21) to give

$$\frac{1}{\Gamma_{meas}^2} = [\rho_{tot}(U_c)]^2\{\sum_J P_J\,\frac{\pi^2}{4}\,\frac{(2J_c+1)^2}{\sigma_c^4\,\exp[J_c(J_c+1)/2\sigma_c^2]G(J,\pi)^2}\}\,/\,\sum_J P_J \qquad (24)$$

From this equation $\rho_{tot}(U_c)$ can be calculated provided we know in addition to the measured level width the following quantities:
a) The spin-cutoff factor σ_c of the compound nucleus at its excitation energy U_c which should be chosen as discussed in sect. 3.2.3.
b) Values of the quantities $G(J,\pi)$, the sums over all open channels must be known.
For obtaining these $G(J,\pi)$ values two methods can be used:
1) If the excitation energy is so high, that a very large number of residual levels is populated, the $G(J,\pi)$ values can be calculated using equ. (11) [71]. In this case we have to know the level densities of all residual nuclei up to the maximum possible excitation energy e.g. the level density of the residual nucleus reached by neutron emission has to be known up to a maximum energy $U_{max\ res} = U_c - B_n$ (B_n = neutron separation energy). B_n being $\sim$ 10 MeV for medium mass nuclei this means that for example we use the residual level densities up to U = 10 MeV if we want to determine U_c at 20 MeV. Using the available information on the level densities from neutron resonances and level counting $G(J,\pi)$ can be calculated with an uncertainty of about a factor of two and accordingly also $\rho_{tot}(U_c)$ can be determined only with this accuracy.
2) The calculation of the $G(J,\pi)$ values and the corresponding large uncertainties can be avoided, if excitation functions used for the fluctuation analysis

are measured on an absolute scale and the absolute value of the average cross section σ_{Lev} is determined. Then the quantities $G(J,\pi)$ can be removed from equ. (18) by combining it with equ. (8). In this way one obtains [49]

$$\rho_{tot}(U_c) = \frac{1}{2\pi\ \Gamma_{Meas}} \sum_J \frac{\sigma_{cJ\pi}.F_b\ (J,\pi,\varepsilon_b,I_b,\pi_b).4\sigma_c^{\ 2}}{\sigma_{Lev}.(2J+1).\exp[-J(J+1)/2\sigma_c^{\ 2}]} \qquad (25)$$

This equation doesn't follow exactly from equ. (18) and (8) as discussed in ref. [2]. In order to be able to eliminate the quantities $G(J,\pi)$ one has to use weight factors P_J' somewhat different from the exact values given by equ. (21). However, as discussed in ref. [49] the error introduced by this approximation is negligible in most cases.

As the average cross-section can be measured easily to an accuracy of about 10%, the use of equ. (25) allows a much more accurate calculation of the compound level densities than use of equ. (18) and calculation of the $G(J,\pi)$ values from the residual level densities. Overall accuracies of $\pm$ 30% (mostly due to the exp. errors of Γ (typically $\pm$ 20%) and the errors due to σ_c uncertainties (typically also $\pm$ 20%) are possible for the compound level densities derived in this way. Thus whenever possible fluctuation measurements should be supplemented by absolute measurements of the corresponding average cross-sections. Of course equ. (25) is only applicable if the excitation function selected for the fluctuation measurements has no contribution from non-compound reactions. If the excitation function used for the fluctuation analysis does contain an unknown contribution from non-compound processes, application of equ. (25) introduces large systematic errors while the method 1 (calculation of the $G(J,\pi)$ values from the residual level densities) is not affected at all by such direct contributions and may thus be preferable in such cases.

Up to now level widths have been measured by fluctuation analysis of excitation functions (mostly for (p,α) or (p,p) reactions) for a large number of nuclei in the mass-range A = 20-60 mostly for excitation energies around 20 MeV [63, 72]. In addition level densities have been derived from total neutron cross-sections for a number of nuclei in the same mass-range for relatively large ranges of excitation energies [76, 77]. Beyond mass 60 measurements become increasingly difficult for two reasons:

a) Due to the increasing level density the cross-sections for any individual exit channel become extremely small.

b) The level width decreases strongly with increasing mass number and above mass 60 Γ becomes smaller than the energy resolution of conventional Tandem-beams.

Thus only one investigation concerning nuclei with A > 65 has been performed to date [64]. Using Tandem-beams of improved energy resolution and stability ($\sim$ 0.5-1 keV) new and improved fluctuation measurements in the mass-range 65 < A < 140 seem possible and desirable. Above A = 140 no fluctu-

ation measurements seem possible at present due to the described difficulties.

SUMMARY AND CONCLUSION

A) NUCLEAR LEVEL DENSITIES BELOW THE NEUTRON BINDING ENERGY

1) Absolute nuclear level densities can be derived from the study of particle emission cross-sections in compound nucleus reactions with an accuracy of 20-30% for the whole mass range and excitation energies below the neutron binding energy.
2) These level density measurements can be performed using conventional experimental techniques and well established methods of analysis, if the experiments are carefully chosen to minimize contributions of non-compound reactions. For heavy nuclei (A >70) this means that the (p,n) and (α,n) reactions should be used, for lighter nuclei (p,α), (α,p), (n,α) and (n,p) reactions will also provide good level density information.
3) Only very limited use has so far been made of these possibilities (s. sect. 3.5). This situation can only to some extent be improved by reanalysis of existing data.
4) The most efficient way to improve our level density information below the neutron binding energy seems to be further measurement of neutron emission cross-sections in (p,n) and (α,n) reactions and analysis of the data by means of the procedures described in sect. 3.2.

B) NUCLEAR LEVEL DENSITIES ABOVE THE NEUTRON BINDING ENERGY

1) Absolute nuclear level densities for energies up to about two times the neutron binding energy can be derived from neutron emission spectra in (p,n) and (α,n) reactions by means of the Grimes method (s. sect. 3.4) with an accuracy of 30-40%.
2) Extraction of level densities from composite evaporation spectra suffers still from lack of adequate procedures for this purpose. For the simplest case of neutron emission of compound nuclei with excitation energies below the 3n threshold it should be possible to develop procedures which permit extraction of level densities of an accuracy comparable to the Grimes method.
3) Thus also for the excitation energy range up to twice the neutron binding energy new measurements of neutron emission cross-sections from (p,n) and (α,n) reactions and analysis both by means of Grimes'method and analysis of the composite neutron spectra seems to be the most promising way to improve our knowledge on level densities.
4) For very high excitation energies (up to 100 MeV) measurement of α-evaporation spectra has been proved a very valuable method especially for heavy nuclei.

REFERENCES

1. A. A. KATSANOS, J. R. HUIZENGA and H. VONACH, Phys. Rev. 141, 1053 (1966)

2. H. VONACH, Habilitationsschrift Techn. Hochschule München (1964)

3. J. R. HUIZENGA and A. A. KATSANOS, Nucl. Phys., A98, 614 (1967)

4. A.A. KATSANOS and J. R. HUIZENGA, Phys. Rev., 159, 931 (1967)

5. T. v. EGIDY et al., Z. Physik, A286, 3411 (1978)

6. J. R. HUIZENGA, Ann. Rev. Nucl. Sc., (1972), p. 901

7. C. C. LU et al., Nucl. Phys., A164, 225 (1971)

8. N. T. PORILE et al., Phys. Rev., C9, 2171 (1974)

9. B. STROHMAIER, Thesis Univ. of Vienna (1974)

10. S. M. GRIMES et al., Phys. Rev., C5, 85 (1972)

11. A. B. SMITH et al., to be published

12. F. G. PEREY, B. BUCK, Nucl. Phys., 32, 353 (1962)

13. D. WILMORE, P. E. HODGSON, Nucl. Phys., 55, 673 (1964)

14. C. A. ENGELBRECHT, H. FIEDELDEY, Ann. Phys., 42, 642 (1967)

15. F. G. PEREY and C. M. PEREY, Phys. Rev., 131, 745 (1963)

16. G. S. MANI et al., Rep. C.E.A. 2379 (1963)

17. L. McFADDEN and G. R. SATCHLER, Nucl. Phys., 84, 177 (1966)

18. H. VONACH, R. C. HAIGHT and G. WINKLER, to be published

19. J. R. HUIZENGA and G. R. IGO, Nucl. Phys., 29, 463 (1962)

20. G. M. BRAGA-MARCCAZZAN et al., Phys. Rev., C6, 1398 (1972)

21. M. BLANN, Ann. Rev. Nucl. Sc., 25, 123 (1975)

22. W. DILG et al., Nucl. Phys., A217, 269 (1973)

23. A. GILBERT and A. G. W. CAMERON, Can. J. Phys., 43, 1446 (1965)

24. B. STROHMAIER and M. UHL, Proc. of Int. Conf. on Nucl. Data f. Science and Technol., Antwerp, Sept. 1982 (in press)

25. S. GRIMES et al., Phys. Rev., C3, 645 (1971)

26. S. GRIMES et al., Phys. Rev., C4, 607 (1971)

27. S. GRIMES et al., Phys. Rev., C6, 236 (1972)

28. J. R. GROVER and J. GILAT, Phys. Rev., 157, 814 (1966)

29. A. C. DOUGLAS and N. MacDONALD, Nucl. Phys., 13, 382 (1959)

30. M. UHL, Acta Physica Austriaca, 31, 245 (1970)

31. H. VONACH et al., Symp. on Neutron Cross-Sections from 10 to 50 MeV, Brookhaven, May, 1980, BNL-NCS-51245, DOE/NDC-21/L, NEANDC(US)-208/L, INDC(USA)-84/L (1980) and references there in

32. R. PLATTNER et al., Helv. Phys. Acta, 36, 1056 (1963)

33. P. HUBER et al., Phys. Lett., 5, 202 (1963)

34. H. SOBOTTKA et al., Helv. Phys. Acta, 43, 559 (1970)

35. K. J. LeCOUTEUR in Nucl. Reactions, ed. by P. M. Endt and M. Demeur (North Holland, Amsterdam, 1959)

36. G. CHENEVERT et al., Nucl. Phys., A122, 481 (1968)

37. E. GADIOLI et al., Nuov. Cim. Lett., 3, 677 (1972)

38. E. GADIOLI et al., Nuov. Cim., 22A, 398 (1974)

39. C. HOLBROW and H. H. BARSHALL, Nucl. Phys., 42, 264 (1963)

40. R. M. WOOD, R. R. BORCHERS and H. H. BARSHALL, Nucl. Phys., 71, 529 (1965)

41. R. R. BORCHERS, R. M. WOOD and C. H. HOLBROW, Nucl. Phys., 88, 689 (1966)

42. G. N. LORVHIKOVA et al., Sov. J. Nucl. Phys., 27, 609 (1978)

43. V. G. PRONYAEV et al., Sov. J. Nucl. Phys., 30, 310 (1979)

44. G. V. KOTEL'NIKOVA et al., Sov. J. Nucl. Phys., 31, 582 (1980)

45. G. N. LOVCHIKOVA et al., Sov. J. Nucl. Phys., 31, 1 (1980)

46. W. PILZ, D. SCHMIDT and D. SEELIGER, Sov. J. Nucl. Phys., 33(4),463(1981)

47. G. N. LOVCHIKOVA et al., Sov. J. Nucl. Phys., 33, 22 (1981)

48. H. VONACH and J. R. HUIZENGA, Phys. Rev., 149, 844 (1966)

49. J. R. HUIZENGA et al., Phys. Rev., 182, 1149 (1969)

50. C. C. LU, L. C. VAZ and J. R. HUIZENGA, Nucl. Phys., A190, 229 (1972)

51. A. KENNEDY et al., Phys. Rev., C5, 500 (1971)

52. A. SPRINZAK et al., Nucl. Phys., A203, 280 (1973)

53. J. WILEY et al., Nucl. Phys., A212, 1 (1973)

54. J. C. PACER et al., Nucl. Phys., A226, 413 (1974)

55. S. M. GRIMES, R. C. HAIGHT, K. R. ALVAR, H. H. BARSCHALL and R. R. BORCHERS, Phys. Rev., C19, 2127 (1979)

56. S. M. GRIMES, R. C. HAIGHT and J. D. ANDERSON, Nucl. Sci. Eng., 62, 187 (1977)

57. R. C. HAIGHT, S. M. GRIMES and J. D. ANDERSON, Nucl. Sci. Eng., 63, 200 (1977)

58. S. M. GRIMES, R. C. HAIGHT and J. D. ANDERSON, Phys. Rev., C17, 508 (1978)

59. U. SEEBECK and M. BORMANN, Nucl. Phys., 68, 387 (1965)

60. M. BORMANN, Habilitationsschrift, Hamburg (1965)

61. T. ERICSON, Ann. of Phys., 23, 390 (1963)

62. T. ERICSON, T. MAIER-KUCKUK, Ann. Rev. Nucl. Sci., 16, 183 (1966)

63. G. M. BRAGA-MARCAZZAN, L. MILAZZO-COLLI, Energ. Nucl., 15, 186 (1968); Progr. Nucl. Phys., 11, 145 (1970)

64. P. FESSENDEN, W. R. GIBBS and R. B. LEACHMAN, Phys. Rev., C3, 807 (1966)

65. E. GADIOLI et al., Nuov. Cim., 44B, 338 (1966)

66. M. MARUYAMA et al., Nucl. Phys., A145, 581 (1970)

67. G. M. TEMMER, M. MARUYAMA, D. W. MINGAY, M. PETRASCU, R. Van BREE, Phys. Rev. Lett., 26, 1341 (1971)

68. G. J. CLARK et al., Nucl. Phys., A173, 73 (1971)

69. F. BROWN, D. A. MARSDEN and R. D. WERNER, Phys. Rev. Lett., 20, 1449 (1968)

70. W. KOENIG, K. W. McVOY, H. A. WEIDENMÜLLER and P. KIENLE, Phys. Lett., 123B, 279 (1983)

71. H. K. VONACH and J. R. HUIZENGA, Phys. Rev., 138, 1372 (1965)

72. J. ERNST et al., Nucl. Phys., A136, 87 (1969)

73. H. K. VONACH, A. A. KATSANOS and J. R. HUIZENGA, Nucl. Phys., A122, 465 (1968)

74. L. W. PUT, J. D. A. ROEDER and A. van der WOUDE, Nucl. Phys., A112, 561 (1968)

75. J. D. A. ROEDER, Thesis, Groningen (1971)

76. A. D. CARLSON and H. H. BARSHALL, Phys. Rev., 158, 1142 (1961)

77. P. KOPSCH and S. CIERJACKS, Proc. of the Internat. Conf. on Statistical Properties of Nuclei, ed. J. B. Garg, Plenum Press, N. Y., (1972), p. 455

ACKNOWLEDGEMENTS

The calculations for the $^{56}Fe(n,\alpha)$ reaction discussed in section 3.2 have been performed by Prof. M. Uhl by means of the Code STAPRE. The author gratefully acknowledges this important contribution and numerous interesting discussions with both Prof. Uhl and Dr. B. Strohmaier.

TABLE I

Level density parameters for the residual nuclei formed in the $^{56}Fe(n,\alpha)$ reaction, which reproduce the α-emission cross-section to the resolved levels in ^{53}Cr in the U = 2.1 - 3.1 MeV range

Res. Nucleus	$a(MeV^{-1})$	Δ(MeV)
^{56}Fe	6.00	.8
^{56}Mn	6.53	- 1.54
^{53}Cr	5.96	- .72

TABLE II

Sources of error in the method of determining the level density of the residual nucleus reached by neutron emission from absolute cross-sections σ_{Lev} for population of resolved levels

Source of error	Estimated Contribution to $\Delta\rho/\rho$ (in %)	
	in general	for specific example $^{56}Fe(n,\alpha)$
exp. error of σ_{Lev}	∿ 5-15	∿ 8
error in estimate for contr. of non-compound reaction to σ_{Lev}	strongly dependent on type of reaction and incident energy	∿ 10
uncertainty in $\sigma_{cJ\pi}$ because of uncert. of opt. model parameters	∿ 5	∿ 7
uncertainty in $\sigma_{cJ\pi}$ because of uncertainties of pre-compound and direct fractions f_{PE} and f_D	∿ 5-20 smaller for incident α-particles than for incid. nucleons	∿ 8
uncertainty of $G(J,\pi)$ because of uncertainty in opt. model parameters	∿ 10	∿ 15
uncertainty of $G(J,\pi)$ because of uncert. of spin distribution of levels	∿ 5-15	∿ 10
uncertainty because of isospin effects neglected in calc.	0-15 except for (p,p') where error may be much larger	∿ 0
total uncertainty	∿ 20-30	∿ 25

TABLE III

Uncertainties in derivation of level densities from $\frac{d\sigma}{d\varepsilon}$ measurements

Source of error	Estimated Contribution to $\Delta\rho/\rho$ (in %)	
	in general	for specific example $^{56}Fe(n,\alpha)$
exp. error in $\frac{d\sigma}{d\varepsilon}$ / σ_{Lev}	∿ 3-10	9-11
error in $\frac{d\sigma}{d\varepsilon}$ / σ_{Lev} because of uncertainty of precompound cont. to both quantities	strongly dependent on type of reaction and incident energy	∿ 10
errors in $(\frac{d\sigma}{d\varepsilon}$ / $\sigma_{Lev})_{calc}$ due to:		
uncertainty in spin distribution of levels	∿ 5-15	∿ 7
uncertainty in optical potential for the measured emitted particle	∿ 5-15	∿ 7
total uncertainty	∿ 15-25	∿ 17

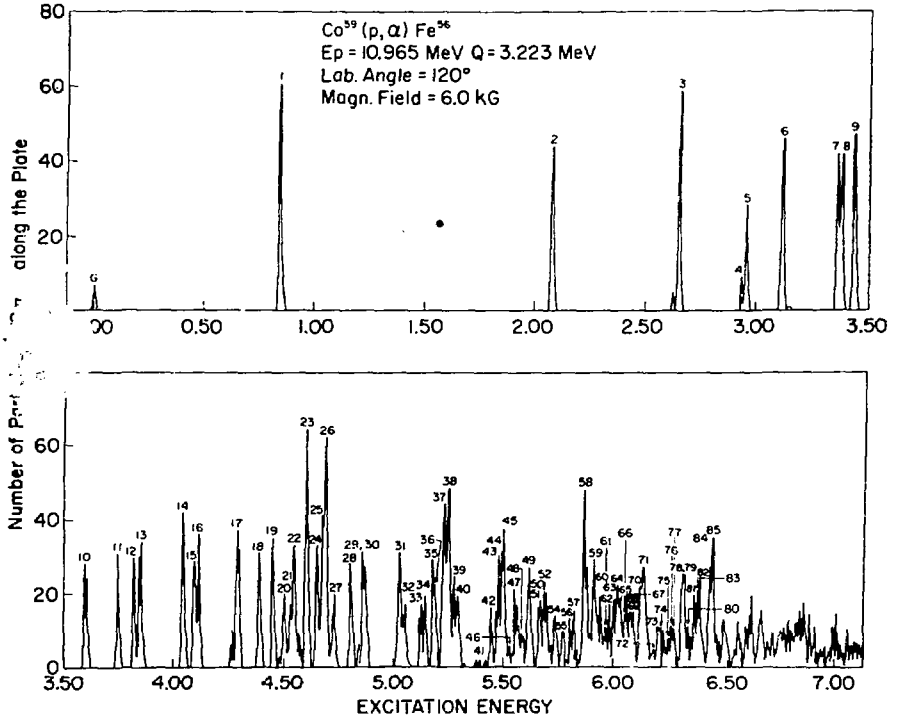

Fig. 1 Identification of nuclear energy levels from high resolution charged particle spectroscopy; α-particle spectrum from the $^{59}Co(p,\alpha)^{56}Fe$ reaction (Fig. 2 of ref. 1)

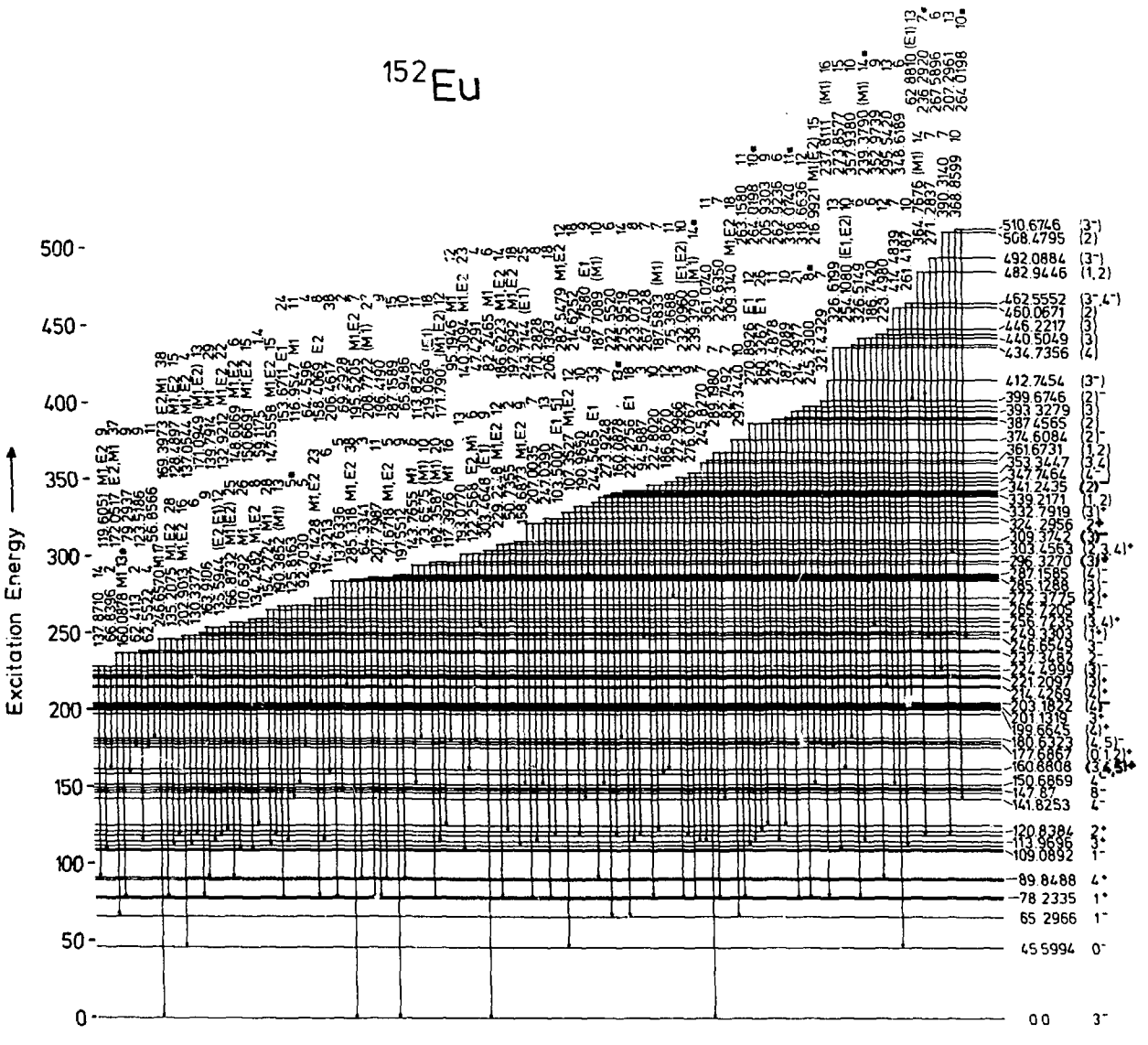

Fig. 2 Identification of nuclear energy levels from high resolution study of γ-radiation following thermal neutron capture in ^{151}Eu (Fig. 4 of ref. 5)

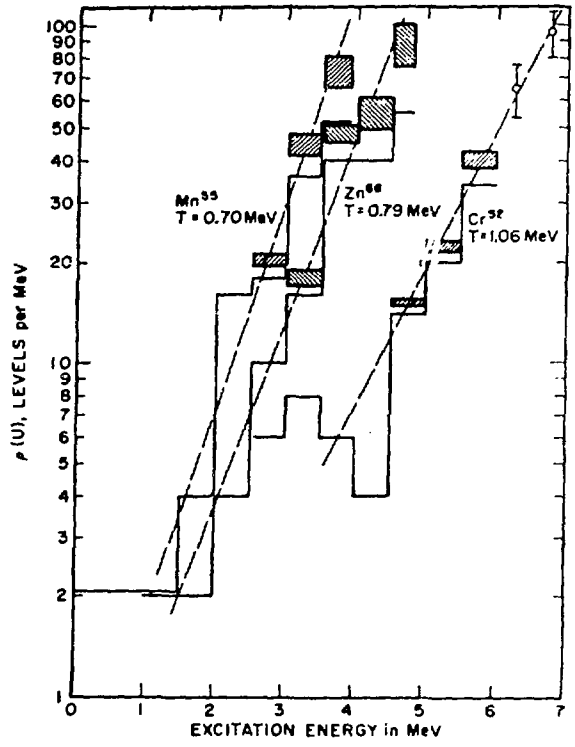

Fig. 3 Level density of medium mass nuclei derived by counting of the levels found in (p,p') and (p,α) reactions. Histogram: observed level density; shaded areas: level density corrected for unresolved doublets (Fig. 8 of ref. 4)

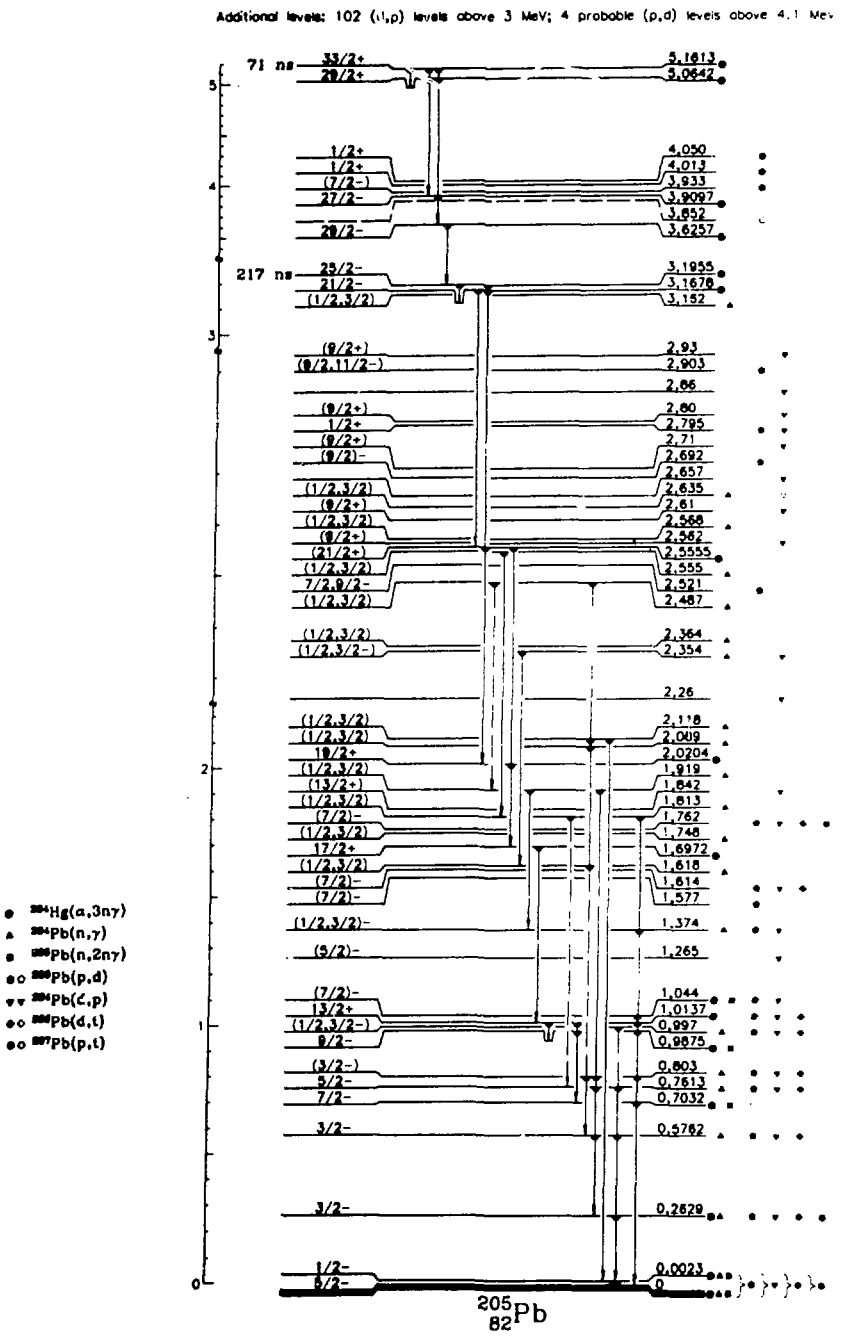

Fig. 4 Level scheme of ^{205}Pb as derived from a variety of nuclear reactions (Table of Isotopes, ed. C.M. Lederer, 7th Ed, Wiley, N.Y., 1978)

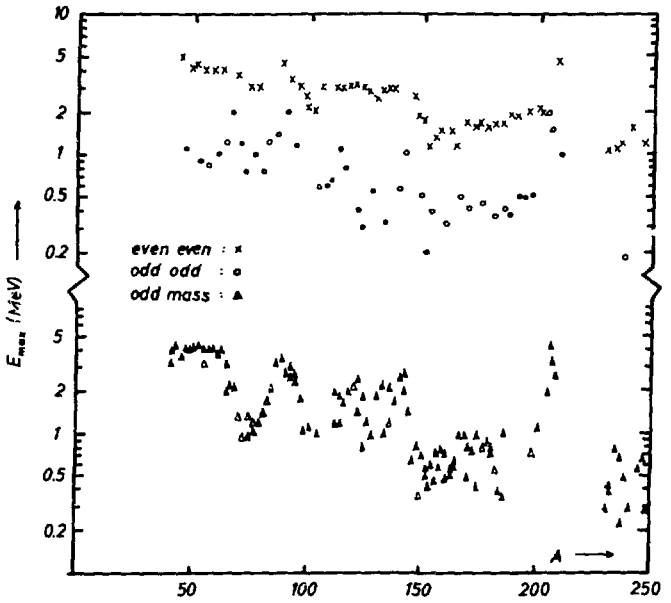

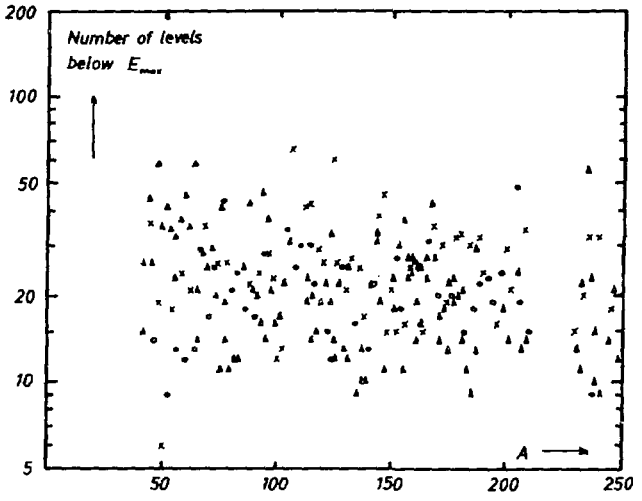

Fig. 5 Summary on the results obtained so far by the level counting method
a) maximum excitation energy E_{Max} up to which almost (> 90%) all levels are believed to be known,
b) number of levels observed below E_{Max}

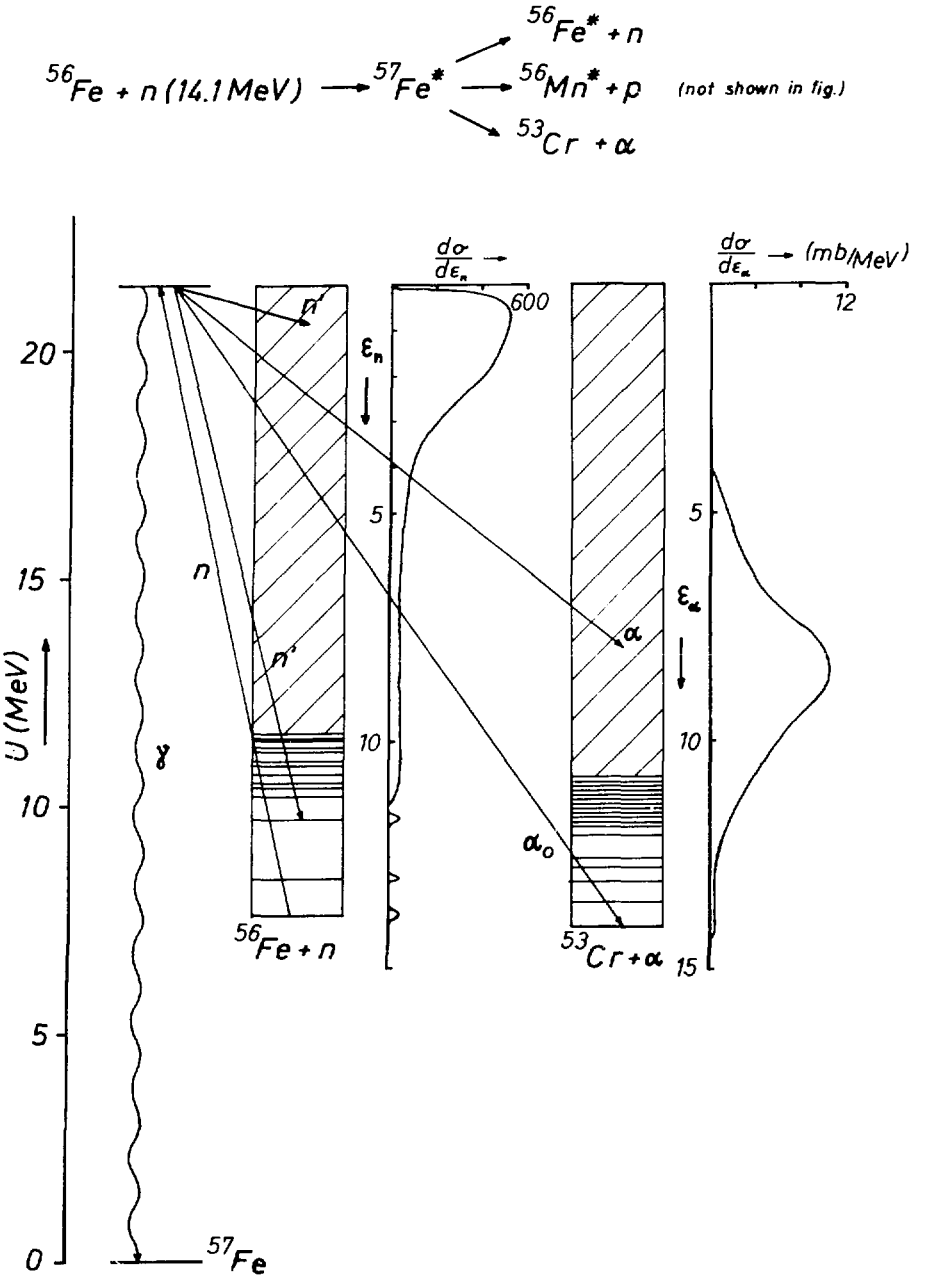

Fig. 6 Scheme of a compound nucleus reaction for the specific example ^{56}Fe + 14.1 MeV neutrons

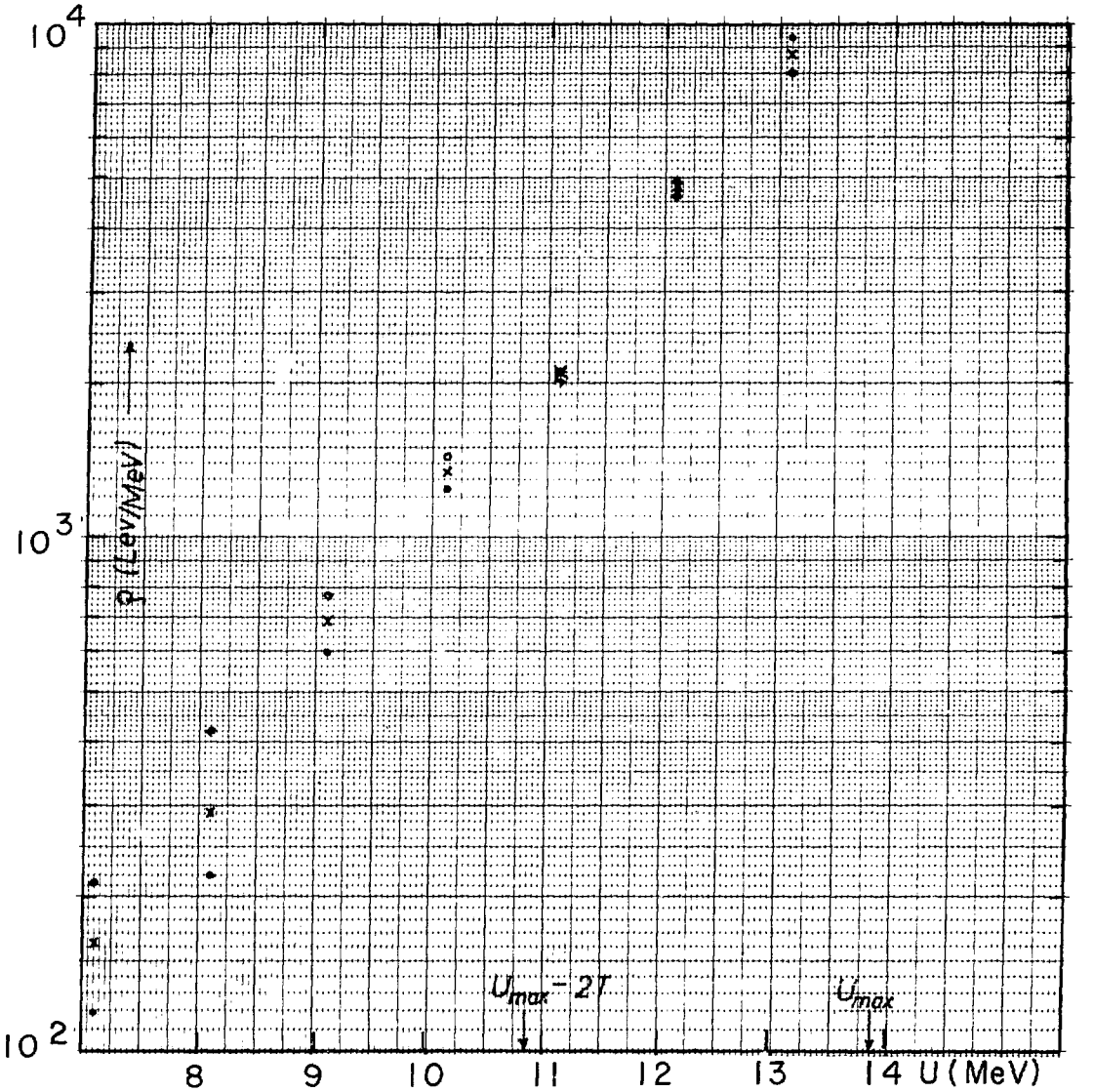

Fig. 7 Comparison of different level density functions ρ(U) for ^{56}Fe which give the same cross-sections for population of resolved levels in ^{53}Cr in the reaction ^{56}Fe + 14.1 MeV neutrons

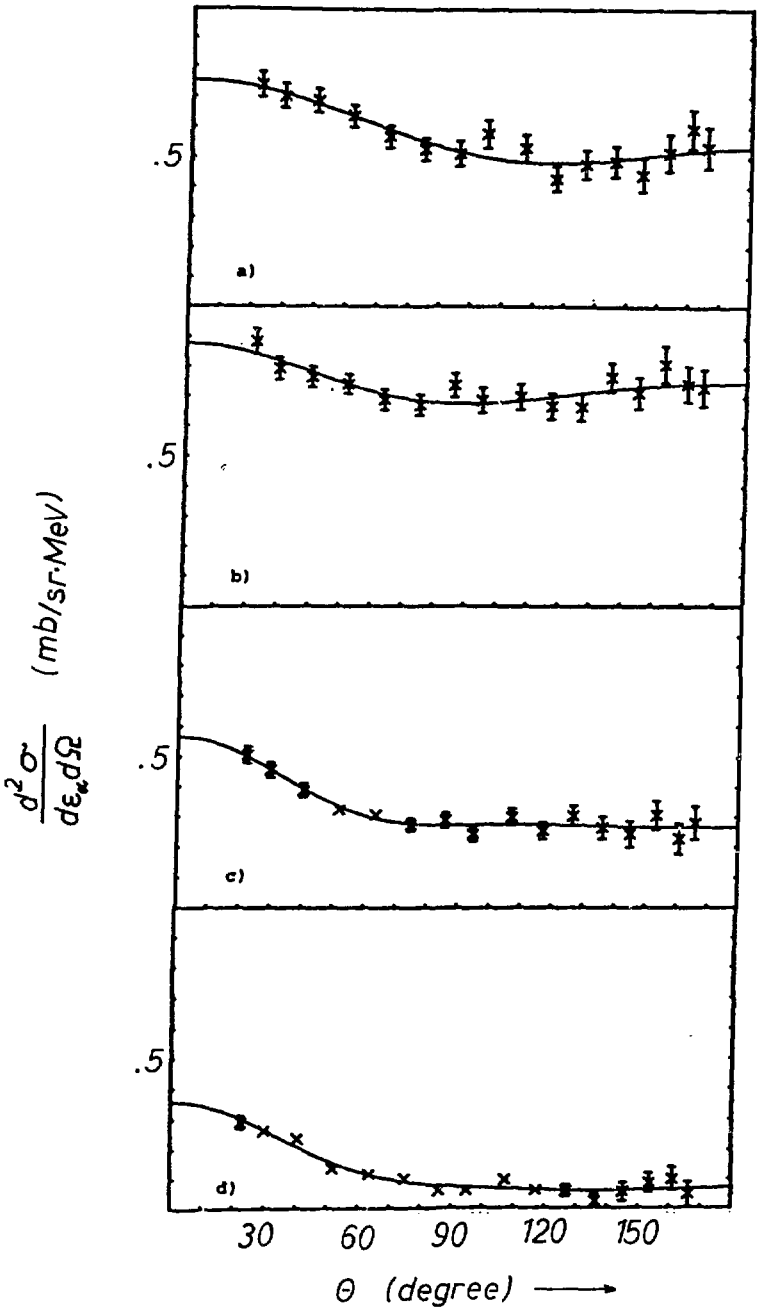

Fig. 8 Angular distribution of α-particles from the reaction $^{56}Fe(n,\alpha)$ at E_n = 14.1 MeV.
(a) $E_{\alpha ch}$ = 6-8 MeV, (b) $E_{\alpha ch}$ = 8-10 MeV, (c) $E_{\alpha ch}$ = 10-12 MeV,
(d) $E_{\alpha ch}$ = 12-14 MeV

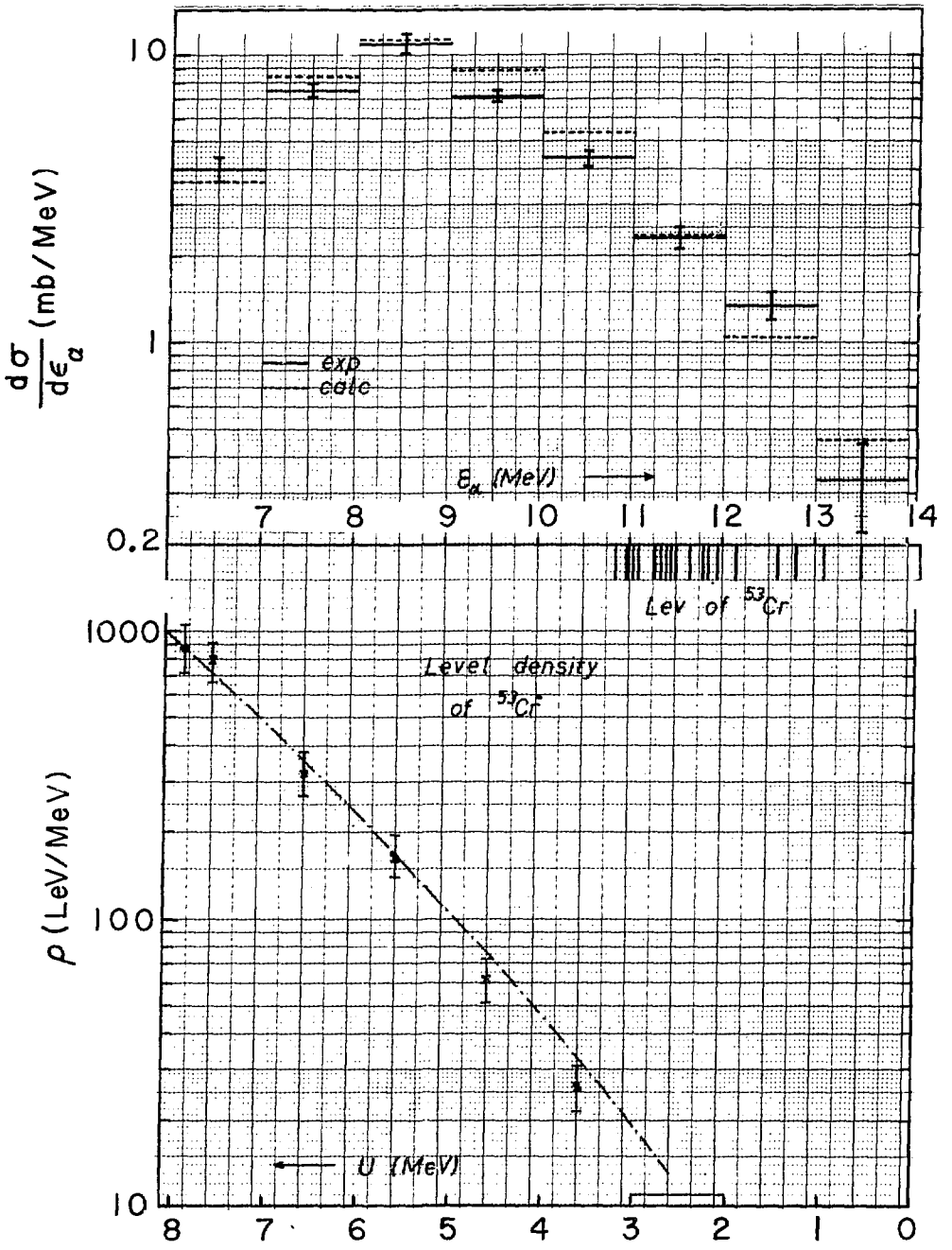

Fig. 9 Extraction of level density information from the α-spectrum observed in the $^{56}Fe(n,\alpha)$ reaction

(a) measured and calculated α-emission cross-sections $d\sigma/d\varepsilon_\alpha$

(b) level densities derived from comparison of experimental and calculated α-emission cross-sections, also shown density of resolved levels at low excitation energy and level density at the neutron binding energy derived from average s-wave resonance spacing assuming a spin cutoff factor $\sigma = 4$

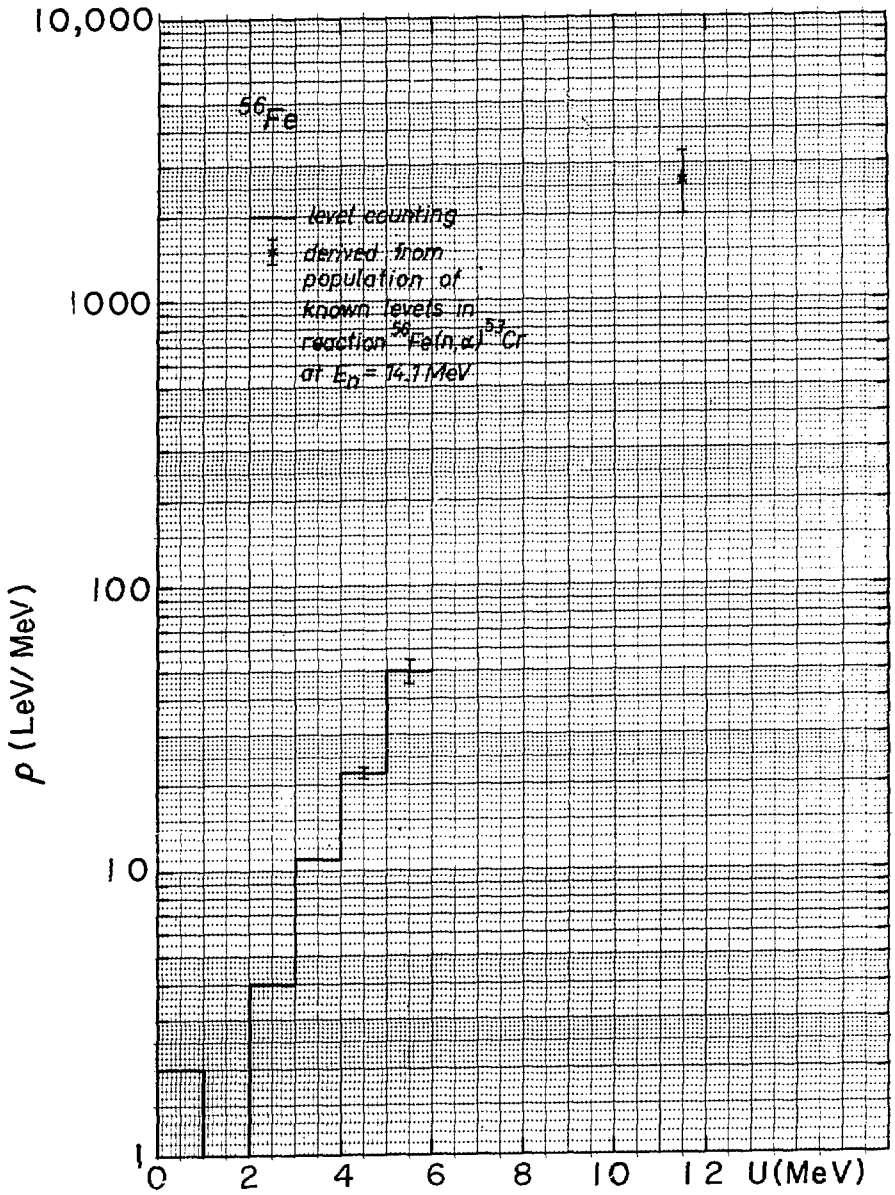

Fig. 10 Level density of ^{56}Fe; comparison of the result obtained from the $^{56}Fe(n,\alpha)$ cross-section to resolved levels in ^{53}Cr with results from level counting

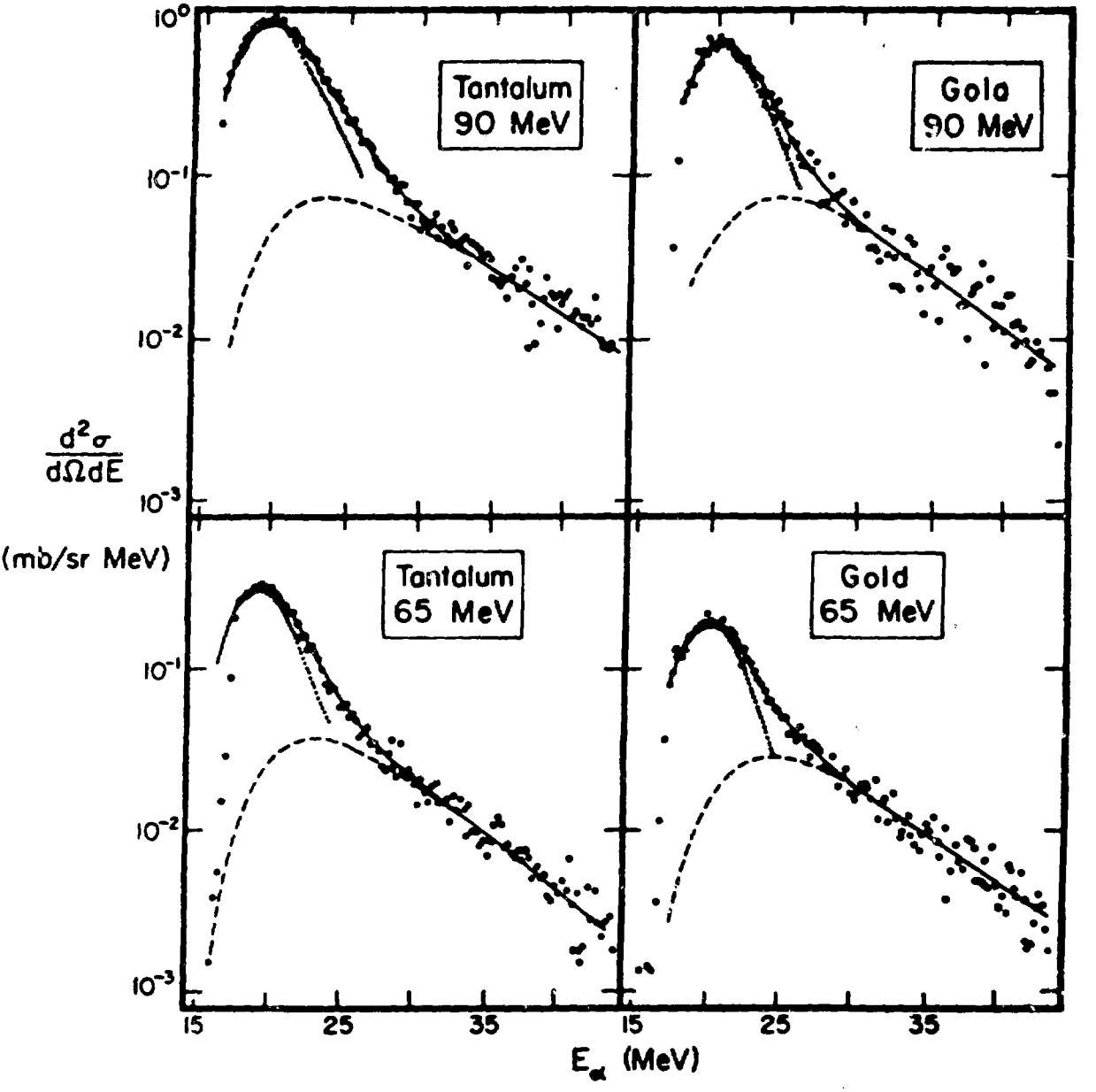

Fig. 11 Energy spectra of α-particles from (α,α') reactions on gold and tantalum at 160° (Fig. 2 of ref. 36)

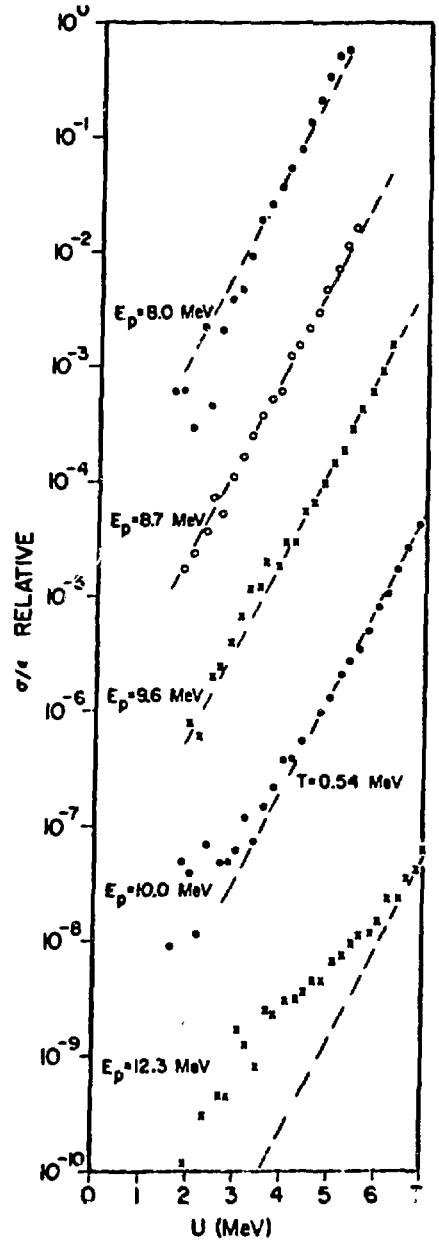

Fig. 12 Relative level density of ^{181}W below the neutron binding energy as derived from the 135° neutron spectra from the $^{181}Ta(p,n)$ reaction at different bombarding energies (Fig. 7 of ref. 27)

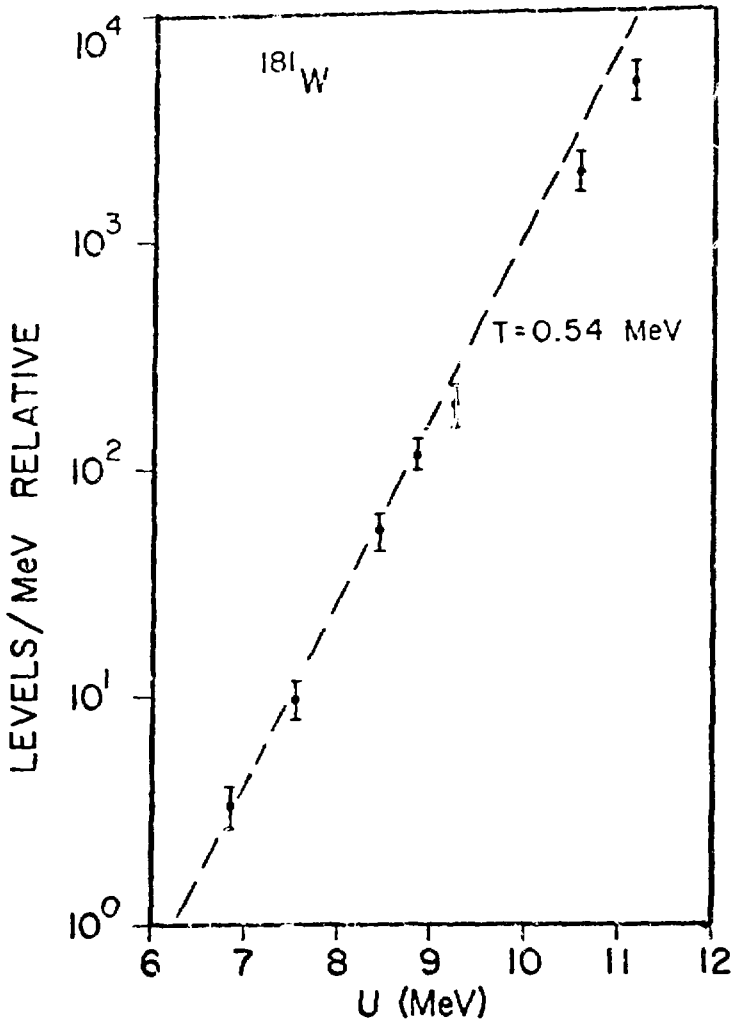

Fig. 13 Relative level density of ^{181}W for energies above the neutron binding energy as derived from study of the $^{181}Ta(p,n)$ reaction by means of Grimes' method (Fig. 13 of ref. 27)

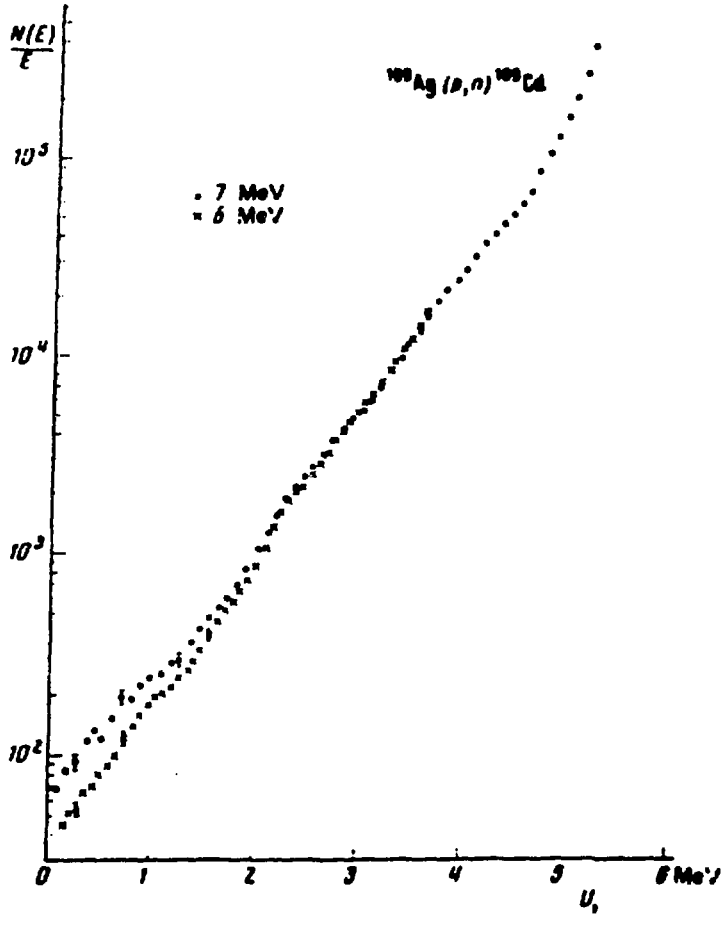

Fig. 14 Relative level density of ^{109}Cd as derived from the neutron spectra of the $^{109}Ag(p,n)^{109}Cd$ reaction at different bombarding energies (Fig. 3 of ref. 42)

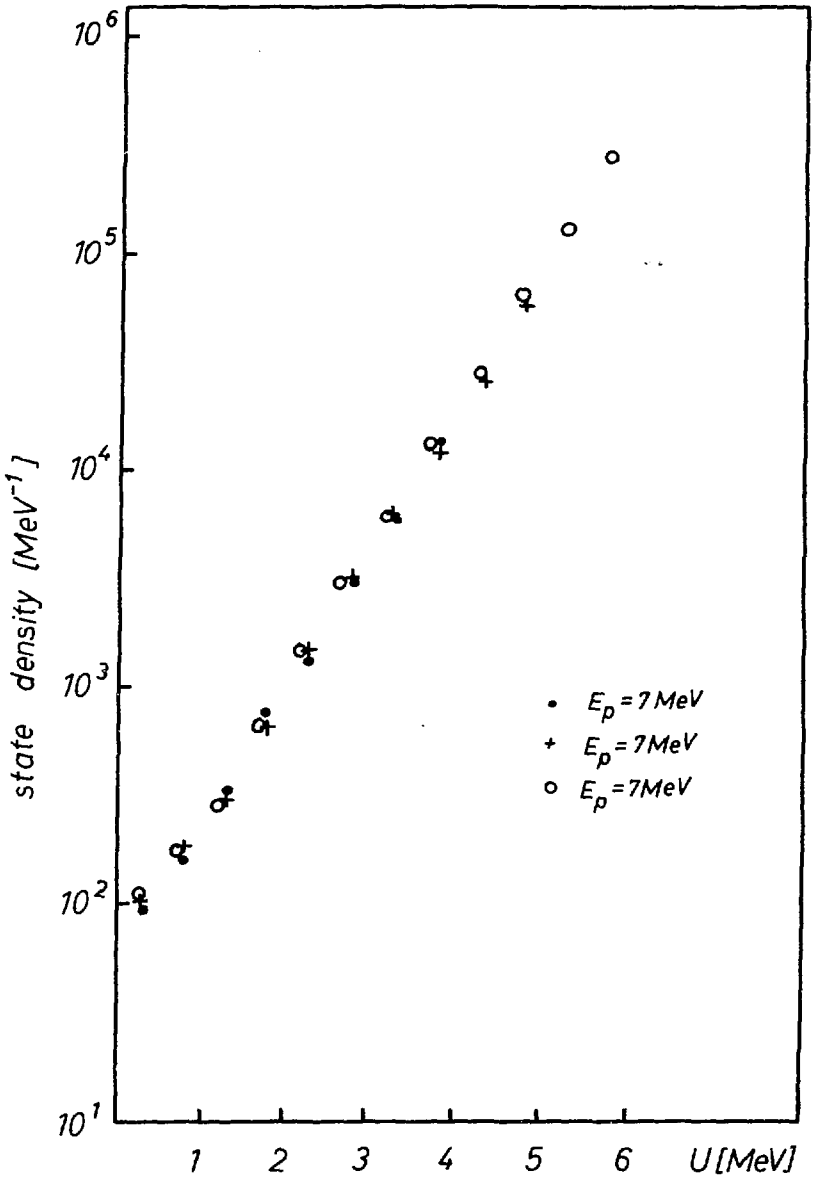

Fig. 15 Absolute state density of ^{109}Cd derived from the neutron spectra of the reaction ^{109}Ag(p,n)^{109}Cd at different bombarding energies (Data from fig. 3 of ref. 46)

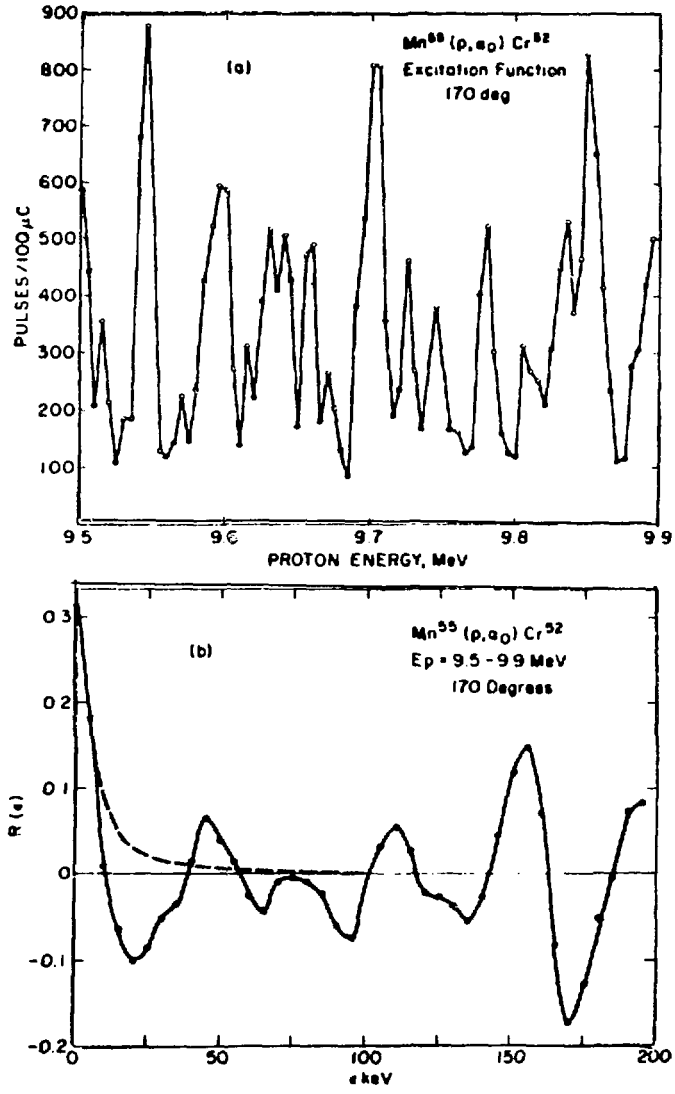

Fig. 16 (a) Excitation function for the $^{55}Mn(p,\alpha_0)^{52}Cr$ reaction
(b) Autocorrelation function derived from the data displayed in (a). The dashed curve is a theoretical Lorentzian curve with Γ = 6 keV

SYSTEMATICS OF THE NUCLEAR LEVEL DENSITIES

G.H. Rohr

Commission of the European Communities - JRC
B-2440 Geel, Belgium

ABSTRACT

Neutron resonance data are applied to study properties of highly excited states in nuclei. A level density systematics of compound resonances for a large number of nuclei of different even-odd character is discussed. The interpretation of the rather complicated structure in the systematics is that there is a step-shaped base line for the level density parameter formed by nuclei with minimal effects from residual interaction and no shell effects. This base line is used to answer questions relevant not only to level densities but also to nuclear physics in general. The step-like behaviour of the base line for light and medium-light nuclei is interpreted as changes in the level density due to changes of the average number of particles and holes participating in the compound excitation. The proof that the "compound states" in light and neutron closed shell nuclei are doorway (2p1h) states and therefore do not fulfil the Bohr assumption for a compound state may explain non-statistical effects observed in the capture process. Deviations of the level density parameter from the base line are interpreted as the effect of short range forces. A few examples are given and discussed for different mass regions. In the neighbourhood A ~ 75 the reduction of the pairing energy is assumed to be due to the blocking effect. In the mass range of the actinides the pairing energy has been readjusted at high excitation energy and at A ~ 105 it is shown that for neutron rich nuclei n-p interactions play the major role. Finally, the question is discussed whether or not there is a collective enhancement at higher excitation energy.

INTRODUCTION

In this contribution neutron resonance data are utilized to study the properties of highly excited states in nuclei. A level density systematics of compound resonances for a large number of nuclei of different even-odd character is investigated. The rather complicated structure of the system-

atics can be interpreted not only with respect to the specific problem of level densities but also to other nuclear physics aspects. These aspects are discussed in the following in connection with nuclear models used for calculations of excited nuclear states. The corresponding level schemes of the nuclear models are drawn schematically in Fig. 1.

The single particle states are explained with the shell model, assuming that the nucleon moves in an average potential including spin-orbit coupling. The calculated single particle level spacing for closed shell nuclei agrees quite well with the observed states at low excitation energy but deviates by several orders of magnitude at neutron separation energy. To allow for an increase of the level density at higher excitation energy a residual interaction, not specified, has to be introduced allowing a nucleon in an excited state to share its energy with other nucleons, resulting in a more complicated state. The conditions that with a collision the energy of the single particle states do not change and that the energy, spin and parity are conserved are the basis of the independent particle model. Then we expect, in an odd nucleon system, that 2p1h states become energetically possible at a certain threshold and with further increase in energy successive states of higher hierarchy (3p2h, 4p3h, ... states) are created.

We may ask, what is the hierarchy of these states at neutron separation energy? Is the hierarchy small enough that steps in the level density systematics may be seen due to the transition from one hierarchy to the next? Are the compound states so complicated that the Bohr assumption (for creation and decay of the compound state) is fulfilled for all nuclei?

For even nuclei the most important residual interaction, the pairing force, has to be included. It consists of a short range attractive force between identical nucleons. In a crude approximation the inclusion of a short range force (delta-force) in the shell model Hamiltonian results in a suppression of the ground state without altering the other single particle states. The application of the independent particle model with the lowered ground state causes an energy gap Δ (Pairing energy) and reduces the level density corresponding to an excitation energy of $(U-\Delta)$ at neutron separation energy. The change in the level density compared to a nucleus with no specified residual interaction can be taken as a measure of short range forces. We may ask, does the pairing energy change with the excitation energy? Have other interactions to be included?

A more accurate description of the pairing interaction is expected with the quasi-particle model. The single particle states will be transformed into quasi-particle states by means of the gap equation and quasi-particles will be treated in the independent quasi-particle model. Do we describe in principle all states with the independent particle model? The answer from the literature is no; the collective states explained with the liquid drop model have to be added. However the vibrational states, for instance the first excited 2^+ state, can also be interpreted in the shell model as a two quasi-particle state obtained from one broken pair. The linear combination of one broken 2^+ terms causes an oscillating deformation of the whole nucleus and results in a shift of energy for one state so that it becomes the first excited state of the nucleus. The two phonon state (second 2^+) corresponds to a four quasi-particle state consisting of 2 broken pairs as indicated in

Fig. 1c). Until now the rotational states cannot be understood in the framework of the shell model, but with the introduction of the IBA model it may become possible. Let us assume that collective excited states are quasi-particle states with a very rhythmic collision pattern which causes its shift in energy. We then expect that the number of states in an interval ΔE at high energy (higher than the shift due to collective character) can be predicted by the particle models. In a first approximation the number of collective states which are shifted out of the interval will be replaced by quasi-particle states of higher energy shifted into ΔE. Whether or not the assumption is justified we hope to answer by means of the level density systematics performed at neutron separation energy.

The talk is organized as follows: In the first part the data used for the level density systematics and its interpretation are presented. In the second part the rather complicated structure of the systematics is interpreted and a base line for the level density parameter a for nuclei with minimized residual interactions and no shell effects is proposed. In the last part examples are given to answer the questions posed in the introduction.

NEUTRON RESONANCES AND CALCULATION OF PARTIAL LEVEL DENSITIES

Neutron resonances

The main sources of information for neutron resonances are the BNL 325 third edition (1973) [1] and Neutron Cross Sections Part 1 (1981) [2], which represents BNL 325 fourth edition and supersedes the resonance data of nuclei up to Z = 60 given in ref. [1]. In both editions lists of recommended resonance parameters for each isotope are presented.

Based on data of ref. [2] and other data published later than 1972, an evaluation for the level spacing and for the s-wave strength function S_0 had been performed at Geel [3]. In preparation of this contribution the data of ref. [2] have been included so that the average level spacing for more than 265 nuclei are now available [4]. The average resonance parameters have been determined by means of a computer programme [3], called MISDO, and is available at the NEA DATA BANK. A method is used which applies the Bayes' theorem to establish a threshold, for a given p-wave strength function S_1, which is used to separate large s-wave resonances from p-wave resonances and small s-wave resonances. The number of small resonances which have been lost are estimated by an iterative procedure assuming a Porter Thomas distribution for the reduced neutron widths. Small modifications of the method have been used for light nuclei ($A < 40$) and nuclei with a large p-wave to s-wave strength function ratio. In the latter case the experimental parity assignment of s-wave resonances has been used.

In Fig. 2 the neutron widths for ^{238}U resonances are plotted against the neutron energy together with threshold curves, which are labelled and determine the 1‰ probability limit of p-wave resonances for the p-wave strength function S_1.

In total 20 S_I values can be used in one run and the results are given in a printed graph. The CPU-time is ~ 9 sec for 400 resonances using the IBM 4341. The influence of the threshold on the results of the level spacing D and s-wave strength function S_0 are plotted in Fig. 3.

The level spacing for low thresholds is contaminated with p-wave resonances up to $S_I = 3 \cdot 10^{-4}$. The average of the first values above this threshold has been used to determine D and S_0. The behaviour of the average parameter for higher thresholds reflects properties of the neutron width distribution, which is an additional information with which to judge the accuracy of the obtained data.

Calculation of partial level densities

In the following the partial density of states for a fixed number of particles (p) and holes (h) are discussed in the framework of the independent particle model. An exact calculation of p-h excitations, assuming uniformly spaced single particle states has been performed by Böhning, using a combinatorial method [5]. The results are compared with those of the level density formula, which are derived by means of statistical approximations in the conventional way. According to this, the Ericson formula agrees better than others with the exact determination for the (p-h) distribution of states at constant excitation energy [6]. The formula is improved by Williams [7] thus:

$$\rho(U,p,h) = \frac{g(gU-A)^{p+h-1}}{p!\ h!(p+h-1)!} \qquad (1)$$

with $$A = \frac{1}{4}(p^2 + h^2) + \frac{1}{4}(p-h) - \frac{1}{2}h.$$

In this equation g is the single particle state density and U the excitation energy. In Fig. 4 the ratio of partial particle level density to single particle level density has been plotted for a specified number of p and h and for fixed excitations ($M = gU$) between M = 9 and 100. The distribution has a sharp maximum at $p \sim \frac{1}{2}\sqrt{M}$ and drops down to zero for $p > \sqrt{M}$. The maxima of level densities for 3p2h, 4p3h and 5p4h states are at M = 20, 36 and 64 respectively. In the following section it will be checked whether these values are relevant in the level density systematics, but we expect that shell effects play a major role for the partial level density of states.

For a more realistic single particle level density distribution only the combinatorial method has been applied to calculate partial level densities of states at neutron separation energy. The starting point of these calculations are in general Nilsson's single particle states and the pairing correlation has been taken into account using the quasi-particle formalism and pairing energies from Cameron [8].

Two and four quasi-particle states of allowed spin and parity have been calculated for 6 nuclei in the 3s resonance range [9]. The predicted level spacing at neutron separation energy is in good agreement with the experimental spacing of ^{47,49}Ti, ^{57}Fe and ^{61}Ni but disagrees for ^{43}Ca and ^{53}Cr.

In another publication [10] the level density of doorway states, that means all states which are obtained by one collision of the incoming neutron with a nucleon of the target-nucleus, has been calculated for 20 nuclei, also in the 3s resonance range, in order to investigate the fluctuations of the experimental strength function values around the average curve predicted by the optical model. These calculations have been extended to more than 240 nuclei spread over the whole atomic weight range [11,12]. The data have been used to get support for the interpretation of the level density systematics and have been included in Fig. 7.

THE LEVEL DENSITY SYSTEMATICS

For many years the observed nuclear states have been interpreted with the level density theory which was mainly initiated by Bethe and based on the framework of the Fermi gas model [13]. The level density, at excitation energy U and spin of the compound state J, is given by:

$$\rho(U,J) = \frac{1}{24\cdot\sqrt{2}} \; \frac{2J+1}{a^{1/4}\sigma^3} \; \frac{\exp\left[2(a(U-\Delta))^{1/2} - J(J+1)/2\sigma^2\right]}{(U-\Delta)^{5/4}} \qquad (2)$$

The parameters in expression (2) are taken as:

spin cut-off factor	$\sigma = \sqrt{0.1045\cdot a\cdot t\cdot A^{2/3}}$
nuclear temperature	$t = \sqrt{(U-\Delta)/a}$
pairing energy	Δ taken from Gilbert and Cameron [8].

According to the Fermi gas model the level density parameter a is proportional to the level density of the single particle states at Fermi surface energy $g = 6\cdot a/\pi^2$ and is expected to be proportional to the atomic number A.

The systematics of a is not strongly dependent on the correct level density expression since a is determined by one value for each nucleus, namely the level density taken at similar excitation energies (between 6 and 10 MeV). It may influence the gross structure of the systematics, but the behaviour of neighbouring nuclei is preserved. This behaviour is expected to be used in the level density systematics.

A level density systematics on the very recent evaluated level spacing of neutron resonances is shown in Fig. 5. For comparison another systematics performed 15 years earlier is given in Fig. 6, a drawing which is taken from reference [14]. In the latter case data from measured resonances and calculated values (open circles) are included. We cannot compare the data in detail but the following properties are common to both sets of data:

1) The level density parameter increases with the atomic number, and has strong minima at nuclei with a magic number of neutrons (N = 28, 50, 82 and 126) and also a strong maximum at A ~ 150 corresponding to a neutron number of N = 90.
2) There are steps (steep increase of a) for light and medium light nuclei at atomic numbers A = 38, 69 and 94 with a ~ 5, 10 and 15 respectively.

3) There are strong fluctuations of a values for nuclei around A ~ 110 and A > 235.

Additional minima are indicated in Fig. 5 at N = 20 (A = 40), Z = 50 (A = 125) and A = 175 and 183. The latter may be explained by subshell structures as could be expected from Nilsson's model for strongly deformed nuclei. The strong maximum observed at A = 150 with N = 90 has its counterpart at A = 230 with Z = 90 seen in Fig. 8 and is therefore interpreted as a shell effect. As shown in Fig. 6 the increasing trend of the level density parameter has been represented by a linear function, which is expected from the Fermi gas model.

A more detailed interpretation based on the framework of the independent particle model is given in Fig. 7,8 [11,12,15] where in Fig. 7 the calculated values for the level density of the doorway states are included. As shown, the doorway state level density agrees quite well with the observed level density of compound resonances for all nuclei A < 37 and approaches the observed values at closed shell nuclei. The deviations from the doorway state density indicate an increase in compound states due to the existence of more complex states created by more than one collision. The number of collisions in the compound reaction process is reflected in a step-like behaviour of the level density parameter a. Therefore the steps at a ~ 5, 10 and 15 may be interpreted as transitions to 3p2h, 4p3h and 5p4h states created by 2, 3 and 4 collisions respectively.

In Table I the excitation energy M_{step} at steps a ~ 5, 10 and 15 has been calculated and compared with the excitation energy M_{max} where the density of 3p2h, 4p3h and 5p4h states have the maximum based on data obtained with the uniform single particle model (expression (1) and Fig. 4). In spite of the simplicity of the model, the agreement is rather good and supports the interpretation given above. The relative change of the level density at the steps decreases with the atomic number and no steps are to be seen for nuclei A > 100. The level density parameter for A > 170 may be described with one line which now has a slope predicted from the Fermi gas model.

TABLE I

The excitation energy at the steps in the systematics are compared with the excitation energy where the partial level density of 3p2h, 4p3h and 5p4h have their maxima

Hierarchy	a_{step} [MeV]$^{-1}$	U [MeV]	M_{step}	M_{peak}
3p2h	5	7.7	23	20
4p3h	10	7.3	44	36
5p4h	15	6.8	62	64

The lines drawn in Fig. 7 and 8 are based on data for odd-odd nuclei (Fig. 8), where the residual interaction is expected to be minimized. In between the steps the slope is based on calculated values for the level density of doorway states in the range A = 20 to A = 100. Finally, the base line assumed as the level density parameter description for nuclei with (almost) no residual interaction and no shell effects is given by:

$$a = 0.071 \cdot A + VAR$$

$$\begin{aligned} VAR &= 1.64 & A &< 38 \\ VAR &= 3.74 & 38 < A &< 69 \\ VAR &= 6.78 & 69 < A &< 94 \\ VAR &= 8.65 & 94 < A &< 170 \end{aligned}$$

and $$a = 0.1080 \cdot A + 2.4 \qquad A > 170 \ .$$

As seen from Fig. 7 the base line is a lower limit for the data points except for nuclei with shell closure and a few nuclei at A > 235.

APPLICATION OF THE LEVEL DENSITY SYSTEMATICS

In this section a few remarks are made concerning the application of the hierarchy concept of the level density systematics in respect to the capture process and the base line of the level density parameter is utilized to answer questions posed in the introduction.

The hierarchy concept

The compound states at neutron separation energy for nuclei A < 37 and neutron closed shell nuclei are formed by only one collision and are in fact doorway resonances. The formation and decay of these simple states are not independent, even when mixing of states is assumed i.e. the Bohr assumption is not fulfilled. Consequently correlations between widths of different reactions, or so-called non-statistical effects, are expected in these resonances. The partial capture widths have been exclusively predicted by means of the valence nucleon model. Deviations from this model are explained by postulating interference between valence and doorway amplitudes [16]. In other examples the observed transition strength is related to valence or doorway amplitude separately.

Until now no doorway-capture calculations have been performed but by knowing the fact that there are compound resonances which decay only in this manner, such calculations are highly recommended. The resonances are present in nuclei A < 37 (2p-resonance range excluded) where capture in (doorway) resonances for neutron closed shell nuclei can be composed of at most two components, namely the valence- and doorway-amplitude. The comparison of experiment and theory will certainly contribute to the understanding of the capture process in resonances.

In a contribution to the γ-ray spectroscopy conference at Grenoble, the known hierarchy of more complicated compound states has been applied to assign collective excited doorway states and to study the pigmy resonances but is not repeated here [15].

Interpretations of the deviations from the base line

The base line of the level density parameter represents nuclei with a minimum of effective interaction and no shell effects. Deviations from this line will be discussed and a few examples given for different mass regions.

i) Nuclei in the neighbourhood of A ~ 75.

The level density parameter for nuclei around A ~ 75, in between the neutron closed shell nuclei 28 and 50, are shown in Fig. 9. These values are systematically higher than the base line for odd-even and even-even nuclei, which may be explained by a reduction of the pairing energy at high excitation energy due to the so-called blocking effect. This effect describes the fact that the excitation of about 4 particles and 3 holes in this mass region reduces the number of quasi-particle states participating in the pairing correlation. The pairing energy has been determined using equation (2) and a values given by the base line. They yielded, an average, a reduction of Δ by 7 % for the even-even nuclei and 35 % for the odd-even nuclei.

ii) Mass range of the actinides.

In contrast to the first example a few a values for the actinides are clearly below the base line. Also here the deviations have been taken as a measure of the pairing energy [12]. The results for proton and neutron pairing energy are drawn in Fig. 10 and Fig. 11 respectively. The average values have been indicated by crosses, assuming that the pairing correlation is limited to an even number of both neutrons and protons. It can be seen that the pairing energy for neutrons determined at high excitation energy (Δ_{Ex}) is systematically higher than that determined at the ground state (Δ_G) of the nucleus, and for protons below Z = 94 it is reduced by about 50 %. Assuming a δ-force for the pairing energy proportional to (2j+1) [17], the reduction of Δ_{Ex} for protons is interpreted as showing that single particles of low spin-values are important in this mass region [12]. In Fig. 12 a level density systematic has been performed using the pairing energy Δ_{Ex} predicted by the base line.

The pairing energy has also been used together with the base line and equation (2) to predict the level density of nuclei ρ_c. The ratio ρ_c/ρ_{obs} (experimental) is plotted in Fig. 13 and Fig. 14 for Δ_G and Δ_{Ex} respectively. The respective figures of merit for 24 resonances are F = 1.6 and F = 1.22, favouring the Δ_{Ex} obtained by the baseline [12]. The prediction of the level density of compound states as described above can be applied to any mass range, even for nuclei far from the stability line. Furthermore the deviation of the observed level density parameter for closed shell nuclei from the base line can be used to determine the shell effect in units of MeV.

iii) Nuclei in the neighbourhood of A ~ 105.

The determination of the pairing energy in the range A = 100 to 110, performed as described in the previous examples, was not successful. This is seen by the fluctuation of the level density parameter in Fig. 12 (Δ_{Ex} determined as described in i), ii) and [12]) not being reduced as compared to Fig. 7 (Δ_G taken from [8]). The reason is shown in Fig. 15 where, in the upper part, the level density parameter for two isotope series (Ru, Pd) are plotted

against the atomic number. The deviation from the base line increases with A, i.e. the residual interaction decreases with increasing odd number of neutrons. In the lower part of Fig. 15 the energy of the lowest 2^+ state is plotted in dependence of A and shows an anticorrelation to the level density parameter. The energy of the 2^+ states decreases with increasing number of neutrons. There are isotopes where the change from spherical to deformed shapes, indicated by a change in the energy of the 2^+ state, is even much stronger. For example, for Zr^{98} and Zr^{100} the energy is 1.22 MeV and 0.21 MeV respectively [18].

The level density parameter of the neutron rich nuclei with the strongest deviation from the base line are presented in Fig. 16. The deviation of the level density parameter corresponds, on average, to an increase of the level density by a factor six. The a values approach the base line if we assume that there is no effective residual interaction in these nuclei ($\Delta = 0$), indicated with the arrow-heads, and there is in addition a change in the moment of inertia from 0.7 I_{rig} to I_{rig}, indicated by the dots on the arrows. We conclude that these nuclei seem to behave like normal matter and that the spherical-to-deformed transition with increasing number of odd neutrons may be explained by a phase transition from superfluid to normal state.

What is the mechanism for this transition? The explanation for the abrupt change to deformed nuclei ($N > 60$) is still a challenge in nuclear physics.

A shape transition due to a second deformed minimum has been excluded by calculations of the potential energy surface using the Strutinsky method [19]. More recently, Federman and Pittel have shown, using explicit shell-model calculations, that the n-p interaction may be responsible for this fact [20]. This interaction is largest for particles in spin orbit-partner orbits of large spatial overlap and counteracts the n-n and p-p pairing correlations which try to stabilize the spherical shape of nuclei. In the mass region $A \sim 100$, according to the authors, the strong attraction between 1g9/2 proton and 1g7/2 neutron can break the pairing correlation by a polarization mechanism which causes mutual promotion of neutrons and protons from lower single particle states into 1g7/2 and 1g9/2 respectively. But the polarization effect can only occur if the gain in the n-p interaction exceeds the loss of single particle plus pairing energy. In contradiction to the observation, this should be indicated by a level density parameter lower than the base line.

But the increase of the level density parameter with odd neutron number supports the n-p interaction. Furthermore, all the nuclei with the strongest deviation from the base line have two or more protons in the 1g9/2 orbit and one or more neutrons in the 1g7/2 orbit (Mo, Ru, Pd), or two or more neutrons in the 2d5/2 orbit (Cd). Therefore no polarization mechanism is needed to explain the n-p interaction in these nuclei.

The spin coupling possibilities are increased for n-p interactions compared to the pairing correlation, where the alignment of the spins of the same nucleons are prevented by the Pauli principle. A coupling to spin zero may also be obtained by two pairs of (n-p) nucleons. Does one of the possible explanations used for the backbending effect of high spin states play a role here too?

The study of residual interaction by means of the level density systematics will be extended to other mass regions where (n-p) interactions have been predicted.

Collective enhancement

Collective enhancement at high excitation energy has been proposed and discussed in several papers. Bjørnholm et al. have studied the dependence of the level density formula on the symmetry of the nuclear shape [21]. Malov et al. used a semi-microscopic approach to study the effect of the rotational motion on the level density [22]. The calculation of the level density at neutron separation energy, with and without accounting for rotational motion, performed for 12 nuclei spread over the mass range $155 < A < 245$ yielded an enhancement of collective states from 1.7 to 6.9, with an average value of 3.2.

The collective enhancement in both papers is large and can be tested with the huge amount of data contained in the level density systematics. The level density parameters for some of the isotopes of Sn, Te, Xe and $_{56}Ba^{130}$ are presented in Fig. 17 together with the base line (full) and the next lower hierarchy line (dotted). This figure contains the nuclei with the largest deformation for stable nuclei and $A < 135$; namely $_{54}Xe^{124}$ and $_{56}Ba^{130}$ where, near the data point of the latter isotope, the rotational spectrum is drawn. Most of the data points, in particular the Sn isotopes, are in between both lines due to the proton closed shell ($Z = 50$), but there are no values which significantly exceed the base line.

In the mass region of nuclei with the strongest deformation $150 < A < 180$ there is also a value significantly larger than the base line except for the data around $A = 150$ ($N = 90$), where the sharp peak has been interpreted as a shell effect with its counterpart at $A = 230$ ($Z = 90$). Furthermore, the fluctuation of the level density parameter in the range $160 < A < 180$ is so small that sub-shell effects, caused by the deformation, can be identified.

In conclusion the study of the level density systematics indicates no enhancement of collective states at high excitation energy as expected (see introduction).

REFERENCES

1. S. F. MUGHABGHAB and D. I. GARBER, BNL-325, Vol. I (1973).

2. S. F. MUGHABGHAB, M. DIVADEENAM and N. E. HOLDEN, Neutron Cross Sections, Vol. 1, Part A., Academic Press 1981.

3. G. ROHR, L. MAISANO and R. SHELLEY, Proc. of the Specialists' Meeting on Neutron Cross Sections of Fission Product Nuclei, Bologna (1979), p. 197.

4. G. ROHR, to be published.

5. M. BÖHNING, Nucl. Phys. A152, 529 (1970).

6. T. E. ERICSON, Advances in Physics 9, 425 (1960).

7. F. C. WILLIAMS Jr., Nucl. Phys. A166, 231 (1970).

8. A. GILBERT and A. G. W. CAMERON, Canadian Journal of Physics 43, 1446 (1965).

9. W. M. GOOD, D. PAYA, R. WAGNER and T. TAMURA, Phys. Rev. 151, No. 3, 912 (1966).

10. K.-N. MÜLLER and G. ROHR, Nucl. Phys. A164, 97 (1971).

11. G. ROHR and R. SHELLEY, Int. Conf. on Neutron Physics and Nuclear Data for Reactors and other Applied Purposes, Harwell (1978) p. 478.

12. G. ROHR, L. MAISANO and R. SHELLEY, see Ref. [3] p. 207.

13. H. A. BETHE, Phys. Rev. 50, 332 (1936), Rev. Mod. Phys. 9, 69 (1937).

14. V. FACCINI and E. SAETTA-MENICHELLA, Energia Nucleare 15, 54 (1968).

15. G. ROHR, Neutron Capture γ-ray Spectroscopy, Grenoble, Inst. Phys. Conf. Ser. 62, 322 (1982).

16. B. J. ALLEN, Nuclear Data for Science and Technology, Antwerp (1982), p. 707.

17. M. G. MAYER, Phys. Rev. 78, 22 (1950).

18. C. M. LEDERER and V. S. SHIRLEY (eds.), "Table of Isotopes" 7th ed., J. Wiley & Sons Inc., N.Y. (1978).

19. R. K. SHELINE, I. RAGNARSSON and S. G. NILSSON, Phys. Letters 41B, No. 2, 115 (1972).

20. P. FEDERMAN and S. PITTEL, Phys. Rev. C20, 820 (1979).

21. S. BJØRNHOLM, A. BOHR and B.R. MOTTELSON, Physics and Chemistry of Fission, Rochester (1973) Vol. I, p. 367.

22. L. A. MALOV, V. G. SOLOVIEV and V. V. VORONOV, Neutron Capture γ-Ray Spectroscopy, Petten (1974), p. 175.

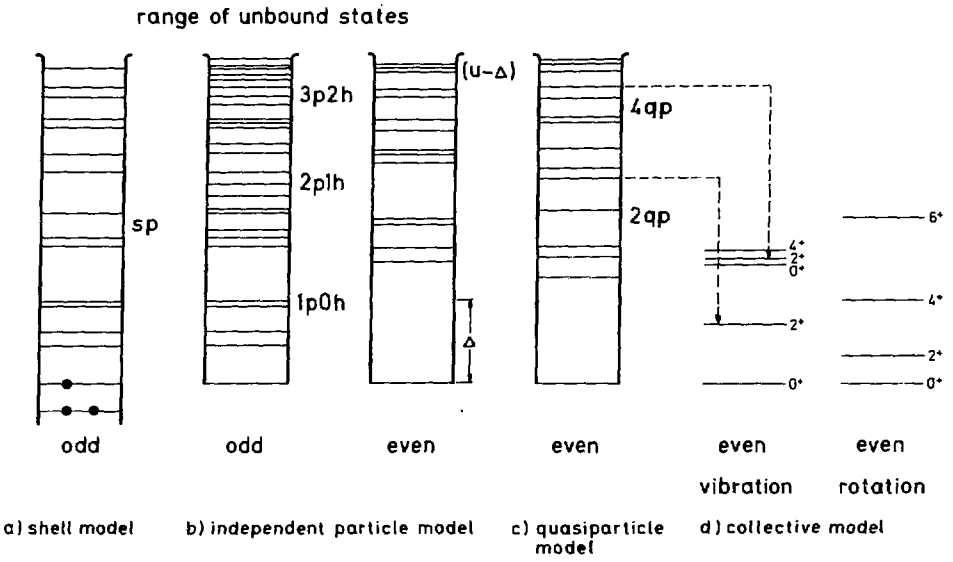

Fig. 1 Level schemes of nuclear models shown schematically.

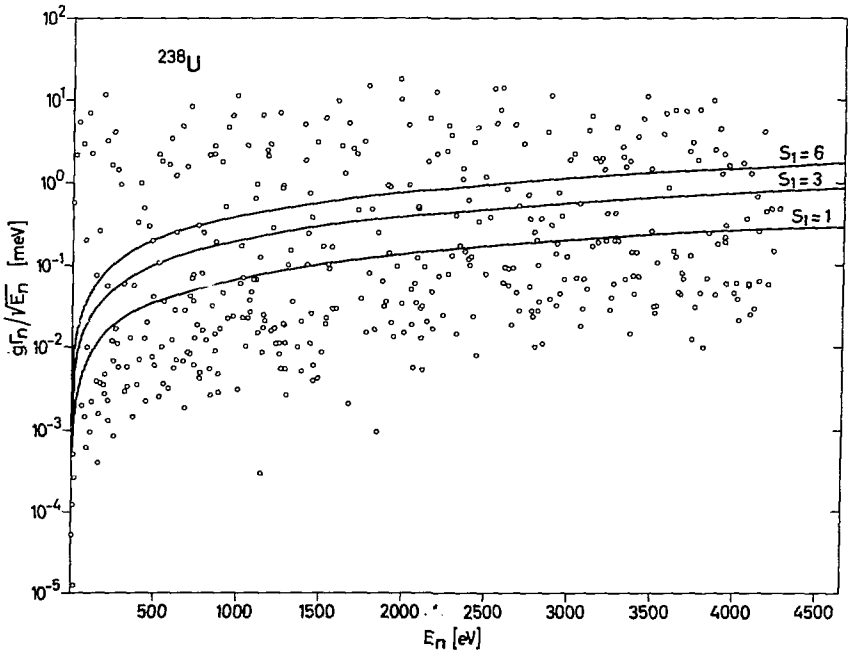

Fig. 2 The reduced neutron widths of ^{238}U resonances are plotted against neutron energy.

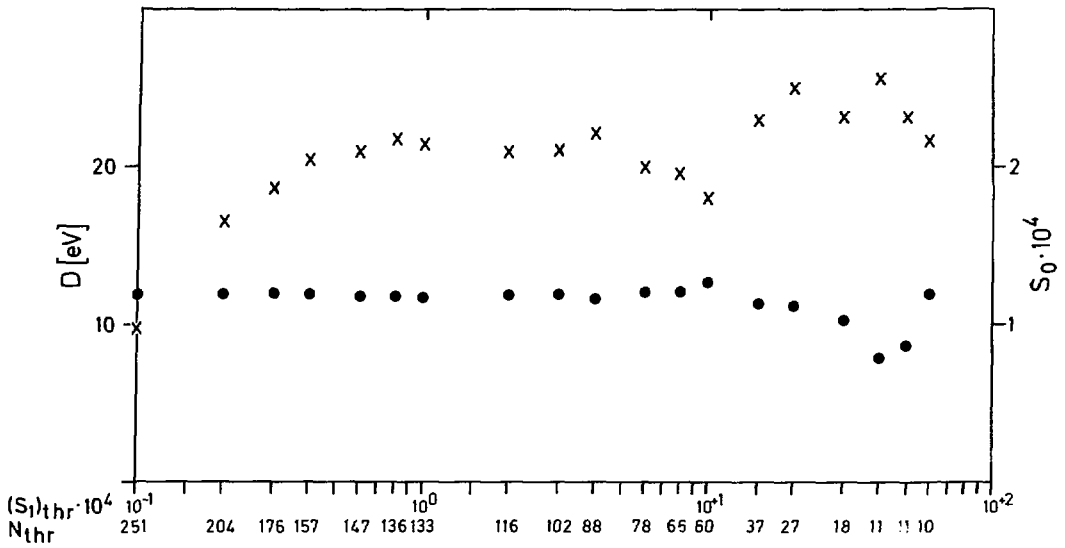

Fig. 3 Level spacing D and strength function S_0 of ^{238}U calculated for different threshold values (S_1).

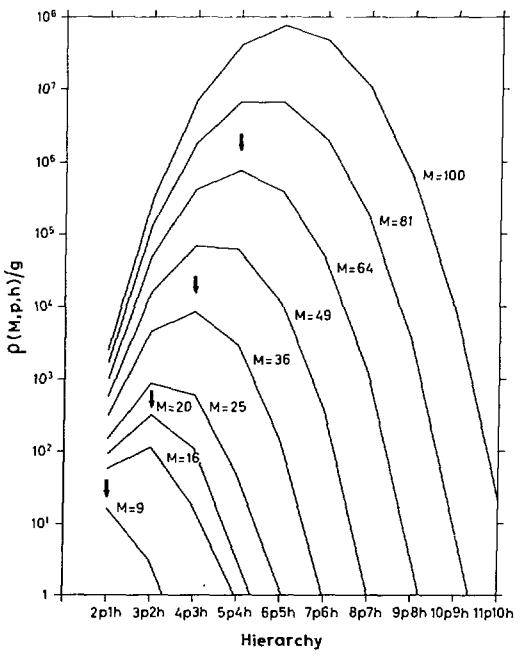

Fig. 4 Distribution of partial level densities at fixed excitation energies: M = g · U.

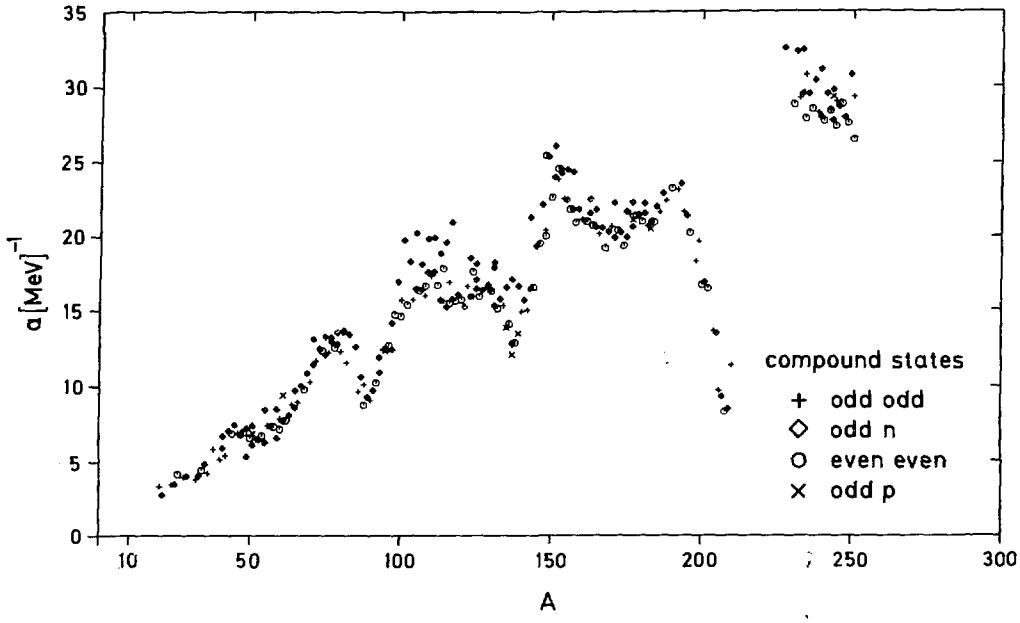

Fig. 5 Level density systematics based on new evaluated data [4].

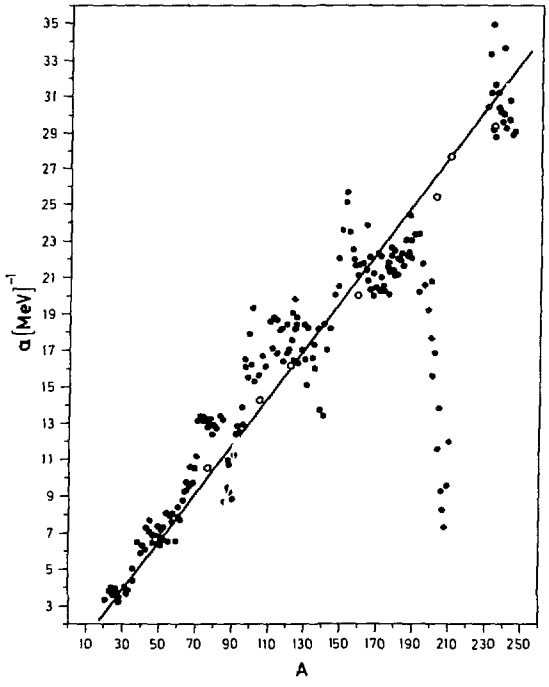

Fig. 6 Level density systematics taken from Ref. [14].

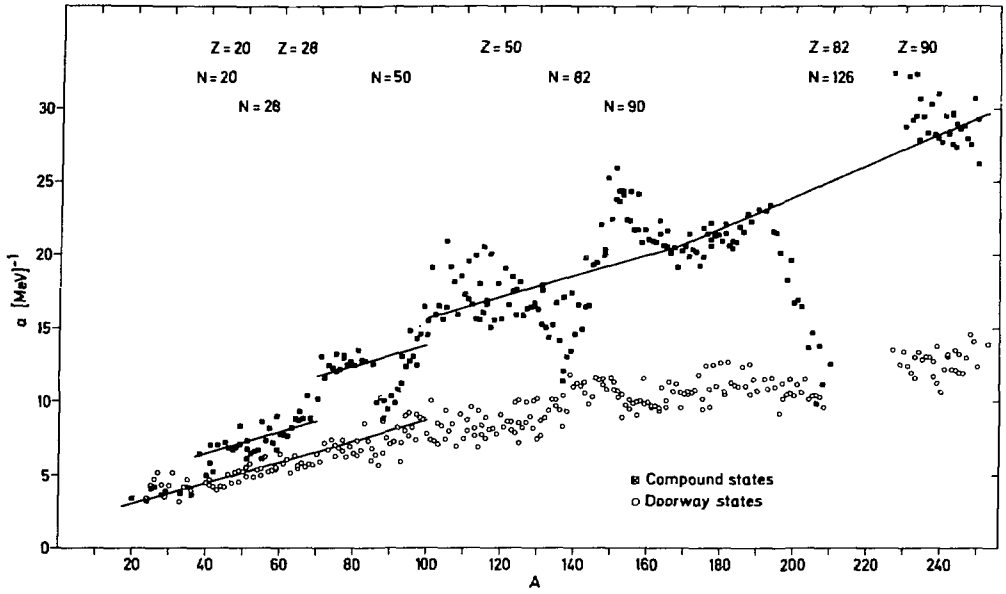

Fig. 7 Level density systematics of compound and doorway states based on pairing energies taken from Ref. [8].

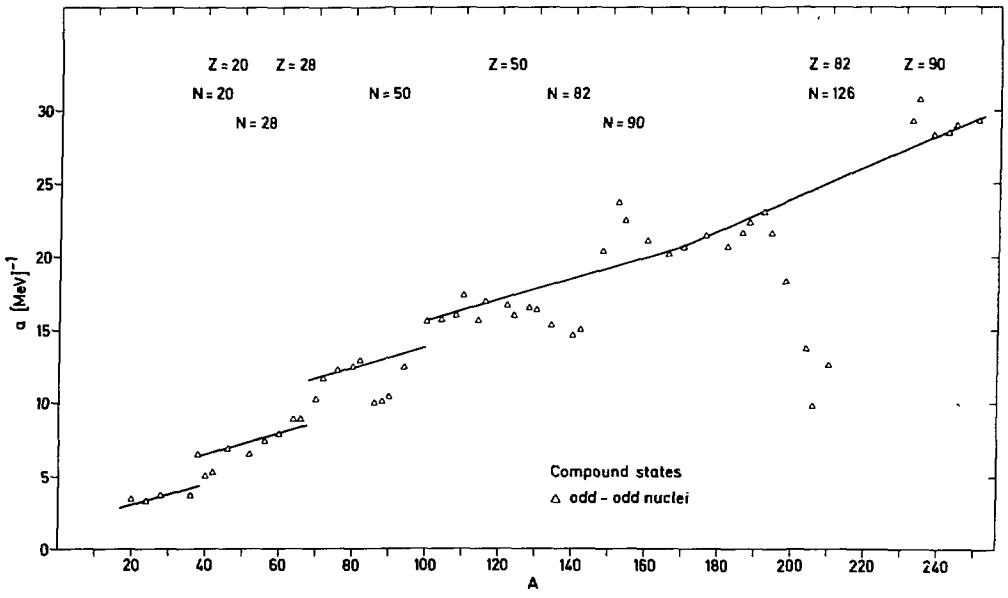

Fig. 8 The level density systematics for odd-odd compound nuclei.

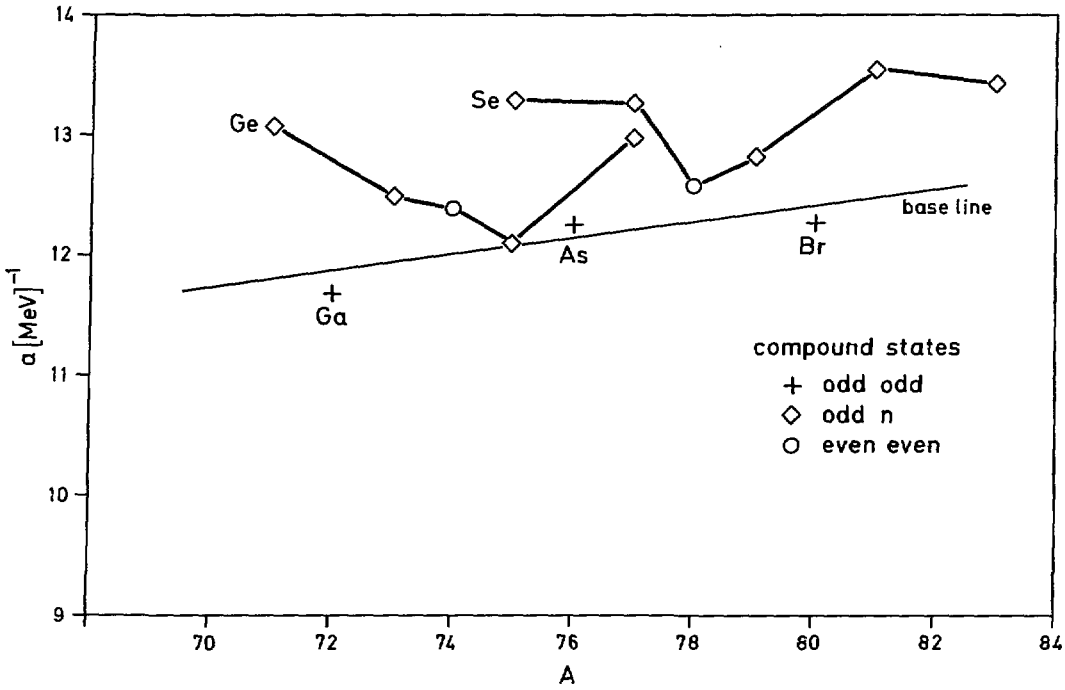

Fig. 9 The level density parameter for nuclei around A ~ 75.

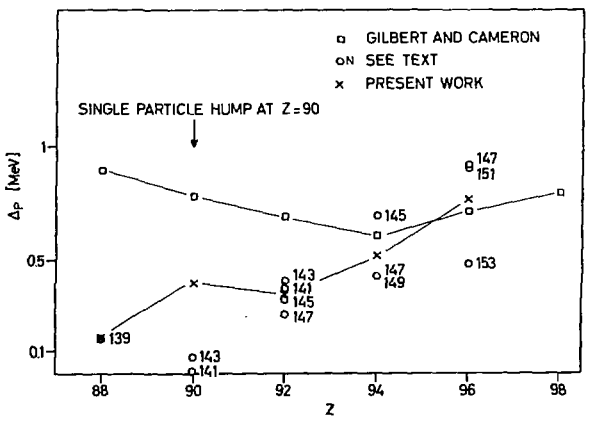

Fig. 10. Proton pairing energy plotted against proton number in the range 220< A < 250.

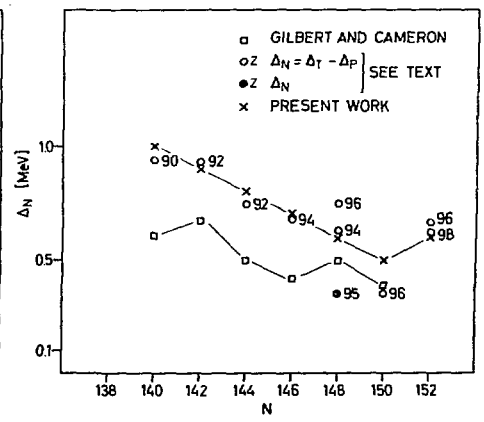

Fig. 11. Neutron pairing energy plotted against neutron number in the range 220 < A < 250.

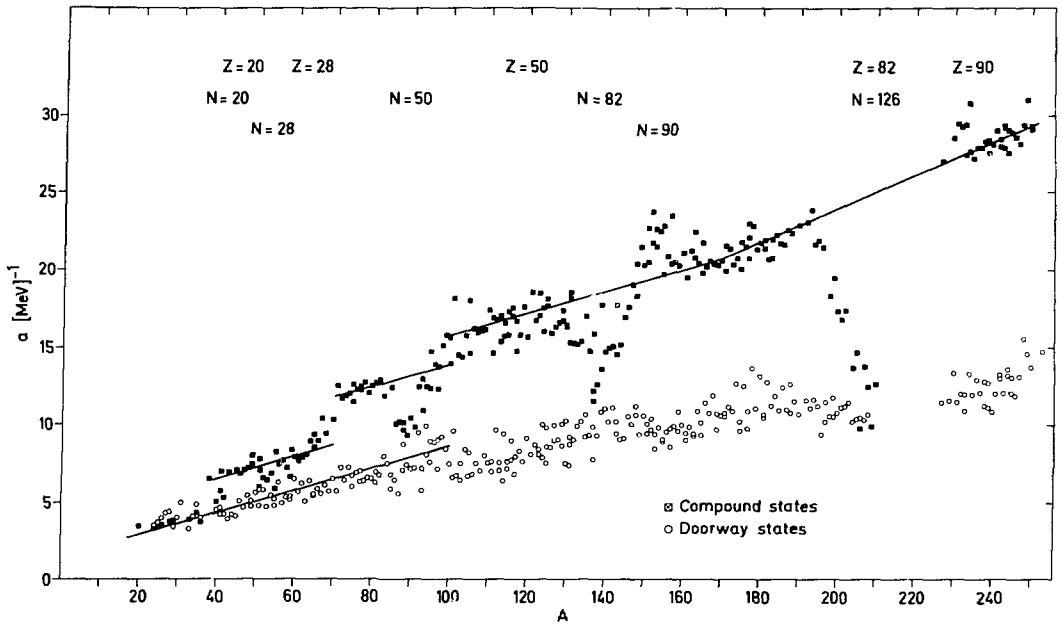

Fig. 12 Level density systematics based on pairing energies defined in Ref. [12].

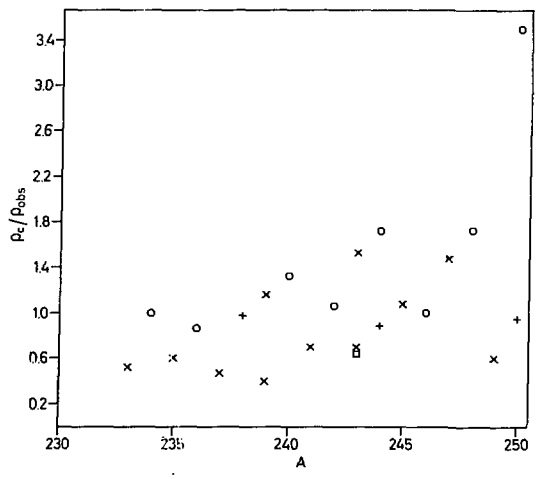

Fig. 13. Ratio of calculated to observed neutron resonance density for actinide nuclei plotted against A. Pairing Δ_G taken from Ref. [8].

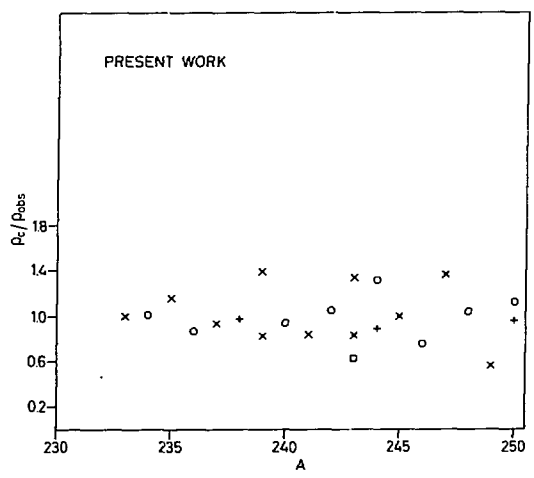

Fig. 14. Ratio of calculated to observed neutron resonance density for acti-nide nuclei plotted against A. Pairing Δ_{Ex} taken from Ref. [12].

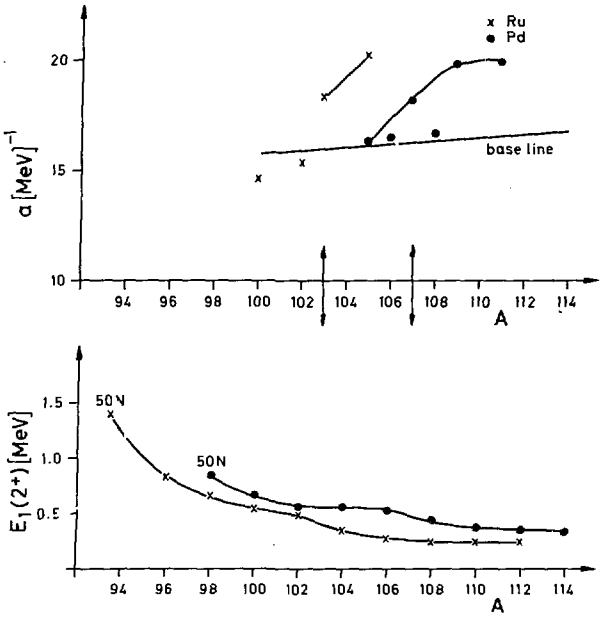

Fig. 15 The level density parameter and the energy of the lowest 2^+ level are plotted in dependence of A in the range $100 < A < 114$.

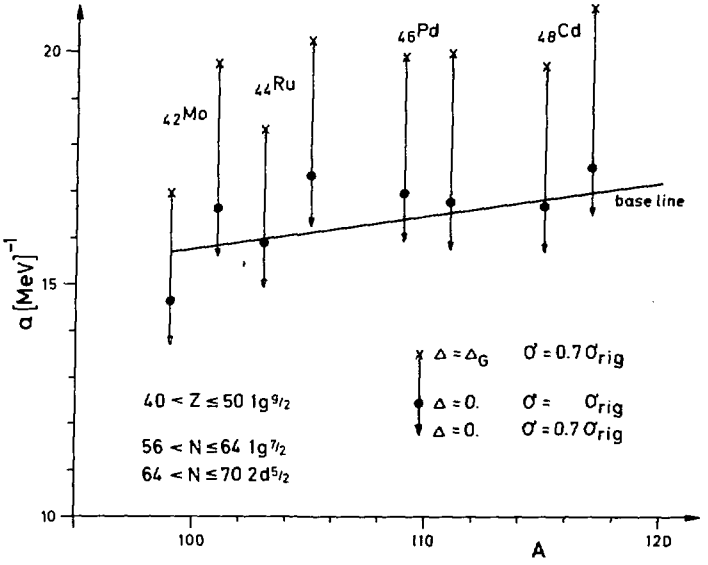

Fig. 16 The level density parameter of the neutron rich nuclei with the strongest deviation from the base line in the range $99 < A < 117$.

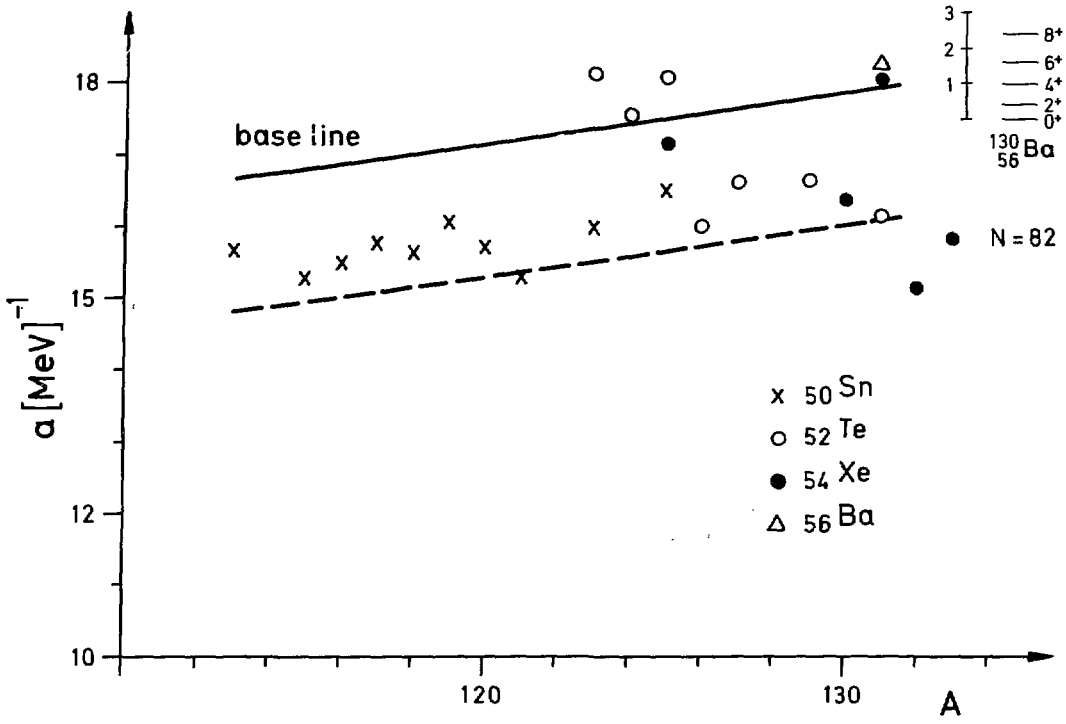

Fig. 17 The level density parameter for nuclei in the range 113 < A < 130.

THE IMPACT OF NUCLEAR LEVEL DENSITY MODELS ON CROSS SECTION CALCULATIONS

E. D. Arthur

Theoretical Division
Los Alamos National Laboratory
Los Alamos, New Mexico 87545

ABSTRACT

The role of different level density formulations in applied Hauser-Feshbach calculations is examined through comparison to varied types of neutron-induced experimental data. Results obtained using two phenomenological models that are widely employed in cross-section calculations, the Gilbert Cameron and back-shifted Fermi-gas models, are compared with each other and to such data. Additionally, results from microscopic level density calculations that use realistic single particle levels are presented. Such calculations provide stringent tests with which the performance of these microscopic models in applied Hauser-Feshbach calculations can be assessed. In the course of such comparisons, experimental data that are particularly sensitive to level density effects are identified. Finally, the question of consistency between state densities occurring in preequilibrium calculations and level densities employed in statistical calculations is addressed. Examples are provided of initial efforts to ensure such consistency in cases where phenomenological density models are used.

INTRODUCTION

Nuclear level densities are an important facet of theoretical calculations that employ the Hauser-Feshbach statistical and preequilibrium models. Since such calculations are used to interpolate or predict nuclear data for applied purposes, reasonable calculational accuracies are required. These accuracies in turn depend to a large degree upon the realistic description of the nuclear level density. Such tasks are complicated by the necessity to know level densities at nuclear excitations or for nuclei where measurements do not exist. Further complications occur because most applied calculations continue to rely upon pheonomenological models developed almost twenty years ago.

This paper examines the most commonly utilized level density models and provides a qualitative assessment of their utility through comparison to several classes of experimental data. Data were selected that provide unique conditions under which these models and their parameters can be tested. These comparisons also include cross sections from calculations that employ microscopic level-density models based on realistic single particle schemes. Such models eliminate simplifying assumptions, such as equidistant level spacing, used in the derivation of closed-form Fermi gas expressions. They also provide the possibility for more realistic extrapolation to unmeasured nuclei or excitation energy regions. They are, however, more complicated to use in nuclear model calculations, and have less flexibility for adjustment in cases where they disagree strongly with experimental data.

Finally, the question of consistency between state densities used in pre-equilibrium calculations and the equivalent level density employed in Hauser-Feshbach models is addressed. Some recent theoretical calculations that represent preliminary attempts to resolve this problem are described.

LEVEL DENSITY MODELS

The majority of theoretical calculations for applied purposes employ phenomenological level-density models, the two most popular being the Gilbert Cameron formalism [1] and the back-shifted Fermi-gas model [2]. The Gilbert-Cameron model dates from 1965 and utilizes a Fermi-gas expression for the level density at higher excitation energies:

$$\rho(E) = \frac{\sqrt{\pi}}{12} \frac{\exp(2\sqrt{aU})}{a^{1/4}U^{5/4}} \frac{1}{\sigma\sqrt{2\pi}} \tag{1}$$

where $U=E-\Delta$ includes empirically determined pairing contributions, Δ. Values of the level density parameter $\underline{a}$ are determined from fitting experimental data for s-wave resonance spacings, $\bar{D}_0$, at the neutron binding energy. Gilbert and Cameron found the systematic behavior of this parameter over a range of atomic masses to be linearly related to shell corrections that they too empirically deduced. The spin cutoff parameter σ is discussed below.

At lower excitation energies, expression (1) does not reproduce cumulative level data or particle emission spectra very well, so instead, a constant temperature expression is used:

$$\rho(E) = (1/T) \exp[(E-E_0)/T] \tag{2}$$

The parameters E_0 and T can be adjusted to reproduce the cumulative number of levels occurring up to a given excitation energy while joining smoothly to the Fermi gas form at some adjustable energy, E_x.

The density of levels of a given angular momentum J (assuming equal contributions from both parities) is then

$$\rho(U,J) = \rho(U)\ (2J+1)\ \exp[-(J+\tfrac{1}{2})^2/2\sigma^2]/2\sigma^2 \quad . \tag{3}$$

The spin cutoff parameter σ has the following systematic behavior:

$$\sigma^2 = 0.0888\ \sqrt{aU}\ A^{2/3} \quad , \tag{4a}$$

where A is the atomic mass. This original Gilbert-Cameron expression has been modified by Reffo [3] to be

$$\sigma^2 = 0.146\ \sqrt{aU}\ A^{2/3} \quad , \tag{4b}$$

which provides a better representation of spin distributions obtained from discrete level information as well as microscopic thermodynamic calculations [3].

The second commonly used formalism is the back-shifted Fermi-gas model proposed by Gadioli and Zetta [4]. This model employs a single Fermi-gas expression for the entire excitation energy range, but treats the fictive ground state position Δ and level-density parameter a as adjustable parameters. Thus,

$$\rho(E) = \frac{1}{12\sigma a^{1/4}\sqrt{2}}\ \frac{\exp[2\sqrt{a(E-\Delta)}]}{(E-\Delta+t)^{5/4}}, \tag{5}$$

where the thermodynamic temperature is defined by

$$E - \Delta = at^2 - t \quad . \tag{6}$$

The level density as a function of J is given by Eq. (3), but in this model, the spin cutoff parameter is related to the rigid body moment of inertia

$$\sigma^2 = I_{rigid}\ t/\hbar^2 \cong 0.015\ A^{5/3}t \quad . \tag{7}$$

The third level density formation considered here is the microscopic Fermi gas model. Its detailed description is not appropriate for this paper (see Refs. 5-7 for such detail), but basically the state density $\omega(E)$ is calculated using realistic sets of single particle levels combined with the grand partition function for a system of interacting fermions. The use of the superconductivity formalism that employs a BCS Hamiltonian [8] allows the inclusion of pairing effects so that, at low excitations, the calculated level

density has roughly a constant temperature energy dependence. At higher energies above the transition point where superconductivity effects disappear, the results return to the Fermi gas form. The model produces state densities and spin cutoff parameters as a function of excitation energy along with energy dependent positive and negative parity ratios. The absence of an analytic form for this model adds a greater degree of complexity to nuclear reaction calculations. Some attempts [9] have been made to circumvent this difficulty through determination of equivalent Fermi gas parameters $\underline{a}$ and $\underline{\Delta}$. These were then employed in Hauser-Feshbach preequilibrium calculations through use of an expression similar to Eq. (3).

Application of these two phenomenological models discussed previously generally requires use of published parameter sets adjusted to reproduce experimental s-wave resonance data (D_0) over a wide mass range. Very complete analyses of such data using the Gilbert-Cameron formalism have been made by Cook et al. [10] to obtain shell and pairing parameter systematics. Their original effort has been updated recently [11] to include new resonance data as well as to incorporate the spin cutoff parameter representation provided by Eq. (4b). The constant temperature parameters and the matching energy E_x can be adjusted to fit discrete level information appropriate to a given calculation. This step is done automatically in several modern Hauser-Feshbach codes [12-14]. If this capability does not exist, then the constant temperature systematics of Gilbert-Cameron or more recent works can be used [15].

A very complete study of the parameters $\underline{a}$ and Δ (and their systematics) for the back-shifted Fermi-gas model was completed by Dilg et al. [2]. These two parameters were adjusted to reproduce simultaneously discrete level and s-wave resonance (D_0) information. Additionally, proton resonance data were employed in some cases. Again, in present-day calculations, some improvement of the model parameters may be achieved through use of up-to-date discrete level information as well as consideration of D_0 data in a restricted mass region pertinent to the problem of interest.

Application of the microscopic level-density model leaves little room for parameter adjustment. In calculations of D_0 values [16,17], the most common practice involves modification of the neutron and proton pairing gaps to optomize agreement to experimental data. Such efforts have a reduced effect around shell closures where the shell gaps are the dominant factors influencing the calculated results. Finally, a judicious choice of single-particle levels appropriate to a given mass region must be made; otherwise striking differences in the calculated density can be obtained [9].

III. COMPARISONS TO DATA

To qualitatively assess the formalisms described in the previous section, calculated cross sections and emission spectra obtained using these models will be compared to a variety of experimental data types. We selected two regions of spherical nuclei for this purpose, one involving the structural materials occurring near the Z = 28 closed shell and the other in the mass 90 region around the N = 50 closed shell. By concentrating on spherical nuclei, we avoid problems (particularly for microscopic calculations) associated with level density enhancements occurring in deformed nuclei that result from

discrete levels built upon rotational or vibrational bandheads [18]. Mass regions around closed shells provide circumstances where level densities fluctuate greatly between nearby nuclei because of such shell effects, and where a plentiful supply of very complete D_0 data exist for several isotopic chains. These conditions can serve as very stringent tests of models or parameter systematics. These two mass regions also have a variety of available experimental data, ranging from neutron and charged-particle emission spectra to isomeric state production cross sections. Furthermore, some nuclei that we examined have large differences between neutron and proton binding energies, a situation that provides some unique illustrations of level-density effects on calculated cross section data.

The mass region encompassing the structural materials is attractive for reasons other than the neutron cross section data available there. It was this region that formed the basis for a rather complete analysis [9] of particle emission spectra using microscopic level density calculations. This study was sensitive to, and examined, regions of the level density at excitations above and below the neutron binding energy. Heretofor many analyses [16,17] employing microscopic level density models concentrated on the region around the binding energy through their comparison to s-wave resonance data to verify such models.

Experimental data exist in this region that span a large range of excitation energies so direct comparisons of level-density calculations can be made. Such a comparison is made in Fig. 1 for one such case, ^{60}Ni. The three curves represent the level-density models described earlier. In particular, the microscopic level-density calculations were made using the Seeger-Perischo single-particle levels [19], along with pairing energy values (at zero excitation) equal to those of Gilbert and Cameron [1]. All three models reproduce the data reasonably well, although the microscopic level-density results are perhaps more impressive considering the lack of adjustable parameters. There are differences in the shape predicted by these models, as illustrated in Fig. 2. The comparison shows the ratio of the Gilbert-Cameron and back-shifted Fermi-gas model results with those from the microscopic calculation for ^{60}Ni. All densities were normalized to each other around the neutron binding energy (~ 11 MeV). Of the two phenomenolocial models, the shape of the back-shifted Fermi-gas results lies closer to the microscopic values. The difference in the low energy shape of the Gilbert-Cameron results can be attributed primarily to the use of the constant temperature expression in this model.

Further tests of these three level-density models appear in Fig. 3, where ratios of calculated to experimental D_0 values [20] are illustrated for several isotopic chains in this mass region. For the two phenomenological models, published parameter systematics [2,10] were used, whereas microscopic calculations were made using the Seeger-Perischo levels. This comparison illustrates a situation one often encounters in multistep Hauser-Feshbach calculations of reaction paths that involve several members of an isotopic chain. If one has available such D_0 information and uses a phenomenological level density expression within their nuclear model calculations, then the level-density parameters can be adjusted locally to optimally reproduce such results. The comparison of Fig. 3 also indicates the predictive capability of microscopic calculations since agreement to within a factor of two or three generally occurs.

To place these level density models under more scrutiny, we examined in detail a series of neutron-induced reactions on ^{65}Cu with comparison to several types of cross-section data. In Fig. 4 the neutron emission spectrum calculated for 8.5 MeV incident neutrons is compared with the data of Kinney et al. [21]. Such data were chosen for comparison because, at these energies, preequilibrium contributions that can camouflage level-density effects are at a minimum. Secondly, for inelastic scattering reactions that dominate, regions of excitation energy are reached in the target nucleus where the description of the level density is important, particularly for an odd-A nucleus such as ^{65}Cu. The ^{65}Cu nucleus is also interesting owing to a lack of experimental resonance information, which causes a reliance upon the predictive capability of the level-density model. In the application of the Gilbert-Cameron expressions, one is constrained by discrete level information available at low excitation energies. At higher excitations, one must rely upon parameter systematics to determine the appropriate value of $\underline{a}$ in expression (1). Similarly, for the back-shifted Fermi-gas model, discrete level information provides low-energy constraints. At higher excitation energies, Dilg et al. [2] determined the level density parameter $\underline{a}$ through use of proton resonance data. For the microscopic calculations shown, the Seeger-Perischo levels were again used.

At first glance the data in Fig. 4 appears to best be reproduced using the back-shifted Fermi-gas model, except for the disagreement for emitted neutron energies around 1.5 MeV. These neutrons correspond to excitations of about 7 MeV in ^{65}Cu and the underprediction there is symptomatic of problems encountered for this nucleus at higher excitation energies with the back-shifted Fermi-gas results. Further evidence for this discrepancy appears in Fig. 5 in which comparisons are made with the proton emission spectrum measured [22] for 14.8-MeV neutron reactions on ^{65}Cu. Such spectra are comprised of protons from three primary sources: (a) (n,np) and (n,pn) reactions that account for most of the low-energy proton emission; and (b) (n,p) reactions that produce higher-energy protons. In this comparison, a sizeable overprediction in calculated results occurs because of the lower level density values for ^{65}Cu (relative to the two other models) produced using the back-shifted Fermi-gas results. This problem can be identified because the (n,p), (n,np+n,pn) and (n,2n) reaction channels produce residual nuclei (^{65}Ni, ^{64}Ni, ^{64}Cu), where D_0 information is available to constrain the level density. Additionally, the (n,np), (npn), and (n,2n) reactions populate, in appreciable amounts, discrete levels in their respective residual nuclei, so that level density effects are reduced. The failure to predict correctly the ^{65}Cu level density results in an underprediction of competition from (n,n'γ) processes. This, in turn, causes the overprediction in proton emission, as shown occurring from (n,p) and (n,np) processes. Figure 6 compares explicitly the level densities calculated for ^{65}Cu using the three models discussed here. The results agree reasonably well at lower excitation energies. At the higher energies that directly impact the calculated proton emission spectrum, the level-density values diverge with a sizeable underprediction occurring for the back-shifted Fermi-gas results. This problem appears to be related to the small value for the Fermi-gas parameter $\underline{a}$ derived for ^{65}Cu by Dilg et al. [2] using proton resonance data [23].

Similar problems occur in the calculation of proton emission spectra induced by 14.8-MeV neutrons on ^{63}Cu, as shown in Fig. 7. In this case, significant contributions originate from (n,np) reactions since the proton binding energy in the ^{63}Cu compound nucleus is 5 MeV lower than that for neutrons. Both phenomenological level density models predict lower ^{63}Cu level densities than does the microscopic model, although values for the other residual nuclei are equivalent. In the case of the Gilbert-Cameron model, the lower ^{63}Cu density produces less (n,nγ) competition so that increased (n,np) emission takes place. The back-shifted Fermi gas model predicts the lowest ^{63}Cu density of the three models and leads to larger (n,p) and (n,pn) contributions. Neutron emission from the first compound nucleus is reduced so that a smaller (n,np) contribution occurs. Again, for this model, the smaller ^{63}Cu level density originates from the a value deduced from proton resonance data.

As was the case for the structural materials, the A = 90 mass region encompassing the N = 50 closed shell provides several unique conditions for level-density tests and assessments. Plentiful s-wave resonance spacing data are available for several isotopic chains. Discrete levels are also known up to relatively high excitation energies so that the magnitude and energy dependence of spin cutoff parameters can be deduced and compared to theoretical predictions. Finally, the existence of measurable isomeric levels provides further experimental data with which to examine the spin cutoff parameter computed using various level-density models.

The value of the spin cutoff parameter σ and particularly its energy dependence can have significant effects upon calculated quantities in instances where sizable differences exist between spin values occurring in competing reaction channels. Reffo [3] illustrated the importance of the assumed energy dependence of σ on calculated $^{100}Mo(n,\gamma)$ cross sections. His results appear in Fig. 8a. The solid curve was obtained from calculations that assume an energy dependence of σ^2 given by the solid curve in Fig. 8b. The cross section represented by the dashed curve was calculated for the assumption of a constant σ^2 below the energy E_x shown in Fig. 8b. This assumption produces a spin distribution peaked at $J \cong 5$, while the linear extrapolation produces a most probable spin of $J \cong 1.5$. Since the target spin is 0 and, at low energies, the target spin distribution is peaked at lower values, the wider spin distribution produced by the constant σ^2 assumption decreases slightly the inelastic competition that mainly populates levels having lower spins. The small change in the inelastic channel is accompanied by a large effect in the capture as seen in Fig. 8a.

A more direct determination of σ and its energy dependence can be obtained through use of discrete level spins and a σ^2_{LEVELS} obtained through the maximum likelihood estimator:

$$\sigma^2_{LEVELS} = \frac{1}{2N} \sum_{i=1}^{N} (J_i + \frac{1}{2})^2 \quad . \tag{8}$$

Such results are shown by the histogram in Fig. 9 for ^{98}Mo. The curves labeled 1 and 2 represent σ values obtained for the Gilbert-Cameron model

(Expression 4a) and the back-shifted Fermi-gas model (Expression 7). Also shown by Curve 3 are the microscopic level density results for σ. In this case (as with others in this mass region), microscopic calculations were made using the Seeger-Howard single particle levels. [24] The Gilbert-Cameron expression underpredicts the magnitude of σ, while the other models reproduce the data in a better fashion. The microscopic model provides the best agreement of theory with the discrete level data. A significant improvement occurs when Reffo's expression for σ^2 is used [Eq. (4b)], the results of which are represented by the curve labeled 4.

Ratios of cross sections for ground to metastable state production are often used to deduce information relating to spin cutoff parameters. To further test the effect of spin cutoff parameters in cross section calculations, we have calculated the m/g ratios populated in the $^{89}Y(n,\gamma)^{90}Y$ and $^{90}Zr(n,p)^{90}Y$ reactions. The calculations were made using a detailed gamma-ray cascade model [13,25] that allowed deexcitation through E1, M1, and E2 transitions. Values of the ^{90}Y metastable to ground state ratios populated in the $^{89}Y(n,\gamma)$ reaction are compared with the data of Grench [26] in Fig. 10. The Gilbert-Cameron results fit these data better than the results of the other two models which produce m/g ratios that are about 20% higher. The spin cutoff parameter from the Gilbert-Cameron expression also agrees with the result of $\sigma \cong 3$-4 deduced by Grench et al. [26], using cruder models for analysis. Figure 11 illustrates the ^{90}Y m/g ratio populated in the reaction $^{90}Zr(n,p)^{90}Y$. The quality of the experimental data [27] is poorer, but the trends in calculated results are similar to those shown in Fig. 10. Again, calculations using the Gilbert-Cameron spin cutoff parameters reproduce these data better than the two other models. This result seems inconsistent with our conclusions and those of others [28] who find an underprediction of the spin cutoff parameter in this mass region when Eq. (4a) is used. However, Fig. 12 shows that the spin distribution obtained by examining ^{90}Y discrete level information up to E_x=2.5 MeV is better fit by the Gilbert-Cameron results. For spin populations in the ^{90}Y residual nucleus, these three data types appear to be consistent in the magnitude of the deduced spin cutoff parameter.

Figure 13 again returns to the use of measured proton emission spectra to illustrate sensitivities to level-density models and parameters. The experimental proton emission spectrum [29] produced by 14.8-MeV neutrons on ^{90}Zr is shown. For the ^{90}Zr compound system, the proton binding energy is about 3 MeV less than that of the neutrons, so that a sizable amount of the (n,np) reaction occurs. Such (n,np) spectral contributions are sensitive to the level density used to describe the ^{90}Zr target nucleus. All of the calculations shown employ the Gilbert-Cameron formalism; however, the Fermi-gas parameter values for ^{90}Zr have been varied by ± 10% to illustrate the effect on the calculated spectrum. Since the ^{90}Zr level density cannot be normalized to experimental D_0 values, the parameters must be deduced from their systematic behavior, and these uncertainties are probably reasonable. Deviations of 30% or more are produced in portions of the calculated spectrum as a result of this change. When the ^{90}Zr level density is reduced, proton production increases mainly due to larger (n,np) contributions. This at first seems inconsistent because this level-density change should produce smaller amounts of neutron emission to populate the ^{90}Zr residual nucleus in the first stage of the (n,np) process. However, (n,np) reactions are enhanced because of less competition

from (n,n'γ) processes. Conversely, a larger level density for ^{90}Zr leads to greater neutron emission to populate the ^{90}Zr residual nucleus. However, the increased (n,n'γ) competition results in a reduction of the calculated (n,np) cross section. While such level-density effects are readily apparent in this comparison with proton emission data, there is little discernable effect on other channels, such as the ^{90}Zr(n,2n) reaction shown in Fig. 14.

Level-density differences that occur between nearby nuclei can cause deviations from their systematic behavior for other types of cross section data. Such an example appears in Fig. 15 where calculated gamma-ray production spectra [30] produced by 6.5-MeV neutron interactions with natural tantalum and tungsten are compared. The significant differences in the portions of the gamma-ray spectra above 2 MeV for these materials arises primarily from level-density effects, as illustrated in Fig. 16. Here the cumulative number of low-lying levels for ^{181}Ta and ^{182}W is shown. The odd-odd ^{181}Ta nucleus (which constitutes 100% of natural tantalum) has a significantly higher level density than does ^{182}W or the other even-even tungsten isotopes that make up most of elemental tungsten. At this incident energy, the great majority of the gamma-production spectrum is made up of contributions from (n,n'γ) deexcitation of the continuum region of these target nuclei. Thus, level densities that accurately describe the excitation energy region from 1 to 6 MeV are necessary to produce valid calculational results.

NUCLEAR DENSITIES IN PREEQUILIBRIUM AND STATISTICAL MODEL CALCULATIONS

This paper has been explicitly concerned with the characterization and effect of nuclear level densities as they appear in Hauser-Feshbach statistical model calculations. However, some of the previous examples shown and many of the calculations performed for applied purposes involve preequilibrium models used in conjunction with such Hauser-Feshbach methods. Until recently, there has been little concern for consistency between state densities involved in the calculation of emission rates in preequilibrium calculations and level densities used in statistical models.

Earlier we showed the general reliance in Hauser-Feshbach codes upon phenomenological level density forms, with parameters adjusted to reproduce experimental data or determined from the behavior of their systematics. In the master equation exciton model, one of the most widely used preequilibrium formalisms for applied calculations, the state density for a system of excited particles p and holes h is given by [31]:

$$\omega(p,h,E) = \frac{g(gE)^{p+h-1}}{p!h!(p+h-1)!} \quad , \tag{9}$$

where g is the density of uniformly spaced single particle levels. In most such preequilibrium calculations, g has the value A/13(MeV^{-1}) where A is the atomic mass. To obtain an expression equivalent to the Fermi-gas level density [(Eq. (1)], a sum must be made over particle-hole pairs so that [32],

$$\rho(U) = \sum_p \frac{1}{\sqrt{2\pi}\,\sigma}\, \omega(p-1,h,U) \quad . \tag{10}$$

Fu [32] has compared level densities for ^{63}Cu calculated using the Gilbert-Cameron formula [Eq. (1)] to values obtained using Eq. (10) above. Figure 17 shows the results. The curve labeled 1 was calculated using Eq. (10). Curve 2 is based on the Gilbert-Cameron formalism. The disagreement between these two curves is symptomatic of the inconsistency that exists between state densities used in preequilibrium models and level densities occurring in Hauser-Feshbach calculations. Fu has produced an improved form for the preequilibrium state density through incorporation of pairing corrections that depend upon the particle-hole numbers of the states involved. Inclusion of such pairing effects improves the agreement of Eq. (10) with the Gilbert-Cameron results, as shown by curve 3 in Fig. 17.

Another attempt to unify the level density description in preequilibrium and Hauser-Feshbach models has been made by Akkermann et al. [33] They modified the state density constants in the initial compound nucleus and residual nuclei, g_c and g_r, respectively, to be more consistent with the behavior of the Fermi-gas parameter a in the Gilbert-Cameron model through the relationship $g = 6a/\pi^2$. Large and unsatisfactory preequilibrium contributions were obtained as a result of this change because of the sensitivity of the preequilibrium transition rates to g_c. Phenomenological determinations [34] of the form of the square of the empirical matrix element of residual interactions, M^2 generally assume $g_c = A/13$. For the change $g_c = 6a/\pi^2$ to be made, new systematics would have to be developed. Instead, Akkermann et al. chose to keep g_c equal to its A/13 value and adjust the state density parameter g_r for each residual nucleus.

The principal emphasis for the prequilibrium model work in Ref. [33] was related to fits obtained to continuum angular distribution data [35] induced by 14 MeV neutrons. In particular, the comparison of experimental and calculated first order Legendre coefficients for neutrons having secondary energies between 6 and 10 MeV was an important facet of this paper. Figure 18 shows the effect upon the fit to such f_1 data after the g_r changes described above were made.

SUMMARY AND CONCLUSIONS

The two major level density models used in applied theoretical calculations have been compared to each other and to experimental data in the A = 60 and A = 90 mass regions. Additionally, results from microscopic level density calculations were included in these comparisons. We provided several examples in which level densities needed for nuclei lacking s-wave resonance data had a significant impact on calculated quantities. Analysis of particle emission spectra, particularly recent results for proton emission, could provide qualitative information needed to adjust Fermi gas parameters.

We subjected microscopic level densities to more severe tests than had generally occurred in previous comparisons to D_0 data. Again, analysis of

emission spectra places stringent constraints on the densities predicted by such models at excitations above and below the neutron binding energy. We found that reasonably good agreement with measured data could be obtained using such microscopic models, although their lack of sensitivity to easily adjustable parameters could possibly cause problems in their general application. Certainly more calculations of this type should be included in nuclear model efforts to further test them, as well as to develop improved systematics.

The lack of consistency between density expressions and results obtained in preequilibrium and Hauser-Feshbach calculations is a significant problem in current nuclear model calculations. Some initial attempts to resolve these discrepancies show promise, but more work is needed to solve the problem in the case of phenomenological density expressions. Furthermore, an even greater effort will probably be needed to achieve consistency with Hauser-Feshbach calculations that employ microscopically calculated state densities.

REFERENCES

1. A. GILBERT and A. G. W. CAMERON, Can. J. of Physics, 43, 1446 (1965).

2. W. DILG, W. SCHANTL, H. VONACH, and M. UHL, Nucl. Phys. A, 217, (1973).

3. G. REFFO, "Parameter Systematics for Statistical Theory Calculations of Neutron Reaction Cross Sections," in Nuclear Theory for Applications, Trieste, International Atomic Energy Agency Report IAEA-SMR-43 (1079), p. 205.

4. E. GADIOLI and L. ZETTA, Phys. Rev., 167, 1016 (1968).

5. J. R. HUIZENGA and L. G. MORETTO, Ann. Rev. Nucl. Sci., 22, 427 (1972).

6. L. G. MORETTO, Nucl. Phys. A, 185, 145 (1972).

7. S. M. GRIMES, "Limits of Thermodynamic Models for Nuclear Level Densities," in Theory and Applications of Moment Methods in Many Fermion Systems, Plenum Publishing Corp. (1980), p. 17.

8. J. BARDEEN, L. N. COOPER, and J. R. SCHRIEFFER, Phys. Rev., 108, 1175 (1957).

9. S. M. GRIMES, J. D. ANDERSON, J. W. MCCLURE, B. A. POHL, and C. WONG, Phys. Rev. C, 10, 2373 (1974).

10. J. L. COOK, H. FERGUSON, A. R. DE L. MUSGROVE, Aust. J. Phys., 20, 477 (1967).

11. J. L. COOK and E. K. ROSE, "Valency Effects in Compound Nucleus Level Spacings," Proc. Conf. Nuclear Data for Science and Technology, Antwerp, Belgium (September 6-10, 1982), to be published.

12. P. G. YOUNG and E. D. ARTHUR, "GNASH: A Preequilibrium Statistical Nuclear-Model Code for Calculation of Cross Sections and Emission Spectra," Los Alamos National Laboratory report LA-6947 (1977).

13. M. UHL and B. STROHMAIER, "STAPRE - A Computer Code for Particle Induced Activation Cross Sections and Related Quantities," ISPRA report, IRK-78/02 (1976).

14. C. L. DUNFORD, "A Unified Model for Analysis of Compound Nucleus Reactions," Atomics International report AI-AEC-12931 (1970).

15. S. IIJIMA, T. AOKI, M. SASAKI, "Study of Systematics and the Determination of Level Density Parameters of Fission Product Nuclei," Nippon Atomic Industry Group preprint (October 1982).

16. J. R. HUIZENGA, A. N. BEHKAMI, J. S. SVENTEK, R. W. ATCHER, Nucl. Phys. A, 223, 577 (1974).

17. V. BENZI, G. MAINO, E. MENAPACE, and A. VENTURA, "BCS Level Density Calculations and a Consistent Estimate of Radiative Widths by Means of a Thermodynamic Model," in Proc. Specialists' Mtg. on Neutron Cross Sections of Fission Product Nuclei, Bologna (1979), NEANDC(E) 209"L", p. 215.

18. S. BJORNHOLM, "Role of Symmetry of the Nuclear Shape in Rotational Contributions to Nuclear Level Densities," in Proc. Physics and Chemistry of Fission, Rochester, IAEA-SM-174 (1974), p. 367.

19. P. A. SEEGER and R. C. PERISCHO, "A Model-Based Mass Law and a Table of Binding Energies," Los Alamos Scientific Laboratory report LA-3751 (1967).

20. S. F. MUGHABGHAB, M. DIVADEENAM, N. E. HOLDEN, Neutron Resonance Parameters and Thermal Cross Sections-Part A, Academic Press, New York (1981).

21. W. E. KINNEY and F. G. PEREY, "^{63}Cu and ^{65}Cu Neutron Elastic and Inelastic Scattering Cross Sections from 5.5 to 8.5 MeV," Oak Ridge National Laboratory report, ORNL-4908 (1974).

22. S. M. GRIMES, R. C. HAIGHT, K. R. ALVAR, H. H. BARSCHALL, and R. R. BORCHERS, Phys. Rev. C 19, 2127 (1979).

23. J. BROWNE, H. W. NEWSON, E. G. BILPUCH, and G. E. MITCHELL, Nucl. Phys., A, 153, 481 (1970).

24. P. A. SEEGER and W. M. HOWARD, Nucl. Phys A, 238, 491 (1975).

25. M. UHL, Physica Austriaca, 31, 245 (1970).

26. H. A. GRENCH, K. L. COOP, H. O. MENLOVE, and F. J. VAUGHN, Nucl. Phys. A, 94, 157 (167).

27. E. D. ARTHUR, "Calculation of Neutron Cross Sections on Isotopes of Yttrium and Zirconium," Los Alamos Scientific Laboratory report LA-7789-MS (1979).

28. D. G. GARDNER, "Recent Developments in Nuclear Reaction Theories and Calculations," in Proc. Symposium on Neutron Cross Sections from 10 to 50 MeV (1980), BNL-NCS-51234, Vol. 2, p. 641.

29. R. C. HAIGHT, S. M. GRIMES, R. G. JOHNSON, and H. H. BARSCHALL, Phys. Rev. C, 23, 700 (1981).

30. E. D. ARTHUR, "Gamma-Ray Production Cross Section Calculations for the Tungsten Evaluation," in Applied Nuclear Data Research and Development October 1-December 31, 1980, C. I. Baxman and P. G. Young, Eds., Los Alamos Scientific Laboratory report LA-8757-PR (1981), P. 3.

31. J. J. GRIFFIN, Phys. Rev. Lett 17, 478 (1966).

32. C. Y. FU, "A Consistent Nuclear Model for Compound and Precompound Reactions with Conservation of Angular Momentum," Oak Ridge National Laboratory report ORNL/TM-7042 (1980).

33. J. M. AKKERMANN, H. GRUPPELAAR, G. REFFO, Phys. Rev. C, 22, 73 (1980).

34. C. KALBACH, Z. fur Phys. A 287, 319 (1978).

35. D. HERMSDORF, A. MEISTER, S. SASSONOFF, D. SEELIGER, K. SEIDEL, and F. SHAHIN, "Differentielle Neutronenemissionsquerschnitte bei 14,6 MeV Einschussenergie," Dresden Report ZfK-277 (1974).

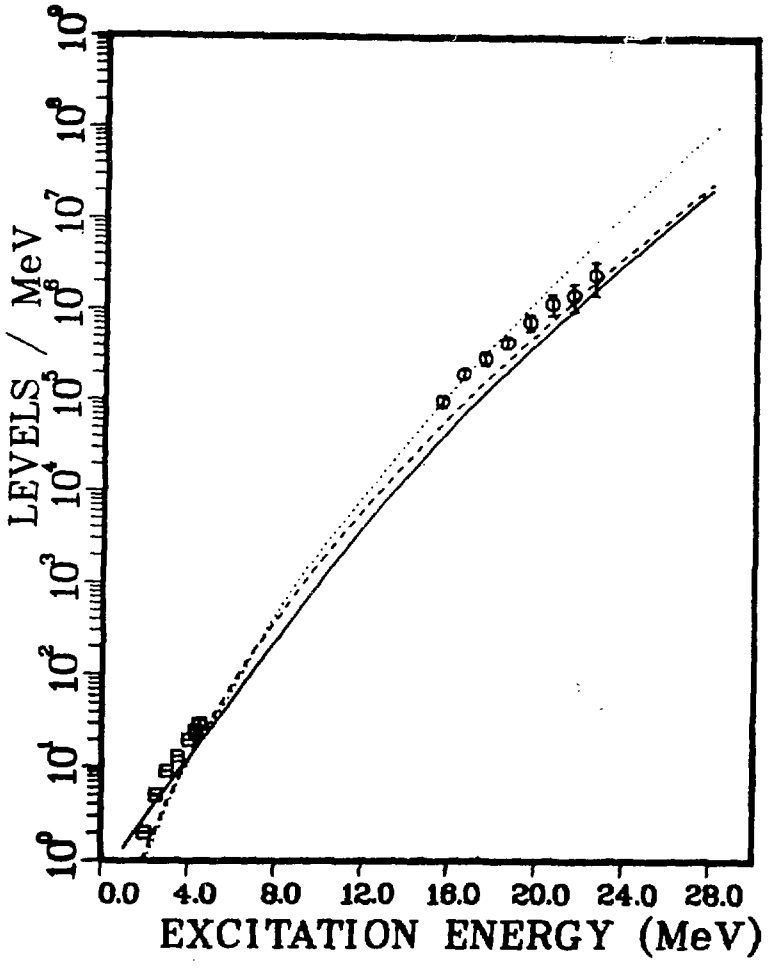

Fig. 1. Comparison of the nuclear level density calculated using the three models described in the text to experimental data for ^{60}Ni. The solid curve was calculated using the Gilbert-Cameron model; the dashed curve, the back-shifted Fermi-gas model; and the dotted curve, microscopic calculations.

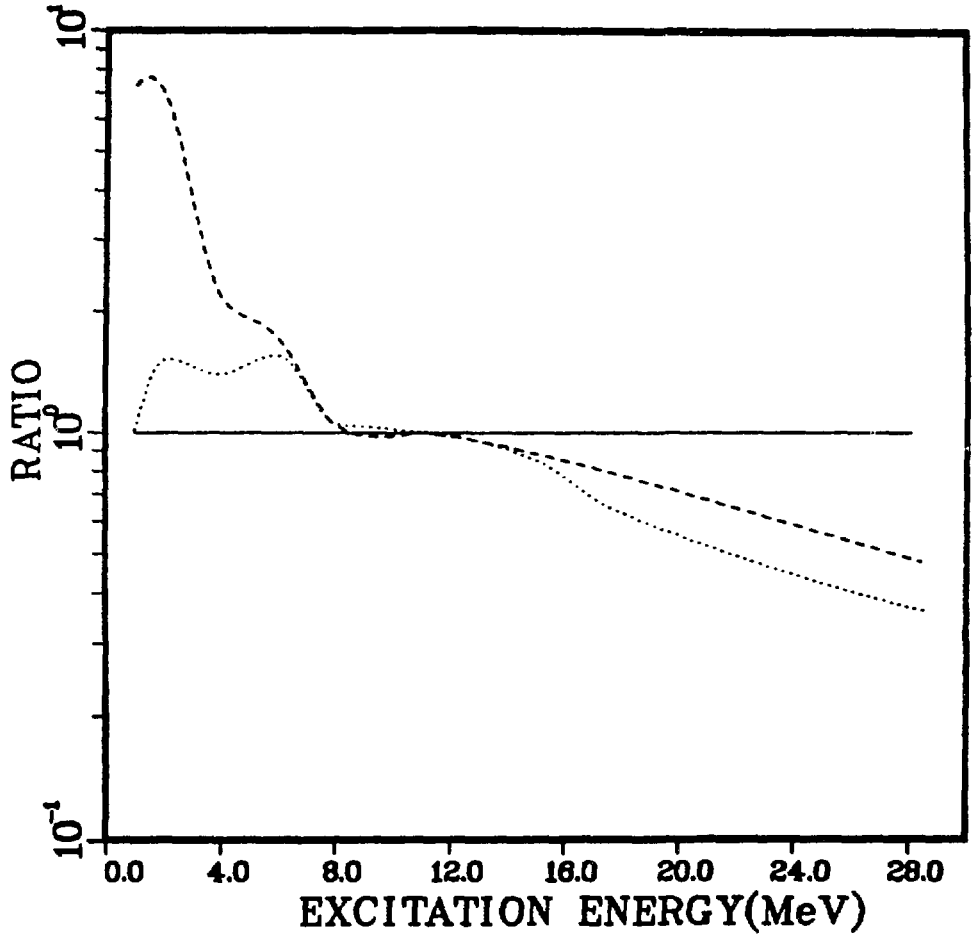

Fig. 2. Level densities calculated using the two phenomenological models are compared to results from microscopic calculations for ^{60}Ni. All calculations were normalized at 11 MeV. The dashed curve represents the Gilbert-Cameron results, while the dotted curve was calculated using the back-shifted Fermi gas model.

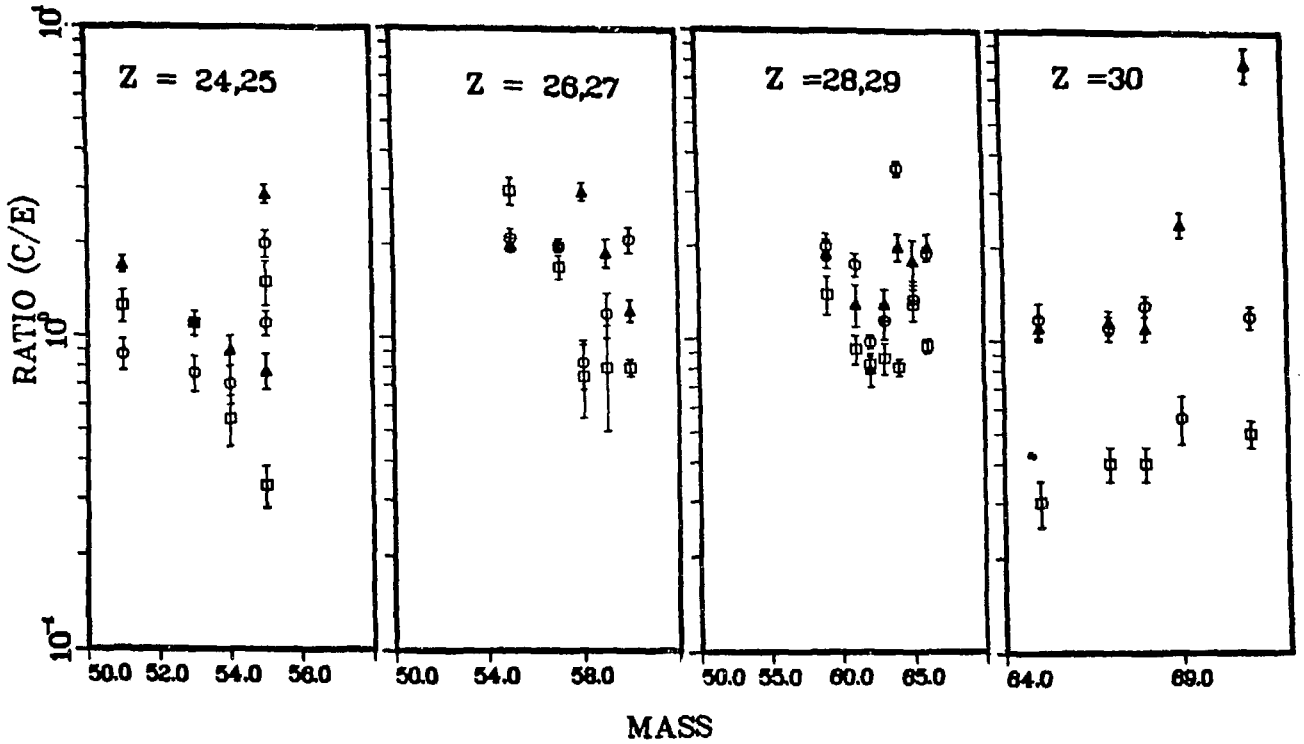

Fig. 3. The ratio of calculated to experimental values for the s-wave neutron resonance spacing, D_0, are presented for several isotopic chains around A=60. The squares represent the microscopic results; the circles are the Gilbert-Cameron results; and the trianges the back-shifted Fermi-gas results.

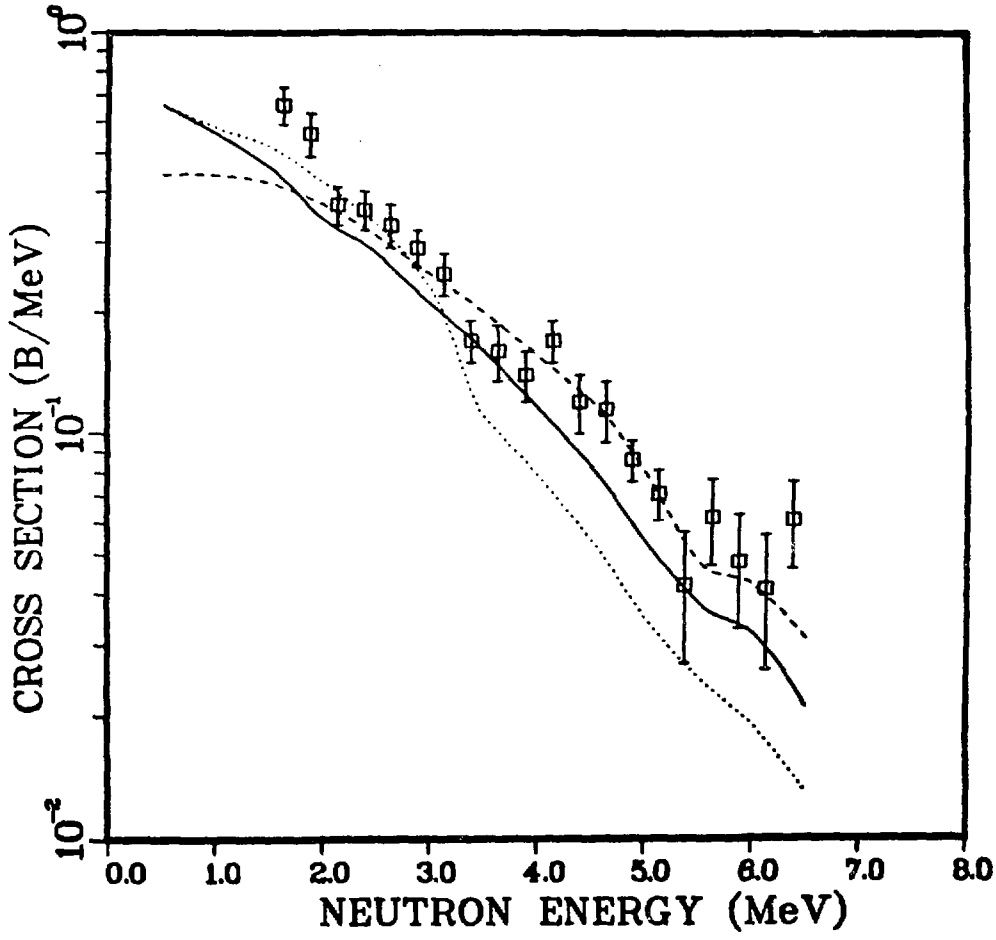

Fig. 4. Calculated neutron emission spectra for 8.5-MeV neutron interactions with ^{65}Cu are compared to the data of Kinney et al. [21]. The solid curve was calculated using the Gilbert-Cameron model; the dashed curve, the back-shifted Fermi-gas model; and the dotted curve, the microscopic model.

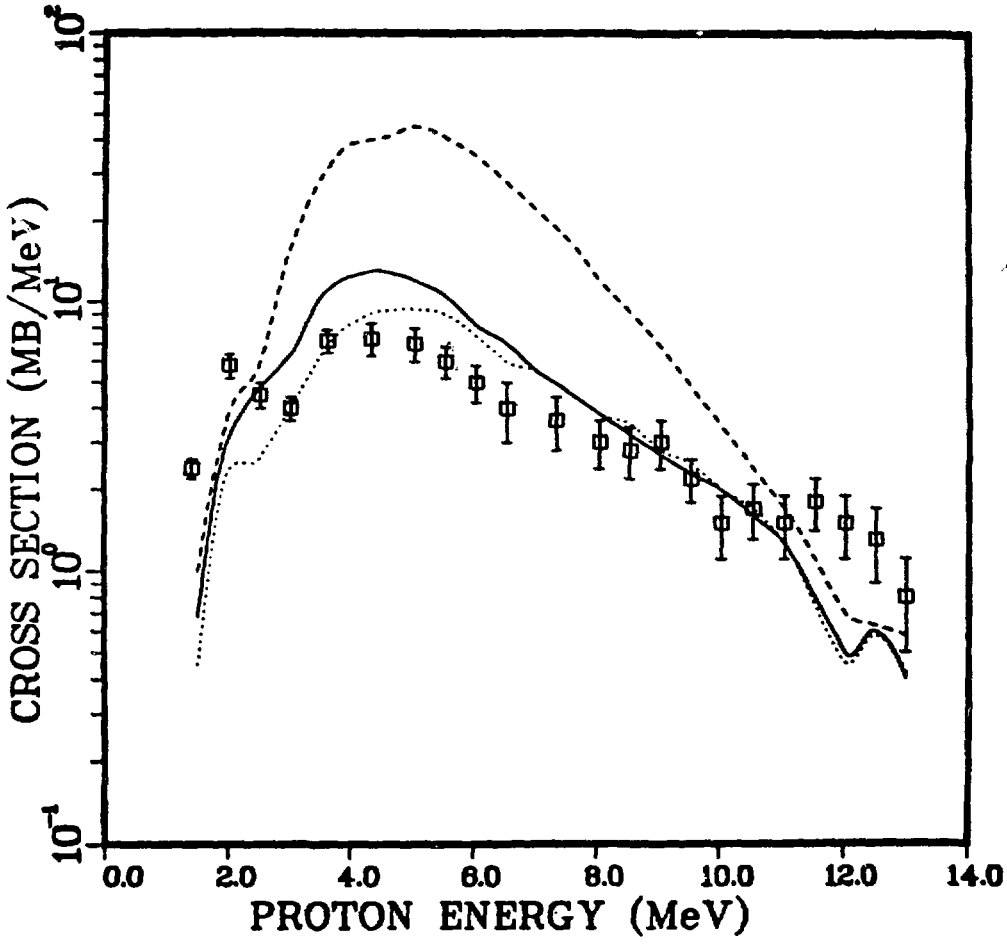

Fig. 5. The calculated proton emission spectra induced by 14.8-MeV neutrons on ^{65}Cu are compared to the data of Grimes et al. [22]. The level-density models associated with each curve are identified in Fig. 4.

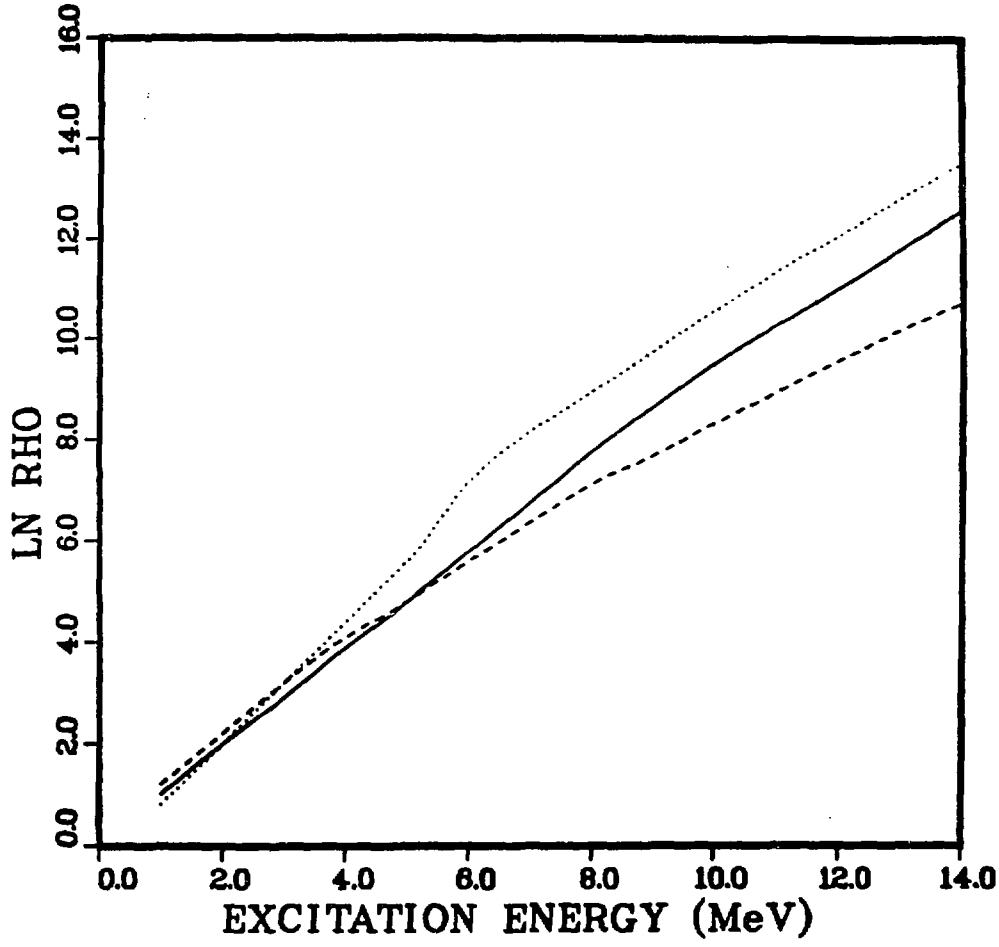

Fig. 6. Calculated level densities for ^{65}Cu. The natural logarithm is shown and the curves are identified as in Fig. 4.

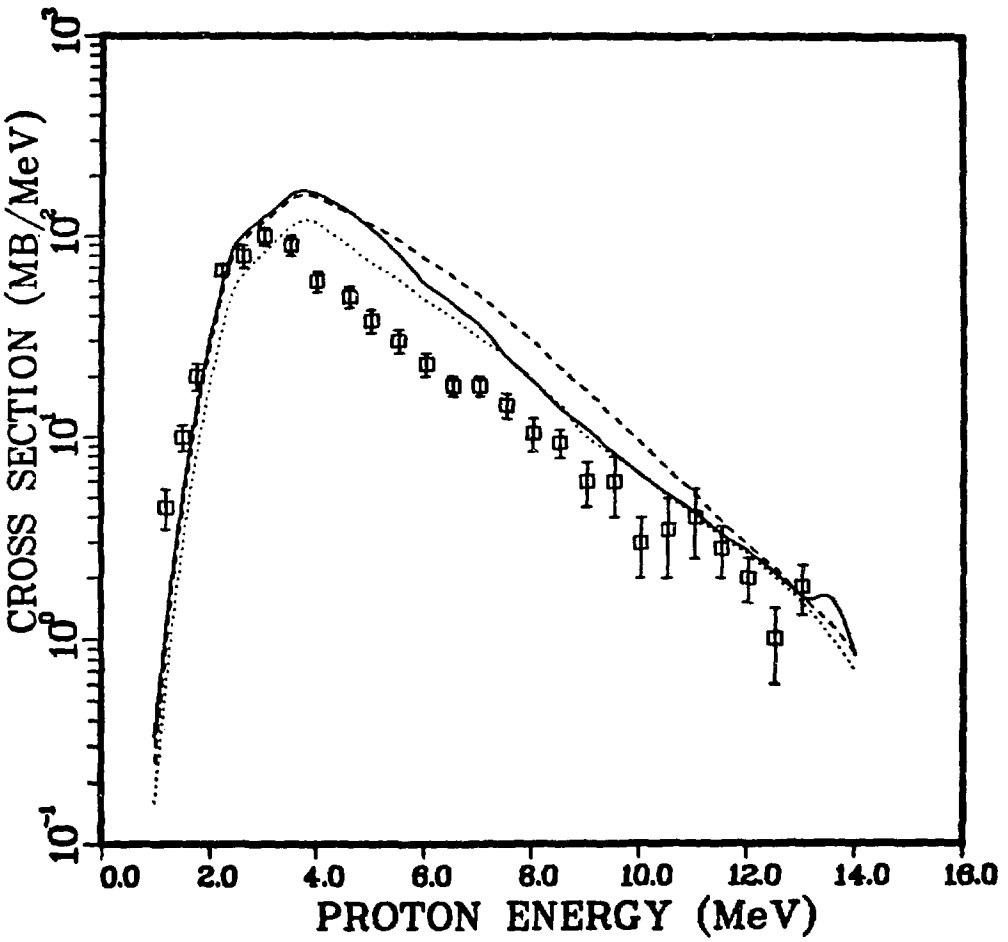

Fig. 7. Calculated proton emission spectra resulting from 14.8-MeV neutrons on ^{63}Cu are compared to the Grimes et al. data [22]. The curves are identified in Fig. 4.

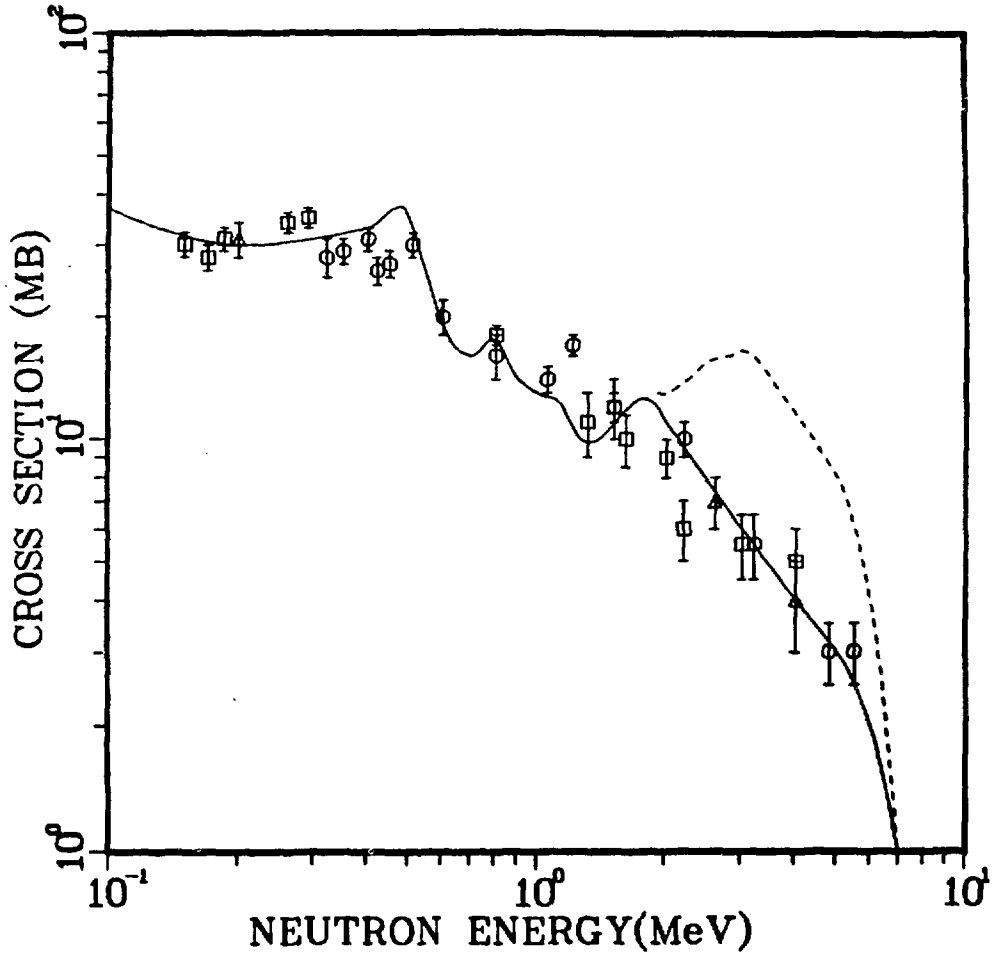

Fig. 8a. The effects of the spin cutoff parameter on the calculated $^{100}Mo(n,\gamma)$ cross section. See Fig. 8b for more details.

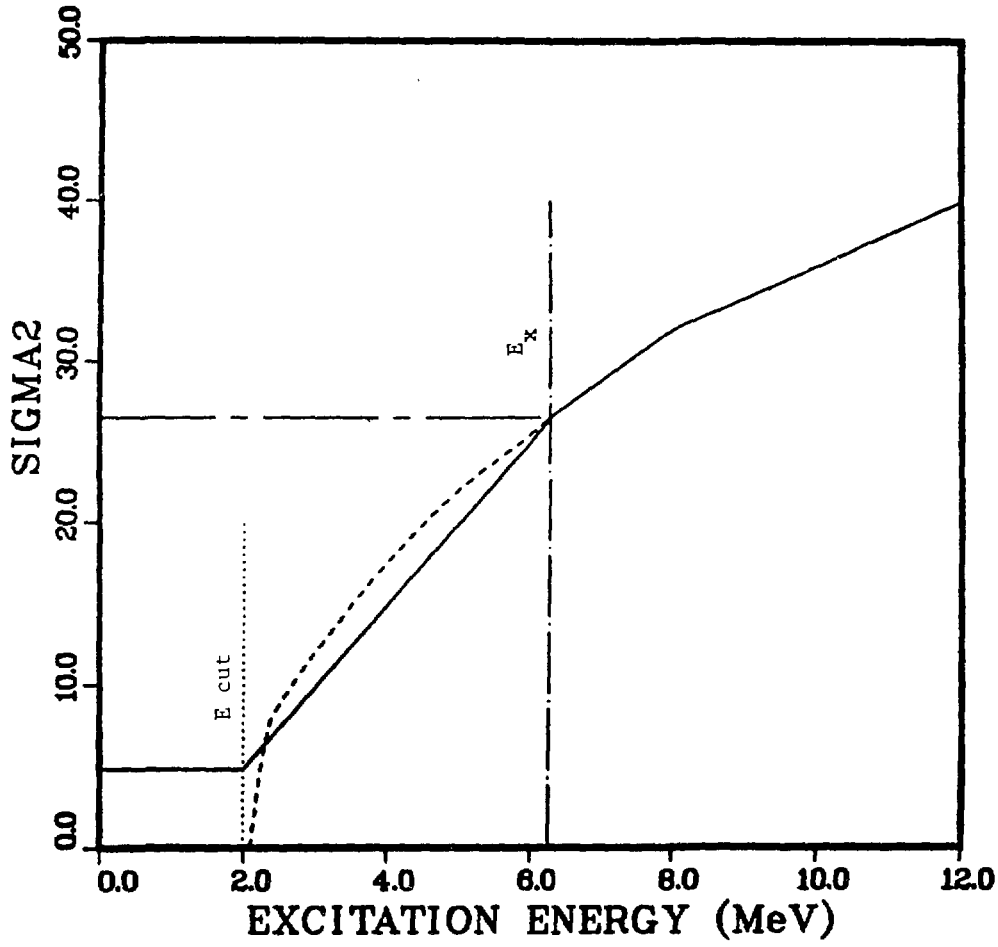

Fig. 8b. Energy dependence assumed for the spin parameter in $^{100}Mo(n,\gamma)$ calculations by Reffo [3]. The solid curve is a linear extrapolation to a constant value of σ^2 at the pairing energy and was used to produce the solid curve in Fig. 8a. The assumption of a constant value for σ^2 for excitation energies below 6 MeV produced the dashed curve shown in Fig. 8a. The dashed curve here represents an extrapolation from higher energies of Eq. (4b).

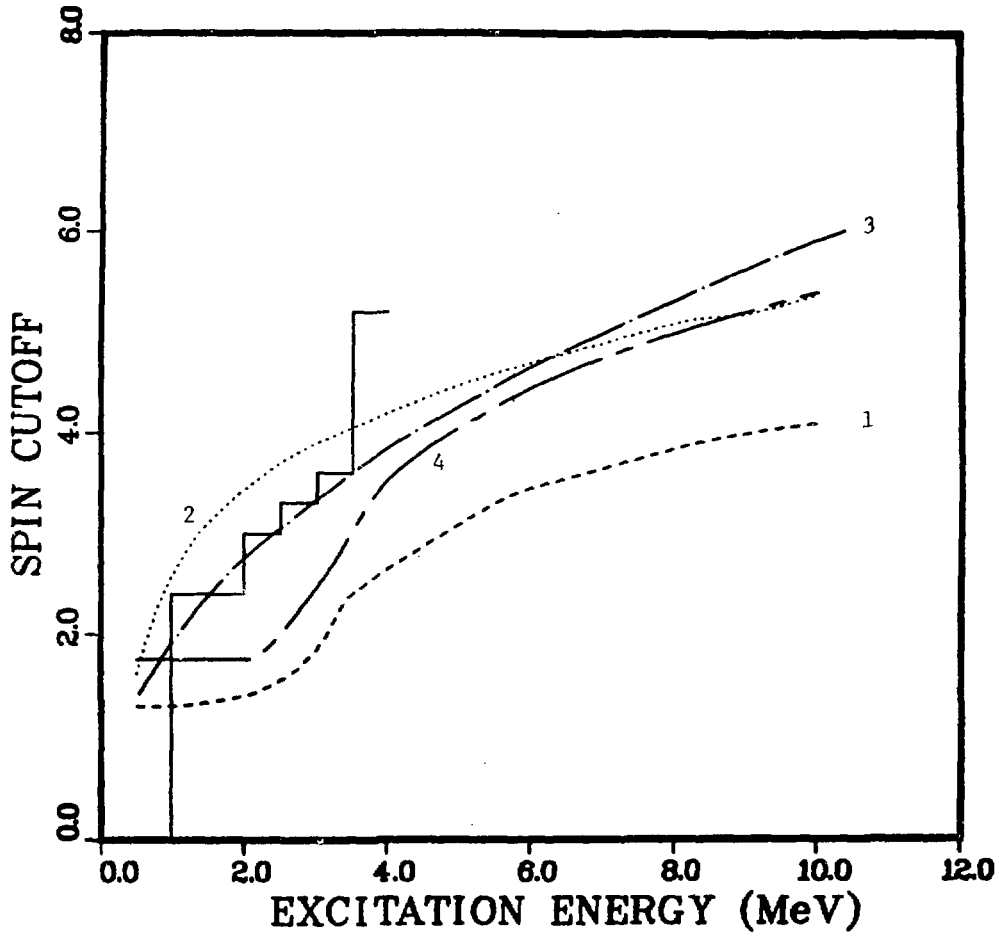

Fig. 9. Spin cutoff parameters calculated for ^{98}Mo are compared to results obtained from discrete level data represented by the histogram. The curves labeled 1 and 2 represent the Gilbert-Cameron and back-shifted Fermi-gas models; Curve 3 results from microscopic calculations; Curve Curve 4 was calculated using Eq. (4b), as suggested by Reffo [3].

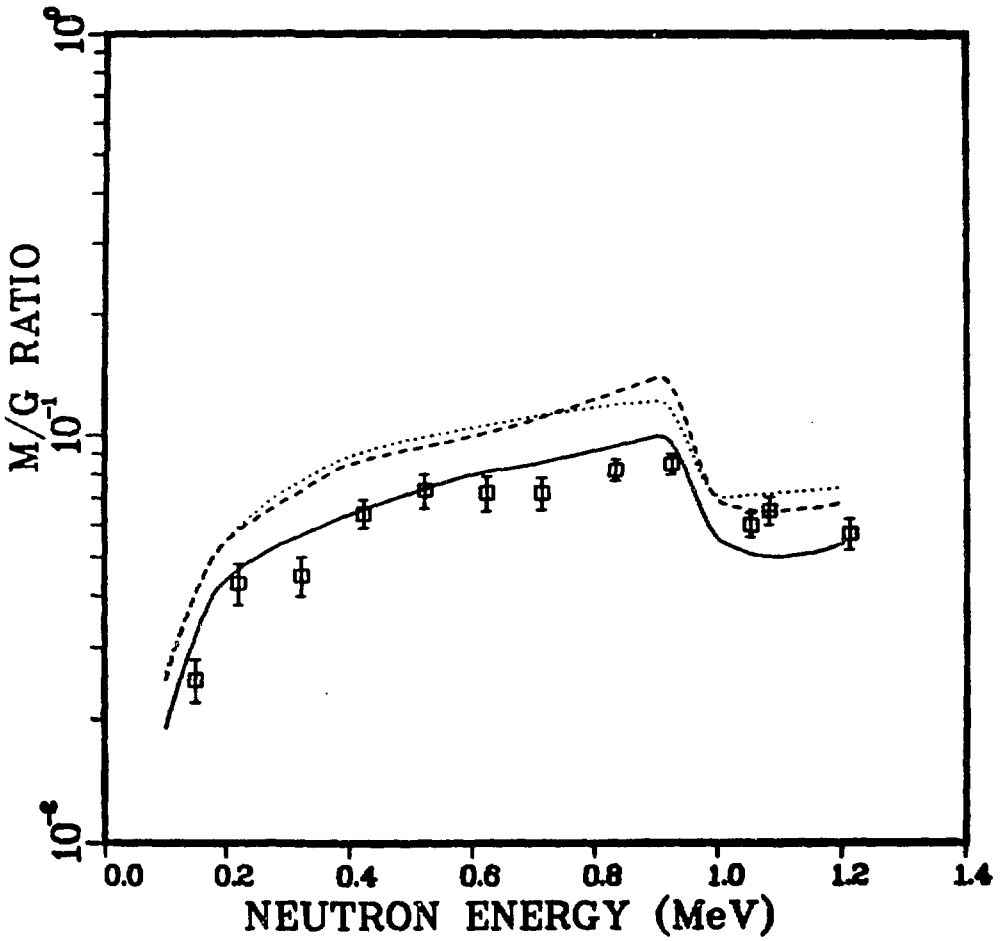

Fig. 10. Ratios of metastable to ground state yields for ^{90}Y produced in the $^{89}Y(n,\gamma)$ reaction are compared to the Grench et al. [26] data. The solid curve was calculated using the Gilbert-Cameron model, the dashed, the back-shifted Fermi-gas model, and the dotted, the microscopic model.

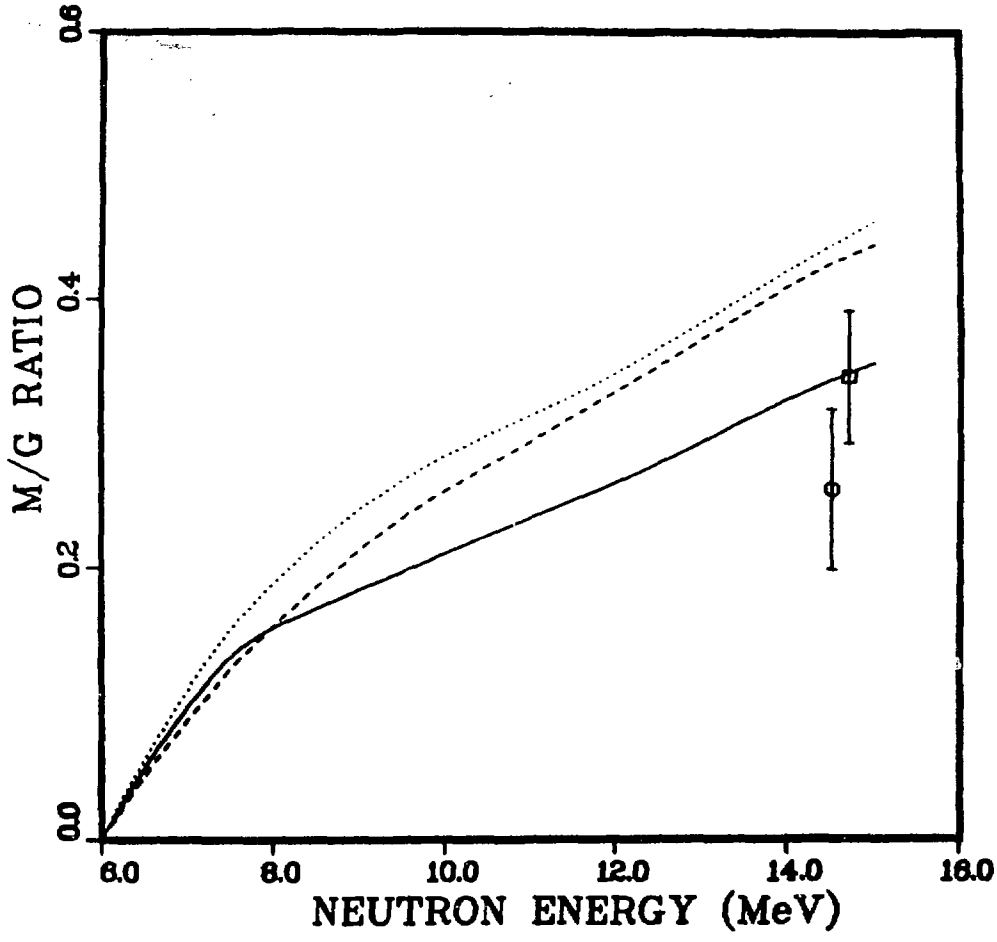

Fig. 11. Metastable to ground state ratios for ^{90}Y populated in the $^{90}Zr(n,p)$ reaction. The curves represent calculations using models identified in Fig. 10.

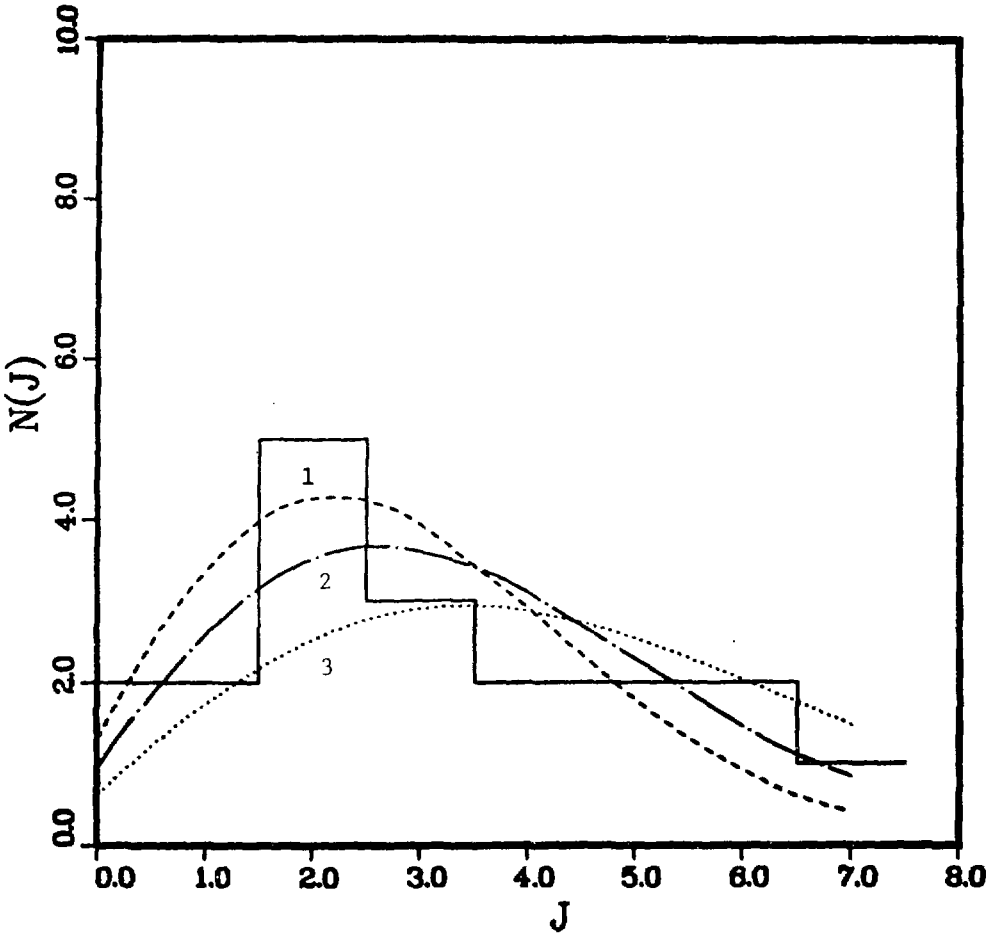

Fig. 12. The ^{90}Y spin distribution (histogram) obtained from discrete level information for excitations up to 2.5 MeV. Curve 1 was produced using the Gilbert-Cameron spin cutoff parameter; that labeled 2 results from microscopic calculations; while Curve 3 was obtained using the back-shifted Fermi-gas spin cutoff parameter.

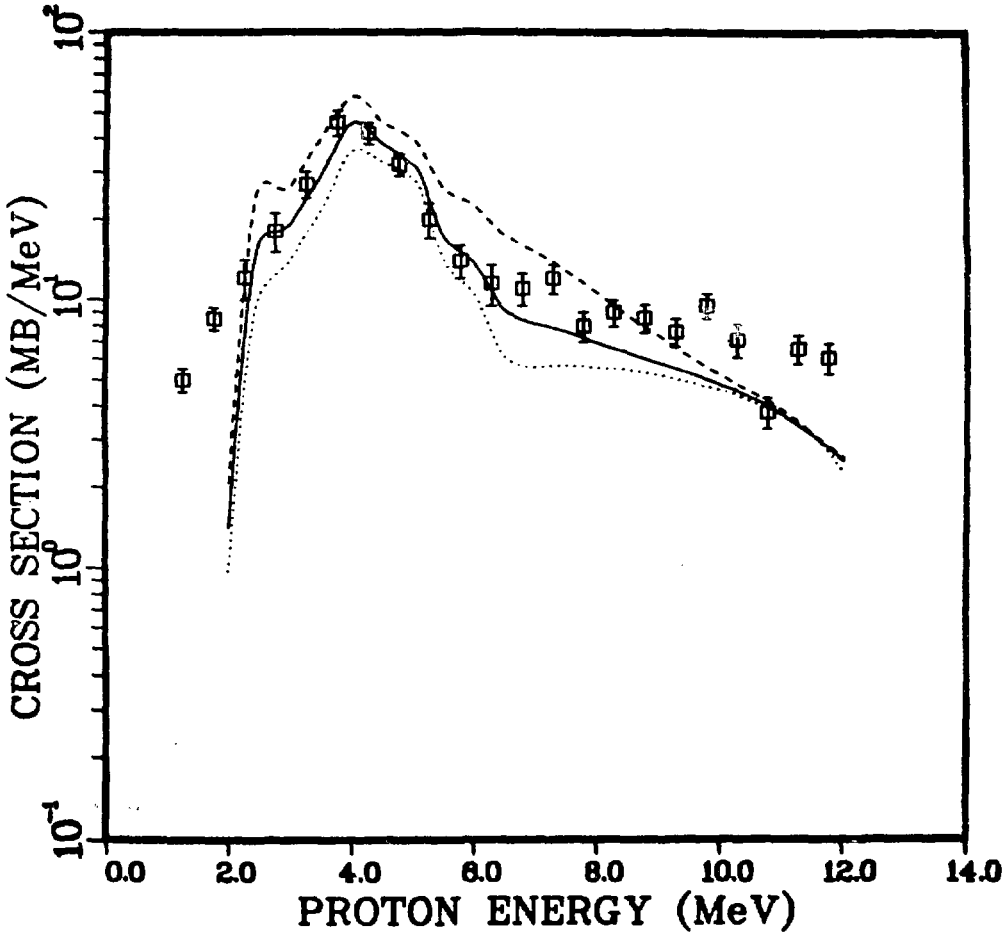

Fig. 13. Calculations of proton emission spectra from 14.8-MeV neutrons on ^{90}Zr are compared to experimental data [29]. All calculations were made using the Gilbert-Cameron model. The solid curve represents results obtained using standard Gilbert-Cameron values for the level density parameter, a; the dashed curve results when the parameter a for ^{90}Zr is decreased by 10%; the dotted curve results when a for ^{90}Zr is increased by 10%.

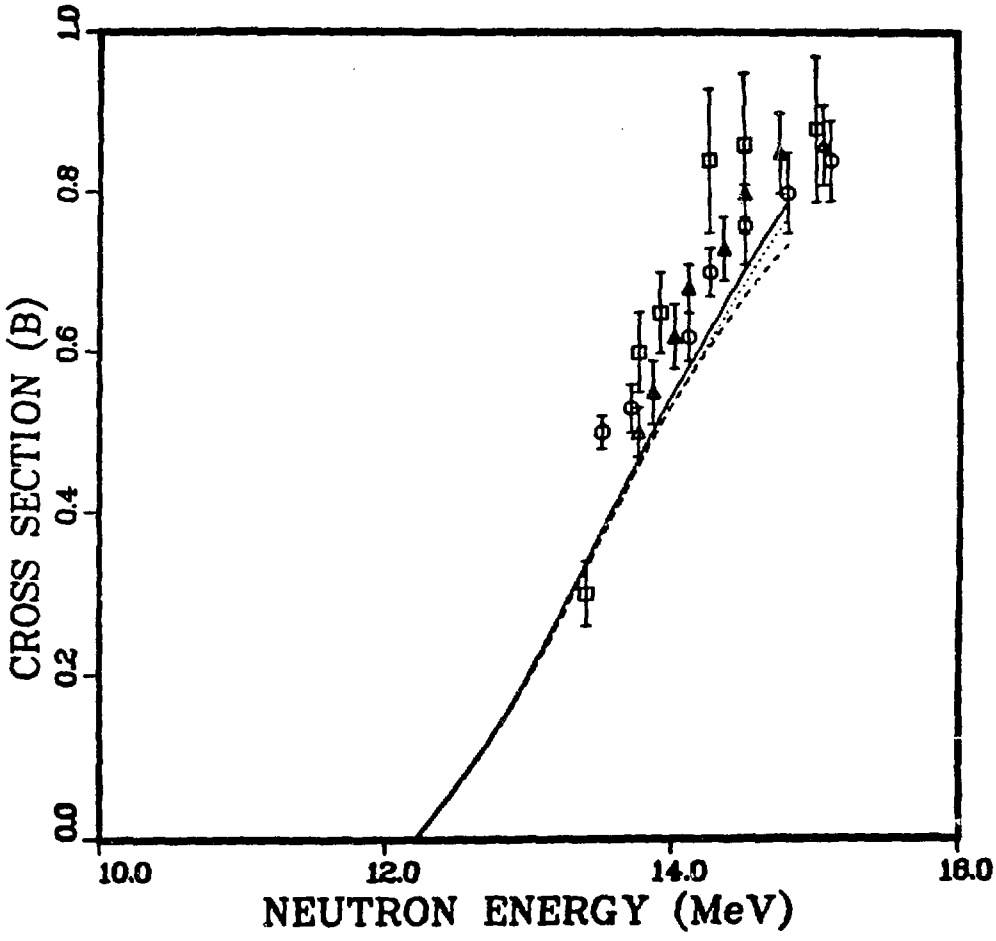

Fig. 14. Calculated $^{90}Zr(n,2n)$ cross sections with the level density parameter a changes described in Fig. 13 are compared to experimental data.

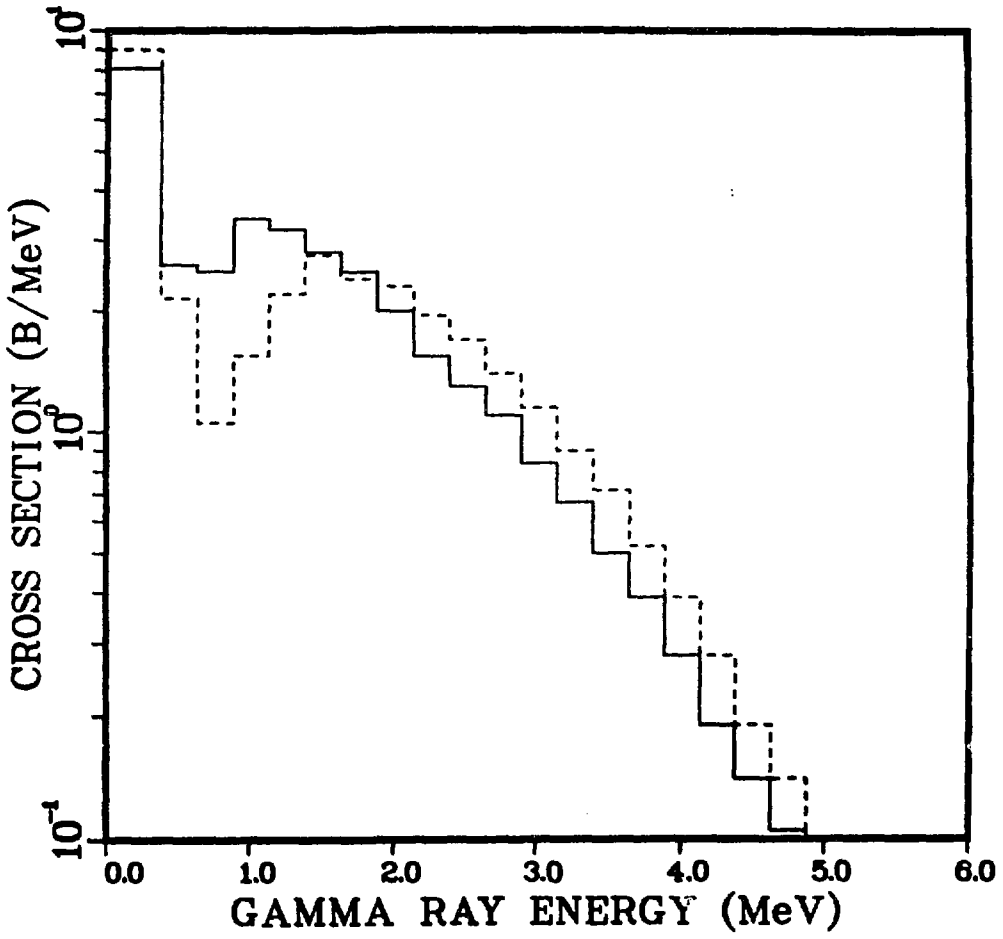

Fig. 15. Calculated tungsten (solid histogram) and tantalum (dashed histogram) gamma-ray production spectra induced by 6.5-MeV neutrons are compared to each other to illustrate level-density effects on such spectra occurring for nearby nuclei.

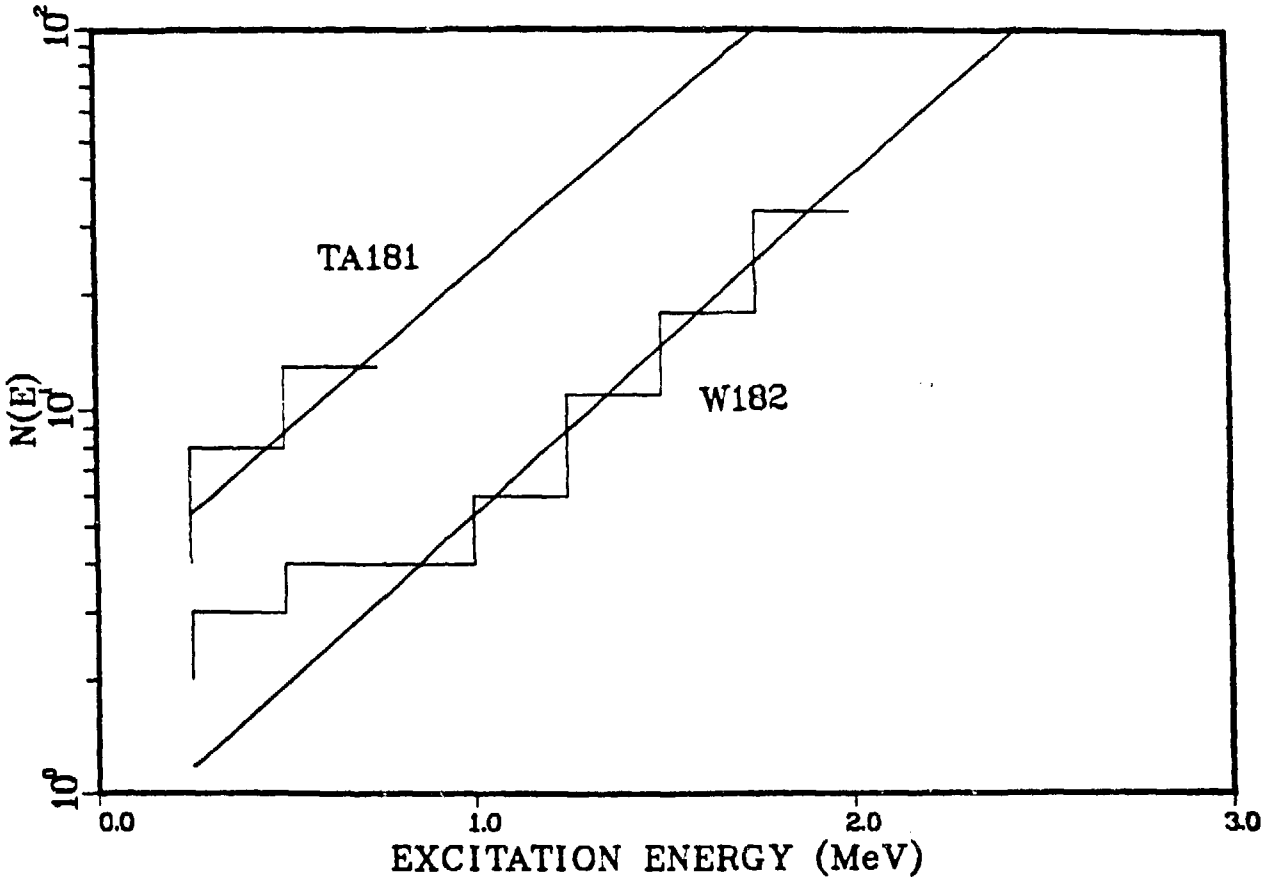

Fig. 16. The cumulative number of low-lying discrete levels of ^{181}Ta and ^{182}W. The solid curves are constant temperature expression fits to these data.

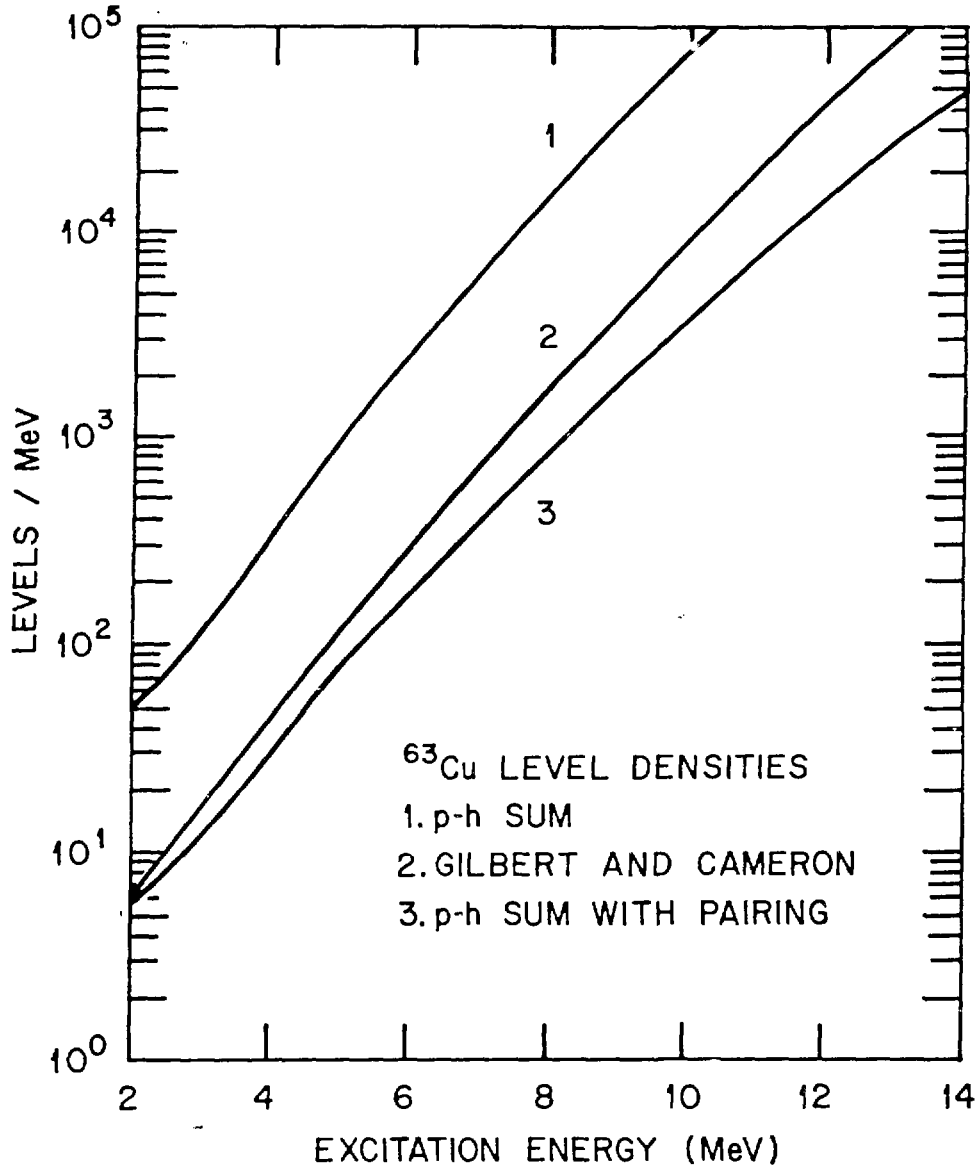

Fig. 17. Level densities for ^{63}Cu calculated by Fu [32]. Curve 1 was calculated using Eq. (10); Curve 2 was obtained using the Gilbert-Cameron expression; while Curve 3 results when pairing effects are introduced into Eq. (10) for particle-hole densities.

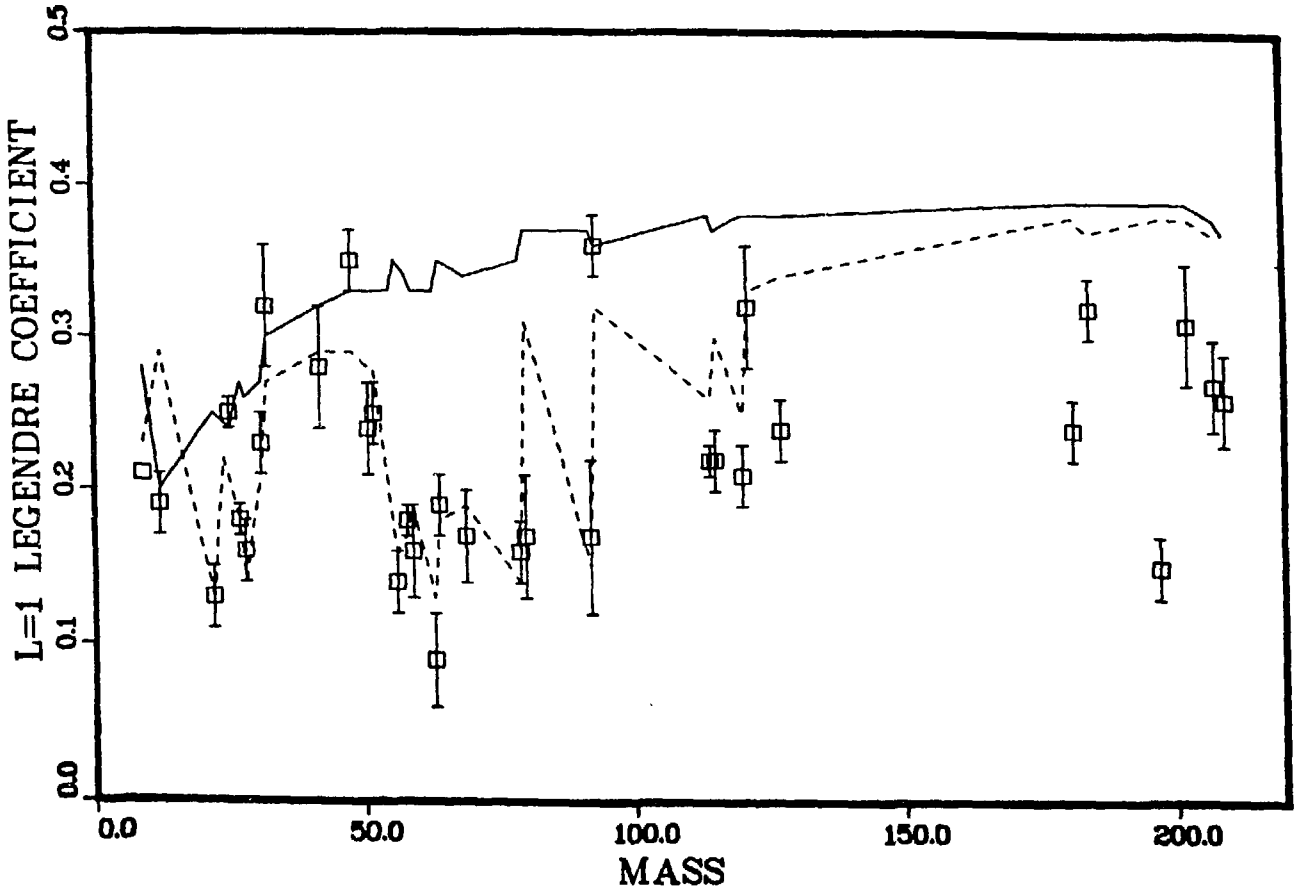

Fig. 18. Fits to $\ell = 1$ Legendre coefficients obtained from an analysis [33] of the Hermsdorf [34] data. The solid curve represents theoretical values obtained with $g = A/13$, while the dashed curve assumed $g = 6a/\pi^2$ for the residual nuclei state density.

FISSION CROSS-SECTIONS AND THE NUCLEAR LEVEL DENSITY

J E Lynn

A.E.R.E, Harwell

ABSTRACT

We have reviewed fission cross-section theory to draw attention particularly to its requirements for information on the nuclear level density and in particular its dependence on nuclear deformation. The status of level density theory is reviewed from this point of view, and it is demonstrated again that collective enhancement factors must play a major role in affecting the magnitude of fission cross-sections. The collective enhancement appears to remain at least partially effective up to excitation energies of at least 20 MeV.

INTRODUCTION

Although the main theme of its solution was formulated almost half a century ago [1], the nuclear level density problem remains one with several controversial aspects, all of which are relevant to the theory of fission cross-sections. Among the important factors that bear upon the magnitude of the level density and its dependence on excitation energy are the influences of nuclear shell effects and pairing correlation energy, the effect of nuclear deformation and the contribution of collective excitations. The last factor also has an important bearing upon the dependence of the level density on angular momentum. The knowledge of level density behaviour is central to the theoretical calculation of fission cross-sections. In gleaning this knowledge, theoretical formulation and understanding is imperative, direct experimental evidence being confined to low excitation energies, to the neutron resonance window at higher excitation energy, and to nuclear deformations mostly confined to values near that of the ground state.

In this paper we review the current knowledge of nuclear level density behaviour and its consequences in the theory of fission cross-sections. We commence, in Section 2, with a summary of the theory of the fission reaction as deduced from compound nucleus theory, including special reference to the actinides and the complicated behaviour of the fission barrier that dominates their fission properties. This section introduces the level density as a central concept and, in particular, explicitly draws attention to its dependence on nuclear deformation. In Section 3, we discuss the evaluation of the

level density from the almost universally used starting point of the Laplace transform of the grand partition function. The normal method, borrowed from statistical mechanics for evaluation of the Laplace transform, depends on the possibility of describing nuclear energy levels as a superposition of independently occupied single particle states. Within this framework we describe shell effects in the level density and deformation effects that are consequent upon the extension of shell concepts to deformed nuclei, and we review attempts that have been made to include the effects of nuclear residual forces that cannot be included within the smooth potential well description of the single particle states.

In Section 4 we extend this discussion to the question of the dependence of level density upon angular momentum. This is crucial for the comparison of theoretical deductions with neutron resonance observations, which are limited to a very narrow range of angular momentum, and is also very important for the evaluation of fission cross-sections at low to moderate excitation energies. A key element in this discussion is the question of collective enhancement, the extent to which the independent particle degrees of freedom are insufficient, at any given excitation energy, to account for the total level density and therefore must be enhanced by rotational and vibrational degrees of freedom.

The comparison of theoretical calculations with direct experimental data on nuclear level density is pursued in Section 5. Comparisons of the theory with observed fission cross-section behaviour or deductions on level densities from fission cross-sections form the main elements of Section 6.

More information on interesting aspects of the level density is drawn together in Sections 7 and 8. In Section 7 we discuss cross-sections of the nuclides in the thorium region of the periodic table. In Section 8 we deal with the extension of level density knowledge to higher excitation energies and the consequent problems in calculating high energy fission cross-sections. Finally, our overall conclusions are given in Section 9.

2. Fission cross-sections

The fission reaction is assumed to proceed almost entirely through the compound nucleus mechanism. In its simplest form this implies that the cross-section for the reaction may be factorised into a part σ_{CN}, representing formation of the compound nucleus in a highly excited state through absorption of the initial projectile by the target nucleus, and a part representing the probability of decay of the excited compound nucleus state by fission. This last factor is commonly written either as the ratio of the fission width to total width of the compound level,

$$P_f = \Gamma_{(f)}/\Gamma \tag{1}$$

or alternatively as the ratio of the corresponding transmission coefficients

$$P_f = T_{(f)}/T \tag{2}$$

Equation (1) is strictly valid only for energies close to a single level; the average over many levels (assuming their widths to be much smaller than their

spacing) is

$$\overline{\sigma_f} = \Sigma_J \left\langle \sigma_{CN,J} \Gamma_{J(f)} / \Gamma_J \right\rangle = 2\pi^2 \lambda\!\!\!^{-}{}_a^2 \, \Sigma_J g_J \left\langle \Gamma_{J(a)} \Gamma_{J(f)} / \Gamma_J \right\rangle \rho(J) \tag{3}$$

where $\lambda\!\!\!^{-}{}_a$ is the de Broglie wave length for projectile a, g_J is the spin statistical factor for forming the compound nucleus with total angular momentum J and $\rho(J)$ ($\equiv D_J^{-1}$) is the density of compound nucleus levels of spin J. This expression is normally written in terms of average widths by use of an averaging correction factor S_{af}:

$$\overline{\sigma_f} = 2\pi^2 \lambda_a^2 \, \Sigma_J g_J (\overline{\Gamma}_{J(a)} / \overline{D}_J)(\overline{\Gamma}_{J(f)} / \overline{\Gamma}_J) S_{af} = \Sigma_J \sigma_{CN,J} (\overline{\Gamma}_{J(f)} / \overline{\Gamma}_J) S_{af} \tag{4}$$

Explicit expressions and methods for calculating the width fluctuation factors S can be found in many references ([2] to [4]).

For overlapping levels, a reasonable generalisation of eq.(4) is

$$\overline{\sigma_f} = \Sigma_J \sigma_{CN,J} (T_{J(f)} / T_J) S_{af} \tag{5}$$

where

$$\sigma_{CN,J} = \pi \lambda_a^2 g_J \, T_{J(a)} \tag{6}$$

Eq.(6) defines the transmission coefficient T_c

The transmission coefficients T can be written in terms of the level widths [5] :

$$T_{J(a)} = 1 - \exp\left(- 2\pi \overline{\Gamma}_{J(a)} / \overline{D}_J\right) \tag{7}$$

While the widths in this expression are, strictly speaking, those of S-matrix theory, no great inaccuracy is normally introduced by using R-matrix widths.

The fission transmission coefficient T_f is often regarded as the sum over the coefficient for individual fission channels, μ:

$$T_{J(f)} = \Sigma_\mu T_{J(\mu)} \tag{8}$$

This is the generalisation of Bohr and Wheeler's concept of the transition state [6], which describes the internal state of the fissioning nucleus, as it passes over the fission barrier, as a superposition of all energetically available states of intrinsic excitation of the nucleus, thus giving

$$T_{(f)} = \int_0^{E^* - V_D} dE \rho_D(E) \tag{9}$$

where E^* is the excitation energy of the fissioning nucleus, V_D is the barrier height and $\rho_D(E)$ is the density of levels of intrinsic excitation at

the barrier deformation. In eq.(8), the individual transmission coefficients include the quantal penetrability factor through the fission barrier. This is normally assumed to have the Hill-Wheeler form [7] for a barrier with quadratic dependence on deformation:

$$T_{(\mu)} = \left[1 + \exp 2\pi\ (E_{\mu} - E^{*})/\hbar\omega\right]^{-1} \tag{10}$$

ω being the circular frequency of an oscillator well of the same curvature and inertial parameter as the barrier. The energy E_{μ} is the sum of the barrier height and the excitation energy of the intrinsic state defining the channel μ.

When only a few channel energies E_{μ} are lower than or close to the excitation energy E^{*} eq.(8) should be used, if possible, to evaluate the total fission transmission coefficient $T_{(f)}$, from a finite number of discrete channels. But even in this situation there can be a contribution from the near-continuum of higher channels, a consequence of the nature of eq.(11). This contribution can be taken into account by the use of the density function for intrinsic states and an integration.

For excitation energies that are much greater than the barrier height it is natural to replace the summation of eq.(8) by integration over a level density function:

$$T_{J(f)} = \int_{0}^{\infty} dE\rho_{D}(E,J)\ \left[1 + \exp 2\pi(E + V_{D} - E^{*})/\hbar\omega\right]^{-1} \tag{11}$$

The evaluation of the fission transmission coefficient is considerably more involved when the barrier has the double-humped form that is common to most of the actinides [8]. The existence of a complex intermediate state of intrinsic motion associated with the secondary well deformation effectively decouples the nucleus from its fission mode of motion at an advanced stage along its path. A statistical treatment of this decoupling gives the approximate expression

$$T_{(f)} = T_{(A)}T_{(B)}/\left[T_{(A)} + T_{(B)} + T_{II(b)}\right] \tag{12}$$

where $T_{(A)}$ and $T_{(B)}$ are transmission coefficients for the inner and outer barriers, respectively, and have the form of the r.h.s of eq.(8), the intrinsic states μ having, in general, different character for the two deformations. The quantity $T_{II(b)}$ is the transmission coefficient for decay of the intermediate states by particle emission and radiation.

Equation (12) implies that the energy average is made over an interval that is large compared not only with the spacing of fine-structure levels but also with that of the intermediate levels (usually called class-II levels) associated with the secondary well. If this latter condition is not met, and the intermediate levels are narrower than their spacing, the fission transmission coefficient will have an intermediate resonance form [9,10]

$$T_{(f)} = \Sigma_{\lambda_{II}}\Gamma_{\lambda_{II}}(c)\Gamma_{\lambda_{II}}(f)/\left[(E - E_{\lambda_{II}})^{2} + (\tfrac{1}{2}\Gamma_{\lambda_{II}})^{2}\right] \tag{13}$$

Here, λ_{II} denotes the class-II level at excitation energy $E_{\lambda_{II}}$ with fission width $\Gamma_{\lambda_{II}(c)}$ for coupling the intermediate state to the fine-structure (class-I) levels, and total width $\Gamma_{\lambda_{II}} = \Gamma_{\lambda_{II}(f)} + \Gamma_{\lambda_{II}(b)} + \Gamma_{\lambda_{II}(c)}$ for total decay plus coupling. These widths fluctuate from level to level just as the class-I level widths do. In consequence the energy average over the resonance terms of eq.(13) must be written in a form involving average class-II widths and fluctuation factors S^{II}_{fc} [11] analogous to that of eq.(5); this is

$$\left\langle T_{(f)} \right\rangle = (2\pi/D_{II})\ (\overline{\Gamma}_{II(c)}\overline{\Gamma}_{II(f)}/\overline{\Gamma}_{II})S^{II}_{fc} = T_{(A)}T_{(B)}/(T_{(A)} + T_{(B)} + T_{II(B)}) \quad (14)$$

where the transmission coefficients $T_{(A)}, T_{(B)}$ and T_{II} can now be expressed in terms of the mean widths and spacing of the class-II levels by the equations

$$T_{(A)} = 2\pi\ \overline{\Gamma}_{II(c)}/D_{II} \quad (15a)$$

$$T_{(B)} = 2\pi\ \overline{\Gamma}_{II(f)}/D_{II} \quad (15b)$$

$$T_{II(b)} = 2\pi\ \overline{\Gamma}_{II(b)}/D_{II} \quad (15c)$$

These expressions are analogous to the first order expansion of eq.(7). If the barriers A and B are assumed to have the inverted harmonic oscillator form, the barrier transmission coefficients $T_{(A)}, T_{(B)}$ take a form, analogous to eq.(10) or, at higher excitation energies, its approximation by an integral eq.(11).

$$T_{J(A)} = \Sigma_{\mu}\left[1 + \exp 2\pi(E_{A\mu} + V_A - E^*)/\hbar\omega_A\right]^{-1} \quad (16a)$$

$$\approx \int_0^{\infty} dE\rho_A(E,J)\ \left[1 + \exp 2\pi(E+V_A - E^*)/\hbar\omega_A\right]^{-1} \quad (16b)$$

with a precisely analogous form for $T_{(B)}$. Here ρ_A, ρ_B represent the densities of intrinsic excitations at the deformations of the inner and outer barriers with barrier heights V_A, V_B and tunnelling frequency parameters $\hbar\omega_A$, $\hbar\omega_B$ respectively.

The nature of the statistical fluctuations of the level widths is worth a note here since they govern the value of the statistical fluctuation factors in the expressions for average cross-sections. It is well known that the fluctuations of fine structure widths for decay processes through a single channel are governed by the Porter-Thomas distribution [12], which is a member (with $\nu = 1$) of the chi-squared family governed by the parameter ν (the "number of degrees of freedom"). The relative variance of a member with parameter value ν is $2/\nu$. This distribution is almost certainly appropriate for the decay widths of the class-II levels also. However, the

coupling width of the class-II state requires special consideration [11]. While it is useful to think of this quantity as composed of contributions from channels analogous to those for the passage over the fission (outer) barrier these are not statistically independent in the same way as the decay channels. Rather, the contributions to coupling from overlapping class-II levels are to be considered statistically independent and the fluctuation factors (like S_{cf}^{II}) are to be computed accordingly.

Thus the level density concept enters the description of fission cross-sections in several different ways. The most obvious is the fine-structure resonance density, requiring the level density ρ_I of the compound nucleus at high excitation energy (several MeV) and with deformation approximately that of the ground state. At near-barrier or sub-barrier energies the prominent intermediate resonance structure is governed by the level density ρ_{II} of the compound nucleus at effective excitation energies a few MeV lower and at the much greater deformation of the secondary well in the barrier. At rather higher excitation energies of the compound nucleus or for computation of average cross-sections the densities of intrinsic states of the compound nucleus at the barrier deformations but at low to medium effective excitation energies are required (eq.16). Other level density functions are required for the calculation of the total transmission coefficient, which includes all the competitive processes. The competing radiation decays are governed by the level density function at normal or secondary deformation.

$$T_{(\gamma)}^{(I)} \approx 2\pi\Gamma_{I(\gamma)}/D_I = \int_0^{E^*} dE_\gamma f(E_\gamma)\rho_I(E^* - E_\gamma) \tag{17a}$$

$$T_{(\gamma)}^{(II)} \approx 2\pi\Gamma_{II(\gamma)}/D_{II} = \int_0^{E^* - E_{II}} dE_\gamma f(E_\gamma)\rho_{II}(E^* - E_{II} - E_\gamma) \tag{17b}$$

where $f(E_\gamma)$ represents the gamma-ray energy dependence of gamma transitions. This depends on the multipolarity L of the transitions and hence on the angular momentum and parity dependence of the level density, e.g.

$$T_{J(\gamma)}^{(I)} = \int_0^{E^*} dE_\gamma \sum_{J_f=|J-L|}^{J+L} f_L(E_\gamma)\rho_I(E^* - E_\gamma, J_f) \tag{18}$$

Particle decay is governed by the level densities of residual nuclei, either at normal or secondary well deformation. Thus the transmission coefficient for neutron emission from class-I states, integrated over all channels, is

$$T_J^{(I)}(n,tot) = \sum_{I''} \sum_{i''} \sum_{s''=|I''-\frac{1}{2}|}^{I''+\frac{1}{2}} \sum_{\ell''=|J-s''|}^{J+s''} T_{J(ni'',\ell'')}(E^* - S_n - E_{i''})$$

$$\approx \sum_{I''} \int dE_n' \sum_{s''} \sum_{\ell''} T_{J(n,\ell)}(E_n')\rho_{A-1,I}(E^* - S_n - E_n', I'') \tag{19}$$

where E_n' is the energy of the emitted neutron and S_n the neutron separation energy of the compound nucleus (mass number A) and $E_{i''}$ is the excitation energy of the residual nucleus state i'', of spin I''.

In all the above expressions parity and parity changes governed by multipolarity and angular momentum selection rules are taken to be implicit.

3. The evaluation of the level density

The nuclear level density is normally evaluated from the grand partition function

$$\exp \Phi = \Sigma_\ell \exp \left[-\beta E_\ell + \sum_k \beta\mu_k C_{k\ell}\right] \tag{20}$$

where the sum is over all the eigenvalues E_ℓ of the nuclear system, each with a set of quantum numbers $C_{k\ell}$ for quantities that are constants of the motion (to the number of N_k). In thermodynamic terms the quantity β plays the role of a reciprocal temperature, the μ_k are a set of chemical potentials and the quantity Φ is then related to the free energy, $\Phi = \beta F$. The level density can be obtained from the Laplace transform of the grand partition function and evaluated by saddle point integration, giving

$$\rho(E, C_1, \ldots, C_k, \ldots) = \left[1/(2\pi)^{(N_k+1)/2}(\det G)^{\frac{1}{2}}\right]\exp(\beta_o E - \Sigma_k x_{ko} C_k + \Phi_o) \tag{21}$$

with the saddle-point conditions defined by

$$E + (\partial\Phi/\partial\beta)_{\beta=\beta_o} = 0 \tag{22}$$

$$C_k - (\partial\Phi/\partial x_k)_{x_k = x_{ko}} = 0 \tag{23}$$

The quantities x_k are the products $\beta\mu_k$. The elements of G are

$$G_{11} = (\partial^2\Phi/\partial\beta^2)_{\beta=\beta_o} \tag{24a}$$

$$G_{1k} = (\partial^2\Phi/\partial\beta\partial x_k)_{\beta=\beta_o, x_k=x_{ko}} \tag{24b}$$

$$G_{kk'} = (\partial^2\Phi/\partial x_k \partial x_{k'})_{x_k=x_{ko}, x_{k'}=x_{k'o}} \tag{24c}$$

The grand partition function can be readily calculated if the eigenvalues and quantum numbers of the levels can be approximated by an independent particle system in the form

$$E_\ell = \Sigma_i n_i^{(\ell)} \varepsilon_i \tag{25a}$$

$$C_{k\ell} = \Sigma_i n_i^{(\ell)} c_{ki} \tag{25b}$$

where the ε_i are the eigenvalues of single-particle (or quasi-particle - see below) levels, the c_{ki} their quantum numbers (of purely scalar type) and $n_i^{(\ell)}$ their occupation numbers within the nuclear state ℓ. For a fermian system with magnetic quantum numbers explicitly included amongst the constants of motion c_k, these equations allow Φ to be written,

$$\Phi = \ell n\ \Pi_i\left[1 + \exp(-\beta\varepsilon_i + \Sigma_k x_k c_{ki})\right] \tag{26}$$

and its derivatives, giving the saddle point conditions for the total energy E and constants of the motion c_{ki} are

$$\partial\Phi/\partial\beta = \Sigma_i\left[-\varepsilon_i \exp(-\beta\varepsilon_i + \Sigma_k x_k c_{ki})\right] / \left[1 + \exp(-\beta\varepsilon_i + \Sigma_k x_k c_{ki})\right] \tag{27a}$$

$$\partial\Phi/\partial x_k = \Sigma_i c_{ki} \exp(-\beta\varepsilon_i + \Sigma_k x_k c_{ki}) / \left[1 + \exp(-\beta\varepsilon_i + \Sigma_k x_k c_{ki})\right] \tag{27b}$$

The introduction of the numbers of neutrons, N, and protons, Z, of the nuclear system as two of the constants of the motion, and of the concept of the single particle level density g_s at the Fermi-levels defined by the ground state occupation of N neutrons and Z protons allows the independent-particle model level density function to be written in the zero-order Fermi-gas approximations

$$\rho(E,M) = e^{-M^2/2\sigma^2}\rho(E)/\left[2\sigma(2\pi)^{\frac{1}{2}}\right] \tag{28a}$$

$$\rho(E) = (\pi^{\frac{1}{2}}/12a^{\frac{1}{4}}\ E^{5/4})\ \exp\left[2(aE)^{\frac{1}{2}}\right] \tag{28b}$$

The spin dispersion coefficient σ entering the distribution of the level density over the magnetic quantum number M and the "Fermi-gas" parameter a are given by

$$a = \pi^2 g_s/6 \tag{29a}$$

$$\sigma^2 = 0.088a\theta\ (N+Z)^{2/3} \tag{29b}$$

$$\theta = (E/a)^{\frac{1}{2}} \tag{29c}$$

The dependence of the level density on total angular momentum J is found by the Bethe device of subtracting the density for M = J+1 from that for M=J, giving

$$\rho(E,J) = \rho\ (E,M=J) - \rho\ (E,M=J+1) \approx (2J+1)e^{-(J+\frac{1}{2})^2/2\sigma^2}\rho(E)/4\sigma^3(2\pi)^{\frac{1}{2}} \tag{30}$$

This form for the nuclear level density has played a dominant role in all discussions of the subject since its first formulation by Bethe [1] in

1937. Important modifications have had to be made to it in the light of major physical effects that have been found to modify the independent-particle system of the nucleus and the comparisons with improved experimental data.

One of these major physical effects is the occurrence of shell gaps in the single-particle state density at the Fermi levels. In first approximation this can be accounted for by employing a reduced value of the density g_s and hence of a, but this will not account for the energy dependence of the level density. The average quantity g_s is in fact to be evaluated around the Fermi levels over an energy interval of the order of the temperature β^{-1} of the system; hence, in a shell nucleus, it can be expected to increase rapidly with excitation energy to some asymptotic value [13], and this increase will be amplified by its appearance in the exponent of the level density. This effect can be accounted for, at least partially, by a development of the independent-particle equations in which the sub-shell magnetic quantum number degeneracy of spherical nuclei is explicitly included [14,15]. An alternative approach is that of the back-shifted Fermi-gas model [16] in which a "normal" single-particle state density is used but the extra binding of the ground state of a closed shell nucleus is taken into account by adjustment of the excitation energy; the effective excitation energy U to be employed in place of E in eqs.(28),(29) is

$$U = E - \Delta \tag{31}$$

In principle, the shell effect can be properly accommodated within the independent-particle model by the numerical evaluation of eqs. (22),(25) and (27) using a realistic single particle level scheme.

Another important physical effect is that of pairing correlation energy. This can be accommodated semi-empirically within the Fermi-gas formula by another adjustment to the effective excitation energy, which depends on the odd-even character of the neutron and proton numbers, the most general form being

$$U = E - P(Z) - P(N) \tag{32}$$

P(Z) and P(N) are zero for odd values of Z and N. Empirically determined values for even arguments of P(Z) and P(N) have been tabulated [17]; normally these empirical values are close to the odd-even differences in nuclear separation energies.

A proper treatment of the pairing correlation effect can be achieved approximately within the independent-particle formulation of the level density by moving to the concept of constructing the nuclear excited states from independent quasi-particles [18,19]

$$E_\ell = \Sigma_j n_j^{(\ell)} e_j - \tfrac{1}{4} g_s \Delta^2 \tag{33}$$

$$C_{k\ell} = \Sigma_j n_j^{(\ell)} c_{kj} \tag{34}$$

where the $n_j^{(\ell)}$ are now the quasi-particle occupation numbers for quasi-

particle excitations

$$e_i = \sqrt{(\varepsilon_i - \lambda)^2 + \Delta^2} \quad ; \tag{35}$$

the gap quantity Δ and the Fermi energy λ are determined from the strength of the pairing interaction, the single-particle energies ε_i and total number of particles (paired and unpaired) in the system. The ground state of an even nucleus contains no quasi-particles and hence has the energy (relative to an independent-particle system) $-\frac{1}{4}g_s\Delta^2$. An odd-mass nucleus necessarily contains one quasi-particle in its ground state, which therefore has energy $\sim \Delta - \frac{1}{4}g_s\Delta^2$. The ground state of a double-odd nucleus has two quasi-particles and energy $\sim 2\Delta - \frac{1}{4}g_s\Delta^2$.

These energy effects in the correlated ground-state are crucial for the description of level densities in two ways. Firstly, they imply odd-even effects in the level density at low excitation energies, and, by implication at higher energies [20]. For example, the low-lying levels of a double-odd nucleus have a two quasi-particle character and a corresponding density. Such levels, and their density, do not occur in even nuclei below an excitation energy of $\sim 2\Delta$. Hence, the semi-empirical adjustment to the effective excitation energy as described in eq.(32) can be understood. Secondly, the gap quantity Δ is dependent on excitation energy and vanishes above a critical excitation energy [19,20]. Above this energy the nucleus can be assumed to revert to a normal independent-particle system, but the effective excitation energy available for distributing particles over the single particle levels is reduced by the extra pair-correlated binding energy of the ground state as given above, i.e.

$$\begin{aligned} U &\approx E - \tfrac{1}{4}g_s\Delta_o^2 \quad , && \text{even nuclides} \\ &\approx E - \tfrac{1}{4}g_s\Delta_o^2 + \Delta_o , && \text{odd-A} \\ &\approx E - \tfrac{1}{4}g_s\Delta_o^2 + 2\Delta_o && \text{double-odd} \end{aligned} \tag{36}$$

where Δ_o denotes explicitly the gap quantity for the ground state. The gap quantity also depends upon the projected angular momentum quantum number of the system [21,22], and in particular Moretto [22] has presented consistent equations for evaluating the grand partition function for the quasi-particle model including the effect of angular momentum on the blocking phenomenon.

The independent-particle (or quasi-particle) formulation, originally developed for spherical nuclei, can readily be extended to deformed nuclei. In this case the main sub-shell degeneracies over angular momentum projection of the spherical shell model are removed, only the two-fold degeneracy associated with the sign of the angular momentum projection Ω_i on the cylindrical symmetry axis of spheroidal nuclei remaining. Hence, the quantum number M, the projection of the total angular momentum of the system on a laboratory-based axis is replaced, as a constant of the motion, by the projection K on the nuclear axis.

With changing deformation of a nucleus the single particle state density

at the Fermi energy varies. From eqs. (28,29) we might expect a qualitatively larger variation, in the same direction, of the level density. In the Strutinsky theory of the deformation energy surface [8] the shell corrections to the basic liquid drop term are fully correlated with the single particle state density. In the actinides the nuclear deformations corresponding to energy minima and maxima are very close to the deformations at which the single-particle state densities have minima and maxima respectively. Hence it might be expected that, for corresponding available excitation energies, level densities at the fission barrier deformations will be considerably greater than those for primary and secondary well shapes. The argument has been generalised by Reisdorf [23], who has employed the theorem of Balian and Bloch [24] for the eigenvalue density in an arbitrary-shaped cavity. With an expansion of the single-particle state density in powers of $A^{-1/3}$, thus including a surface area and a curvature dependence, Reisdorf can reproduce neutron resonance state densities reasonably well for spherical and deformed nuclei, provided a shell correction, dependent on excitation energy, is also taken into account, and shows that the same procedure with empirically-adjusted and deformation-dependent shell corrections, can account for experimental fission probabilities at 11 MeV excitation energy.

The simple argument ignores, however, the dependence of the energy gap quantity Δ on the single-particle density. For constant nuclear volume this dependence is significant. The consequent effect of this change in Δ on the level density at low and medium excitation energies is opposite to and greater than the change in the effective Fermi-gas parameter, partly (at low energies) because of its effect on the quasi-particle energy and partly because of the change in effective excitation energy from the pair-binding effect in the ground state. This has been demonstrated in calculations of Britt et al [25] and Dossing and Jensen[26]. With single-particle state densities that are realistic for the actinides it appears that intrinsic barrier state densities can be lower than those for the primary and secondary wells up to excitation energies of the order of 8 MeV.

More general characteristics of the residual nuclear forces are important for the consideration of the deformation dependence of the nuclear energy. The dependence of the energy of independent-particle states on the deformation is found to be realistic only over a limited range of small deformation from the spherical. It was demonstrated by Strutinsky[8] that the overall deformation dependence of the ground state could be represented by adding a shell-correction energy to a smoothed liquid-drop energy which contains the full effect of the short-range residual nuclear forces, the shell-correction being prescribed as the difference between the actual independent-particle state energy and smoothed independent-particle energy computed from a smoothed single-particle state spectrum. It has been shown[27] that this prescription is equivalent, in second order approximation to a Hartree-Fock representation of the energy.

In actinide nuclides these methods lead to a double-peaked form (the double-humped fission barrier) of the dependence of "ground" state energy on deformation owing to the superposition of the oscillating shell-correction upon a broadly-peaked liquid-drop term. The shell-correction term is dependent upon the single-particle state density at the Fermi-energy, peaks corresponding to high density, and troughs to low. The shell-binding

corresponding to the trough close to the liquid-drop peak gives rise to the secondary well of the fission barrier.

If the same concept is applied to the states at high excitation energies the shell-correction term can be expected to be washed out, the averaging of the single-particle state spectrum now being defined over a wide energy interval around the Fermi-energy; the fission barrier is said to revert to the liquid-drop form. Gottschalk and Ledergeber [28] have considered this effect in the procedure for calculating the level density. Starting from Hartree-Fock theory they show that the grand partition function can be written, in zero-order, as the sum of a term derived from a uniform single-particle state density and one derived from the energy-fluctuating component of the single-particle density. Application of the saddle-point equations for the energy leads to the interpretation of the first derivative of the g.p.f. as the sum of the smooth part of the excited energy surface plus a temperature-dependent shell correction. Gottschalk and Ledergeber argue that if the excitation energy is calculated from the prescription,

total energy = shell model energy at local deformation

ground state energy = Strutinsky renormalized ground-state energy,

the residual-interaction term in the ground-state energy does not have its counterpart in the excited state energy and the level density calculation will be erroneous. This omission will not be felt however if excitation energies are adjusted to experimentally observed barrier energies rather than calculated ones.

4. Angular momentum dependence

The formal development of Section 2 can only treat angular momentum correctly for spherical systems. The dependence of level density on angular momentum projection, M, on an arbitrary axis can be used to yield its dependence on total angular momentum in such a system (eq.30). In a spheroidal system however only the dependence on angular momentum projected along the cylindrical symmetry axis K can be found. To proceed to the total spin dependence, strong assumptions must also be made about the nature of the components on the remaining axis.

At very low excitation energies the independent-particle (or quasi-particle)states determined by the method of Section 2 can be regarded as the band-head states for bands of collective rotational states of increasing angular momentum. The extension of this concept to higher excitation energies allows us to develop an expression for the angular momentum dependence of the level density within a unified, independent-particle plus rotation, model. Close to a given excitation energy E^* it is assumed that the density of independent-particle (band-head) states can be expressed as

$$\rho_{BH}(E,K) = \rho_{IP}(E,K) = (1/\sigma_k(2\pi)^{\frac{1}{2}})\ e^{-K^2/2\sigma_k^2}\ \rho_{IP}(E^*)\ e^{(E-E^*)/\theta} \qquad (37)$$

where $\theta \approx (\partial \ln\rho/\partial E)_{E=E^*}$. If, at excitation energy E^* the rotational energy

$$E_{rot} = (\hbar^2/2\mathcal{I})\left[I(I+1) - K^2\right] \tag{38}$$

is unavailable then the total level density for total angular momentum I is

$$\rho(E^*,I) = \sum_{K=-I}^{I} \rho_{BH}(E^* - E_{rot},K) \tag{39a}$$

$$= (1/\sigma_k(2\pi)^{\frac{1}{2}})\rho_{IP}(E^*)\exp\left[-(\hbar^2/2\mathcal{I}\theta)I(I+1)\right]\sum_{K=-I}^{I}\exp\left[-K^2(1/2\sigma_k^2 - \hbar^2/2\mathcal{I}\theta)\right] \tag{39b}$$

$$\approx (1/\sigma_k(2\pi)^{\frac{1}{2}})\rho_{IP}(E^*)(2I+1)\ \exp\left[-(\hbar^2/2\mathcal{I}\theta)I(I+1)\right] \tag{39c}$$

provided $(1/2\sigma_k^2 - \hbar^2/2\mathcal{I}\theta)$ is much smaller in magnitude than I^{-2}. This is to be contrasted with the expression that would be obtained if K were simply assumed to be an arbitrary projection of the angular momentum; from eq.(30)

$$\rho(E,I) = (2\sigma_k^3(2\pi)^{\frac{1}{2}})^{-1}\rho_{IP}(E)(2I+1)\exp\left[-(I+\tfrac{1}{2})^2/2\sigma_k^2\right] \tag{40}$$

Thus the enhancement of the level density from collective rotations in the spheroidal model is roughly by the factor $2\sigma_k^2$ (assuming that $\sigma_k^2 \approx \mathcal{I}\theta/\hbar^2$).

The validity of such a rotational enhancement at medium to high excitation energies is controversial. In principle all degrees of freedom of motion are comprised in the independent particle system. In practice only at extremely high excitation energy are they effectively exhausted in describing the state wave-functions. At medium excitation energies (such as the neutron separation energy) in heavy actinides only perhaps about six particles are excited in the typical independent-particle states. On the other hand rotations, involving as they do a collective motion of many nucleons will require a description in terms of a coherent superposition of very many excited particles, hence of independent particle states drawn from a very much higher excitation range. Bjornholm, Bohr and Mottelson [29] indicate that the characteristic temperatures involved for such states will be of the order of 1.5 MeV, and hence the excitation energies are an order of magnitude greater than the neutron separation energies.

Support for the hypothesis of the rotational enhancement factor comes from an analysis by Huizenga et al [30]. Neutron resonance densities were calculated using eqs. (21) to (26) with realistic single particle energies. With angular momentum dependence based on eq.(30) the experimental data on spherical nuclides were closely reproduced [31], but those on deformed nuclei required the rotationally enhanced form, eq.(39c). Other workers [32,33] consider that the rotational enhancements are not required to explain the data, but these analyses employ semi-empirically determined (yet systematic) shell energy correction terms. The balance of evidence best supports

the concept of rotational enhancement at moderate excitation energies.

The concept of rotational enhancement can be generalised as one of enhancement due to symmetry-breaking in the shape of the nucleus [29]. The factor $2\sigma_k^2$ represents the enhancement due to breaking spherical symmetry, reducing the nuclear shape to one of axial symmetry. A further stage of symmetry breaking is introduced when the shape is not symmetric with respect to rotation about an axis perpendicular to the major axis (this operation is referred to as $\mathcal{R}$) but is symmetric with respect to reflection in a plane containing the major axis. This has the effect of doubling the state density; for every intrinsic state of definite parity a rotational band of opposite parity is introduced. Such a shape is energetically favoured in calculations of the deformation energy of an actinide nucleus as it passes over the outer barrier [33].

Maximum enhancement of the rotational states is obtained when the nuclear shape is completely lacking in symmetry. In this case the nucleus will be able to make collective rotations about the three perpendicular body-fixed axies, with the result that there will be $2I+1$ different states for every value of rotational angular momentum I in each rotational band. If each of these states is labelled by a number τ, the total level density based on a density of bandhead states $\rho_{BH}(U)$

$$\rho(E,I) = \sum_{\tau=1}^{2I+1} \rho_{BH}(E - E_{rot}(\tau,I)) \tag{41a}$$

$$\approx (2I+1)\rho_{BH}(E) \tag{41b}$$

if $E_{rot}(\tau,I)$ is much less than the temperature θ of the level density formula (37) for ρ_{BH}. For this expression we note that the density of band-head states will be double that for an axially symmetric nucleus, because K is no longer a good quantum number, and negative values of K can occur independently in the basis states; the quantity $\rho_{BH}(E)$ is to be taken as the sum of the densities of the basis states over all values of K. Eq.(41) is thus higher by a factor $\sim \sigma_k(8\pi)^{\frac{1}{2}}$ than the density for an axially symmetric nucleus with $\mathcal{R}$-invariance.

The rotational states of the completely asymmetric nucleus can be built up from basis states of specified symmetry with respect to rotations through π about the three body-fixed axes. The quantum numbers for these rotations (r_1, r_2, r_3) $(r_i = \pm 1)$ fall into four sets. Any one of these sets is appropriate for the description of a single rotational band of a nucleus that lacks axial symmetry but otherwise possesses the symmetry of an ellipsoid. This is expected [34] to be the condition of a deformed actinide nucleus as it passes over the inner peak of the double-humped fission barrier. The density of its rotational states is therefore expected to be one quarter of the density for the completely asymmetric nucleus i.e. $\sigma_k(\pi/2)^{\frac{1}{2}}$ times that of the axially symmetric nucleus with $\mathcal{R}$-invariance.

5. Comparison of level density data with theory

The availability of direct experimental data against which theory can be

checked is strictly limited. For the actinides data are limited to the s-wave neutron resonances at the neutron separation energy and the low-lying excited states confined to an energy interval of about 1 to 1.5 MeV or lower. These data are limited to normal deformation ($\varepsilon \sim 0.2$). The data on class-II levels from fission intermediate structure relate to the secondary well deformation ($\varepsilon \sim 0.56$), but the effective excitation energy which is taken to be the difference of the neutron separation energy and the spontaneously fissioning isomer is poorly known for these states, the energy of the isomer having to be inferred from data on neighbouring nuclides. Level density data for the barrier deformations are not, of course, available and the theory can only be checked at these deformations by its adequacy in reproducing fission cross-sections; this comparison is made in the next section.

We have made calculations of the level density of the actinides using a simplified version of the independent quasi-particle, or particle, level density theory of Section 3 to check that the neutron resonance densities can be reproduced with reasonable values of the parameters. The basic equations that have been used are the following:

$$\Phi = \ln \Pi_i \Big\{ 1 + \sum_{s=o}^{1} \exp\left(-\beta e_i + \Sigma_{k\neq p} x_k c_{ki} + (-)^s x_p |\Omega_i|\right.$$
$$\left. + \exp\left[-2\beta(\varepsilon_i - \lambda) + 2\,\Sigma_{k\neq p} x_k c_{ki}\right]\right\}$$
$$+ \tfrac{1}{4}\beta\left[\, g_{sn}\Delta^2(E,K) + g_{sz}\Delta_z^2(E,K)\right] \qquad (42a)$$

where p labels projection of angular momentum and $|\Omega|$ is the absolute value of this quantum number for the generalised quasi-particle or single-particle level, i, written here as

$$e_i = \left[(\varepsilon_i - \lambda)^2 + \Delta^2\,(E,K)\right]^{\frac{1}{2}} + (\varepsilon_i - \lambda) - |\varepsilon_i - \lambda|$$
$$E_g = \Sigma_{i=o}^{h_n}\, 2\varepsilon_i + \left[N - 2h_n\right]e_j - \tfrac{1}{4}\, g_{sn}\Delta_{no}^2 +$$
$$\Sigma_{i=o}^{h_z}\, 2\varepsilon_i + \left[Z - 2h_z\right]e_k - \tfrac{1}{4}\, g_{sz}\,\Delta_{zo}^2 - \delta_{nz} \qquad (42b)$$

where K is the total spin-projection. The ground-state energy is written

$$E_g = \Sigma_{i=o}^{h_n}\, 2E_i + \left[N_n - 2h_n\right]e_j - \tfrac{1}{4}\, g_{sn}\Delta_{no}^2 +$$
$$\Sigma_{i=o}^{h_z}\, 2E_i + \left[N_z - 2h_z\right]e_k - \tfrac{1}{4}\, g_{sz}\Delta_{zo}^2 - \delta_{nz} \qquad (43)$$

where h_n, h_z denote the largest integers less than or equal to the numbers of

neutrons N and protons Z in the nucleus, $j = h_n + 1$, $k = h_z + 1$ and $e_\ell = [(\varepsilon_\ell - \lambda)^2 + \Delta_o^2]^{\frac{1}{2}}$. The quantity δ_{nz} is an additional binding effect available to odd-odd nuclides from the residual interaction between the final unbound neutron.

In these calculations the fermi energy is taken to be just that for an independent particle system of a given number of nucleons. The energy gap quantities $\Delta_n(E,K)$, $\Delta_z(E,K)$, are taken from the numerical behaviour as a function of excitation energy and spin projection K determined in other work [20,22]; the ground-state values Δ_{no}, Δ_{zo} are input parameters. The main purpose for the use of eq. (42,(43) in the Darwin-Fowler expressions is to allow the calculation of the independent-particle model of the state density and its trend downwards into the "superconducting" region. The Darwin-Fowler expressions are solved by iteration, starting with input approximations to β and the x_k, adjustments being made to these according to the magnitude of the differences between the successive approximations and target aims of the excitation energy and constants of the motion.

For large (but physically reasonable) values of the ground state gap quantities for neutrons and protons, Δ_{no}, Δ_{zo} the dependence of the level density on these quantities is very considerable. This is shown in Fig.1 for some typical actinides at the neutron separation energy. The single-particle level scheme used for the calculation are taken from ref.[33]. In Fig.1 the deformation $\varepsilon = 0.205$. The dependence of level density on deformation is shown for 240 Pu in Fig.2 for fixed excitation energy (E=6.52 MeV) and pairing gaps. The qualitative correlation with single-particle state density is obvious, the level density being much greater at the barriers than at the primary and secondary wells.

If the values of the pairing gap parameters Δ_{no} and Δ_{zo} are taken from neutron separation energy differences (with some smoothing) the level density results for a selection of actinides at their neutron separation energies is shown in Table 1. The calculated densities for values of the axial spin projection K=0 or $\frac{1}{2}$ agree with observation reduced to minimum J using eq. 40 within a factor of 6 or so at worst, which is about the usual degree of scatter agreement that any theory achieves. If the single particle level scheme is adjusted to give agreement with quasi-particle energies observed for 233-Pa and 231-Th, the results are improved in that immediate mass region.

This suggests reasonable validity for the model, at least at medium excitation energies, with the corollary that the collective rotation represent a full ingredient of the level density at these energies.

We are thus encouraged to extend this simplified model of independent-particle excitations to the barriers and secondary well deformation regions. Typical behaviour of the level density so calculated as a function of excitation energy with various deformations is shown in Fig.3. In these calculations the pairing gap quantities are assumed to depend on single-particle state density according to the statistical expression [35]:

$$\Delta \propto (\sinh d/G)^{-1} \tag{44}$$

where d is the single particle level spacing and G the pairing coupling constant.

The effect observed in ref.[26,25] i.e. the lower level density for the barrier deformations up to quite high excitation energies is very apparent. The calculations can be made for a range of K-values and from these the spin dispersion parameter σ_K can be deduced. These are shown in Table 2 for a range of deformations; they increase at first with increasing deformation, reflecting the fact, for the actinides, that high Ω single particle states from higher shells are brought down at the greater deformation. The σ_K value decreases markedly with decreasing excitation energy; this is shown for 233Th in Fig.4. However the level density calculations can be expected to be inaccurate at very low excitation, firstly because of the general behaviour of the Darwin-Fowler approximation, but mainly because of the treatment of the pairing gap in the calculation of the grand partition function; the energy-dependent quantity is effectively factorised out of the sum-of-states to allow the treatment of the latter as a product of independent particle factors in the usual way. Combinatorial calculations indicate considerably smaller level densities at very low energy, particularly for odd-odd nuclides.

Comparison of the calculated level density with the recommended forms of ref.[36] are shown in Table 3, in the form of ratios. The level density recommendations for actinides [36] are, for normal deformation, essentially the Gilbert-Cameron parameters [17] with a modification of the first MeV range of excitation for even and odd-A nuclides. For barrier deformations the level densities in ref.[36] are adjusted so that the fission cross-sections of a few key nuclides can be reproduced. However these parametrisations can only be good up to excitation energies of a few MeV or so. Above that they are likely (from the observation of near-constancy of fission probabilities to excitation energies of at least 10 to 20 MeV) to be similar to those of the normally deformed nucleus, but with an enhanced constant of proportionality. This enhanced constant of proportionality, which is particularly noticeable at low energies in the parametrisations of ref.[36], seems very likely to represent the rotational enhancement due to axially deformed shapes at barrier A and reflection asymmetric (pear) shapes at barrier B.

In Table 3 it is apparent that the level density computed from the microscopic model and the assumption of a normal rotational enhancement is not too different (to within a factor of 3 either direction) from the forms used in ref.[35] for normal deformation. On the other hand, for high excitation energies at barrier deformations the ratio is large, implying that the rotational enhancement is very substantial.

6. Calculation of fission cross-sections from microscopic level densities

Pioneering calculations of this kind, but applied to the excitation cross-sections for yielding spontaneously fissioning isomers were originally carried out by Britt et al [25]. Here we have used a similar, but simplified level density model to compute fission cross-sections.

Results of the present computations are shown in Figs. 5 and 6 in comparison with experimental data on the fission cross-sections of ^{240}Pu and ^{241}Am. The results of the level density calculations on the compound nucleus at barrier deformations and on the residual nucleus at normal deformation have been approximated by constant temperature forms over specific energy ranges. These parametrisations have been employed to calculate fission and neutron

transmission coefficients and hence fission cross-sections in the computer programme EVAPF described in ref.[36].

In the cases shown in Figs. 5 and 6 the computed cross-sections are clearly inadequate. At some energy the calculation approaches the data in magnitude but then falls away by up to an order of magnitude over several MeV.

In a semi-quantitative way the nature of this discrepancy may be ascribed partially to the rotational enhancement of the level density at the dominant inner barrier of axially asymmetric shape. The factor of enhancement is there $\sigma_k(\pi/2)^{\frac{1}{2}}$. Allowing for the energy dependence of the dispersion coefficient σ_k (see Fig.4) the energy dependence and magnitude of the cross-section data will to some extent be matched.

7. Cross-sections of low charge actinides

The cross-section behaviour of actinides with low charge, such as the isotopes of thorium and protoactinium, is anomalous as viewed from the framework of the double-humped fission barrier. The "giant" resonance structure exhibited by these cross-sections is explained by their correspondence to simple states of vibrational motion within a well of the fission barrier structure, but the relatively undamped nature of these resonances implies a much shallower well than the usual secondary well that is calculated from Strutinsky theory. Quite sophisticated calculations[33] in fact indicate the possible existence of a shallow well bifurcating the outer hump in the fission barrier of thorium nuclides.

A number of implications for cross-sections follow from the hypothesis of a tertiary minimum. The first is the relative lack of damping of the vibrational resonances that appear in the cross-section. The second is the overall magnitude of the fission cross-sections at above-barrier energies; this is now governed almost entirely by the level density factors at the outer barrier (the inner barrier being much lower, according to theory [39]). The collective enhancement factor for the state density at the outer barrier is only 2, the nuclear shape being reflection-asymmetric and axially-symmetric. Calculations indicate that this effect could lower the cross-section in the first few MeV above the barrier by a factor of about 2 compared with the double-humped barrier model. The third effect is that a fluctuation might be superposed on the cross-section for a limited energy range ($\sim$1-2 MeV) above the inner barrier; the modulation and amplitude for such fluctuations will be governed by the state density at the inner barrier deformation.

The vibrational resonance structure is governed very closely by the available single-particle states near the Fermi energy associated with the tertiary well. Calculations that include the effect of vibrational motion on the single-particle behaviour[36] have demonstrated that the single-particle level scheme of[33] gives a very reasonable picture of the vibrational resonances at these extreme deformations.

8. Fission cross-sections at much higher excitation energies

The calculation of fission cross-sections up to some tens of MeV of excitation energy demands a range of level density information over a wide range of energy and quite extensive chain of nuclides. Barrier densities are

required for the initially excited compound nucleus up to high excitation energy, and normal densities are required for the residual nucleus formed after emission of one neutron, in order to calculate the primary fission cross-section. To this cross-section must be added the energetically allowed (n,xnf) cross-sections; the level densities of lower mass nuclides are required not only for calculating the branching ratios along the chain, but also the distribution of excitation energy in the residual nuclei.

Our insight into the behaviour of the level density functions at these higher excitation energies is, from a quantitative point of view, severely limited. The general indications from the independent-particle model with pairing is that the barrier state densities will rise rather more rapidly (above 5 to 10 MeV excitation) than the primary well densities, owing to the greater single-particle level densities at the Fermi energy. Eventually however these differences in single-particle level density will be washed out with increasing temperature and the rates of increase at different deformations should be similar. The tendency of barrier state densities to increase especially rapidly in the intermediate excitation energy range (say 10 to 20 Mev) could well be cancelled, however, by the onset of the disappearance of the collective enhancement factor.

Extraction of empirically adjusted level density functions from neutron-induced fission cross-section data up to about 20 MeV suggests that the compensation from these two trends must be remarkably close. In ref.[38] barrier level density functions were deduced from the fission cross-sections of ^{235}U, ^{238}U, ^{237}Np and ^{239}Pu. For an odd-A nuclide the temperature deduced at about 20 MeV excitation is about 0.82, very close to the value given by the Fermi-gas formulation, eq.(29c), on the assumption that $a \approx 30$ MeV^{-1}.

Examples of level densities calculated for normal deformation and barrier deformation from our model at excitation energies up to 18 MeV are shown in Figs.7 and 8 for ^{239}Pu and ^{242}Am. The parametrised forms deduced in ref.[38] for the inner barrier are also shown for comparison. It is apparent that although the general energy dependence is very similar over a very large range of excitation energy, the calculated density lies a factor of about 3 to 5 below the empirical curve, suggesting that the rotational enhancement effect is still operating. By contrast the parametrisation for normal deformation [36], which was used in the analysis of ref.[38] by extrapolating the Fermi-gas form to these high excitation energies, is remarkably close to the curve marked $\varepsilon = 0.205$ in Fig.7.

9. Conclusions

We have surveyed the requirements of fission cross-section theory for knowledge of level densities at different deformations of the nucleus. In the normal framework of a microscopic independent-particle or quasi-particle model using realistic pairing gaps and calculated Nilsson single-particle orbitals from deformed folded Yukawa potential it is apparent, as observed in earlier work [31], that neutron resonance spacings can be reproduced within a reasonable factor, provided that the independent-particle states are taken as the band-heads of rotational states associated with an axially- and reflection-symmetric body. Although this approach represents therefore a

reasonable one to understanding the nature of level densities it is clear from the calculations of level densities at barrier deformations that it is not yet sufficiently developed to give reliable quantitative estimates of fission cross-sections.

The greatest difficulties seem to occur at lower excitation energies. Here we can expect the rotational enhancement factor for the barrier state densities to be quite strongly energy dependent, even when fully operational. At much higher excitation energies where sub-shell and pairing effects become almost fully damped out we can be more confident in the correctness of the independent-particle model, but we become increasingly uncertain of the legitimacy of including a collective enhancement effect in the barrier state densities. Our comparisons of calculation with empirically deduced barrier level densities suggest that collective enhancement is still partially operative even at excitation energies of about 18 MeV.

REFERENCES

1. H.A. BETHE, Rev.Mod.Phys.9 (1937)69

2. A.M. LANE and J.E. LYNN, Proc.Phys.Soc.A70(1957)557

3. L. DRESNER, Proc.Int.Conf.on Neutron Interactions with Nucleus, New York, USAEC Report TID-7547, p.71.

4. P.E. HODGSON, Nuclear Reaction & Structure, Clarendon, Oxford, 1971.

5. P. MOLDAUER, Phys.Rev.157(1967)907.

6. N. BOHR and J.A. WHEELER, Phys.Rev.56(1939)426.

7. D.L. HILL and J.A. WHEELER, Phys.Rev.89(1953)1102.

8. V.M. STRUTINSKY, Nucl.Phys.A95(1967)420.

9. J.E. LYNN, in Nuclear Structure, Proc.of Symposium at Dubna, (I.A.E.A., Vienna, 1968)p.463

10. H. WEIGMANN, Z.Phys.214(1968)7.

11. J.E. LYNN, in Nuclear Fission and Neutron-Induced Fission Cross-Sections, ed.A.Michaudon (Pergamon,Oxford, 1981)p.157.

12. C.E. PORTER and R.G. THOMAS, Phys.Rev.104(1956)483.

13. T.D. NEWTON, Can.J.Phys.34(1956a)804.

14. N. ROSENZWEIG, Phys.Rev.107,817(1957)

15. N. ROSENZWEIG, Proc.Int.Conf.on Study of Nuclear Structure with Neutrons, Antwerp (North-Holland,Amsterdam,1965).

16. W. DILG et al., Nucl.Phys.A217(1973)269

17. A. GILBERT, and A.G.W. CAMERON, Can.J.Phys.43(1965)1446

18. S.T. BELYAEV, Camptes rendus du congres international de physique nucleaire, ed.Gugenheimer (Dunod, Paris, 1958)p.713.

19. M. SANO and YAMASAKI, Prog.theor.Phys.29(1963)397.

20. G. KLUGE, Nucl.Phys.51(1964)41.

21. T. KAMMURI, Prog.theor.Phys.31(1964)595.

22. L.G. MORETTO, Nucl.Phys.A185,145(1972)

23. W. REISDORF, Z.Phys.A300(1981)227

24. R. BALIAN, and BLOCH, C.Ann.Phys.60(1970)401,64(1971)271,69(1972)76

25. H.C. BRITT et al, Phys.Rev.C7(1973)801.

26. T. DOSSING and A.S. JENSEN, Nucl.Phys.A222(1974)493.

27. M. BRACK et al, Rev.Mod.Phys.44(1972)320.

28. P.A. GOTTSCHALK and T. LEDERGEBER, Nucl.Phys.A278(1977)16.

29. S. BJØRNHOLM et al in Physics and Chemistry of Fission, Proc.Int.Conf. Rochester (I.A.E.A., Viennna,1974)Vol.1.,p.367.

30. J.R. HUIZENGA et al, Nucl.Phys.A223,589.

31. J.R. HUIZENGA et al, Nucl.Phys.A223,577.

32. S.K. KATARIA, V.S. RAMAMURTHY and S.S. KAPOOR, Phys.Rev.C18(1978)549.

33. P MÜLLER and J.R. NIX, Nucl.Phys.A229, 292(1974).

34. S.E. LARSSON and G. LEANDER in Physics and Chemistry of Fission Proc.Int.Conf.Rochester (I.A.E.A.,Vienna,1974)Vol.1 p.177.

35. A. BOHR and B. MOTTELSON, Nuclear Structure (Benjamin, Reading Mass) Vol.2,p652(1975).

36. S. BJØRNHOLM and J.E. LYNN, Revs.Mod.Phys.52,725(1980).

37. J.E. LYNN, J.Phys.G., in press, 1983.

38. J.E. LYNN et al, Prog.in Nucl.Ener.5, 255(1980).

39. P. MÜLLER and J.R. NIX, Proc.Int.Symp.in Physics and Chemistry of Fission, Rochester (I.A.E.A., Vienna,1974)vol.1, p.103.

TABLE I

Calculated independent quasi-particle model level densities for some actinides, using realistic gap quantities and the Nilsson orbitals of ref.[33]. The excitation energy is the neutron separation energy S_n and the compared neutron resonance data are reduced to J=0 or ½(both parities). The deformation assumed e = .205

Nucleus	S_n (MeV)	K	Δ_{no} (MeV)	Δ_{zo} (MeV)	$\rho(S_n K)$		$\rho(S_n, J=K$
					Orbitals of ref [33]	Adjusted orbitals	Expt.
^{233}Th	4.79	½	0.65	0.86	0.247×10^5	0.218×10^5	0.12×10^6
^{232}Pa	5.57	0	0.66	0.93	$.694\times10^6$	0.458×10^6	0.61×10^6
^{234}U	6.85	0	0.61	0.78	1.15×10^6	0.42×10^6	0.28×10^6
^{235}U	5.30	½	0.64	0.82	0.11×10^6	0.75×10^5	0.19×10^6
^{238}Np	5.49	0	0.62	0.86	1.73×10^6	1.42×10^6	0.24×10^6
^{239}Pu	5.66	½	0.61	0.79	0.45×10^6		0.21×10^6
^{242}Pu	6.31	0	0.58	0.72	0.37×10^6		0.48×10^6
^{242}Am	5.54	0	0.59	0.77	1.21×10^6		0.22×10^6
^{245}Cm	5.52	½	0.56	0.66	0.12×10^6		0.14×10^6

TABLE II

Calculations of the spin-projection dispersion coefficient σ_k as a function of deformation and excitation energy for ^{240}Pu Gap quantities assumed to be $\Delta_{no} = \Delta_{zo} = 0.75$

E (MeV) \ ε	.21	.42	.56	.82
5.5	5.96	6.56	7.3	6.64
6.5	6.47	7.4	7.56	7.1
7.5	7.0	8.0	7.8	7.4

TABLE III

Ratio of level density recommendation of ref.[35] to level density computed on present microscopic model

ρ[ref.35]/ρ(model)							
Nuclide	^{239}Pu	^{240}Pu		^{241}Pu		^{241}Am	^{242}Am
ε	.205	.205	.42	.205	.42	ε=.205	ε=.42
E*							
1.0							1.54
1.5	3.62	2.66	0.79	3.8	5.4	1.6	
2.0			1.28				3.5
3.0	3.02	2.45	8.61	2.13	8.3	0.3	6.0
4.0		0.67	13.4	0.83			
5.0	0.69		21.4		26.7		19.2
5.24				0.71			
5.66	0.61						
6.52		0.34				0.32	

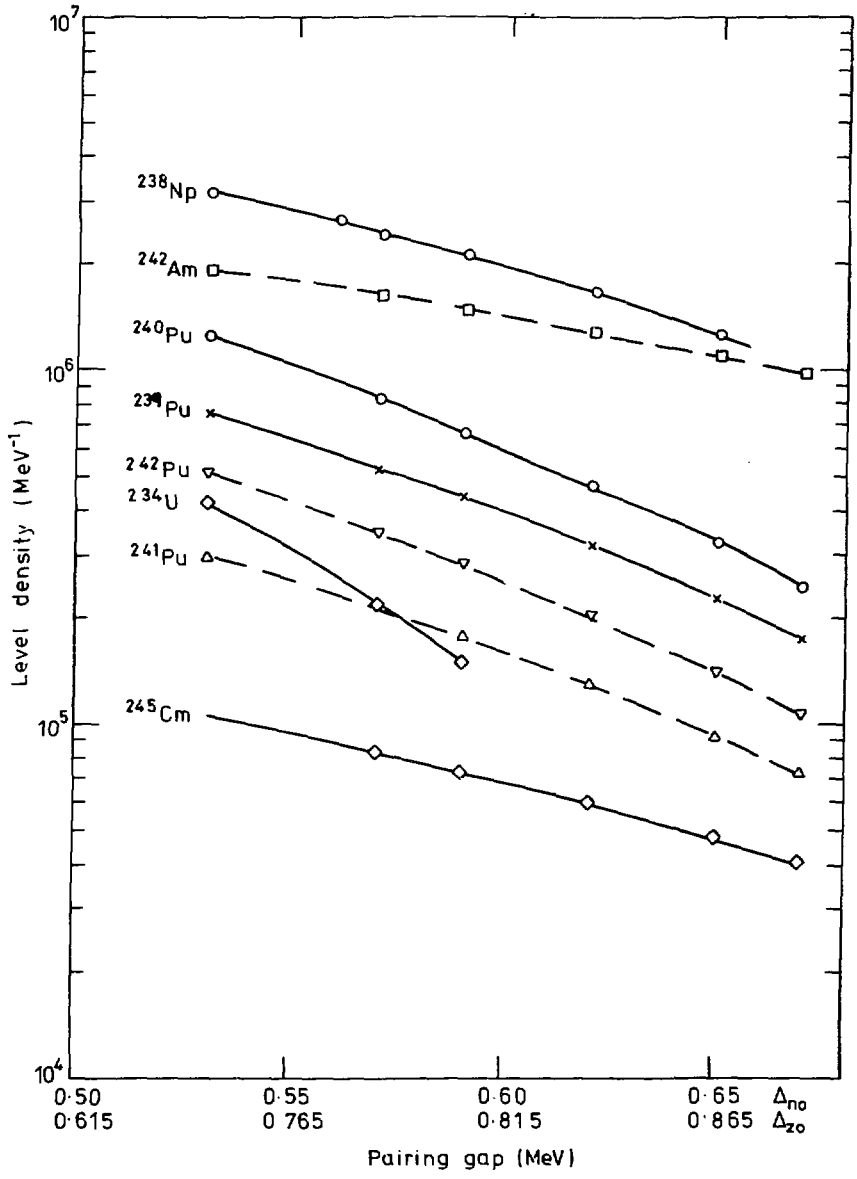

Fig.1 Level density (at the neutron separation energy) of a number of nuclides as a function of Δ_{no} and Δ_{zo}. The chosen deformation is $\varepsilon = 0.205$ (close to normal ground state deformation).

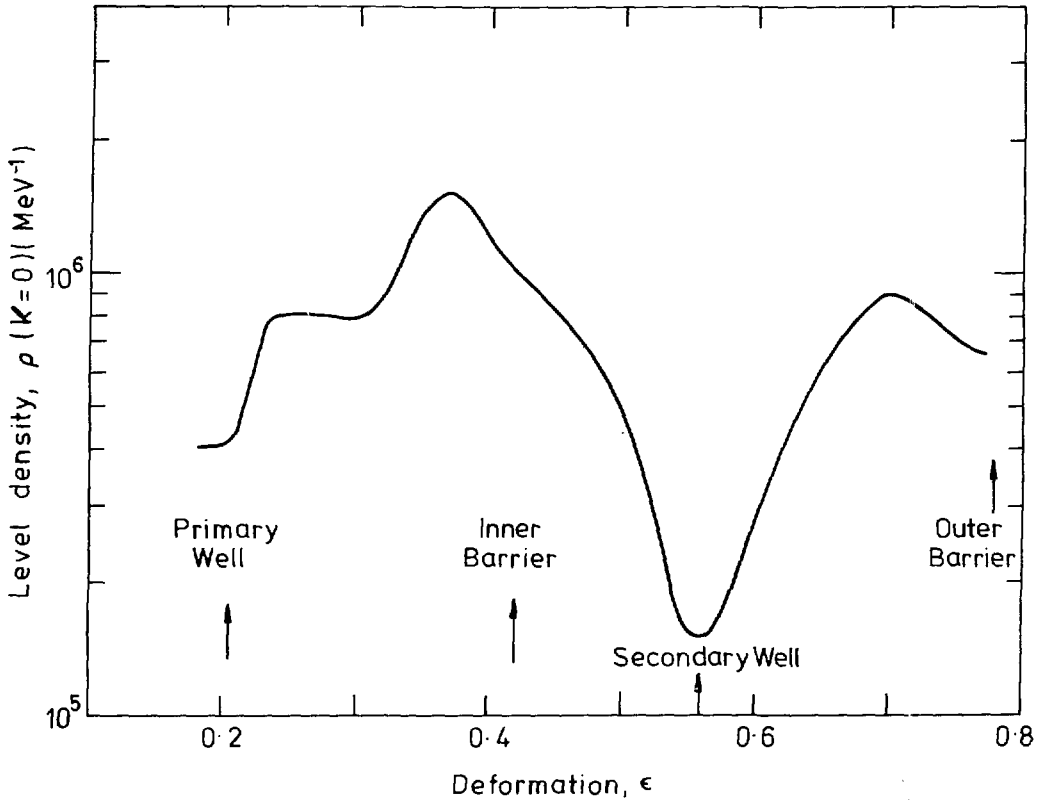

Fig.2 Level density (at the neutron separation energy) of ^{240}Pu as a function of nuclear deformation, on the assumption that $\Delta_{no} = \Delta_{zo} = 0.75$ MeV.

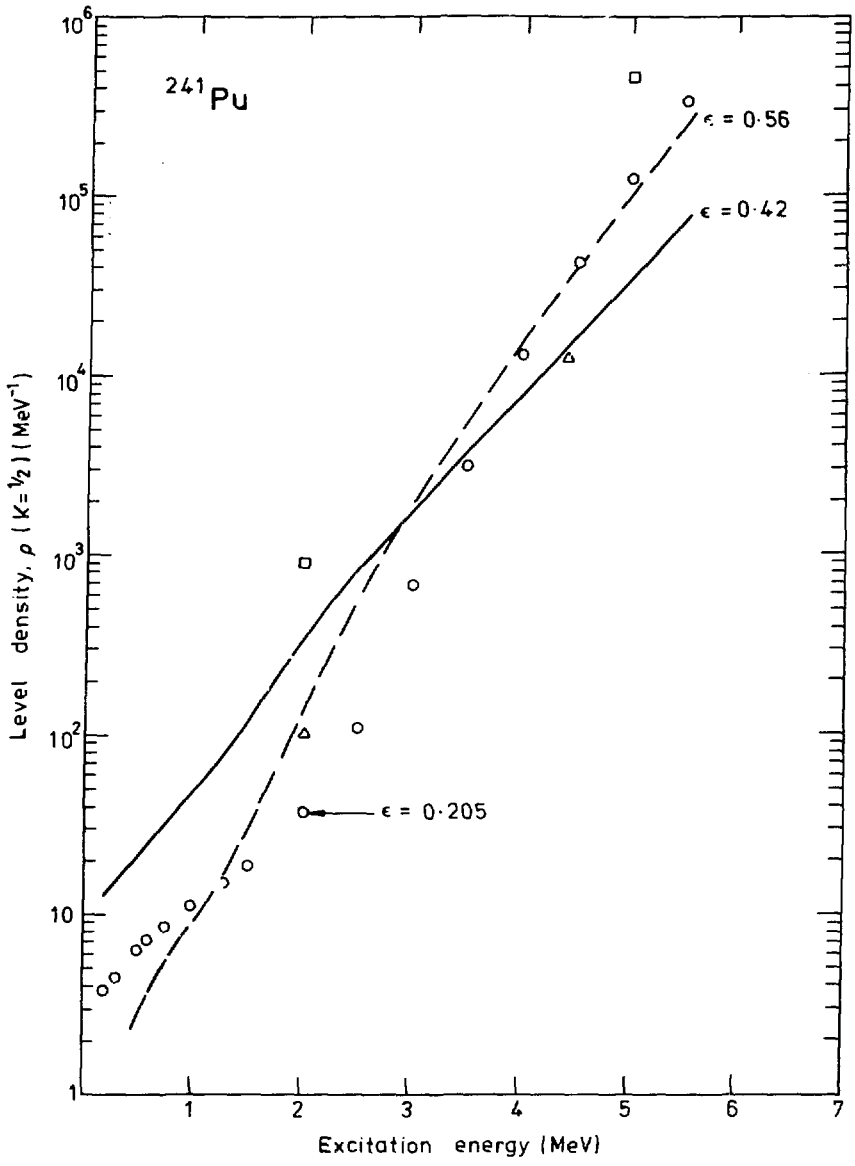

Fig.3 The level density of ^{241}Pu for K = ½ for normal, secondary well and barrier deformations. The quantities Δ_{no}, Δ_{zo} are assumed to depend on the single-particle state densities at the Fermi energies through eq.(44). Triangles (for ε = .205) and squares (for ε = .42) indicate the comparable constant temperature parametrisation of ref.[36].

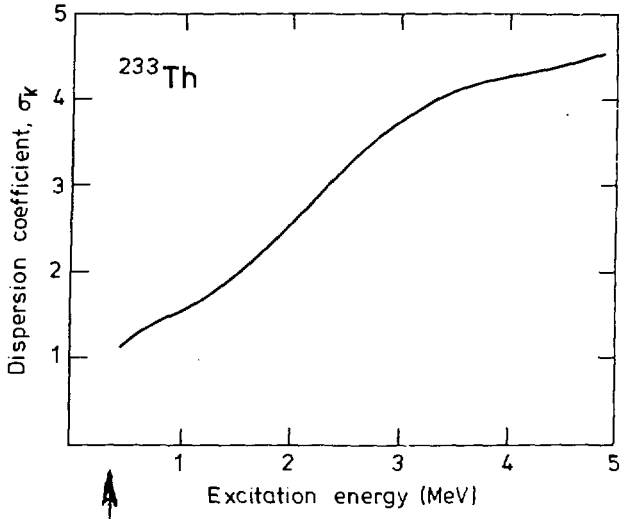

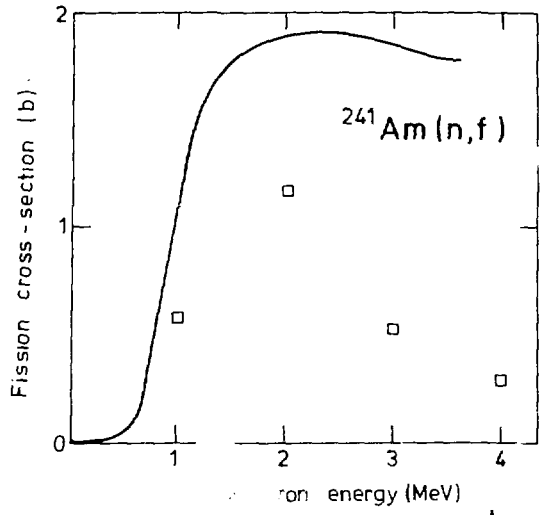

Fig.4 The calculated dependence of K-dispersion coefficient $_K$ as a function of excitation energy for ^{233}Th. The coefficient is calculated from level densities for different values of K and the assumption of a gaussian dependence on K.

Fig.6 Calculations (squares) of the fission cross-section of ^{241}Am using the model level density functions. The observed cross-section is shown by the continuous line.

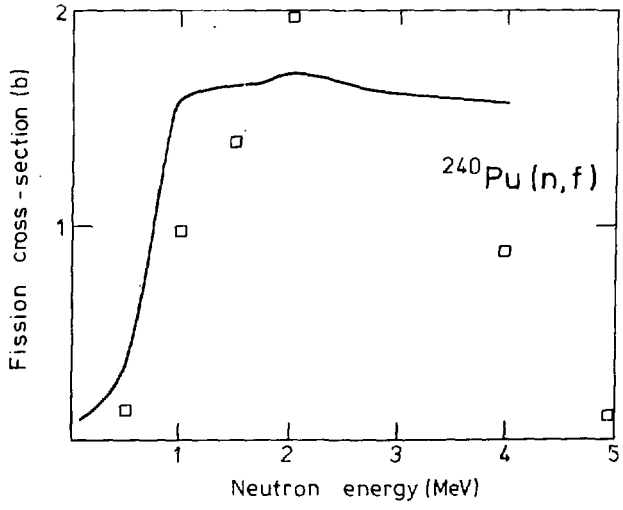

Fig.5 Calculations (squares) of the fission cross-section of ^{240}Pu using the model level density functions. The observed cross-section is shown by the continuous line.

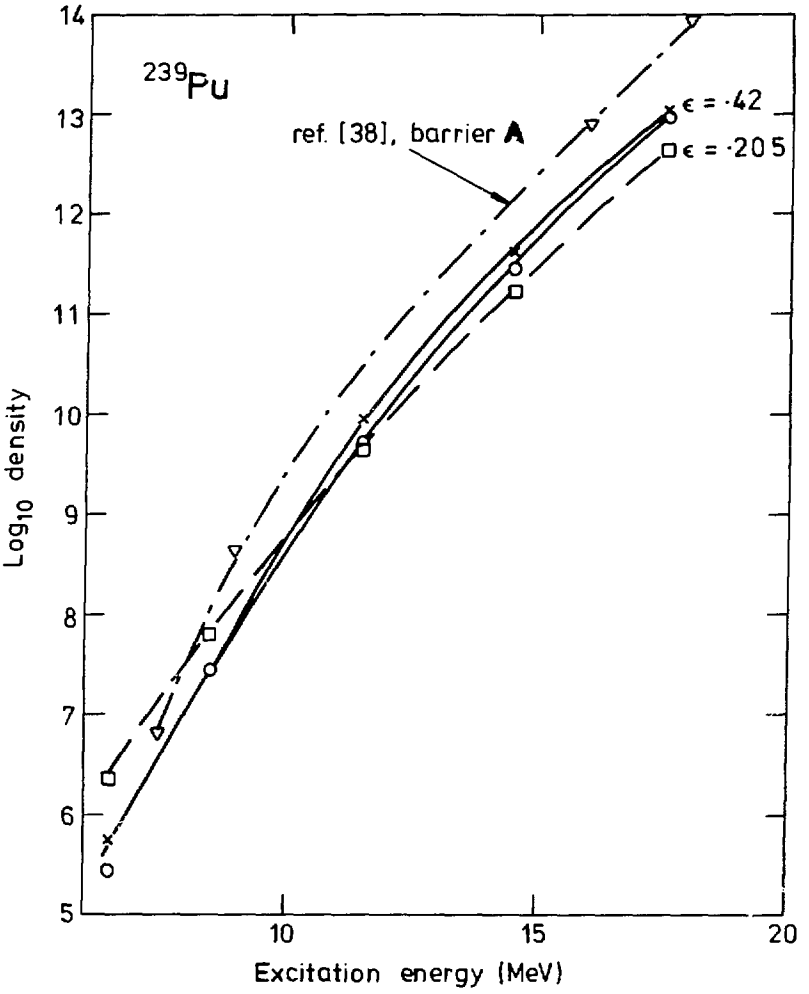

Fig.7 Calculated level density of ^{239}Pu at higher excitation energies. The empirical form of ref.[38] is also shown.

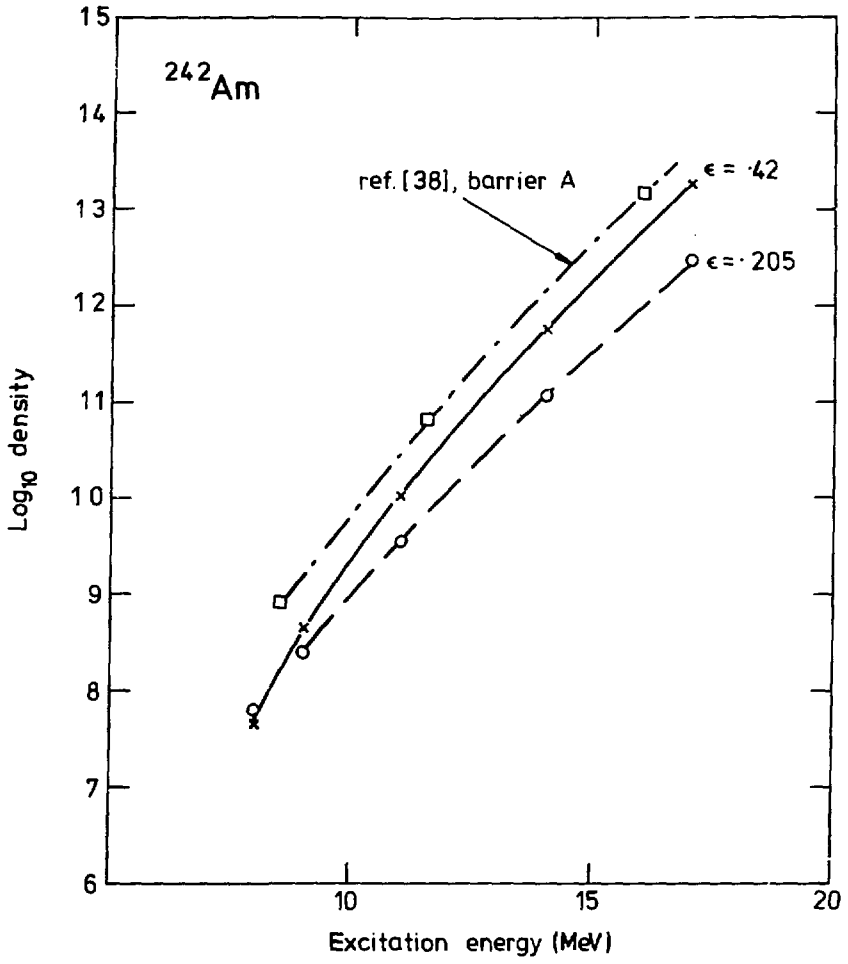

Fig.8 Calculated level density of ^{242}Am at higher excitation energies. The empirical form of ref.[38] is also shown.

TEMPERATURE-INDUCED DEFORMATION - A POSSIBLE MECHANISM FOR WASHING OUT OF SPHERICAL SHELL EFFECTS

K.-H. Schmidt, J.G. Keller, D. Vermeulen

Gesellschaft für Schwerionenforschung mbH, GSI
D6100 Darmstadt, Federal Republic of Germany

ABSTRACT

The interplay of shell structure and rotational motion in the nuclear level density is discussed. The result of a schematic calculation reveals a washing out of spherical shell effects at much lower excitation energies than expected if only the intrinsic level density is considered.

INTRODUCTION

In a recent analysis of the cross sections of heavy evaporation residues, it was deduced that the influence of spherical shells on the level density is much weaker than that of deformed shells (1).

Microscopic calculations of the intrinsic nuclear level density are well established now, and recently also the justification of analytic expressions (e.g. ref 2) has been shown (3). From this work, a different behaviour of spherical and deformed shells as a function of excitation energy is not expected.

We will discuss the interplay of shell structure and collective effects in the nuclear level density. As the role of collective effects is still under discussion, we intend only to show up some important effects in a schematic way. In particular we will investigate the possibility of a different behaviour of spherical and deformed shells as a function of excitation energy.

A SCHEMATIC MODEL FOR THE NUCLEAR LEVEL DENSITY

The intrinsic level density represents all levels of a nucleus. Collective motions may, however, lower several levels considerably. This leads to an increase of the level density at low excitation energies. Rotational motions may be included at low excitation energies by superposing a rotational band on each intrinsic level. This "rotational enhancement" is expected to be damped into the intrinsic background at higher energies. Qualitative considerations about this damping are published by Bjørnholm, Bohr and Mottelson (4). They discuss that a separation between rotational motion and intrinsic motion can only be preserved at temper-

atures low enough to ensure a well defined deformation of the nucleus. Bjørnholm et al. propose a limit of $T = 40\ \mathrm{MeV}\ A^{1/3}\ \delta$. The dependence of the limiting temperature T on the deformation δ causes an interesting interplay of shell effects and rotational enhancement.

For a qualitative consideration, the rotational enhancement was assumed to be exponentially washed out (in analogy to the influence of shell effects on the level density). This was achieved by an additional factor $1+\sigma^2\exp(-E^*/aT^2)$ in the nuclear level density with σ being the spin cutoff parameter and a being the level density parameter. Only axially symmetric shapes were considered.

Guided by microscopic calculations, we treated the deformation dependence of the shell effects by the following analytic expression:

$$\delta U = \delta U_o \cos(\Theta/0.47 - \Theta_o)\ \exp(-\Theta^2/2.2)$$
$$\text{with } \Theta = 0.671\ \delta\ A^{1/3}$$

The parameters δU_o and Θ_o were adjusted to reproduce the experimental shell effect and deformation of the ground state including the liquid drop energy.

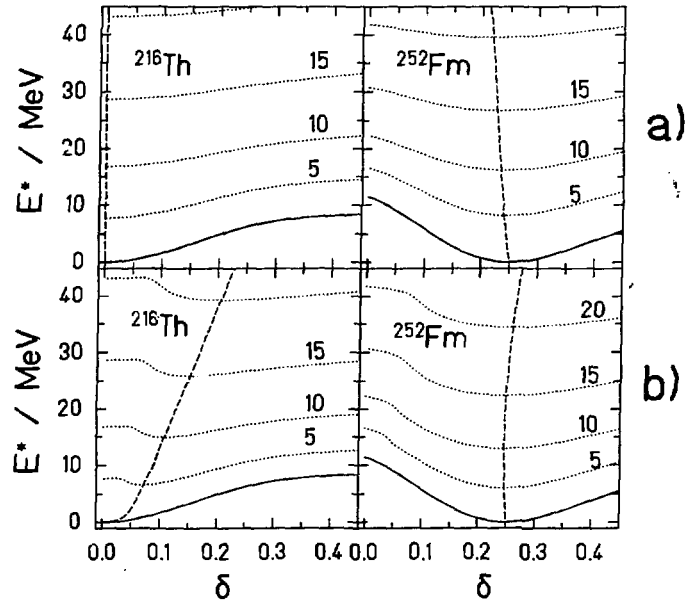

Fig. 1: The schematically calculated nuclear level density without a) and with b) the inclusion of rotational levels for a spherical (^{216}Th) and a deformed nucleus (^{252}Fm). The dotted contour lines are labeled with the height of the nuclear level density ($\log^{10}(\rho/\mathrm{MeV}^{-1})$) for zero angular momentum. The dashed lines connect the configurations with a maximum level density.

In fig. 1, the calculated nuclear level density is shown as a function of excitation energy and deformation for a spherical and a deformed magic

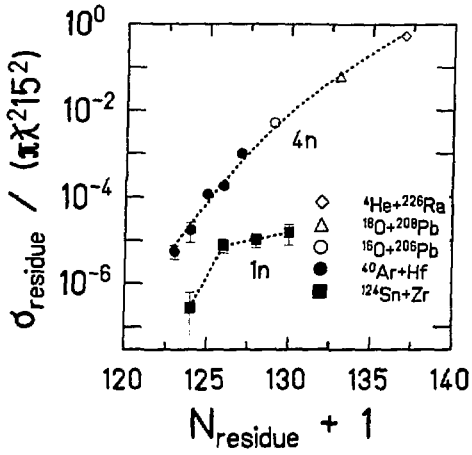

Fig. 2: The maxima of the 1n- and the 4n-cross sections as a function of the neutron number(6-8). The factor $1/(\pi\lambda^2 15^2)$ was applied in order to remove trivial entrance channel effects for different target projectile combinations and to make the abcissa approximately equal to the survival probability $\Pi(\Gamma_n/\Gamma_{tot})$ times the transmission coefficient of the fusion barrier for low angular momentum (7).

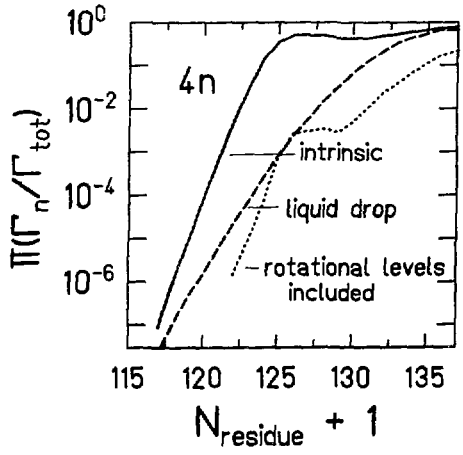

Fig. 3: The survival probability $\Pi(\Gamma_n/\Gamma_{tot})$ for zero angular momentum, calculated for the systems shown in fig. 2, using different level densities.

nucleus. The inclusion of rotational enhancement changes things drastically. As the limiting temperature increases with deformation, a nucleus which is spherical in the ground state will be driven to deformation at higher excitation energies because of the gain of rotational levels. This fact was already stated in ref. (5), however, without considering shell effects. Consequently, spherical shell effects will be washed out at much lower excitation energies when the rotational enhancement is included, whereas the influence of deformed shells remains nearly unchanged.

COMPARISON WITH EXPERIMENTAL DATA

For Thorium, evaporation residue cross sections have been measured over a long isotopic chain, crossing the spherical N=126 shell. The maxima of the 1n- and the 4n-cross sections are shown in fig. 2. While the 1n cross sections show a pronounced structure at N=126, the 4n cross sections seem to be influenced only little by the strong shell effect around ^{216}Th. The calculated survival probability, shown in fig. 3, reproduces this behaviour when only liquid drop properties of the nuclei are considered. As the existence of the shell effect in the ground state masses is known experimentally, a mechanism is needed to wash out the shell structure in the level density at low excitation energy. The inclusion of the rotational levels brings the survival probability in the range of the experimental data. However, the remaining shell structure seems still to be somewhat too strong.

CONCLUSION

The rotational enhancement leads to a temperature-induced deformation which tends to destroy a spherical shell effect in the nuclear level density at rather low excitation energies. This general statement is independent of the special schematic model used in this work, if only collective motions tend to enhance the total level density with increasing deformation. At energies above 20 to 30 MeV where the shell effect in the intrinsic level density is destroyed by the nuclear temperature, the behaviour of the collective levels is not essential for the described additional shell smearing mechanism.

REFERENCES

(1) J.G. KELLER et al.,
Report IKDA 81/7, Institut für Kernphysik, TH Darmstadt, 1981

(2) A.V. IGNATYUK et al., Sov. J. Nucl. Phys. 21 (1975) 255

(3) K.-H. SCHMIDT et al., Z. Phys. A308 (1982) 215

(4) S. BJØRNHOLM, A. BOHR and B.R. MOTTELSON,
Proc. Conf. Phys. a. Chem. of Fission,
Rochester 1973, IAEA Vienna 1974, Vol. I, p. 367

(5) S.E. VIGDOR and H.J. KARWOWSKI, Phys. Rev. C26 (1982) 1068

(6) C.C. SAHM, Private Communication (1983)

(7) K.-H. SCHMIDT et al., Proc. Conf. Phys. a. Chem. of Fission,
Jülich 1979, IAEA Vienna 1980, Vol. 1, p. 409

(8) J.G. KELLER et al.,
Report IKDA 81/5, Institut für Kernphysik, TH Darmstadt, 1981

PAIRING CORRECTION FOR PARTICLE-HOLE STATE DENSITIES

C. Y. Fu

Oak Ridge National Laboratory
Oak Ridge, Tenn. 37830 U.S.A.

ABSTRACT

The pairing correction proposed by Ignatyuk and Sokolov for particle-hole state densities has been examined. It has been found that the accuracy of the correction is sufficient for practical applications only if the system is in its normal state ($\Delta = 0$). In the superfluid state ($\Delta \neq 0$), a consistent pairing-Pauli correction is developed here for improved accuracy. Practical implementations of the pairing correction are given and further developments are outlined.

INTRODUCTION

The particle-hole state density formula widely used for preequilibrium reaction calculations is given by Williams [1]:

$$\omega(p,h,U) = \frac{g(gU - A)^{n-1}}{p!h!(n-1)!} \quad , \tag{1}$$

with the usual notations. The Pauli correction, A, is given by [1]:

$$A = (p^2 + h^2 + p - 3h)/4g \quad . \tag{2}$$

A pairing correction, to be added to A, has been proposed by Ignatyuk and Sokolov [2]:

$$P = \frac{1}{4}\, g(\Delta_0^2 - \Delta^2) \quad , \tag{3}$$

where Δ_0 and $\Delta(U,n)$ are, respectively, the ground-state and the excited-state gap parameters; $\Delta(U,n)$ is calculated from a set of pairing equations in the uniform model [2,3].

However, the accuracy of the pairing correction is unknown. Calculations of Δ for given U and n are difficult. The corrections, P and A, are inconsistent where $\Delta \neq 0$. These are problems that inspire the present work.

CONSISTENT PAIRING-PAULI CORRECTION

The Pauli correction, A, was derived [1] on the basis of a uniform single-particle level spacing, 1/g. If the system is in a region where $\Delta \neq 0$, one has to deal with quasiparticle energies and the level spacing can no longer be considered as uniform. However, an effective level spacing, $1/g_e$, may be inferred from the minimum excitation energy for given n, which has been derived by Moretto [3]:

$$U_{min} = \frac{1}{4} g(\Delta_0^2 - \Delta^2) + \frac{n}{2} \sqrt{(n/2g)^2 + \Delta^2} \quad , \tag{4}$$

where the first term is the change in condensation energies from the ground state to the excited state. This change is an energy loss and is the pairing correction proposed by Ignatyuk and Sokolov. The second term is the additional energy needed to excite n/2 particles from just below the Fermi surface to just above. Compairing this energy with $n^2/4g$, the minimum excitation energy for a system without the pairing interaction, one obtains the effective level spacing:

$$\frac{1}{g_e} = \sqrt{(1/g)^2 + (2\Delta/n)^2} \quad . \tag{5}$$

Replacing 1/g in Eq. (2) by $1/g_e$ leads to a modified Pauli correction:

$$A_p = A \sqrt{1 + (2g\Delta/n)^2} \tag{6}$$

that is consistent with P and U_{min}.

ACCURACY OF THE PAIRING CORRECTION

Calculations using Eq. (1) with A replaced by $P + A_p$ are shown in Fig. 1 in comparison with a calculation by Moretto [3] using the saddle-point approximation. Except for n = 2, the agreement is good. For n = 2, the saddle-point approximation lacks accuracy [3] while the present calculation above 3 MeV (where $P \approx 0$ and $A_p = 0$) is nearly exact [1]. Thus the present pairing correction may be considered sufficiently accurate. The dashed lines were calculated with the original Pauli correction A only, to illustrate the importance of the pairing correction.

Use of P + A instead of $P + A_p$ in Eq. (1) results in an increase in the state densities up to a factor of two where $\Delta \neq 0$, so the consistent pairing Pauli correction derived here is the more accurate.

PRACTICAL IMPLEMENTATIONS

All relevant quantities were solved numerically and iteratively from a set of pairing equations in terms of reduced variables so that the results depend only on U and n, but not on the parameters g and Δ_0. The results were then parameterized as explicit functions of U and n. In term of $C = (1/4) g\Delta_0^2$, $n_c = (\ln 4) g T_c$ with $T_c = 2\,\Delta_0/3.5$, the minimum excitation energy (threshold), U_{min}, is calculated from:

$$\frac{U_{min}}{C} = \begin{cases} 3.23\,\dfrac{n}{n_c} - 1.57\,(n/n_c)^2 & \text{if } n/n_c \leqslant 0.446\,, \\ 1 + 0.627\,(n/n_c)^2 & \text{if } n/n_c > 0.446. \end{cases}$$

The pairing gap parameters, $\Delta(U,n)$, are calculated from:

$$\frac{\Delta}{\Delta_0} = 0.996 - 1.76\,(n/n_c)^{1.60} \Big/ (U/c)^{0.68}$$

if $U/c \geqslant 0.716 + 2.44\,(n/n_c)^{2.17}$, otherwise $\Delta = 0$. These results define the pairing correction P to 3% on the average up to $U/c < 80$.

FURTHER DEVELOPMENTS

Several useful developments involving pairing effects are in progress and have to do with spin distributions, two kinds of particles, and consistency with the Fermi-gas level density formulas.

ACKNOWLEDGEMENTS

This work was performed under the auspices of the U.S. Department of Energy under contract W-7405-eng-26 with the Union Carbide Corporation.

REFERENCES

1. F. C. Williams, Nucl. Phys. A166, 231 (1971).

2. A. V. Ignatyuk and Yu. V. Sokolov, Sov. J. Nucl. Phys. 17, 376 (1973).

3. L. G. Moretto, Nucl. Phys. A243, 77 (1975).

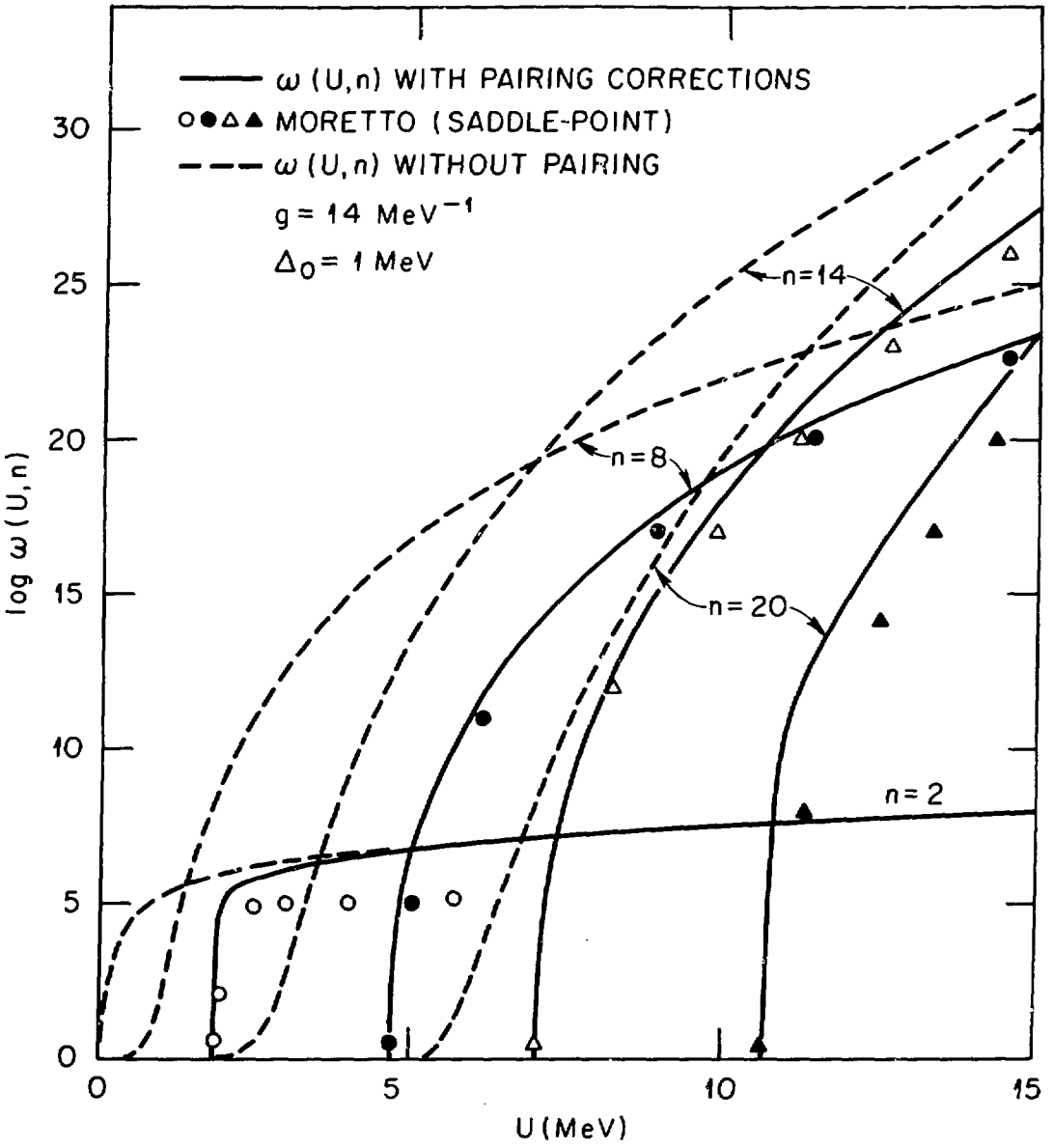

Fig. 1. Calculated particle-hole state densities with and without pairing correction and comparison with a direct calculation by Moretto [3]. The present calculation with pairing correction (solid curves) and Moretto's calculation (symbols) have the same thresholds.

SEMI CLASSICAL APPROACH TO NUCLEAR LEVEL DENSITIES

J. TREINER

Division de Physique Théorique[x], Institut de Physique Nucléaire,
F-91406 ORSAY CEDEX

A significant progress has been achieved, within the past decade, in the study of the shell effects on nuclear level densities. This is illustrated in fig.1, where are plotted the values of the level density parameter extracted from neutron resonance level spacings using either (fig.1-b) Bethe's expression —which is derived assuming an equidistant single particle (s.p.) spectrum— either (fig.1-a) a method incorporating in a simple way the shell structure of the s.p. spectrum [1.a]. The method is sketched in Dr. Ramamurthy's contribution to this conference.

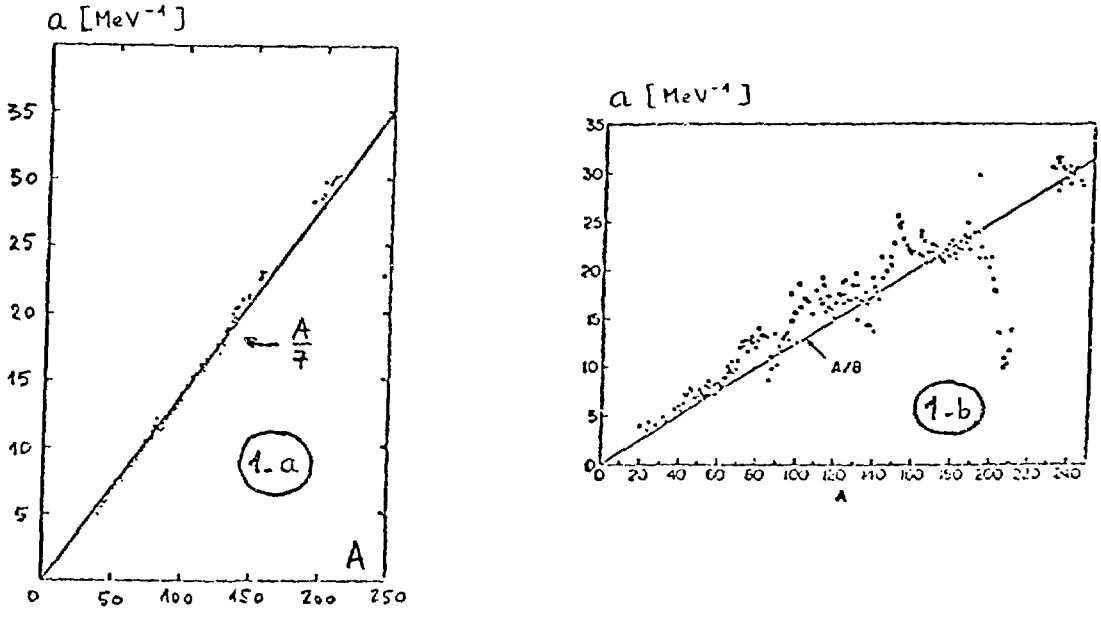

Fig.1 : systematic of level density parameters a) from ref [1.a] b) from ref [1.b]

[x] Laboratoire associé au C.N.R.S.

One can see that no fluctuations remain in the systematics of a : one may thus consider that the macroscopic part of a which we shall denote a_{LDM} is now well determined experimentally ; indeed a rather detailed and interesting feature of the systematics of the level density parameter could even be pinpointed in ref [1a], namely the fact that, when one considers a series of isotopes, a_{LDM} shows a minimum for the β-stable element. Another interesting aspect is the determination of the variation of the surface energy coefficient with excitation energy : from the data plotted on fig.1-b a negative temperature correction was found, whereas model calculations using a Hill-Wheeler box as well as a harmonic oscillator predict an increase of surface energy with temperature [2,3]. Different studies using Woods-Saxon potentials [4] have discussed these various aspects and a dependence of a_{LDM} on the separation energies has been proposed. However if one is to explain such a refined effect as the isospin one mentioned above, a self-consistent approach is clearly necessary.

We shall now present some of the recent theoretical results obtained using a semi classical approach —the Thermal Thomas Fermi (TTF) method. A very simple formula can be given for a_{LDM} which exhibits the properties of the nuclear effective interaction involved. Notice that the method does not allow to treat shell effects so that it is essential to have at our disposal experimental values where these effects have been removed.

The TTF method [5]

Let us first briefly sketch how the Hartree-Fock (HF) method is generalized to finite temperature (THF). The semi classical approximation is then straightforward. The system is described by a HF hamiltonian H which, in the case of a Skyrme type effective interaction, is a function of the density and the kinetic energy density only. The equilibrium state at temperature T is calculated by minimizing the free energy $F = H - TS$, where S is the entropy. S is calculated using the non-interacting Fermi gas expression :

$$S = - \sum n_\alpha \ln n_\alpha + (1-n_\alpha) \ln (1-n_\alpha) \qquad (1)$$

where n_α is the occupation number of particle state α with energy ε_α :

$$n_\alpha = \frac{1}{1 + \exp \frac{\varepsilon_\alpha - \mu}{T}} \tag{2}$$

The chemical potential μ is determined by the normalization condition

$$\sum_\alpha n_\alpha = A$$

The density ρ_α and the kinetic energy density τ_α are given by

$$\rho_\alpha = \sum_\alpha n_\alpha |\phi_\alpha|^2 \tag{3}$$

$$\tau_\alpha = \sum_\alpha n_\alpha |\nabla \phi_\alpha|^2 \tag{4}$$

and the ϕ_α 's and ε_α 's are solutions of a set of HF equations

$$\left[- \vec{\nabla} \frac{\hbar^2}{2m^*} \vec{\nabla} + U \right] \phi_\alpha = \varepsilon_\alpha \phi_\alpha \tag{5}$$

$$U = \frac{\delta H}{\delta \rho} \tag{6}$$

$$\frac{\hbar^2}{2m^*} = \frac{\partial H}{\partial \tau} \tag{7}$$

where m^* denotes the nuclear effective mass, whose origin lies in the non locality of the HF potential (in the case of a Skyrme type interaction, $\hbar^2/2m^*$ is a linear function of ρ). The TTF method is now straightforwardly derived : one assumes plane waves with momentum k for the states ϕ_α and replaces the discret sums in eqs (3) and (4) by integrals over k . One gets the following equations :

$$\rho = \frac{1}{2\pi^2} \left(\frac{2m^* T}{\hbar^2} \right)^{3/2} J_{1/2}(\eta) \tag{8}$$

$$\tau = \frac{1}{2\pi^2} \left(\frac{2m^* T}{\hbar^2} \right)^{5/2} J_{3/2}(\eta) + \beta \frac{(\nabla \rho)^2}{\rho} + \gamma \Delta \rho \tag{9}$$

(the corrective terms in β and γ in eq.(9) represent the $\hbar^2$- corrections to the pure Thomas-Fermi functional).

$$S = \frac{5}{3}\frac{\hbar^2}{2m^*}\frac{1}{T}\frac{1}{2\pi^2}\left(\frac{2m^*T}{\hbar^2}\right)^{5/2} J_{3/2}(\eta) - \eta\rho \tag{10}$$

where
$$J_\nu(\eta) = \int_0^\infty \frac{x^\nu}{1+\exp(x-\eta)} \tag{11}$$

$$\eta = \frac{1}{T}(\mu - U) \tag{12}$$

One can now make a low temperature expansion of the Fermi integrals $J_\nu(\eta)$:

$$J_{1/2}(\eta) \sim \frac{2}{3}\eta^{3/2}\left(1+\frac{\pi^2}{8\eta^2}\right) \tag{13}$$

$$J_{3/2}(\eta) \sim \frac{2}{5}\eta^{5/2}\left(1+\frac{5\pi^2}{8\eta^2}\right) \tag{14}$$

This allows one to write for the energy and the free energy

$$E(T) = E_0 + a_{LDM}T^2 \tag{15}$$

$$F(T) = E_0 - a_{LDM}T^2 \tag{16}$$

where E_0 is the ground state energy and a_{LDM} is given by

$$a_{LDM} = \frac{\pi^2}{4}\sum_{n,p}\int \rho_q^0 \frac{2m_q^*}{\hbar^2 k_{F_q}^2}\, d\vec{r} \tag{17}$$

Notice that a_{LDM} is expressed in function of the equilibrium nucleon densities ρ_q^0 at $T=0$ which makes it particularly easy to calculate. The change in ρ_q will appear at the order T^4 only in the expansion of the free energy. Consequently the effective interaction appears explicitely

through the effective mass only (of course it plays an indirect role in determining the equilibrium density profiles).

Temperature dependence of the surface and curvature energy coefficients

Next, assuming a Fermi shape for the nucleon density, we can derive from eq.(17) an $A^{-1/3}$ expansion of a_{LDM}, by use of the following theorem [6] : if f denotes a Fermi distribution with radius R and surface diffuseness d, then for any value of ν and for integer μ's,

$$\int f^{\nu} r^{\mu} dr = \frac{R^{\mu+1}}{\mu+1}\left[1+(\mu+1)\sum_{k=0}^{\mu}\binom{\mu}{k}\eta_{\nu}^{(k)}\left(\frac{d}{R}\right)^{k+1} + o\left(e^{-\frac{R}{d}}\right)\right] \tag{18}$$

with

$$\eta_{\nu}^{(k)} = (-)^{k}\int_{0}^{\infty}\left[\frac{1+(-)^{k}e^{-u\nu}}{(1+e^{-u})^{\nu}} - 1\right]u^{k}du$$

writing

$$a_{LDM} = a_{v}A + a_{s}A^{2/3} + a_{c}A^{1/3} \tag{19}$$

one gets

$$a_{v} = \frac{\pi^{2}}{4}\frac{2m^{*}}{\hbar^{2}k_{F}^{2}} \tag{20}$$

$$a_{s} = \frac{m}{m^{*}}a_{v}\left[\frac{3d}{r_{0}}\left(\eta_{1/3}^{0} - \left(1-\frac{m^{*}}{m}\right)\eta_{4/3}^{0}\right) - 6\frac{\varepsilon_{s}}{K}\left(1-\frac{1}{3}\frac{m^{*}}{m}\right)\right] \tag{21}$$

In eq.(21) ε_{s} denotes the surface energy and K the incompressibility modulus. An expression can also be derived for a_{c} but we shall not write it with full length here as it is rather involved, due to the fact that, besides the leading term, which writes :

$$a_{c}^{L} = \frac{m}{m^{*}}a_{v}\frac{6d^{2}}{r_{0}^{2}}\left[\eta_{1/3}^{(1)} - \eta_{1}^{(1)} - \left(1-\frac{m^{*}}{m}\right)\left(\eta_{4/3}^{(1)} - \eta_{1}^{(1)}\right)\right] \tag{22}$$

a number of small corrective terms, arising from the central compression of the nucleus, have to be added to a_{c}^{L} (they involve in particular the surface and the curvature energy coefficients).

The values of the $\eta_{\nu}^{(k)}$'s are the following

$\eta^{(0)}_{4/3} = 2.55482$ $\qquad$ $\eta^{(0)}_{4/3} = -0.44518$

$\eta^{(1)}_{4/3} = 9.13381$ $\qquad$ $\eta^{(1)}_{1} = \frac{\pi^2}{6}$ $\qquad$ $\eta^{(1)}_{4/3} = 1.46935$

Taking some typical values $m^*/m \simeq 0.8$, $k_F \simeq 1.35\ \mathrm{fm}^{-1}$, $\varepsilon_s = 20$ MeV, $d = 0.55$ fm, $K = 200$ MeV, one gets

$$a_v = 0.052\ \mathrm{MeV}^{-1}$$
$$a_s = 0.22\ \mathrm{MeV}^{-1}$$
$$a_c^L = 0.67\ \mathrm{MeV}^{-1}$$

One thus sees that the temperature dependence of both the surface and the curvature energy coefficient is positive, and large (compared to the volume contribution). For example for A = 216 one gets

$$a_{LDM} = 0.052 \times 216 + 0.22 \times 36 + 0.67 \times 6$$
$$= 11.23 + 7.92 + 4.02 = 23.17\ \mathrm{MeV}^{-1}$$

Although surface and curvature corrections appear to contribute as much as the volume term (this is due to the fact that the integrand in eq.(17) goes like $\rho^{1/3}$, i.e. decreases very slowly), the value of a_{LDM} is still too small compared to the experimental value $a_{LDM} = 30\ \mathrm{MeV}^{-1}$ (see fig.1). Self consistent calculations including Coulomb and asymmetry effects show that the discrepancy of $\sim$ 25% cannot still be removed. Clearly a physical effect is missing, which will be analyzed below. Let us first briefly show how the isospin behaviour of a_{LDM} in a series of isotopes can be understood from eq.(17).

Isospin behaviour of a_{LDM}

We have already mentioned that it seems that a_{LDM} shows a minimum value for the β-stable isotope. We shall now see that this effect is related to the behaviour of the surface contribution to a_{LDM}. Eq.(21) shows that is roughly proportional to the surface diffuseness d which is different for neutrons and protons in the case of a neutron excess. Now the internal and external part of the surface are determined by different nucleon properties [7] : in particular the external part of the surface d_{out} is directly related to the separation energy S_q $(q = n, p)$: $d^q_{out} \sim 1/\sqrt{S_q}$: As S_n decreases

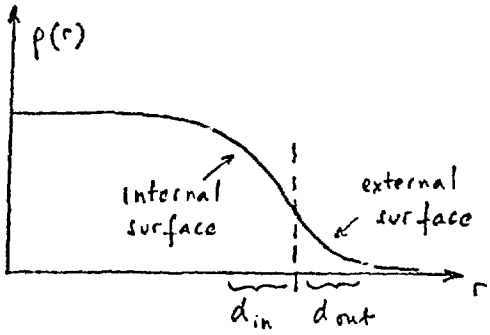

and S_p increases (both roughly linearly) with increasing asymmetry it follows that d^n_{out} increases while d^p_{out} decreases. As for the internal surface thickness one can show, from semi classical arguments [7] that d_{in} is the same for neutrons and protons (i.e. varies as I^2), so that the difference between the total neutron and proton surface thickness is due to the differences in S_n and S_p. As a result a^n_{com} increases and a^p_{com} decreases with increasing asymmetry. This explains the dependence of a_{com} on the separation energies proposed in ref.[1.a]. Besides, one understands qualitatively that these opposite behaviours of a^n_{com} and a^p_{com} may produce a minimum in the sum a_{com}. This minimum is indeed obtained when one feeds eq.(17) with the self consistent extended Thomas-Fermi ground state densities. It is interesting to note that the semi classical interpretation of this fact involves a rather detailed feature of the nucleon densities, indeed not established experimentally, namely the evolution of the nuclear surface thickness with asymmetry.

Effective masses in nuclei

Let us now turn to the analysis of the discrepancy of ~ 25% observed between experimental values and values calculated using eq.(17). As the equilibrium densities cannot be at fault, the origin of the discrepancy must lie in the effective mass.

In the HF scheme, the effective mass m^* arises from the non locality of the potential. The smaller the value of m^*, the smaller the corresponding density of states ; a value of m^* in the range (0.6 - 0.8) leads to a reasonable agreement with experiment concerning the deep states but not in the vicinity of the Fermi surface ; optical model analysis show that m^* should show an energy dependence [8], raising its value up to ~ 1.2 near the Fermi surface. This effect is beyond the HF approach and is not present in the

starting assumptions leading to eq.(17). However it can be incorporated simply as follows:

In a semi classical picture, the Fermi surface corresponds to the geometrical surface, in the sense that the nuclear surface is built up mainly by the states near the Fermi level (high angular momentum means less bound states). Thus the energy dependence of the effective mass can be converted into a modified r -dependence, schematically represented in fig.2 :

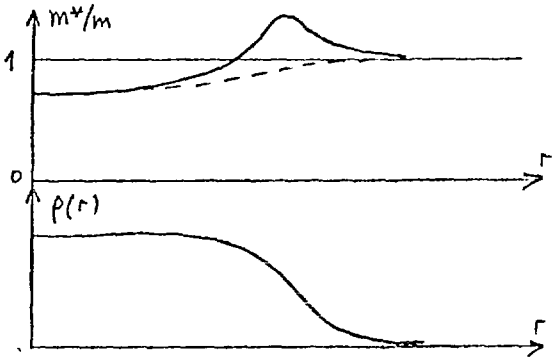

fig.2

such a modified $m^*(r)$ incorporated in a HF calculation leads to a density of particle states in good agreement with experiment near the Fermi surface as well as for the deep states, and removes the discrepancy in the calculated a_{LDM} Of course the volume term a_v (eq.(20)) remains unchanged. The change appears in the surface and curvature contributions, which are increased by $\sim$ 50%. Analysis along these lines have been carried out recently in refs.[9-10]. One of the interesting consequences pointed out in ref.[9] concerns the fission barrier : a rapid evaluation shows for example that the fission barrier in ^{240}Pu is reduced by a factor of ~ 2 at a temperature of $T = 1.5$ MeV, i.e. at an excitation energy of $\sim$ 70 MeV.

To summarize, one can say that the semi classical approach provides a satisfactory scheme explaining the known features of the macroscopic systematics of the level density parameters. The transparency of the method makes it easy to incorporate the experimental information in the nuclear effective interaction used in more microscopic approaches.

REFERENCES

[1.a] S.K. Kataria, V.S. Ramamurthy and S.S. Kapoor, Phys. Rev. C18 (1978) 549

[1.b] A. Gilbert and A.G.W. Cameron, Can. J. Phys. 43 (1965) 1446.

[2] J. Treiner, Workshop on semi classical methods in Nuclear Physics, *ILL Grenoble 1981*

[3] J. Töke and W. Swiatecki, Nucl. Phys. A372 (1981) 141

[4] S.K. Kataria and V.S. Ramamurthy, Nucl. Phys. A349 (1980) 10

[5] J.R. Buchler and R.I. Epstein, Ap. J. Lett. 235 (1980) 73
M. Barranco and J. Treiner, Nucl. Phys. A351 (1981) 269

[6] H. Krivine and J. Treiner, J. Math. Phys. 22 (1981) 2484

[7] J. Treiner and H. Krivine, Orsay preprint IPNO/TH 82-18

[8] G.E. Brown, J.H. Gunn and P. Gould, Nucl. Phys. 46 (1963) 598
J.P. Jeukenne, A. Lejeune and C. Mahaux, Phys. Reports 25C (1976) 83
V. Bernard and N.V. Giai, Nucl. Phys. A348 (1980) 75

[9] X. Campi and S. Stringari, Z. Phys. A309 (1983) 239

[10] M. Prakash, J. Wambach and Z.Y. Ma, Stony Brook preprint.

Chairman's Concluding Remarks

J.E. Lynn

I have discovered since coming here that one of the duties as Chairman is to give a closing talk. I believe that this is due to the excellent organizing ability of Dr. Pronyaev, who anticipated correctly that time would remain after the summaries of the Working Group meetings before the official closing time of 12 noon. That gives me 52 minutes: however, I shall disappoint Dr. Pronyaev by refusing to use all this time.

I do not wish to give here anything that may be interpreted as a definitive summary of this meeting, but rather to give my personal impressions as a physicist who has not specialized particularly deeply in its subject matter.

May I first of all say that if this meeting is typical of the Advisory Group meetings held by the Agency, then they are extremely hard-working meetings. Even on Wednesday, for example, our excursion day, some of us found ourselves subjected to a mathematical minimization project, organized by Sol Pearlstein. The objective of this project was to minimize the time we spent in the Atlantic City Casinos. The process adopted was to walk the full length of the Atlantic City board-walk in both directions. This certainly achieved its stated aim, which is just as well, for the experimentally determined

results of the rate of increase of density of funds close to the Casino gaming tables turned out to be very high, but, unlike the level density function, also negative, although it was observed that there were fluctuations in this rate; but these, being statistical Ericson-type fluctuations, rather than predictable intermediate structure resonances, could not be used to any advantage. However, it seems particularly appropriate that the only member of our group who comes from a non-capitalist society was the only one to make a net profit; it amounted, I believe, to 50 cents.

The subject of this Advisory Group meeting should be viewed within the overall political and financial climate surrounding nuclear technology at the present time. Over many years there have been increasing pressures from governments to decrease expenditure in this field, especially in the basic research that is directly relevant to it. At the same time it is apparent that with the increasing sophistication and extension of technological developments in nuclear power, the demands in range and quality of nuclear data are certainly going to continue and probably increase in the longer term. To meet these demands when, at the same time, the amount of experimental effort that is being funded in this field is markedly decreasing, the importance of being able to calculate many of the required nuclear data from nuclear theory, or to be able to use theory as a reliable tool in helping to evaluate the available experimental data (including its interpolation and extrapolation) is now very great.

Within this context the role of knowledge of the nuclear level density is of paramount importance, and it is most timely in view of the problems and difficulties of the subject, and at the same time the significant progress

that is nevertheless being made on these problems, that the IAEA should have called this meeting.

I believe that this meeting has brought much illumination to the perspectives of the subject. The way in which level density theory can be used in data applications, applications that arise in several fields of science and technology, were admirably summarized in the opening paper and enlarged upon subsequently by several speakers. The theory itself was approached from several angles. The importance of phenomenological approaches to the problem was emphasized both from the point of view of the simplicity of the analytical formulae produced for level density description, and from that of the surveyability of the parameterization required. Within this approach, some of the mathematical developments that we heard about were most impressive.

The so-called microscopic approaches seem to be based on two distinct philosophies. One is the belief that the use of a realistic representation of single-particle level schemes will allow a more realistic calculation of the level density for an individual nucleus, especially if some account is taken of the major residual two-body forces that are not included in the potential well used to describe the single-particle scheme. Normally this is taken to be the pairing force. We heard about the developments in this field and the important attempts to link the results to those of phenomenological approaches. The other philosophy concentrates especially upon the residual forces, and techniques, such as the moment methods, important progress in which was described at this meeting, attract much interest. The computer time required for such calculations is clearly high, and probably prohibits their

use in large general reaction codes. But nevertheless I feel that developments along these lines will be most important in underpinning our understanding of these level density problems and hence our confidence in using simpler methods for actual calculations.

A very important sub-area of methods that seek to incorporate the more subtle features of the Hamiltonian into the derivation of level densities concerns the treatment of angular momentum, particularly in deformed nuclei. The question of the validity of the rotational enhancement factor at moderate to high excitation energies is a controversial one. The work described at this meeting that seeks to investigate the question quantitatively from a fundamental basis is therefore clearly a valuable new departure. In relation to this, there was also much discussion about the spin cut-off factor, a quantity which appears in all kinds of problems ranging from calculation of nuclear reaction cross sections to the interpretation of resonance level sequences.

We also heard about significant progress in evaluating level densities for specified particle-hole number combinations, a topic that has assumed much importance as the role of pre-equilibrium mechanisms for higher energy reactions has become identified.

The difficulties found in the theoretical study of the nuclear level density are mirrored in the experimental study of the problem and these in turn interact with and complicate the verification of theory. This meeting has concentrated particularly on the means by which reliable information on level densities can be deduced from raw experimental data, and again

considerable progress has been reported, both in the direct (resonance region) data and the less direct (evaporation spectra) data. Brute force measurements of level spectrum data were also discussed in one talk, but this is a topic to which we were unable, in the time available, to give full attention.

I shall not attempt to summarize the summaries of the Workshop sessions that occupied the second part of our meeting. It is sufficient to say that these seem to me to give an excellent overall and definitive view of the state of the subject and several valuable recommendations for future work to resolve presently seen problems, particularly those that relate to the use of level density knowledge in the field of technology.

Finally, on behalf of the participants in this meeting, may I express our deep thanks to the Nuclear Data Section IAEA particularly Dr. Pronyaev, for organizing the program of this meeting in very difficult circumstances, and to all our hosts at Brookhaven National Laboratory for the excellent local organization, and the fine hospitality, social arrangements, and care that they have lavished upon us.

IAEA ADVISORY GROUP MEETING ON
BASIC & APPLIED PROBLEMS OF NUCLEAR LEVEL DENSITIES

Brookhaven National Laboratory, U.S.A.
11 - 15 April 1983

PROGRAM

(I = Invited; C = Contributed)

Monday morning, 11 April

9:00 - 9:15	Opening of the Meeting Election of Chairman and Secretaries
9:15 - 9:55	R. C. Haight (Lawrence Livermore National Laboratory) (I) APPLIED USES OF NUCLEAR LEVEL DENSITIES
9:55 - 10:05	Discussion
10:05 - 10:45	S. M. Grimes (Ohio University) (I) MOMENT METHOD CALCULATIONS OF NUCLEAR LEVEL DENSITIES
10:45 - 10:55	Discussion
10:55 - 11:10	(Coffee break)
11:10 - 11:50	G. Maino and E. Manapace (ENEA, Bologna) (C) A NILSSON-BCS MICROSCOPIC APPROACH FOR LEVEL DENSITIES, EXTENDED TO ODD NUCLEI AND RELATED PHENOMENOLOGICAL PARAMETERS
11:50 - 12:00	Discussion
12:00 - 14:00	(Lunch)

Monday afternoon, 11 April

14:00 - 14:15	T. Raya Halemane (State University College, Fredonia) (C) LEVEL DENSITY APPROACH TO PERTURBATION THEORY AND INVERSE-ENERGY-WEIGHTED SUM-RULES

14:15 - 14:25	Discussion
14:25 - 14:40	S. Raman (Oak Ridge National Laboratory) (C) BRUTE FORCE LEVEL DENSITY
14:40 - 14:50	Discussion
14:50 - 15:30	A. M. Anzaldo Meneses (Inst. fur Neutronenphysik, Karlsruhe) (I) APPLICATION OF NUMBER THEORETICAL METHODS FOR THE CALCULATION OF NUCLEAR LEVEL DENSITIES
15:30 - 15:40	Discussion
15:40 - 15:55	C. Jacquemin (Inst. de Physique Nucleaire, Orsay) (C) EXACT CALCULATION OF LEVEL DENSITIES FOR NON INTERACTING MANY-FERMION SYSTEMS
15:55 16:05	Discussion
16:05 - 16:20	(Coffee break)
16:20 - 17:00	C. Kalbach (Triangle Universities, Durham) (I) PARTICLE-HOLE STATE DENSITIES FOR PRE-EQUILIBRIUM REACTION CALCULATIONS AND FOR CLOSED AND OPEN CONFIGURATIONS
17:00 - 17:10	Discussion
17:10 - 17:25	H. Gruppelaar (ECN, Petten) (C) LEVEL DENSITY IN UNIFIED PREEQUILIBRIUM AND EQUILIBRIUM MODELS
17:25 - 17:35	Discussion
18:00	Mixer (North Room, Brookhaven Center) Courtesy of the IAEA

Tuesday morning, 12 April

9:00 - 9:40	G. Hansen and A. S. Jensen (University of Aarhus) (I) ENERGY DEPENDENCE OF THE ROTATIONAL ENHANCEMENT FACTOR IN THE LEVEL DENSITY
9:40 - 9:50	Discussion
9:50 - 10:30	V. S. Ramamurthy, S. K. Kataria, S. S. Kapoor (BARC, Bombay) (I) REVIEW OF RECENT PHENOMENOLOGICAL APPROACHES TO THE DESCRIPTION NUCLEAR LEVEL DENSITIES

10:30 - 10:40	Discussion
10:40 - 10:45	(Coffee break)
10:45 - 11:25	G. Reffo (ENEA, Bologna) (I) LIMITS AND VALIDITY OF THE PHENOMENOLOGICAL GILBERT-CAMERON LEVEL DENSITY APPROACH
11:25 - 11:33	Discussion
11:33 - 12:13	F. H. Fröhner (Inst. fur Neutronenphysik, Karlsruhe) (I) STATISTICAL INFERENCE OF LEVEL DENSITIES FROM RESOLVED RESONANCE PARAMETERS
12:13 - 12:35	Discussion
12:35 - 14:00	(Lunch)

Tuesday afternoon, 12 April

14:00 - 14:40	P. Ribon (C.E.N. Saclay) (I) EXTRACTION OF INFORMATION ON NUCLEAR LEVEL DENSITIES FROM THE RESONANCE REGION
14:40 - 14:50	Discussion
14:50 - 15:30	H. Vonach (Inst. fur Radiumforschung und Kernphysik, Vienna) (I) EXTRACTION OF LEVEL DENSITY INFORMATION FROM NON-RESONANT REACTIONS
15:30 - 15:40	Discussion
15:40 - 15:55	(Coffee break)
15:55 - 16:35	G. H. Rohr (CBNM, Geel) (I) SYSTEMATICS OF THE NUCLEAR LEVEL DENSITIES
16:35 - 16:45	Discussion
17:30 - 18:30	Cocktail Party (Berkner Hall) Courtesy of the Associated Universities Inc.
18:30 - 20:30	Banquet
20:30	Concert (Berkner Hall)

Wednesday morning, 13 April

9:00 - 9:40	E. D. Arthur (Los Alamos National Laboratory) (presented by Dave Madland (LANL)) (I) THE IMPACT OF NUCLEAR LEVEL DENSITY MODELS ON CROSS SECTION CALCULATIONS
9:40 - 9:50	Discussion
9:50 - 10:30	J. E. Lynn (AERE Harwell) (I) FISSION CROSS-SECTIONS AND THE NUCLEAR LEVEL DENSITY
10:30 - 10:40	Discussion
10:40 - 10:55	(Coffee break)
10:55 - 11:10	K-H. Schmidt, J. G. Keller and D. Vermeulen (GSI, Darmstadt) (C) TEMPERATURE - INDUCED DEFORMATION - A POSSIBLE MECHANISM FOR WASHING OUT OF SPHERICAL SHELL EFFECTS
11:10 - 11:20	Discussion
11:20 - 11:35	C. Y. Fu (Oak Ridge National Laboratory) (C) PAIRING CORRECTION FOR PARTICLE-HOLE STATE DENSITIES
11:35 - 11:45	Discussion
11:45 - 12:15	J. Treiner (Institut de Physique Nucleaire, Orsay) (C) SEMI-CLASSICAL APPROACH TO NUCLEAR LEVEL DENSITIES

Wednesday afternoon, 13 April

12:15 SHARP	Coach leaves for excursion to Atlantic City from Berkner Hall. (Boxed lunch served in the coach.)

Thursday, 14 April

Working Group discussions and drafting of reports.

Friday morning, 15 April

9:00 - 10:00	WORKSHOP I: S. M. Grimes NUCLEAR LEVEL DENSITY THEORIES AND NUCLEAR MODEL REACTION CROSS-SECTION CALCULATIONS
10:00 - 11:00	WORKSHOP II: F. H. Fröhner and H. Vonach EXTRACTION OF NUCLEAR LEVEL DENSITY INFORMATION FROM EXPERIMENTAL DATA
11:00	J. E. Lynn CHAIRMAN'S CONCLUDING REMARKS
12:00	Adjournment

LIST OF ATTENDEES

DR. A.M. ANZALDO MENESES
KERNFORSCHUNGSZENTRUM
KARLSRUHE. INR.
POSTFACH 3640
D-7500 KARLSRUHE
WEST GERMANY

DR. M. R. BHAT
BLDG. 197D
NATIONAL NUCLEAR DATA CENTER
BROOKHAVEN NATIONAL LABORATORY
UPTON, NY 11973

DR. THOMAS BURROWS
BLDG. 197D
NATIONAL NUCLEAR DATA CENTER
BROOKHAVEN NATIONAL LABORATORY
UPTON, NY 11973

DR. ROBERT E. CHRIEN
BLDG. 510A
PHYSICS DEPT.
BROOKHAVEN NATIONAL LABORATORY
UPTON, NY 11973

DR. M. DIVADEENAM
BLDG. 197D
NATIONAL NUCLEAR DATA CENTER
BROOKHAVEN NATIONAL LABORATORY
UPTON, NY 11973

DR. CHARLES L. DUNFORD
BLDG. 197D
NATIONAL NUCLEAR DATA CENTER
BROOKHAVEN NATIONAL LABORATORY
UPTON, NY 11973

DR. F.H. FROEHNER
INST. FUER NEUTRONENPHYSIK
AND REAKTORTECHNIK
KERNFORSCHUNGSZENTRUM
KARLSRUHE
POSTFACH 3640
D-7500 KARLSRUHE
WEST GERMANY

DR. C. Y. FU
NEUTRON PHYSICS DIV.
OAK RIDGE NATIONAL LAB.
P. O. BOX X
OAK RIDGE, TN 37830

DR. DONALD G. GARDNER
LAWRENCE LIVERMORE NAT. LAB.
P.O. BOX 808
LIVERMORE, CA. 94550

DR. M.A. GARDNER
L-234
LAWRENCE LIVERMORE NAT. LAB.
P.O. BOX 808
LIVERMORE, CA. 94550

DR. STEVE M. GRIMES
DEPT. OF PHYSICS
OHIO UNIVERSITY
ATHENS, OH 45701

DR. HARM GRUPPELAAR
NETHERLANDS ENERGY RESEARCH
FOUNDATION ECN
P.O. BOX 1
NL-1755 ZG
PETTEN NH
THE NETHERLANDS

DR. R.C. HAIGHT
L-405
LAWRENCE LIVERMORE NAT. LAB.
P.O. BOX 808
LIVERMORE, CA. 94550

DR. THIRUMALA RAYA HALEMANE
PHYSICS DEPT.
STATE UNIV. COLLEGE
FREDONIA, NY 14063

DR. M. HILLMAN
BLDG. 815
BROOKHAVEN NATIONAL LABORATORY
UPTON, NY 11973

DR. NORMAN E. HOLDEN
BLDG. 197D
NATIONAL NUCLEAR DATA CENTER
BROOKHAVEN NATIONAL LABORATORY
UPTON, NY 11973

DR. C. JACQUEMIN
INSTITUT DE PHYSIQUE NUCLEAIRE
UNIVERSITY PARIS SUD
I.P.N. BP 1 91406
ORSAY CEDEX FRANCE

DR. HELMUT JAHN
KERNFORSCHUNGSZENTRUM
KARLSRUHE. INR.
POSTFACH 3640
D-7500 KARLSRUHE
WEST GERMANY

DR. AKSEL S. JENSEN
INSTITUTE OF PHYSICS
UNIVERSITY OF AARHUS
DK-8000 AARHUS C
DENMARK

DR. C. KALBACH
T.U.N.L-PHYSICS DEPT.
DUKE UNIVERSITY
DURHAM, NC 27706

DR. ROBERT R. KINSEY
BLDG. 197D
NATIONAL NUCLEAR DATA CENTER
BROOKHAVEN NATIONAL LABORATORY
UPTON, NY 11973

DR. J. E. LYNN
NUC. PHYSICS DIVISION
HANGAR 8
AERE HARWELL
CHILTON,DIDCOT
OXON, GREAT BRITAIN

DR. DAVID G. MADLAND
T2 MS-B243
LOS ALAMOS NATIONAL LAB.
P.O. BOX 1663
LOS ALAMOS, NM 87545

MR. B. A. MAGURNO
BLDG. 197D
NATIONAL NUCLEAR DATA CENTER
BROOKHAVEN NATIONAL LABORATORY
UPTON, NY 11973

DR. F. M. MANN
W/A-4
WESTINGHOUSE HANFORD
P. O. BOX 1970
RICHLAND, WA 99352

DR. E. MENAPACE
CENTRO DE CALCOLO DEL CNEN
VIA MAZZINI 2
I-40138 BOLOGNA
ITALY

DR. P.A. MOLDAUER
BLDG. 316
ARGONNE NATIONAL LAB.
9700 SOUTH CASS AVE.
ARGONNE, IL 60439

DR. S. F. MUGHABGHAB
BLDG. 197D
NATIONAL NUCLEAR DATA CENTER
BROOKHAVEN NATIONAL LABORATORY
UPTON, NY 11973

DR. S. PEARLSTEIN
BLDG. 197D
NATIONAL NUCLEAR DATA CENTER
BROOKHAVEN NATIONAL LABORATORY
UPTON, NY 11973

DR. V. PRONAJAEV
WAGRAMERSTRASSE 5
NUCLEAR DATA SECTION
I.A.E.A.
P.O. BOX 100
A-1400 VIENNA
AUSTRIA

DR. V.S. RAMAMURTHY
NUCLEAR PHYSICS DIVISION
BHABHA ATOMIC RESEARCH CENTRE
BOMBAY-400085
INDIA

DR. S. RAMAN
PHYSICS DIVISION
OAK RIDGE NATIONAL LAB.
P. O. BOX X
OAK RIDGE, TN 37830

DR. G. REFFO
CENTRO DE CALCOLO DEL CNEN
VIA MAZZINI 2
I-40138 BOLOGNA
ITALY

DR. PIERRE RIBON
DPRMA-SERMA
CEN-SACLAY
B.P. NO 2
F-91190 GIF SUR YVETTE
FRANCE

DR. G. ROHR
BUREAU CENTL DES MESURES
NUCLEAIRES
STEENWEG NAAR RETIE
B-2440 GEEL
BELGIUM

DR. P. ROSE
BLDG. 197D
NATIONAL NUCLEAR DATA CENTER
BROOKHAVEN NATIONAL LABORATORY
UPTON, NY 11973

DR. ROBERT SCHENTER
HANFORD ENG. DEVEL. LABORATORY
WESTINGHOUSE HANFORD
P. O. BOX 1970
RICHLAND, WA 99352

DR. KARL-HEINZ SCHMIDT
GES. FÜR SCHWERIONENFORSCHUNG
GSI DARMSTADT POSTFACH 110541
D 6100 DARMSTADT
WEST GERMANY

DR. BRIGITTE STROHMAIER
UNIV. WIEN
INST. FUER RADIUMFORSCHUNG
UND KERNPHYSIK
BOLTZMANNGASSE 3
A-1090 VIENNA IX
AUSTRIA

DR. JACQUES TREINER
INSTITUT DE PHYSIQUE NUCLEAIRE
UNIVERSITY PARIS SUD
I.P.N. BP 1 91406
ORSAY CEDEX FRANCE

DR. J.K. TULI
NUC. DATA PROJECT
BLDG. 197D
NATIONAL NUCLEAR DATA CENTER
BROOKHAVEN NATIONAL LABORATORY
UPTON, NY 11973

DR. H. VONACH
UNIV. WIEN
INST. FUER RADIUMFORSCHUNG
UND KERNPHYSIK
BOLTZMANNGASSE 3
A-1090 VIENNA IX
AUSTRIA

NEUTRON DATA REFERENCES

Element	Quantity	Energy (eV) Min	Max	Type	Documentation Ref	Page	Date	Lab	Comments
^{40}Ca	Lvl Density	5.0+5	8.0+6	Theo	BNL-NCS-51694		Apr83	BOL	Reffo.PG203.GRPH CALC CFD LVL SCHEME
^{40}Ca	Lvl Density	1.2+7	7.6+7	Theo	BNL-NCS-51694		Apr83	PAR	Jacquemin.PG105.GRPHS CALC CFD EXACT
^{56}Fe	$\sigma_{dif.inl}$	2.5+6	8.5+6	Theo	BNL-NCS-51694		Apr83	BOL	Reffo.PG203.GRPHS ANGDIST CFD EXPT.
^{60}Ni	Lvl Density	8.5+6	4.0+6	Theo	BNL-NCS-51694		Apr83	BOL	Reffo.PG203.GRPHS SPIN CUTOFF E DEP.
^{60}Ni	Lvl Density		2.8+7	Theo	BNL-NCS-51694		Apr83	LAS	Arthur.PG311.GRPHS CALC CFD EXPT
^{63}Cu	$\sigma_{n,p}$	1.5+7		Theo	BNL-NCS-51694		Apr83	LAS	Arthur.PG311.GRPH CALC CFD EXPT
^{63}Cu	Lvl Density	NDG		Theo	BNL-NCS-51694		Apr83	LAS	Arthur.PG311.GRPH DIFF.CALC.CFD
^{65}Cu	σ_{nem}	8.5+6		Theo	BNL-NCS-51694		Apr83	LAS	Arthur.PG311.GRPH CALC CFD EXPT
^{65}Cu	$\sigma_{n,p}$	1.5+7		Theo	BNL-NCS-51694		Apr83	LAS	Arthur.PG311.GRPH CALC CFD EXPT
^{65}Cu	Lvl Density	1.0+6	1.4+7	Theo	BNL-NCS-51694		Apr83	LAS	Arthur.PG311.GRPH CALC LVL DENSITY
^{89}Y	$\sigma_{n,\gamma}$	1.0+5	1.2+6	Theo	BNL-NCS-51694		Apr83	LAS	Arthur.PG311.CALC M/G CFD EXPT
^{90}Zr	$\sigma_{n,2n}$	1.2+7	1.5+7	Theo	BNL-NCS-51694		Apr83	LAS	Arthur.PG311.CALC CFD EXPT
^{90}Zr	$\sigma_{n,p}$	6.0+6	1.5+7	Theo	BNL-NCS-51694		Apr83	LAS	Arthur.PG311.P SPECT.CALC M/G CFD EX
^{93}Nb	Lvl Density	2.0+5	2.0+7	Theo	BNL-NCS-51694		Apr83	RCN	Gruppelaar.PG143.TBL.CALC CFD CALCS.
^{100}Mo	$\sigma_{n,\gamma}$	1.0+5	7.0+6	Theo	BNL-NCS-51694		Apr83	LAS	Arthur.PG311.GRPH SPIN-CUTOFF
^{116}Sn	Lvl Density	5.0+5	4.0+6	Theo	BNL-NCS-51694		Apr83	BOL	Reffo.PG203.GRPH CALC CFD LVL SCHEME
^{124}Te	Lvl Density	4.0+6	2.0+7	Theo	BNL-NCS-51694		Apr83	BOL	Maino+PG75.GRPHS,TBL.PHENOMEN.PARS.
^{126}Te	Lvl Density	4.0+6	2.0+7	Theo	BNL-NCS-51694		Apr83	BOL	Maino+PG75.GRPHS,TBL.PHENOMEN.PARS.
^{127}Te	Lvl Density	4.0+6	2.0+7	Theo	BNL-NCS-51694		Apr83	BOL	Maino+PG75.GRPHS,TBL.PHENOMEN.PARS.
^{130}I	Lvl Density	4.0+6	2.0+7	Theo	BNL-NCS-51694		Apr83	BOL	Maino+PG75.GRPHS,TBL.PHENOMEN.PARS.
^{132}Xe	Lvl Density	4.0+6	2.0+7	Theo	BNL-NCS-51694		Apr83	BOL	Maino+PG75.GRPHS,TBL.PHENOMEN.PARS.
^{131}Ba	Lvl Density	4.0+6	2.0+7	Theo	BNL-NCS-51694		Apr83	BOL	Maino+PG75.GRPHS,TBL.PHENOMEN.PARS.
^{136}Ba	Lvl Density	4.0+6	2.0+7	Theo	BNL-NCS-51694		Apr83	BOL	Maino+PG75.GRPHS,TBL.PHENOMEN.PARS.
^{136}Ba	Lvl Density	2.5+6	1.8+7	Theo	BNL-NCS-51694		Apr83	BOL	Reffo.PG203.GRPHS SPIN CUTOFF E DEP.
^{137}Ba	Lvl Density	4.0+6	2.0+7	Theo	BNL-NCS-51694		Apr83	BOL	Maino+PG75.GRPHS,TBL.PHENOMEN.PARS.
^{137}Ba	Lvl Density	5.0+5	3.0+6	Theo	BNL-NCS-51694		Apr83	BOL	Reffo.PG203.GRPH CALC CFD LVL SCHEME
^{138}Ba	Lvl Density	4.0+6	2.0+7	Theo	BNL-NCS-51694		Apr83	BOL	Maino+PG75.GRPHS,TBL.PHENOMEN.PARS.
^{139}Ba	Lvl Density	4.0+6	2.0+7	Theo	BNL-NCS-51694		Apr83	BOL	Maino+PG75.GRPHS,TBL.PHENOMEN.PARS.
^{139}La	Lvl Density	4.0+6	2.0+7	Theo	BNL-NCS-51694		Apr83	BOL	Maino+PG75.GRPHS,TBL.PHENOMEN.PARS.
^{141}Ce	Lvl Density	4.0+6	2.0+7	Theo	BNL-NCS-51694		Apr83	BOL	Maino+PG75.GRPHS,TBL.PHENOMEN.PARS.
^{142}Pr	Lvl Density	4.0+6	2.0+7	Theo	BNL-NCS-51694		Apr83	BOL	Maino+PG75.GRPHS,TBL.PHENOMEN.PARS.
^{143}Nd	Lvl Density	4.0+6	2.0+7	Theo	BNL-NCS-51694		Apr83	BOL	Maino+PG75.GRPHS,TBL.PHENOMEN.PARS.
^{144}Nd	Lvl Density	4.0+6	2.0+7	Theo	BNL-NCS-51694		Apr83	BOL	Maino+PG75.GRPHS,TBL.PHENOMEN.PARS.

Element	Quantity	Energy (eV) Min	Max	Type	Documentation Ref	Page	Date	Lab	Comments
^{145}Nd	Lvl Density	4.0+6	2.0+7	Theo	BNL-NCS-51694		Apr83	BOL	Maino+PG75.GRPHS,TBL.PHENOMEN.PARS.
^{145}Nd	Lvl Density		4.2+3	Theo	BNL-NCS-51694		Apr83	KFK	Froehner.PG219.GRPH 'STARA' EST.LVLS
^{146}Nd	Lvl Density	4.0+6	2.0+7	Theo	BNL-NCS-51694		Apr83	BOL	Maino+PG75.GRPHS,TBL.PHENOMEN.PARS.
^{147}Nd	Lvl Density	4.0+6	2.0+7	Theo	BNL-NCS-51694		Apr83	BOL	Maino+PG75.GRPHS,TBL.PHENOMEN.PARS.
^{151}Nd	Lvl Density	4.0+6	2.0+7	Theo	BNL-NCS-51694		Apr83	BOL	Maino+PG75.GRPHS,TBL.PHENOMEN.PARS.
^{148}Pm	Lvl Density	4.0+6	2.0+7	Theo	BNL-NCS-51694		Apr83	BOL	Maino+PG75.GRPHS,TBL.PHENOMEN.PARS.
^{143}Sm	Lvl Density		2.4+2	Theo	BNL-NCS-51694		Apr83	KFK	Froehner.PG219.GRPH 'STARA' EST.LVLS
^{150}Sm	Lvl Density	4.0+6	2.0+7	Theo	BNL-NCS-51694		Apr83	BOL	Maino+PG75.GRPHS,TBL.PHENOMEN.PARS.
^{151}Sm	Lvl Density	4.0+6	2.0+7	Theo	BNL-NCS-51694		Apr83	BOL	Maino+PG75.GRPHS,TBL.PHENOMEN.PARS.
^{152}Sm	Lvl Density	4.0+6	2.0+7	Theo	BNL-NCS-51694		Apr83	BOL	Maino+PG75.GRPHS,TBL.PHENOMEN.PARS.
^{153}Sm	Lvl Density	4.0+6	2.0+7	Theo	BNL-NCS-51694		Apr83	BOL	Maino+PG75.GRPHS,TBL.PHENOMEN.PARS.
^{155}Sm	Lvl Density	4.0+6	2.0+7	Theo	BNL-NCS-51694		Apr83	BOL	Maino+PG75.GRPHS,TBL.PHENOMEN.PARS.
^{152}Eu	Lvl Density	4.0+6	2.0+7	Theo	BNL-NCS-51694		Apr83	BOL	Maino+PG75.GRPHS,TBL.PHENOMEN.PARS.
^{153}Eu	Lvl Density	4.0+6	2.0+7	Theo	BNL-NCS-51694		Apr83	BOL	Maino+PG75.GRPHS,TBL.PHENOMEN.PARS.
^{153}Eu	Lvl Density		1.1+2	Theo	BNL-NCS-51694		Apr83	KFK	Froehner.PG219.GRPH 'STARA' EST.LVLS
^{154}Eu	Lvl Density	4.0+6	2.0+7	Theo	BNL-NCS-51694		Apr83	BOL	Maino+PG75.GRPHS,TBL.PHENOMEN.PARS.
^{155}Eu	Lvl Density	4.0+6	2.0+7	Theo	BNL-NCS-51694		Apr83	BOL	Maino+PG75.GRPHS,TBL.PHENOMEN.PARS.
^{156}Eu	Lvl Density	4.0+6	2.0+7	Theo	BNL-NCS-51694		Apr83	BOL	Maino+PG75.GRPHS,TBL.PHENOMEN.PARS.
^{153}Gd	Lvl Density	4.0+6	2.0+7	Theo	BNL-NCS-51694		Apr83	BOL	Maino+PG75.GRPHS,TBL.PHENOMEN.PARS.
^{155}Gd	Lvl Density	4.0+6	2.0+7	Theo	BNL-NCS-51694		Apr83	BOL	Maino+PG75.GRPHS,TBL.PHENOMEN.PARS.
^{156}Gd	Lvl Density	4.0+6	2.0+7	Theo	BNL-NCS-51694		Apr83	BOL	Maino+PG75.GRPHS,TBL.PHENOMEN.PARS.
^{157}Gd	Lvl Density	4.0+6	2.0+7	Theo	BNL-NCS-51694		Apr83	BOL	Maino+PG75.GRPHS,TBL.PHENOMEN.PARS.
^{158}Gd	Lvl Density	4.0+6	2.0+7	Theo	BNL-NCS-51694		Apr83	BOL	Maino+PG75.GRPHS,TBL.PHENOMEN.PARS.
^{159}Gd	Lvl Density	4.0+6	2.0+7	Theo	BNL-NCS-51694		Apr83	BOL	Maino+PG75.GRPHS,TBL.PHENOMEN.PARS.
^{161}Gd	Lvl Density	4.0+6	2.0+7	Theo	BNL-NCS-51694		Apr83	BOL	Maino+PG75.GRPHS,TBL.PHENOMEN.PARS.
^{160}Tb	Lvl Density	4.0+6	2.0+7	Theo	BNL-NCS-51694		Apr83	BOL	Maino+PG75.GRPHS,TBL.PHENOMEN.PARS.
^{181}Ta	$\sigma_{n,X\gamma}$	6.5+6		Theo	BNL-NCS-51694		Apr83	LAS	Arthur.PG311.GRPH CFD W
W	$\sigma_{n,X\gamma}$	6.5+6		Theo	BNL-NCS-51694		Apr83	LAS	Arthur.PG311.GRPH CFD TA
^{208}Pb	Lvl Density	3.0+6	2.4+7	Theo	BNL-NCS-51694		Apr83	PAR	Jacquemin.PG105.GRPHS.PART.STATE DEN
^{234}U	Lvl Density	NDG		Theo	BNL-NCS-51694		Apr83	HAR	Lynn.PG345.GRPH VS PAIRING GAP
^{238}U	Res.Params.		4.5+3	Theo	BNL-NCS-51694		Apr83	GEL	Rohr.PG291.GRPH. RED. WN VS E
^{238}U	$\langle\Gamma\rangle/D$	NDG		Theo	BNL-NCS-51694		Apr83	GEL	Rohr.PG291.GRPH.SO VS DIFF S1 THRESH
^{238}U	Lvl Density		4.2+3	Theo	BNL-NCS-51694		Apr83	KFK	Froehner.PG219.GRPH 'STARA' EST.LVLS

NEUTRON DATA REFERENCES

Element	Quantity	Energy (eV) Min	Max	Type	Documentation Ref	Page	Date	Lab	Comments
^{238}Np	Lvl Density	NDG		Theo	BNL-NCS-51694		Apr83	HAR	Lynn.PG345.GRPH VS PAIRING GAP
^{239}Pu	Lvl Density	NDG		Theo	BNL-NCS-51694		Apr83	HAR	Lynn.PG345.GRPH VS PAIRING GAP
^{240}Pu	$\sigma_{n,f}$	5.0+5	5.0+6	Theo	BNL-NCS-51694		Apr83	HAR	Lynn.PG345.GRPH CALC CFD EXPT
^{240}Pu	Lvl Density	NDG		Theo	BNL-NCS-51694		Apr83	HAR	Lynn.PG345.GRPH VS PAIRING GAP
^{241}Pu	Lvl Density	NDG		Theo	BNL-NCS-51694		Apr83	HAR	Lynn.PG345.GRPH VS PAIRING GAP
^{242}Pu	Lvl Density	NDG		Theo	BNL-NCS-51694		Apr83	HAR	Lynn.PG345.GRPH VS PAIRING GAP
^{241}Am	$\sigma_{n,f}$	1.0+6	4.0+6	Theo	BNL-NCS-51694		Apr83	HAR	Lynn.PG345.GRPH CALC CFD EXPT
^{242}Am	Lvl Density	NDG		Theo	BNL-NCS-51694		Apr83	HAR	Lynn.PG345.GRPH VS PAIRING GAP
^{245}Cm	Lvl Density	NDG		Theo	BNL-NCS-51694		Apr83	HAR	Lynn.PG345.GRPH VS PAIRING GAP
Many	Lvl Density	NDG		Theo	BNL-NCS-51694		Apr83	GEL	Rohr.PG291.GRPHS.LVL PAR 'A' VS MASS